The long-term development of peatlands in Peruvian Amazonia

Thomas James Kelly

Submitted in accordance with the requirements for the degree of Doctor of Philosophy

The University of Leeds

School of Geography

January 2015

The candidate confirms that the work submitted is his/her own, except where work which has formed part of jointly authored publications has been included. The contribution of the candidate and the other authors to this work has been explicitly indicated below. The candidate confirms that appropriate credit has been given within the thesis where reference has been made to the work of others.

The work in Chapter 5 of the thesis has appeared in publication as follows:

Thomas J. Kelly, Andy J. Baird, Katherine H. Roucoux, Timothy R. Baker, Eurídice N. Honorio Coronado , Marcos Ríos, and Ian T. Lawson. 2014. The high hydraulic conductivity of three wooded tropical peat swamps in northeast Peru: measurements and implications for hydrological function. *Hydrological Processes*, 28:3373–3387

I was responsible for collecting the hydrological data, writing the text and drawing the diagrams. Euridice N Honorio Coronado contributed the vegetation data and this is acknowledged separately in the thesis. The contribution of the other authors consisted of comments on the drafts of the text.

The work in Chapter 5 of the thesis has also appeared in publication as follows:

Lawson, I.T., Jones, T.D., Kelly T.J., Honorio Coronado, E.N., & Roucoux, K.H. 2014. The geochemistry of Amazonian peats. *Wetlands.* DOI: 10.1007/s13157-014-0552-z

I contributed the water table data, including the description given in the text. This is the only data from this paper which also appears in this thesis. The other authors collected the data and wrote the majority of the text, which I commented on.

Acknowledgements

I would like to give a big thanks my two main supervisors, Ian Lawson and Katy Roucoux, for their steadfast support, and in particular for accompanying me on my first field season to Peru. Without the small NERC grant, "Long-term forest dynamics in Peruvian Amazonia" which they secured in 2010, none of this research would ever have happened. Working as a scientist in the Amazon is a privilege which I do not take for granted. Along with Tim Jones, we also set up the tropical pollen reference collection during late 2010, which has proven to be an invaluable investment. Many thanks to Tim for his early contributions to the project.

I would also like to thank my third supervisor Tim Baker for his help with statistics, floristic identifications, and logistical help with organising fieldwork. Euridice Honorio Coronado provided me with invaluable information on the ecology of floodplain forests. I would especially like to thank Andy Baird for being part of my research support group and for giving so much of his time to discussions on peat hydrology, for his help with peatland modelling, and for field training in Wales which taught me the skills that I later used in Peru.

I would also like to thank Charlotte Bryant for consultation on Radiocarbon sampling and on the application process; Nicole Sanderson and Steve Haley at Exeter University for processing the ^{210}Pb samples; Bill Baker at Kew Gardens for arranging and supporting me during my herbarium visit; Kalle Ruokolainen and Hanna Tuomisto for advice prior to my first fieldwork season and for supporting my visit to take samples from their herbarium in Turku; Oliver Clark, Esme Shattock and Wayne Murphy who accompanied me during my fieldwork in 2012; Hugo Vasquez, Julio Iriarica, Jhon del Aguila Pasquel, and Gian Carlo Padilla Tenazoa who also gave invaluable help during fieldwork; Paul Beaver and the staff at the Tahuayo Lodge; many colleagues at the Instituto de Investigaciones de la Amazonia Peruana, but especially Angel Salazar and Ricardo Faranñay; and David Ashley, Rachel Gasior, and Martin Gilpin for their support and advice during my lab work here in Leeds. I would also like to thank my fellow PhD students, staff, and researchers in Geography, especially Freddie Draper, Greta Dargie, Liz Watson, Dylan Young, Dom Emery, Calum Carson, Jacqui Manton, Ant Blundell, Carol White, Gemma Dooling, Joey Talbot, Jorge Ramirez, Lauren Parry, Ed Turner, Tom Collins, Patrick Rolfe (RIP), Chris Williams, Wannes Hubau, and Nikee Groot. It would have been a much lonelier road without you all.

I would like to acknowledge NERC for my PhD studentship, and for additional funding in the form of three radiocarbon grants (Numbers: 1612.0312, 1558.0411, 1747.1013). A Royal Geographical Society Dudley Stamp award helped to fund the hydrological work at

San Jorge and Buena Vista. Leeds University helped to fund my geochemical analyses. Graeme Swindles kindly funded one of the radiocarbon dates on the San Jorge core.

I would like to acknowledge the Ministerio de Turismo in Iquitos who gave their permission for the work at Quistococha, and the Dirección General Forestal y de Fauna Silvestre of the Peruvian Ministerio de Agricultura who granted me my broader research permit (No. 352-2011-AG-DGFFS-DGEFFS).

Finally much love and thanks to my Mum and Dad, and my Nan who have given me so many things, far beyond measure. Also, love to my girlfriend Claire who has been of great support to me through my PhD; I daren't think how many miles we've both put in to travelling between Leeds and Kent over the last four years! In many ways it has been a difficult time, and my Mum sadly passed away during the summer of 2013, followed by my Nan in the summer of 2014. It is a source of some sadness that they aren't here to see this thesis finished, but they knew me and they knew that I would reach the end of the road. My Mum was a Proust fan, amazing the curators at a museum in in France with the fact that she had read all of his work (!), so I will finish on this quote: *"The real voyage of discovery consists not in seeking new landscapes but in having new eyes".* Onwards and upwards.

ABSTRACT

Amazonian peatlands are carbon dense ecosystems which also contribute to the biological diversity of the western Amazon. Their existence remained unconfirmed until scientific studies in the last decade revealed extensive peatlands in the Pastaza-Marañón basin of Peru. This study sought to investigate the palaeoecological history and hydrological behaviour of peatlands in the Pastaza-Marañón basin. The aims of the study were to determine the key drivers of past vegetation change in two Amazonian peatlands, to produce the first explicit conceptual model of Amazonian peatland development, to improve our understanding of the hydrological behaviour of Amazonian peatlands, and to improve interpretations of the late Quaternary tropical pollen record.

Field data were collected in order to determine the saturated hydraulic conductivity (*K*), an essential parameter for hydrological models, in three Amazonian peatlands. Measured *K* at 50 cm depth varied between 0.00032 and 0.11 cm s^{-1}, and at 90 cm, it varies between 0.00027 and 0.057 cm s^{-1}. Simulations using a simple hydrological model suggest that under current climatic conditions, even with high *K*, peatlands would be unable to shed the large amount of water entering the system via rainfall through subsurface flow alone. An annual record of water table variation from one site, Quistococha, shows that the water level can fall rapidly (c. 1.6 cm d^{-1}) in the absence of rainfall. The main conclusions to be drawn from this part of the study are that most of the water leaves these peatlands via overland flow and/or evapotranspiration, and that regular rainfall is essential for maintaining the moist conditions necessary for continued peat accumulation.

Palaeoecological data were collected from two peatlands: Quistococha and San Jorge. The data from Quistococha constitute the first multiple-core study of an Amazonian peatland, and form the basis of a developmental model. These data show that a well-placed single core can represent the main vegetation changes, although multiple cores add valuable detail to the picture of site development. Lateral growth mostly occurred through 'primary mire formation', where peat begins accumulating simultaneously across a site: the expansion of Quistococha therefore differs from many temperate and sub-arctic peatlands, where primary mire formation is mostly confined to coastal areas. Differences in the subsurface topography are shown to have affected vegetation development, and likely resulted in higher beta diversity than present during the early stages of Quistococha's development. At San Jorge, radiocarbon dating has revealed a period of slow accumulation between 1300 and 450 cal yr BP which is also associated with a major change in vegetation from a *Pistia* dominated aquatic pollen assemblage to a *Mauritia* and *Mauritiella* dominated palm swamp assemblage. This is amongst the first

evidence suggesting an effect of late-Holocene climatic change on ecosystems in the western Amazon, but will require confirmation through further work at other sites in the region.

Contents

List of Figures

List of Tables

Abbreviations

a.s.l.	corresponds to 'above sea level'
ANOVA	corresponds to 'analysis of variance'
d.b.h.	diameter at breast height (tree diameter measurements)
ENSO	stands for 'El Niño-Southern Oscillation'
ITCZ	stands for 'intertropical convergence zone'.
K	refers to hydraulic conductivity.
Ka	corresponds to thousands of years.
LIA	stands for 'Little Ice Age'
LOI	corresponds to loss-on-ignition
Ma	corresponds to millions of years.
MCA	stands for 'Medieval Climate Anomaly'.
Mel./Comb.	stands for 'Melastomataceae and Combretaceae undifferentiated'.
NMDS	stands for 'non-metrical multidimensional scaling'
PAZ	stands for 'pollen assemblage zone'.
s.d.	stands for 'standard deviation'
SEM	stands for 'scanning electron microscope/microscopy'.
t.	In the context of a Latin name 't.' is the abbreviation for 'type'.
Undiff.	stands for 'undifferentiated'

1. Introduction

1.1 Project background

Recent research has shown that tropical forests, already known to be substantial carbon stores, may be acting as carbon sinks which are offsetting anthropogenic greenhouse gas emissions (Phillips et al. 1998; Baker et al., 2004; Lewis et al., 2004). With an estimated 120 ± 30 Pg C stored in biomass in the Amazon (Malhi et al. 2006a), of which 93 ± 23 Pg C is in above-ground biomass (Malhi et al. 2006b), the Amazon rainforest plays a significant role in the terrestrial component of the global carbon cycle.

However, this above-ground living component is only one part of the story with respect to carbon storage in tropical regions. Large quantities of carbon are stored in tropical soils (Sierra et al., 2007), lake sediments (Aniceto et al., 2014), and peatlands (Page et al., 2011). Tropical peatlands are estimated to cover an area of around 441,000 km^2, and to store at least 88.6 Pg C (Page et al., 2011). This makes them one of the largest terrestrial stores of organic carbon in the tropics (Jaenicke et al., 2008). Carbon released from tropical peatlands (and wetlands more broadly) affects the Earth's climate through the addition of carbon dioxide and methane to the atmosphere (Page et al., 2002; Li et al., 2007; Sjögersten et al. 2014). In Amazonia, Southeast Asia, and Africa peatlands also add to the between-habitat (beta) diversity, and provide important habitats for threatened animal species (Nicholson, 1997). Indeed, the mono-dominant stands of fruit-producing trees such as *Mauritia flexuosa* frequently found in Amazonian peat swamps are important for endangered animals such as the lowland tapir (*Tapirus terrestris*; Bodmer, 1990).

The majority of tropical peat (~77% by volume) is thought to occur in Southeast Asia, and it is estimated that Southeast Asian peatlands alone store around 55 Pg C (Jaenicke et al. 2008; Page et al., 2011). However, there are few intact peatlands remaining in Southeast Asia, due to significant human impact in the form of deforestation, drainage, fire damage, and changes in land use (Ballhorn et al., 2009; Danielsen et al., 2009; Hooijer et al. 2010; Koh et al., 2011). In Peninsular Malaysia, Sumatra, and Borneo, it is estimated that around 30% of peatlands have been deforested since 1990 (Miettenen and Liew, 2010), with many being degraded through conversion to oil palm (most often *Elaeis guineensis*) plantations (Mietinnen et al., 2012). Yet recent studies have shown that there are also substantial intact peat deposits in the Peruvian Amazon and Brazil (Lähteenoja et al., 2009a,b; Lähteenoja and Page, 2011), and research into peatland carbon storage is ongoing in the Congo Basin (Dargie et al. 2012). The latest published estimate for peatland area in Amazonia is around 150,000 km^2 (Schulman et al., 1999),

although this is based on little field evidence. It is thought that 35,600 ± 1,088 km^2 of this is in Peru (Draper et al., 2014), with studies showing peat there up to 7.3 m thick (Lähteenoja and Page, 2011). While remote sensing data indicate that there are hundreds of peatlands distributed across Amazonia (Lähteenoja et al., 2009a,b, 2013; Lähteenoja and Page, 2011; Lähteenoja, 2011; Householder et al., 2012; Draper et al., 2014), only a small fraction of these have been subjected to any kind of detailed on-the-ground investigation.

In the tropical lowlands of South America, peatland formation is closely tied to the large river systems which occupy the Amazon basin, as these create waterlogged areas where organic matter can be stored under anaerobic conditions. Most recent research has been focused in and around the Pastaza-Marañón basin of north-east Peru (Lähteenoja and Page, 2011). This area (c. 120,000 km^2) is a mosaic landscape, with floodplains and river systems belonging to the Ucayali, Marañón, and Amazon rivers and their tributaries surrounded by higher, older terraces that have a different vegetation and underlying geology (Räsänen *et al*., 1992). The peatlands found in this area vary in age; the number of radiocarbon dates is limited (see Chapter 3), but all that have been dated so far began to accumulate peat in the Holocene, and no peatlands older than 9 ka BP have been identified (Lähteenoja et al., 2012).

The uncertainty in estimates of carbon storage in the peatlands of the Pastaza-Marañón basin remains large (0.44-8.15 Pg C; Draper et al., 2014), but the total carbon storage of Peruvian peatlands is small relative to the amount stored in other tropical peatland areas, and very small relative to the global peatland carbon pool (c. 610 Pg C; Page et al., 2011). However, it appears that the carbon density of these peatlands is greater than that of the adjacent *terra firme* (dry-land) forest (Draper et al., 2014). *Terra firme* forest has a biomass of c. 293 Mg ha^{-1} or c. 144 Mg C ha^{-1} (based on data from 59 forest plots across Amazonia; see Baker et al., 2004), with estimates of an additional c. 227 Mg C ha^{-1} stored as soil organic carbon (Sierra et al. 2007); the best estimate for the above- and below-ground carbon storage in the Pastaza-Marañón peatlands is 892 ± 535 Mg C ha^{-1} (Draper et al., 2014). This pattern is not unique to the tropics: Buffam et al. (2011) found, in a forested North American wetland, that peatlands and lakes occupied less than a third of the landscape but stored more than 80% of the carbon. Therefore, the high carbon density of Amazonian peatlands makes them a priority for conservation in order to prevent and reduce emissions of CO_2 to the atmosphere, as argued for tropical peatlands in general by Murdiyarso et al. (2010).

Given their role as carbon stores and as habitats which contribute to the rich biodiversity of the Amazon region, it is important that we increase our understanding of the processes which operate within Amazonian peatlands, and particularly how they may respond to future climate change. Gloor et al. (2013) showed that the hydrological cycle has changed since 1990, with the wet season becoming wetter due to increasing Atlantic sea surface temperatures. Conversely, Amazonia also experienced two exceptional drought years in 2005 and 2010 (Lewis et al. 2011), and climate models and observations have predicted a future increase in drought frequency (Malhi et al. 2008; Hilker et al., 2014).

This study seeks to investigate the palaeoecological history and hydrological behaviour of peatlands in the Pastaza-Marañón basin, with the intention that this will provide insights into the vulnerability of these ecosystems to future environmental changes. Nine sites were explored as part of this work (see Chapter 3). Given the lack of previous research (reviewed in Chapters 2 and 3), this study sought first to investigate three different peatlands in order to examine their hydrological sensitivity. The hydrological properties of peatlands also have implications for the interpretation of the peatland archive. Taxonomic research was also undertaken to better describe key peatland pollen and spore types found in the peatland record. However, the focus of the palaeoecological analysis has been on two sites, Quistococha and San Jorge: the main focus of this work has been on establishing the vegetation history of these two peatlands through pollen analysis. These palaeoecological data have been used to test hypotheses relating to peatland development, including the nature of internal processes and the influence of external drivers. Later discussion chapters look in detail at the applicability of conceptual models previously developed for other peatlands, the variety of internal processes especially those related to lateral expansion of the peatlands, and the potential roles of late Holocene climatic change and river channel dynamics in driving peatland vegetation changes.

1.9 Conventions

1.9.1 Terminology

Details of terminology specific to the study area are discussed in more detail in Chapter 3, particularly those associated with forests and Amazonian floodplain systems.

The term ‘bog’ is used to refer exclusively to ombrotrophic (rain fed) peatlands.

The term ‘clayey peat’ used in other studies (*see* Wüst et al., 2003) is broadly synonymous with ‘mixed clay and organic matter’ used here. A mixture of clay and organic matter can be laid down in open-water sedimentary environments as well as

under vegetation, and so to avoid confusion the author prefers the latter, more descriptive term.

'Amazonia' is used here as a synonym for the Amazon River basin.

The suffix '-cocha' means lake in the Quechua language.

The term 'aguajal' refers to a palm swamp dominated by *Mauritia flexuosa* (Nicholson, 1997).

The term 'allogenic' refers to factors external to the (peatland) system being described, such as climate (Charman, 2002).

The term 'autogenic' refers to factors internal to the system being described; for example, hydroseral succession has been described as an autogenic process in wetlands (Charman, 2002).

1.9.3 Chronology

Unless clearly marked AD or BC, calibrated or known ages are provided in calendar years before present (cal yr BP), where the 'present' is defined according to the radiocarbon timescale (i.e. AD 1950). Negative ages therefore refer to periods after AD 1950. Uncalibrated radiocarbon ages are given in radiocarbon years before AD 1950 (^{14}C yr BP).

The Quaternary Period is defined as the last 2.58 million years of Earth's history, as ratified by the International Union of Geological Sciences (Gibbard et al., 2010).

The Holocene Epoch is defined as a sub-division of the Quaternary and refers to the most recent warm period which began 11.65 cal yr BP (Walker et al., 2009).

1.9.4 Taxonomic nomenclature

In pollen analysis, identifications are occasionally made to species level, but more commonly to genus or family. In the text, to avoid repetition, the abbreviation for species (sp.) is not used, so for example *Cecropia* is equivalent to *Cecropia* sp.

The term 'type' refers to a pollen taxon which does not perfectly map onto a single biological species, genus or family. For example, in European palynology '*Corylus*-type' includes pollen of *Corylus* and *Myrica.*

Family names, such as Moraceae, stand for undifferentiated pollen that has been identified to family level only.

In this thesis, families refer to those used in the main pollen keys for Amazonia, as discussed in Chapter 4. For example, many species in the Tiliaceae have been re-assigned to the Malvaceae (e.g. *Luehea*), but have been kept within the Tiliaceae in the

present study to prevent complications when comparing the diagrams in this study and previous work.

1.10 Layout of the Thesis

Chapter 2. Literature review detailing the conceptual framework of the thesis, existing research on tropical peatland palaeoecology and hydrology, Holocene climate change in Amazonia, and current knowledge of pollen taxonomy. Research gaps are identified prior to the presentation of the main thesis aims and hypotheses.

Chapter 3. Provides details of the region and field sites studied, including local climate, geology and the results of previous work.

Chapter 4. Describes the methodological framework and details the methods used in the thesis.

Chapter 5. Presents results relating to the hydrological behaviour of the sites. No prior published work exists on the hydrology of Amazonian peats and so this provides novel data which is also of relevance to understanding past behaviour.

Chapter 6. Presents the results of pollen and phytolith taxonomic investigations for peat swamp taxa, which provide the basis for identifications made later in the thesis.

Chapter 7. Presents the available chronological data for the cores obtained, including radiocarbon and ^{210}Pb based age-depth models

Chapter 8. Presents the pollen and stratigraphic data obtained at Quistococha, including a site survey, pollen analyses for four peat cores and one lake sediment core.

Chapter 9. Presents the pollen, geochemical, and stratigraphic data obtained at San Jorge, as well as site-level interpretations.

Chapter 10. Discusses the applicability of previous developmental models before putting forward a detailed conceptual model of site development for Quistococha. This includes an examination of the synchroneity of key changes in pollen abundance.

Chapter 11. Discusses potential drivers of peatland vegetation change using data from Chapters 7, 8, 9, and 10 as well as palaeoclimatic data from other studies. The discussion is structured as a series of developmental phases.

Chapter 12. Conclusions and a summary of the main findings.

2. Tropical peatlands, wetlands and the Holocene history of Amazonia

2.1 Introduction and theoretical framework

Peat is a form of soil which consists of partially decomposed organic matter that has accumulated in a waterlogged or subaqueous environment (Charman, 2002). Peat will accumulate in any situation where accumulation (litter input) exceeds the rate of decay (Charman, 2002). The precise definition of 'peat' varies (see Wüst et al., [2003] for a review), but in this thesis the definition follows that of Page et al. (2011) who undertook the most recent and most comprehensive review of tropical peatlands. Page et al. (2011) define 'peat' as a layer more than 30 cm thick consisting of at least 65% organic matter. Peatlands are found throughout the tropics in both upland and lowland environments, in Western Africa, Southeast Asia, and Central and South America (Page et al., 2011).

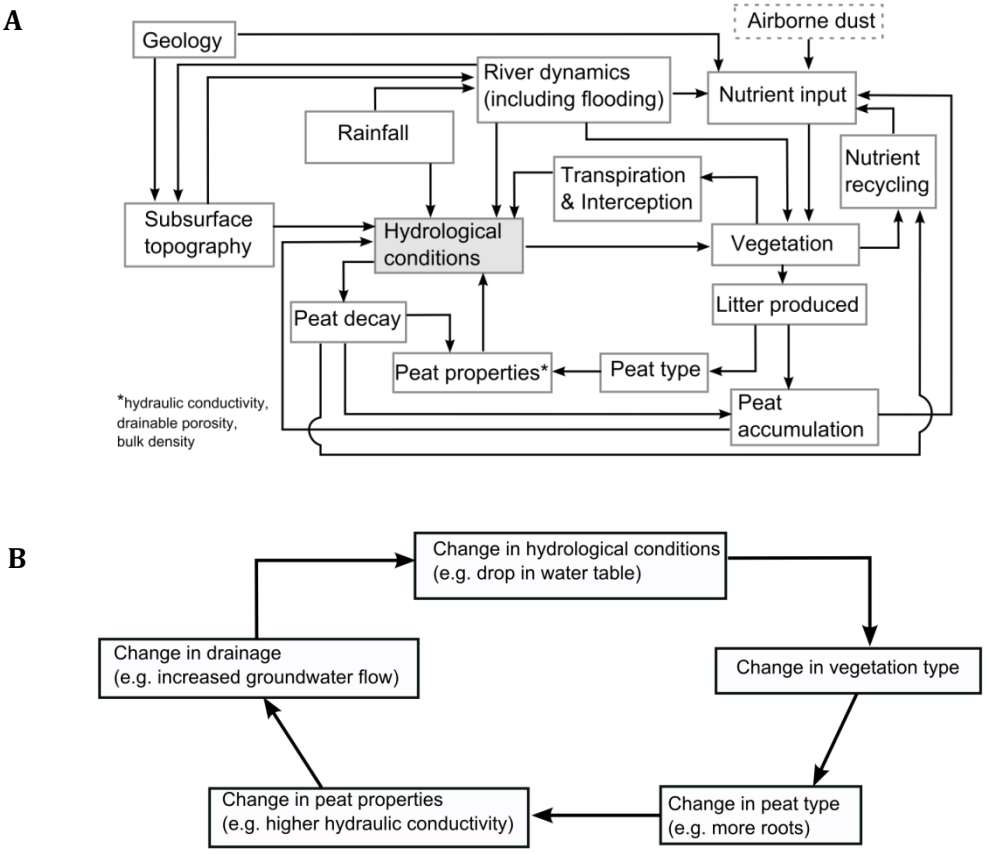

Figure 2.1: A: Relationships between different factors involved in the development of a peatland. The subsurface topography is one of the main starting conditions in a peatland and initialises a chain of further interactions through its effect on the local hydrology. The potential influence of airborne dust, especially on low nutrient (ombrotrophic) peatlands, has also been tentatively inferred. **B:** An isolated loop from within (A) showing a potential ecohydrological feedback linking peat properties such as hydraulic conductivity and peatland vegetation change. (Both diagrams are based on the author's analysis of the literature in this chapter, but draw particularly on: Charman et al., 2002; Morris et al., 2011; Baird et al., 2012).

There is a growing literature on tropical peatlands, but due to their general inaccessibility, the number of studies is still more limited than for northern peatlands. However, there is a great breadth of literature on temperate and subarctic peatlands (Charman, 2002), and this can be used to establish lines of enquiry in the tropics. The conceptual framework which underlies numerical models of peatland development produced for temperate peatlands summarises our understanding of peatland processes derived from measurements and observations (Frolking et al., 2010; Baird et al. 2012), and can be used to establish which areas of research may be the most important for understanding tropical peatlands. For example, the conceptual model in Morris et al. (2011) shows connections between the hydraulic conductivity, drainage, and oxic zone thickness, highlighting the importance of peat hydraulic properties to the development of a peatland as a whole. Few changes in peat accumulation can occur in a peatland without affecting either the hydrology or the vegetation, and these two elements are also intimately linked to one another through ecohydrological feedbacks (Figure 2.1; Waddington et al., 2014). It is beyond the scope of a single study to investigate all the factors relating to peatland development, and therefore this thesis has prioritised studying hydrology and vegetation as a way to advance our understanding of the developmental history of Amazonian peatlands.

Hydrology has a fundamental effect on almost all aspects of peatland function, including nutrient supply and plant distributions (Bunting and Warner, 1998). For example, the depth of the water table strongly affects the rate at which organic matter decomposes, and therefore the rate at which peat accumulates. Decaying organic matter not only releases gases (CO_2, CH_4), which can alter the rate of water flow through the peat by blocking pores (Beckwith and Baird, 2001), but also results in nutrient release that can alter the peatland vegetation (Page et al., 1999).

In turn, peatland vegetation can alter the hydrology of the peat: the type and quantity of litter produced by a given plant community has an effect on the hydraulic properties (see below) of the peatland (Boelter, 1969; Charman, 2002), and the rate at which water is transferred to the atmosphere through evapotranspiration (Schellekens et al., 2000). Vegetation type also affects the amount of material that will be stored as peat due to differences in decay rates and root litter addition (Frolking et al., 2010). As such, ecological succession has the potential to act as an internal driver in any peatland system through alterations to the litter input, hydrology and water balance, which then feed back to cause further vegetation change.

Peatlands are among the few ecosystems to record their own history (Walker, 1970), and the palaeoecological record can be used to reconstruct succession in peatlands over

long timescales (decades to millennia). This study seeks to combine knowledge of peatland vegetation change gained from the palaeoecological record with an understanding of peatland hydrology based on modern measurements. Together these two elements are capable of providing insights into past and future peatland development. To the best knowledge of the author, the only other study to have integrated modern hydrology and palynology is that of Glaser et al. (2004) in Canada, where an understanding of the modern hydrology allowed interpretations of the palaeoecological record to be greatly improved.

This chapter reviews the existing literature, drawing on research in northern peatlands as well as the tropics, with the aim of identifying current knowledge gaps. Throughout, this review focuses on the literature of most relevance to understanding the developmental history of the lowland, predominantly forested peatlands of the Pastaza-Marañón basin, though it also draws on information from other types of peatland around the world. This review examines previous research into tropical peatland hydrology, conceptual models of peatland development, and the palaeoecological and palaeoclimatic literature for Amazonia. The rationale for the research undertaken in the present study, and the main aims and hypotheses for the thesis are given at the end of this chapter.

2.2 Tropical peatland hydrology

There have been few studies of tropical peatland hydrology, and they have mostly focused on Southeast Asian peatlands degraded by fire and drainage. For example, Nagano et al. (2013) provide water table records for peatlands in Thailand which have been affected by peat subsidence (caused by drainage for agriculture). One of the main knowledge gaps in tropical peatlands is the lack of data for the two main peat hydraulic properties, drainable porosity (or specific storage; the amount of water which will drain from an aquifer under the force of gravity, in cm cm^{-1}) and hydraulic conductivity (*K:* the rate at which water will flow through an aquifer where there is a hydraulic head of 1, in cm s^{-1}) (see Shaw, 1994). Dommain et al. (2010) reviewed previous research into *K* for Southeast Asian peatlands, and there are just six studies (discussed further in Chapter 5). Several authors also provide values of *K* for tropical peat without clearly describing their method, particularly in terms of the depth at which the measurements were made(e.g. Hoekman, 2007; Sayok et al., 2007; Nugroho et al., 1997). While a wide range of values is reported (discussed further in Chapter 5), the method used to derive *K* estimates can have a significant effect on the data obtained (Surridge et al., 2005). Pajunen (1997) provides a detailed account of the physical properties (bulk density, hydraulic conductivity) of some peatlands in Rwanda. However, the vegetation of these

upland (>1000 m a.s.l.) Rwandan peat swamps is very different to most peatlands described for the lowland tropics (see Chapter 3, and Section 2.4), consisting of reeds such as *Cyperus papyrus* and *Cladium mariscus* (Pajunen, 1997). This may mean that they differ in terms of their hydrological behaviour.

Interactions between the many elements of the peatland system mean that numerical models can be especially useful with respect to testing hypotheses and predicting future changes in, for example, peat accumulation rate (Yu et al., 2001). However, there have been relatively few studies which have sought to model the hydrology of tropical peatlands, which may in part be a result of the lack of physical data discussed above. Wösten et al. (2008) highlighted the paucity of peat hydraulic data with which to parameterise their models, and due to the lack of any data on drainable porosity, were forced to use an estimated value. Modelling efforts have been concentrated in Southeast Asia and have sought to predict which areas are most vulnerable to fire damage, with the aim of directing preventative management. Wösten et al. (2008) modelled groundwater levels for a peatland area in Kalimantan, revealing the resilience of natural, undisturbed peatland to climatic perturbations (such as low rainfall in El Niño years). Conversely, areas which had been drained by canals or subjected to logging produced low modelled water tables, and were found to correlate with fire scars seen in satellite imagery (also see Wösten et al., 2006). Jaenicke et al. (2010) used a hydrological model to predict the effect of restoration measures (canal blocking) on water tables for a peatland area in Kalimantan, and thereby calculated the reduction in greenhouse gas emissions resulting from the decrease in peat decay.

While the response of peatlands to man-made drainage is likely to be similar in both Peru and Southeast Asia, the models of Wösten et al. (2008) and Jaenicke et al. (2010) are unlikely to be transferable to intact peatlands in Amazonia. The catchments (occupied by almost continuous peatland) modelled by these studies are very large: c. 150 x 140 km for Wösten et al. (2008), and 590 km^2 for Jaenicke et al. (2010). Rivers often form the boundary of these peatland areas, and may even drain them directly, but they are much smaller than the rivers of the Amazon floodplain. The peat thickness of the sites studied by Wösten et al. (2006, 2008) was up to c. 10 m, twice the depth of most Amazonian peatlands currently known (see Chapter 3). The peatlands of the Pastaza-Marañón basin of Peru (Lahteenoja et al., 2009a) and the Madre de Dios region (Householder et al., 2012) are not continuous in the same way as in Southeast Asia; instead, they are scattered throughout the basin. Application of a model such as that of Wösten et al. (2008) would require an accurate digital elevation model, but the available datasets, such as that from the Shuttle Radar Topography Mission, are based on remote sensing techniques which reflect the vegetation canopy height, not the ground level. In

Southeast Asia the thick (c. 10 m) peat domes create observable differences in topography; in Amazonia, the topographic difference from the margin of a peat dome may be only 1-2.5 m (Lähteenoja et al. 2009b; Swindles et al., 2014), and systematic changes in canopy height across a peatland may add significant uncertainty. Nevertheless, while the applications of landscape-scale hydrological models may be currently impractical, in principle there is no reason why long-term (thousands of years) site-level developmental models created for temperate peatlands (e.g. Frolking et al., 2010; Baird et al., 2012) could not be adapted for use in Amazonia. These models could be used to help predict the response of peatlands to projected future climatic changes.

In Amazonian peatlands, only limited hydrological data were available at the start of the present study. Lähteenoja and Page (2011) took spot measurements of water table depth at nine different sites. Swindles et al. (2014) have since measured water tables across Aucayacu peatland, and found that values range from c. 12 cm above the surface (pools) to 48 cm below the surface (under litter hummocks around the base of trees). However, river levels and rainfall fluctuate throughout the year in the Peruvian Amazon (Chapter 3), which will likely also affect peatland water tables. Peatland water tables in other regions can vary from day to day and week to week as a result of changes in rainfall (e.g. Oughtershaw peatland, UK; Holden, 2006). Continuous water table records are therefore preferable to spot measurements in most peatlands. With respect to modelling the hydrology of Amazonian peatlands, and by extension peatland development, knowledge of peat hydraulic properties is paramount (Baird et al., 2012; Rosa and Larocque, 2008; Page et al., 1999). The lack of hydrological data at the outset of this study was therefore an important research gap as hydrological processes are critical to peatland function.

2.3 The Holocene in Amazonia

2.3.1 Holocene climate change

Sections 2.1 and 2.2 explained the importance of hydrology to peatland function. In Section 2.2, the emphasis was on the influence of internal properties which affect water flow in peatlands and on peatland models which have looked at the effect of short-term changes in hydrology. However, hydrological changes can also be caused by climatic change which can persist for long periods of time (centuries to millennia). Climate is known to be one of the main factors which drives peatland development across the world (Figure 2.1), and the response of peatlands to known Holocene climate events can provide analogues for the effect of projected future climate change (Charman, 2002). This section summarises the available palaeoclimatic data for this region for the Holocene, focusing on the time period covered by this study (i.e. from c. 4 ka BP).

2.3.1.1 Migration of the ITCZ

It has been said recently that, in relation to its size, there is a shortage of palaeoenvironmental records spanning the Holocene in Amazonia (Bush et al., 2007a). Recent reviews of mid- to late Holocene (last 6000 years) climate reveal Central and South America to be amongst the most data-poor regions of the world (Wanner et al., 2008). Based on evidence from palaeoenvironmental records outside of Amazonia, there have been significant changes in South American climate during the last 11,700 years. An increasing body of evidence shows that the Intertropical Convergence Zone (ITCZ) has moved southwards over the course of the Holocene (Curtis et al., 1999; Seltzer et al., 2000; Haug et al., 2001; Cruz et al., 2005; van Breukelen et al., 2008). There is a general consensus that this shift was caused by changes in insolation, orbitally driven by the precessional cycle (Haug et al., 2001; van Breukelen et al., 2008; Mayle and Power, 2008), and there is a strong correlation between insolation (January, 10°S) and many isotopic records of precipitation from South America (Bird et al., 2011a,b). The evidence for migration of the ITCZ comes from a variety of sources. To the north of Amazonia, records indicate a gradual decrease in precipitation over the course of the Holocene. For example, the Cariaco Basin record of titanium (Ti) and iron (Fe) shows that conditions were wet in northern South America between 10.5-5.4 ka BP, and that this was followed by a general drying trend (Haug et al., 2001). There was an especially marked reduction in rainfall just after 4000 cal yr BP (Haug et al., 2001). This trend is supported by isotopic evidence from Lake Valencia (Venezuela), which shows that the lake level has been falling since around 3,000 cal yr BP (Curtis et al., 1999). Conversely, records from more southerly areas (i.e. those south of 10°S) experienced dry conditions in the early Holocene, followed by an increase in rainfall during the late Holocene. At Lake Titicaca, lake levels were lowest during the early and mid-Holocene, but high lake levels were recorded after 4,500 cal yr BP (Baker et al. 2001). Likewise, the speleothem record from Botuvera cave (Cruz et al., 2005) in southeast Brazil shows that $\delta^{18}O$ values become increasingly negative over the course of the Holocene, indicating a gradual increase in precipitation. In summary, the movement of the ITCZ has resulted in shifting rainfall patterns on long timescales, with relatively drier conditions in the northern Amazon and relatively wetter conditions in the southern Amazon since c. 4000 cal yr BP.

Pollen-based evidence indicates that these Holocene climatic changes had an impact on Amazonian ecosystems. As might be expected, southern areas near to modern ecotonal boundaries were occupied by dry forest and savanna during the early Holocene (Mayle et al., 2000). Records from Bolivia, at Lagunas Bella Vista and Chaplin, have shown that the rain forest expanded to occupy these areas over the last 2000 to 3000 years (Mayle et al., 2000). However, away from these ecotonal areas, the impact of Holocene climate

change is harder to discern. Palynologically, large changes in vegetation type as recorded in Bolivia are more straightforward to interpret than subtle changes in composition, which can also be masked by a lack of taxonomic precision.

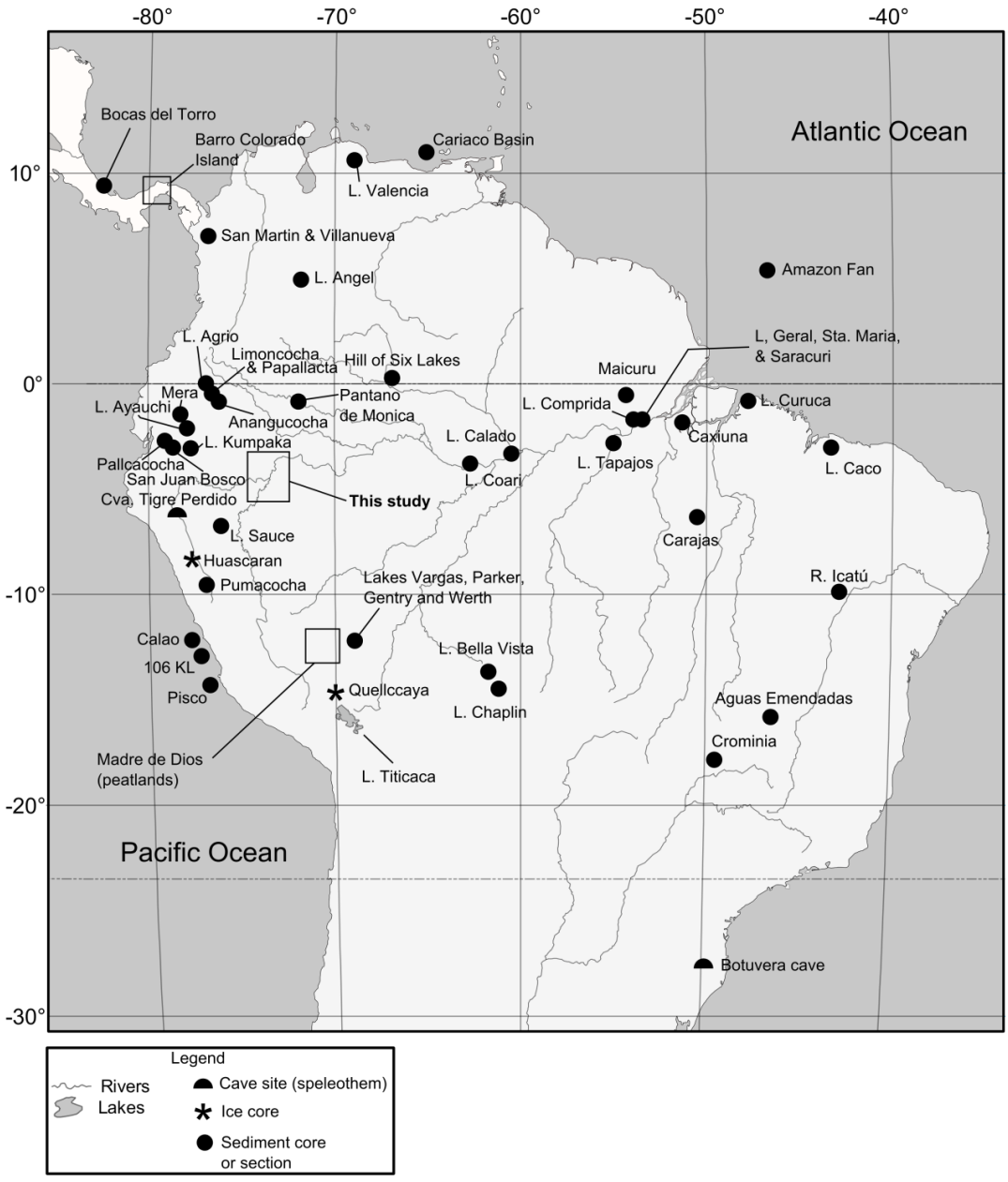

Figure 2.2: Key late Quaternary palaeoenvironmental records from across South America discussed in this thesis. The area of the present study has also been shown, as well as the location of Barro Colorado Island, the area from which the pollen Atlas of Roubik and Moreno (1991) originated, and the location of the Madre de Dios peatlands (currently no palaeoecological data).

Peatlands could help to reconstuct Holocene climate change away from ecotonal areas in the south of Amazonia. Tropical peatland sites can contain numerous different vegetation zones (see Section 2.4), and therefore when they respond to climatic change it is more likely that this will lead to shifts in vegetation which can be seen in the palaeoecological record. However, most peatlands currently known are less than 4000

years old (see Chapter 3), and as such they are more likely to record changes on shorter timescales (centennial scale) which are superimposed on the longer, precessionally-driven changes discussed in this section.

2.3.1.2 El Niño- Southern Oscillation (ENSO)

ENSO, characterised by shifts in atmospheric pressure and sea surface temperatures in the eastern and western Pacific (Rasmussen & Wallace, 1983), is the main source of inter-annual and decadal climatic variability across South America (Poveda et al., 2006; also see Chapter 3 for details of the modern phenomenon). The frequency and magnitude of ENSO cycles are thought to have changed on Holocene timescales (Haug et al., 2001). In some cases, these changes are difficult to distinguish from the southerly movement of the ITCZ discussed above, and changes in the frequency and amplitude of ENSO cycles are often superimposed on a longer-term trend which follows changes in insolation through the Holocene (Bird et al., 2011b).

During the very early Holocene (before 8 ka BP), El Niño events were frequent (every 2-8 years) and strong, and it is thought that eastern Pacific sea surface temperatures (SST) were c. 2 ˚C warmer than modern (core 106KL; Rein et al. 2005). However, during the mid-Holocene (c. 8-5.6 ka BP), El Niño events seem to have been weaker and less frequent (Rodbell et al., 1999; Rein et al., 2005; Donders et al., 2008). In a recent review of proxy data (particularly mollusc shell stable isotopes) from the mid-Holocene (c. 8-5 ka BP), Carré et al. (2012) concluded that SST was between 1 to 4˚C cooler than present, with predominantly La Niña-like conditions. Shell middens along the coast of Peru (Sandweiss et al., 2001), and numerical models (Clement et al., 2000), also support the evidence for weaker ENSO during the mid-Holocene.

In a study of a lake core from southern Ecuador (Pallcacocha), Rodbell et al. (1999) inferred that the 'modern' El Niño periodicity only became established after 5 ka BP, on the basis that clastic horizons associated with El Niño events occur at the modern frequency of 2 to 8.5 years after this point. Evidence from the west Pacific also shows an increase in ENSO at 5 ka BP (Gagan et al., 2004), but Rein et al. (2005) suggest this may have occurred slightly earlier at c. 5.6 ka BP. McGregor et al. (2013), in an isotopic study of a short coral record from the central Pacific, suggest that ENSO variance was lower than present by up to 79% as late as 4.3 ka BP. Hansen et al. (2003) record changes in vegetation on the eastern side of the Andes after c. 4 ka BP (e.g. a decline in *Podocarpus*) which indicate a shift to moister conditions around this time. In a review of terrestrial palaeoecological records from Africa and South America, Marchant and Hooghiemstra (2004) found a marked environmental change c. 4 ka BP, which they also attribute to the onset of stronger ENSO cyclicity. In summary, although there are some differences in

timing between different studies, most studies find that ENSO variance was weaker during the mid-Holocene and became fully established between 5 ka BP and 4 ka BP.

Several authors have also suggested that there was a marked increase in the amplitude of the 2 to 8.5 year ENSO cycle after around 2-3 ka BP (Gagan et al., 2004; Donders et al., 2008; Makou et al., 2010). In the western Andes, El Niño is associated with wetter conditions (see Chapter 3), and there is some evidence that these changes can be seen in terrestrial records, such as the pollen record from the Quimsacocha area (Andean Ecuador; Jantz and Behling, 2012) which shows a shift to moister conditions at around 2,200 cal yr BP, and the lake record from Laguna Blanca (Andean Venezuela; Polissar et al., 2013) which shows an increase in lake level from c. 2,000 cal yr BP onwards.

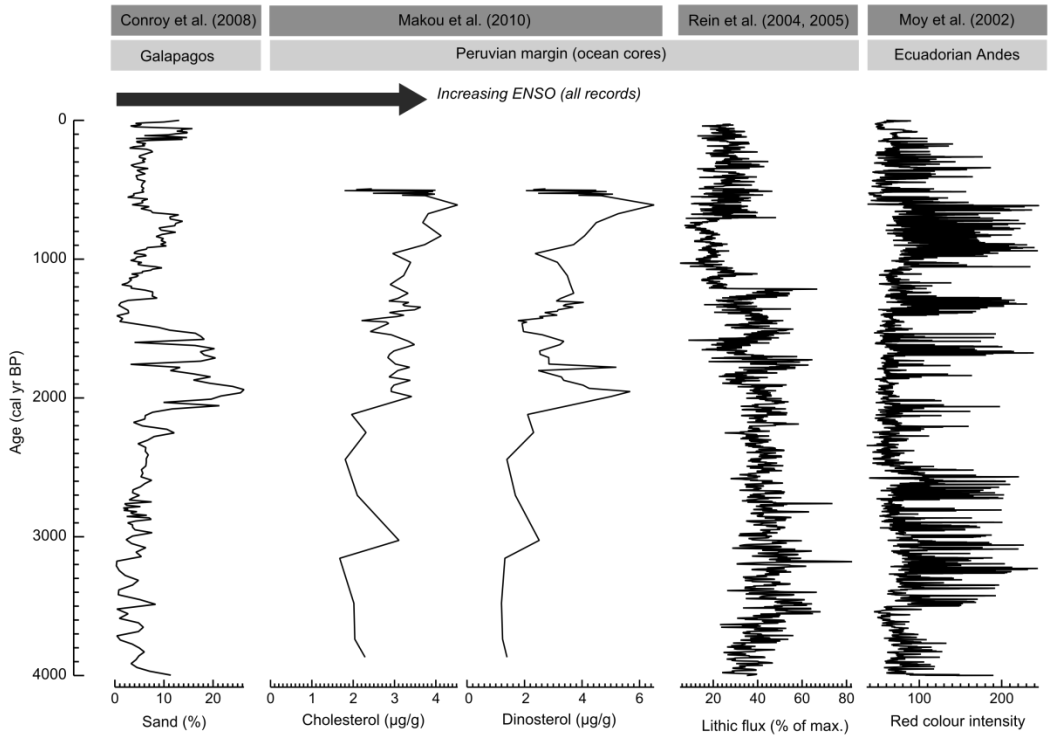

Figure 2.3: Principle ENSO proxy records from the South American region showing the last 4,000 years (note: records are arranged in order from west to east). The ability of palaeoenvironmental records to resolve the difference between ENSO frequency and amplitude is limited, and so these records reflect both of these elements (for example, in the Moy et al. [2002] record the relative intensity of the colour of the sediment is not directly proportional to differences in ENSO amplitude).

Yan et al. (2011) found a correlation between ENSO proxy records from Indonesia and the Galapagos (cf. Conroy et al., 2008; Oppo et al., 2009), and found that ENSO variance generally decreased during the period corresponding to the Little Ice Age (AD 1400-1850; Table 1). Although problems with dating marine sediments (e.g. ^{14}C reservoir effects) can mean that precise synchroneity is difficult to establish, there is also evidence that changes seen in ENSO proxy records correlate with distant archives such as those in the Arabian Sea (Rein et al., 2004). However, reconstructed ENSO fluctuations after 2 ka

BP vary somewhat between different proxy records; although all appear to show increased variability after 2 ka BP, correlating events between records is often difficult (Figure 2.2). This is not simply due to issues of chronology; many ENSO proxy records from South America correlate poorly with one another not simply in terms of the fine detail of change but also in broad terms (Figure 2.2). For example, in the record of Moy et al. (2002) from Pallcacocha (Ecuador), ENSO appears to peak at c. 1,000 – 700 cal yr BP, whereas in the Rein et al. (2004, 2005) record, ENSO is weak over this period. In the Conroy et al. (2008) record from El Junco in the Galapagos, little activity can be seen between 4 and 2 ka BP, but the record of Moy et al. (2002) indicates many ENSO events throughout this period.

In tropical South America, there are almost as many different proxies for ENSO as there are proxy records, including red pigment intensity (Moy et al., 2002), lithic flux and percentage sand content (Rein et al., 2004, 2005; Conroy et al., 2008), chlorins and carotenoid concentrations (Rein et al., 2004, 2005), and cholesterol and dinosterol concentrations (Makou et al., 2010). Some records are continuous up to the present day, and others are curtailed (e.g. Makou et al., 2010). Different proxies function in different ways and are not always easily comparable; for example, the pigment found in the record of Moy et al. (2002) only records the occurrence of an El Niño year, not its strength.

The importance of ENSO in the global climate system (see Section 2.3.1.3) means that long-term changes in its amplitude and frequency cannot be ignored when interpreting terrestrial records (including peatlands), especially in the tropics. The linkages between archives from across the world are becoming increasingly well established for the last c. 2,500 years (Rein et al., 2004), corresponding to the period following the increase in ENSO amplitude and frequency in the late Holocene discussed above. It could therefore be argued that many of the climatic changes which are well-known from proxy records in Europe and North America (see Table 2.1) originated in the tropics (Rein et al. 2004). If there were large changes in ENSO during the last 2000 years, it is likely that these would have affected peatlands in the western Amazon. However, the inconsistencies between records point to the need for caution when inferring ENSO as an explanation of past changes. These inconsistencies not only result from problems with chronology, but from the varying proxies used to reconstruct ENSO, each of which responds in a different way to El Niño conditions.

2.3.1.3 Amazonian palaeoclimatology in the global context

Observations of the modern climate have shown that ENSO has a definite effect on North American climate (e.g. Helama et al. 2009), and there is growing evidence for its

influence on European climate as well through the effect of ENSO on the stratosphere (Ineson and Scaife, 2009). Using a number of sources, including early instrumental data, the significant influence of ENSO on European climate has been demonstrated for at least the last 300 years (Brönnimann et al., 2007).

In the palaeoenvironmental record, there are clear similarities between reconstructed North Atlantic sea surface temperature anomalies and Ti concentrations in Cariaco basin sediments (a proxy for the position of the ITCZ) which demonstrate linkages between climate in tropical South America and the North Atlantic (cf. Bird et al., 2011a). Mayewski et al. (2004) also note that there have been connections between polar climate and the tropics throughout the Holocene.

Yan et al. (2011) and Rein et al. (2004) have shown that several climatically distinct periods, such as the Medieval Climate Anomaly (MCA), coincide with periods of changed ENSO activity in the tropics. The MCA is defined by generally warmer conditions in Europe, but MCA was probably global in extent and different regions experienced varying temperature and rainfall anomalies (Graham et al., 2011); the precise timing of the MCA remains a matter for debate. Helama et al. (2009) observed that the MCA, as seen in the low lithic flux of the Rein et al. (2005) record from coastal Peru (Figure 2.3), was coincident with a period of reduced rainfall reconstructed from tree rings in Europe. Graham et al. (2011) state that the MCA ran from c. AD 900 to 1350. Others would argue that the climate had already begun to change long before AD 1350, and that in fact the end of the MCA probably should be placed in the late 1200s AD (see Table 2.1). Seager et al. (2007) found that climate was generally drier across South America during the MCA, but data are very sparse. In several Andean archives there is little evidence for the MCA (Figure 2.4), whereas in others there is a clearer signal, such as the evidence for glacial retreat in the Andes at Queshquecocha (Stansell et al. 2013). Stansell et al. (2013) interpreted the glacial retreat as being the result of drier and warmer conditions, and as the rainfall feeding these sites is derived from the Amazon basin this implies that the lowlands were also drier at this time. However, whether this affected Amazonian peatlands remains to be examined.

Recent debates have also centred on the start of the Little Ice Age, a global climatic anomaly characterised by cooler temperatures in Europe (Graham et al., 2011). Some authors have suggested that a large volcanic eruption in AD 1257/1258 may mark the beginning of the LIA (Miller et al., 2012). Until recently the volcano responsible for this eruption was unknown, but it is now believed that the source was the Samalas volcano of Lombok Island in Indonesia (Lavigne et al., 2013). This exceedingly large tropical eruption is thought to have been one of the largest of the last 7000 years (Lavigne et al.,

2013), and was substantially larger than the eruption of Krakatau in 1883 (Mann *et al*., 2012). Models predict an initial cooling of c. 2 ˚C immediately after the eruption, with the effects continuing for several years until at least AD 1262 (Mann *et al*., 2012), with evidence for an El Niño-like response (i.e. "a warmer eastern equatorial Pacific and increased ENSO variability"; Mann et al., 2005, p.448). Whilst it is likely that low solar activity during this period helped to prolong any initial cooling (see Steinhilber et al., 2009), it is possible that the LIA began in the tropics.

Table 2.1: Summary of the main climatic periods for the last c. 2500 years which are commonly referred to in the literature. Ages have been given as calendar dates (AD/BC). Temperatures generally refer to the expression of a given event in Europe, where these events have been most thoroughly discussed; in the tropics the hydrological effect is likely to be of more importance.

Period	Timing (AD)	Overall window	References
Current Warm Period	1870 onwards [1], 1900 onwards [2]	AD 1870 onwards	[1] Hendy et al. (2002), [2] Bird et al. (2011a)
Little Ice Age	c. 1300-1900 [1], c. 1350-1850 [2], c. 1400-1850 [3], c. 1500-1900 [4], 1400-1700 [5]	c. AD 1300-1900	[1] Ljungqvist (2010), [2] Wanner et al. (2008), [3] Yan et al. (2011), [4] Thompson et al. (1986), [5] Mann et al. (2009)
Medieval Climate Anomaly (a.k.a. Medieval Warm Period)	c. 900-1350 [1], c. 800-1300 [2], c. 1000-1300 [3], c. 950-1250 [4], 950-1250 [5].	c. AD 800-1350	[1] Graham et al. (2011), [2] Ljungqvist (2010), [3] Yan et al. (2011), [4] Goosse et al. (2012), [5] Mann et al., (2009)
Dark Ages Cold Period	c. 300-800 [1], c. 500-900 [2], c. 720-930 [3]	c. AD 300-930	[1] Ljungqvist (2010), [2] Yan et al. (2011), [3] Helama et al. (2009)
Roman Warm Period	c. 1-300 [1], c. 50-400 [2]	c. AD 1-400	[1] Ljungqvist (2010), [2] Yan et al. (2011)

In spite of inconsistencies seen in ENSO records discussed above, the LIA appears distinctive in many proxy climate records from across South America; the LIA appears to be one of the most consistently observed events of the last 4,000 years (Figure 2.4). Evidence for the LIA can be seen in reduced Ti concentrations in the Cariaco Basin (Haug et al., 2001), in the $\delta^{18}O$ record from Lake Pumacocha (Bird et al., 2011a), in the Quelccaya and Huascaran ice cores (Thompson et al., 1986; 1995; 2013), and in the Cascayunga speleothem record (Reuter et al., 2009). Sediment cores from proglacial lakes in the Peruvian Andes also show a period of glacial advance during the LIA (Figure 2.4; Stansell et al., 2013), and there is evidence for cooling in the Andean pollen record from Quimsacocha (Jantz and Behling, 2012). In mangrove swamps around the mouth of the Amazon (Bragança peninsula) there was a period of reduced flooding between AD 1560 and the end of the 1800s (Cohen et al., 2005).

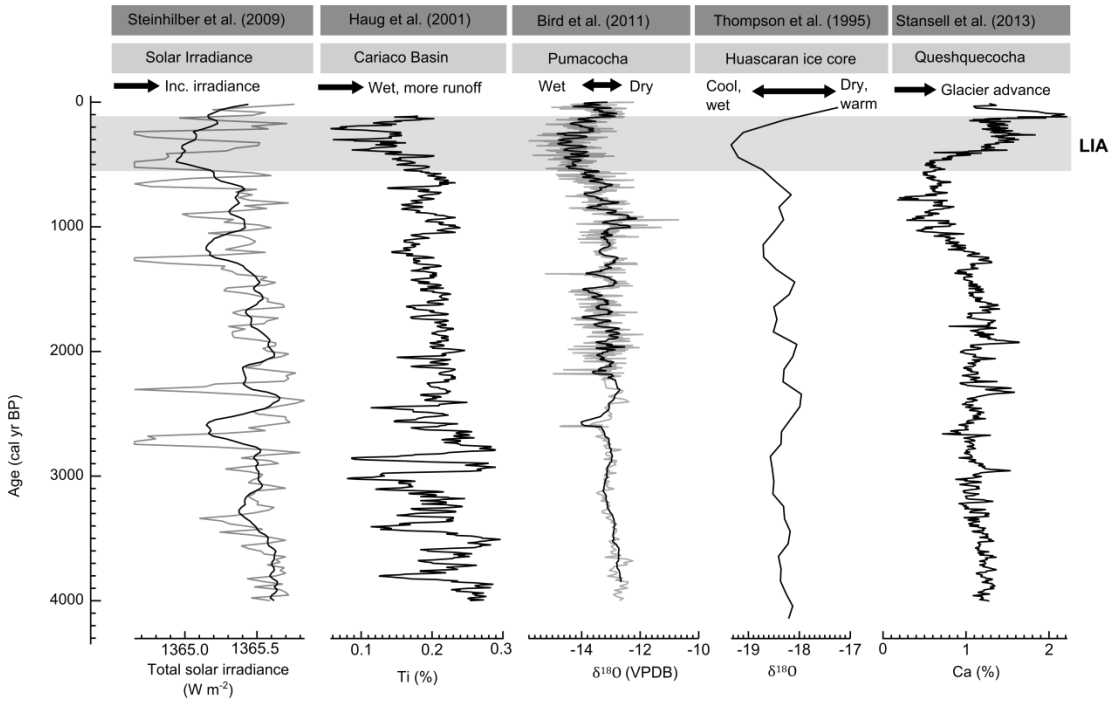

Figure 2.4: Records for the last 4000 years, illustrating the evidence for Little Ice Age (LIA) climatic change across different proxy records from Andean Peru (Pumacocha, Huascaran, Queshquecocha) and Venezuela (Cariaco Basin). Solar Irradiance has also been shown for reference. (Note: a ten point moving average [solid black line] is shown over the un-averaged data [grey line] for Solar Irradiance and Pumacocha).

In summary, there is evidence for late Holocene climate changes, especially around the time of the Little Ice Age as observed in other regions of the world. The degree to which the Medieval Climate Anomaly might have affected Amazonian peatlands is also of particular interest, as this period of possibly drier climate in the Amazon may be an analogue for near-future climatic change. In records covering the Last Glacial, drier climate has been inferred on the basis of depositional hiatuses (which imply low lake level), such as those at Carajas, Maicuru and the Hill of Six Lakes (Ledru et al., 1998; d'Apolito et al., 2013). Currently, available data are not capable of revealing evidence for centennial-scale hiatuses in accumulation in Amazonian peatlands (cf. Lähteenoja et al. 2009a, 2012). Extending our knowledge of the palaeoecological record is the only way to examine in detail whether the events summarised in Figure 2.4 had an effect on peatlands.

2.3.2 History of human occupation in Amazonia

Interpreting palaeoecological records requires knowledge of all the processes at work in the landscape, including those which result from the actions of people. Palaeoecology has also provided important insights into the debate surrounding Pre-Columbian populations that could not have been gained through site-based archaeology (Athens and Ward, 1999; Mayle & Iriarte, 2014). The evidence for human occupation in the

Iquitos area will be examined in detail in Chapter 3, with a particular focus on the site at Quistococha where there is archaeological evidence for pre-Columbian settlement. In this section, the broader context of human settlement in Amazonia is discussed, along with the debates surrounding the size of pre-Columbian populations, their distribution, their impact on Amazonian ecosystems, and finally an analysis of how this may be of relevance to Amazonian peatland research.

Evidence from Caverna da Pedra Pintada (Brazil) shows that there have been people in Amazonia for the entirety of the Holocene (Roosevelt et al., 1996). Indeed, if the radiocarbon dates obtained by Roosevelt et al. (1996) are calibrated, the oldest date for human occupation is around 12,995 ± 290 cal yr BP, which precedes the onset of the Holocene epoch. The archaeological evidence indicates that this community was living largely on forest resources, such as nuts, seeds, and game animals (Roosevelt et al., 1996). Evidence from other sites also confirms that there have been human populations in Amazonia for most of the Holocene, with worked quartz and amethyst from Lapa do Gaviao (Amazonian Brazil) occurring in contexts dated to 7900-8140 cal yr BP (Prous & Fogaca, 1999). At another site near Taparinha (Brazil), pottery associated with freshwater shells dates to c. 7800-8000 cal yr BP (Roosevelt et al., 1991). The Central Amazon Project (CAP) working near Manaus has also established that there are at least 67 archaeological sites in the 1000 km^2 area that they have studied (Neves & Petersen, 2006). Of these, ten are early, pre-ceramic sites, some dating back to c. 7700 cal yr BP (Neves & Petersen, 2006).

The size of pre-Columbian populations has been the subject of intense debate for many years (Heckenberger et al., 1999; 2003). It is now well established that the native population of South America collapsed dramatically following first contact with Europeans in AD 1492 (Bacci, 2011). The lack of resistance to many European diseases, such as smallpox and measles, meant that the number of native people living in South America, and in Amazonia specifically, may have fallen by more than 90% in just 50 years (Bush and Silman, 2007). While the indigenous population of Amazonia in 1972 was around 500,000 (Denevan, 2006), some have estimated that during the Pre-Columbian period it may have been as high as 11 million (Bush and Silman, 2007). This raises the possibility that Amazonian forests may have been significantly affected by human activity during the Holocene. Whilst some have suggested a so-called 'bluff' settlement model where human populations and their impacts were focused on terraces along the main rivers (Denevan, 1996), others have cited evidence from areas such as the Xingu region of Brazil as suggesting that Amazonian environments far beyond the floodplains may also have been extensively altered by pre-Columbian peoples (Heckenberger et al., 2003). Other evidence has been cited of extensive human

occupation along the lower Negro River, where there is evidence for settlement at 31 different sites. One of these (Açutuba) has an area of *terra preta* (highly fertile anthropic soil) and artefacts that covers over 30 ha (Heckenberger et al., 1999). Radiocarbon dating at this site indicates occupation over the last 1000 years, with some indication that it may extend much further back into prehistory (c. 4900 cal yr BP).

The impact of pre-Columbian cultures must have been limited by a lack of metal tools (Denevan, 1996). Recent studies have even suggested that some areas of the Bolivian Amazon were never cleared, but were already occupied prior to the expansion of rainforests c. 2 ka BP and kept open (Carson et al., 2014). Experimental archaeology has shown that it would have required a large investment of time and effort to clear even a small area of *terra firme* forest for agriculture (Denevan, 1996). It is therefore likely that pre-Columbian methods of agriculture differed from those used in Amazonia today, as the limited capacity for clearing forest would have made shifting agriculture impractical (Denevan, 2004). Indeed, it has been hypothesised that the *terra preta* soils found across Amazonia are the result of continuous cultivation around permanent settlements (Denevan, 2004). Agroforestry techniques, where useful trees are encouraged to grow or are deliberately planted, would also have been of lower impact than the establishment of totally open clearings. Trees are certainly widely used by modern indigenous groups in Amazonia, one example being the *Iriartea* palm which is used both as a construction material (poles and thatch) and as a source of food (Macia, 2004). Although difficult to detect in the archaeological record, at Araracua in Columbia there is evidence of an abundance of fruit trees in the form of pollen, alongside that of maize and manioc (Denevan, 1998). Clement (2006) presented evidence for the domestication of tree species which looks at the size and nutritional value of the peach palm (*Bactris gasipaes*). The yield for this palm is much higher in parts of Brazil than in populations found along the Ucayali River (Peru), which could indicate that some populations have been modified as a result of domestication (Clement, 2006).

As part of the debate surrounding the impact of Pre-Columbian peoples, palaeoecology has provided important insights that could not have been gained through other methods, such as site-based archaeology (Athens and Ward, 1999; Mayle & Iriarte, 2014). Palaeoecology has also provided a way of determining the environmental and climatic context of occupation (Mayle and Iriarte, 2014), which is some cases has substantially altered our understanding of the degree to which pre-Columbian people were responsible for forest clearance, as opposed to maintaining existing open areas (Carson et al. 2014). Palaeoecology and archaeology have been applied together in regions such as the Bolivian Amazon and the Guianas to determine when geoglyphs, raised fields, or other earthworks were constructed, and the period over which they

were occupied (e.g. McKey et al., 2010; Iriarte et al., 2012; Whitney et al., 2013; Carson et al., 2014). At several sites, pollen and charcoal records have also been used to infer human impact by burning or to support other more fragmentary evidence of human presence (Iriarte et al., 2012; Mayle & Iriarte, 2014). For example, evidence of *Zea mays* pollen and phytoliths in Ecuador has indicated that it has been cultivated in Amazonia for at least 5000 years (Bush et al., 1989). Fire histories have shown that human impact was often localised, and centred around lakes and other water sources (e.g. Bush et al., 2007a,b). This supports the inferences made from archaeological sources by authors such as Denevan (1996).

As an agent of ecosystem disturbance and vegetation change, fire is important in many parts of Amazonia, and it has been suggested that fire has altered swamp successions in Venezuela (e.g. Rull, 1999; see Section 2.5.3). However, by comparison with more southerly (ecotonal) areas, natural fires have likely been less significant in the western Amazon where the fire return interval is estimated at > 900 yrs (i.e. fires may never occur naturally in some areas; Mayle and Power, 2008). Modern studies, such as that of Nepstad et al. (2004) have shown that even small increases in evapotranspiration (c. 15%) or decreases in rainfall can dramatically alter the flammability of forests and so cause an increased probability of fire, and fire frequencies have likely changed during the Holocene (Mayle and Beerling, 2004). Bush et al. (2008) argued that under dry conditions, man-made fires are also more likely to escape and cause widespread burning. However, while man-made fires could also have been more prevalent during the pre-Columbian period, Iriarte et al. (2012) did not find this to be the case in their study of raised fields in French Guiana. In the seasonally dry forests of southern and northeast Brazil, soil profiles contain significant quantities of charcoal of Holocene age (Pessenda et al., 2004, 2010), but this is in contrast to a recent study in the western Amazon where soil pits in *terra firme* areas were found to contain little or no charcoal in most cases (McMichael et al., 2012). While there is a need for further soil pit surveys and lake charcoal data, this would *a priori* suggest that fire has not been a significant agent of ecosystem disturbance in the western Amazon during the Holocene, in contrast to Venezuela (cf. Rull, 1999). However, charcoal counts will be used to test this idea for the peatlands in this study.

In Chapter 3, further details will be presented which summarise the archaeological research previously undertaken in the study region. The research reviewed in this section has shown that people have lived in Amazonia throughout most of the Holocene, that pre-Columbian indigenous populations may have been much larger in the past than at present, that they were likely concentrated along rivers (as are peatlands in the western Amazon; Lähteenoja et al., 2009a), and that they made use of a wide range of

forest resources. There is therefore the possibility that human resource use could have affected peatlands in prehistory, and this must be considered when interpreting vegetation changes reconstructed in peatland palaeoecological records. However, these records may also record pre-Columbian land-use in adjacent areas, as particles such as pollen and microscopic charcoal can travel on the wind and be preserved in peatlands (Mayle and Iriarte, 2014). In particular, while the archaeological record may be fragmentary or be limited by poor stratigraphic integrity, lake and peatland records can offer a more continuous record in some circumstances, allowing greater chronological precision (Iriarte et al., 2012; Mayle & Iriarte, 2014).

2.4 Succession and the terminology of vegetation change

Succession can be defined as 'vegetation change through time' (Cooper, 1926). Hydroseres have been a focus for the study of succession as they are amongst the few successions to preserve their history in pollen and other plant remains (Walker, 1970; Burrows, 1990). Although plant species have long been known to behave in an individualistic manner in terms of migration, dispersal, and succession (*cf.* Gleason, 1917), authors such as Tansley (1935; 1939) have argued that ecosystems can develop as a series of predictable phases. Indeed, Tansley (1935) would disagree with the initial definition of succession given above:

> *"But I think that the concept of succession involves not merely change but the recognition of a sequence of phases (admittedly continuous from one phase to another) subject to ascertainable laws: otherwise why do we employ the term succession instead of change?"*
>
> *Tansley (1935), p. 286*

In Tansley's (1935) lexicon, 'catastrophes' are effectively not a part of the normal, predictable, autogenically-driven successional processes but serve only to interrupt them, and as initiating causes. Tansley (1935) argues that prediction achieved through the application of general rules is paramount in the study of succession, and excludes 'catastrophes', thereby making it simpler to theorise and elucidate successional rules.

The conceptual importance of succession in peatland development is supported by a body of palaeoecological data from northern hemisphere peatlands. Abrupt changes in carbon accumulation rate are often associated with changes in vegetation (Belyea and Malmer, 2004), a finding that has been supported by numerical models (e.g. Bauer, 2004). The change from minerotrophic to ombrotrophic plant communities in particular has been found to have an impact on organic matter accumulation. Several studies have shown higher rates in raised bogs than in fens (Tolonen and Turunen, 1996; Turunen et al., 2002), with some suggesting that this is related to the change in vegetation (Witte and van Geel, 1985), but the pattern is far from straightforward and other factors, such as hydrology, are clearly important (Bauer, 2004; Figure 2.1).

The work of Walker (1970) in particular critiqued much of the classical thinking about hydroseral succession, including notions such as oakwood 'climax' communities developed by authors such as Tansley (1939). In a review of twenty pollen records, chosen because they were not obviously affected by allogenic processes, Walker (1970) found a variety of different vegetation successions. For example, reed swamp generally transitioned into fen, but also occasionally transitioned directly to a bog community (Walker, 1970). In a later review of peatland successions in Ontario (Canada), Bunting and Warner (1998) also found that some transitions were more common than others. In this sense, succession can be seen as a probabilistic process (Walker, 1970).

There is also an increasing recognition that changes observed in palaeoecological records, particularly peatlands, can be caused by a combination of both allogenic and autogenic processes (Lavoie et al., 2013). The term 'allogenic' refers to factors external to the system being described, such as climate in the case of peatlands (assuming that feedbacks from individual peatlands to the climate system are negligible), and the term 'autogenic' refers to factors internal to the system being described (Charman, 2002). Hydroseral succession has been described as an autogenic process (Charman, 2002). Allogenic factors can be "interpreted as an overlay" on internally driven processes (Foster & Wright, 1990; p.460), and may decrease the rate of an internal process, 'stabilise' it, 'reverse' it, or 'reinforce' it (Charman, 2002; p.144). As such, since the 1970s, ecologists have tended to move away from equilibrium-based paradigms such as those of Tansley (1935, 1939), and have instead sought to study the drivers and mechanisms of vegetation change (Glenn-Lewin *et al*., 1992). Episodes of climatic change can have an effect on plant succession and a modern plant community may continue to be influenced by an event which happened hundreds of years before (Payette, 1988). For example, at Titus Bog (Pennsylvania, U.S.A), Ireland and Booth (2011) have shown that rapid change in plant assemblages can occur during a shift in climatic conditions. Similarly, they showed that physical expansion of a peatland can occur during short, favourable climatic periods, without shrinking again when climatic conditions become less favourable again because of stabilizing ecohydrological feedbacks (also see Morris et al., 2011). In the peat core, this may be observed as a quick transition from (for example) aquatic to more terrestrial plant communities.

In summary, the meaning of 'succession' can vary considerably, with different authors applying different definitions (Burrows, 1990). While successional sequences cannot always be used to predict future changes, they can provide indications of the most likely phase which will follow a current vegetation community (Walker, 1970). If we combine an understanding of autogenic succession with one that takes into account the effect of

allogenic drivers, then 'succession' is a powerful concept which can provide important insights into peatland development through time.

2.5 Tropical peatland palaeoecology

2.5.1 Palaeoecology of Central American and Southeast Asian peatlands

There has been a sustained interest in the palaeoecology of tropical peatlands for over forty years (e.g. Anderson and Muller, 1975; Haseldonckx, 1977; Morley, 1981), and indeed the first palynological investigation of a tropical peatland was conducted more than 80 years ago (Polak, 1933). This section reviews previous research into the palaeoecology of tropical peatlands (Tables 2.3 and 2.4), and where possible comparisons are made with Amazonian peatlands with the aim of identifying research gaps. Some sites in Colombia (Pantano de Monica) have been subject to pollen analysis, and show evidence for peat-like accumulations in parts of the core; however, these are relatively thin, near surface 'root mats' overlying clay-rich sediments and muds more typical of sedimentary accumulations (Behling et al., 1999). As such, they have been included in a summary of lake records in Table 2.4.

Geographically, the nearest lowland tropical peatland area to the Amazon is that of Central America and the Caribbean. *Sphagnum*-dominated peatlands have been reported from Belize. A core was taken at the Sarstoon-Temash peatland in 2010, the preliminary results for which showed that pollen preservation was good and that the modern *Cyrilla*-Cyperaceae-*Sphagnum* vegetation could be a 'climax' community (Jarosz, 2011). The peatland here is thought to be around 3,000 years old, but detailed results have not yet been published.

The coastal peatlands of Costa Rica are dominated by *Raphia taedigera* (the only Neotropical *Raphia* species) and reportedly range in thickness from 0.5 to 15 m depth (Obando and Malavassi, 1993; Dransfield et al., 2008). Some of these are likely to have formed in abandoned river channels similar to many in Amazonia, within large-scale tectonic basins (Obando and Malavassi, 1993). One particular site that has been the focus of study is the Changuinola peatland on the east coast of Panama, which is domed and more than 7 m thick in places (Phillips et al., 1997). The formation of this peatland is thought to have been affected by tectonic subsidence (Phillips et al., 1997). Phillips et al. (1997) produced a vegetation classification based on field data for Changuinola which recognised seven 'phasic communities' (Table 2.2). More recent research has shown that the vegetation patterns observed in the Changuinola peatland are related to a phosphorous (P) gradient, with changes in vegetation and microbial communities from the P-rich areas of shallow peat at the margins towards the more P-depleted areas in the centre where peat accumulations are deeper (Troxler et al., 2012). Pollen analysis has

revealed that this spatial succession is also found down-core i.e. it is also a temporal succession (Phillips et al., 1997; Table 2.2).

Table 2.2: Comparison of spatial and temporal succession in a domed peatland at Changuinola, Panama (summarised from Phillips et al, 1997). Arrow denotes continuity of pollen assemblage across two different vegetation phases (i.e. they are indistinguishable in the pollen record). Note that this table does not follow geological convention, and places the oldest phase at the top to better facilitate comparison with Tables 2.3 and 2.4.

Phase	Spatial vegetation zonation	Temporal zonation (pollen)	Temporal zonation (pollen)
		Core ED-3	Core BDD-23
I	*Rhizophora* (mangrove)		
II	*Raphia-Laguncularia* (back-mangrove)		*Rhizophora, Laguncularia, Acrostichum*
III	*Raphia* (palm swamp)	Arecaceae aff. *Raphia*	*Raphia/Euterpe, Myrica, Sagittaria,* Cyperaceae/Poaceae
IV	*Raphia-Symphonia-Euterpe-Campnosperma* (mixed swamp forest)	↓	*Campnosperma, Raphia/Euterpe, Myrica*
V	*Campnosperma* (swamp forest)	*Campnosperma*	*Campnosperma, Raphia/Euterpe*
VI	*Rhynchorspora-Cyperus-Poaceae* (saw-grass/stunted forest)	Cyperaceae, Poaceae, *Ilex*	
VII	*Myrica-Cyrilla* (bog-plain)	*Cyrilla-Myrica*	

Most of the pollen sequences studied in tropical peatlands are from Southeast Asia (Table 2.3). As in Panama, a spatial succession has been observed in Southeast Asian peatlands, with a higher diversity community found on shallow peat around the margins of peat domes, grading towards a pole forest over thicker peat at the centre (Page et al., 2006). Anderson (1961) describes six different phasic communities in Sarawak culminating in an '*Ombretocarpus-Dactylocladus* association', although a smaller number of phases are found in other regions (e.g. Sumatra; Morley, 2013). Whilst there is only a small amount of data available for comparison (see Chapter 3), this shows that on the whole Southeast Asian and Amazonian peatlands differ in their arboreal composition at the genus level. Many Amazonian peatlands are dominated by palms in the genus *Mauritia* (Nicholson, 1997; Lähteenoja et al., 2009a), although trees in the genus *Calophyllum* have been found to be abundant at some domed peatland sites (see 'San Jorge' in Chapter 3). As in Panama, Anderson and Muller (1975) found that the spatial succession of Anderson (1961) can be seen down-core, although some of the phases seen in space were difficult to separate palynologically. In Sarawak, the later vegetation phases have been found to be similar in composition and growth form to open dwarf forests found elsewhere on white sand areas (Morley, 2013); a similarity between peatland pole forests and white sand forests is also found in Peru (Lähteenoja et al., 2009b; Chapter 3).

In the case of Southeast Asian peatlands, their successional histories have been controlled largely by eustatic changes in sea level since the end of the last glacial. Indeed, it has been suggested that sea level change has been a significant driver of peat initiation (Neuzil, 1997; Wüst, 2001; Dommain et al., 2014): the pollen of *Rhizophora*, a genus of typical coastal mangrove trees, can sometimes be found towards the peat/substrate contact (e.g. Anderson and Muller, 1975; Hillen, 1984). Pollen zones in many of the Southeast Asian records are dominated by a small number of genera (Table 2.3). Some common genera include *Campnosperma*, *Calophyllum*, and *Pandanus*; other genera are known to be common in Southeast Asian peatlands but are poorly represented in the pollen record (e.g. *Nypa*; Hillen, 1984).

Although most peatlands in Southeast Asia formed after c. 5 ka BP (Dommain et al., 2014), some are much older than their Amazonian counterparts: Anshari et al. (2001, 2004) found that the Pemerak peatland is > 30 ka in age, meaning that peat also accumulated during the last glacial period. At present, no Amazonian peatlands have produced basal dates older than 9 ka (Lähteenoja et al., 2012). The peatlands of Central America are similar in many ways to those of Southeast Asia, in that their development has been influenced by sea level change and coastal processes, although Phillips et al. (1997) found that the Changuinola peatland lacked the early mangrove phase of development.

As such, it would seem that successional histories from other parts of the tropics cannot necessarily be transferred to Amazonian peatlands in a straightforward way. Sites elsewhere are frequently older, have been affected by a different set of allogenic factors, and are occupied by different plant assemblages. The first peatland record from Quistococha shows that peat can accumulate under a diverse range of different vegetation types (Roucoux et al., 2013), and establishing whether there are consistent successional pathways in Amazonian peatlands (as in Central America and Southeast Asia; Table 2.2) remains a research gap.

2.5.2 Palaeoecological records from Amazonian lakes

As Amazonian peatlands are positioned on the floodplains of the Ucayali, Marañón, and Amazon Rivers (Lähteenoja and Page, 2011), information on long-term vegetation changes recorded in wetland lakes from other parts of Amazonia has been compiled to examine existing knowledge of floodplain vegetation succession in the region (Table 2.4). These records are not directly comparable to peatlands, in particular because the pollen source area of lakes and peatlands is different. The focus has been on sites which are likely to be of use in understanding Western Amazonian sites (hence sites from very arid areas in the South of Brazil have not been tabulated).

In some senses, the records summarised in Table 2.4 are not comparable to one another, because they occupy ecologically different parts of the Amazon Basin, an area which is roughly the size of Europe (Colinvaux et al., 2000). In the case of wind-borne pollen types such as Cyperaceae and Poaceae, their abundance can reflect local presence only (as part of marginal wetland vegetation), or savannas (wet or dry) which fill the landscape (such as the L. Carimagua record from Colombia; Behling and Hooghiemstra, 1999). It is difficult to find a general successional pattern across these records; many show similarity to one another only due to spatial autocorrelation as they are from similar wetlands in a single region (e.g. the records of Absy, 1979). Conversely, although some studies looked at more than one core from a given area, it is uncertain as to whether these studies have fully captured the local variability of a single site or river system (the issue of multiple-core sampling is discussed in Section 4.1.2). Some taxa occur across many of the records, such as *Symmeria paniculata*; (endemic to floodplain habitats; Kubitzki, 1989), *Cecropia* (common to disturbed areas and anemophilous; Parolin, 2002), and Cyperaceae and Poaceae (found in macrophytic communities; Kalliola et al., 1991). Palms are common throughout many of the records (e.g. *Mauritia, Mauritiella, Euterpe*), but do not occupy a consistent position in a 'succession'. In the Maxus 4 core (Weng et al., 2002), a *Mauritia* phase occurs towards the top of the core, but at Pantano de Monica (1), it is present throughout the core (Behling et al., 1999).

Comparison with the only available record for the region around Iquitos (Roucoux et al., 2013; Table 2.2) reveals some similarities with records from elsewhere in Amazonia. For example, the Myrtaceae phase has parallels in the records of Absy (1979), and *Cecropia* phases are common to many records (e.g. Frost, 1988; Weng et al., 2002). However, the Rubiaceae are not a common constituent in the lake records compiled in Table 2.3, and nor is *Ilex*, which is found more frequently in Southeast Asian peatland records (Table 2.2). There is a lack of data for the region around Iquitos, and a need for data which relates specifically to the wetlands and peatlands of the Western Amazon.

2.5.3 Palaeoecology of palm swamps in Amazonia

Many peatlands in the study region of this project can also be described as *Mauritia flexuosa* palm swamps (Lähteenoja et al., 2009), and this section reviews the literature with the aim of gaining insights into the formation of this forest type. Pollen of the palm genus *Mauritia* is common in the recent palaeoecological record, and where its pollen is abundant it is generally taken as an indicator of the presence of palm swamp habitat. De Lima et al. (2014) identified a total of 32 Quaternary records from across Amazonia where *Mauritia*-type pollen was found, and Rull & Montoya (2014) identified 41 but included ocean cores. Several of these are unlikely to provide insights into *Mauritia*

flexuosa swamp development in the western Amazon; some records are from > 1000 m elevation (e.g. Vereda das Águas Emendadas, Barberi et al., 2000), from southern parts of Amazonia with pronounced seasonality of rainfall, including a dry season > 6 months (e.g. Icatú River, De Oliveira et al., 1999; Crominia, Ferraz-Vicentini and Salgado-Labouriau, 1996), or contain only small percentages of *Mauritia*-type pollen which are not indicative of *Mauritia* swamp at the core site (e.g. L. Chaplin, Mayle et al., 2000; L. Angel, Behling and Hooghiemstra, 1998; L. do Caçó, Ledru, 2002).

Very few palaeoecological studies have looked at palm swamps, or more specifically *Mauritia* swamps, for their own sake. However, Rull & Montoya (2014) recently reviewed the available literature on *Mauritia* palm swamps. They found that *Mauritia* swamps had expanded during the mid- to late-Holocene, particularly in northern South America (Colombia, Venezuela), and were far less widespread during the last glaciation.

Other studies have looked at hydroseral succession in these habitats, either deliberately or incidentally. *Mauritia* 'phases' can be identified in a number of Holocene pollen records (Table 2.3). In the Maxus 4 core (Weng et al., 2002), from a lowland wetland in Ecuador, a significant *Mauritia* phase is visible in the record which lasts for around 3,000 years. In this case, the increase in abundance of *Mauritia* was interpreted as indicating an interruption of the 'normal' hydroseral succession driven by an increase in flooding, which favoured the growth of *Mauritia*. They also noted peat accumulations at this site, with the onset of peat accumulation following the infilling of the lake. As with the study by Ferraz-Vicentini and Salgado-Labouriau (1996), Weng et al. (2002) inferred that many of the vegetation changes observed in the palaeoecological record were caused by a combination of climatic change and river dynamics (flood energy and frequency).

In other records which contain evidence of a palm swamp phase, authors have also inferred that river dynamics have had a dominant impact on vegetation history in these habitats. Urrego et al. (2006) found that the succession on the floodplain in the Chocó of Colombia could also be seen down-core. However, hydrological changes driven by eustatic sea level change are also thought to have been significant in determining the pathway of vegetation change. For example, at Lake Comprida Bush et al. (2000) inferred that sea level rise caused a rise in water table during the early Holocene, which led to the formation of a *Mauritia* palm swamp which dominated the local vegetation for around 1000 years. A further example is that of Behling and Da Costa (2000), who inferred that sea level changes had a significant impact on the physical and successional development of a site on the Rio Curuá. At this site there is a significant *Mauritia* phase in the early part of the record (c. 7-6 ka BP), with a main peak which lasts for around

500 years. After this point, *Mauritia* declines, with Behling and Da Costa (2000) inferring that this was as a result of rising water levels.

However, the interpretation of *Mauritia* in the palaeoecological record has not been entirely consistent. Whilst Weng et al. (2002) interpreted the increase in *Mauritia* as being the result of increased flooding, at Anangucocha, Frost (1988) attributed the *decline* of *Mauritia* to an increase in flooding. In another study on Lake Sauce, Correa-Metrio et al. (2010) took *Mauritia* to be a taxon with an affinity for dry conditions, an inference which is somewhat at odds with its swamp habitat preference. It is possible to reconcile all of these interpretations, in that they are all expressions of relative shifts in hydrology and climate. However, these relative interpretations can make it difficult to make comparisons between records. Furthermore, whilst the habitat preferences of *Mauritia* mean that its occurrence in the palaeoecological record can generally be interpreted in hydrological terms, some have also suggested that its occurrence may be related to human impact. *Mauritia* is valued for its fruits, and is still widely harvested (Rull & Montoya, 2014; Chapter 3, this thesis). Although there is no direct evidence for deliberate *Mauritia* cultivation, its expansion has been connected to human influence on the landscape (Rull & Montoya, 2014). In the Gran Sabana (Venezuela), *Mauritia* expansion during the late Holocene is associated with charcoal indicative of extensive burning at many sites (Rull, 1999; Rull & Montoya, 2014). At Lake Geral, the increase in *Mauritia* is associated with other possible indicators of human impact such as *Cecropia* pollen and charcoal indicative of cooking fires (Bush et al. 2000).

These examples demonstrate some important points which relate directly to this study. Firstly, the pervasive impact of active river systems on Amazonia floodplains often leads to the disruption of 'normal' successional pathways. Sea level change, climate, and human activity have also affected vegetation histories, and so often overly successional processes. Secondly, the occurrence and persistence of *Mauritia* in the pollen record must be interpreted in the context of the other available sedimentological and palaeobotanical evidence. Depending on the preceding conditions, its appearance may indicate an increase or decrease in water level, successional change, or even human impact.

Reference	Anderson & Muller (1975)	Anshari *et al.* (2004)	Anshari *et al.* (2001, 2004)	Hasseldonckx (1977)	Hillen (1984)	Hope et al., (2005)	Morley (1981)
Site	Marudi	Pemerak (A)	Pemerak (B)	Pekan Nanas	Lower Perak	Enggelam E2P23	Palangkaraya (PR2)
Region	Southeast Asia	Southeast Asia	Southeast Asia	Southeast Asia	Southeast Asia	Southeast Asia	Southeast Asia
Age range (cal. yrs BP)	4.8 ka to present	37.6 ka to present	31 ka to present	5.6 ka to present		8.3 ka to present	n.a.
Zone 1 (oldest)	*Rhizophora*, *Nypa* , *Oncosperma*	*Calophyllum*	Arecaceae	*Oncosperma*	*Oncosperma*, Rubiaceae	*Pandanus,* Meliaceae, *Campnosperma*	Poaceae, *Pandanus*
Zone 2	*Campnosperma*, *Stenochlaena*	*Calophyllum*, Sterculeaceae	*Palaquium*, *Gluta*	Cyperaceae	*Campnosperma, Ilex*	*Campnosperma, Acalypha*	*Lithocarpus, Garcinia*
Zone 3	*Gonystylus*, *Garcinia*	Sterculeaceae, *Gluta*	*Calophyllum*, *Planchonella*	*Calophyllum*	*Ilex, Stemonurus*	Mel./Comb.	
Zone 4	*Pandanus*, *Dactylocladus*	*Gluta*	*Calophyllum*, *Palaquium* Dipterocarpaceae	*Campnosperma*, *Calophyllum*		*Campnosperma, Elaeocarpus*	
Zone 5		Dipterocarpaceae, *Madhuca, Calophyllum*	*Gymnostonia*, *Calophyllum*	*Gluta, Calophyllum*		Mel./Comb., *Elaeocarpus*	
Zone 6		*Madhuca, Gluta*				*Dacrydium*	
Zone 7		*Gymnostonia*					

Table 2.3: Summary of successional sequences based on pollen data from peatlands throughout the tropics (excluding data from lake sequences). Taxa are listed in order of numerical dominance in the pollen assemblages. Note that pollen zones do not always follow those given in the original publications; some zones have been sub-divided to better illustrate associations that were contemporaneous. Zone 1 represents the base of each sequence (i.e. is the oldest). Abbreviations: Mor./Urt. = Moraceae/Urticaceae. Mel./Comb. = Melastomataceae/Combretaceae. The author contends that *Mauritia* and *Mauritiella* are palynologically indistinguishable without grain size data (see Chapter 6), but the original identifications from the referenced studies have been retained. The pollen types listed are a simplification of the original datasets, and as with all pollen data, the pollen abundance is not always equivalent to the real abundance of a taxon in the palaeo-vegetation assemblage.

Reference	Morley (1981)	Morley (1981)	Phillips *et al.* (1997)	Pudjoarinto &Cushing (2001)	Roucoux *et al.* (2013)	Sémah *et al* . (2004)	van der Kaars *et al.* (2001)
Site	Palangkaraya (PR4)	Palangkaraya (PR8)	Changuinola	Telaga Balekambang	Quistococha	Pojoksari (G)	Rawa Danau
Region	Southeast Asia	Southeast Asia	Central America (Panama)	Southeast Asia	Amazon (Peru)	Southeast Asia	Southeast Asia
Age range (cal. yrs BP)	n.a.	n.a.	c. 3 ka to present	1.3 ka to present	2.3 ka to present	25 ka BP to present	15.7 ka to present
Zone 1 (oldest)	Poaceae	Pteridophyta	Arecaceae aff *Raphia*	Mor./Urt., Poaceae	Cecropiaceae	(Poaceae; no peat)	Mor./Urt., *Macaranga-Mallotus* t., *Gironniera*
Zone 2	*Lithocarpus*	*Pandanus, Campnosperma*	*Campnosperma,* Pteridophyta	Poaceae, Cyperaceae, Mor./Urt., *Lithocarpus*	Cyperaceae	Poaceae, *Typha*	*Elaeocarpus,* Mor./Urt., *Macaranga-Mallotus t.*
Zone 3	*Lithocarpus, Garcinia*	*Dacrydium*	Cyperaceae, Poaceae, *Ilex*	Poaceae, Cyperaceae, *Cyathea* type	Moraceae, *Mauritia/Mauritiella*	Elaeocarpaceae, Myrtaceae, *Ilex, Canthium*	*Macaranga-Mallotus t.*
Zone 4	*Calophyllum*	*Combretocarpus*	*Cyrilla*, *Myrica*, Cyperaceae, Poaceae		Myrtaceae and Rubiaceae	*(overlain by clays)*	*Elaeocarpus, Ilex*
Zone 5					*Mauritia/Mauritiella* and *Ilex*		*Arenga, Cocos nucifera* type, *Ilex*
Zone 6					*Mauritia/Mauritiella*		

Table 2.3 contd.

Reference	Absy (1979)	Absy (1979)	Absy (1979)	Behling *et al.* (1999)	Behling *et al.* (1999)	Behling *et al.* (1999)	Behling and Lima da Costa (2000)
Site ***Country (region)*** ***Age range (cal. yrs BP)***	Lago do Cajú Brazil (Amazonas) 2.2 ka to present	Lago Surara Brazil (Amazonas) 6 ka to present	Costa da Terra Nova Brazil (Amazonas) 2.9 ka to present	Panatano da Monica (1) Colombia (Quinché) 11 ka to present	Panatano da Monica (2) Colombia (Quinché) 4.5 ka to present	Panatano da Monica (3) Colombia (Quinché) 3.5 ka to present	Rio Curuá N. Brazil (Pará) 8.7 ka to present
Zone 1	Poaceae, *Alchornea*, Myrtaceae, Mel./Comb.	*Ouratea, Symmeria, Alchornea*, Myrtaceae	Poaceae, *Alchornea, Cecropia, Symmeria*	Mauritia, *Lycopodium*	*Caryocar*, *Protium*	Fabales, Malpighiaceae, *Eurterpe/Geonoma* t.	Moraceae
Zone 2	*Alchornea, Symmeria, Aldinia*	*Cecropia, Symmeria, Alchornea*, Myrtaceae	Poaceae, *Alchornea, Cecropia, Symmeria*, Cyperaceae	*Mauritia*, *Casearia*	Fabales, *Cecropia*	*Euterpe/Geonoma* t., *Banara/Xylosma t* Moraceae	*Mauritia*, Cyperaceae, *Sagittaria*
Zone 3	Myrtaceae, Cecropia	*Alchornea, Symmeria*	*Cecropia*	*Mauritia*, Moraceae, Anacardiaceae,	*Psychotria*	*Euterpe/Geonoma* t., Fabales	Cyperaceae, *Sagittaria*
Zone 4	Myrtaceae, Mel./Comb.	Myrtaceae, *Symmeria, Alchornea.*	*Cecropia, Piper,* Asteraceae		*Euterpe/Geonoma* t., *Caryocar*		Fabaceae, *Virola, Ilex*
Zone 5	*Symmeria*, Myrtaceae, *Aldinia*	Poaceae, *Symmeria, Alchornea*			Fabales, Moraceae		*Euterpe/Geonoma* t., *Virola,* Fabaceae
Other notes				**n.b.** Melastomataceae is abundant through			**n.b.** Melastomataceae and Moraceae are abundant throughout

Table 2.4: Summary of successional sequences taken from lake records in Amazonia (< 1000 m a.s.l.). None of these sites have confirmed peat accumulations, however they have been included due to the shortage of peatland pollen records from this region to provide an indication of typical floodplain pollen assemblages. For abbreviations, see Table 2.1.

Reference	Behling *et al.* (2001)	Behling (1996)	Bush *et al.* (2000)	Bush *et al.* (2000)	Colinvaux et al (1988)	Frost (1988)	Horbe *et al.* (2011)
Site	Lago Calado	Lago Curuça (B)	Lake Geral	Lake Comprida	Limoncocha	Anañgucocha	Lake Coari
Country (region)	Brazil (nr. Manaus)	N. Brazil (Pará)	N. Brazil (Pará)	N. Brazil (Pará)	Ecuador	Ecuador (Napo)	N.Brazil (R. Solimões)
Age range (cal. yrs BP)	9.3 ka to present	10.5 ka to present	8.2 ka to present	9.5 ka to present	1.1 ka to present	3.2 ka to present	10 ka to present
Zone 1	Cyperaceae, Poaceae, *Alchornea, Symmeria*	Arecaceae, *Ilex*, Mel./Comb.	*Symphonia*	*Mauritia* type	*Cecropia*, *Mauritia*	*Cecropia*	Cyperaceae, Poaceae
Zone 2	Cyperaceae,*Symmeria,* Poaceae, *Alchornea*	*Ilex*, Arecaceae, Mel./Comb.	*Amanoa*	*Mauritia* type, Poaceae	*Cecropia, Mauritia*, Elaeocarpaceae, Poaceae, Pteridophyta	*Cecropia*, *Mauritia* type, Pteridophyta	*Alchornea*, Mor./Urt., *Salix*
Zone 3	*Symmeria, Alchornea*, Mor./Urt.	Arecaceae	*Symphonia, Mauritia*	*Mauritia* type, Poaceae, Mel./Comb.	*Cecropia*	*Cecropia*, Pteridophyta	*Symmeria, Amanoa*
Zone 4		Arecaceae, *Rhizophora*, Poaceae	*Mauritia* type, *Cecropia*, Cyperaceae, Poaceae	Cyperaceae, Poaceae		*Cecropia*, Mor./Urt., Pteridophyta	*Symmeria, Alchornea, Mabea* type.
Zone 5				Cyperaceae, Poaceae, *Cecropia*			

Table 2.4 Contd.

Reference	Urrego (1997)	Urrego (1997)	Urrego (1997)	Urrego (1997)	Urrego *et al.* (2006)	Urrego *et al.* (2006)	Weng *et al.* (2002)
Site	Mariñame (1)	Mariñame (2)	Quinché (1)	Quinché (2)	San Martin	Villaneuva	Maxus 4
Country (region)	Colombia (Caquetá)	Colombia (Caquetá)	Colombia (Caquetá)	Colombia (Caquetá)	Colombia (Chocó)	Colombia (Chocó)	Ecuador (Yasuni)
Age range (cal. yrs BP)	n.a.	n.a.	n.a.	n.a.	4.4 ka to present	3.7 ka to present	8.1 ka to present
Zone 1	Mor./Urt., Bignoniaceae, *Mauritia*	*Cecropia*, Mor./Urt., Mel./Comb.	Papilionaceae, *Cecropia*, Mor./Urt.	*Cecropia*, Mel./Comb.	*Mauritiella*, *Campnosperma*	*Mauritiella, Campnosperma, Cecropia*	*Polypodium,* Malpighiaceae*, Ficus*
Zone 2	*Cecropia*	*Mauritia*, Mel./Comb., Anacardiaceae, Papilionaceae	Liliaceae, Mel./Comb.	Cyperaceae, *Virola*, Mel./Comb., *Mauritia* type, Pteridophyta	*Campnosperma*	*Euterpe* t., *Campnosperma*, *Mauritiella*, *Pterocarpus*	*Cecropia*
Zone 3	*Cecropia, Mauritia, Virola, Symphonia, Hedyosmum,* Malpighiaceae	Myrtaceae, Mel./Comb., *Macrolobium*	*Cecropia*, Papilionaceae	*Virola*, *Symphonia*, *Iriartea*, Pteridophyta	*Pseudobombax*, *Vantanaea*	*Mauritiella, Cecropia, Campnosperma, Piper*	Fabaceae
Zone 4	*Hedyosmum, Virola,* Mel./Comb., Mor./Urt.	*Mauritia*, *Euterpe/Geonoma* t.	Mel./Comb., Malpighiaceae	*Mauritia*, *Virola*, *Symphonia*	*Mauritiella*, *Vantanaea*, *Campnosperma*	*Mauritiella, Campnosperma*	*Ficus*
Zone 5	*Mauritia*, *Euterpe/Geonoma* t.		Mel./Comb., *Mauritia-t.*, Mor./Urt.		*Ilex, Pseudobombax, Campnosperma*	*Campnosperma*, Cyperaceae	*Sloanea*
Zone 6					*Mauritiella*, Mel./Comb.	*Mauritiella*, Cyperaceae, *Ilex*	*Mauritia*
Zone 7					*Guazuma, Ilex*	*Mauritiella,* Mel./Comb., *Ilex, Pseudobombax, Cecropia*	Myristicaceae
Zone 8					*Mauritiella, Amanoa*	*Mauritiella, Alchornea*	

Table 2.4 Contd.

2.6 Conceptual models of peatland development

The term 'conceptual model' in this thesis is taken to refer to a model reconstructing the development of a real peatland over time. In this case, conceptual models are therefore based on palaeoecological, stratigraphic, and chronological data collected from site surveys of peatlands (i.e. they are inductive). As such, this definition excludes simplified, hypothetical models of peatland development or conceptual frameworks which may form the basis of numerical model simulations (e.g. Belyea & Baird, 2006; Baird et al., 2012).

The model of Anderson (1961) was the first put forward for tropical peatlands, but was developed for sites in Southeast Asia where sea level change has been a significant driver of peat initiation (also see Neuzil, 1997; Dommain et al., 2014), and the succession described is not applicable to Amazonian peatlands (which have not been subjected to marine influence during the Quaternary). In the Anderson (1961) model, peat initiates on clay-rich alluvium due to the impermeability of the substrate, and the flat topography (which hinders drainage). Seaward migration of the coastline then affects the drainage of tidal rivers, causing an increase in the mean river level as peat also continues to accumulate. This process continues until sufficient peat has accumulated to form a flat 'bog plain' and a series of phasic plant communities (Anderson, 1961). There are elements of Anderson's (1961) model which may be relevant to Amazonian peatlands, such as the observation that the subsurface was unlikely to have been level prior to peat initiation and that therefore small areas of higher land would be occupied by forest of differing composition to lower depressions. Anderson (1961) also found that in the Rajang Delta, peat was always underlain by clay which helps to create the waterlogged conditions ideal for peat formation. Anderson (1961) discussed other factors which might be aid peat formation, such as the possible role of sulphur as an agent to reduce microbial breakdown (Anderson suggests that high concentrations of sulphur may be toxic to microbial organisms). Investigations into the role of micro-organisms in peat formation (or degradation) are still few (although see Dungait et al., 2012; Troxler et al., 2012).

Philips and Bustin (1996) put forward a model for the Changuinola peatland in Panama, but like the model put forward by Anderson (1961), this is a coastal peatland whose development has been affected by both marine processes and tectonic subsidence. There is evidence for Holocene tectonic subsidence in southern parts of the Pastaza depression (cf. Dumont, 1993) which has led to the formation of lakes, but at present there is no evidence that this could have affected the development of the peatlands in this area. The potential influence of subsidence on peatland formation in Peru is worthy of investigation.

The work of Lähteenoja *et al*. (2009a,b; 2011; 2012), and Householder *et al*. (2012) has laid a good foundation of research from which to build our understanding of Amazonian peatlands (synthesised in Chapter 3). However, as yet, data are not abundant and only a handful of sites (e.g. CICRA peatland in Madre de Dios, Peru; Householder *et al*., 2012) have been studied in detail. Householder et al. (2012) for example, provide a detailed map of the basin geomorphology of the CICRA peatland, but no radiocarbon dates or stratigraphic information which could be used to infer a developmental history. As such, there are no published conceptual or numerical models of peat development for Amazonian peatlands.

In northern peatlands, conceptual models have been put forward for a number of different peatlands, such as those in North America (e.g. Heinselman, 1963; Kratz and Dewitt, 1986; Futymar and Miller, 1986; Klinger, 1996; Anderson et al., 2003; Comas *et al.* 2004; Ireland et al., 2013) and Europe (e.g. Sjörs, 1983; Foster and Wright, 1990). These models mostly describe the ways in which peatlands expand laterally as a function of two processes; terrestrialisation and paludification. As plants colonise different areas they create a different kind of environment ('hydrophytic habitat'; Tansley, 1935) which can be colonised by other plant species. Terrestrialisation is where a peatland expands by converting open water into peatland through the accumulation of organic material (Tansley, 1939; Anderson et al., 2003), and paludification is where peatland expands onto surrounding areas of land (Sjörs, 1983; Anderson et al., 2003). There are two different kinds of paludification. The first is where plants and increasing peat accumulation alter the conditions at the peatland margins, resulting in impeded drainage and gradual peatland expansion (Heinselman, 1963; Klinger, 1996).The second kind of paludification is referred to by Sjörs (1983) as 'primary mire formation'; this can be thought of as spontaneous peat initiation where conditions are suitably waterlogged and poorly drained. In some cases, it has been suggested that a change in vegetation and edaphic conditions as a result of anthropic burning could also have caused this kind of peat initiation (Charman, 1992).

The 'classic model' of peatland development (Klinger, 1996; Ireland et al., 2012), and the similar 'expanded classic model' (Kratz and Dewitt, 1986), involves the lateral expansion of floating vegetation across the surface of a lake. This fills in the lake basin from the margin, resulting in the growth of peatland and the eventual expansion of the peatland onto marginal areas of land by paludification (Klinger, 1996; Anderson, 2003). Heinselman (1963) produced an opposing 'Myrtle Lake' model showing the persistence of the lake through time; there is also no "invasion zone" of sedges around the margin of Myrtle Lake at present (Heinselman, 1963; p. 350). In the 'Myrtle Lake' model, peat

accumulation occurs through gradual paludification of the surrounding area, and the lake persists, its level rising as the surrounding peat thickens.

Ireland et al. (2012, 2013) have argued that peatland expansion can also be accelerated by periods of climatic change; periods of terrestrialisation were found to correlate with drier climatic episodes. Ireland et al. (2012) also point to evidence from modern observations; peatlands encroached on lakes due to dry climatic periods in the 20th century (Buell et al., 1968). Indeed, recent debates have been partly focused around the relative importance of allogenic and autogenic drivers (Anderson et al., 2003).

These models for peatland development may have some applicability in the Amazon, but this remains to be tested with field data. Without data on peat stratigraphy, multiple basal ages, and palaeoecological data, establishing the degree to which any autogenic developmental pathways have been affected by allogenic factors is also currently impossible for Amazonian peatlands.

2.7 Palynology in Amazonian peatlands

2.7.1 Pollen and spore taxonomy

Having established the need for further palaeoecological research in Amazonia peatlands, this section aims to identify whether increased taxonomic knowledge is also required. In neotropical palynology, taxonomic difficulties have been a major obstacle to the formation of detailed palaeoecological interpretations. Some authors have estimated that the Brazilian portion of the Amazon forest alone may contain more than 11,000 tree species (Hubbell *et al*., 2008), and this sheer diversity coupled with the similarity of many pollen types has made the study of past vegetation changes taxonomically challenging. The low taxonomic resolution of many palaeoecological records has fuelled debates, especially those surrounding the composition of the Amazon forest during the Last Glacial (*cf.* Colinvaux *et al*. 2000, 2001; Van der Hammen and Hooghiemstra, 2000). In many diagrams, identifications are made only to the family level. While there have been important improvements in palaeoecological interpretations thanks to the production of pollen keys (e.g. Roubik & Moreno, 1991; Colinvaux *et al*., 1999), taxonomic studies of particular groups of taxa (*cf.* Burn and Mayle, 2008), and studies of the modern pollen rain (e.g. Gosling *et al*., 2005, 2009), difficulties still remain. With respect to peatlands, most of the taxa found in the peatland forests today are represented in pollen keys at the genus level (Table 2.5). However, distinctions between some ecologically important species are not yet possible; for example, the palm *Mauritia* is abundant in many peatlands (e.g. Lähteenoja et al., 2012), but its echinate pollen is generally held to be indistinguishable from that of *Mauritiella* which is also known from peatland areas (see Chapter 6).

In terms of the herbaceous vegetation in peatlands, the taxonomy of fern spores also requires further research. There is already a body of information on neotropical fern spores in existing pollen keys (*cf*. Colinvaux et al., 1999; Roubik and Moreno, 1991), but many of the species found in floodplain areas are not represented. Furthermore, it is not often clear where identifications to family, genus or species level can be made with confidence. Whilst fern spores are wind dispersed and therefore abundant in the palaeoecological record (e.g. Behling et al. 2000; Weng et al. 2002), in many pollen diagrams they are grouped morphologically (e.g. Colinvaux et al. 1988, 1997, 2001; Behling et al. 2000; Bush et al. 2007b). In general such groupings prevent comparison with available data on modern fern habitat preferences and forest type associations.

Table 2.5: Species common to peatlands in the study region (after Honorio Coronado; see Chapter 3), and the availability of pollen descriptions. Only a few taxa have published descriptions to species level, but all taxa have been described to genus. Reference abbreviations: CDM = Colinvaux et al., (1999), RM = Roubik & Moreno (1991), NPD = Neotropical Pollen Database, And. = Anderson (1993), DS = Dias Saba (2007), H = Haselhorst et al. (2013), F = Ferguson (1986)

	Availability of descriptions		
Peatland taxa	**Genus**	**Species**	**References**
Amanoa aff. guianensis	x		CDM
Calophyllum brasiliense	x		RM
Dendropanax cf. resinosus	x		CDM, RM, H
Diospyros poeppigiana	x		RM
Elaeoluma glabrescens	x		CDM
Eschweilera ovalifolia	x	x	NPD
Hevea guianensis	x		NPD
Inga stenoptera	x		RM, H
Mauritia flexuosa	x	x	CDM
Mauritiella armata	x		CDM, F
Matayba sp.	x		CDM
Pachira aff. brevipes	x		CDM, DS
Remijia aff.ulei	x		And.
Symphonia globulifera	x	x	RM
Tabebuia insignis var. monophylla	x		CDM, RM, H
Triplaris weigeltiana	x		RM

2.7.2 Phytoliths

Phytoliths are microscopic particles secreted in the leaves and other organs of plants (Piperno, 2006). They are known variously as 'plant opal' and 'silica cells', but 'phytolith' (literally 'plant stone') seems to be the most appropriate term as plants can manufacture both siliceous and calcareous particles (Piperno, 2006). The silica used by plants to create siliceous phytoliths is obtained from groundwater and transported as monosilicic acid before being deposited in the growing cells (Pearsall, 1994). Phytoliths are produced by a large number of tropical plant families (Piperno, 2006), including many which are abundant in peatlands. Taphonomically, phytoliths differ greatly from pollen; whereas pollen must be dispersed by plants as part of their reproductive cycle, phytoliths form part of the plant structure and play no part in the reproductive process

(Piperno, 2006). Phytoliths enter the soil when a plant dies and degrades, and the durable phytoliths are released (Piperno, 2006). Phytoliths, being composed of biogenic silica, are exceedingly resistant to decay. As such, as the normal processes of decay work on the plant material deposited on the peat surface, the phytoliths remain. In a peatland, they largely reflect the local vegetation and in many cases they reflect vegetation which has died in situ; they can therefore be seen as acting like plant macrofossils (Piperno, 2006), in that they represent the very local vegetation (unlike some pollen types).

Many palms produce spherical, spinulose phytoliths (e.g. *Oenocarpus*; Silva and Portiguara, 2009; also Figure 2.5) which differ from the phytoliths of all the other major phytolith-producing plant families (Piperno, 2006). Recent phytolith keys include that published by Watling and Iriarte (2013) for the coastal savannas of French Guiana, which illustrates the spinulose phytoliths of *Euterpe* and *Mauritia*. Palms in the sub-family Calamoideae, which includes *Mauritia* and *Mauritiella*, do not produce phytoliths in their roots (Prychid et al., 2004); this suggests that in the palaeoecological record their phytoliths only reflect surface litter inputs.

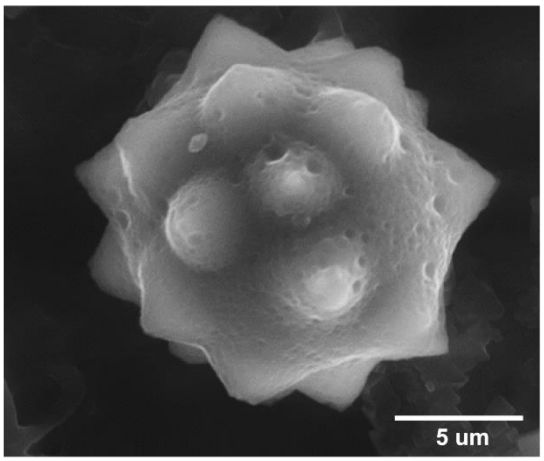

Figure 2.5: Palm phytolith from 64 cm depth at Quistococha core QT-2010-1, likely *M. flexuosa* or *M. armata*. This image reveals some small dissolution pits across the surface of the phytolith which probably occurred following deposition (sample had not been prepared using acids prior to SEM).

Some palms also produce 'hat-shaped' phytoliths (cf. Piperno, 2006); in rare cases (e.g. *Socratea*) palm species produce both 'hat-shaped' and elliptical spinulose phytolith types (Piperno, 2006). In terms of taxonomy, differentiating between different genera which produce spinulose phytoliths can be difficult, and in the Neotropics this area requires further taxonomic study which is beyond the scope of this thesis. However, at the family level the only other plant family known to produce similar phytoliths is the Bromeliaceae (Piperno, 2006), and in peatlands these are unlikely to contribute a sufficient quantity of litter to be a significant source of taxonomic confusion (bromeliads are small epiphytic plants).

The abundance of phytoliths found in a given sample from a peat core is a function of several different factors. For a given cohort of peat, the phytolith concentration is

determined by the amount of litter containing phytoliths which fell on the peat surface when the cohort was laid down, the concentration of phytoliths in that original litter, the rate of phytolith dissolution, and the proportion of the non-phytolith litter removed by decay following deposition. Provided dissolution rates remain low, the final concentration of phytoliths will largely reflect the amount of litter lost to decay and the original concentration of phytoliths in the litter (Figure 2.6).

Whilst pollen might be used in a similar manner, with high pollen concentrations indicating a period of high decay in the profile, pollen concentrations are not equivalent to those of phytoliths in this instance. Firstly, pollen will decay under oxic conditions, and as such low pollen concentrations may also be indicative of high peat decay rates. Secondly, pollen concentrations can be affected by production levels and taphonomic processes, such as dispersal potential or the openness of the canopy. In order to interpret pollen concentration data these effects must be taken into account. Phytoliths rarely travel far from where they are produced, and therefore can usefully complement pollen data.

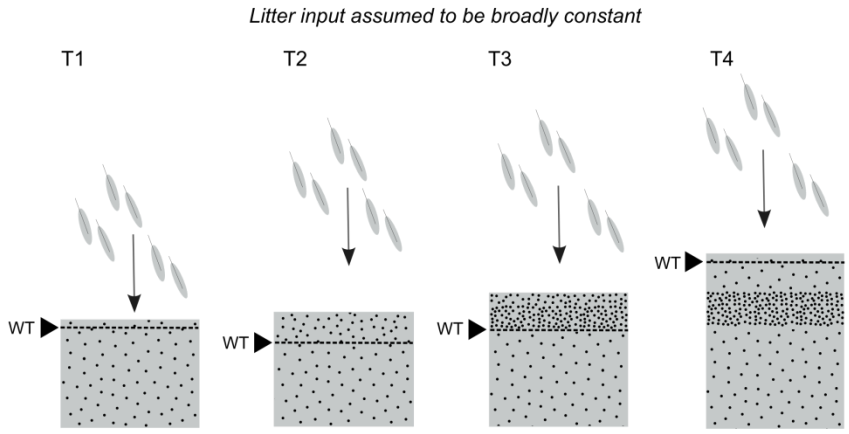

Figure 2.6: Possible effect of hydrological conditions on the concentration of phytoliths found in the peat profile. It is hypothesised that drier conditions could lead to an increase in the concentration of phytoliths in the peat profile which is independent of increases in phytolith input. **T1:** Litter falls on the peat surface under wet conditions. There is reduced decay of the litter, and the phytolith concentration more closely resembles the parent material. **T2:** Water table falls allowing higher anaerobic decay, releasing more phytoliths from the litter. **T3:** Due to the high decay rate caused by the lower water table, the accumulation rate is slow. This creates a zone of very humified peat with a high phytolith concentration. **T4:** Return to wetter conditions. The layer with a high concentration of phytoliths is preserved beneath newly accumulating peat layers.

2.8 Summary of research gaps

There has been little research into tropical peatland hydrology, especially those hydraulic properties essential for the construction of hydrological models, and almost none in Amazonia. Existing data from Amazonia comprise spot measurements of water

table only. Hydrology and succession are central to understanding the development of peatlands, and are closely connected to one another through ecohydrological feedbacks. Most of our knowledge about tropical peatlands is derived from sites in Southeast Asia, which have a very different flora to sites in Amazonia and which have mostly been formed as a result of eustatic sea level change. In terms of their temporal succession, this research is essentially not transferable to Amazonia due to their differing floras and allogenic drivers. There are peatlands in central America, but these too are occupied by very different vegetation to that found on the Amazonian floodplain. This review has also summarised changes in late Holocene climate seen in South American proxy records, but whose effect on Amazonian peatlands remains unknown. Existing peatland development models mostly deal with northern peatlands, and those developed for the tropics have focused on sites close to the coast.

In the following section, the aims and hypotheses for this thesis, which have been tailored in an attempt to fill these research gaps, are outlined. With respect to palaeoecology, improved interpretations can be gained through a more precise taxonomy. As Birks (1993) argues, this is also essential to strengthen links between Quaternary palaeoecology and modern ecology, and attempts to improve Neotropical pollen taxonomy have been made with the hope that this will aid the accomplishment of the main thesis aims.

2.9 Thesis aims and hypotheses

2.9.1 Thesis aims

In some senses, geology is a science which defies the classic scientific model, whereby a hypothesis is put forward and then data is collected in order to test it (Frodeman, 1995). Most geologists have continued to apply the method of 'multiple working hypotheses' (Chamberlain, 1897), whereby one collects data for a particular time period and then examines all of the possible interpretations to create a narrative. In some senses this can be seen as a defence against equifinality; different events can often leave a similar trace in the geological record, and without examining all of the possible causes, a false conclusion may be drawn. However, this ignores the fact that geologists, often in an iterative way, apply the classic scientific method. An initial dataset is often added to in order to test a particular hypothesis and hence the strength of the interpretations. In reference to the palaeoecological research in this thesis, a number of key hypotheses were put forward which help to test particular interpretations of the peatland record, while also maintaining a broader framework of 'multiple working hypotheses' encompassed by the thesis aims.

2.9.1.1 Determine the key drivers of past vegetation change in two Amazonian peatlands.

As discussed in this chapter and in Chapter 1, the future of peatlands in Amazonia may be affected by a combination of autogenic succession, man-made land-use changes, changing climate, and river dynamics. Modern ecological studies rarely extend over more than 50 years (Willis et al., 2007), and as Davies and Bunting (2010) discuss, on decadal timescales the long lives of trees can mask population shifts which result from climate change. As such, conservation initiatives must incorporate long-term perspectives on environmental change from other sources. Our understanding of how peatlands will react to projected future changes can be informed by data from the palaeoecological record (Willis et al., 2007; Bunting and Whitehouse, 2008). However, at present, we have little knowledge of how Amazonian peatlands have changed in the past. The main aim of this project is to develop site histories for two Amazonian peatlands. Within this, a particular aim was to understand the long-term development of the pole forest at one of the two sites selected for palaeoecological study in this thesis, San Jorge (see Chapter 3 for site description). Initially identified as a hitherto undescribed vegetation community by Lähteenoja et al. (2009b), it was suggested that this forest type could be analogous to white sand forests (cf. Fine et al., 2010), a rare and unusual forest type. Research by E. Honorio Coronado et al. (see Chapter 3) showed that San Jorge was indeed dominated by species such as *Pachira brevipes* common to white sand forests (Fine et al., 2010), and this study sought to establish whether this was a late-successional community related to low nutrient availability (as in Southeast Asian peatlands; cf. Morley, 2013).

2.9.1.2 Produce the first explicit conceptual model of Amazonian peatland development

Conceptual models help to identify key processes responsible for change in peatlands, and therefore help to predict responses to future environmental changes. Although conceptual models of peatland development through time have been produced for peatlands elsewhere (Section 2.6), there are very few conceptual models of peatland development for tropical peatlands, and no explicit models specifically produced for peatlands in Amazonia. Existing studies, including the detailed survey of the CICRA peatland by Householder et al. (2012) in southern Peru, and existing studies on the palaeoecology of floodplain lakes (see Section 2.5) provide a useful starting point. However, studies from northern peatland sites have produced conceptual models based on multiple peat basal dates in combination with site surveys and palaeoecological data (e.g. Ireland et al., 2013), and this study seeks to emulate this more detailed approach.

2.9.1.3 Improve our understanding of the hydrological behaviour of Amazonian peatlands.

The hydrology of tropical peatlands in general remains poorly studied, and at the outset of this study there were no published studies of the hydrology of Amazonian peatlands. An understanding of peatland hydrology is essential to understanding the peatland palaeoecological record, firstly because it aids in understanding ongoing processes (such as peat decomposition and commensurate changes in peat hydraulic properties) which may have affected peatland vegetation change on longer timescales, and secondly because it provides an understanding of how hydrological processes can affect the palaeoenvironmental record through taphonomic processes (e.g. movement of soluble chemical species). It is therefore of potential importance with respect to the development of conceptual models of peatland development (see above).

2.9.1.4 Improve interpretations of the recent tropical pollen record

Current knowledge of Amazonian pollen types is far from comprehensive (Section 2.7). One of the aims of this thesis is to improve interpretations of the Neotropical pollen record, with a particular focus on peatland pollen types. At the outset of this project, some common peatland pollen taxa were generally considered inseparable (e.g. *Mauritia* and *Mauritiella*) or undescribed (e.g. *Tabebuia insignis*), and so this thesis aims to use reference materials to improve pollen and spore identifications.

2.9.2 Hypotheses tested

As discussed above, several specific hypotheses were framed and tested during the course of this project. These are presented below in order to show how the research aims were translated into testable predictions. The study sites and rationale for their selection are discussed in more detail in Chapter 3 and methods in Chapter 4. The *Mauritia* and *Mauritiella* dominated swamp at Quistococha was chosen for a detailed multiple core palaeoecological study; the site at San Jorge (c. 25 km from Quistococha) was investigated using a single core; hydrological measurements were made at these two sites and one other, Buena Vista.

2.9.2.1 Peatland palaeoecology

Hypothesis 1: *Key events in the pollen stratigraphy at Quistococha (e.g. the* Mauritia *rise) occurred synchronously across the site.* This hypothesis, if accepted, would imply the dominance of an external driver (e.g. climatic change or river channel migration) in the development of the Quistococha peatland, rather than autogenic terrestrialization and/or paludification which would result in diachronous changes across the site.

Hypothesis 2: *Key changes in the pollen records at San Jorge and Quistococha were synchronous.* Acceptance of this hypothesis would imply that climate change is the likely driver of ecosystem change; river channel migration is unlikely to affect two sites simultaneously and in the same way.

Hypothesis 3: *Key changes in the pollen records at these two sites were synchronous (within dating uncertainties) with climate events identified in other records from the region.* Acceptance of this hypothesis would lend weight to the argument that climatic change is the main driver of ecosystem change at the two sites and help to identify likely consequences of future climatic changes.

2.9.2.2 Peatland hydrology

Hypothesis 4: K *varies within the uppermost c. 1m of the peat profile.* In many peatlands *K* decreases with depth (*cf.* Armstrong, 1995), although this is not always the case (e.g. Chason and Siegel, 1986) and *K* can both increase and decrease abruptly between different peat layers (e.g. Baird *et al.*, 2008). For tropical peatlands there is no published information on variation in *K* near the peat surface where it is likely that *K* is highest and there is a substantial flow of groundwater (*cf*. Takahashi and Yonetani, 1997).

Hypothesis 5: K *varies spatially between different parts of the Quistococha peatland.* Models of groundwater flow in temperate peatlands have shown that it is important to consider spatial heterogeneity in physical properties such as *K* (*cf*. Beckwith *et al.*, 2003; Belyea and Baird, 2006). As such, this project sought to examine the spatial heterogeneity of *K* in a tropical peat swamp (Quistococha) by testing whether there was a significant difference in *K* values from three contrasting locations on the peatland.

Hypothesis 6: K *varies between different wooded tropical peatlands.* The distribution of major elements in tropical peat profiles has shown that the zone of elemental recycling by vegetation could extend from 50 to 200 cm (Weiss et al., 2002; Lawson et al., 2014). If vegetation has a significant effect on *K* through controls on the litter input (cf. Boelter, 1969; Päivänen, 1973), then this raises the possibility that there is a link between the vegetation which has grown over the last c. 200 years (cf. Weiss et al., 2002; Lähteenoja et al., 2009a), and the hydraulic properties (including *K*) in the top metre of the peat. Acceptance of this hypothesis would raise the possibility that peatland vegetation can initiate autogenic changes through changes in the quality of the leaf litter.

2.10 Summary

This chapter has reviewed the key literature that informed the development of research questions and which is relevant to the ensuing discussions, including a detailed examination of late Holocene environmental change in Amazonia. The next chapter

introduces the study region and sites, and chapter 4 discusses how the methodology was developed to meet the aims and objectives.

3. Field Sites

3.1 Overview

This chapter first provides a summary of the previous work undertaken in the peatlands on the Pastaza-Marañón basin. Details are then given of the regional setting, including the geology, palaeogeography, climate, hydrology, vegetation, archaeology, and modern human impact. Nine sites were visited as part of this study, and this chapter goes on to provide information from previously published work regarding their age, vegetation, and geochemistry as well as relevant observations made by the author during fieldwork. Three were selected for hydrological study, and two for palaeoecological analysis. In some cases, sites were explored during fieldwork but were not subjected to detailed laboratory analyses, and a brief summary of this work has also been included.

3.2 Peatlands of the Pastaza-Marañón Basin: previous work

Some of the sites investigated as part of this work are among 22 peatlands in the Pastaza-Marañón basin of North East Peru known from previous investigations undertaken by Lähteenoja et al. (2009a,b; 2011; 2012: see Figure 3.4). This basin covers an area of c. 120,000 km^2, and contains two of the main tributaries of the Amazon River; the Ucayali and the Marañón. These two rivers join c. 76 km south of the city of Iquitos. Some small areas of peatland have also been found along the R. Yaguas and R. Cotuhé in northeast Peru as part of a Chicago Field Museum rapid inventory (Pitman et al., 2011), and these appear to be similar botanically to those in the main area of the Pastaza-Marañón basin.

As Lähteenoja (2011: p. 9) states in her doctoral thesis, her aim was to "initiate peatland research in Amazonia", and therefore much of that work was designed to collect a broad range of data on peat thickness, the long term rate of carbon accumulation (LORCA), peatland distribution, and geochemistry from multiple sites. In the Pastaza-Marañón basin Lähteenoja et al., (2012) estimated peatland area at c. 43,800 km^2, with below-ground carbon storage estimated 1.67-18.92 Pg C. Draper et al. (2014) have refined this estimate using an expanded dataset of peat depths and vegetation surveys, coupled with multiple remote sensing products; their estimate of peatland area in the Pastaza-Marañón basin is 35 600 ± 2133 km^2, with a total above and below-ground carbon storage of 0.44-8.15 Pg C.

Ten of Lähteenoja's sites currently have radiocarbon dated profiles (Lähteenoja et al., 2009a, 2012). The oldest site discovered so far is that of Aucayacu, the base of which has been dated to 8870 ± 110 cal yr BP (Lähteenoja et al., 2012), but most of the dated sites are significantly younger than this (see Table 3.1). The range of different peat basal ages

has been taken to suggest that river dynamics are responsible for peatland creation, rather than climate change (Lähteenoja et al. 2009a; Figure 3.2). Lahteenoja et al. (2009b) described the use of Ca concentrations as indices of trophic status: five of the ten sites can be defined as minerotrophic and four ombrotrophic (no Ca concentration data is provided for Lagunas), but the surface peat Ca concentration ranges from 90 mg kg^{-1} to 17400 mg kg^{-1} (Table 3.1). Sites such as Quistococha occupy an intermediate position between these two extremes (Lähteenoja, 2011); minerotrophic sites can be subdivided to form a third category of peatland (Figure 3.3). The existing, relatively limited information summarised here can be used to produce a hypothetical classification system for Amazonian peatlands (Figure 3.3). In Figure 3.3, the two extreme ends of the range are minerotrophic sites which receive sediment input from annual flooding, and sites which are entirely ombrotrophic. An intermediate stage (Figure 3.3C) includes sites which are relatively isolated from riverine sediment input, but which have not yet become domed, and therefore still receive some nutrients from groundwater flow. This classification will require refinement through further research; at present, details of flooding regime for most sites are limited, and not founded on abundant observations. The potential developmental trajectory implied in Figure 3.3 also requires testing using palaeoecological data.

Table 3.1: Summary details for peatland sites which were subjected to detailed study by Lähteenoja *et al.* (2009, 2012), illustrating the Holocene age of all currently dated peatlands and their wide range of Ca values (low values are an indicator of ombrotrophy; Shotyk, 1996). Sites included in this study are marked*. Calibrated ages are given to one sigma (as in Lähteenoja *et al.* 2009, 2012). Sites are marked on the map in Figure 3.4.

Peatland Name	Age (cal yr BP)	Max peat thickness (cm)	Surface Ca average (mg kg^{-1})
Lagunas	3900-4070	155	n.a.
Charo*	660-685	170	16770
Buena Vista*	1175-1260	290	17400
San Jorge (centre)*	1900-2005	350	370
Rinon	1540-1690	390	1330
Maquia	1945-2005	475	5905
Quistococha*	2320-2350	490	1460
Roca Fuerte (centre)	5050-5290	540	158
San Roque	7670-7740	635	9898
Aucayacu	8760-8980	745	90

Peat depths occupy the full range from 30 cm (the minimum peat depth required to be defined as a peatland; Page et al., 2011) to 745 cm (Figure 3.1). The distribution is relatively uniform, which likely reflects the range of ages for the different sites (Table 3.1), and the varying depths of the accumulating basins. Peat accumulation rates are often high, and vary from 0.46 to 9.31 mm yr^{-1} (Lähteenoja et al., 2012). However, it is

possible that the very high peat accumulation rates observed are distorted by the input of mineral material. For example, the highest 'peat accumulation rates' reported by Lähteenoja et al. (2009a) are in the lowest part of the San Jorge profile where C content is low (36.7%; also see Chapter 9). Peat accumulation rates in the upper parts of San Jorge and Quistococha are between 1-2 mm yr^{-1} (Lähteenoja et al., 2009a), and are likely to be typical of other peatlands in this region where mineral input is minimal, although further research is required to test this. As for peatland areas in Indonesia (cf. Page et al., 2004), the peat accumulation rates so far obtained for Amazonian peatlands are greater than those calculated for many boreal, subarctic, and temperate peatlands (cf. Aaby & Tauber, 1975; Turunen et al., 2001; Borren et al., 2004).

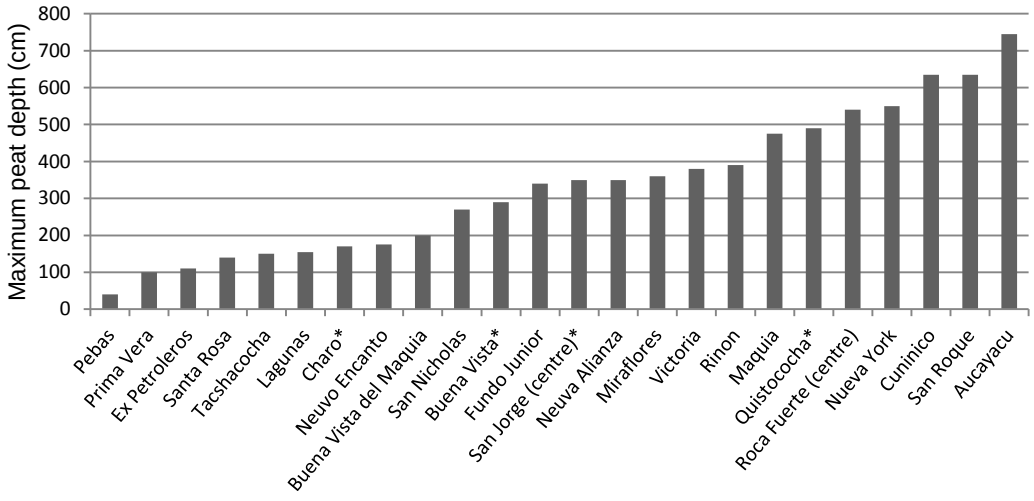

Figure 3.1: Maximum peat depth for the peatlands of the Pastaza-Maranon basin compiled from Lähteenoja et al. (2009, 2011). A uniform distribution is apparent, ranging from c. 30 cm to more than 700 cm. Sites investigated as part of the present study have been marked *.

Lähteenoja et al. (2009b, 2011) also collected data on the chemical composition of the peats at multiple sites, although at a lower resolution by comparison with the detailed single site study of Weiss et al. (2002) in Indonesia. The first detailed single core study of Amazonian peat chemistry was undertaken at Quistococha by Lawson et al. (2014). This work showed that the nutrient enrichment is deeper at Quistococha than in typical northern peatlands, a similar finding to that made by Weiss et al. (2002). Lawson et al. (2014) argued that bioaccumulation and elemental recycling was one of the main controls on the concentration of metals (e.g. Ca, K, Mg) in the top c. 150 cm of the peat profile, and highlighted the problems of using C/N ratios as a proxy for decomposition at sites where past vegetation assemblages have varied substantially.

The pollen record generated by Roucoux et al. (2013) for Quistococha is the first for a peatland in lowland Amazonia, and this thesis seeks to build on that work by adding

further spatial and temporal detail. The record from core QT-2010-1 shows that peat has accumulated under a variety of different vegetation types, including sedge fen, flooded forest with Myrtaceae, and palm swamp forest (Figure 3.2; Roucoux et al., 2013). The pollen data show that a *Mauritia*-dominated swamp has existed at Quistococha since c. 1000 cal yr BP (Roucoux et al., 2013). Lawson et al. (2014) found that vegetation changes seen in the pollen record from Quistococha (QT-2010-1) were accompanied by changes in peat chemistry.

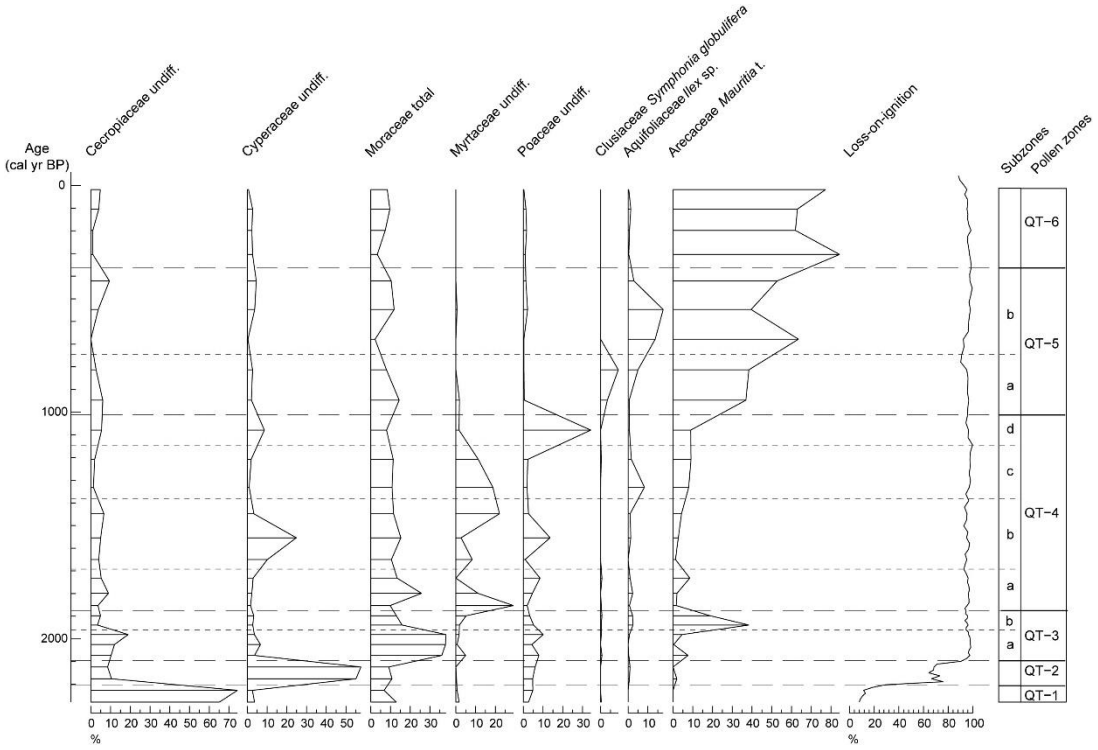

Figure 3.2: Pollen diagram showing taxa chosen to represent the main vegetation phases plotted against time for QT-2010-1, with LOI shown for reference (reproduced from Roucoux et al., 2013).

So far palaeoecological research as part of the present study and generally throughout lowland Amazonia has focused on pollen (Chapter 2), with proxies such as diatoms and testate amoebae rarely being applied. In some cases, this is because of poor preservation (Swindles et al., 2014; Chapter 4), but is also because a lack of knowledge of present distributions has limited palaeoecological interpretations. However, recent work has also been undertaken on the ecology of testate amoebae at one site (Aucayacu; Swindles et al., 2014). This is the first study of testate amoebae in a tropical peatland, and may allow the future application of transfer functions to establish past hydrological changes independently of pollen data.

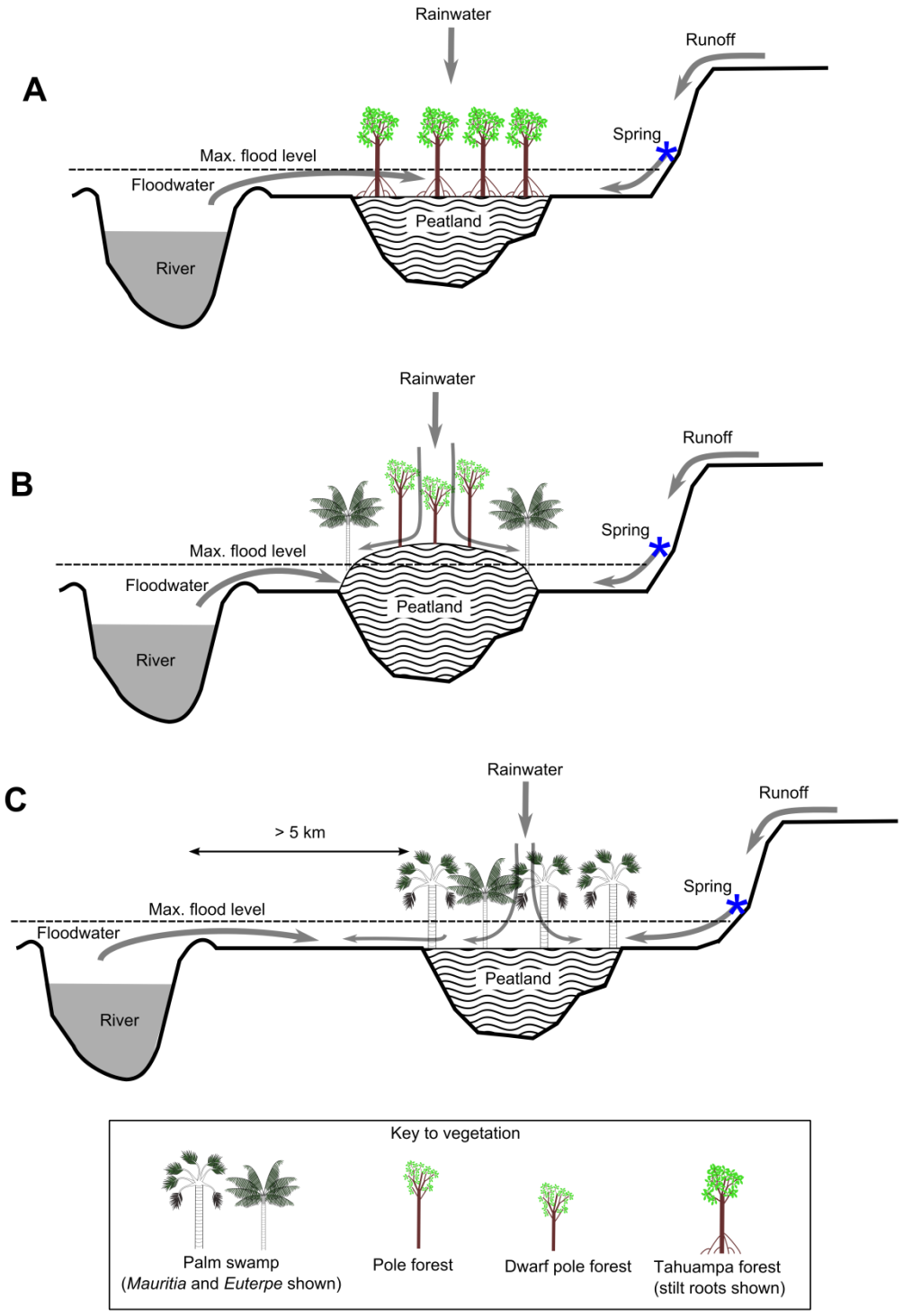

Figure 3.3: A proposed classification system for Amazonian peatlands (based on data in Lähteenoja et al., 2009b; Lähteenoja, 2011). Note that vegetation is purely illustrative and does not cover the full range of complexity encountered. A: Minerotrophic peatland flooded annually by the river with allochthnous sediment input (e.g. Buena Vista). B: Domed peatland with a centre which is never flooded and which has become ombrotrophic. The margins of the peatland are still flooded and are occupied by a different forest type (e.g. San Jorge). C: Site which is not domed and is not above the flood level and which may be flooded annually. However, the long distance from the site to the river means that it is locally derived rainwater, dammed against the rising level of the river, which floods the site (cf. Mertes, 1997). This site would be intermediate between A and B in terms of nutrients, depending on sediment type and load (e.g. Quistococha).

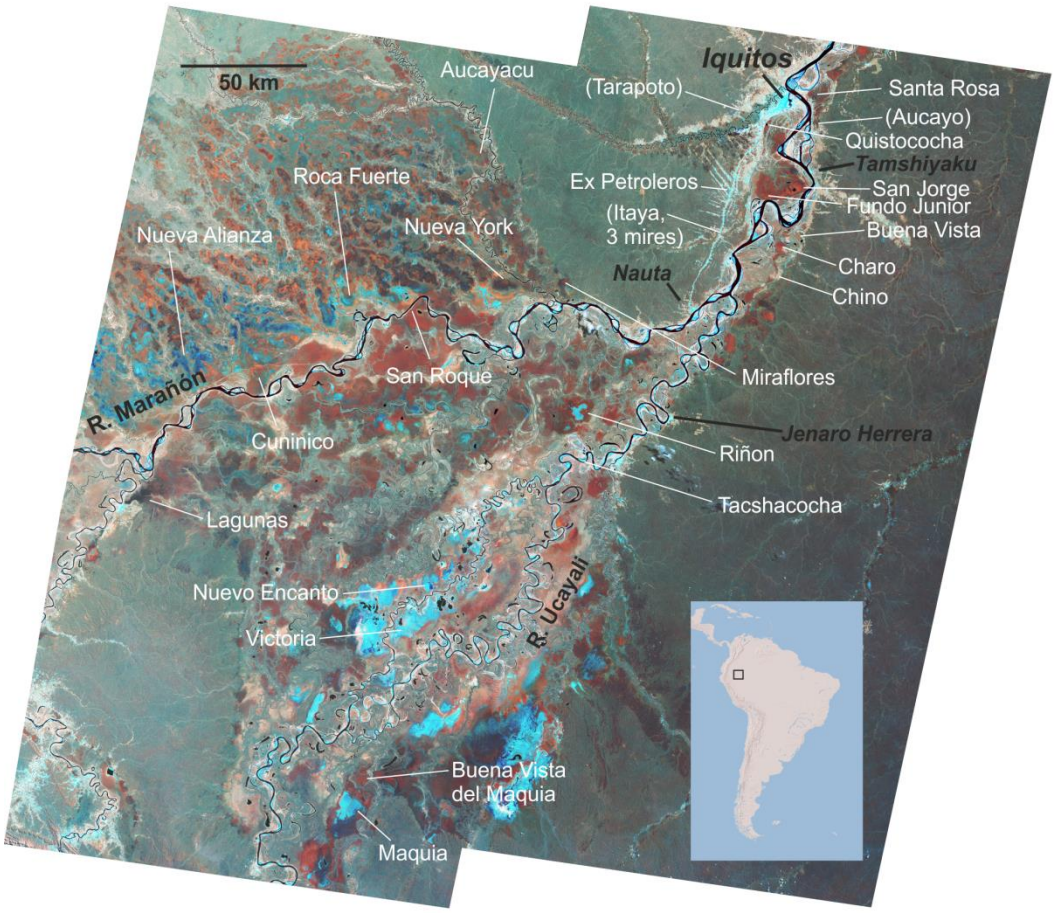

Figure 3.4: Landsat satellite map (false colour) of sites investigated by Lähteenoja et al. (2009, 2012) across the Pastaza-Marañón foreland basin of Peru (position of the region in South America is shown on the inset map). Sites in brackets were investigated but did not contain organic accumulations > 30 cm thick. Red areas generally correspond to peatlands and palm swamps. Green areas correspond to *terra firme* rainforest. The blue/grey areas mark open areas, the city of Iquitos, and other disturbed land associated with roads, agriculture, and fluvial sediments (image processed by F. Draper following Lähteenoja et al. 2009: band 4 = red, band 5 = green, band 7 = blue). Towns have been marked in black italics.

3.3 Regional setting

3.3.1 Geology and palaeogeography

The geology and palaeogeography of this region are essential underlying factors explaining the presence and distribution of peatlands in northeast Peru. The Quaternary age (2.6 Ma – present) deposits in this region are mostly confined to the floodplains of large rivers such as the Amazon, Ucayali, and Marañón, and as such are subject to frequent re-working as a result of channel migration. In Amazonia, sediments deposited during interglacials are heavily eroded during periods of glacial low sea-level (Irion *et al*., 1995). This may, to a large degree, explain why no peatland sites with pre-Holocene basal dates have yet been found.

The pre-Quaternary geology is dominated by deposits of Neogene age (23-2.6 Ma), and these formations constitute the underlying geology of the upland *terra firme* areas (Räsänen et al., 1998). During the early Miocene, large parts of western Amazonia were occupied by the Pebas system (Figuerido et al., 2009), which is amongst the largest and longest-lived lake and wetland systems to have existed in the Cenozoic (Wesselingh et al., 2001). The reason that this region has been occupied by large wetland areas since the Miocene is largely related to tectonics, and particularly to the uplift of the Andes. The Pastaza-Marañón basin is a subsiding basin which lies to the east of the sub-Andean Thrust and Fold Belt, and forms part of the Andean foredeep (Dumont, 1993). The continued subsidence aids the formation of wetlands and peatlands in this region by creating a low gradient for water flow, and hence slower drainage at a regional scale.

Studies of Miocene deposits from the Iquitos area have revealed the presence of lignites at depths of more than 250 metres (Hoorn, 1993), which suggests that the subsiding basin acts as a long-term carbon store in circumstances where organic deposits (including peatlands) escape re-working by lateral river movement. The palynology of the sediments shows some similarities with Holocene-age floodplain sediments, with a high abundance of *Mauritiidites franciscoi* pollen, which is probably a direct ancestor of the modern genus *Mauritia* (Rull, 2001), throughout the sequences analysed (Hoorn, 1993). However, the occasional presence of *Rhizophora* pollen and other marine palynomorphs shows that there was a periodic marine influence (Hoorn, 1993; Hoorn, 1994), an inference supported by strontium isotope ratios in mollusc specimens (Wesselingh et al., 2006).

Amber recovered from sections near Tamshiyaku (Figure 3.4) has revealed a microbial and insect fauna which suggests that moist tropical forest was already established in this part of Amazonia by the mid-Miocene (Antoine et al., 2006); this supports isotopic studies of bivalves that show evidence of a humid climate in the western Amazon by c. 16 Ma BP at the latest (Kaandorp et al., 2005).

Another important geological structure in this area is the Iquitos arch, which is one of several in the Amazon drainage basin; others include the Carauari arch in western Brazil (cf. Roddaz et al., 2005; Gupta, 2011). There has been some debate as to the exact position of the Iquitos arch (cf. Wesselingh et al., 2006), which separates the Marañón from the Solimoes basin, but like all the major arches in Amazonia it broadly trends from the northwest to the southeast. The Iquitos arch is a geologically recent feature, and it has deformed Miocene and Pliocene age deposits (Roddaz et al., 2005). Wesselingh et al., (2006) give the position of the arch as a north-south line just to the east of Iquitos; this can be used as a marker for the eastern boundary of the Pastaza-Marañón basin.

Many of the large-scale drainage features in Amazonia are tectonically controlled (Gupta, 2011). The underlying geology is known to control the regional drainage at a range of scales, for example causing a NW-SE orientation of some of the major rivers to the west of Iquitos. Studies have also shown that the underlying geology can affect vegetation patterns in this region (Higgins et al., 2011). The palaeogeography of Amazonia has also likely had an effect on species distributions; for example the drainage basin of the Orinoco, now largely occupying Venezuela, could well have extended much further into what is now western Amazonia in the Miocene and Pliocene (cf. Hoorn et al., 1995). Communities are now separated, such as those found in the swamps of Guiana (van Andel, 2003) and Peru (this study), which would have been joined by a common drainage network until a few million years ago. This long-term palaeogeographical perspective may explain floristic similarities between sites in different parts of the Amazon basin, including wetlands and peatlands.

3.3.2 Climate and hydrology

All of the sites studied lie within 60 km of the city of Iquitos. This region is one of the wettest parts of Amazonia, with rainfall > 3000 mm yr^{-1} (Marengo, 1998). Whilst there is a dry season which peaks during June, July and August, the seasonal variability is low in this part of the Amazon basin and rainfall does not drop below c. 100 mm $month^{-1}$ (Espinoza Villar et al., 2009a). As the decay of organic matter is slower under waterlogged conditions, peatlands are more likely to occur in regions where rainfall exceeds evaporation (Charman, 2002). Marengo (1998) showed that potential evapotranspiration (c. 1040 mm yr^{-1}) never exceeds precipitation through the year at Quistococha, although accurately calculating evapotranspiration in Amazonia is not straightforward and the applicability of Penman's (1948) method is questionable. The Penman-Monteith equation (Monteith, 1965), which incorporates vegetation, is likely to produce more accurate values (Shuttleworth, 2007). However, this equation is more difficult to parameterise in tropical forest (Mallick et al., 2013). More recent approaches have used eddy covariance data to estimate evapotranspiration, and in Indonesia these have produced values of >1600 mm yr^{-1} in undisturbed palm swamp forest (Hirano et al., 2014).

The wet season runs from November to May, and is accompanied by large scale flooding. At Tamshiyaku gauging station (near San Jorge; Figure 3.4), the 1974–2004 averages indicate that the peak river discharge occurs in April-May and that the lowest river discharges are in August, September, and October (Espinoza Villar et al., 2009b). Mean annual temperature is c. 25˚C, with high relative humidity of 80–90% throughout the year (Marengo, 1998).

Whilst the description given above is representative of the mean state of climate in this region, there are also distinct inter-annual differences in rainfall. Due to the generally high rainfall throughout the year, interannual variability may be considered as more significant than seasonal variation (Espinoza et al., 2009). This variability is, in large part, caused by ENSO (Marengo, 1992). Marengo (1992, 1998, 2004) notes that only years which experience strong El Niño conditions experience below-average rainfall (e.g. 1912, 1926, 1983, 1987, 1998), whereas the opposite La Niña phase is generally associated with higher rainfall in the northern part of the Amazon basin. This variation in rainfall is also reflected in the river levels recorded throughout northern Amazonia (Marengo, 1998). It is believed that this reduced rainfall results from the reduced strength of the northeast trade winds over the tropical Atlantic in El Niño years, thereby reducing moisture transport into the basin (Marengo, 2004). This pattern is the opposite to that seen on the other side of the Andes (e.g. equatorial islands such as the Galapagos), where El Niño years are generally characterised by torrential rainfall (Rasmusson & Wallace, 1983; Bendix, 2000).

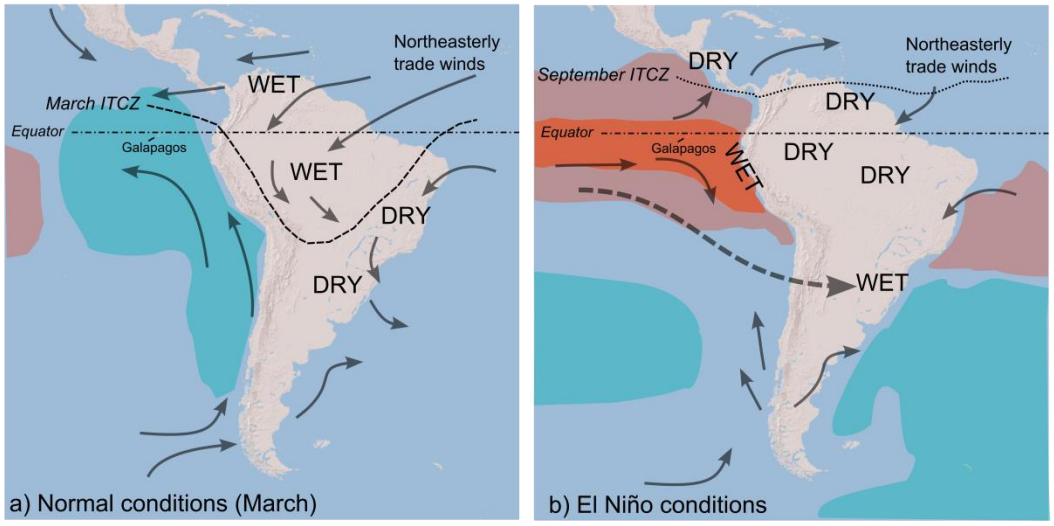

Figure 3.6: Diagram illustrating the difference between a) normal and b) El Niño years under current climatic conditions. Coloured areas indicate sea surface temperatures. During El Niño, the decreased pressure difference between the tropical Atlantic and Pacific causes decreased moisture transport into the Amazon basin, resulting in generally drier conditions. In the Galapagos and along the coast west of the Andes, warm sea surface temperatures result in increased evaporation and heavy rains, something which must be considered when interpreting proxy records from different sides of this divide. The dashed arrow in b) indicates the increased jet stream which carries evaporated moisture from the Pacific to south-east Brazil, causing the heavy rains during El Niño years. In the Pastaza-Marañón basin, El Niño years are relatively dry (figure based on Martin et al., 1993; Schwing et al., 2002; Garcia, 1994; Wang et al., 2004; Cane, 2005).

3.3.3 Floodplain vegetation

3.3.3.1 Seasonally flooded forests

Forests found in the floodplain of the Amazon and its tributaries are often flooded in the wet season, and are compositionally different to the surrounding *terra firme* forest. Inundated forests can often tolerate a rise in river level of around 12m, which can last for up to 7 months, although different areas are subject to varying levels and periods of flooding (Parolin et al. 2010). This lengthy inundation places considerable stress on the plant species which inhabit these habitats (Ferreira & Prance, 1998); in species such as *Tabebuia barbata* this stress can lead to the formation of annual rings (Worbes, 1997).

Whilst some authors have recognised up to seven different inundated forest types in Amazonia on the basis of floodwater composition (Prance, 1979), the focus here is on seasonally flooded freshwater forests as opposed to those which are inundated either diurnally or permanently. Seasonally flooded forests can be divided into two types; 'varzéa' and 'igapó' (Morley, 2001). This distinction marks a difference in the nutrient supply from the different floodwaters. Varzéa forests are flooded by 'white' water, which is laden with silt from eutrophic rivers, whereas igapó forests are flooded by 'black' or 'clear' water, which is generally oligotrophic, highly acidic, and nutrient poor (Morley, 2001).

The floras of these flooded forests have been characterised by several studies. On the Rio Manu, Foster (1990) described the composition of a varzéa forest. Whilst it is often stated that these forests are less diverse than *terra firme* forest (e.g. Dumont et al., 1990; Nebel et al., 2001), Foster (1990) identified 1,215 species in this forest, excluding those found in beach and lake habitats. In terms of family composition, the Leguminosae are the dominant taxon, but this family still constitutes less than 10% of the total flora (c. 90 species). The Moraceae are the second most important family (c. 65 species), followed by the Rubiaceae (c. 60 species) and the Pteridophyta, which were treated as a single family (c. 55 species). This family-level composition seems to be very similar to that of varzéa forests studied by other authors. Although the study of Wittman et al. (2004) only looked at tree species, they also found that the Leguminosae were the dominant taxon. Similarly, in a wider study from across Amazonia, Wittman et al. (2006) found that the Leguminosae were the dominant family in varzéa forests, followed by the Euphorbiaceae. However, this similarity between different plots at the family level can disguise an underlying heterogeneity in species composition. Wittman et al. (2006) found that the floristic similarity between low-varzéa forests more than 1000km apart was around 20%. This demonstrates some level of similarity, but indicates a more substantial level of difference. Yet in high-varzéa, the similarity between plots 1000 km

apart was generally much lower, and averaged only 10%. Furthermore, they found a distinct difference in the composition of varzéa in western and eastern Amazonia. In igapó forests, there is also a high level of endemism, and Parolin et al. (2004) found that around 30% of the species found in igapó forests are not common in other habitats.

It has been hypothesised that flooding duration has an effect on the diversity of these forests. Ferreira (1997) tested this by performing inventories of several igapó forests in an area roughly 200 km north east of Manaus. This study supported the original hypothesis, with lower diversity being associated with greater flood duration. In the plot where flooding duration was greatest, and the flood waters deepest, the ten most abundant species accounted for c. 75% of the total species found. The five most dominant species were *Eschweilera tenuifolia*, *Hevea spruceana*, *Macrolobium acaciaefolium*, *Burdachia prismatocarpa* and *Amanoa oblongifolia*. These species are therefore most able to cope with the extreme conditions of this habitat (Ferreira, 1997).

In high-varzéa where inundation is less extreme, diversity can approach that of the surrounding *terra firme* forest (Salo, 1986; Wittman et al., 2004). In terms of tree species alone, over 900 flood tolerant species have been identified in varzéa forest across Amazonia (Wittman et al., 2006). When compared with the diversity of floodplain forests in other parts of the tropics, Amazonian varzéa is ten times more diverse than forests found in Cambodia, for example (Wittman et al., 2006).

3.3.3.2 Swamp forests

Swamp forests can distinguished from floodplain forests (varzéa and igapó) on the basis of drainage; swamps occur in depressions, and so remain waterlogged for longer periods than adjacent floodplain forests (Terborgh & Andresen, 1998). These forests also differ in species composition when compared to *terra firme*, *varzéa* and *igapó* forest types (Terborgh & Andresen, 1998). Locally, such forests have been called 'tahuampa', 'restinga', 'bosque de quebrada' or when the *Mauritia* palm is abundant, 'aguajal' (Kahn & Mejia, 1990). The term 'restinga' is generally used to refer to periodically flooded forests on alluvial soil, whereas *tahuampa* refers to swamp forests that are periodically flooded by black water streams (and unlike igapó forests remain waterlogged between flooding). The term 'bosque de quebrada' refers to seasonal swamp forest in upland valleys (Kahn & Mejia, 1990). In some cases, swamps can also occupy depressions in *terra firme* areas, and therefore can be found outside of the main floodplain (see Section 3.7.1). The terminology relating to swamp vegetation is often inconsistent, and as the various local terms demonstrate, classifications are usually made along either physical or ecological lines as opposed to a combination of both (Kalliola et al., 1991). It might be

concluded from this that accurate description, rather than accurate terminology, is more important when discussing these ecosystems.

Kahn and Mejia (1990) studied an area of permanently waterlogged swamp forest near Jenaro Herrera in the Ucayali River valley, and found eleven different palm species in the one hectare surveyed. Of these, *Mauritia flexuosa* made up more than half of the individuals (54.5%) greater than 1 m in height. Together with *Geonoma acaulis* (21.3%), *Oenocarpus mapora* (10.2%) and *Euterpe precatoria* (4.2%), just four species made up c. 90% of the palm community at this site (Kahn & Mejia, 1990). Palm basal area contributed more than half (55%) the total basal area covered by trees, demonstrating their importance to this swamp forest community (Kahn & Mejia, 1990). The low diversity of these systems, and the dominance of a small number of different species, is an attribute of these swamp forests that has been noted by other authors (Terborgh and Andresen, 1998; Ter Steege et al., 2000). Of all the Amazonian forest types discussed here, they have the lowest plant diversity (Ter Steege et al., 2000). Those plants which are abundant in these swamps often have special adaptations; in the case of *Mauritia flexuosa*, pneumatophores (breather roots) allow oxygen to reach the roots allowing the tree to function in permanently waterlogged soils (de Granville, 1974; Seubert, 1996; Pereira et al., 2000). A similar adaptation has also been observed in many other palm genera such as *Euterpe* (de Granville, 1974).

3.3.3.3 Aquatic vegetation

Abandoned river channels are a common feature of river floodplains, and form oxbow lakes cut off from the main channel. These may be surrounded by floodplain forest, palm swamp or even *terra firme* forest in some cases. They have their own macrophytic communities, as the gradual infilling of oxbow lakes constitutes another important successional process. Macrophytic plant communities may form floating mats or 'meadows' of vegetation in oxbow lakes. These communities are tolerant of water level fluctuations, and although they may disappear during periods of low water, they quickly re-establish from seed (Kalliola et al., 1991). Lakes associated with rivers that have little suspended load frequently lack this floating vegetation (Kalliola et al., 1991). Junk and Piedade (1997) found that floating aquatics such as *Pistia stratiotes* and *Salvinia auriculata* do not grow well in acid, nutrient poor black water. For example, along the Rio Negro, almost no aquatic and semi-aquatic plants are found (Junk and Piedade, 1997).

Where they do occur, Kalliola et al. (1991) divided these communities into three zones: a zone of free floating species (e.g. *Azolla, Salvinia, Pistia*), a zone of floating species which are rooted to the bottom of the lake (e.g. *Victoria*), and a final zone of species which root

either directly into the ground in the shallows or into the floating mats created by other species (e.g. *Cyperus, Panicum, Thelypteris*). Thus, these communities create an aquatic succession which may result in the slow conversion of open water into forested swamp and peatland in some places (as in, for example, temperate wetlands; Ireland et al., 2012).

3.3.3.4 Pioneer trees

Although early-successional floodplain forests contain an array of different pioneer taxa, the genus *Cecropia* is worthy of individual attention. This genus of pioneer trees contains around 60 species, all of which are typical of early secondary forest succession (Parolin, 2002). It is an efficient coloniser of open ground and monospecific stands are not uncommon in recently disturbed habitats (Salo, 1986). In their study of varzéa forest, Wittman et al. (2006) found that the Cecropiaceae were the seventh most dominant family. However, *Cecropia* is rarely found in nutrient poor, blackwater areas, and so is more characteristic of varzéa than igapó forests (Parolin, 2002). The seeds will not germinate when submerged, and so *Cecropia* is not found at permanently flooded sites. Although *Cecropia* forms a closed canopy very rapidly, individuals live for only c. 20 years, so these low diversity stands are quickly replaced by more diverse vegetation unless the forest is subjected to continual disturbance (Parolin, 2002).

In the central Amazon floodplain around Manaus, other pioneers are also common such as *Salix humboldtiana* and *Senna reticulata* (Parolin et al., 2002), and *Ficus insipida* Willd. (Salo, 1986; Schöngart et al., 2007). However, all of these species are more common to white water areas and current data suggest that they are less abundant in peatlands and along black-water rivers.

3.3.4 Archaeology

Recent studies have suggested that pre-Columbian populations in the Iquitos area were small, with only localised impacts focused in areas close to rivers (McMichael et al., 2012). Phytoliths recovered from soils containing charcoal reveal a mostly arboreal assemblage, implying few cultivated crop-plants. The rarity of palm phytoliths at many sites also implies that these too were not selectively managed (McMichael et al., 2012).

However, archaeological investigations continue to reveal more pre-Columbian settlements in the Western Amazon. Settlements have been excavated in regions adjacent to Loreto, such as the site at Omé (Colombia) and Maicura (Brazil). Human occupation at Omé is dated to between c. 1350-660 yrs BP, and the site at Maicura was occupied between c. 1100-750 yrs BP (Morcote-Rios, 2008). Areas of prolonged occupation have also been identified on the Ucayali and Napo Rivers (Myers, 2004).

To some extent, the evidence presented by McMichael et al., (2012) is contradicted by evidence from detailed archaeological investigations of sites such as these. Immediately adjacent to Quistococha, fragments of pottery, charcoal, and phytoliths have been discovered in recent years, and plant fragments produced radiocarbon dates for occupation of 1740-1880 and 2350-2690 cal yr BP (Rivas Panduro et al., 2006; Rivas Panduro, 2006). This is a site of regional archaeological importance, being the nearest archaeological site to Iquitos, and one of the few in Western Amazonia to have *terra preta* or *terra mulata* (dark, man-made) soils. At this site, *Zea mays* cobs were found, as well as abundant spinulose and 'hat-shaped' palm phytoliths which indicate exploitation of palms such as *Bactris* (S. Bozarth, unpublished data).

A **B**

Figure 3.7: Pre-Columbian pottery on the *terra firme* terrace to the west of Quistococha. **A:** Fragment of a large pot (c. 45 cm wide) observed in a section in 2012 by the author. **B:** Fragment of pottery found during official excavations in 2005, with 5 cm scale bar (photograph courtesy of S. Rivas Panduro).

The difficulty of detecting ancient human settlements in a landscape covered in vegetation, where evidence may only be preserved in the form of charcoal and pottery (Figure 3.7), and where much has probably been destroyed by the movement of large rivers, is considerable. The site at Quistococha has itself been 80% destroyed as material has been removed for use as aggregate in construction (Rivas Panduro, 2006; Rivas Panduro et al., 2006). Many surveys have also yet to reach some of the more remote areas. For this reason, the lack of evidence at the present time for extensive human settlement in the western Amazon, as opposed to the east (McMichael et al., 2012) and the Xingu region (Heckenberger et al., 2003), does not necessarily imply that human populations were markedly lower in this area. Further integrated archaeological and palaeoecological studies are clearly needed in this region.

3.3.5 Recent human impact near Iquitos

Recent human impact near Iquitos is of interest for several reasons:

i) The high accumulation rate in some Amazonian peatlands means that recent anthropogenic changes can potentially be resolved in the palaeoecological record.

ii) Resources exploited at the present day have often been exploited over long periods of time and hence can provide insights into human impact in prehistory.

iii) The present study aims to use past changes to provide insights into future changes, particularly as a result of projected climate change, but in other tropical peatland areas, man-made disturbance has been a significant factor.

The road from Nauta to Iquitos had only begun being built in 1996 (Kalliola and Paitán, 1998). As has been illustrated in many parts of Amazonia, deforestation and settlement quickly follow on from road-building as access, particularly to markets, is made more straightforward. Once forest products face the demands of national and international trade, resources used sustainably at a local level can be quickly depleted. As infrastructure increases, so does the risk to natural ecosystems, and therefore there is always a need for enforced protection and conservation in key areas (e.g. Allpahuayo-Mishana National Reserve).

Perhaps one of the main potential future threats is drilling for oil, which requires the laying of long pipelines and therefore disturbance along large strips of land (Finer et al., 2013). This could have negative impacts on peatlands if this disturbs their hydrology, or if poor management leads to oil leaks and spills. The sites in this study and those in the central area between the Marañón and Ucayali rivers are not yet directly threatened, but the majority of Loreto has been sold off as oil concessions (see Finer et al., 2013) and much of this area contains peatlands.

Peatlands can also be affected as a result of local or regional resource use. One example of this is the harvest of the *Mauritia* palm for its fruit (Vasquez and Gentry, 1989). In the region near Iquitos, this has had a substantial effect on the gender balance of the population of this palm in many wetland sites (Kahn, 1988). The female trees are cut during the process of harvesting the fruit, which may not only have an effect on the species composition of some peatlands over the long term but also results in an increased level of disturbance and creation of tree fall gaps (Figure 3.14). As such *Mauritia* is often 'locally depleted', as are many other trees which can be used as construction material, for the production of charcoal for local use or sale, or for food (Figure 3.9; Vasquez and Gentry, 1989; Kvist and Nebel, 2001; Arce-Nazario, 2007).

Figure 3.8: Examples of human impact in and around peatlands in the region of Iquitos. **A**: Cleared clay levee with remnant crop plants at the eastern margin of Quistococha peatland. **B**: Fire wood piled in preparation for the production of charcoal, San Jorge. **C**: Palm fronds ready for use as roofing material, San Jorge. **D**: *Mauritia flexuosa* fruits collected from the peatland laid out to dry before being taken to Iquitos for sale, San Jorge (All photos by the author).

Mauritia seed dispersal is carried out mostly by large mammals, such as the tapir (*Tapirus terrestris*), but large long-lived mammals such as this are often locally rare as a result of hunting (Bodmer, 1990; Bodmer et al., 1997; Nuñez-Iturri & Howe, 2007). At Quistococha, the author observed squirrel monkey (*Saimiri* sp.), but did not observe any larger monkeys such as the howler monkey (*Alouatta* sp.) which might act as more effective seed dispersers. Medium to large monkey species can often be detected by sound as well as sight, and the lack of observations during the several weeks the author spent at Quistococha strongly suggests that this reflects a real absence. Over long timescales, the combination of felling for fruit and poor seed dispersal may affect populations of *Mauritia* both at peatland sites and more widely, just as poor seed dispersal has affected other tropical trees reliant on large vertebrates for their dispersal (Nuñez-Iturri & Howe, 2007).

Farming along levees adjacent to peatlands may have some impact, possibly through the input of nutrients and fertilisers (Figure 3.8). Observations by the author during fieldwork have not revealed any large scale impact on peatlands resulting from human activity in the region near Iquitos, although this may change in the future as the city continues to expand. However, the case of *Mauritia* highlights the potential effect of selective resource use on peatlands, as well as the potential, indirect effects of over-hunting on plant populations.

In summary, although tropical peatland areas in other parts of the world have been heavily affected by modern land-use change (Chapter 1), at present direct human impact on peatlands appears to be more limited in the western Amazon. The main impacts stem from unsustainable resource use in areas near to population centres. Future impacts from oil exploitation remain uncertain, but at present man-made climatic change remains a more definite threat, particularly for peatlands in the more remote parts of the Pastaza-Marañón basin.

3.4 Quistococha lake and peatland (3°50' S, 73°19'W)

Quistococha peatland is named after the lake at its centre; the centre of the site lies 10 km west of the main channel of the Amazon River (Figure 3.11). The site was chosen for detailed study both for its ease of access and because, on floristic grounds (Table 3.2), it may represent one of the most common types of peatland ecosystem in western Amazonia (Lähteenoja et al., 2009a). The site consists of an approximately circular lake with a surface area of 1 km^2 (Räsänen et al., 1991), around which are substantial (> 4 m depth) peat accumulations (Lähteenoja et al., 2009a). The peatland abuts the edge of the lake, and field evidence suggests that this margin may be eroding in places. The peat lies on an impermeable substrate of riverine or lacustrine clayey silt. The eastern margin of the peatland is defined by a clay ridge which creates a low hydrological barrier between the peatland and the rest of the floodplain (Figures 3.10 & 3.11). There is also an archaeological site on the river terrace immediately to the west of Quistococha (see Section 3.3.4; Figures 3.7 & 3.9).

Lähteenoja et al. (2009a) gave a radiocarbon date for the basal age of the peat in a core (3.90–4.00 m depth) of 2320-2350 cal yr BP (1σ). Roucoux et al. (2013) also obtained a similar basal date of 2308-2056 cal yr BP (2σ) from 4.00 m depth in a core taken at approximately the same point. Lähteenoja *et al.* (2009b) showed that the elemental composition of the peat at Quistococha is consistent with a dominantly rain-fed system, although the moderately high Ca/Mg ratio suggests that there is at least some groundwater input (Ca/Mg ratios as an indicator of minerotrophy are discussed in Chapter 4). Two small springs were observed on the margins of the site, and therefore

there may be some groundwater input originating from the western margin, as observed at sites in Madre de Dios by Householder et al. (2012).

Figure 3.9: Aerial photograph of Quistococha lake and peatland looking east, with the inhabited upland in the foreground and the uninhabited floodplain in the background (courtesy of S. Rivas Panduro). Towards the western edge of the site, large quantities of sand have been removed for use as aggregate. A ring marks the area where archaeological digs have revealed pottery associated with a pre-Columbian settlement. The clay ridge which marks the eastern site boundary, and the Itaya River beyond, have also been marked (these can be seen in Figure 3.10).

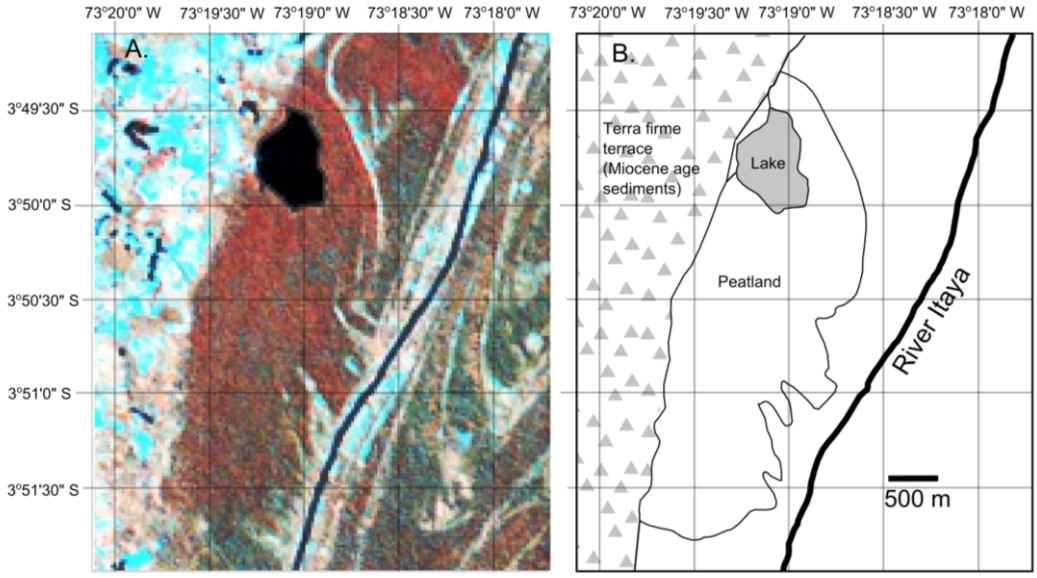

Figure 3.10: A: Landsat image (false colour) for Quistococha (follows processing used in Figure 3.4; processed by F. Draper). **B:** Inferred Quistococha peatland margins based on Landsat imagery and field observations. The Landsat imagery indicates that there may be peatland areas to the northeast (red colour), but these are separated from the main Quistococha peatland by a levee, which acts as a hydrological barrier.

The tree flora in the forest inventory plot at Quistococha appeared to be representative of the vegetation across the studied part of the peatland (Table 3.2; data published in

Roucoux et al., 2013). Three species, *Mauritia flexuosa, Mauritiella armata* (Mart.) Burret (both Arecaceae) and *Tabebuia insignis* Sandwith (Bignoniaceae), together represent 82% of the individuals (Table 3.2). Species richness was much lower than would be expected for *terra firme* rain forest (*cf.* De Oliveira and Mori, 1999).The aquatic plants at Quistococha occupy small patches mostly within 10 m of the shore line (Figure 3.11). There are small (c. 5 x 5 m) floating mats of Cyperaceae and Poaceae near to the eastern shore line, and larger patches of floating Nympheaceae around the lake margin (aff. *Nymphaea amazonum*).

Figure 3.11: Photographs showing vegetation at Quistococha lake and peatland. A: Peatland vegetation with dense canopy, including *Mauritia flexuosa* and *Tabebuia insignis.* B: View looking east across Quistococha lake showing palm swamp on the opposite shore and the clear open water of the lake itself. C: The peatland margin on the eastern shore, showing some aquatic plants (Nymphaeaceae), and low-growing swamp herbs (Araceae). D: Floating aquatic mat near the eastern shore, consisting of mixed Poaceae and Cyperaceae. (All photos by the author).

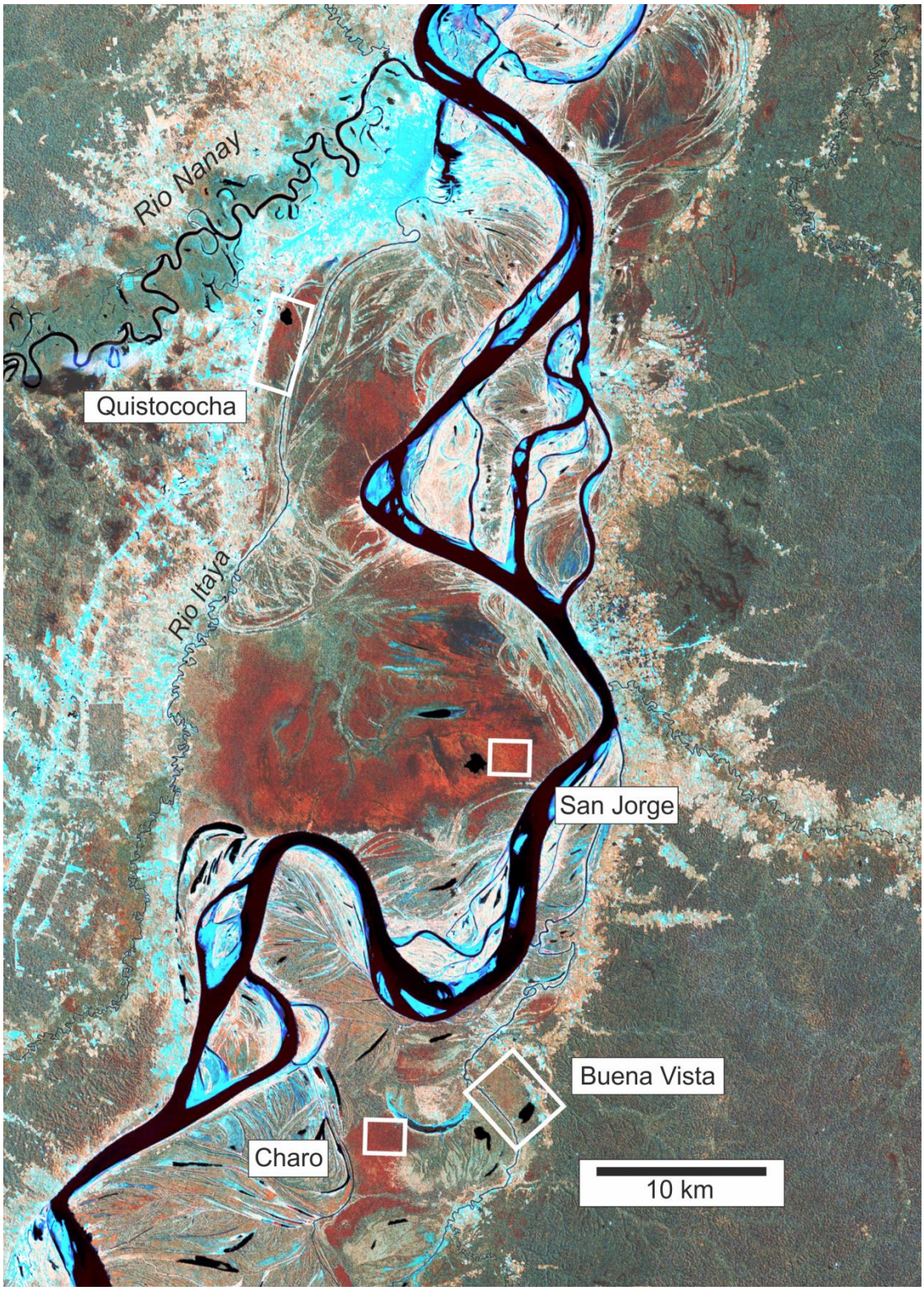

Figure 3.12: Landsat satellite map (false colour) of San Jorge, Quistococha, Buena Vista, and Charo (processed by F. Draper), processed following Lähteenoja et al. 2009 (band 4 = red, band 5 = green, band 7 = blue). Red areas correspond to peatlands and palm swamps. The sites at are shown with a white box indicating the approximate area of study in each case. The blue/grey areas mark the city of Iquitos and other disturbed, un-vegetated land associated with roads, agriculture, and fluvial sediments. Green areas correspond to *terra firme* rainforest.

Table 3.2. List of the ten most important species ranked by the Importance Value Index (IVI) which were found in the 0.5-ha plots at Quistococha (Area B in Figure 1B), San Jorge, and Buena Vista. IVI was calculated as the sum of the relative (Rel.) values of abundance of individuals (Ab.), basal area (BA) and frequency (Fr., 50 subplots). Only individuals with ≥ 10 cm diameter are included. Data were collected during the first survey of above-ground peatland carbon storage in Amazonian peatlands as part of the NERC-funded project "Long-term forest dynamics in Peruvian Amazonia" (Data courtesy of E. Honorio Coronado – data available via RAINFOR at www.rainfor.org).

Quistococha					(%)	(%)	(%)	(%)
Species	Family	Ab.	BA	Fr.	Rel. Ab	Rel. Do	Rel. Fr	IVI
Mauritia flexuosa	Arecaceae	92	6.29	41	22.38	53.86	23.16	99.41
Tabebuia insignis	Bignoniaceae	131	2.77	46	31.87	23.69	25.99	81.56
Mauritiella armata	Arecaceae	113	1.17	26	27.49	10.02	14.69	52.20
Symphonia globulifera	Clusiaceae	31	0.76	23	7.54	6.51	12.99	27.05
Hevea guianensis	Euphorbiaceae	11	0.19	10	2.68	1.62	5.65	9.95
Amanoa aff. *guianensis*	Phyllanthaceae	11	0.16	10	2.68	1.37	5.65	9.70
Virola surinamensis	Myristicaceae	4	0.06	4	0.97	0.49	2.26	3.72
Brosimum utile	Moraceae	4	0.04	4	0.97	0.35	2.26	3.58
Alchornea schomburgkii	Euphorbiaceae	3	0.06	3	0.73	0.51	1.69	2.94
Alchorneopsis floribunda	Euphorbiaceae	3	0.04	2	0.73	0.35	1.13	2.21
Other 6 species		8	0.14	8	1.95	1.22	4.52	1.95
Overall total	16 species	411	11.7	177	100	100	100	300

San Jorge					(%)	(%)	(%)	(%)
Species	Family	Ab.	BA	Fr.	Rel. Ab	Rel. Do	Rel. Fr	IVI
Pachira aff. *brevipes*	Malvaceae	225	3.35	45	38.79	25.24	21.74	85.78
Remijia aff. *ulei*	Rubiaceae	143	4.68	46	24.66	35.30	22.22	82.18
Calophyllum brasiliense	Clusiaceae	116	1.92	47	20.00	14.45	22.71	57.16
Mauritia flexuosa	Arecaceae	51	2.69	31	8.79	20.30	14.98	44.07
Dendropanax aff. *resinosus*	Araliaceae	28	0.37	23	4.83	2.79	11.11	18.73
Mauritiella armata	Arecaceae	6	0.08	5	1.03	0.63	2.42	4.08
Oxandra riedeliana	Annonaceae	6	0.08	5	1.03	0.58	2.42	4.03
Ormosia coccinea	Fabaceae	2	0.05	2	0.34	0.40	0.97	1.71
Hevea guianensis	Euphorbiaceae	2	0.03	2	0.34	0.25	0.97	1.56
Tabebuia insignis	Bignoniaceae	1	0.01	1	0.17	0.06	0.48	0.71
Overall total	10 species	580	13.3	207	100	100	100	300

Buena Vista					(%)	(%)	(%)	(%)
Species	Family	Ab.	BA	Fr.	Rel. Ab	Rel. Do	Rel. Fr	IVI
Inga aff. *stenoptera*	Fabaceae	89	1.22	31	20.32	11.07	10.84	42.22
Matayba sp.	Sapindaceae	38	1.85	25	8.68	16.86	8.74	34.28
Diospyros poeppigiana	Ebenaceae	54	1.40	26	12.33	12.73	9.09	34.15
Triplaris weigeltiana	Polygonaceae	26	0.49	17	5.94	4.50	5.94	16.38
Elaeoluma glabrescens	Sapotaceae	23	0.48	19	5.25	4.34	6.64	16.23
Hydrochorea corymbosa	Fabaceae	17	0.50	12	3.88	4.53	4.20	12.61
Amanoa aff. *sinuosa*	Phyllanthaceae	17	0.42	13	3.88	3.82	4.55	12.24
Terminalia aff. *oblonga*	Combretaceae	9	0.66	9	2.05	6.01	3.15	11.22
Myrtaceae sp2.	Myrtaceae	16	0.32	11	3.65	2.94	3.85	10.44
Eschweilera aff. *ovalifolia*	Lecythidaceae	11	0.50	9	2.51	4.51	3.15	10.17
Other 32 species		138	3.15	114	31.51	28.68	39.86	100.05
Overall total	42 species	438	11	286	100	100	100	300

3.5 San Jorge peatland (4°03' S, 73°11' W)

San Jorge is a domed peatland (Lähteenoja *et al.,* 2009b), which is not subjected to annual flooding at the point where the measurements were taken for this study. San Jorge lies 35 km south of Iquitos, adjacent to the Amazon River (Figure 3.11). Observations made during fieldwork in 2012 indicate that the margin of the peatland along the Amazon may be eroding rapidly, although the area where the core was taken (2 km east of the lake) remains some distance from the river. The margins of the peatland are occupied by palm swamp (including *Mauritia flexuosa*); standing water is found on this part of the site even during the dry season. San Jorge is also associated with a lake but this is located to the west of the core site and was not reached, largely due to the difficulty of the terrain.

The low Ca/Mg ratio of the peat suggests that this is a strictly ombrotrophic system (Lähteenoja et al., 2009b). In a core taken in approximately the same part of the peatland as the present study, Lähteenoja et al. (2009a) obtained a basal date of 2945 ± 65 cal yr BP from a depth of 560-570 cm, although it is clear that this predates the initiation of pure peat at the site. Further radiocarbon dates were obtained by this study and are provided in Chapter 7.

The diversity of the peatland pole forest at San Jorge is very low, with only 10 species identified in the 0.5 ha inventory plot (Table 3.2). As at Quistococha, the assemblage is dominated by individuals from three (different) species, which make up 83% of the individuals; *Pachira* aff. *brevipes* (A. Robyns) W.S Alverson (Malvaceae), *Remijia* aff. *ulei* K.Krause (Rubiaceae), and *Calophyllum brasiliense* Cambess (Clusiaceae). Palms are much less abundant at this site, and the slender growth form typical of 'dwarf' or 'pole' forest (E. Honorio Coronado, pers. comm.) was exhibited by most species (including *M. flexuosa*). Many of these species are also commonly found in 'white sand forests', which are also nutrient poor (and are found growing in *terra firme* areas such as the forest near Jenaro Herrera; Section 3.7.1). Examples of species which are also common or dominant in white sand forests include *Pachira brevipes* and *Calophyllum brasiliense* (*cf.* Fine et al., 2010), which are especially abundant at San Jorge. Lähteenoja et al. (2009b) also observed understorey plant species of the Melastomataceae family and bird species common to white sand forests. Draper et al. (2014) found that peatland pole forests such as San Jorge are the most carbon dense forest type in Amazonia.

Figure 3.13: San Jorge peatland. A: Palm swamp at the eastern margin, where standing water covers much of the site. Palm trees have been felled here to make a pathway through the forest. B: The centre of the peatland, showing the slender 'pole forest'. (All photos by the author).

3.6 Buena Vista (4°14' S, 73°12' W)

The Buena Vista peatland lies 55 km south of Iquitos (Figure 3.12), adjacent to the Tahuayo River, which is a tributary of the Amazon. The site was investigated by Lähteenoja et al. (2009a) who found peat accumulations of up to 290 cm. A radiocarbon date from the base of the peat produced an age of 1175-1260 cal yr BP (1σ). Unlike Quistococha, Buena Vista is flooded on an annual basis; this additional source of nutrients is reflected in a much higher Ca/Mg ratio in the peat chemistry (Lähteenoja et al., 2009b; Table 3.1), and markedly different vegetation presumably reflecting a greater supply of nutrients, as well as different flood regime and site history (Table 3.2).

The forest at Buena Vista is more diverse than that at San Jorge and Quistococha, with 42 species. Whereas at Quistococha and San Jorge the three most abundant species account for >80% of the individuals, at Buena Vista the ten most abundant species make up 41% of the individuals (Table 3.2). Buena Vista is also the only site where the palms *M. flexuosa* and *M. armata* were absent from the 0.5-ha plot; the only palm species observed was *Astrocaryum jauari* Mart., represented by one individual. The growth habit of the trees at Buena Vista is also different; many more species have the stilt roots typical of black-water seasonally-flooded *tahuampa* forests (Figure 3.14).

Figure 3.14: Photographs showing environments along the Tahuayo River. A: The Tahuayo river, flanked by a stand of Myrtaceae. B: Buena Vista peatland, showing the dense tangle of stilt roots typical of seasonally flooded forest. (All photos by the author).

3.7 Other sites investigated.

Other sites and areas were investigated, with the possibility that these might have been used to expand the scope of this study. Several other wetland sites, identified as possibly peat-forming on the basis of their floristic composition and Landsat imagery, were visited but not selected for further hydrological or palaeoecological study. However, observations at these sites may add to our understanding of peat accumulation more generally in the region and are reported here**.**

3.7.1 Jenaro Herrera

Jenaro Herrera is a large village with an adjacent research station 160 km south of Iquitos. Previous investigations of the vegetation in this vicinity indicated that there were sites with vegetation characterised by *Mauritia flexuosa* which are similar to that found at some peatland sites (*cf*. Honorio et al., 2008). An example of recent subsidence can be seen to have affected the area near to Jenaro Herrera (Dumont et al., 1990), and this is clearly visible in the geology and in digital elevation models. This study sought to investigate whether the subsided area was associated with peat ('aguajal 1' in Figure 3.15).

The opportunity was also taken to investigate a white sand forest here; the structure of this forest was found to be very similar to that of the forest at San Jorge. All of the trees had a slender growth form and low stature. A small accumulation of peat was identified in an area of apparent poor drainage (forest hollow); deposits such as this may be of use palaeoecologically as a means of establishing long-term forest histories. Subsequent dating of the core taken at the deepest point (70 cm) revealed a basal date of 1283-1304 cal yr BP (K. Roucoux, unpublished), which means that peat initiation occurred earlier than in some of the peatlands on the floodplain (e.g. Charo).

Investigations at three Arecaceae dominated sites on the river terrace revealed that there were no substantial organic accumulations. While the site on the floodplain ('aguajal 1'; Figure 3.15) is situated in a similar geological position to sites such as Buena Vista, it too did not yield substantial organic accumulations. Dumont et al. (1990) date the tectonic subsidence of this area, which was formally part of the adjacent terrace, to c. 13, 850 cal yr BP. Therefore the lack of thick organic accumulations is less likely to be related to the age of the site (although re-working by the Ucayali River is possible), and more likely to be the result of inappropriate conditions for the accumulation of organic matter (e.g. sediment input too high). Although shallow, the organic accumulations found at these sites sometimes reached c. 30 cm. This is not dissimilar to accumulations reported by Lähteenoja et al. (2013) at sites described as peatlands in the central Amazon. They may also act as records of ecosystem change over centennial timescales, and provide a means of answering palaeoecological questions which cannot be addressed by widely spaced, albeit deeper, accumulations.

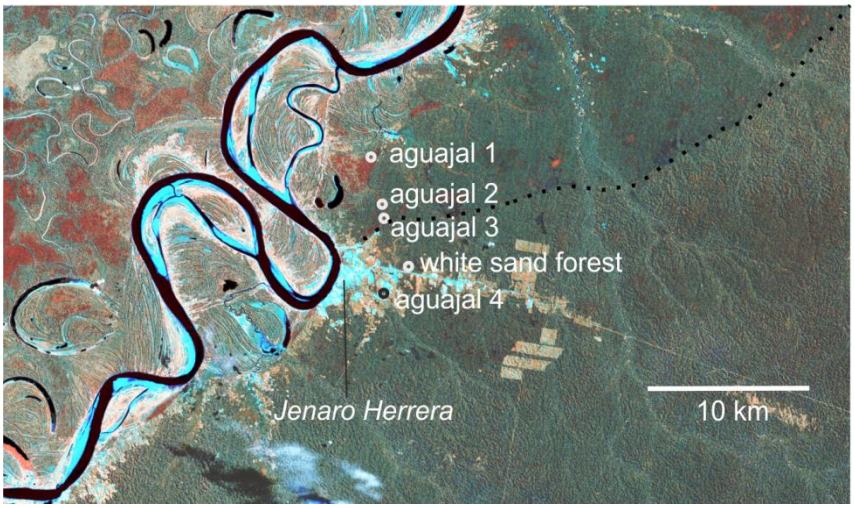

Figure 3.15: Landsat satellite map (false colour) of sites investigated as part of the present study in the vicinity of Jenaro Herrera (see Figure 3.4 for wider context). Red areas generally correspond to peatlands and palm swamps. The blue/grey areas mark open areas, the city of Iquitos, and other disturbed land associated with roads, agriculture, and fluvial sediments. (image processed by F. Draper following Lähteenoja et al. 2009: band 4 = red, band 5 = green, band 7 = blue). Dotted line indicates the division between *terra firme* and an area of tectonic subsidence (cf. Dumont et al., 1990).

3.7.2 Charo

Charo peatland lies to the southwest of Lake Charo, a large oxbow lake connected indirectly to the main Amazon channel by a narrow connection to the Tahuayo River (Figure 3.12). Lähteenoja et al. (2009a) obtained an age of 660-685 cal yr BP (1σ) from a depth of 168-176 cm (base of the peat). Detailed forest plot data are not available for Charo peatland, but the author observed some differences relative to San Jorge, Quistococha and Buena Vista. In particular the palm *Attalea* was present at this site, in

addition to the familiar *Mauritia flexuosa. Mauritiella armata* was absent. The palm *Bactris* was common at the site margins near to Lake Charo, but was less abundant in the peatland interior. The depth of the 2012 flood, as deduced from the mark on tree trunks, was around 2.7 m. This is much higher than at Quistococha, and may indicate that Charo is situated lower down on the floodplain.

A core was obtained from Charo for further study (CHA-2012-1), but it was apparent during field sampling that the clay content of the substrate is very high. Loss-on-ignition analyses revealed that the soils at Charo have a low organic content through large parts of the core. Around 70% of the samples had LOI values of <75%. Investigatory hydraulic conductivity tests were also conducted at Charo (see Chapter 4 for method), but the clay content of the peat at this site meant that the recovery times for some tests were very long and therefore full recovery was not reached. These data were therefore discarded, but this indicates that the hydraulic conductivity is lower at this site.

3.8 Summary

As a result of the geological setting and wet climate, the Pastaza-Marañón foreland basin of north-eastern Peru is conducive to the formation of extensive wetland and peatland areas, and this has likely been the case since the Miocene. The presence of Miocene lignites at depths of more than 250 m also suggests that the basin can act as a long-term (millions of years) store of organic carbon. This section has provided details of the peatland sites which have been studied and for which detailed hydrological and palaeoecological data are provided later in the thesis. It has also provided in outline some information relating to areas and sites which were explored but which were not subjected to further study. Key points outlined in this chapter have been the importance of inter-annual climate variability resulting from El Niño, the variety of different floodplain vegetation types, and the lack of knowledge of pre-Columbian people and their impact in this region.

4. Methods: background and details

4.1 Introduction

4.1.1 Overview

This chapter details the approaches and methods used by this study. The chapter begins by describing the overarching methodological approach before giving details of the specific methods and techniques used. This includes a short section on certain palaeoecological techniques that were investigated but later rejected as lines of inquiry. Where appropriate, a short overview of the technique and assessment of its suitability is also given.

4.1.2 Palaeoecology: Multi-core approach

This study applied a multi-core approach to examining vegetation development through pollen analysis at one site (Quistococha). Multi-core analysis is surprisingly rare in peatland pollen studies, despite the fact that different cores rarely show identical changes through time. Apart from the desire to add further detail regarding site development, it could also be argued that multiple cores are important simply for establishing how representative a single core is of a whole site (cf. Edwards, 1983), especially in terms of the timing of vegetation changes.

A multi-core approach has been used by some other studies in northern peatlands, such as that of Waller (1998) who looked at four cores from a fen in the Brede valley (England), and Lawson (2001) who examined five cores from Nisi fen (Greece). Lawson et al. (2007) also looked at pollen in multiple basal cores for sites in the Faroe Islands in order to examine the processes determining blanket peat initiation. Hu and Davis (1995) examined three cores to examine the synchroneity of hydroseral changes across Caribou bog in Maine. Morley (1981), who looked at a site in Indonesia, and Taylor et al. (2001) who looked at a site in Singapore, are the only studies to have undertaken pollen analysis on multiple cores in tropical peatlands. Morley (1981) found a relatively high level of consistency between cores during the early stages of succession (dominated by Poaceae and *Lycopodium*), but more variable proportions for later successional pollen taxa such as *Garcinia cuspidata*. Although there was a substantial degree of consistency between cores, Taylor et al. (2001) found the proportion of some pollen taxa differed significantly (e.g. *Macaranga*). In both cases, study of multiple cores led to ecologically significant observations which would not have been possible in a single core study.

Hughes and Dumayne-Peaty (2002) examined the visual stratigraphy in multiple cores to study the successional patterns of Crymlyn Bog in Wales, and it can be argued that a

combination of detailed microfossil study and less quantitative observations can be used to develop better site models. Phillips and Bustin (1996), and Phillips et al. (1997) used a combination of pollen analysis and stratigraphic data to formulate a model for the formation of a tropical peatland (Changuinola/Bocas del Toro) in Panama. The development of this coastal peatland has been strongly influenced by periodic subsidence and is unlikely to provide a model which can be applied to floodplain peatlands, but the approach to model development is certainly applicable.

The integration of pollen analysis into studies of site development in tropical peatlands is arguably essential if detailed models are to be produced. Stratigraphic data may not reveal the spatial variability of vegetation phases shown through pollen analysis, especially in tropical peatlands where identifying plant macrofossils can be difficult and there are few such identifiable remains (excluding roots and bark). As discussed in Chapter 6 in the context of *Tabebuia insignis* var. *monophylla*, it may not be possible to effect an identification of a tree without a flower, even where the whole tree can otherwise be examined in detail. The plant macrofossil record in tropical peatlands is likely to be biased towards those plant groups which produce easily preserved remains, or whose remains are especially distinctive. This limits plant macrofossil study to addressing questions of peatland openness (i.e. distinguishing between grasses/sedges and trees).

4.1.3 Hydrology: a field-based approach

Previous studies have used a variety of methods to estimate peat hydraulic conductivity (K). In the laboratory, K can be measured using the modified cube method (MCM) outlined by Beckwith et al. (2003a), and this method has been applied by several authors (e.g. Surridge et al., 2005; Rosa and Larocque, 2008). The MCM has one main advantage over field measurements in that it can provide estimates of the anisotropy of K in the peat; i.e., it can reveal differences in the horizontal (K_h) and vertical (K_v) components of K (Beckwith et al., 2003a). Although some have suggested that field measurements of K mostly reflect the horizontal component (K_h), in reality it reflects an undefined mixture of both K_h and K_v (Surridge et al., 2005).

In this case, the transport of large numbers of samples from the field to the laboratory was impractical and so only field measurements were undertaken. Previous studies have shown that field based and laboratory methods can produce very similar results (e.g. Surridge et al., 2005), and that the difference in the results obtained is small compared to the overall variability of K through a peatland (e.g. Rosa and Larocque, 2008).

4.2 Field Methods

4.2.1 Coring methods

All peat cores collected during the summers of 2011 and 2012 were collected by the author using a 50 cm long Russian type corer (Jowsey, 1966). Cores were obtained by sampling using parallel boreholes c. 1-2 m apart, with a 10 cm overlap between the core sections taken from each borehole (this prevents contamination of adjoining core sections by the nose cone of the Russian corer). The majority of core sections were sub-sampled in the field at 16 cm intervals, but cores containing the contact between the peat and the underlying clay were retained for laboratory analysis. This was the result of a compromise between achieving a temporal resolution which allowed the observation of major vegetation changes (c. 90 yrs between 16 cm samples, as estimated using Lähteenoja et al., [2009a] and Roucoux et al. [2013]), and the difficulties of transporting large quantities of material back to the UK.

The cores from San Jorge (SJO-2010-1) and the lake at Quistococha were collected by I. Lawson, K. Roucoux, T. Baker and T. Jones in the summer of 2010 using a Russian corer; in the case of the lake core this was operated from a small catamaran-type coring platform. The top ~30 cm of the lake sediments were sampled by the author using a short gravity corer during 2011 (Renberg, 1991). Where complete core sections were taken, these were wrapped in cling-film and placed into protective plastic gutters before being wrapped in a further layer of thick plastic sheeting. Core locations were recorded using a Garmin handheld GPS. All cores were stored under license at 4°C at Leeds University once they had been transported to the UK.

4.2.2 Long-term water-table monitoring

As there is a pronounced change in rainfall throughout the year, a single measurement of water-table depth is generally not representative, although it will provide a reasonable indication of minimum water level if taken at the peak of the dry season. Although resources were not available to examine long-term water-table changes at all three sites (Quistococha, San Jorge, Buena Vista), variations in water-table were recorded in the forest plot at Quistococha for one year.

The water table at Quistococha was monitored from the end of July 2011 to mid-July 2012 using a pair of self-logging pressure transducers, set to take measurements every two hours. The pressure transducers record total pressure (atmospheric plus water), and so when used to record water table changes, values need to be corrected for changes in atmospheric pressure (A.J. Baird, pers. comm.). The background atmospheric pressure was therefore recorded using a Schlumberger 'Baro-Diver', and these values were used

to calculate the position of the water table relative to the peat surface. The barometric pressure logger was installed c. 1.5 m above the peat surface, and the water pressure logger was installed 46 cm below the surface.

4.2.3 Hydraulic conductivity (*K*) measurements

In the field, *K* is generally estimated using piezometer slug tests, although the specific design of the piezometer intake, the method used to install the piezometer tubes, and the means of measuring the head response may vary (e.g. Hvorslev 1951; Price, 1992; Baird et al., 2008). A piezometer is a tube with a screened opening at the base used to measure the hydraulic head at a certain location and depth (see Hendricks, 2010). In this case, a slug refers to a small weight which displaces a set volume of water in the piezometer tube. During a slug withdrawal test, the water level is displaced and the time over which the water level in the piezometer takes to equilibrate provides a measure of *K* (Baird et al., 2004). For this study, piezometers were made of polyvinyl chloride (PVC) piping with an outer diameter of 34 mm and an internal diameter of 30 mm (*cf*. Surridge et al. 2005). The intake at the base of the pipe was 9 cm in length, and the pipe was sealed at the base. The intake was not screened with mesh, and was constructed such that 65% of it was open to water flow, following Baird et al. (2004). This design was chosen because it provides the best balance between maintaining the structural integrity of the tube (as well as the wall of the well) and the openness of the intake (the intake is assumed to be completely open in the calculations described below).

K was estimated using slug withdrawal tests (Baird et al., 2004) and by applying the equation of Hvorslev (1951):

$$K = -\frac{A}{Ft} ln\left(\frac{h}{h_0}\right) \quad (1),$$

where *A* is the inside cross-sectional area of the piezometer (units cm^2; in this case 7.07 cm^2); *t* is the time (in seconds) at which the head difference (*h*, measured in cm) was recorded between the water level in the piezometer during the test and that prior to the test; h_0 is the initial head difference (at $t = 0$); and *F* is the shape factor of the piezometer intake (in this case a value of 36.2 cm was used). For all of the piezometer tests t_{95}, the time taken for the head to recover by 95%, was used in the calculation of *K*. *F* was calculated using the formula of Hvorslev (1951) as altered by Brand and Premchitt (1980):

$$F = \frac{2.4\pi l}{log_e[\frac{1.2l}{d}+\sqrt{1+\left(\frac{1.2l}{d}\right)^2}]} \quad (2),$$

Where *l* is the length of the intake, and d is the outer diameter of the piezometer. The shape factor is an expression of the way in which flow into the piezometer tube is altered by its dimensions, and is not affected by the hydrological conditions in the soil unless the intake is positioned close to the water table (Brand and Premchitt, 1980).

K was standardised to a temperature of 20°C using the equation of Klute (1965):

$$K_{ST} = K_T \left(\frac{N_T}{N_{ST}}\right) \quad (3),$$

where K_{ST} is the hydraulic conductivity at the standard temperature (ST) (cm s^{-1}), K_T is the hydraulic conductivity at the temperature of measurement (T) (cm s^{-1}), and N is the viscosity (g s^{-1} cm^{-1}). Actual temperatures recorded in the piezometer tubes ranged from 24–26 °C when the middle of the intake was at 50 cm depth, and from 24.5–27 °C when it was at 90 cm depth.

Figure 4.1: Photograph showing piezometer tubes installed one metre apart at Quistococha peatland. Branches were used to limit compaction of the peat in adjacent areas by the operator during the insertion of the tubes. A *Mauritia flexuosa* hummock can be seen in the background formed from large palmate leaves; this kind of microtopography was avoided during sampling.

The piezometers were inserted into holes made using a gouge auger with a slightly smaller diameter than the piezometers. A 'blocker' (Baird *et al.*, 2004) was used during installation to prevent material becoming entrained in the intake holes or entering the piezometer tube. Following installation, the piezometers were 'developed' (Surridge et al., 2005). Development involves the removal of water from the piezometer tube to

create large (>> 1) hydraulic gradients towards the piezometer, thus encouraging water to flow into the tube and unblock any pores which may have become obscured during installation. In particular, smearing around the intake can lower the recovery rate, and so cause erroneously-low values of *K* (Surridge et al., 2005). Development is not always straightforward; it is possible to over-develop a piezometer, thereby eroding a cavity around the intake that can also lead to erroneous *K* calculations (Hvorslev, 1951; Surridge et al., 2005). The peats at Quistococha were very fibrous, and so smearing around the intake is unlikely to have been a significant source of error. Therefore, the extensive development used by some previous studies (e.g. Baird et al., 2004, 2008; Surridge et al., 2005) was deemed unnecessary. Approximately 100 cm^3 of water (measured using a volumetric bailer) was removed from the tube in order to ensure that no large peat fragments had become entrained in the piezometer intake during installation. At San Jorge and Buena Vista, a larger volume of water was removed during development, as suspended material could still be seen after having removed 100 cm^3 of water. At San Jorge 200 cm^3 of water was removed, while at Buena Vista the figure was between 200 and 400 cm^3.

Following installation, piezometers were allowed to settle for 20 minutes before the pressure transducer and slug were inserted. The piezometer was then left for a minimum of twenty minutes to allow the water level to equilibrate with pore water pressures in the peat before the slug withdrawal test was undertaken. The slug itself was made from acrylic rod, and when withdrawn caused a drop in head of c. 4 cm. The water level during head recovery was measured using Schlumberger 'Mini-Diver' and 'Micro-Diver' self-logging pressure transducers, set to take measurements at 0.5 Hz. The two types of pressure transducer have nominal full-range (10 m) accuracies of 0.5 and 1.0 cm respectively, and a resolution of 0.2 cm. However, laboratory tests showed that the accuracy was similar to the resolution (A. Baird, pers. comm.).

4.3 Laboratory Methods

4.3.1 Pollen, phytoliths and charcoal

4.3.1.1 Background

The presence of pollen and other palaeobotanical remains in tropical peatland profiles was first established by Polak (1933); therefore studies of peatland pollen records in the tropics have a long history, dating back to the birth of pollen analysis as a palaeoecological technique (generally considered to be 1916; Manten, 1966). The application of phytoliths to the study of past environments has a more recent history,

and it was Rovner (1971) who first drew the attention of palaeoecologists to their potential as a palaeobotanical proxy. Until now, in the tropics phytoliths have been most widely applied in archaeology (e.g. Pearsall, 1994; Piperno & Stothert, 2003). In particular, the phytoliths of *Zea mays* (maize) have frequently been found in archaeobotanical studies, and are an important indicator of ancient agriculture (e.g. Bush et al., 1989; Perry et al., 2006). Studies of phytolith dissolution have shown that preservation should be good as long as acidity remains below pH 6 (Fraysse et al., 2009). Phytolith dissolution appears to be at a minimum at pH 3 (Fraysse et al., 2009), which suggests that preservation in peats should be good.

4.3.1.2 Pollen and phytolith preparation

Samples of sediment of 1 cm^3 volume were taken using a brass volumetric sampler. Sample preparation followed standard methods (e.g. Faegri and Iversen, 1989; Berglund & Ralska-Jasiewiczowa, 1986), and is outlined in Table 4.1. HF treatment was used on some near-basal samples in order to remove clays and other mineral materials where these were abundant. Samples were not sieved to remove fine sediments such as clays, as even fine mesh (7 μm) can cause loss of small pollen types, such as *Cecropia* (see Haberle, 1997).

Lentfer and Boyd (1998) reviewed at length the methods used for the separation of phytoliths from their host sediments. There are two commonly applied techniques; 'wet oxidation' and 'dry ashing' (Piperno, 2006). However, in the case of peatlands, where minerogenic components generally constitute <5 wt%, phytoliths can also be viewed in pollen slides. This extraction method is likely to be less efficient than methods which remove all non-siliceous organic matter, and indeed phytolith abundances may also closely reflect the decomposition of the peat itself (see Chapter 6 for further discussion).

Unless HF is used to treat pollen samples, biogenic silica bodies such as phytoliths will survive the pollen preparation and so can be counted at the same time as the pollen for a given sample. In this case, spinulose palm phytoliths were counted alongside pollen.

Pollen samples obtained from herbarium material were also prepared according to standard methods (Faegri and Iversen 1989), but without HF treatment. The methodology used for modern fern spores involves a slightly modified method, where sieving is not undertaken (this helps to avoid loss of sample).

Table 4.1: Pollen preparation method (phytoliths and charcoal were also examined from the pollen slides). Protocol follows that of the University of Leeds School of Geography and Berglund & Ralska-Jasiewiczowa (1986).

1. *Lycopodium* spore tablets (x2) added as a "spike" to allow pollen concentrations to be calculated (Stockmarr, 1971).
2. Hot (c. 80 ˚C) 7% HCl for 20-30 minutes to remove carbonates and break up *Lycopodium* tablets
3. Centrifuge, decant, wash with deionised water
4. Hot 10% NaOH for 2-4 minutes to remove organic acids.
5. Centrifuge, decant, wash with deionised water. This prevents damage to pollen from remaining in NaOH during sieving.
6. Sieve through a 180 μm mesh to remove large plant fragments
7. Wash repeatedly with deionised water to remove remaining humic acids and fine clays.
HF TREATMENT
8. Acidify samples using 7% HCl prior to HF treatment
9. Hot HF treatment was at 80 ˚C for 2 hours.
10. Use hot 7% HCl to remove fluorosilicates. Treat samples for at least one hour.
11. Centrifuge, decant, wash with deionised water.
ACETOLYSIS
12. Wash with CH_3COOH – Concentrated (glacial) Acetic acid to remove water prior to acetolysis
13. Make acetolysis mixture using one part H_2SO_4 (Sulphuric acid) to nine parts acetic anhydride. Add 6 ml to each sample, and place each sample in the water bath for 7 minutes.
14. Wash samples with glacial acetic acid to cool and stop the reaction
STAINING AND MOUNTING
15. Wash samples with water, and then with dilute c.1% NaOH to increase the alkalinity prior to addition of safranin dye.
16. Wash samples with water, add two drops of 0.2% safranin dye
17. Wash samples twice with tertiary-butyl alcohol (TBA) to remove water
18. Transfer samples to glass vials and add silicone oil. Leave samples to allow remaining TBA to evaporate
19. Mount samples on glass slides using paraffin wax to seal the slides ready for microscope study.

4.3.2 Pollen reference materials

Samples of modern pollen reference material were obtained from established tropical pollen reference collections (University of Edinburgh), herbaria (University of Turku [TUR]; Jenaro Herrera; Royal Botanical Gardens, Kew [K]) and in the field. Only samples which had been confidently identified to genus or species level were prepared. For field samples, identifications were made with the assistance of experienced tropical botanists T.R. Baker, E. Honorio Coronado, and M. Rios.

4.3.3 Microscopy

Slides for normal light microscopy were made using silicone oil as the mounting medium, and were sealed using paraffin wax. Pollen, phytolith and charcoal analysis was

undertaken using a Leica DMLS binocular microscope. Routine counting was undertaken at 1000x; identification of pollen in the tropics is more straightforward at higher magnification and this also allowed easy counting of phytoliths down to a minimum of 5 µm. Several pollen types (e.g. *Cecropia*, *Begonia*) are also typically small (often <10 µm; 6 µm in polar view) and reliable detection is best accomplished at high magnification.

Scanning electron microscopy (SEM) was used in the examination of pollen reference materials. Herbarium samples examined using scanning electron microscopy were air dried and mounted on a metal stub using graphite paste. They were then gold coated prior to analysis with an FEI Quanta 650 environmental SEM.

4.3.4 Pollen taxonomy

In Amazonia, an optimistic estimate of the number of taxa sampled for pollen (e.g. 1,210 types in Roubik and Moreno, 1991) is still far short of covering half the plant species which occupy the lowland tropics. In the present study, identifications were simplified because peatlands are generally less diverse than other forest types. Family level identifications were also usually possible, even where genus and species level identification was difficult.

During the course of this study, the research group at Leeds have gradually expanded their tropical pollen reference collection to cover the pollen/spores of many plants which occupy Amazonian peatlands (also see Chapter 6). These were used to support the identifications made, which were based on the pollen atlases of Roubik and Moreno (1991) and Colinvaux et al. (1999), the thesis of Absy (1979), and those types described in the Neotropical Pollen Database (NPD; Bush and Weng, 2006). Nowicke and Takahashi (2002) were used to provide additional details on the pollen of *Acalypha*. The heterogeneity of *Acalypha* pollen is only partly covered in other pollen guides. References relating to fern spore taxonomy are discussed in Chapter 6. Van Geel (2001) was used as a guide to some non-pollen palynomorphs, specifically *Spirogyra.* In an environment where a total taxonomy is not available, eliminating or identifying common non-pollen types is also important.

Further details on the pollen of the Moraceae/Urticaceae family were taken from Burn and Mayle (2008). Not all the morphotypes defined in Burn and Mayle (2008) were accepted by the present author as distinct types in the north-western Amazon. The flora in the north of Amazonia is generally more diverse, and the Moraceae family is amongst the most diverse and ubiquitous of all the tree families. As such, whilst grains with distinct morphologies can be identified to genus (e.g. *Ficus*, *Cecropia*, *Brosimum*, *Coussapoa*), many triporate types are too similar between different genera to allow

confident identification (e.g. *Poulsenia*, *Perebea*). This is particularly true where grains are damaged.

Weber et al. (1999) were used as an additional source for the identification of pollen from the Araceae family. In particular, the pollen of *Pistia stratiotes* (water lettuce) was identified using this paper as a guide rather than Roubik and Moreno (1991). The latter describe *Pistia* as an inaperturate grain without any surface sculpture (i.e. psilate), but the author found that the striae described from SEM study by Weber et al. (1999) were faint but still visible in most cases. Weber et al. (1999) also provide additional detail on the pollen of *Spathiphyllum*, which has a more prominent surface sculpture and less elongated grain shape than *Pistia*.

The Melastomataceae and Combretaceae were generally found to be indistinguishable from one another, but the pollen of *Adelobotrys* (Melastomataceae) is quite distinct (cf. NPD), being small in size and having a rounded grain shape with very indistinct pseudocolpi, and a small square pore. *Adelobotrys adscendens* is common in lowland wet forest (Almeda, 1981), and probably the most common species in this genus, but pollen of this type was conservatively denoted *Adelobotrys* sp.

Descriptions of *Remijia* were not available in atlases or the NPD and identification followed Anderson (1993). SEM images of *Virola* were obtained from Walker and Walker (1979), normal light images of *Dendropanax* from Haselhorst et al. (2013), and images of taxa in the Tileaceae, especially *Luehea* and *Pachira*, from Dias Saba (2007).

Further investigations into the pollen taxonomy of peatland pollen and spore types were undertaken as part of this study (see Chapter 6).

4.3.5 The pollen sum

A minimum total of 300 total land pollen (TLP) was counted for all samples. The pollen sum excluded spores of the Pteridophyta, and pollen of the aquatic *Pistia stratiotes* which was extremely abundant in many samples from San Jorge. In the calculation of pollen percentages, unknown pollen types were also included. In a single instance, low pollen concentrations meant that a pollen sum of 150 grains was counted as it would have been impractical to reach 300, a method which has been used previously by other tropical palynologists working with samples where pollen concentrations are low (Haberle et al., 1997). A lower total was also counted for individual pollen surface samples (>100), but several surface samples were studied, and amalgamated pollen totals were > 300 (see Chapter 6).

A count of 300 grains is considered optimal by many palynologists as it balances the reduced errors which come through increasing the pollen sum against the increased labour which this involves (Birks and Birks, 1980). Confidence intervals (95%) can be calculated using the equation given in Maher (1972):

$$p = \frac{\hat{p}+\left[\frac{(1.96)^2}{2n}\right] \pm (1.96)\sqrt{\left[\frac{\hat{p}(1-\hat{p})}{n}\right]+\left[\frac{(1.96)^2}{4n^2}\right]}}{1+\left[\frac{(1.96)^2}{n}\right]} \quad (3)$$

Where n = the pollen count; and $\hat{p}$ = x/n where x is the estimate of the proportion of the given taxon following a count of n grains.

Figure 4.2 provides an example of how the confidence intervals from this equation can be displayed, and Table 4.2 shows how this can be converted into percentage errors. The confidence interval narrows rapidly up to a pollen sum of c. 300 grains but declines more slowly above this.

Given the uncertainty involved in the counting process (which are a function of count size), a count of 300 TLP should allow a change in the abundance of a given taxon of >10% to be detected in most samples (Table 4.2). In a study of current pollen assemblages in South Africa, Hill (1996) found no statistically significant difference between counts of 250, 500 and 1,000 grains for most vegetation types, although in more diverse areas higher counts were found to improve the precision. The diversity of the vegetation in Hill's (1996) South African study (max. 37 different taxa) is of a similar number to peatlands such as Quistococha (24 taxa > 2.5 cm stem diameter; Roucoux et al., 2013).

Although the errors are greater, counts of 150 TLP may also be adequate, and Madanes and Dadon (1998) found that 150 TLP is frequently sufficient to characterise the main pollen types (those totalling 70-80% of the pollen sum). As such, counts of this size are appropriate where pollen concentrations are low. One reason that tropical palynologists might count a larger number of grains would be to allow for the detection of rare pollen taxa (Madanes & Dadon, 1998). The alpha diversity of floodplain forests is generally less than that for terra firme forests (see Chapter 3), and in many cases a small number of taxa dominate the assemblage. However, as will be shown in Chapter 6, some common taxa are poorly represented in the pollen record and therefore increased counts may be beneficial. In this case, expanding the count to > 300 TLP to more accurately quantify very rare taxa (those < 2%) was beyond the scope of this study, and other approaches were taken to improve the interpretation of the palaeoecological record in tropical peatlands.

Table 4.2: Summary of the percentage error associated with pollen counts depending on i) the total pollen sum and ii) the proportion of a given taxon in the assemblage. The maximum confidence interval is shown (i.e. the upper limit), although as shown in Fig. 4.2 the 95% confidence interval is not symmetric. A total count of >300 was used in this study (highlighted). Values calculated according to Maher (1972).

Total	Confidence intervals (95%) for a given proportion					
pollen sum	2%	5%	10%	25%	50%	80%
75	8.21	9.26	10.59	13.04	14.34	12.41
100	6.41	7.40	8.64	10.86	12.03	10.30
150	4.56	5.47	6.56	8.47	9.46	7.98
200	3.61	4.45	5.44	7.13	8.01	6.70
250	3.03	3.81	4.72	6.26	7.05	5.87
300	2.64	3.37	4.21	5.63	6.36	5.28
400	2.13	2.79	3.54	4.79	5.42	4.47
500	1.81	2.42	3.10	4.22	4.80	3.94
1000	1.13	1.59	2.08	2.89	3.30	2.69

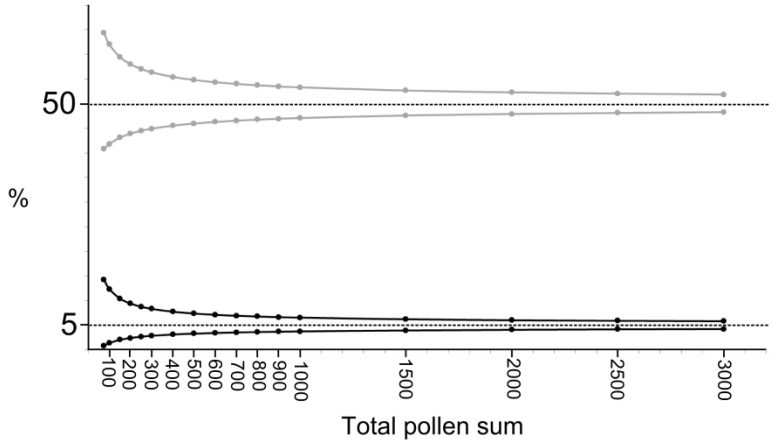

Figure 4.2: Diagram indicating pollen confidence intervals where taxa constitute 5% and 50% of the pollen sum. The 95% confidence intervals (dotted lines) narrow asymptotically towards the true percentage as the pollen count increases. Note that errors are smaller for populations which make up a lesser proportion of the pollen sum (5% in this case), but are proportionally more significant than for larger populations. Values calculated according to Maher (1972).

4.3.6 Charcoal counts

Microcharcoal > 5 μm in length was counted in the pollen slides, but was sparse in all of the peat sequences, as in Roucoux *et al.* (2013). Statistical analysis of charcoal counts from pollen slides has shown that a minimum sum of 200 charcoal particles plus spike is required to gain an accurate (± 5%) measure of charcoal abundance (Finsinger & Tinner, 2005). As such, in some of the diagrams the errors attached to counts are likely to be large relative to the proportions counted. In the case of the peat cores, charcoal counts are generally not indicated on the pollen diagrams as the absolute abundances serve only to show that charcoal was rare in the sequences. Charcoal was more common in parts of the lake core, and therefore charcoal abundance has been shown for this core (QT-2010-3).

4.4 Sedimentology

4.4.1 Sediment description

A number of different schemes have previously been applied to the description of peat, including those of Von Post (1924), Troels-Smith (1955), and Esterle (1990). Wüst *et al*. (2003) reviewed some of this terminology in the context of tropical peats, and formulated a scheme similar to that of Esterle (1990). At its most basic level, this scheme describes the peat on the basis of its fibre content, ranging from fibric (66–100% fibres), and hemic (33–66% fibres) to sapric (0–33% fibres). Whilst the simplicity of this method has some advantages, it is somewhat difficult to assess fibre content in the field. The Troels-Smith system also has a number of advantages over the Wüst *et al*. (2003) classification; for example it is capable of describing lake sediments and inorganic sediments which may lie at the base of a peat profile. As such, core stratigraphies were described using the Troels-Smith (1955) system. These are presented alongside the palynological data. During *K* measurements (see above), humification was recorded semi-quantitatively according to the Von Post (1924) scheme (after Hobbs, 1986).

4.4.2 Loss on ignition

Loss-on-ignition (LOI) has been widely applied to assess the moisture and organic content of peat and sediments (Heiri *et al*., 2001). Samples are weighed and then dried overnight at 105 °C to provide a measure of the moisture content. The samples are then heated to 500-550 °C which causes any organic carbon to oxidise, leaving behind only mineral ash (although this may still contain siliceous particles of biological origin). Heiri *et al.* (2001) showed that there are a number of potential sources of error in LOI measurements, including the exposure time and temperature differences in the furnace. Seventeen pairs of repeat measurements produced a mean difference of 1.6% between pairs of samples (s.d.: 1.3%).

4.4.3 Magnetic susceptibility

Hatfield and Stoner (2013) provide an overview of the application of magnetic susceptibility (MS) in palaeoenvironmental studies, summarised here. A measure of how magnetisable a core sample becomes when placed in a weak external magnetic field (c. 0.1 mT), the MS is also affected by sample density (Hatfield and Stoner, 2013). The concentration of ferromagnetic minerals within the core is thought to be the main control on MS values (Hatfield and Stoner, 2013). Equally, MS responses can be reduced where biogenic carbonate is a significant component of the sample, as carbonate is diamagnetic (Hatfield and Stoner, 2013).

Volumetric magnetic susceptibility (κ, dimensionless; Hatfield and Stoner, 2013) measurements of cores QT-2010-3 and SJO-2010-1 were undertaken by T.D. Jones in 2010 using a Bartington MS2 meter and and MS2C loop sensor. Background MS was measured before and after each core section to account for sensor drift (assumed to be linear). The measurement interval was 2 cm. The results of these analyses are presented alongside other core data in Chapters 8 and 9

The method was not applied to the shorter peat cores as wet peat (which contains >90 % water in most instances) is a dielectric and therefore measurements taken are frequently dominated by noise (and drift in the instrumentation) rather than real signal. Furthermore, MS measurements undertaken with a loop sensor will smooth readings over approximately twice the loop diameter (Hatfield and Stoner, 2013). This not only makes boundary detection less accurate than visual core description and loss-on-ignition, but creates 'edge effects' near the end of each core section (Hatfield and Stoner, 2013). Investigations were undertaken by the author on cores taken from Quistococha in 2011, but MS measurements served only to distinguish clay and peat, a distinction which can be made more reliably using loss-on-ignition measurements.

4.5 Elemental analysis

4.5.1 Carbon and Nitrogen

4.5.1.1 Background

In lakes, C/N ratios can be used to help establish the extent to which sediments are composed of the autochthonous organic matter of lake algae or allochthonous organics from inwashed terrestrial plant matter (Meyers 1994). For example, both marine and lacustrine algae have C/N ratios of <10, and both C_3 and C_4 plants have ratios >20 (Meyers 1994; Meyers and Lallier-Vergès 1999).

Diagenesis is generally assumed to be minimal in lacustrine environments (Meyers and Lallier-Vergès 1999), although nitrogen can be more labile and therefore higher nitrogen concentrations may be found in sediments close to the sediment-water interface (Talbot, 2001). C/N ratios can therefore be a useful aid to interpreting lacustrine pollen records, as if there was significant input of from inwashed organics, it can be inferred that a proportion of the pollen is probably being washed in from the surrounding catchment. Conversely, if this is not the case and the C/N ratios remain low, then the input of wind-blown pollen onto the lake surface is likely to be a more important source of pollen relative to surface inwash. This technique was used by

Sifeddine et al. (2001) used C/N to determine the origins of the organic matter in lake sediments from Carajás.

In peatlands, there is a greater potential for diagenesis, and C/N ratios may be seen as a measure of decomposition over time, especially where the peat has been produced under a constant vegetation type (*see* Kuhry and Vitt, 1996). However, Lawson et al. (2014) challenged this assumption in light of data from Quistococha which did not show a straightforward decrease in C/N ratio with depth, as would be expected if decomposition had exerted a strong control on C/N values.

4.5.1.2 C/N method

Samples of 1 cm^3 were dried at 105 ˚C and milled to ensure that the sample was sufficiently homogenised. Each sub-sample was then weighed into a tin cap by the author, prior to analysis with a Eurovector Turboflash CNS combustion analyser by Leeds School of Geography laboratory staff. Vanadium pentoxide was used as a catalyst. The peat standard NJV942 was used with all sample batches. The experimental values for carbon and nitrogen were within 95% of the certified value for NJV942 for all sample runs. Eleven repeat measurements produced a mean difference of 0.55wt% for carbon and 0.02wt% for nitrogen between pairs of samples.

4.5.2 Major elements

4.5.2.1 Background to the use of major elements in peatlands

Peatlands can be broadly divided into 'minerotrophic' and 'ombrotrophic' (Heinselman, 1970; Shotyk, 1988), although there is a gradient within this broad division (Lähteenoja et al., 2009b; Chapter 3). There are three main ways of establishing whether a peatland is ombrotrophic; by establishing the 'domed' topography of the peatland (and particularly that the top of the dome is above the maximum flood level), through examining the vegetation (ombrotrophic peatlands harbour characteristic plant species), and by examining the pH and major cations of the surface waters (Shotyk, 1996). In Amazonia, peatlands are forested and therefore it is difficult to establish whether they are domed; the canopy partially obscures the signal from satellites required by differential GPS units, and the soft substrate and limited line-of-sight also hinder the use of traditional levelling techniques. The use of plant species to determine ombrotrophy is potentially circular, especially in Amazonia where the current floristic composition of domed peatlands is relatively unknown.

However, surface water or peat chemistry by definition provides an indication of the degree of minerotrophy, and peatlands are generally described using this approach

(Bridgham et al., 1996). Peat chemistry has already been applied to define Amazonian peatlands (Lähteenoja et al., 2009b, Lähteenoja & Page, 2011). Although nitrogen and phosphorus are frequently the main limiting nutrients in peatlands (Bridgham et al., 1996; Troxler et al., 2012), ions such as calcium (Ca^{2+}) are also correlated with minerotrophy and plant distributions (Heinselman, 1970; Waughman, 1980; Wassen et al., 1989). In particular, the Ca/Mg ratio can be compared with that of regional rain water to establish whether a peatland is ombrotrophic (Lähteenoja et al., 2009b; Proctor et al., 2009; Keimowitz et al., 2013; Furch and Junk [1997] review the metal content of rainwater for the Amazon basin). Previous authors have also used down-core measurements of peat geochemistry to establish past changes in nutrient availability (Lawson et al., 2014), and specifically the point in time at which a peatland became ombrotrophic (e.g. Chapman, 1964; Shotyk, 1996; Martínez Cortizas et al., 2002). This is a useful technique, although it can be complicated by biological recycling of nutrients in forested peatlands with deep root zones (Weiss et al., 2002; Lawson et al., 2014).

4.5.2.2 Background to ICP-OES

ICP-OES (inductively coupled plasma optical emission spectroscopy) has been widely applied to establish the quantity of major and trace elements present in a variety of different situations (Hou & Jones, 2000), including peatlands (e.g. Le Roux et al., 2005). Full details of the technique are provided by Hou and Jones (2000), some details of which are summarised here.

In ICP-OES, samples are introduced using a nebuliser before being heated to a temperature of between 6000-7000 Kelvin (Hou and Jones, 2000). This causes the excitation of electrons within the atoms of elements in the sample, and when these then decay back to a more stable state they emit light. Elements have individual emission spectra, and the ICP-OES measures the intensity of single wavelengths of light emitted as a result of this process, thereby allowing the quantity of a given element in each sample to be determined. The light is generally detected by a photomultiplier tube, with a focus on wavelengths between 160-800 nm (Hou and Jones, 2000).

Solid samples must be subjected to a chemical extraction in order to produce a liquid form suitable for analysis. In this study, the method followed the pure aqua regia (HCl mixed with $HN0_3$) extraction of the British Standard BS 7755 (1995), which was also used by Lawson et al. (2014) in the study of core QT-2010-1 from Quistococha peatland.

Lähteenoja et al. (2009b) and Lähteenoja and Page (2011) used an aqua regia extraction with HF (sometimes referred to as a total extraction). However, a standard aqua regia extraction is often used rather than a total extraction as it is thought that this provides a

better indication of the availability of nutrients to plants, and is often used in agricultural applications (Vercoutere et al., 1995). As Chen and Ma (2001) note, the aqua regia only method (without HF) can result in extractions of < 75% for many common elements (e.g. Ca, Fe, Al, K, Mn, Ni, Pb, Zn). Others have argued that neither of these methods is likely to reflect the actual biological availability of elements in the soil profile; even a standard aqua regia extraction is far more powerful than any normal biological mechanism (British Standard BS 7755, 1995). In this case, a standard aqua regia extraction was chosen as the main purpose was to determine the biological availability of elements to peatland vegetation, and to establish the main down-core trends in Ca and Mg.

4.5.2.2 Major element sample preparation and analysis

Sample preparation followed the method outlined in Table 4.3 and was carried out by the author. Samples were analysed by staff at the University of Leeds School of Geography using a Perkin Elmer model 5300DV ICP-OES (with simultaneous spectrometer).

Table 4.3: Aqua regia extraction method for analysis of metals in peat using ICP-OES (after Leeds School of Geography protocol and British Standard BS 7755, 1995).

1. Dry samples at 60 ˚C, then grind samples to a fine powder
2. Weigh a minimum of 0.3 g (preferably 0.5 g or greater) for each sample into an extraction beaker.
3. Weigh certified reference material into extraction beakers (for peats, NJV942 was used). Use weight approximating that used for the samples being analysed. Also prepare reagent blanks.
Extraction
4. Add small quantity of deionised water (< 0.5 ml) to moisten the samples
5. Add 10.5 ml HCl, followed by 3.5 ml HNO3. Gently swirl flask to ensure reagents are mixed in. For peats, add a further 5 ml HNO3 in quantities of c. 1 ml
6. Cover each beaker with 'tear-drop' shaped watch glass and leave overnight (16 hours) at normal room temperature
7. Place the samples on the hotplate and gradually increase the temperature. Once reflux temperature has been reached, maintain for 2 hours. Rotate samples on the hotplate to ensure that all are evenly heated (temperature is generally cooler towards the margins).
8. Remove samples from the hotplate. Leave to cool and settle until insoluble particles are no longer suspended.
9. Pass the supernatant through a Watman 542 filter paper and collect the filtrate in a 50 or 100 ml volumetric flask.
10. Use deionised water to wash the insoluble particles onto the filter paper, and rinse with more deionised water.
11. Make up to 50 ml or 100 ml mark and seal the flask. Shake well.
12. Transfer an aliquot of each sample into plastic 15 ml tubes ready for ICP-OES analysis

4.6 Chronology

4.6.1 Radiocarbon dating

4.6.1.1 Background

Radiocarbon dating has been widely applied to provide absolute chronologies in archaeology and palaeoenvironmental studies since its initial development by Willard Libby and others in the 1940s (Arnold and Libby, 1949). In Amazonian peats, radiocarbon (^{14}C) dating is the only effective means of establishing an absolute chronology over Holocene timescales. Other techniques, such as tephrochronology, have not yet been fully developed as chronological tools in Peru (although Rodbell *et al.* [2002] studied visible tephras in Andean lakes in Ecuador and there may be some potential for the future application of tephrochronology in the western Amazon).

The central theory behind radiocarbon dating and recent advances are described in detail in Lowe and Walker (1997) and Bronk Ramsay (2008), some aspects of which will be summarised here. ^{14}C is a radioactive isotope of carbon which is mainly formed in the upper atmosphere, and which decays through emission of beta (β) particles over time to become stable ^{14}N. ^{14}C in the atmosphere rapidly oxidises to form $^{14}CO_2$, which is then incorporated into organic tissues. An organism remains in isotopic equilibrium with the ^{14}C in its surrounding environment until it dies (or particular cells die, such as those in tree rings), at which point decaying ^{14}C atoms are no longer replaced (Lowe and Walker, 1997). As the ^{14}C in the dead organism decays to form ^{14}N at a steady rate, and the age of the organic matter can be determined by measuring the remaining amount of ^{14}C.

Eight half-lives, or around 45 ka, is considered to be the limit of radiocarbon dating (Lowe and Walker, 1997). In this study, the sites form part of the Holocene floodplain and therefore are unlikely to be more than 11.7 ka in age. In most cases, modern radiocarbon dating uses accelerator mass spectrometry (AMS) to count the number of ^{14}C atoms in a sample. Earlier beta (β) emission counting methods (see Lowe and Walker, 1997) required as much as ten grams of material (Arnold and Libby, 1949), but AMS allows reliable dates to be obtained from samples of as little as a few milligrams.

Production of ^{14}C varies through time, largely as a result of solar activity, and hence it was realised early on in the history of the technique that a means of calibration would be required (e.g. Willis et al., 1960). The initial error associated with an uncalibrated radiocarbon date represents the analytical error only. After calibration, the error associated with a radiocarbon date generally increases, and the normally distributed analytical error becomes a non-normally distributed error (described by a probability density function). Calibration of a radiocarbon date to produce a calendar age can be

achieved by comparing a radiocarbon determination with one obtained from an archive which has also been dated using a different absolute dating technique (Lowe and Walker, 1997). Dendrochronology has been extensively used for this purpose (Lowe and Walker, 1997); the ^{14}C from a tree ring can be compared to the absolute age obtained by ring-counting in trees which produce annual rings. The internationally ratified tree ring based calibration curve INTCAL13 is based on data collected from the northern hemisphere (Reimer et al., 2013).

Due to the more limited atmospheric mixing between the northern and southern hemispheres, there are interhemispheric differences in the amount of ^{14}C that mean a different calibration curve is required for the southern hemisphere (SHCal13: Hogg et al., 2013a). The difference between calibrating with the two different curves is c. 40 years (Hogg et al., 2013a), with southern hemisphere samples emerging as older than northern hemisphere samples. In this case, the northern hemisphere calibration curve has been used, as the study area of this thesis is crossed annually by the ITCZ; this means that during the wet season the ITCZ lies further south and there is mixing with air from the northern hemisphere (McCormac et al., 2004). There are further reasons for using the northern hemisphere curve:

i) SHCal13 is based largely on tree ring chronologies from Tasmania and New Zealand; given that there can be intrahemispheric offset within the southern hemisphere (Hogg et al., 2013b), there is uncertainty over whether the offset in SHCal13 also reflects that for South America.

ii) The measured SHCal13 curve only extends to 2145 cal yr BP (Hogg et al., 2013a). Beyond this point, the offset is modelled by applying an offset to the northern hemisphere calibration curve. The author contends that awareness of a potential offset between different calibration methods is of equal use to a calibration curve which is only loosely based on actual data.

iii) An agreed southern hemisphere calibration curve has only been available since 2004 (McCormac et al., 2004), and has not been widely applied in published records from South America (cf. Urrego et al., 2006; de Toledo & Bush, 2008; Lähteenoja et al., 2009a; Whitney et al., 2011). Although the difference between SHCal13 and northern hemisphere curves is only small, the application of different curves can create artificial diachroneity.

4.6.1.2 Sample preparation and analysis

Samples for radiocarbon dating were prepared using powder-free gloves, and glassware and spatulas were washed with HCl and deionised water. All peat samples were sieved

at 180 µm to ensure the removal of large roots, and then centrifuged before being sent for analysis. Metal sieves were flamed with a Bunsen burner and then washed with deionised water in order to remove any potential contamination from organic residues. Lake samples were either left unprocessed or were picked using tweezers and a low-powered light microscope to remove visible organic fragments where these were in a mineral-rich matrix.

The $\delta^{14}C$ and $\delta^{13}C$ content of the samples was determined through accelerator mass spectrometry (AMS) by staff at the NERC Radiocarbon Facility in East Kilbride. Samples were treated with 2M HCl at 80 ˚C for 4 hours, before being washed with deionised water, dried, and homogenised. The samples were then heated with CuO in order to obtain the total carbon for a given mass of sample as CO_2. Via Fe/Zn reduction, the CO_2 gas was then converted to graphite suitable for AMS analysis.

4.6.2 Fallout radionuclides: ^{210}Pb dating

4.6.2.1 Background

Due to the substantial anthropogenic input of ^{14}C into the atmosphere from nuclear bomb testing, radiocarbon dating cannot be applied straightforwardly to 20th century peats (Lowe and Walker, 1997). Although it is theoretically possible to date such young material, there is no internationally agreed calibration curve for the period after AD 1950 (Turetsky et al., 2004). This presents a problem in tropical peatlands, where the frequently rapid accumulation of peat can mean that the upper 50-100 cm have been laid down in the last c. 200 years (cf. Weiss et al., 2002; Roucoux et al., 2013). Spheroidal carbonaceous particles (SCPs) from high temperature combustion are often used to date profiles across this time interval in Europe (Rose et al., 1995; Turner et al., 2014), but do not occur in significant numbers in the western Amazon (Swindles et al., 2014).

In northern peatlands, anthropogenic fallout radionuclides such as ^{137}Cs, ^{207}Bi, and ^{241}Am, as well as naturally produced ^{210}Pb, have been used to provide absolute age estimates in recent peats (Turetsky et al., 2004; Parry et al., 2013). These have not been used in Amazonian peatlands before, but have been applied in Andean peatlands (cf. Benavides et al., 2013) and lakes (Bird et al., 2011b), and have the potential to be applied in lowland sites such as those in this study.

Immobility is a key assumption underlying the use of these radionuclides to obtain a chronology, and recent studies in northern peatlands have shown this assumption may be violated in some cases. In particular, Parry et al. (2013) found that ^{137}Cs is highly mobile in ombrotrophic peats where there is no clay to bind it. As will be shown through research into the hydrology of several peatlands in Chapter 5, the high hydraulic

conductivity and the changes in water table throughout the year mean that it would not be advisable to use ^{137}Cs to date ombrotrophic Amazonian peatlands. A further potential problem is that the peaks in ^{137}Cs activity in 1958 and 1963 are generally less pronounced in the southern hemisphere than in the northern hemisphere (*see* Appleby, 2001), although Bird et al. (2011b) observed a pronounced ^{137}Cs peak at Pumacocha (Andean Peru), possibly as a result of the movement of the ITCZ discussed above in the context of ^{14}C (Section 4.5.1.1). ^{241}Am is relatively immobile in peats, but is often not present in detectable quantities (Parry et al., 2013).

While there is evidence for ^{210}Pb mobility in peats (e.g. Urban et al., 1990; Belyea and Warner, 1994; Olid et al., 2013), it is certainly less mobile than ^{137}Cs (Parry et al., 2013). Where ^{210}Pb is leached from the peat, Urban et al. (1990) argue that this can introduce errors (generally age overestimates, where ^{210}Pb is removed) on the order of 30 years. However, ^{210}Pb should be relatively immobile in peats, as it is an inert isotope and generally combines with sulphur under anoxic conditions to form insoluble PbS (Damman, 1978; Parry et al., 2013).

^{210}Pb has a half-life of 22.26 years, and can be used to provide dates for the last c. 150 years (El-Daoushy, 1986; Lowe and Walker, 1997; Parry et al., 2013). ^{210}Pb lies near the end of the ^{238}U decay series, with ^{210}Pb decaying to the short-lived isotopes ^{210}Bi and ^{210}Po before finally decaying to stable ^{206}Pb (Lowe and Walker, 1997). The half-life of ^{238}U is extremely long (c. 4.5 x 10^9 years; Lowe and Walker, 1997), and therefore there is a constant source of ^{210}Pb in the natural environment as the ^{238}U in the earth's crust continues to decay.

4.6.2.2 Sample preparation and analysis

After completing other analyses, the San Jorge core (SJO-2010-1) was divided into 2 cm sections by the author. Either 5 or 6 cm^3 of peat was sampled volumetrically from each 2 cm sub-section, and dried for two days at 50 ˚C (this moderate temperature helps to prevent loss of volatile compounds of Pb). Samples were then weighed in order to estimate their dry bulk density before being sent to the University of Exeter for ^{210}Pb analysis.

Samples were chemically treated with aqua regia (HNO_3 and HCl) and H_2O_2 at the University of Exeter in order to extract ^{210}Pb and remove organic matter before being transferred to silver plates. The ^{210}Pb content of the samples was then determined indirectly through counting alpha particle emissions from its granddaughter isotope ^{210}Po (for details on this approach see Appleby, 2001). As is standard practice (Le Roux and Marshall, 2011), a spike of ^{209}Po was added to each sample to determine whether

there was any loss of ^{210}Po during the preparation. Measurements were made using a combination of 'TENNELEC TB 3LB' and 'ORTEC OCTÊTE-Plus Integrated Alpha-Spectroscopy System' emission counters, with a measurement time between 70 and 285 hours. Analyses were undertaken by Nicole Sanderson at the University of Exeter, UK. Two samples were re-analysed, but due to the low bulk density of the peat sufficient material could not be obtained for true replicate samples.

4.7 Statistical analyses

4.7.1 Ordination

Ordination techniques, such as principle components analysis (PCA), provide a straightforward way of summarising pollen datasets (Birks, 2007). Ordination takes a multivariate dataset and reduces it to a number of artificial axes, each of which explains a proportion of the variance. The first axis explains the largest proportion of the variance, the second axis the second largest and so on. Proximity of a sample to an axis relates to the amount of variance in that sample explained by the axis. Samples grouped together have a similar pollen assemblage; in a standard ordination, this grouping is done regardless of their position in the core (Birks, 2007).

In the case of pollen data, there are frequently no environmental variables (e.g. pH) included in this analysis. However, the artificial gradients formed purely by examining the species data can be interpreted in ecological terms; this is sometimes referred to as "indirect gradient analysis" (ter Braak and Prentice, 1988; p. 244). The first axis, which explains most of the variation in the data, can be seen as the unknown environmental gradient which drives most of the change in the pollen data (ter Braak and Prentice, 1988).

Minchin (1987) found that LNMDS (local non-metrical multidimensional scaling) performs better than PCA, detrended correspondence analysis (DCA) and Gaussian ordination (GO) for indirect gradient analysis. In PCA, indirect gradient analysis always produces an arch effect, although modified version of PCA can help to mitigate against this (Minchin, 1987). This is because the other axes of the ordination are generally associated (although uncorrelated) with the first axis, and indeed this was the rationale behind the development of other approaches such as DCA (see Hill and Gauch, 1980). While DCA generally performs better than PCA and GO, Minchin (1987) found that DCA only provides better results than LNMDS in a limited number of circumstances, such as for unimodal species response curves. As such, LNMDS was chosen as the preferred form

of ordination for the pollen data in this study. Analyses were undertaken in R 2.15.0 (www.R-project.org).

4.7.2 Pollen diagram zonation

4.7.2.1 Varying approaches to pollen zonation

The complex nature of pollen data means that zonation serves an important purpose by making description, interpretation, and correlation more straightforward (Birks, 1973; Gordon and Birks, 1972). A pollen zone can be defined as a body of accumulated material with "a consistent and homogeneous fossil pollen and spore content" (Birks, 1973; p.273). The numbering of pollen zones is generally done from the bottom of the sequence upwards, in keeping with geological convention.

In early pollen studies, pollen assemblage zones were frequently determined by eye with no assistance from numerical techniques at all (e.g. Pennington, 1964). Numerical methods arguably provide more repeatable results (Gordon and Birks, 1972), which is particularly important where pollen zones are being compared between multiple sequences (as in this study). In reality, there may be very little difference between numerically derived zones and those derived visually, and most numerical techniques will place pollen zones in roughly the same position in a sequence (Gordon and Birks, 1972). Ultimately it must be remembered that pollen zones are there purely as an aid to interpretation; all pollen zonation schemes will create the impression of a sudden break in assemblage which may not reflect real and frequently gradual changes in vegetation type that can be seen in pollen data (Lawson, 2001).

Psimpoll (Bennett, 2007), the program used to produce the pollen diagrams in this thesis, provides several possible methods for statistical pollen zonation:

Group 1: 'Splitting' methods

a. Binary splitting by sum-of-squares
b. Binary splitting by information content
c. Optimal splitting by sum-of-squares
d. Optimal splitting by information content

Group 2: 'Agglomeration' methods

a. Constrained cluster analysis by sum-of-squares (CONISS)
b. Constrained cluster analysis by information content (CONIIC)

In general, the greatest difference in the pollen zones produced will be found between the group 1 and group 2 methods, which each have a fundamentally different underlying approach (Bennett, 1996; Bennett, 2007). It is good practice to make comparisons between methods before choosing a pollen zonation method (e.g. Lawson, 2001).

Binary splitting divides the data into two and then sub-divides further until the desired number of zones has been created. As such, if a diagram is produced with four zones and an additional zone is added, that zone boundary will sub-divide an existing zone and the other boundaries will remain unchanged (Bennett, 1996). Optimal splitting will examine all the data and place the zone boundaries at once (Bennett, 1996). In this situation a diagram with four zones may be divided totally differently to a diagram with five zones. Both approaches (binary/optimal splitting) seek to place the boundary where it will create the greatest reduction in variance as determined by sum-of-squares or information content (Bennett, 1996).

'Agglomeration' approaches, such as CONISS (Grimm, 1987), produce a bottom-up grouping based on cluster analysis, whereby samples adjacent to one another in a core are grouped together until the desired number of zones is attained (Bennett, 1996). Results are often presented as a dendrogram (e.g. Behling et al., 2000). The choice of taxa used in the analysis is also somewhat subjective. Previous studies have used a cut-off of 5% (e.g. Gordon and Birks, 1972; Bennett, 1996), whilst others have used only a subset of the main taxa (e.g. Lawson, 2001).

The optimum number of pollen zones used to describe a sequence can be established statistically (*see* Bennett, 1996), but is often set subjectively by the analyst. The number of pollen zones required is predominantly a function of the number of samples. As a rule of thumb, one zone is needed for about every ten samples (Bennett, 1996), although in some sequences where there are substantial changes in composition a larger number of zones may be used relative to the sample number (e.g. at Quistococha; Roucoux et al., 2013). Subzones can be defined by eye wherever it might be useful to highlight a change within a statistically defined zone, such as where a poorly represented taxon might be environmentally significant (Bennett, 1996; e.g. Roucoux et al., 2013).

4.7.2.2 Pollen zonation method

Lawson (2001) examined all of the different approaches before choosing a particular zonation scheme; in general it is best to choose the zone boundary identified by the majority of methods. In this case, pollen records were developed for several different sequences and it was important to balance both the comparability of the zonation schemes with the need to obtain the scheme which best suited each individual core.

Pollen zonation schemes were produced for all of the cores using the different methods noted above and tabulated to assess which zones boundaries were the most consistent. Only taxa > 5% in one or more samples were included. In general, binary splitting and

optimal splitting by information content produced zonation schemes where one of the pollen zones contained only one sample. The rest of the schemes were remarkably consistent and therefore any of these might have been chosen, but optimal splitting by sum of squares was chosen in order to allow better comparison with the zonation of Roucoux et al. (2013).

4.7.3 Indicator species analysis

In ecology, indicator species are those which are particularly associated with a certain habitat, either in terms of abundance or occurrence (i.e. they are either abundant in, or only occur in, a particular habitat) (Dufrene and Legendre, 1997). In palynology, the same approach can be used to identify pollen taxa which are particularly associated with different sections of the core. These taxa are frequently the most useful when attempting to interpret the nature of the past environments recorded in the pollen data. The method used here follows that proposed by Dufrêne and Legendre (1997), which has generally replaced earlier approaches such as TWINSPAN (Hill, 1979). In a comparison of their method and that of TWINSPAN, Dufrene and Legendre (1997) found that TWINSPAN was less sensitive and that it can therefore fail to identify some useful indicator species or underestimate their indicativeness.

To determine indicator species, the data must first be classified into different groups. Dufrêne and Legendre (1997) provide their own methods of achieving this, but in this case, the groups used were the same as the pollen zones obtained by optimal splitting by sum-of-squares (see above). The abundance and occurrence of a species is then compared to itself through the whole dataset. For each species an 'indicator value' (IndVal; Dufrêne and Legendre, 1997) is produced according to the formulae (after Dufrêne and Legendre, 1997):

$$A_{sz} = \frac{Ngrains_{sz}}{Ngrains_{s}} \quad (4a)$$

Where $Ngrains_{sz}$ is the mean number of pollen grains for species *s* across samples in zone *z*, and $Ngrains_{s}$ is the total of the mean number of grains of species *s* across all of the zones.

$$B_{sz} = \frac{Nsamples_{sz}}{Nsamples_{z}} \quad (4b)$$

Where $Nsamples_{sz}$ is the number of samples in pollen zone z where species s is present and $Nsamples_{z}$ is the total number of samples in that zone.

$$Ind\_value_{sz} = A_{sz} \times B_{sz} \times 100 \quad (4c)$$

Equation (4c) shows the final formula for calculating the indicator value for species *s* in pollen zone *z* through the combination of formulas (4a) and (4b). Formula 4a provides a means of examining the 'specificity' of an individual species (i.e. how abundant a species is in one zone relative to the other zones in the dataset), and formula 4b provides a means of examining the 'fidelity' of a species (i.e. the degree to which a species is confined to one zone). In short this method identifies 'symmetrical' indicator species, which are found mostly in one zone and whose presence can be predicted in most of the samples in that zone (Dufrêne and Legendre, 1997). Species with an indicator value greater than 50 can generally be thought of as indicative of a particular pollen zone, although Dufrêne and Legendre (1997) listed all species with a value > 25.

4.7.4 Linear mixed models

Linear mixed models were used to test hypotheses relating to the hydrological characteristics of the peatland (see Chapter 5), with the measured hydraulic conductivity (*K*) as the response variable, and the depth, site, area and batch where the measurements were taken as the predictor variables (incorporated as fixed or random effects in the model). All analyses were conducted using R 2.15.0 (www.R-project.org). A standard linear model can incorporate a single random effect (Fox, 2002), but in this case the incorporation of further random effects was required and hence a linear mixed model was used.

A fixed effect can be defined as one which is experimentally determined, and random effects can be defined as 'factors which are sampled from a larger population' (Bolker et al., 2011). In this case therefore, in the study of peatland hydrological properties, random effects are the hydraulic conductivity measurements taken for different sites, areas, and batches. The only fixed effect is the depth at which the measurements were taken.

Once constructed, models can be compared using a standard ANOVA to establish which provide the best fit for the data. Where a more complex model (e.g. a model incorporating area, batch, and depth) is not significantly different from a simpler model incorporating fewer factors (e.g. depth and area), then this indicates that the additional factor (the batch of piezometers within an area, in this example) does not contribute significantly to the variation in the dataset.

Further criteria which can be used for model selection are the Akaike information criterion (AIC) and the Bayesian information criterion (BIC). Burnham and Anderson (2004) provide an overview of these criteria and their mathematical basis. Bayesian 'information criterion' is a slight misnomer as unlike the AIC it is not based on information theory (Burnham and Anderson, 2004). In both cases, the model with the lowest value is generally 'better' than models with higher values; this model should be the one which provides the least amount of lost information when compared to the real dataset (Burnham and Anderson, 2004).
AIC and BIC values have been shown but did not play a major role in model selection in this study. Given that the values did not differ substantially between the models being compared they provided a poor means of comparison and hence ANOVA was preferred.

4.8 The DigiBog peat model

4.8.1 Background

Numerical simulations examining peatland sensitivity to varying hydraulic conductivity values and boundary water table positions were run using the hydrological part of the DigiBog model (Baird et al., 2012; Morris et al., 2012). In particular, this served to establish whether the hydraulic conductivity alone could create differences in hydrological behaviour at the peatland sites studied.

The code for the hydrological sub-model of DigiBog (written in Fortran 95) was made available to the author by A. J. Baird and P.J. Morris, along with a full instruction manual (Baird et al., unpublished). DigiBog has advantages over other numerical peat models in that it is capable of producing 2D and 3D models, whereas previous models such as the Holocene Peat Model are strictly 1D (they simulate a column of peat at a single point; *see* Frolking et al., 2010) and are therefore incapable of looking at water table positions through space in a peatland (Baird et al., 2012). The DigiBog model has four main outputs; peatland height, water-table depth, degree of decomposition through the peat profile, and the dry bulk density. DigiBog has five separate submodels which are:

i. The hydraulic properties submodel.

ii. The hydrological submodel.

iii. The plant-succession submodel.

iv. The plant litter production submodel.

v. The decomposition submodel.

The structure of the DigiBog model is presented in Figure 4.3. In the full DigiBog model, the outputs of these submodels feed into one another to simulate ecohydrological feedbacks. For example, the hydraulic properties submodel feeds into the hydrological submodel, thereby affecting water-table behaviour. This feeds into the decomposition submodel which calculates cumulative decay, and this in turn feeds back into the hydraulic properties submodel (Baird et al., 2012).

Sufficient knowledge is not yet available to parameterise many of the submodels; for example, plant litter production rates remain uncertain for Amazonian peatland vegetation types. In this instance, the aim was purely to examine how properties measured in the field affected hydrological behaviour on short timescales (< 1 yr) and so the full model was not used, only the hydrological sub-model.

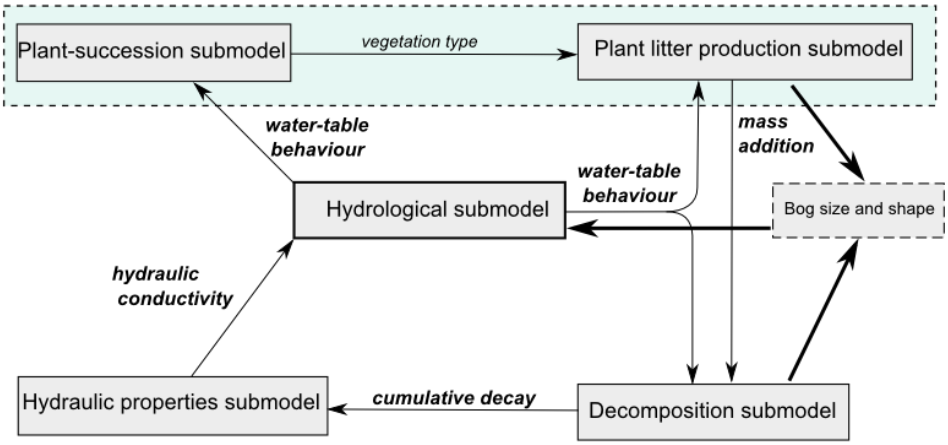

Figure 4.3: Full schematic representation of the DigiBog model showing the connections between the different sub-models (redrawn from Baird et al., 2012).

4.8.2 Summary of the hydrological submodel in DigiBog

The hydrological submodel of DigiBog simulates subsurface flow using the Boussinesq equation (Baird et al., 2012). This equation assumes that the peatland is broadly flat (< 5°), a valid assumption in this case as the models were parameterised as a peatland which had accumulated on a flat surface (see Section 4.7.3). DigiBog also uses the Dupuit-Forchheimer approximation, i.e. it assumes that all flow is horizontal. This is generally valid for shallow aquifers such as peatlands (Baird et al., 2012), and is certainly valid in the model scenario used here. Currently, the boundary water table position must be set as a constant in DigiBog (Figure 4.4).

The parameters used as inputs into the model can either be set as constants using an input file or can be altered through the course of the model run by linking the

hydrological submodel to the other submodels of DigiBog. In this case, simulations were undertaken to examine behaviour over a short time period (30 and 90 days). Peatland growth is unlikely to be significant over such short timescales, and the properties being examined are unlikely to change substantially as a result of, for example, peat decay. As such, input parameters were set as constants in this instance.

4.8.3 Specific details of the model used in this study

The median *K* values obtained as part of this study (see Chapter 5) were used to parameterise the models in order to examine whether the differences in *K* observed at the three sites might have a discernible effect on hydrological behaviour. This was achieved by using two or three separate peat layers for each column of peat, which were assigned different hydraulic properties. Two further models were also constructed in order to:

i) Assess the sensitivity of the models to differences in drainable porosity. Because no data are available for the drainable porosity of Amazonian peats, a value of 0.42 was used in several cases (see Chapter 5), as given by Boelter (1969) for fibric (≥ 66 wt. % fibre) peats in North America. However, this is at the upper end of values quoted for peats. The true drainable porosity of the peat at the sites studied may well be lower, which would lead to a more extensive drawdown zone. As such, two models were run with a lower (0.3) drainable porosity.

ii) Assess the potential impact of a 10 cm thick zone of high *K* in the upper part of the peat profile on water table draw down (K = 0.11 cm s^{-1}).

The model scenarios comprised simple, two-dimensional representations of a virtual peatland 500 m long positioned between two water bodies, with a maximum peat thickness of 1 m (each individual column was 250 cm square). The base of the peatland was represented as a flat impermeable bed, and the water table at the start of the model run was positioned at the peat surface. The models constructed were not intended as entirely realistic representations of actual peatlands; real peatlands in Amazonia have undulating substrates (Householder et al., 2012), peat accumulations thicker than 1 m (Lähteenoja et al., 2009b) and may be domed at their centre (Swindles et al., 2014). These models served mainly to show the effect of hydraulic conductivity on water loss, whilst controlling for other variables.

No net precipitation input was used in any of the model runs, but a water level was set for the two constraining water bodies. In each of the model runs, the water levels in both

water bodies were the same (both either 0 or 75 cm above the base of the peat). In effect, therefore, the models simulated the loss of water from the peatland purely by flow through the peat itself. From the initial condition of a surface water table, the model runs considered drainage over 30 days or 90 days. At the end of each model run, the total amount of water lost from the peatland via groundwater flow was calculated as a percentage of the water present at the beginning of the simulation.

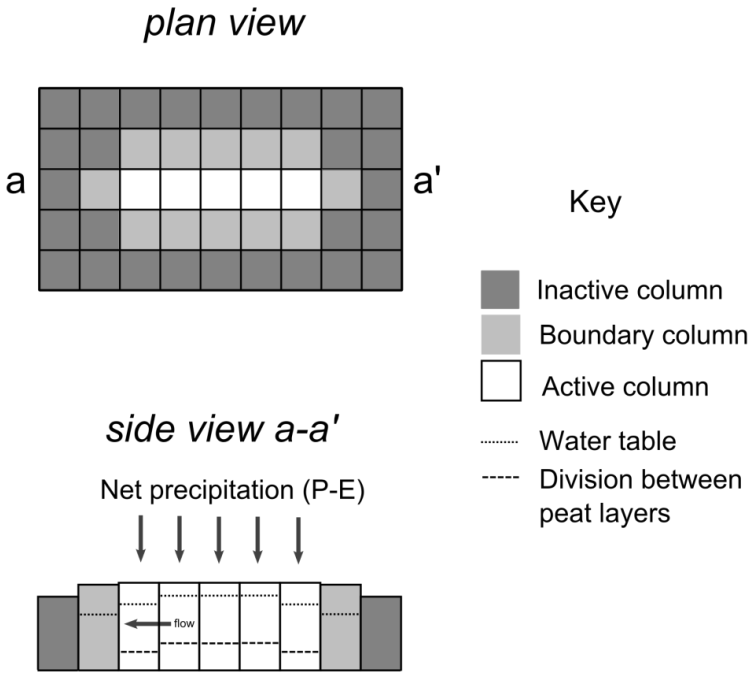

Figure 4.4: Simplified representation of the DigiBog 'strip' model used in this study. The model runs a hydrological simulation for a single strip of peat to simulate water flow along a virtual peatland transect from the centre towards the margins, where a boundary water level is set. Net precipitation can be included or set to zero. (diagram after Baird et al., 2012).

4.9 Other microfossil proxies

Other microfossils, such as diatoms, chironomids, and testate amoebae, are frequently used in palaeoecology to reconstruct past environmental conditions either qualitatively (e.g. Jones et al., 2013), or semi-quantitatively through the use of transfer functions (e.g. Turner et al., 2014). As such, the potential of these proxies to guide interpretation of changes seen in the pollen diagram was examined. Investigation of samples from the lake and peatland revealed that the abundance of diatoms is very low, possibly as a result of unsuitable preservation conditions (T. Jones, *pers. comm*.). As a result, no diatom analyses were undertaken.

Testate amoebae are known to be preserved in Amazonian peatlands, and initial investigations have revealed a new morpho-species *Arcella peruviana* (G. Swindles, *unpublished data*). Recent studies have revealed that it may be possible to use the testate

amoebae record to reconstruct peatland palaeohydrology in Amazonia (Swindles et al., 2014), although studies at further sites are required and there are potential taphonomic issues (e.g. testate amoebae inhabiting the canopy, where conditions are different to those at the peat surface, could form part of the final testate amoebae assemblage in the peat archive).

Investigation of testate amoebae species in the lake at Quistococha (undertaken in collaboration with colleagues at Carleton University, Canada) has revealed a low diversity, low abundance assemblage including species such as *Cucurbitella tricuspis* and *Centropyxis aculeata* (Figure 4.5; T. Patterson, *pers. comm*.). These species are often associated with eutrophic environments in the northern hemisphere, and are probably indicative of low oxygen conditions in the benthic zone. The low abundance and low diversity of testate amoebae found at Quistococha also seems to be typical of other tropical lakes, such as Lake Sentani in Indonesia (Dalby et al., 2000). The testate amoebae assemblages found at Quistococha are unlikely to be sensitive to changes in the wider environment (such as nutrient input), as they are already under stress as a result of the low oxygen levels (Dalby et al., 2000).

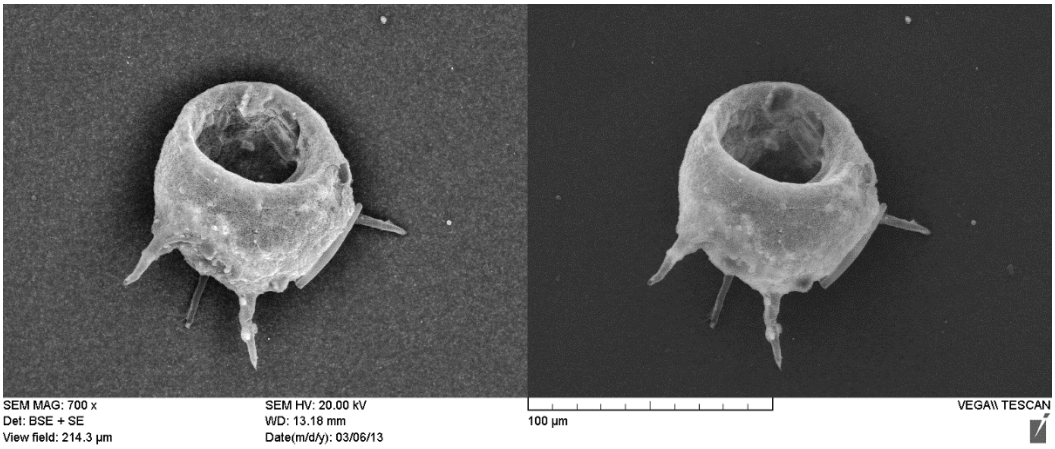

Figure 4.5: SEM image of *Centropyxis aculeata* sampled from the top 4 cm of the lake sediment at Quistococha (Patterson et al., unpublished data).

4.10 Summary

This chapter has provided detailed descriptions of the field and laboratory methods used in this thesis, including a review of previous multiple-core pollen studies. The next chapter is the first results chapter in the thesis, and describes and discusses research into the hydrological behaviour of three Amazonian peatlands.

5. The hydrology of three Amazonian peatlands

5.1 Introduction

While the focus of this study is on understanding the late Holocene vegetation development of the two peatlands at Quistococha and San Jorge, the lack of data describing the modern hydrological behaviour of these peatlands is a great hindrance when interpreting evidence of past behaviour obtained from proxy records.

As discussed in Chapter 2, the hydraulic conductivity (*K*) is part of an ecohydrological feedback loop which is fundamental to the functioning of any peatland (Morris et al., 2011). As such, an understanding of *K* is essential for understanding peat accumulation and soil carbon dynamics (e.g. Frolking et al., 2010; Morris et al., 2011; Baird et al., 2011). Despite its importance as a factor in the ecohydrological functioning and development of peatlands, there are few published data on the *K* of tropical peats (e.g. Takahashi and Yonetani, 1997; Nugroho, 1997; Pajunen, 1997; Hoekman, 2007; Sayok et al., 2007). Indeed, to the best knowledge of the present author, there are no *K* data for Amazonian peatlands. Therefore, the aims of this study were to determine *K* in three typical Amazonian peatlands; to compare these values with measurements from peatlands in other parts of the world; and to explore the implications in terms of the likely functioning of Amazonian peatlands, including their likely response to climatic change. The modern hydrological behaviour of the peatland at Quistococha was also studied through the installation of an automatic water-table logger.

This chapter reports the field measurements, and then uses hydrological modelling to explore their significance. The results and subsequent discussion in this chapter inform the palaeoecological interpretations later in the thesis. Large parts of this study have been published in Kelly et al. (2014).

5.2 Results

5.2.1 Normal and non-normal slug-test recoveries

Piezometers were installed in the permanent forest plots at San Jorge and Buena Vista (see Chapter 3 for site details), and at three points across Quistococha at varying distances from the lake, including the permanent forest plot (Figure 5.1). A total of 108, 28 and 30 piezometer measurements were undertaken at Quistococha, San Jorge and Buena Vista, respectively. Of these, 91, 27 and 23 respectively were used to calculate *K.* A 'normal' recovery was defined as one where the head returned to h_0 by the end of the test (Normal recovery type A: Figure 5.2). Non-normal recoveries fell into four categories (Figure 5.2). In the case of non-normal recovery type A, it was possible to re-define h_0 as the stable head level observed at the end of the *K*-test. In several cases

recovery was less than half that of the initial head difference (non-normal recovery B). One possibility is that, as the slug was removed at the start of the test, the pressure drop caused any gas bubbles around the piezometer intake to increase in size thereby blocking pores (*cf.* Beckwith and Baird, 2001). Non-normal recoveries of type B were thus excluded from the final analysis.

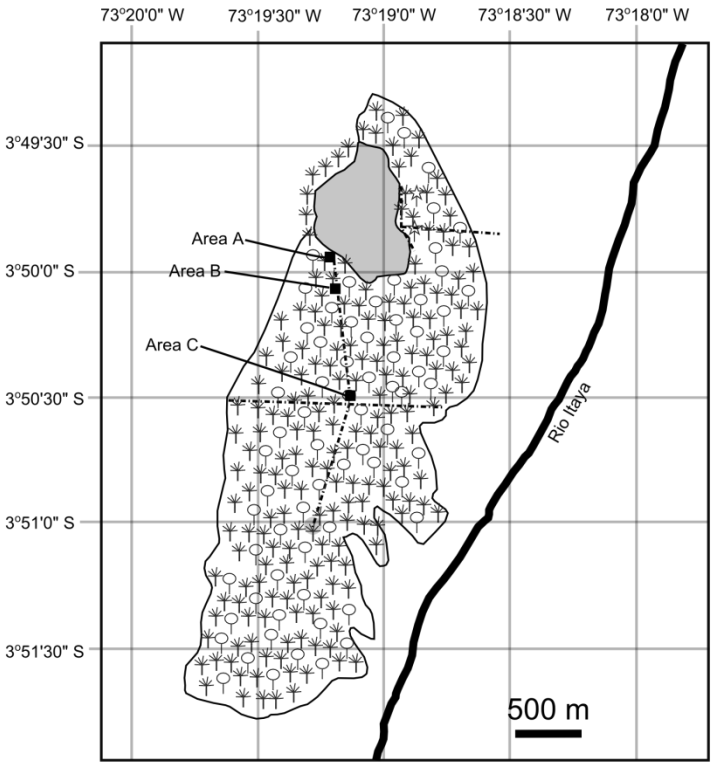

Figure 5.1: Sketch map of Quistococha showing the areas where piezometers were installed. The 0.5-ha forest plot is located in area B. Further details of the geomorphological context are given in Chapter 3.

Non-normal recoveries C and D (Figure 5.2) were most likely caused by atmospheric pressure change over the course of the test which makes it more difficult to identify t_{95}. Between 10:00 and 15:00 on most days there was a considerable drop in air pressure of 5–6 cm water equivalent (Figure 5.2). In such cases, the head recoveries can be corrected by subtracting the atmospheric pressure from the pressure recorded by the transducer in the piezometer. The corrected data can then be used to calculate K in the same way as for the other recovery types. An alternative approach is to use the inflection point to re-define h_0. In this study recoveries were corrected using the atmospheric pressure data.

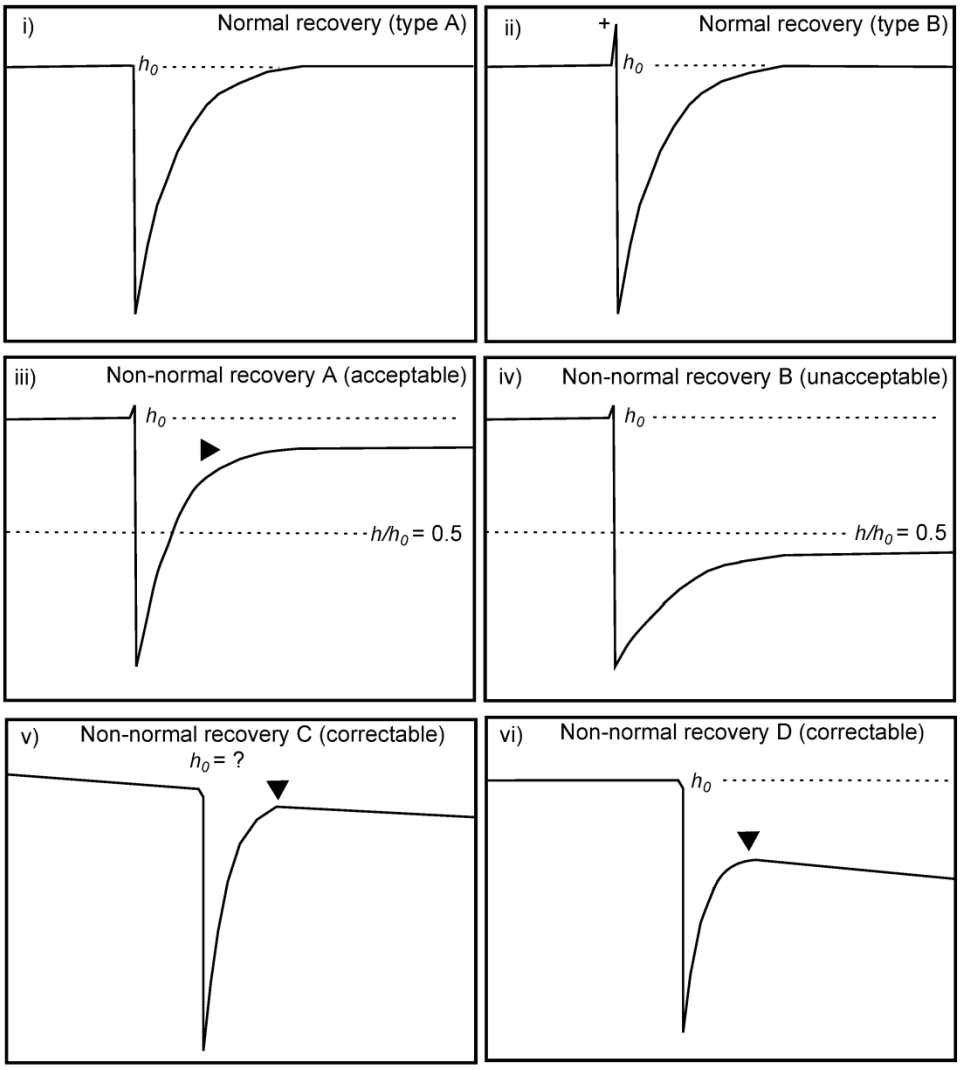

Figure 5.2: Figure showing the six main recovery types, as discussed in the text. (i) Normal recovery: the head fully recovers to its original position before slug removal (h0). (ii) Normal recovery: the head fully recovers to its original position before slug removal, but there is a slight increase in head at the point where the slug is removed (marked +). (iii) Non-normal recovery A (acceptable): in this case, the head does not fully recover to h0.However, it does reach a stable level that can be used to redefine h0 (marked►) and so produce an estimate of t95. (iv) Non-normal recovery B (unacceptable): in this case, the head does not fully recover to h0. Although it does reach a stable level, this level is below h/h0 = 0.5. (v) Non-normal recovery C (correctable): the level of the water is apparently unstable either before or after slug removal; h0 can be redefined using the inflection point (marked ▼) or the recovery can be corrected using atmospheric data. (vi) Non-normal recovery D (correctable): although the head is stable prior to slug removal, allowing h0 to be defined, the head does not fully recover during the K test; h0 can be redefined using the inflection point (marked ▼) or the recovery can be corrected using atmospheric data.

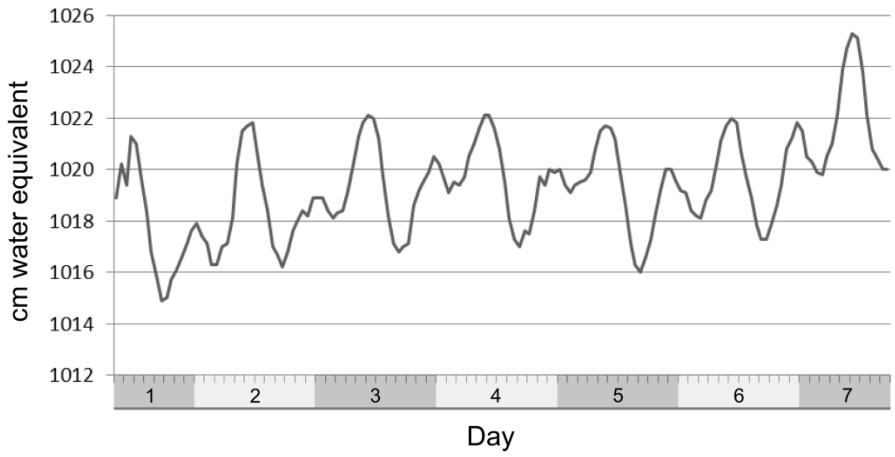

Figure 5.3: Atmospheric pressure over the course of 7 days in the vicinity of Quistococha, beginning at 08:00 on 29 July 2011 and ending at 17:00 on 4 August 2011 (tick marks every 2 h). On all days, there was a substantial drop in pressure between 10:00 and 15:00. Measurements were taken once every hour

5.2.2 Hydraulic conductivity (*K*) estimates

The *K* estimates for Quistococha, San Jorge and Buena Vista are presented in Table 5.1, Table 5.2, Figure 5.6, and Figure 5.7; Figure 5.6 also shows some comparable data from other published sites. Figures 5.4 and 5.5 show some illustrative head recoveries. In this section, the hypotheses described in Chapter 2 are tested.

5.2.2.1 Testing Hypotheses 4 and 5 (K varies within the uppermost 90 cm of the peat profile and K varies spatially between different parts of the peatland)

At the three study areas at Quistococha, there is a significant difference in *K* at 50 and 90 cm depth (Figures 5.4-5.7). In each area, the median value for *K* was higher at 50 cm than at 90 cm and when the data for all areas are combined there is an order of magnitude difference in median *K* for the two depths (Table 5.1). *K* also appears to vary with area (Table 5,1; Figure 5.7). In the area of the swamp nearest to the lake (area A), the median *K* is 0.0037 cm s^{-1} at 50 cm, and 0.0018 cm s^{-1} at 90 cm. These values are substantially lower than those obtained for area B, where the median *K* is 0.016 cm s^{-1} at 50 cm and 0.0063 cm s^{-1} at 90 cm. *K* values for area C are most similar to those for area A (Table 5.1). Indeed, area B differs most from the other two areas, and the *K* values at 50 cm for area B have a smaller variance than areas A and C (Figure 5.7).

The model incorporating area, batch, and depth (Model A: Table 5.3) was not significantly different ($p > 0.05$) from a simpler model incorporating only depth and area (Model B; Table 5.3), suggesting that small-scale spatial variation (within individual areas) did not contribute systematically to the variation. The Akaike Information

Criterion (AIC) and the Bayesian Information Criterion (BIC) were almost identical between models, which confirmed that there was little difference between the two models. However, a model incorporating only area (Model C: Table 5.3) was significantly different ($p < 0.001$) from the model incorporating both depth and area (Model B: Table 5.3). This demonstrates that depth makes a significant difference to the variation in *K* at Quistococha. In Model B, area was found to explain 20.4% of the variance. Therefore, the preferred linear model supports both Hypothesis 1 and 2 (see Chapter 2).

Examination of the data from San Jorge and Buena Vista showed that depth did not exert a significant influence on *K* at these sites. A model incorporating only site (Model G: Table 5.3) was not significantly different from a model incorporating both site and depth (Model E: Table 5.3). Hypothesis 1 was therefore not supported by the data from these two sites.

5.2.2.2 Testing Hypothesis 6 (K varies between different wooded tropical peatlands)

Figure 5.6 suggests that there are substantial differences between the *K* values obtained from the different sites. As discussed in Section 3.5, the variation in *K* with depth at San Jorge is not significant, whereas *K* does vary significantly with depth at Quistococha; this in itself constitutes a difference between the sites. Model C (Table 5.3) also showed that site explained 18.7 % of the variance in the data. This result supports Hypothesis 3, and shows that there are variations in *K* between different wooded tropical peatlands.

5.2.3 Simulations

The results of the simulations are shown in Figure 5.8, with details of the outputs summarised in Table 5.4. The extent of the draw down zone, as defined by a lowering of the water table by > 10 cm, varied slightly between the different model runs. The draw down zone was most extensive for models Quistococha type 2 & 3, and least extensive for the San Jorge type model. The most extensive draw down zone extended 72.5 m into the peatland, the least extensive 25 m. Similarly, the greatest proportion of water was lost from the Quistococha type 3 model, and the lowest proportion from the San Jorge type model. In all model runs, the water table at the centre of the peatland was not greatly lowered (< 0.5 cm).

5.2.4 Water table logger

During the dry season, water levels varied from 27 cm below the peat surface to 9 cm above the surface (Figure 5.9). In the absence of rainfall, peatland water levels fell by c. 1.6 cm day^{-1}. During the wet season in 2012, the site was flooded to a height of c. 1 m above the peat surface. This extent of flooding is rare, with no similar events during the

previous decade (V. Reategui, pers. comm. 2012). Excluding this event, wet season variation in the peat water table was from 5 cm below the surface to 18 cm above the surface. The peak flood height (c. 1 m) occurred on the 19th April 2012, which coincided with the peak for the Amazon River recorded upstream at Tamshiyaku gauging station (cf. Espinoza et al., 2013).

Table 5.1: Summary statistics for the hydraulic conductivity (*K*) estimates for areas A-C at Quistococha as determined using equation (1) and standardised to 20 °C using equation (2). The summary statistics for *K* data from all areas have also been included. *K* values are given in cm s^{-1}.

Quistococha	Area A		Area B		Area C	
Depth (cm)	50	90	50	90	50	90
Median	0.00369	0.00167	0.01606	0.00627	0.00387	0.00164
Lower Quartile	0.00099	0.00099	0.00948	0.00241	0.00255	0.00063
Upper Quartile	0.01036	0.00434	0.02252	0.01072	0.01865	0.00400
Max	0.02761	0.00982	0.05695	0.03735	0.05586	0.00751
Min	0.00038	0.00035	0.00236	0.00043	0.00081	0.00027
n	11	10	21	23	13	13

Table 5.2: Summary statistics for *K* estimates from the three sites studied; Quistococha, San Jorge, and Buena Vista. In the case of Quistococha, this summarises all *K* data from areas A-C. *K* values are given in cm s^{-1}.

	Quistococha		San Jorge		Buena Vista	
Depth (cm)	50	90	50	90	50	90
Median	0.01247	0.00278	0.00464	0.00414	0.00664	0.00624
Lower Quartile	0.00315	0.00106	0.00134	0.00119	0.00576	0.00450
Upper Quartile	0.01899	0.00737	0.00579	0.00748	0.01753	0.01569
Max	0.05695	0.03735	0.05657	0.01409	0.11248	0.05638
Min	0.00038	0.00027	0.00032	0.00039	0.00380	0.00125
n	45	46	14	13	10	13

Table 5.3: Summary of the linear mixed effects models used to test the initial hypotheses (*section 1*). AIC = Akaike Information Criterion, BIC = Bayesian Information Criterion. The models which best fit the data have been marked *.

Model	Data used	Fixed	Random effects	Log Likelihood	AIC	BIC
A	QT	Depth	Area (batch)	-143.7	297.3	309.9
B*	QT	Depth	Area	-145.1	298.1	308.2
C	QT		Area	-153.4	312.7	320.3
D*	QT, SJO,	Depth	Site	-233.6	475.3	487.0
E	QT, SJO,		Site	-238.5	482.9	491.8
F	SJO, BVA	Depth	Site	-79.75	167.5	175.1
G*	SJO, BVA		Site	-79.62	165.2	171.0

Table 5.4: Outline of the main parameters used in the five hydrological models. Summarised outputs of the models are given to supplement the diagrams in Figure 8. The percentage water loss is given, followed in parentheses by the extent of the draw down zone in metres (water table drop > 10 cm). *K* = hydraulic conductivity of the layers (*K* is given in cm s^{-1} with values listed from the base upwards), DP = Drainable porosity.

				Water loss, % (extent of drawdown zone in m) 30 days		90 days	
Model	**No. of layers**	***K* (base → top)**	**DP**	**0 cm**	**75 cm**	**0 cm**	**75 cm**
San Jorge type	2	0.0041, 0.0046	0.42	3.3 (35)	0.7 (25)	6.5 (55)	1.7 (35)
Buena Vista type	2	0.0062, 0.0066	0.42	5.1 (42.5)	1.1 (30)	8.9 (67.5)	2.6 (45)
Quistococha type 1	2	0.0027, 0.0125	0.42	4.7 (42.5)	1.2 (30)	7.7 (62.5)	2.8 (45)
Quistococha type 2	2	0.0027, 0.0125	0.3	5.5 (47.5)	1.6 (32.5)	9.0 (72.5)	3.4 (52.5)
Quistococha type 3	3	0.0027, 0.0125, 0.11	0.3	5.8 (45)	2.1 (35)	9.3 (70)	4.0 (52.5)

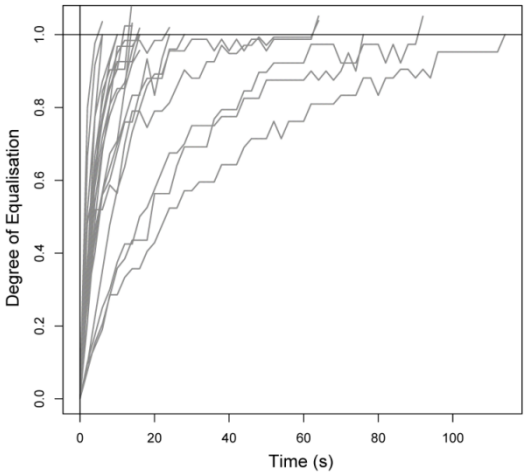

Figure 5.4: Normalized head recovery data for piezometers installed at 50 cm in area B at Quistococha (n = 21). Note that x-axis scale is different from that in Figure 5.5.

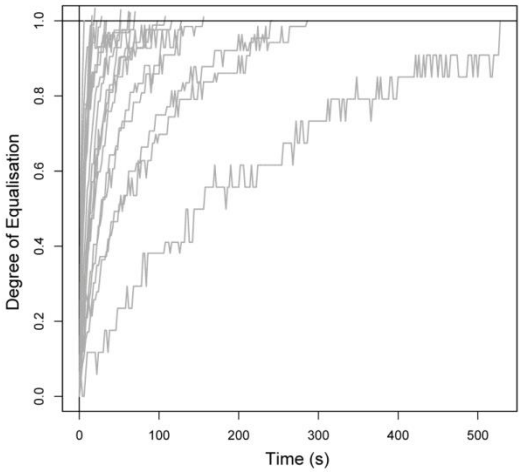

Figure 5.5: Normalized head recovery data for piezometers installed at 90 cm in area B at Quistococha (n = 23). Note that in some cases, the degree of equalization exceeds one because of the typical errors associated with the use of pressure transducers.

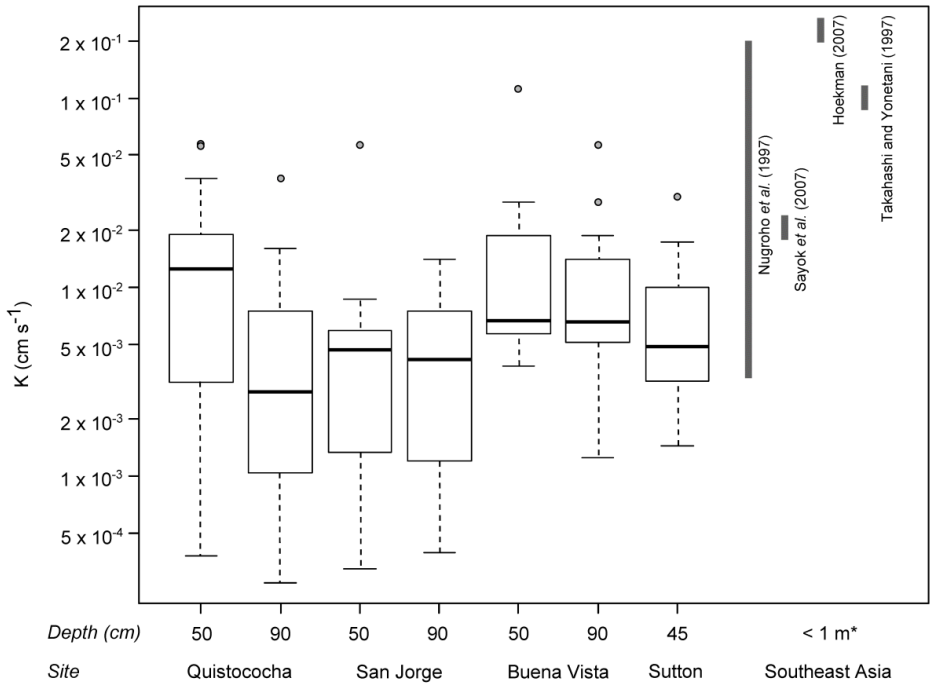

Figure 5.6: Summary of hydraulic conductivity (K) data for Quistococha (n = 91), San Jorge (n = 27), Buena Vista (n = 23) and for a fen root mat at Sutton Fen in Norfolk, UK (n = 14; Baird et al., 2004). The diagram shows the median (bold bar) and the interquartile range (white box). The full range of the data (minimum to maximum value) is shown by a dotted line, except where there are outliers that lie more than 1.5 times the interquartile range from the upper or lower quartile. In this case, outliers are shown as grey circles, and the dotted lines indicate the range of the rest of the data. Note that K estimates have been standardized to 20 °C to aid comparison. K values from four studies in Southeast Asian peatlands have been included for comparison, but these values were generated using different field methods. * Nugroho et al. (1997) did not specify the measurement depth.

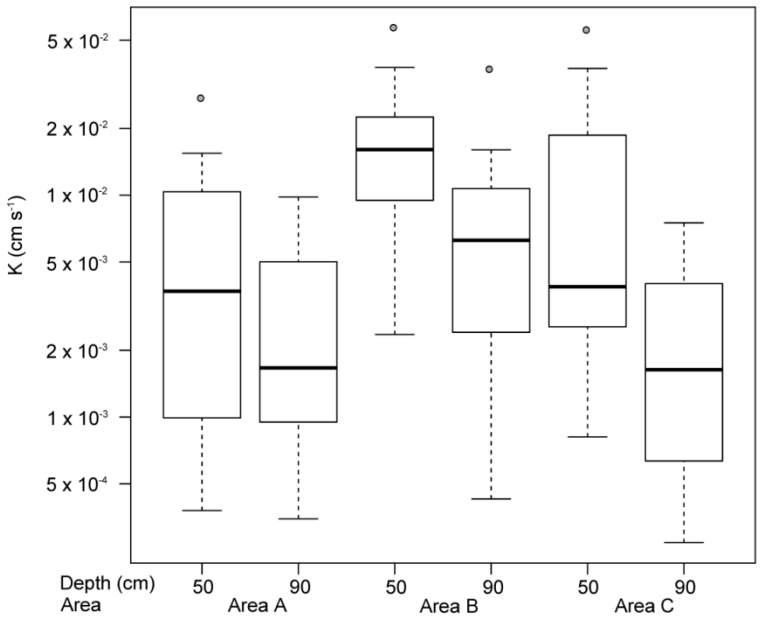

Figure 5.7: Box plots summarizing K data for the three different areas of Quistococha situated at varying distances from the lake edge. Format follows that described in Figure 5.6.

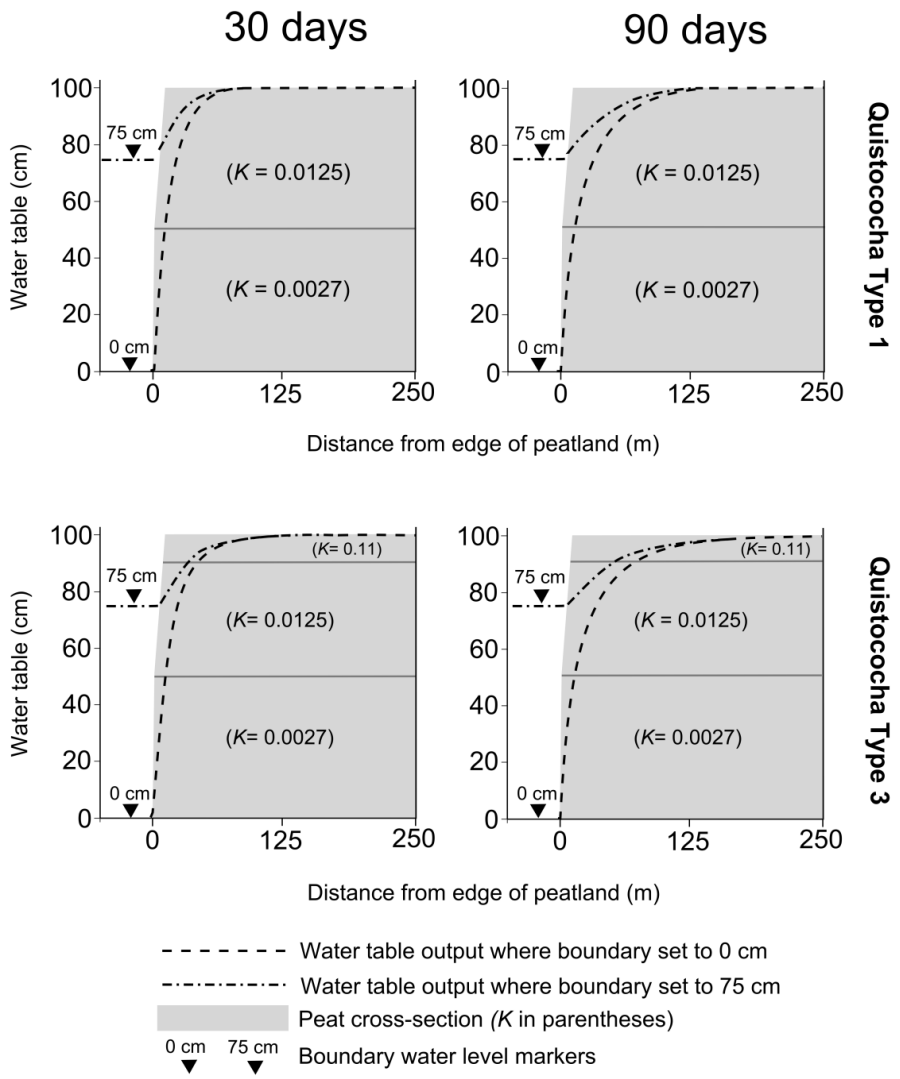

Figure 5.8: Two-dimensional representation of hydrological simulations. The diagrams represent a vertical plane running from the modelled peatland edge to the centre. Two different models are shown: Quistococha type 1 and Quistococha type 3 (for details, see Table V). The models were run for 30 days (left) and 90 days (right) without rainfall or evapotranspiration to examine water losses due to subsurface flow alone. For each model setup and run time, the water table was simulated assuming two different boundary water table positions (0 and 75 cm), and these outputs are shown using dashed lines. The peat is denoted by the shaded area, which also represents the initial water table position. K for the different layers has also been indicated. The other models produced outputs which were not significantly different from that of Quistococha type 1, and have not been shown.

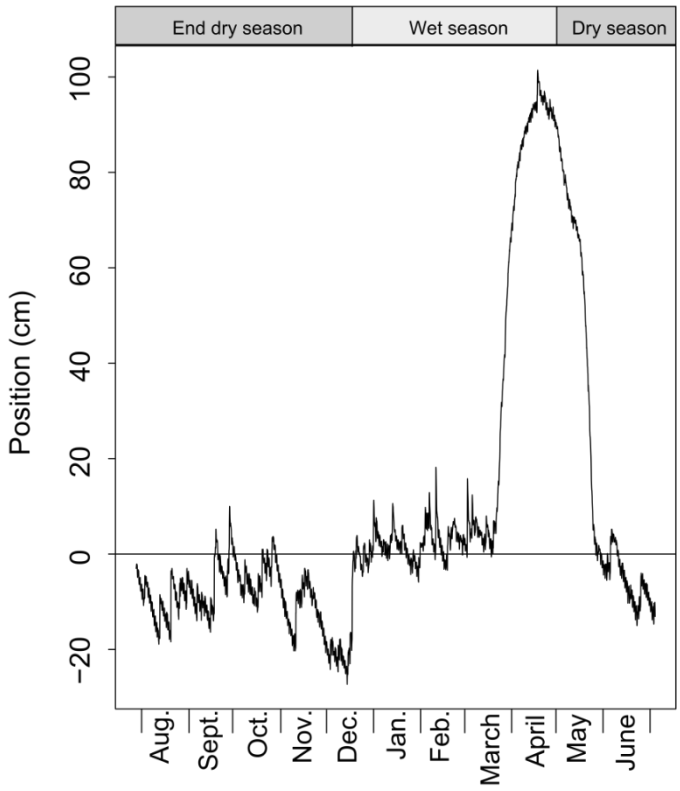

Figure 5.9: Annual record of water table variation from Quistococha peatland. Values were recorded automatically every two hours from July 2011 to July 2012. Values are relative to the surface (0 cm). Quistococha does not flood on an annual basis, but during the extreme flood of 2012, this part of the site was flooded to a depth of 1 m. During the dry season, the water table did not fall more than 25 cm below the peat surface. Sudden increases in water table are interpreted as rainfall events.

5.3 Discussion

5.3.1 Tropical peatland *K* values

Relative to other peatlands, the *K* values reported here are typically an order of magnitude higher than those estimated for northern hemisphere ombrotrophic bogs (see Lewis et al., 2012 for a review), although recent work at an ombrotrophic peatland in Wales has shown that high *K* values can be obtained in fibrous *Sphagnum* peat at depths of 40–60 cm (Baird et al., unpublished data). The tropical *K* values reported closely resemble those estimated for the root mat at the temperate Sutton Fen site (Norfolk, UK) reported by Baird et al. (2004), who used a similar *K*-measurement method to that used here. The root mat at Sutton Fen was composed predominantly of roots and rhizomes of the sedge *Cladium mariscus* (L.) Pohl and the grass *Phragmites australis* Cav. (Streud), along with some well-decomposed plant matter (an observation confirmed by the author on a visit to the site in 2012). The median value for *K* at 50 cm for Quistococha is slightly higher than at 45 cm for Sutton Fen, but the median values from Buena Vista and San Jorge are very similar (Figure 5.6). Pajunen (1997), who utilised the seepage tube methodology of Kirkham (1945), produced estimates of *K* for upland Rwandan swamps dominated by reeds (including one species found at Sutton) such as *Cyperus papyrus* L. and *Cladium mariscus* (L.) Pohl (Pajunen, 1997). *K* values ranged from 0.0006 to 0.0135 cm s^{-1} at 80 cm, and from 0.0018 to 0.0255 cm s^{-1} at 40 cm. These are also of a similar magnitude to those produced by the present study, and

Baird et al. (2004). Despite the obvious floristic dissimilarities, the peat at the three Peruvian sites and in the Sutton Fen root mat is structurally similar, being composed of poorly-decomposed roots, wood and other coarsely fibrous material, which accounts for their hydraulic similarities. In the case of the Rwandan swamps, they also contain a high proportion of root fibres, and data for the dry bulk density are similar; 0.061 g cm^{-1} (70-80 cm) at Quistococha and around 0.086 g cm^{-1} for the Rwandan peatlands (Lähteenoja et al., 2009a; Pajunen, 1997).

Measurements of *K* have also been made at a number of tropical peatlands in Southeast Asia. Some caution is needed in comparing our data with these results, primarily because many of the published studies do not provide a detailed description of the measurement method. This is potentially problematic because small differences in method, such as using an open sided auger hole instead of a piezometer tube, can be significant when measuring *K* (Surridge et al., 2005).

Takahashi and Yonetani (1997) measured *K* from 1.0–1.7 m depth in a wooded peat swamp in Kalimantan (Indonesia) using piezometers, but published only a rounded value ($K \geq 0.01$ cm s^{-1}) for depths < 1 m. Hoekman (2007), studying a peatland in Kalimantan, found a much higher value of *K* of 0.23 cm s^{-1}, but gave no details of how this estimate was obtained. For a peatland in Sumatra, Nugroho et al. (1997) provided a more extensive data set, and gave a list of *K* estimates which range from 0.0035 to 0.19 cm s^{-1} ($n = 28$). However, they did not indicate how their *K* estimates were derived, and provide no depths to accompany their data. Sayok et al. (2007) presented *K* values for peatlands in Sarawak (Malaysia) derived from 59 auger hole slug tests (*cf.* Bouwer, 1989) with a mean value of 0.039 cm s^{-1} for swamp forest peatland (*n = 15*). In all four cases, these estimates are larger than the values obtained at Quistococha, San Jorge, and Buena Vista, but it is unclear whether this represents a real difference or simply an artefact of differing measurement methods.

5.3.2 Simulated groundwater flow

This study has found evidence that *K* can vary both within and between sites, and that *K* measurements from different areas and sites contribute 20 % and 18 % of the variance in the data respectively. However, the majority of the *K* values obtained fall between 0.001 and 0.02 cm s^{-1}, and models show that this variation may only have a minor impact on hydrological function. The difference in *K* observed between the different peatlands does not seem to have a substantial effect on the amount of water lost or the extent of the draw down zone (Table 5.4), although the models here do not take into account peatland geometry. Nevertheless, further models show that as yet unexplored hydrological properties could have a significant effect on hydrological behaviour in

tropical peatlands. In particular, lower drainable porosity values can create more extensive draw down zones. A higher *K* surface layer does not always result in a more extensive draw down zone (Table 5.4), in part because it allows water to travel from more central parts of the peatland to raise water levels at the margins.

The main purpose of the model runs (Figure 5.8) was to examine subsurface flow and whether this might create differences in the hydrological behaviour of these peatlands; this was most simply achieved by running the models without a precipitation input. However, the DigiBog simulations also provide insights into how the high *K* of forested tropical peatland systems might affect peatland water balance during a drought. Although there is some debate, climate models show substantial reductions in rainfall (1 mm day -1) in north western Amazonia by 2080 (e.g. Betts et al., 2004), and others have suggested the possibility of reduced dry season rainfall in particular (Malhi et al. 2009).

The model setup more closely reflects the behaviour of a domed peatland such as San Jorge than that of a peatland like Quistococha, which is bounded on two sides by an impermeable clay ridge and terrace. The simulations show that flow out of the modelled peatland causes water-table lowering for 30–50 metres into the peatland within 30 days (Figure 5.8). Where there is a prolonged dry season, this could result in substantial lowering of the water-table if there is no water entering the system from other sources, such as groundwater springs (e.g. Householder et al., 2012). However, prolonged droughts are unlikely to occur under current climatic conditions. The simulations also suggest that, with *K* set to the values obtained from the three sites in this study, groundwater flow alone would be unable to shed the large quantity of water currently entering Amazonian peatlands from rainfall (> 3000 mm yr^{-1}; Marengo, 1998). Even without rainfall, over a 90-day period the modelled water table in the centre of the peatland remains at the surface. Therefore a large proportion of the water entering Amazonian peatlands must exit the system via overland flow or evapotranspiration. Hoekman (2007) came to a similar conclusion in Indonesia using a combination of remote sensing and terrain relief modelling. Although connected drainage channels were not apparent at the sites visited, water has been observed flowing out from the margins of other peatland sites in Amazonia (e.g. Aucayacu peatland; G. Swindles, pers. comm.; see Lähteenoja et al. 2012 for details). Rapid drops in water level have also been observed in long term data from Quistococha when water levels have risen above the peat surface (Figure 5.9), and this may be due to surface flow. Pool features can also become connected during heavy rainfall events.

During large rainfall events the water table rises to the peat surface and a substantial proportion of the water exits the peatland (or is re-distributed to lower areas) via overland flow. Following a large rainfall event, the water-table will continue to fall as a result of groundwater flow and evaporation. Evaporation rates are also likely to be high, and in peatlands bounded by impermeable barriers (e.g. Quistococha) the majority of water may leave the system via this pathway. Published estimates for evaporation rates are in the region of 1500 mm yr^{-1} for lowland tropical forests with > 3000 mm yr^{-1} of rainfall (*cf*. Bruijnzeel, 1990; Hirano et al., 2014). Schellekens et al. (2000), in a study of a tropical forest in Puerto Rico, also found that evapotranspiration values were very high (2180-2420 mm yr^{-1}), which they attribute to a high rate of interception. This suggests that regular rainfall may be more important for maintaining tropical peatland wetness than individual large rainfall events.

5.4 Summary and conclusions

The results of this study have shown that there is within-site variation in *K,* and that *K* also varies between sites with different vegetation assemblages, although whether there are systematic spatial patterns (e.g. lower *K* at the peatland margin; similar *K* values across similar vegetation types) must be the subject of future work. *K* can also vary with depth in the top metre of the peat profile, but evidence of this was found at only one of the three sites studied. However, hydrological modelling demonstrates that the level of variation in *K* encountered at the different sites may not necessarily result in large differences in hydrological behaviour. The modelling process also indicated the need for further research into peat properties, such as specific yield.

The *K* values obtained from the three peatlands studied are at least an order of magnitude higher than *K* values reported for many northern peatlands (*cf.* Lewis et al., 2012), and are similar to the *K* of a temperate sedge fen (*cf*. Baird et al., 2004). They are an order of magnitude lower than the few existing *K* estimates for Indonesian peatlands, but it is difficult to tell whether this represents a real or a methodological difference. Although the *K* values appear high relative to those obtained at some other sites, hydrological modelling suggests that under current climatic conditions, the peatlands are unable to shed the water entering the system via rainfall. The rapid drop in water tables observed between rainfall events (c. 1.6 cm d^{-1}) at Quistococha is not possible through subsurface flow alone. This suggests that most of the water in these tropical peatlands is lost through overland flow and evapotranspiration. Groundwater flow likely plays a relatively minor role in controlling the water table of a site such as Quistococha. Sustained rainfall may be more important for maintaining tropical peatland wetness than individual large rainfall events due to rapid losses from evapotranspiration.

6. Palynomorph taxonomy and interpretation in Amazonian peatlands

6.1 Introduction

Although many Amazonian peatland plant taxa are represented at the genus level in existing pollen keys (see Chapter 2), identification of some key taxa was not possible at the outset of this study, and there was clear scope to improve the taxonomic resolution of the palaeoecological record in these contexts. This chapter presents details of taxonomic and taphonomic studies undertaken to allow better interpretation of Neotropical peatland pollen and spore types. It reveals that some key distinctions can be made which will shed new light on the vegetation development of peatlands in the Pastaza-Marañón basin. The chapter begins with results from a study of pollen types for peatland trees common to the site which has been a focus for research in the present study (Quistococha), including the palm genera *Mauritia* and *Mauritiella* and the peatland *tree Tabebuia insignis* var. *monophylla.* A detailed study of spores from ferns known to inhabit *aguajal* habitats follows. A description of spinulose palm phytoliths and some hypotheses relating to their interpretation are then given. A full study of pollen taphonomy in peatlands was beyond the scope of the present study, but surface samples from Quistococha and San Jorge were examined in order to gain an insight into pollen representation at these sites. Finally, descriptions and tentative identifications are provided for unknown pollen types found in the peat cores studied.

6.2 Peatland trees

6.2.1 Sample materials

Reference materials for *Tabebuia insignis* were obtained in the field from Quistococha and a second site near to Nauta (Veinte de Enero; 4°41'45"S, 73°49'23"W) in July 2012 by the author and T.R. Baker. Reference samples for all *Mauritia* and *Mauritiella* species were obtained from the herbarium collection at the Instituto de Investigaciones de la Amazonia Peruana (IIAP) research station at Jenaro Herrera (Loreto, Peru) and the Royal Botanical Gardens at Kew (see Table 6.1). Not all proved suitable for analysis; in several cases the specimens obtained either provided pollen which was too damaged (or possibly immature), or which contained insufficient pollen to produce a representative sample for grain size measurements. The material for *Mauritiella aculeata* was deemed too poorly preserved for use, but specimens were obtained for all four of the other species. In relation to the study area of this thesis, the lack of material for *Mauritiella*

aculeata is not critical, as this species is endemic to the Upper Negro River (Kubitzki, 1989).

Peat surface samples were obtained from within the permanent forest plots at San Jorge and Quistococha (see Chapter 3), and a surface sample from a 0.5 ha forest plot at Ollanta (4°26'53"S, 74°50'53"W) was provided by F.C.H. Draper. Samples were taken from the centre of each 20 x 20 m sub-plot. For herbarium samples studied under normal light, 100 grains were measured for each specimen at 1000x magnification (precision of measurements 0.5 μm).

Table 6.1: Summary of the *Mauritia* and *Mauritiella* herbarium reference materials examined (Imm. = immature). Only those samples with good pollen preservation were studied further. The majority of samples were obtained from Kew Gardens ('K' herbarium codes).

Species	Bot. authority	Herbarium no.	Origin	Notes
Mauritiella aculeata	(Kunth) Burret	K000526900	Brazil	Pollen degraded/ imm.
Mauritiella armata	(Mart.) Burret	K000526907	Brazil	Little to no pollen
Mauritiella armata	(Mart.) Burret	K000526904	Brazil	Pollen degraded/ imm.
Mauritiella armata	(Mart.) Burret	K000526910	Brazil	Little to no pollen
Mauritiella armata	(Mart.) Burret	n.a. (Jenaro Herrera)	Peru	Good preservation
Mauritiella macroclada	Burret.	K000526929	Colombia	Good preservation
Mauritia carana	Wallace	K000526864	Brazil	Good preservation
Mauritia flexuosa	L.f.	n.a. (Jenaro Herrera)	Peru	Good preservation
Mauritia flexuosa	L.f.	K000526882	Guyana	Good preservation
Mauritia flexuosa	L.f.	K000526872	Guyana	Good preservation
Mauritia flexuosa	L.f.	K000526878	Brazil	Good preservation
Mauritia flexuosa	L.f.	K000526879	Brazil	Good preservation
Mauritia flexuosa	L.f.	K000526868	Guyana	Good preservation

6.2.2 Differentiating between *Mauritia* and *Mauritiella*

6.2.2.1 Background

The two palm genera *Mauritia* and *Mauritiella* are found across tropical South America and are common to the floodplain of the Amazon river (Figure 6.1). *Mauritia* and *Mauritiella*, or their close relatives have probably been a feature of the Amazon for many millions of years (Rull, 2001), and their pollen is also found in many Quaternary records (e.g. Behling et al., 1999; Bush et al., 2000; Weng et al., 2002; Roucoux et al., 2013). They are important species in the swamps of the Peruvian Amazon (Pitman et al., 2014); they are known to co-occur but they also occur separately (Chapter 3), and *Mauritia* is the more widespread of the two genera (Endress et al., 2013). While a detailed knowledge of their modern ecology is not currently available, their differing distribution in the Holocene floodplains of the Pastaza-Marañón basin implies that they have subtly

different environmental preferences. In particular, the available peatland floristic data indicate that *Mauritiella armata* may be absent from pole forests occupying domed sites (see Chapter 3).

The pollen of these two genera is morphologically so similar (see Appendix A for descriptions) that in the majority of pollen records, they are lumped into a single category, such as *'Mauritia*-type' (e.g. Behling and Hooghiemstra, 2000; Roucoux et al., 2013). Previous studies have used grain morphometry to distinguish between closely related taxa, such as *Isoetes echinospora* and *I. lacustris* (Birks, 1973), or *Betula nana* and *B. pubescens* (Mäkelä, 1996), and the present study aims to test whether this can be achieved for *Mauritia* and *Mauritiella*. Behling et al. (1999) split these two genera on the basis of echinae width and number (H. Behling, pers. comm.), but whilst this might be locally valid the robustness of this approach has not been thoroughly tested. Previous pollen keys have indicated that a distinction can be made between *Mauritia flexuosa* and *Mauritiella aculeata* on the basis of grain size (cf. Colinvaux et al., 1999), but have used glycerine as a mounting medium; it has been demonstrated by morphometric studies that this causeands the pollen grains to swell leading to variation in measurements (Mäkelä, 1996). Ferguson (1986) studied the pollen of *M. flexuosa* using scanning electron microscopy (SEM) and compared this to the pollen of *Mauritiella pacifica* Dugand (syn. *Mauritiella macroclada*), but the pollen of *M. pacifica* has a very different morphology to that of *M. armata*.

This study sought to make a distinction between these two genera. There are three extant species of *Mauritiella* (*M. armata*, *M. aculeata*, *M. macroclada* [syn. *M. pacifica*]) and two of *Mauritia* (*M. flexuosa* [syn. *M. vinifera*] and *M. carana*) in Amazonia according to Dransfield et al. (2008), and efforts were made to sample all of these species so that the findings made are applicable across South America (and more applicable through time). Many other species of these palms have been named in the literature, but all are now generally considered synonyms of these five species (www.theplantlist.org; Dransfield et al., 2008).

The main focus is on grain size parameters which will allow distinction using normal light microscopy. However, the potential for SEM to make distinctions in sub-fossil samples is also explored. Flenley et al. (1991) used SEM to refine identifications of the palm formerly dominant on Easter Island, which was thought to be *Pritchardia* but which SEM revealed to be an extinct species related to *Jubaea chilensis.* SEM has otherwise rarely been applied in Neotropical palynology. Recent research has shown that 'environmental' SEM could allow the study of wet material (cf. Donald, 2003), and thereby allow a more routine analysis of palaeoecological samples. In the Neotropics

pollen taxonomy is challenging and therefore the present study sought to examine whether environmental SEM study could aid in making distinctions using micron and sub-micron scale pollen features.

The implications of this study go beyond the need to make distinctions in the Holocene palaeoecological record. According to Dransfield et al. (2008), there is no fossil record for *Mauritiella* due to the current impossibility of separating its pollen from that of *Mauritia*. Furthermore, de Lima et al. (2014) used pollen data to examine the late Quaternary demographic history of *Mauritia*, but did not make clear the fact that *Mauritiella* pollen is generally not separated from *Mauritia* in palaeoecological records and therefore in places past populations may have been of one or other of these palm genera.

6.2.2.2 Other similar pollen types

The closest relative of *Mauritia* and *Mauritiella*, also in the subtribe Mauritiinae, is *Lepidocaryum* (Baker et al., 2000). *Lepidocaryum* is a small understorey palm (Gentry, 1993), whose modern distribution does not extend into the Pastaza-Marañón basin (Figure 6.1; Dransfield et al., 2008). However, the possibility that its range may have been more extensive in the past cannot be ruled out, as it is known to inhabit nearby regions such as Amacayacu national park in Colombia (Rudas Llleras & Prieto Cruz, 2005). Normal light images of *Lepidocaryum tenue* are given in the Neotropical Pollen Database (NPD; Bush and Weng, 2006), and SEM images are shown in Ferguson (1986). Its pollen is similar to that of *Mauritia* and *Mauritiella* in that it is echinate, and of a similar size or a little smaller (30-35 μm, NPD; 28 – 41 μm, M. Harley, unpublished; 33 – 40 μm, Ferguson, 1986). However, it is clearly monosulcate rather than monoporate and so can easily be distinguished from *Mauritia* and *Mauritiella* in the recent palaeoecological record

The pollen of *Bactris* can also appear similar to that of *Mauritia* and *Mauritiella.* A large genus, *Bactris* contains around 240 species (Gentry, 1993), and the pollen shape and sculpture is highly variable (cf. Roubik and Moreno, 1991; NPD; M. Harley, unpublished). Species such as *Bactris riparia* have a similar floodplain habitat to *Mauritia* and *Mauritiella*, as well as echinate pollen. However, like *Lepidocaryum*, the pollen of *Bactris* is monosulcate and therefore easy to separate from *Mauritia* type pollen.

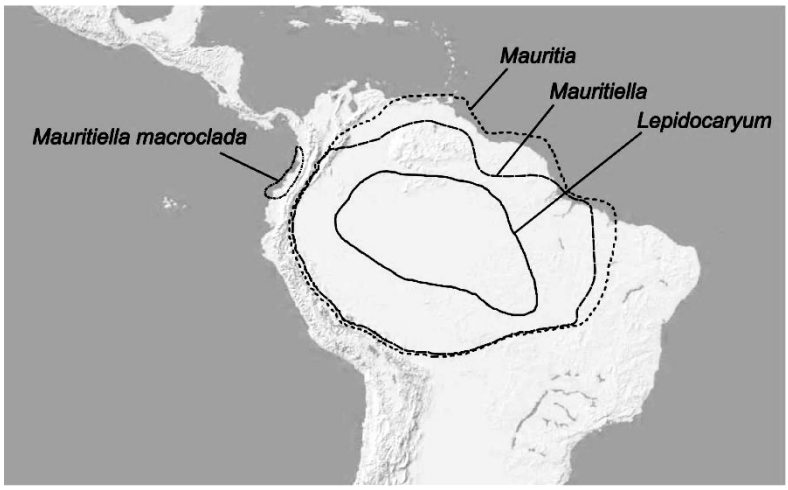

.

Figure 6.1: Map of South America showing the distribution of the three genera in the subtribe Mauritiinae (*Mauritia*, *Mauritiella*, *Lepidocaryum*). Of these only *Mauritiella macroclada* is found to the west of the Andes, and also note that *Mauritia* is found outside of mainland South America on the island of Trinidad (Redrawn from Dransfield et al., 2008).

6.2.2.3 Approach to distinguishing *Mauritia* and *Mauritiella*

Taxonomic distinctions were based primarily on collections made from material obtained from herbaria. However, *Mauritia*-t. grain size data for soil surface samples were also gathered from sites where *Mauritia* and *Mauritiella* were present. In this case, the detailed forest plot inventories undertaken at San Jorge and Quistococha revealed that *Mauritiella armata* was almost entirely absent at San Jorge (6 individuals). Conversely, the inventory at Ollanta revealed that *Mauritia flexuosa* was entirely absent in plot 4 and that only *Mauritiella armata* was present (F. Draper, pers. comm.). In combination with the small pollen transport distance for *Mauritia flexuosa* (Rull, 1998; discussed further in 6.4.3), this means that pollen preserved in soil surface samples from San Jorge and Ollanta is probably of *Mauritia* and *Mauritiella* only (respectively), whereas at Quistococha the population should be mixed. Comparison of grain size data from the three sites can therefore be used to test whether the pollen of *Mauritiella armata* and *Mauritia flexuosa* can be easily distinguished in the palaeoecological record.

6.2.2.4 *Mauritia* and *Mauritiella* grain lengths

A summary of grain measurements is given in Table 6.2. Analysis of variance conducted on the whole dataset strongly suggested that the specimens were not all drawn from the same population ($p < 0.001$), and therefore post-hoc t-tests were undertaken to compare the grain sizes for the different specimens (Table 6.3). Both *Mauritia flexuosa* and *Mauritia carana* were similar in size, and were not significantly different (t-test: $p = 0.826$). The pollen size data from San Jorge were indistinguishable from the *Mauritia*

flexuosa (p = 0.268) herbarium data, as would be predicted. The t-tests showed that the size distributions from San Jorge and Quistococha were distinguishable from one another, although there was considerable overlap in their values.

All other samples were shown to be statistically distinguishable from one another (p < 0.001) and were separable in the plot of the mean and standard deviation. Therefore the data indicate that a distinction can be made between all *Mauritia* and *Mauritiella* types on the basis of grain size. The Ollanta grain size data were significantly smaller than all the Mauritia types, but were also significantly different from the *Mauritiella armata* herbarium data. This may be the result of long-distance dispersal of *Mauritia flexuosa* pollen, and the present author argues that the herbarium collections are a more reliable basis for making distinctions.

Table 6.2: Summary of results from morphometric study of herbarium materials for the four *Mauritia* and *Mauritiella* species (s.d.: standard deviation). Exine thicknesses were derived from a smaller number of measurements (n > 30). As the precision of the measurements was 0.5 µm, full data were not collected as the error would preclude the production of a normally distributed dataset. All measurements in µm.

		Grain length				Echinae length				Exine thickness
Species	n	Mean	s.d	max.	min.	Mean	s.d	max.	min.	min-max
Mauritiella armata	100	34.9	2.5	45	28	6.07	0.9	8.5	4	1-3
Mauritiella macroclada	100	31.1	2.3	38	25	3.4	0.5	5.5	3	1.5-2.5
Mauritia carana	101	44.4	2.7	55	37	4.05	0.8	6	2.5	1
Mauritia flexuosa	601	44.4	3.2	59	38	6.1	1.9	10.5	2	1-2

Table 6.3: Results of Welch's unpaired t-test for comparison of the means of the grain length data obtained (analysis undertaken in R 2.15.2). Non-significant results have been marked in bold.

	Mauritiella macroclada	*Mauritiella armata*	*Mauritia flexuosa*	*Mauritia carana*	Ollanta (*Mauritiella*)	Quistococha (mixed)
M. macroclada						
M. armata	< 0.001					
M.flexuosa	< 0.001	< 0.001				
M. carana	< 0.001	< 0.001	**0.826**			
Ollanta	< 0.001	< 0.001	< 0.001	< 0.001	< 0.001	
Quistococha	< 0.001	< 0.001	< 0.001	< 0.001	< 0.001	
San Jorge	< 0.001	< 0.001	**0.268**	**0.291**	< 0.001	< 0.001

Mauritiella macroclada was clearly smaller than both *Mauritia* species, and most *Mauritiella armata* grains were less than 40 µm in length whereas the opposite was the case for *Mauritia flexuosa* and *Mauritia carana.* The Ollanta sample contained a greater proportion of grains above 40 µm in length than the *Mauritiella armata* herbarium material, but the average remained below 40 µm.

As would be expected (Andersen, 1960), samples of *Mauritia flexuosa* measured by previous studies using glycerine as a mounting medium all gave larger grain size measurements than those in this study. Ferguson (1986) reported grain length ranging from 55-60 μm with echinae 2-3 μm long; Colinvaux et al. (1999) reported grain sizes ranging from 60-68 μm but included sculptural elements (i.e. echinae) in their measurements. Subtracting the echinae lengths given (c. 3μm), this places the grain size of *Mauritia* at between 54-62 μm in Colinvaux et al. (1999); the two glycerine-based studies are therefore consistent with one another.

6.2.2.5 *Mauritia* and *Mauritiella* echinae lengths

Specimens were shown to have been drawn from different populations (ANOVA: $p < 0.001$), and post-hoc t-tests revealed that most collections were significantly different from one another (see Table 6.4). Echinae lengths for the *Mauritia flexuosa* and *Mauritiella armata* reference materials were inseparable from one another ($p = 0.828$). The data for Quistococha were shown to be inseparable from both the herbarium data for *Mauritiella armata* (p=0.144) and *Mauritia flexuosa* (p=0.178), as would be predicted as the forest at Quistococha contains both species.

Table 6.4: Results of Welch's unpaired t-test for comparison of the means of the echinae length data obtained (analysis undertaken in R 2.15.2). Non-significant results have been marked in bold.

	Mauritiella macroclada	*Mauritiella armata*	*Mauritia flexuosa*	*Mauritia carana*	Ollanta (*Mauritiella*)	Quistococha (mixed)
M. macroclada						
M. armata	< 0.001					
M.flexuosa	< 0.001	**0.828**				
M. carana	< 0.001	< 0.001	< 0.001			
Ollanta	< 0.001	< 0.001	< 0.001	< 0.001	< 0.001	
Quistococha	< 0.001	**0.144**	**0.178**	< 0.001	< 0.001	
San Jorge	< 0.001	< 0.001	< 0.001	< 0.001	< 0.001	< 0.001

A similar pattern can be seen between the three sites as is seen in the grain length data, with Ollanta possessing the smallest echinae, Quistococha being intermediate, and San Jorge being the largest of the three. It is possible therefore that echinae length could provide some support for inferences based on grain length, but the results are less clear cut, and therefore using echinae length alone may provide ambiguous or misleading taxonomic information. The variation in echinae length seen in *M. flexuosa* encompasses that seen in all of the other samples (see Figure 6.7). The recommendation is therefore that grain length data provide the best means of taxonomic distinction between *Mauritia* and *Mauritiella* pollen types.

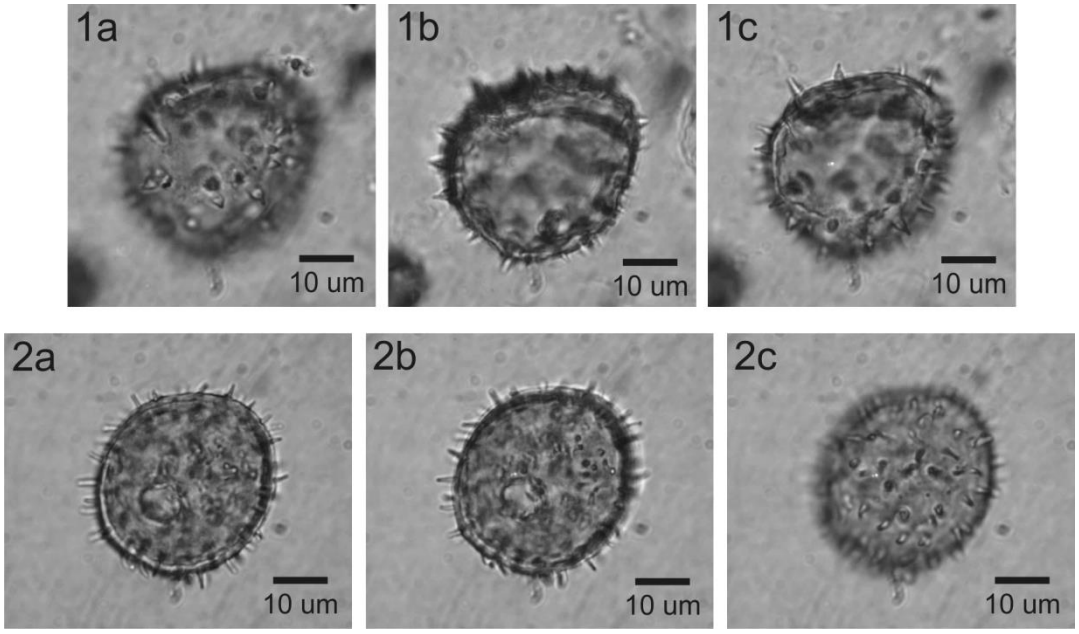

Figure 6.2: *Mauritiella* pollen types obtained from reference specimens seen in normal light (polar view). 1: *Mauritiella armata*. 2: *Mauritiella macroclada*.

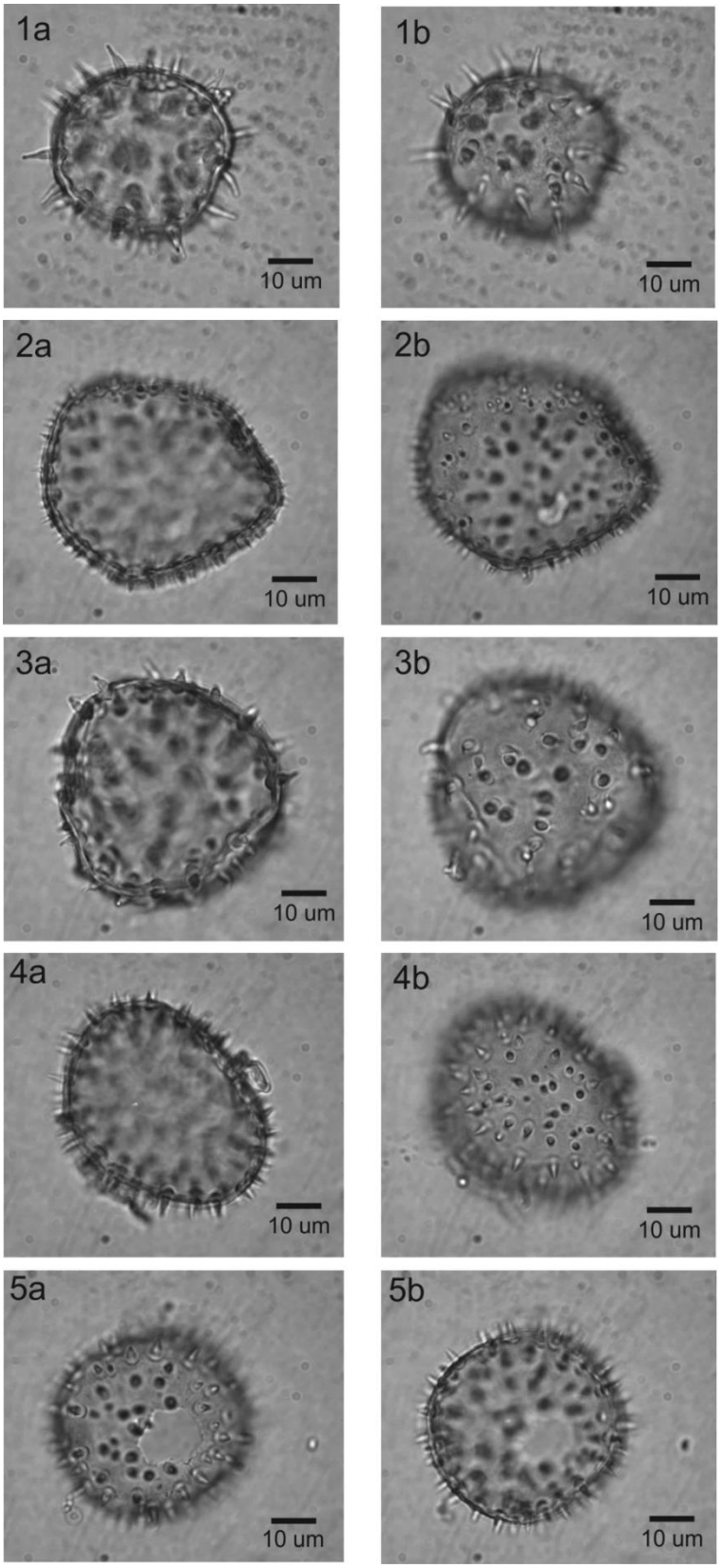

Figure 6.3: *Mauritia* type-pollen obtained from reference collections seen in normal light. 1-3: *Mauritia flexuosa*. 4-5*: Mauritia carana.*

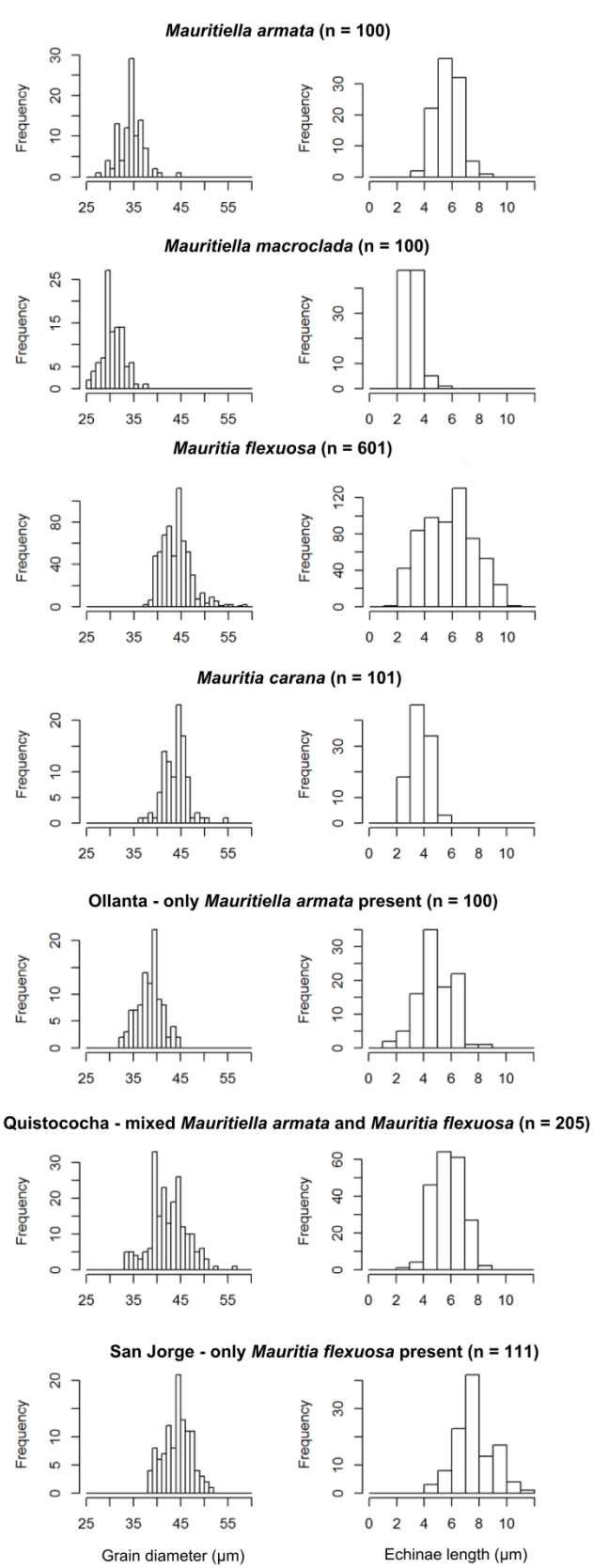

Figure 6.4: Histograms showing collected pollen size data (grain diameter and echinae length) for *Mauritiella armata* (n = 100), *Mauritiella macroclada* (n = 100), all six *Mauritia flexuosa* collections (n = 601), *Mauritia carana* (n = 101), and the three sets of surface samples from Ollanta (n = 100) ,Quistococha (n= 205), San Jorge (n = 111).

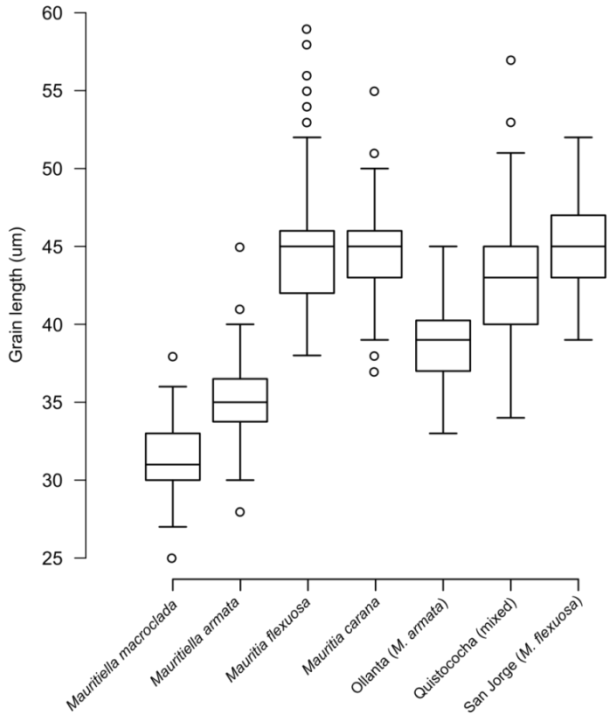

Figure 6.5: Summary boxplot of grain lengths for *Mauritia*-type pollen obtained from herbarium specimens and soil surface samples.

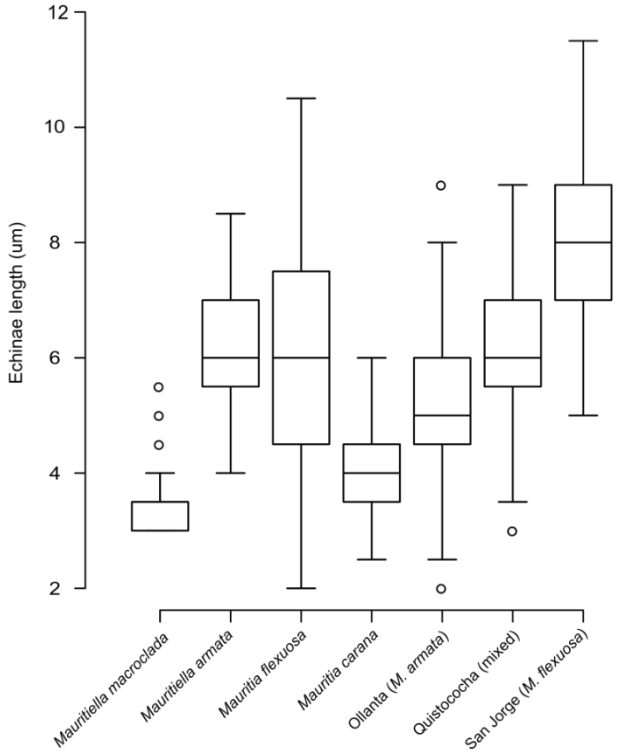

Figure 6.6: Summary boxplot of echinae lengths for *Mauritia*-type pollen from herbarium specimens and soil surface samples. Format follows Figure 6.6

6.2.2.6 *Mauritia* and *Mauritiella* SEM imagery

SEM images (Figures 6.7 & 6.8) show further morphological differences between the two genera. Although the echinae of *Mauritiella armata* are shorter than those of *Mauritia flexuosa*, they are morphologically very similar. The echinae of *Mauritia flexuosa* differ in being more obviously capitate than both *Mauritiella armata* and *Mauritiella macroclada* (see Ferguson, 1986 for *M. macroclada* SEM imagery; Figure 6.2.). Colinvaux et al. (1999: p. 246) reported "small tectate depressions" across the surface of the echinae in *Mauritia flexuosa*, but these were not observed by SEM or light microscopy in this study. I therefore conclude that these were likely an artefact of the preparation process. *Mauritiella macroclada* also differs from *Mauritia flexuosa* and *Mauritiella armata* in that it has echinae which do not taper and are of uniform thickness along their length. There is also a difference in the fine (sub-micron scale) surface sculpture: the micro-gemmae of *M. flexuosa* are more elliptical in plan view than those of *M. armata*.

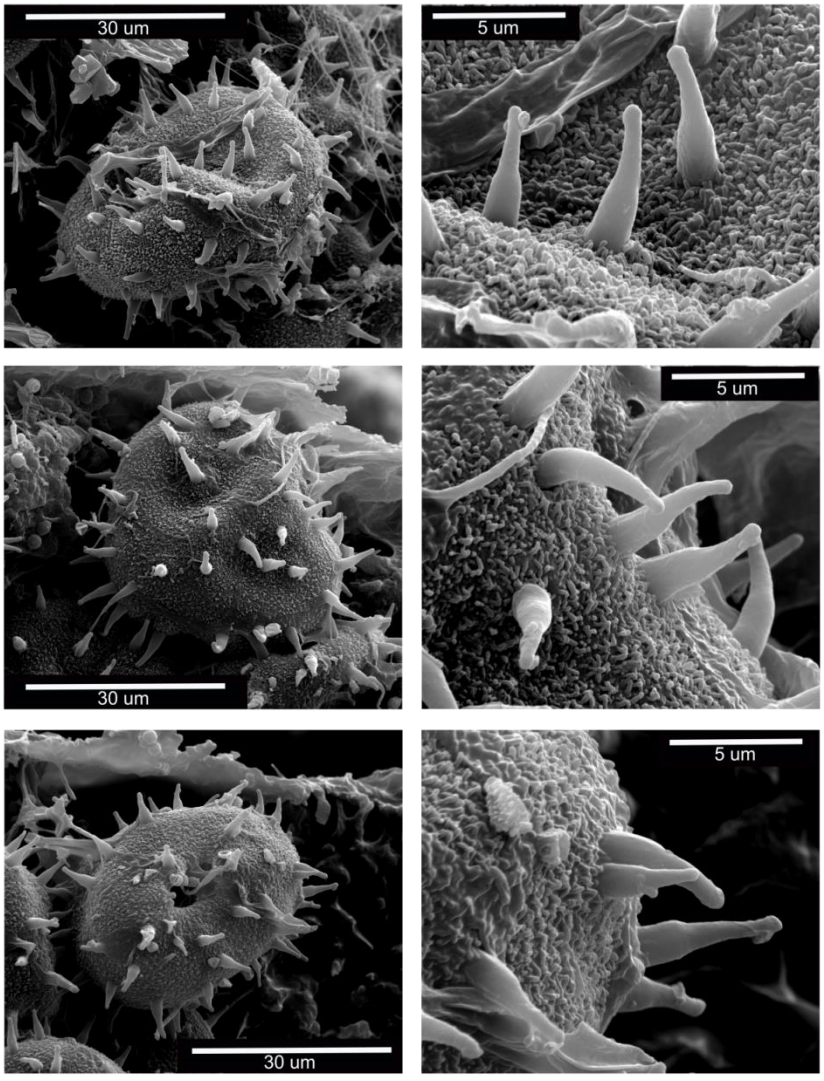

Figure 6.7: Images of *Mauritia flexuosa* taken using SEM. Left hand images show entire grains (5000x); right hand images show close-ups of the fine surface sculpture and echinae (20,000x).

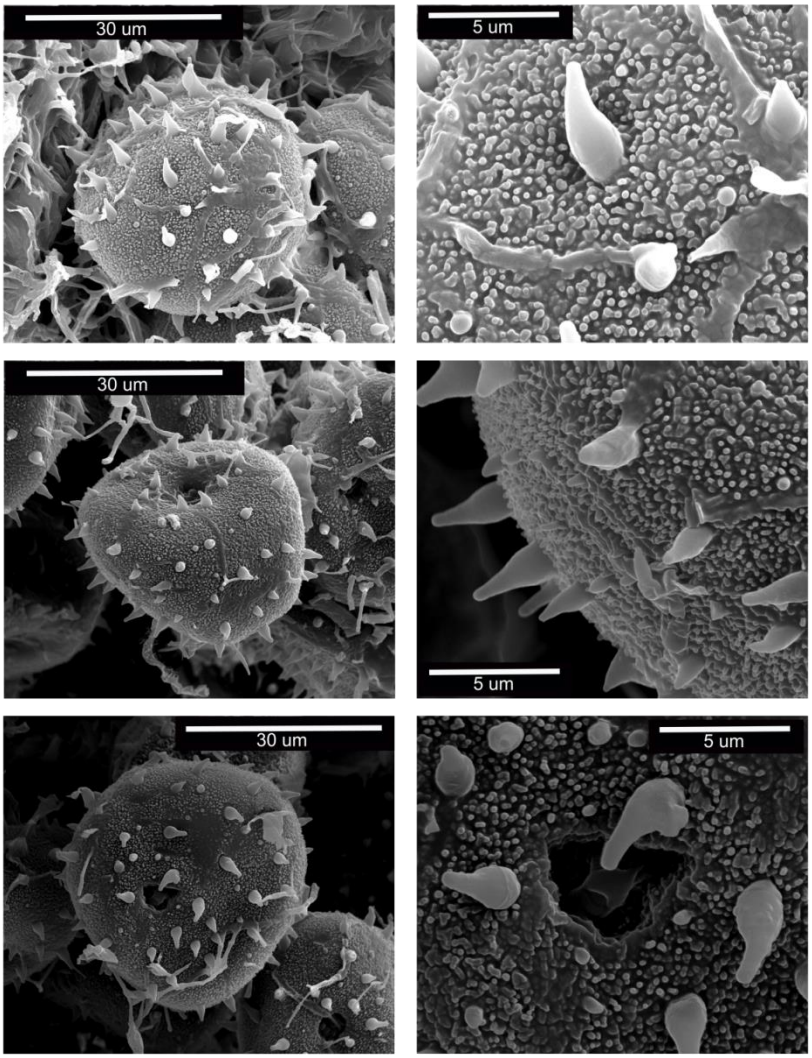

Figure 6.8: Images of *Mauritiella armata* taken using SEM. Left hand images show entire grains (5000x); right hand images show close-ups of the fine surface sculpture and echinae (20,000x).

6.2.3 Pollen description for *Tabebuia insignis* (var. *monophylla*) Sandwith

6.2.3.1 Background

Tabebuia insignis is the most abundant tree in the forest plot at Quistococha, represented by 131 individuals (d.b.h. > 10 cm; data from E.N. Honorio Coronado, see Chapter 3). There are currently few published details on the botany of this tree; Polak (1992) describes the same species in the swamps of Guyana. Initial identification of this species in the field (by T.R. Baker & E.N. Honorio Coronado) was difficult and firm identification was only possible in 2012 following a mass flowering event (typical of this genus; see Barros, 2001); this also afforded a rare opportunity to collect specimens for palynological study. The reason that identification was so difficult was due to the unusual leaf arrangement of *Tabebuia insignis* var. *monophylla* in comparison to other trees in its family (Bignoniaceae; Polak, 1992).

The pollen of several members of the Bignoniaceae is described in Roubik and Moreno (1991). Other work specifically on *Tabebuia* has been undertaken by Gentry and Tomb (1979), who described the pollen of *T. donnell-smithii* Rose, *T. rigida* Urb, *T. rosea* (Bertol.) DC, and *T. stenocalyx* Sprague. Bove (1993) described the pollen of the Bignoniaceae found in the Atlantic forests of Brazil, including five *Tabebuia* species. However, no images or descriptions could be found in the literature for *T. insignis* var. *monophylla*, and given the physical differences in the structure of the tree relative to other Bignoniaceae it was deemed important to describe the pollen in detail.

6.2.3.2 *T. insignis* description

Pollen taken from the flowers of *Tabebuia insignis var. monophylla* was studied for both Quistococha and Veinte de Enero (two individual trees). Photomicrographs of pollen of collected from the flowers of two individuals are shown in Figure 6.10, and SEM images are shown in Figure 6.9. A full description of the pollen is given in Appendix A. *Tabebuia insignis* has tricolporate, finely reticulate pollen with a distinct margo along the colpus, and wide colpi. It also shows a range of morphological variation (Figure 6.10).

The pollen of *T. insignis* closely resembles that of *T. guayacan*, described by Roubik and Moreno (1991). It has a relatively long polar axis and narrow equator, meaning that it is clearly prolate, which separates it from *T. rigida* (Gentry and Tomb, 1979)*, T. chrysotricha* and several other *Tabebuia* species (Bove, 1993; Roubik & Moreno, 1991).

SEM images show subtle differences in the pollen between these two collections. Whilst the grain size and shape are comparable, the surface sculpture is noticeably different in these two samples. The *T. insignis* pollen from Quistococha shows a larger, more irregular reticulum. This likely reflects variation between individuals (or possibly pollen maturity), but could also indicate some underlying genetic variation in *Tabebuia insignis*, an inference which would require further confirmation. It also illustrates the importance of sampling pollen from different individuals when forming reference collections, and when attempting to make taxonomic distinctions using micron-scale features.

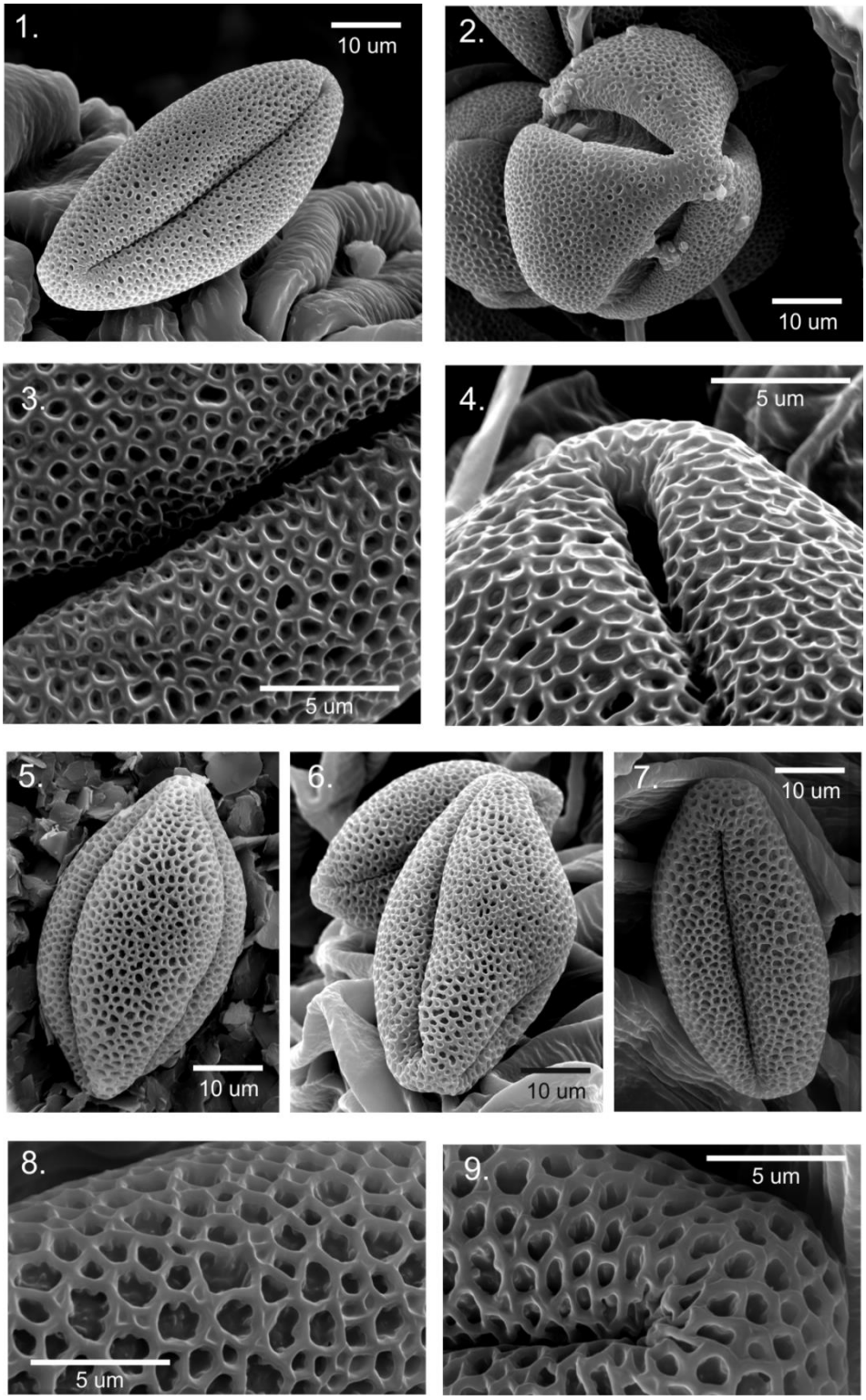

Figure 6.9: SEM micrographs of pollen of *Tabebuia insignis* var. *monophylla* for samples taken from the peatland forests at Veinte de Enero (1-4) and Quistococha (5-9). Grains in equatorial view (1) and polar view (2). Detail of reticulum for the Veinte de Enero sample along the colpus (3) and towards the polar area (4). Examples of differing grain shapes for the Quistococha sample (5-7). Detail of the reticulum for the Quistococha sample showing columellae (8), and towards the polar area (9).

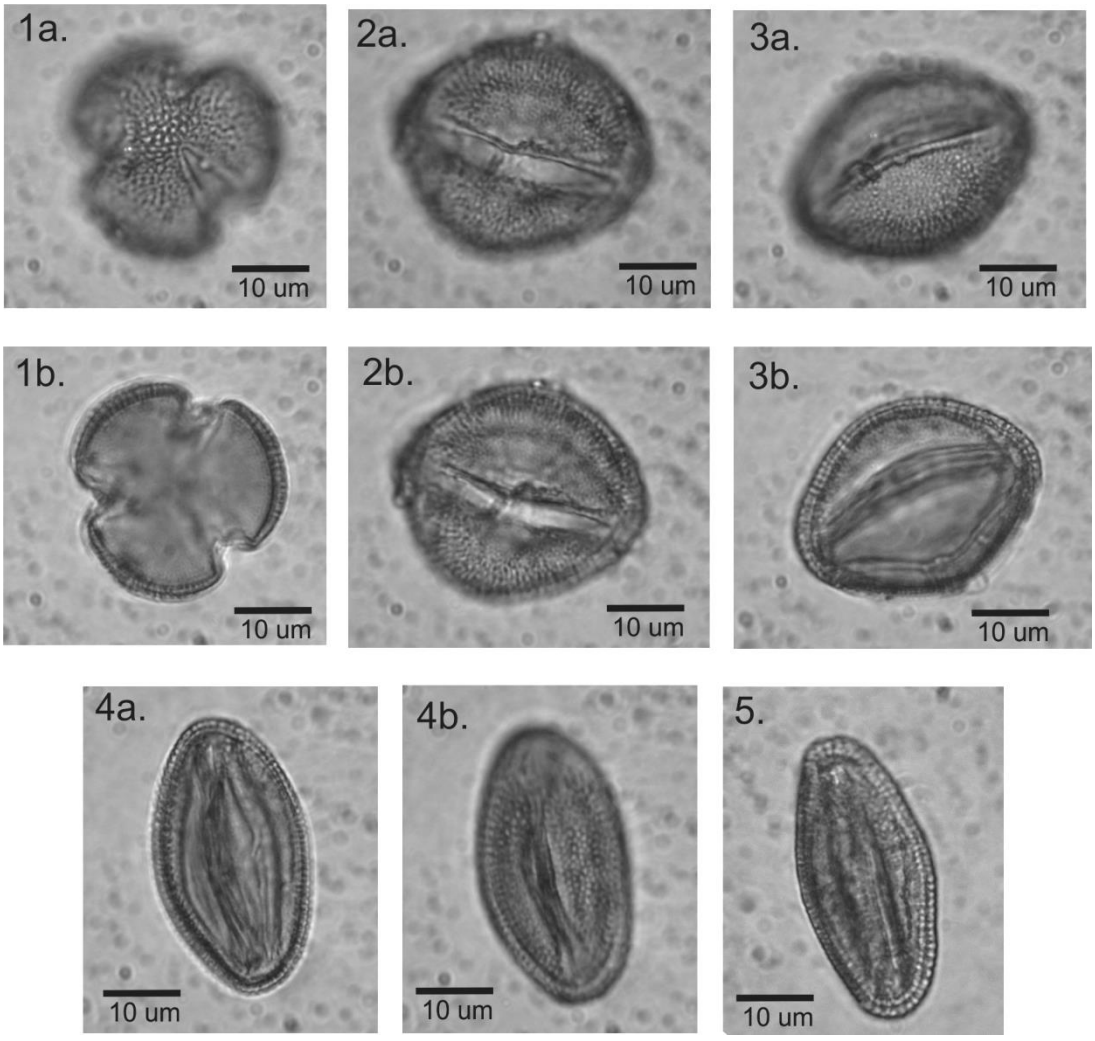

Figure 6.10: Pollen of *Tabebuia insignis* var. *monophylla* viewed in normal light. 1) Polar view showing detail of reticulum (a) and wall structure (b). 2) Rounded grain showing view of pore area. 3) Sub-prolate grain showing view of margo (a) and wall structure (b). 4) Prolate grain showing wall structure (a) and reticulum (b). 5) A second example of a prolate grain showing the wall structure.

6.3 Peatland pteridophytes

6.3.1 Background on tropical pteridophytes

The ferns (part of the pteridophyta) are a diverse group of plants, with an estimated 3,500 species inhabiting the neotropics (Poulsen and Nielsen, 1995), and indeed new species continue to be identified (e.g. Salino et al., 2008; Matos et al., 2009). They have succeeded in a wide range of habitats, including inundated and *terra firme* forest areas (Salovaara et al., 2004), and exhibit a variety of growth forms (Tuomisto and Ruokolainen, 1994). Where the diversity of herbaceous plants has been studied, ferns have been found to be an important part of the flora in *terra firme* and floodplain forest (Gentry & Dodson, 1987; Foster, 1990; Poulsen, 1991). Studies have also shown that

ferns often possess particular edaphic preferences (Tuomisto and Ruokolainen, 1994; Tuomisto et al. 1998; Pacienda and Prado, 2005), and that there is a significant correlation between the distribution of ferns and other plant groups (Ruokolainen et al., 2007). This implies that it may be possible to use ferns to identify different floristic patterns and edaphic conditions in the modern forest (Ruokolainen et al., 2007), and by extension the Quaternary palaeoecological record. This has the potential to be useful in circumstances where the characteristic tree species for a given forest type produce little pollen or are palynologically 'silent'. In this section, new observations from type material are reported and used, along with information in the literature (e.g. Murillo & Bless, 1978; Colinvaux et al., 1999; Roubik and Moreno, 1991; Coelho & Esteves, 2008; Márquez et al., 2010), to highlight distinctive spore morphotypes, and evaluate the degree to which these can be identified in the palaeoecological record.

6.3.2 Sample selection

A list of fern species was obtained from the Aguajal Project database (2011), which contains species composition data for palm swamps in the Madre de Díos region of Peru. From this list, 60 species of ferns in 28 different genera were identified, and this was used as the dominant guide for sample selection. However, other species known to inhabit neighbouring habitats such as river terraces were also sampled in some cases, as fern spores are wind dispersed and it is hypothesised that these may also be found in palaeoecological records from floodplain areas. In some cases, it was not possible to sample species listed by the Aguajal Project database (2011) as they were either not present in the herbarium at Turku, or were not represented by fertile individuals. Nevertheless, a total of 21 genera and 37 species were sampled as part of this study, representing around 50% of the total genera and 40% of the fern species listed in the Aguajal Project database (2011).

6.3.3. Methods

Descriptions followed the form used by Colinvaux et al. (1999) in their pollen atlas, with the terminology following that outlined in Punt et al. (2007). Features measured for all spore types included grain length (equatorial axis) and spore wall thickness, in this case taken as the exine, and excluding the perine. In monolete types, spore length included sculpture which formed a part of the exine, and in trilete types spore length included the zona where present. For monolete types, the spore depth (polar axis) was also measured (Figure 6.11). For trilete types, the radius of the grain and the length of the laesurae were also measured. A minimum of 25 spores were measured per sample where possible.

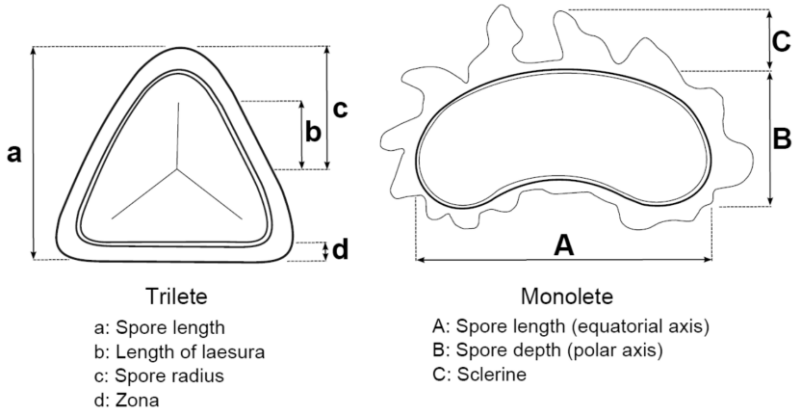

Figure 6.11: Diagram of the main spore parameters measured for trilete and monolete spores.

6.3.4 Results

Results are summarised in Tables 6.5 & 6.6. Spore depths are also presented as box plots in Figures 6.18 & 6.19. Photomicrographs of the spores are shown in Figure 6.13 & Figure 6.17, and full descriptions are provided in Appendix A. SEM images were also obtained for spores with distinctive surface sculptures which had not been examined using SEM by previous studies (Figure 6.12).

Spore size varied substantially in both monolete and trilete spore types. Trilete spores varied in length from a minimum of 24 µm to a maximum of 74 µm. However, most of the spores measured were 30 – 40 µm in length. *Cyathea macrosora* produced the largest trilete spores, and *Adiantum tomentosum* the smallest (Figure 6.19). Monolete spores varied in length from 25 µm to 73 µm, with most of the spores measured lying between 30 – 50 µm. *Campyloneurum phyllitidis* produced the largest monolete spores, and A*splenium pearcei* and *Nephrolepis biserrata* both produced the smallest.

There was very little variation in spore shape in the monolete spore types. All of the spores measured had P/E ratios between 0.5 and 0.7, except those of *Asplenium pearcei* and *Bolbitis nicotianifolia* (P/E > 0.7) and *Campyloneurum phyllitidis* (P/E < 0.4).

Surface sculpture varied considerably amongst the monolete spore types. Many of the spores possessed a microreticulum (e.g. *Elaphoglossum discolor*) on the perine, obscured by other forms of surface sculpture in some cases. Verucae were also common, especially in the family Polypodiaceae, and were observed in six species and three different genera (*Microgramma* spp*, Polypodium caceresii, P. adnatum, Campyloneurum fuscosquamatum*). Reticulate and microreticulate surface sculpture was observed in two genera. Species of the genus *Nephrolepis* all have a very similar surface sculpture. Although described as reticulate, the spores of this genus often appear 'pitted' or pock-

marked, and the reticulate sculpture lie beneath this other form of surface sculpture, obscuring it in many cases.

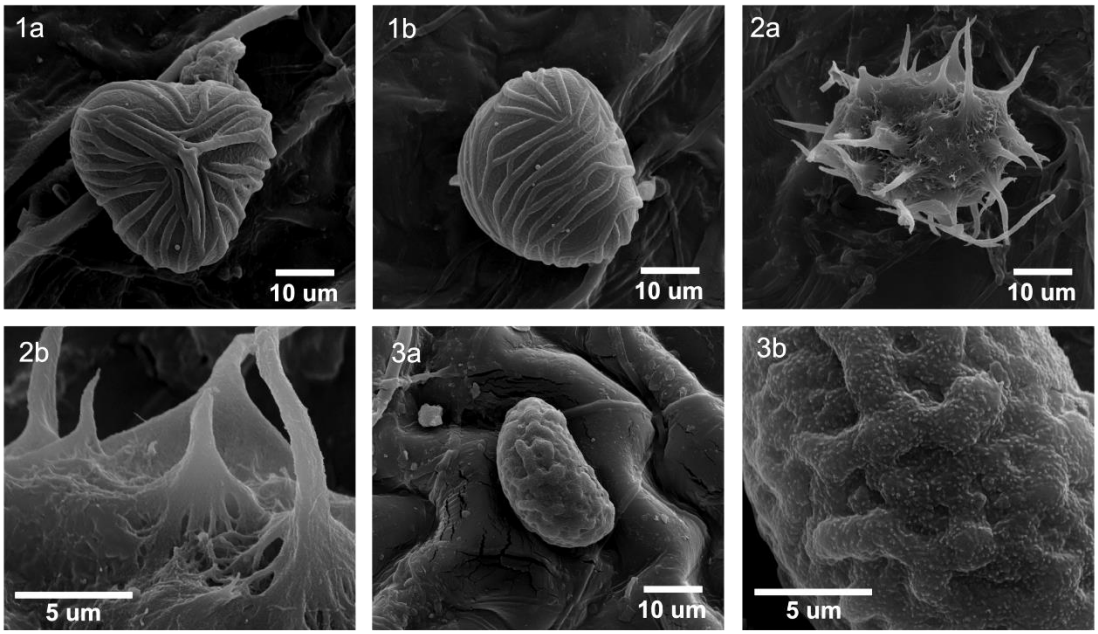

Figure 6.12: SEM images for spore types with distinctive surface sculptures. 1: *Saccoloma inaequale* in a) proximal view, and b) distal view. 2: *Asplenium pearceii* showing a) equatorial view, and b) close view of surface sculpture ('wings'). 3: *Nephrolepis rivularis* showing a) equatorial view, and b) close view of surface sculpture.

Surface sculpture varied considerably amongst the trilete spore types. The most common form of surface sculpture were scabrae, which were observed in four spore types (*Cyathea macrosora, Adiantum obliquum, A.tomentosum, A terminatum*). Three spore types possessed a rugulate surface sculpture on at least part of the sclerine (*Pteris propinqua, P. altissima, Pityrogramma calomelanos*), and two exhibited a microreticulate surface sculpture (*Adiantum humile, Metaxya rostrata*). The microreticulate patterning was often very subtle and difficult to observe in some cases. The only spore type to exhibit a prominent reticulate structure was *Pityrogramma calomelanos.* Similarly, striae and verrucae were also uncommon, with striae only observed in the spores of *Saccoloma inaequale*, and verrucae only observed in the spores of *Pteris altissima* where they merged to form a rugulate sculpture.

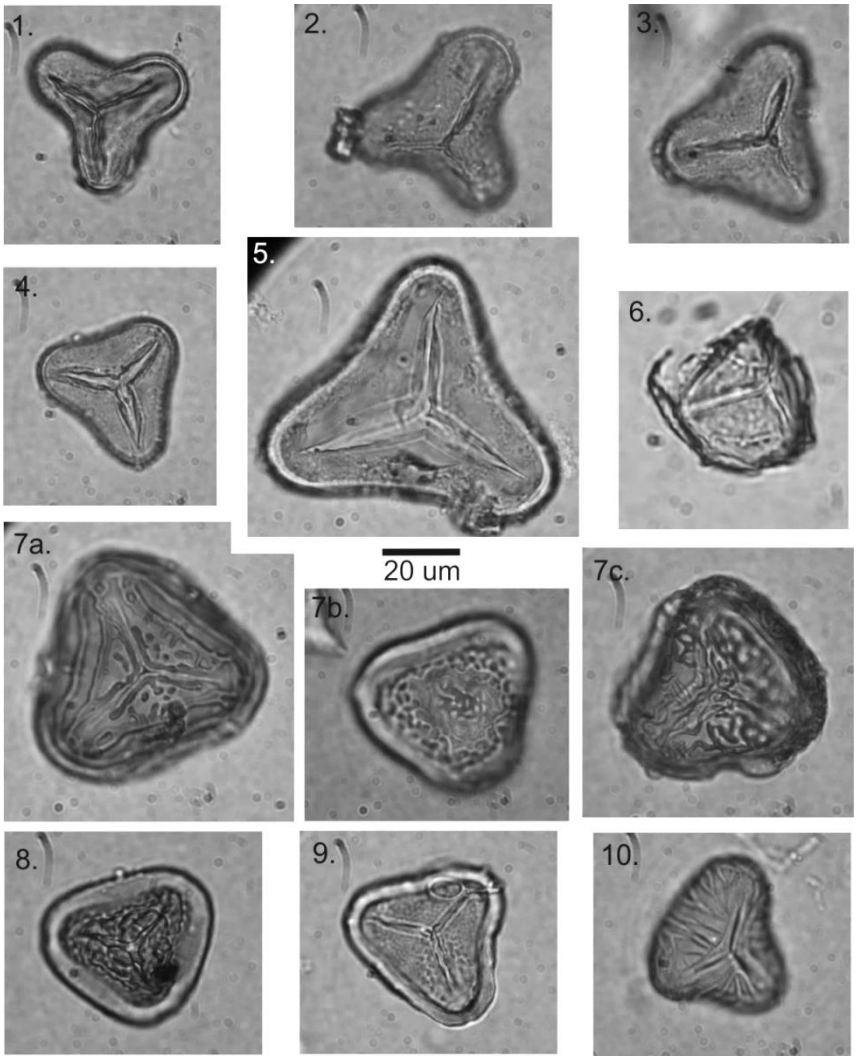

Figure 6.13: Photomicrographs of trilete fern spores from this study. 1: *Adiantum humile*; 2: *Adiantum obliquum*; 3: *Adiantum terminatum*; 4: *Adiantum tomentosum*; 5: *Cyathea macrosora*; 6: *Metaxya rostrata*; 7: *Pityrogramma calomelanos* (note 7b. shows distal face); 8: *Pteris altissima*; 9: *Pteris propinqua*; 10: *Saccoloma inaequale*.

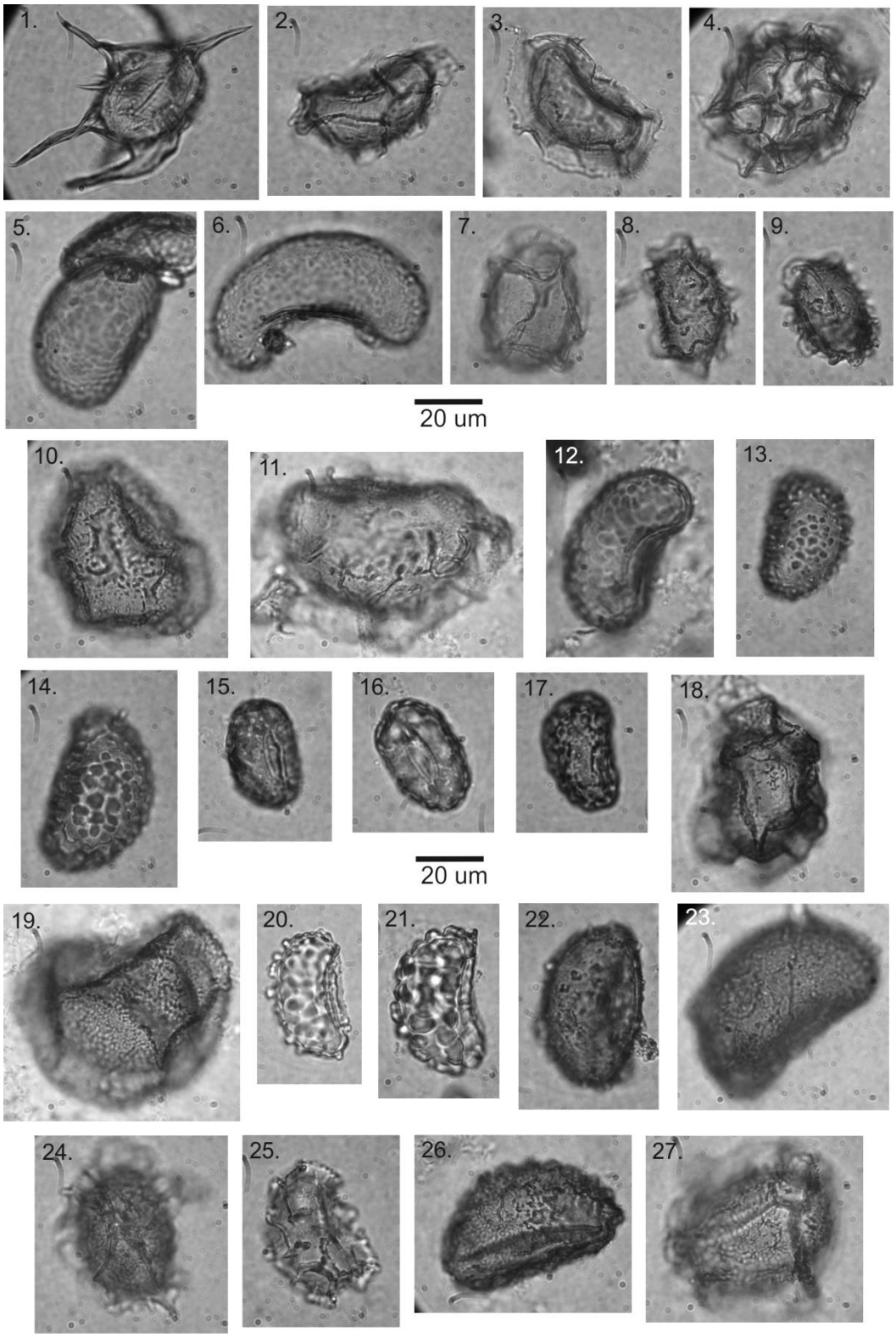

Figure 6.14: Photo micrographs of monolete fern spores from this study. 1*: Asplenium pearcei*; 2: *Asplenium serratum*; 3: *Asplenium cirrhatum*; 4*: Bolbitis nicotianifolia*; 5: *Campyloneurum fuscosquamatum*; 6: *Campyloneurum phyllitidis*; 7: *Diplazium bombanasae*; 8*: Elaphoglossum discolor*; 9*: Elaphoglossum flaccidum*; 10: *Elaphoglossum nigrescens*; 11: *Lomagramma guianensis*; 12: *Microgramma percussa*; 13: *Microgramma reptans*; 14: *Microgramma thurnii*; 15: *Nephrolepis biserrata*; 16: *Nephrolepis pectinata*; 17: *Nephrolepis rivularis*; 18: *Polybotrya caudata*; 19: *Polybotrya osmundacea*; 20: *Polypodium adnatum*; 21: *Polypodium caceresii*; 22: *Polypodium polypodioides*; 23: *Polypodium bombycinum*; 24: *Tectaria antioquiana*; 25: *Thelypteris ancyriothrix*; 26*: Thelypteris interrupta*; 27: *Triplophyllum funestum*.

Species	Family	Herbarium no.	Habit	*n*	Mean length (E)	s.d	Mean depth (P)	s.d.	P/E	Perine	Sculpture
Asplenium cirrhatum	Aspleniaceae	353916	Ep.(t) [a]	26	32.3	2.3	18.6	1.8	0.58	Present	Scabrate
Asplenium pearcei	Aspleniaceae	585244	Ep.(t) [tf]	30	29.7	1.9	19.8	2.1	0.67	Present	Scabrate
Asplenium serratum	Aspleniaceae	356305	Ep.(t) [a]	26	36.9	2.1	21.3	1.2	0.58	Present	Scabrate
Bolbitis nicotianifolia	Lomariopsidaceae	586078	C [a]	30	37.2	2.3	26.2	1.6	0.70	Present	Scabrate
Campyloneurum fuscosquamatum	Polypodiaceae	586626	Ep. [a]	40	49.5	5.2	29.6	2.9	0.60	Absent	Verrucate
Campyloneurum phyllitidis	Polypodiaceae	356120	Ep. [a]	25	61.4	5.2	24.5	3.1	0.40	Absent	Verrucate
*Diplazium bombanasae**	Athyriaceae	587103	T(ep.)	9	36.1	2.6	22.0	2.3	0.61	Present	Scabrate
Elaphoglossum discolor	Lomariopsidaceae	354392 & 316887	E, W(t), G [tf]	57	31.0	1.9	18.9	1.8	0.61	Present	Microreticulate
Elaphoglossum flaccidum	Lomariopsidaceae	353985	Ep. [a]	25	29.9	1.6	18.5	1.1	0.62	Present	Microreticulate
Elaphoglossum nigrescens	Lomariopsidaceae	579343	Ep.	25	44.4	2.3	28.4	2.1	0.64	Present	Scabrate
Lomogramma guianensis	Lomariopsidaceae	316881	C [a]	25	49.3	4.0	31.6	3.4	0.64	Present	Scabrate
Microgramma percussa	Polypodiaceae	587240	E, T [a]	25	48.8	3.0	30.8	2.4	0.63	Absent	Verrucate
Microgramma reptans	Polypodiaceae	587263	[a]	25	39.8	2.3	25.0	2.1	0.63	Absent	Verrucate
Microgramma thurnii	Polypodiaceae	355966 & 587251	Ep. [a]	50	46.4	3.0	29.2	2.9	0.63	Absent	Verrucate
Nephrolepis biserrata	Davaliaceae	354071	[a]	27	29.4	2.3	17.4	1.8	0.59	Absent	Reticulate/pitted
Nephrolepis biserrata	Davaliaceae	587265	[a]	25	37.0	2.0	22.1	2.2	0.60	Absent	Reticulate/pitted
Nephrolepis pectinata	Davaliaceae	587266	Ep. [a]	25	31.3	2.4	18.2	1.5	0.58	Absent	Reticulate/pitted
*Nephrolepis rivularis**	Davaliaceae	317252	Ep. (w), G [a]	17	31.1	3.2	19.0	1.6	0.61	Absent	Reticulate/pitted
Polybotrya caudata	Dryopteridaceae	318422	T, C [a]	30	43.1	4.7	26.9	4.2	0.62	Present	Scabrate
Polybotrya osmundaceae	Dryopteridaceae	317956	C [a]	25	39.4	4.0	21.9	2.4	0.56	Present	Scabrate
Polypodium adnatum	Polypodiaceae	587182	Ep. [a]	25	40.6	2.4	23.8	1.5	0.59	Absent	Verrucate
Polypodium bombycinum	Polypodiaceae	587199	Ep. [a]	25	50.6	4.2	31.5	2.7	0.62	Absent	Verrucate
Polypodium caceresii	Polypodiaceae	587211	Ep. [a]	26	41.8	1.9	24.5	1.7	0.59	Absent	Scabrate
Polypodium polypodioides	Polypodiaceae	587437	Ep.	25	43.5	3.8	24.9	3.1	0.57	Absent	Scabrate
Tectaria antioquiana	Dryopteridaceae	587578	T [a]	30	35.1	2.1	21.9	1.8	0.62	Present	Scabrate
Thelypteris ancyriothrix	Thelypteridaceae	587795	T	35	30.1	1.6	17.8	1.8	0.59	Present	Scabrate
Thelypteris interrupta	Thelypteridaceae	317713	[a]	30	44.4	4.9	26.2	3.7	0.59	Present	Scabrate
Triplophyllum funestum	Dryopteridaceae	585864	T [a]	25	41.7	2.8	26.9	2.2	0.65	Present	Scabrate

Table 6.5: Summary information for monolete spore types, including known growth habits: Ep. = epiphytic, C = climber, T = terrestrial (less common growth habits are marked in brackets). Samples for which fewer than 25 grains were measured have been marked *. Where species are known to occur in aguajal habitats, they have been labelled [a]. Species known to be more common to *terra firme* forest have been labelled [tf]. Species known to colonise forest gaps are marked 'G'. The perine may be lost in subfossil grains (e.g. Lacourse et al. 2003); in this instance, absence of perine could indicate genuine absence or absence resulting from the acetolysis process.

Species	Family	Herbarium no.	Habit	*n*	Mean length (Eq)	s.d.	Mean radius (R.)	s.d.	Laesura length (L)	s.d.	L/R	Zona	Sculpture
Adiantum humile	Pteridaceae	588462	T [tf]	25	29.6	2.1	17.9	1.5	13.8	1.6	0.77	Absent	Microreticulate
Adiantum obliquum	Pteridaceae	588470	T [a]	26	45.8	3.2	25.3	2.2	16.3	1.8	0.64	Absent	Scabrate
Adiantum terminatum	Pteridaceae	586314	T [a]	30	34.1	1.7	19.8	1.7	14.2	2.2	0.71	Absent	Scabrate
Adiantum tomentosum	Pteridaceae	317412	T	30	28.2	1.7	15.7	1.2	12.3	1.4	0.78	Absent	Scabrate
Cyathea macrosora	Cyatheaceae	585950	[tf]	28	55.3	7.6	32.2	5.3	24.2	4.4	0.75	Absent	Scabrate
Metaxya rostrata	Metaxyaceae	317562	T(w) [a]	26	30.3	2.2	17.1	1.6	15.5	1.7	0.91	Absent	Microreticulate
Pitryogramma calomelanos	Pteridaceae	587323	T [a]	30	42.3	3.3	20.6	2.6	13.6	2.3	0.66	Present	Rugulate/reticulate
Pteris altissima	Pteridaceae	587480	T [tf]	30	33.0	2.4	19.7	1.7	12.6	1.6	0.64	Present	Rugulate
Pteris propinqua	Pteridaceae	587458	[a]	45	34.7	2.4	18.8	2.0	13.2	2.0	0.70	Present	Scabrate/rugulate
Saccoloma inaequale	Saccolomataceae	354222	T [tf]	30	32.7	2.6	18.2	1.9	11.1	1.6	0.61	Absent	Striate

Table 6.6: Summary information for trilete spore types, including known growth habits: T = terrestrial, W = fallen wood (less common growth habits are marked in brackets). Samples for which less than 25 grains were measured have been marked *. Where species are known to occur in aguajal habitats, they have been labelled [a]. Species known to be more common to *terra firme* forest have been labelled [tf].

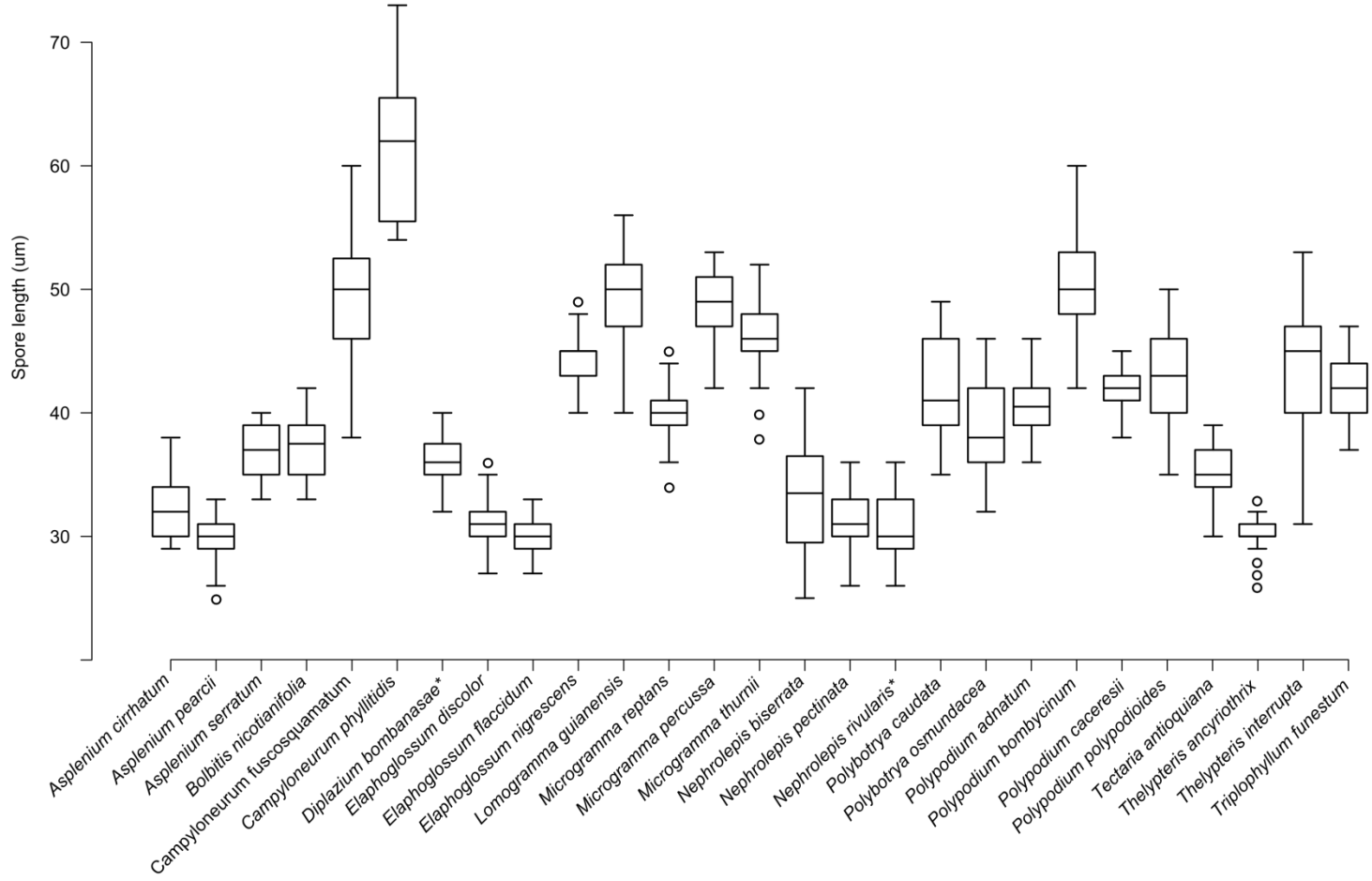

Figure 6.15: Box plots of spore lengths for the monolete Pteridophyte species studied. Species are shown in alphabetical order according to genus. For those species marked with an * fewer than 20 spores were measured.

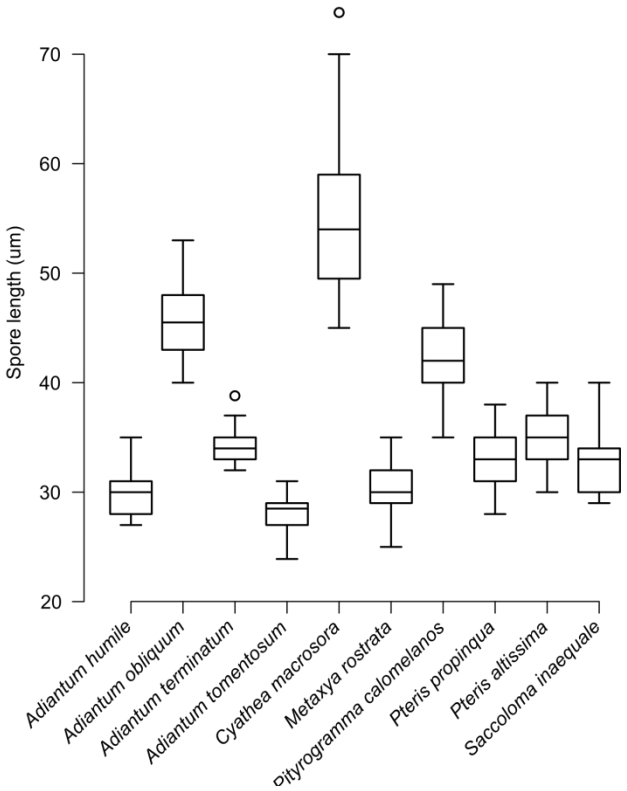

Figure 6.16: Box plots of spore lengths for the trilete fern species studied. Species are shown in alphabetical order according to genus.

Table 6.7: Fern species for which spores have been studied by both this study and by Roubik and Moreno (1991). This table shows the difference in equatorial spore length measurements obtained in each case (μm), with the final column (‡) indicating whether the spore sizes (2σ size range) obtained in this study were smaller (S), or larger (L) than those obtained by Roubik and Moreno (1991). All samples of Roubik and Moreno (1991) were mounted in glycerine, and all samples from this study were mounted in silicone oil. Measurements are in μm.

Species	Roubik and Moreno (1991)	This study (2σ)	Smallest Difference	‡
Asplenium serratum	56	35 – 39	17	*S*
Bolbitis nicotianifolia	32	35 – 40	3	*L*
Nephrolepis biserrata	44	27 – 32	12	*S*
Polypodium polypodioides	59 – 64	40 – 47	12	*S*
Adiantum humile	42 – 50	28 – 32	10	*S*
Adiantum obliquum	43	43 – 49	0	-
Metaxya rostrata	39	28 – 33	6	*S*
Pityrogramma calomelanos	60-75	33 – 40	20	*S*
Pteris altissima	52	32 – 37	15	*S*
Pteris propinqua	40	31 – 35	5	*S*

Table 6.8: Fern species for which spores have been studied by both this study and by Murillo and Bless (1974, 1978). This table shows the difference in equatorial spore length measurements obtained in each case, with the final column (‡) indicating whether the spore sizes (2σ size range) obtained in this study were smaller (S), or larger (L) than those obtained by Murillo and Bless (1974, 1978). Samples which were mounted in glycerine are marked with a †. All other samples were mounted in silicone oil. All measurements are in μm.

Species	Murillo & Bless (1974, 1978)	This study (2σ)	Smallest Difference	‡
Metaxya rostrata	32	28 – 33	0	-
Pteris altissima	35 – 40 †	32 – 37	0	-
Saccoloma inaequale	34 – 35	30 – 35	0	-
Bolbitis nicotianifolia	50 †	35 – 40	10	S
Nephrolepis biserrata	34 – 37	27 – 32	2	S
Polypodium adnatum	42 – 50	38 – 43	0	-
Polypodium bombycinum	40 – 50	46 – 55	0	-
Polypodium caceresii	40 – 45	40 – 44	0	-

6.3.5 Discussion

6.3.5.1 Comparison with previous studies

Ten of the species studied here had previously been studied by Roubik and Moreno (1991) using samples taken from Barro Colorado Island (Panama). A comparison was made between the equatorial measurements (spore length) obtained by Roubik and Moreno (1991) and this study for the ten species (Table 6.7). In eight out of the ten spores compared, the measurements obtained for spore length in this study were smaller than those obtained by Roubik and Moreno (1991). The two exceptions were *Bolbitis nicotianifolia* and *Adiantum obliquum.* Whilst it is possible that there is some difference in spore size for ferns collected in Panama, it is unlikely that this would lead to the systematic difference observed. As Roubik and Moreno (1991) used glycerine jelly as their mounting medium, it seems most likely that this was the reason for the differing results. It was also possible to make some comparison with data obtained by Murillo and Bless (1974, 1978). The values obtained by this study overlapped with most of the values from those studies, except for one of the samples for which glycerine had been used as the mounting medium. It has long been known that using glycerine jelly can cause pollen and spores to swell in size (Andersen, 1960). The comparisons made here reinforce the need to use silicone oil as the mounting medium, which does not affect grain size in the same way. Where silicone oil is used, even measurements obtained from small samples appear to produce broadly similar results (Table 6.8).

6.3.5.2 Distinctive monolete spore types

Nephrolepis

The spore morphology of various *Nephrolepis* species is discussed in Hovenkamp and Miyamoto (2005), and there are some descriptions of *N. biserrata* and *N. cordifolia* in Murillo and Bless (1978). There are also SEM images of *N. cordifolia* in Moy (1988). Colinvaux and Schofield (1976) identified *Nephrolepis* as having distinctive spores in their palaeoecological study of El Junco Lake (Galapagos Islands), but gave no detailed description of the spore morphology.

Of all the monolete spore types studied here, *Nephrolepis* is particularly distinctive. It is relatively small in size by comparison to many of the other spore types (Figure 6.18), although the spores of *Thelypteris ancyriothrix, Elaphoglossum discolor, E. flaccidum, Asplenium pearcei* and *A. cirrhatum* all fell into a similar size range. In terms of its surface sculpture, however, it is very distinctive. The reticulate, semi-foveolate 'pitted' sculpture sets it apart from all of the other spore types of similar size. Unfortunately, it does not seem to be possible to make distinctions below the genus level, as all three *Nephrolepis* species examined were indistinguishable morphologically, and overlapped considerably in terms of their size ranges. Nevertheless, some distinctions may be possible within this genus, as the morphology of *N. cordifolia* in SEM (*cf.* Moy, 1988) was different to that of *N. rivularis* and *N. biserrata* in this study (*N. cordifolia* appears less foveolate, and instead has regular verrucae).

Generally epiphytic in habit (Tuomisto and Ruokolainen, 1994; Tuomisto et al., 2002), ferns of the genus *Nephrolepis* have been encountered in studies of both *terra firme* forest (Tuomisto et al., 2002), and *Mauritia* palm swamp habitats (Aguajal Project, 2011). In a study of *terra firme* forest in Ecuador, *Nephrolepis rivularis* was one of the most common fern species, and was found mainly in forest gaps (Tuomisto and Ruokolainen, 1994). It may therefore be possible to use the spores of this genus as a proxy for small-scale disturbance, although this would require further studies of their modern ecology.

Campyloneurum

Two species within the genus *Campyloneurum* were examined; these varied in both size and morphology. *Campyloneurum phyllitidis* produces the most distinctive spores of these two, as it was the largest of all the monolete spores studied (mean length 61 μm). Giudice et al. (2004) note that the large size of *Campyloneurum,* relative to other spores of the Polypodiaceae, could be the result of polyploidy. There is some overlap

with the spores of *Polypodium bombycinum*, but these can be separated on the basis of their surface sculpture (*P. bombycinum* is not verrucate).

In the case of *C. fuscosquamatum*, its spores bear a close resemblance to those of *Microgramma reptans* and *M. percussa,* as all of these fern species have verrucae which are similar in size and spacing (all c. 1-3 μm, with c. 1 μm between verrucae). Although the spores of *C. fuscosquamatum* are mostly larger in size than those of *M. reptans,* there is some overlap and indeed there is a large overlap in size with the spores of *M. percussa.* As Bush et al. (2001) note it is better to be conservative when making taxonomic distinctions. Both of these genera are in the family Polypodiaceae, and many spore types within this wider family are similar to one another, and so *Campyloneurum* may be indistinguishable from other *Polypodium*-type spores.

Both *C. fuscosquamatum* and *C. phyllitidis* were observed in swamps and aguajal wetlands by the Aguajal Project (2011). Indeed, Salovaara et al. (2004) also found that *C. fuscosquamatum* was especially indicative of wet sites and inundated forest types.

Asplenium

Thirteen species of *Asplenium* are described in Murillo and Bless (1978), although none of these overlap with this study. In general, the spores of *Asplenium* are not especially distinctive, and some produce spores which are similar to those of other genera such as *Blechnum* (*cf.* Colinvaux and Schofield, 1976; Murillo and Bless, 1978). However, there are some distinctive spores within this genus: examples include *Asplenium falcinellum* (which has long, round, protruding echinae-like structures), and possibly *A. praemorsum,* which has an irregularly striate perine (Murillo and Bless, 1978). This study has shown that the spores of *Asplenium pearcei* are also distinctive, as the spores of this species possess very long, pointed 'wings' up to 25 μm in length (Figures 6.15 & 6.17).

Ferns of the genus *Asplenium* are mostly epiphytic in habit, and *A. pearcei* is only rarely observed growing on the ground (Tuomisto et al. 2002). Whilst *A. serratum* and *A. cirrhatum* have both been observed growing in *Mauritia* palm swamps (Aguajal Project, 2011), *A. pearcei* is currently only known from *terra firme* forest (Tuomisto et al. 2002).

6.3.5.3 Distinctive trilete spore types

Saccoloma

The spores of *Saccoloma* have been described previously by Esteves and Coelho (2007), and it is clear from this work that *S. inaequale* possesses a different spore

morphology to that of *S. elegans*, although both are striate. In the present study it was very distinctive, being the only spore type observed to possess a striate surface sculpture. On the basis of the photomicrographs of *Saccoloma elegans* and *S. domingense* given in Roubik and Moreno (1991) and Murillo and Bless (1974), this striate sculpture seems to be a shared feature of spores from this genus. Striae are known to be a feature of spores from other neotropical fern genera such as *Alsophila* and *Cyathea* (Murillo and Bless, 1974; Gastony, 1974). However, the striae of *Saccoloma* appear to differ in size, pattern, spacing and orientation, from those in these other genera.

Saccoloma inaequale is frequently encountered in studies of the modern forest, although it is not always abundant (Tuomisto and Ruokolainen, 1994; Tuomisto and Poulsen, 1996, 2000). Although this species was recorded by the Aguajal Project (2011), it was observed in terrace forest rather than palm swamp. Other studies have also shown that this terrestrial species is most typical of *terra firme* forest (Salovaara et al. 2004), and that it prefers intermediate to rich soils in areas of intermediate drainage on the lower parts of slopes (Tuomisto and Poulsen 1996, 2000).

Pityrogramma

The spore morphology of *Pityrogramma calomelanos* has been described by Coelho and Esteves (2008), and SEM images of this spore type can be found in Wagner (1974). Based on the study of Coelho and Esteves (2008), the spore morphology of *P. calomelanos* is very different to that of *P. trifoliata*. The spores of *Pityrogramma calomelanos* were morphologically different to the spores of the other species studied here (Figure 6.17), and Colinvaux and Schofield (1976) also identified this as a distinctive type in the Galapagos Islands. With their mixture of rugulate and reticulate surface sculpture, and thick zona, the spores of *Pityrogramma* can easily be distinguished from micro-reticulate and rugulate spores of similar size, such as those of *Pteris.* However, it is important to note the variability in the sculpture found on the proximal face.

Terrestrial in habit (Young & León, 1989), *Pityrogramma calomelanos* is a habitat generalist, and has been found in seasonally flooded habitat types in south western Amazonia (Daly et al., 2006), as a part of the floating macrophytic community of oxbow lakes (Aguajal Project, 2011), and even in semi-arid regions (Ambrósio and De Melo, 2001).

Cyathea

The spores of *Cyathea* are amongst the few which have been identified in previous neotropical pollen diagrams (e.g. Colinvaux and Schofield, 1976; Behling et al., 2000; Bush et al., 2004). In this study *Cyathea macrosora* was one of the few spore types distinguished on the basis of grain size. *Cyathea macrosora* was by far the largest trilete type, with some spores exceeding 70 μm in length. Comparison with other studies of this genus seem to show that this large spore size is not untypical, and indeed the minimum spore length of *Cyathea* is greater than 37 μm in most cases (Márquez et al., 2010).

However, morphologically the spores of *Cyathea* are very similar to other trilete scabrate types, and because of this it is important to ensure that any distinctions based on morphometry are robust. Whilst the use of '*Cyathea*-type' in pollen diagrams may be valid, a more extensive survey of different spore types from the Amazonian lowlands is required if definite species level or genus level identifications are to be made. There are a number of other species of *Cyathea* in lowland Amazonia including *C. pungens*, *C. bradei*, and *C. lasiosora* (Tuomisto and Ruokolainen, 1994; Tuomisto & Poulsen, 2000; Duque et al., 2005), and any future investigation should start by looking at the spores of these three species.

Metaxya

In their SEM study, Gastony and Tryon (1976) noted that the spores of *Metaxya* are distinct from other spores in the Cyatheaceae. They do, however, bear some resemblance to spores from some species in the genus *Grammitis* (*cf.* Murillo and Bless, 1974). In this study, the spores of *Metaxya rostrata* were the only ones which could be distinguished on the basis of their scar length (Table 6.6). As Roubik and Moreno (1991) observed, the laesurae are generally long in relation to the radius, and occasionally extend all the way to the equator. The laesurae also protrude above the surface of the spore, unlike most other trilete spore types. The grain shape of *Metaxya* is very rounded, and this alone allowed it to be distinguished from other spores in this study. Due to the potential for confusion with *Grammitis*, a conservative taxonomy would probably assign spores of this type to a category such as '*Metaxya/Grammitis* – type'. Nevertheless, there may be potential for distinction between these two genera in the future, possibly using SEM.

Metaxya rostrata is terrestrial in habit, although it has been known to grow on decaying wood (Tuomisto and Ruokolainen, 1994). It is known to occur in *Mauritia* palm swamp forest (Aguajal Project, 2011), but has also been found to be common on

poorly drained soils in terra firme forest (Tuomisto and Ruokolainen, 1994), and is most common on nutrient poor soils (Tuomisto and Poulsen, 1996).

Pteris

Spores of the genus Pteridaceae have been studied previously by Coelho and Esteves (2008), Martínez and Morbelli (2009), and Murillo and Bless (1974). In Coelho and Esteves (2008) *Pteris splendens*, *P. decurrens* and *P. vittata*, all have potentially distinctive morphologies. The two species investigated by this study were also markedly different to each other, and to those previously studied. *Pteris propinqua* had a characteristic combination of scabrae/verrucae on the proximal face and rugulae on the distal face. *Pteris altissima* had a slightly different sculpture, with pronounced rugulae on both proximal and distal faces. Indeed, the spores of this genus possess a diverse range of differing surface sculptures, which opens up the potential for species-level identifications. Further work may be required as there are still a number of species in this genus which require study. Martínez and Morbelli (2009) also demonstrated that some species can exhibit polymorphism in their spores, which suggests that spores from several individuals may have to be examined to gain an indication of spore morphological variability.

Pteris propinqua is known from *Mauritia* palm swamp habitat (Aguajal Project, 2011), and is known to prefer rich soils (Tuomisto and Poulsen, 1996). *Pteris altissima* is terrestrial in habit and is also known to prefer rich soils (Tuomisto and Poulsen, 1996; Tuomisto et al., 2002).

6.4 Pollen representation

6.4.1 Background and approach

Pollen surface samples were studied at both San Jorge and Quistococha to establish the degree to which the main taxa in the modern forest are represented in the pollen record. Full data for the forest plot (see Chapter 3) and pollen samples have been shown alongside one another in Figures 6.17 and 6.18. Three samples from the centre of separate sub-plots were analysed for the two sites, with the amalgamated total exceeding 300 pollen grains (>100 grains were counted for each sub-plot). Counting of multiple soil surface samples allows a better characterisation of the pollen signal for a particular vegetation type than a single sample (Hill, 1996). Fern spores have been shown, but the forest inventory did not include herbaceous taxa.

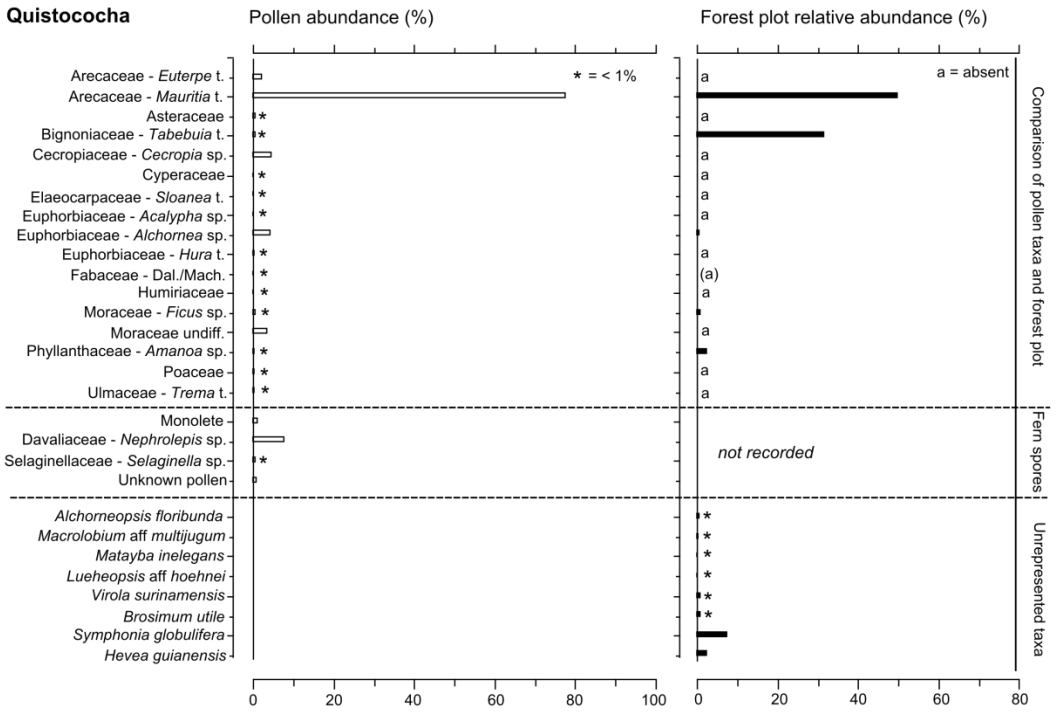

Figure 6.17: Comparison of the pollen assemblage in surface samples with the forest plot inventory data (taxa > 10 cm diameter) for Quistococha peatland. Three surface samples were analysed and the results combined in this diagram (total pollen sum = 389).

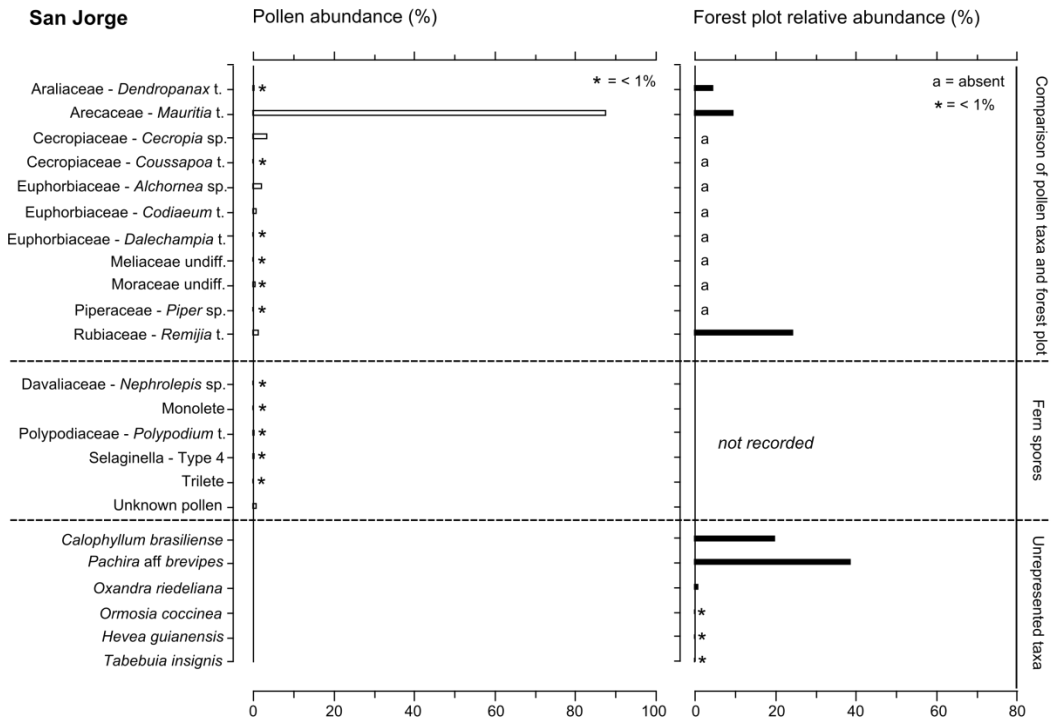

Figure 6.18: Comparison of the pollen assemblage in surface samples with the forest plot inventory data for San Jorge peatland. Three surface samples were analysed (total pollen = 438).

6.4.2 Results

Both at San Jorge and Quistococha, *Mauritia* t. dominates the pollen assemblage. *Mauritia* t. pollen is particularly overrepresented at San Jorge, where it constitutes 8.8% of the individuals in the plot but reaches an abundance of 89% in the surface samples. At both sites, there are a number of taxa which are abundant in the forest plot but are low in abundance or absent from the pollen record. At Quistococha, *Tabebuia* t. is very poorly represented; it constitutes c. 32% of the individuals in the forest plot but makes up < 1% of the total pollen. At San Jorge, most of the main pole forest species are not represented in the pollen record. *Remijia*, which constitutes c. 25% of the individuals in the plot makes up c. 1.5% of the total pollen. *Dendropanax* is also relatively abundant in the plot (4.8%) but is rare in the pollen samples (< 0.5%). Taxa such as *Calophyllum* and *Pachira* are absent from the pollen samples.

At both Quistococha and San Jorge, small quantities of pollen from taxa which were absent from the forest plots were found in the surface samples. At Quistococha, taxa such as *Cecropia,* Moraceae undiff. and *Euterpe* t. were all observed in the pollen record but were absent from the plot. At San Jorge, *Alchornea* and *Cecropia* were both found in the pollen samples but were absent from the plot.

6.4.3 Discussion

Several of the species found in the pollen record at Quistococha which were absent from the plot are found elsewhere on the site, including *Euterpe* and *Cecropia.* Other pollen types found in the peatland probably represent trees found on adjacent terra firme areas or pollen which forms a part of the regional pollen rain (e.g. Moraceae).

Mauritia flexuosa is clearly a prolific pollen producer; this may lend some support to the study of Rosa and Koptur (2013) which found that *Mauritia* is wind pollinated. Weng et al. (2004) also found that *Mauritia* was abundant in the floodplain pollen rain. Where *Mauritia* t. pollen forms the majority of the pollen in a sample, *Mauritia flexuosa* may still only be a minor part of the forest flora. Although this is not an issue when attempting to detect the presence of an aguajal in the palaeoecological record, it makes the distinction between aguajal and pole forest much harder to achieve. *Mauritiella* is largely absent from the pole forest, and therefore the taxonomic distinction between *Mauritia* and *Mauritiella* is more critical given that this may be a key line of evidence in making this distinction.

Other important peatland trees such as *Tabebuia* are almost silent in the pollen record, and wherever they are found it probably indicates that they were abundant at the site. In the case of *Tabebuia*, which is entomophilous, the main means by which pollen is

transferred to the peat surface is when the flower dies and falls to the forest floor. This will create a more patchy pollen distribution across the peat surface than for anemophilous species and hence limit the chance of detection.

There is a need for further work in order to establish the pollen representation of species in different wetland forest types, which was beyond the scope of this study, but the data collected indicate the need for caution when interpreting the pollen record. Just as in European forests (e.g. Bradshaw, 1981), pollen abundance does not always straightforwardly equate to the abundance of individuals, and the presence of taxa which are silent or almost silent in the pollen record presents significant challenges in tropical palynology (Gosling et al., 2005).

6.5 Unknown palynomorphs

6.5.1 Common pollen types

In some instances, firm identifications were not possible and so pollen grains were assigned a type number, and their most likely identities are discussed below. Photographs of the frequently occurring unknown pollen types discussed here are given in Figure 6.19. Full descriptions of all unknown types are given in the Appendix.

6.5.1.1 Type 1

Unknown type 1 is small and spherical (c. 10 μm), tricolporate, and has small (c. 1x 3 μm) but clearly lalongate pores. This pollen type is observed in some abundance in several of the cores, and is synonymous with type K5 in Roucoux et al. (2013). As yet, even tentative identification has not proven possible.

6.5.1.2 Type 2

Unknown type 2 is tricolporate, microreticulate, suboblate to round in shape (PD: 15-16 μm, ED: 16-17 μm). The pore morphology is somewhat variable and pores are not always clearly apparent.

This pollen types bears some resemblance to types within the Rubiaceae family such as *Borreria* and *Sabicea* (see Roubik and Moreno, 1991), but is not a perfect match for these taxa. It also resembles some taxa within the Menispermaceae family such as *Abuta*, but the shape of the grain is a poor match in polar view. At present, the most likely attribution is with the Rubiaceae, but its precise identification remains unknown.

6.5.1.3 Type 3

Unknown type 3 is triporate (pores lolongate, occasionally 4-porate), microreticulate, oblate (ED: c. 15 μm). Although superficially this pollen type appears similar to taxa

within the Moraceae, its thick exine and unusual pore shape are not a close match for any taxa currently known from within this family. The pore shape and elements of the grain shape more closely resemble those of *Celtis schippi* in Roubik and Moreno (1991), and therefore the most likely attribution is with the Ulmaceae.

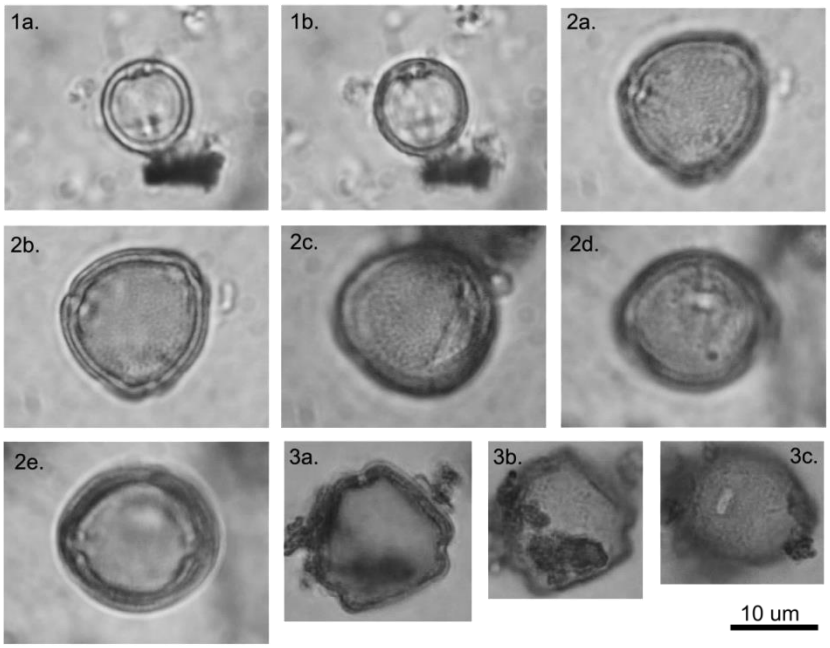

Figure 6.19: Unknown pollen types. 1a and 1b: Type 1 equatorial view. 2a: Type 2 Polar view showing colpi. 2b: Type 2 polar view showing microreticulate surface sculpture. 2c: Type 2 equatorial view; in this example pores are indistinct. 2d: Type 2 equatorial view showing pores and colpi. 3a: Type 3 polar view showing exine structure and pores. 3b: Type 3 polar view showing surface sculpture. 3c: Type 3 equatorial view showing lolongate pores. (Type 3 photos courtesy of K. Roucoux).

6.5.2 Common spore types

6.5.2.1 Type 4

Clearly a trilete spore (Figure 6.20), this type does not key out straightforwardly in the available pollen keys. However, it is distinctive and appears to be associated with the later successional stages (SJ-5). It is likely a species of *Selaginella* sp. and closely resembles *Selaginella aff. exaltata* as described by Colinvaux et al. (1999). However, this description and the accompanying photomicrographs differ somewhat from those in Roubik and Moreno (1991) for this species, and so this type has been conservatively attributed to the Selaginellaceae until a firmer identification can be made.

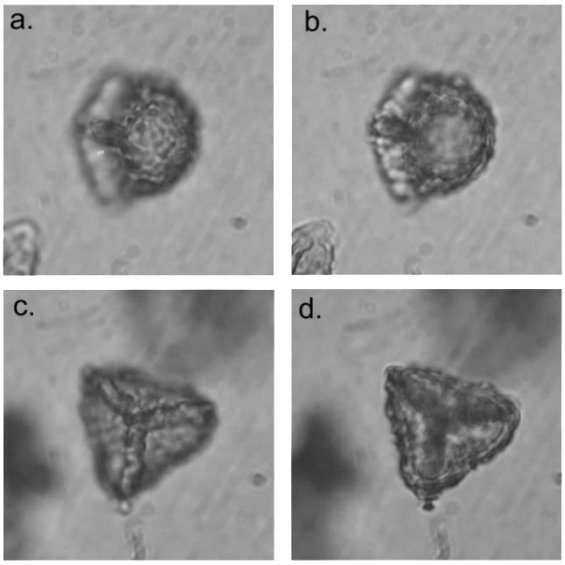

Figure 6.20: Type 4, identified as a species within the Selaginellaceae. a) Side view showing sculpture. b) side view showing laesura. c) Proximal view showing laesura. d) proximal view showing sculpture.

6.5.3 Non-pollen palynomorphs (NPPs)

Two commonly occurring non-pollen palynomorphs were encountered in the cores from San Jorge and Quistococha (Figure 6.21), and these have been described below. These were counted as they potentially strengthen interpretations based on the main sum pollen taxa.

6.5.3.1 Algal spores

Superficially, these are similar to pollen types such as the Ameranthaceae (e.g. *Gomphrena* sp.), however they have no clear columellae and therefore a simpler surface sculpture. They closely resemble the NPPs identified as algal spores illustrated in the Lake Suigetsu pollen atlas (Demske et al., 2013), and this is their most likely identity.

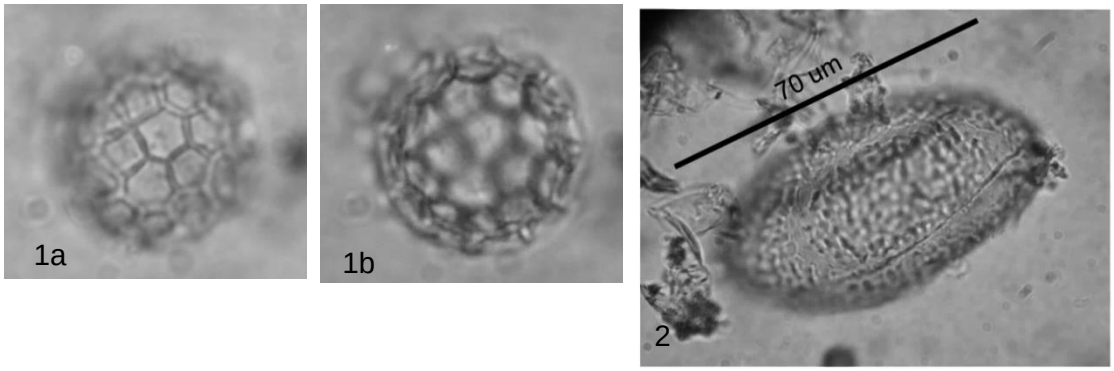

Figure 6.21: Algal spore types (note scales differ). 1(a & b): Algal spores: Spheroidal, c. 12 µm in diameter, inaperturate with reticulate surface sculpture, but no columellae or tectum. 2: Example of *Spirogrya* from 104 cm depth in core SJO-2010-1.

6.5.3.2 *Spirogyra* sp.

The genus *Spirogyra* is a member of the family Zygnemataceae, which are unbranched filamentous green algae (Van Geel, 2001). Although low in number in the samples studied here, they are potentially indicative of standing water. The identification is based on the guide to NPPs of Van Geel (2001), and the microfossil plates in Kuhry (1988).

6.6 Summary

The main aim of the work outlined in this chapter was to facilitate better taxonomic distinctions in the palaeobotanical record preserved in Amazonian peat accumulations. This chapter has summarised studies made into the taxonomy of Amazonian peatland trees, found to be common on the basis of forest plot inventories (see Chapter 3), and ferns as listed in the Aguajal Project database (2011).

This chapter demonstrates that the pollen of *Mauritia* and *Mauritiella*, which has previously been considered inseparable by most authors, can be distinguished both through SEM and through morphometry using normal light microscopy. Few *Mauritiella* pollen grains are greater than 40 µm and few *Mauritia* pollen grains are smaller than 40 µm; if the mean grain size is greater than 40 µm then *Mauritia* is likely the dominant pollen type, and vice versa. It also appears to be possible to distinguish between *Mauritia* and *Mauritiella* more confidently on the basis of micron-scale features by SEM. This is an important finding given that these two trees are both common in the peatlands of Loreto, and in wetlands throughout the Amazon.

Several distinctive fern spore types have been identified; morphometry proved useful in making some taxonomic distinctions (*Cyathea, Metaxya, Campyloneurum*), but the most distinctive spore types were those with characteristic surface sculptures. *Nephrolepis* and *Pityrogramma* were identified as distinctive spore types by Colinvaux and Schofield (1976) in the Galapagos, and this study has shown that these types are also distinctive relative to other types in Amazonian peatlands. Further work is required to establish the distribution of fern taxa in floodplain forests, but the improved identification of pteridophyte spores could improve palaeoecological interpretations in some cases (e.g. *Nephrolepis* may be indicative of gap formation).

Investigations into pollen representation at San Jorge and Quistococha have shown that several tree species present at these two sites are poorly represented in the pollen record, whilst *Mauritia* type pollen is highly overrepresented. This presents some challenges when interpreting the palaeoecological record; for example at San Jorge the

poor representation of pole forest indicator taxa makes determining the point at which this forest type became established more difficult.

7. Core chronologies

7.1 Introduction

In order to facilitate comparisons with records in the wider region, as well as between cores from within the same site, radiometric chronologies were produced for the cores studied at Quistococha and San Jorge. The chronological data presented address several of the main thesis aims, but in particular enable the main hypotheses relating to Amazonian peatland palaeoecology to be addressed, as outlined in Chapter 1:

- *Key events in the pollen stratigraphy at Quistococha (e.g. the* Mauritia *rise) occurred synchronously across the site.*
- *Key changes in the pollen records at San Jorge and Quistococha were synchronous.*
- *Key changes in the pollen records at these two sites were synchronous (within dating uncertainties) with climate events identified in other records from the region.*

This chapter outlines age models for cores which contain more than three radiocarbon dates, and summarises results for the cores at Quistococha which have ≤ 3 radiocarbon determinations. As part of these analyses, some duplicate dates from bulk samples and picked dates are compared, and the implications of this for radiocarbon-dated lake profiles in Amazonia is briefly discussed. ^{210}Pb dating was also applied to date the top c. 40 cm at San Jorge, the first time this dating method has been applied to a peatland in the lowland Amazon Basin.

7.2 Age modelling

The cost of radiometric dating, or the lack of suitable material across parts of a sequence, mean that it is almost always impossible to provide absolute dates for all points in a core. As such, it is common for an age model to be produced which uses a method of interpolation to establish the ages of points between dated horizons (see Blaauw, 2010 for a review of different approaches).

'Classical' age modelling involves simple linear interpolation between points, and is the most commonly applied method (Blaauw, 2010). However, linear interpolation does not clearly display the uncertainties between dated levels which relate to the underlying assumptions in any age model (see Figures 7.2 and 7.3). Furthermore, where the errors attached to a radiocarbon date are particularly large (e.g. due to calibration plateaux; Lotter et al., 1992), other kinds of age model can help to reduce the chronological uncertainty.

One alternative to linear interpolation is to produce a Bayesian age model. A detailed overview of Bayesian age-modelling is provided in Bronk Ramsey (2009), but some details will be summarised here. Although, as in a linear model, there are uncertainties in the ages between dated levels, in a Bayesian model these inherent model uncertainties are more clearly illustrated. Bayes' theorem allows reasonable assumptions to be incorporated into a model (e.g. the assumption that age increases with depth) in order to refine the modelled uncertainty. These assumptions are often referred to as the 'prior' model, and can be thought of as the known behaviour of a system before we undertake any additional analyses (Bronk Ramsey, 2008). Bayesian modelling combines this information with the measurements taken (in this case, ^{14}C determinations) to produce a 'posterior' probability incorporating all of the information (Bronk Ramsey, 2008).

As such, Bayes' theorem can be expressed accordingly (after Bronk Ramsey, 2009):

$$p(t|y) \propto p(y|t)p(t) \quad (1)$$

Where t refers to a set of parameters (i.e. events in a record) and y the measurements associated with them (e.g. radiocarbon dates). $p(t)$ is the 'prior' (e.g. the assumption that age increases with depth), $p(y|t)$ is the 'likelihood' (information from the measurements), and $p(t|y)$ is the 'posterior' probability. Markov Chain Monte Carlo sampling is used produce a range of solutions for the posterior probability which can be expressed as a probability density function (Bronk Ramsey, 2008).

In this case, Bayesian age models were constructed using the BACON software program (Blaauw and Christen, 2011). In addition to the assumption that age increases with depth, BACON incorporates priors for the accumulation rate and the rate at which this can change through the sequence ('memory'). Where the 'memory' is strong, BACON assumes that the accumulation rate varies little from sample to sample (i.e. accumulation rate is autocorrelated). BACON can also incorporate prior information about hiatuses in accumulation. In this instance, the BACON default values for the memory and accumulation rate priors were used. In the case of the memory priors (strength: 4, mean: 0.7), these avoid constraining the model and allow for a range of posterior values to be produced (Blaauw and Christen, 2011). In the case of the accumulation rate (yr cm^{-1}), the posterior values did not depart significantly from the default settings (acc. shape: 1.5, acc. mean: 10). In both cores, the basal dates indicated that a mean accumulation rate prior of 10 yr cm^{-1} was appropriate.

7.3 Quistococha peatland dates

7.3.1 Background

Radiocarbon dates were obtained from ten cores taken across the Quistococha peatland. This served to test the hypotheses outlined in Chapter 1 and listed above. In particular, dates were used to establish the timing of peat initiation across the site, and to determine whether events in the pollen stratigraphy from four peat cores were synchronous. These dates form an important basis for the developmental model produced for Quistococha and described in Chapter 10.

7.3.2 Results

The results of radiocarbon determinations are presented in Table 7.1, and probability density functions for the peat basal dates are also shown in Figure 7.1 with a map showing the location of all the cores analysed across the site. A total of 15 radiocarbon dates were obtained for peat cores collected by the author in 2011 and 2012. These include ten peat basal dates, and five further radiocarbon dates which were used to determine the timing of changes seen in the pollen stratigraphy (mainly the increase in *Mauritia* t. towards the top of the cores). Peat basal dates were obtained from depths ranging from 130 to 352 cm.

Table 7.1: Radiocarbon age determinations for Quistococha peat cores. AMS radiocarbon dates were obtained from the NERC facility at East Kilbride. Calibration was undertaken using the INTCAL13 curve. All samples are the < 180 μm peat fraction. (*Sample inferred to have been affected by young carbon contamination from root penetration.) Four dates were targeted specifically at dating the main increase in *Mauritia*-t. pollen, and three at the lower peak in *Mauritia*-t (marked Ψ) seen in some of the cores studied (see Chapter 8).

Core	Laboratory code	Depth (cm)	14C age (yrs BP)	s.d.	δ13C	Calibrated age (cal yr BP)
Peat basal dates						
QT-2011-1*	SUERC-44988	130	859	37	-30.3	709-891
QT-2011-2 Ψ	SUERC-44989	196	2155	35	-30.1	2067-2301
QT-2011-3	SUERC-44990	178	2234	37	-16.1	2159-2325
QT-2011-4	SUERC-44991	352	2253	35	-29.8	2181-2337
QT-2011-5	SUERC-44992	226	1988	37	-30.7	1897-1987
QT-2011-6	SUERC-44995	320	2061	37	-30.2	1953-2109
QT-2011-7	SUERC-44996	262	2228	35	-29.7	2159-2315
QT-2012-9	SUERC-54428	256	2,324	41	-29.6	2209-2315
QT-2012-10 Ψ	SUERC-54429	180	2,290	41	-30.8	2186-2352
QT-2012-18	SUERC-54432	144	2,059	41	-30.3	1952-2111
Main* Mauritia-t. *increase						
QT-2011-2	SUERC-54423	130	1,164	40	-30.0	1008-1174
QT-2012-9	SUERC-54424	96	684	39	-30.1	566-676
QT-2012-10	SUERC-54425	112	1,144	40	-31.2	978-1172
QT-2012-18	SUERC-54426	96	1,030	41	-30.7	916-980
Lower* Mauritia-t. *peak (also Ψ above)						
QT-2012-9	SUERC-54427	192	1,771	41	-29.5	1615-1733

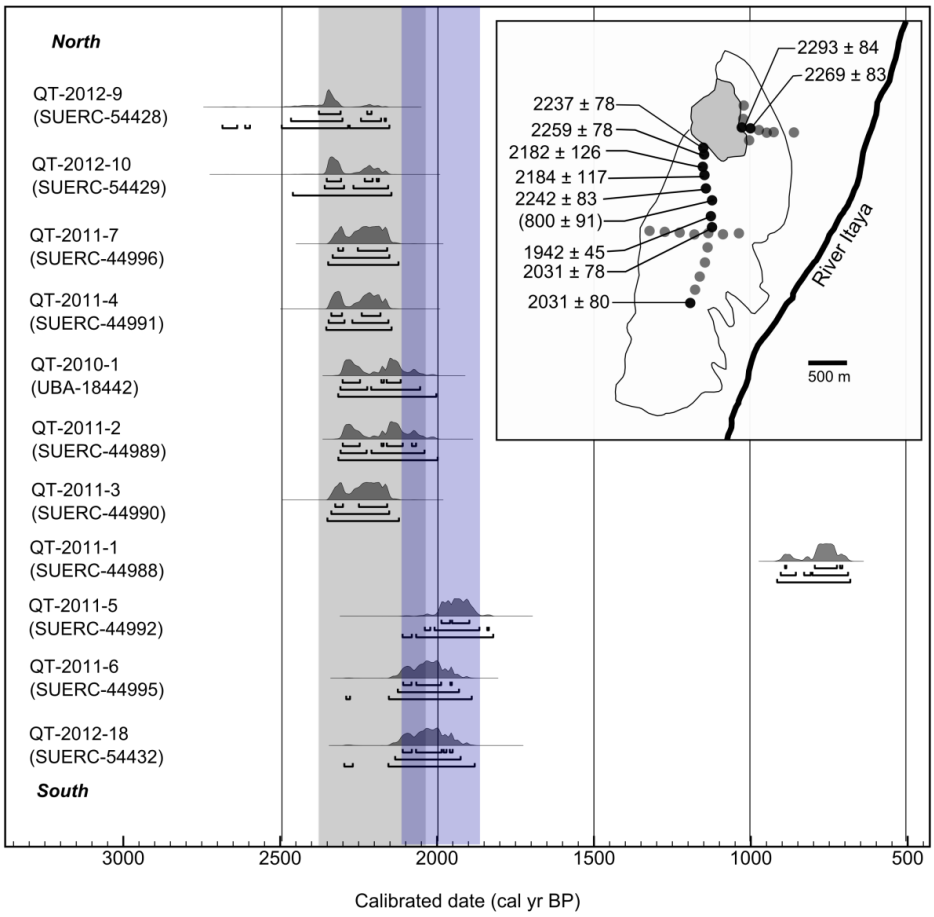

Figure 7.1: Probability density functions for basal radiocarbon dates for the Quistococha peat cores (including core QT-2010-1 of Roucoux et al., 2013), plotted using OxCal (Bronk Ramsey, 1995; Bronk Ramsey & Lee, 2013). Dates have been arranged in sequence, with basal dates from the north of the site at the top and from the south of the site at the bottom. The grey band shows the range of the initiation dates for the area within 800 m of the lake, and the blue band shows the (later) dates from cores on the more southerly parts of the site. Inset map shows the position of all the cores taken, with radiocarbon-dated cores marked in black.

A basal sample from one of the cores (QT-2011-1) returned a date which is substantially younger than all of the other basal peat ages. It was inferred that, in spite of efforts to remove roots through sieving, this sample has been affected by young carbon contamination. Although it is the shallowest core from the site, all other shallow cores returned much older ages and therefore this seems to be the most likely explanation for this outlier. If the date is a correct estimate of the point of peat initiation, then this would affect the model of peatland development in Chapter 10; one possibility might be peat erosion at this point removed earlier accumulations, but isolated erosion at a single point is unlikely. Alternatively, it could represent the path of a former drainage stream across the site (as seen at the Changuinola peatland, Panama; Phillips & Bustin, 1996). Further coring in adjacent areas (or re-analysis of the ^{14}C sample)could establish whether this is indeed the case, but this would not have significant implications for the development of the site.

7.4 Quistococha lake core chronology

7.4.1 Background

A reliable chronology was required in order to facilitate within-site and between-site comparisons, particularly with the existing, well-dated pollen record from QT-2010-1 (Roucoux et al., 2013). However, Räsänen et al. (1991) suggest that dates from floodplain lakes could be affected by 'old' carbon in the form of recycled organic particles. This applies especially to inorganic sediments, such as clays and silts, which have low quantities of authogenic carbon and therefore may contain high proportions of allogenic re-worked material. While the existing bulk ^{14}C dates from a depth of c. 250 cm in Quistococha suggest that the lake is at least 5961 ± 314 cal yrs old (Räsänen et al., 1991), this date is likely much older than the true age (M. Räsänen, pers. comm.). The key recommendation of Räsänen et al. (1991) was therefore to date visible organic fragments (as opposed to bulk samples) where possible.

When samples were prepared for radiocarbon dating, one of the key aims was to test whether there was a significant offset as a result of old carbon input. As many Amazonian palaeoenvironmental records originate from floodplain lakes, and use bulk dates as a basis for their chronology (e.g. Frost, 1988; Berrio et al., 2000; Irion et al., 2006), the results of this section have implications which go beyond this project.

7.4.2 Results

A total of twelve AMS radiocarbon determinations were obtained from QT-2010-3 (Table 7.2). The date obtained from 88-89 cm was slightly out of sequence, but the high pollen concentration across this interval implies that this represents a genuine decrease in the sedimentation rate. Below the upper part of the lake core where the core was composed of organic gyttja, some of the dates obtained were not in sequence (discussed further below).

The sample from 280-282 cm (SUERC-46369) returned an age of 5333-5603 cal yr BP, significantly older than the basal sample (SUERC-37523). Sample SUERC-46369 was composed of small picked fragments and despite best efforts to extract as much material as possible from the core section the final sample size available for ^{14}C determination was < 300 μg C. This can result in an analytical error greater than the stated analytical error (which is based on repeat analyses). As such the calibrated date for this depth was rejected as being unreliable. The maximum age obtained for the sequence is therefore 4833-4967 cal. year BP from a depth of 357-360 cm.

Three further dates were also rejected. Two bulk peat samples returned dates which were > 1000 years older than those obtained from paired picked plant macrofossil

samples from the same levels. This indicates that, in the clay-rich part of the core, dates are likely to be affected by old carbon that has been recycled in the environment. As such, only picked samples were used for the age model in the lower part of the sequence and samples SUERC-37522 and SUERC-37524 were rejected.

Table 7.2: Results of radiocarbon dating analyses undertaken on samples from the lake core at Quistococha (QT-2010-3). Analytical uncertainty is shown to 1 standard deviation (s.d.). Samples were analysed at the NERC facility at East Kilbride. (Note that sample marked ‡ contained < 300 μgC). * denotes sample rejected from age model.

Laboratory code	Depth (cm)	Material	^{14}C age (yrs BP)	s.d.	δ^{13}C	Calibrated age (cal yr BP)
SUERC-44979	40-41	Bulk gyttja	703	37	-25.9	560-710
SUERC-44980	60-61	Bulk gyttja	927	35	-26.2	765-927
SUERC-44981	88-89	Plant macrofossil	1357	37	-31.6	1182-1357
SUERC-38477	95-96	Bulk gyttja	1710	37	-29.0	1540-1705
SUERC-37520	127-128	Bulk gyttja	1942	37	-32.3	1830-1930
SUERC-44982	152-153	Bulk gyttja	2117	37	-31.3	1992-2299
SUERC-37521	196-198	Picked plant fragments	2669	37	-21.8	2748-2838
SUERC-37522*	196-198	Bulk	3728	35	-22.9	3914-4070
SUERC-37523*	229-231	Picked plant fragments	2678	37	-16.3	2751-2842
SUERC-37524*	229-231	Bulk	3667	35	-21.2	3926-4082
SUERC-46369*	280-282	Picked plant fragments ‡	4792	78	-37.1	5333-5603
SUERC-44986	357-360	Picked plant fragments	4311	36	-28.2	4833-4967

However, one of the picked dates was also out of sequence with the rest of the radiocarbon dates. The sample from 229-231 cm returned an age almost identical to that from 196-198 cm, although the δ^{13}C values were different indicating that the material was not the same. There are at least three possible explanations for this:

i. Operator error during coring meant that the same horizon was sampled twice. This is more likely when sampling lakes because, if the coring platform moves, the coring rod may not be vertical and therefore the coring depth could be overestimated (i.e. a shallower layer would be sampled but would appear to have been taken from a greater depth).
ii. Rapid accumulation in this part of the sequence. The accumulation of c. 33 cm of sediment in 80 years (the error associated with the dates) is entirely plausible in the Amazon floodplain. Examination of varvites in varzea lakes has shown accumulation rates can average 3.5 mm yr^{-1} (Irion et al., 1997).

iii. The material further up the sequence (196-198 cm) contained old carbon which was washed in from the catchment and is therefore older than the level from which is was taken.

As the pollen signal is dominated by *Cecropia* in this part of the core, use of the palynostratigraphy to establish which of these scenarios is more likely is difficult. If the first scenario is correct, then the upper date is the 'correct' age, and the sample from 229-231 should be rejected. If the second scenario is correct then both dates are correct and indicate a period of rapid sediment accumulation. If the final scenario is correct then it is the lower date which is correct and the upper date which is out of sequence. As the upper date from 196-198 cm is in sequence with the other dates obtained, this date has been used in the age model; it is the opinion of the author that the first scenario is the most likely, given the similarity of the dates obtained. There is clearly chronological uncertainty in this part of the core; however, this is not critical with respect to peatland development, as the sediments in this part of the core precede the onset of peat accumulation.

In total eight radiocarbon dates were used to produce an age model for the lake core, which is particularly robust in the upper part of the sequence. This is the period of most interest as the dates obtained so far (see Section 7.3) indicate that this is the period during which the peatland formed.

7.4.3 QT-2010-3 age model

Two different age models were developed and compared, in order to find the best possible model and to establish how this process can affect the interpretation of the raw ^{14}C dates obtained. The first model is a simple linearly interpolated age model developed using CLAM (Blaauw, 2010). This procedure was used to develop the published age model for QT-2010-1 (Roucoux et al., 2013). The second model is a bayesian age-depth model produced using BACON (Blaauw and Christen, 2011).

As can be seen in Figures 7.2 and 7.3, both models produce a very similar 'best-fit' result. However, the Bayesian model probably provides a better indication of the uncertainties associated with this model fit (Blaauw and Christen, 2011). Errors can be seen to be larger where a part of the sequence is stratigraphically further from a dated sample, whereas this source of uncertainty is not visible in the linearly-interpolated model.

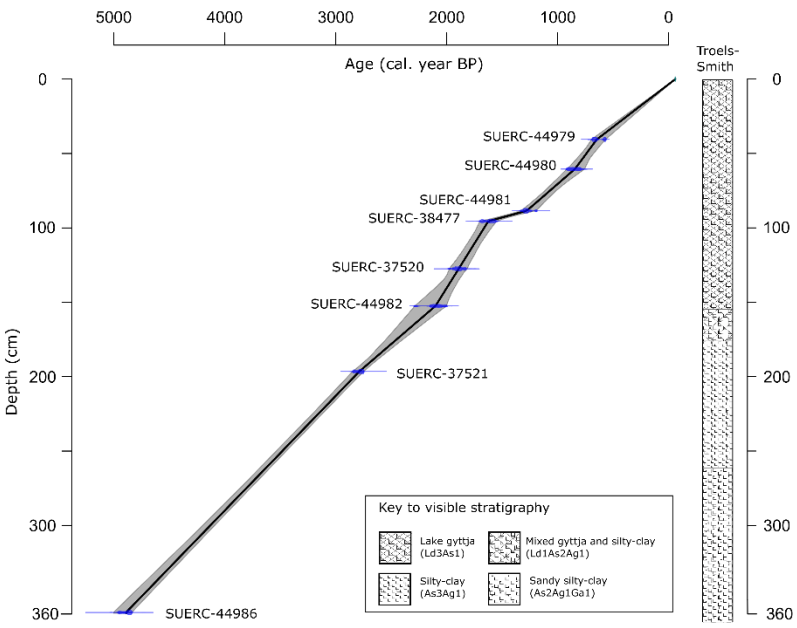

Figure 7.2: Linear age-depth model developed for QT-2010-3 using CLAM software (Blaauw, 2010). Troels-smith stratigraphy has also been shown for reference.

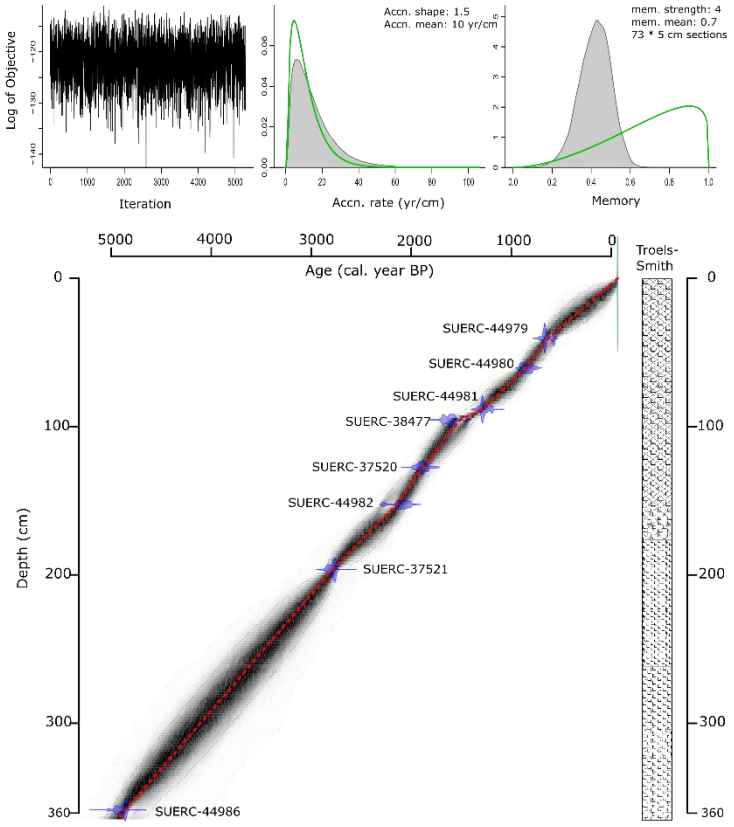

Figure 7.3: Bayesian age-depth model for the lake core (QT-2010-3), developed using the BACON software (Blaauw and Christen, 2011). The shaded area indicates the 95% probability interval of the model, given the assumptions underlying it (i.e. the prior information specified). The red line indicates the best-fit (most probable) age-depth relationship. Plots at the top of the figure show the Markov Chain Monte Carlo iterations, the accumulation rate prior (green) and posterior (shaded) curves, and the 'memory' prior (green) and posterior (shaded) curves. Troels-smith stratigraphy has also been shown for reference (see Figure 7.2 for key).

7.5 San Jorge chronology

7.5.1 Background

A robust age model is essential in order to link the palaeoecological and geochemical data collected at San Jorge with the sequences at Quistococha . This was essential for the testing of hypotheses relating to several of the main thesis aims (see Section 7.1). A further thesis aim was to determine the age of the pole forest at San Jorge. Pollen analysis revealed that this transition likely occurred within the top 50 cm of the core (see Chapter 9), and therefore an alternative to radiocarbon dating was sought to allow more accurate dating of this part of the sequence. ^{210}Pb was chosen, as discussed below.

7.5.3 Results

7.5.3.1 Lead-210 dating

The total ^{210}Pb inventory is 7275 Bq m^{-2} and the annual ^{210}Pb flux (the supply rate) is 226.5 Bq m^{-2} yr^{-1}. The total inventory is towards the upper end of the values obtained by some studies undertaken in the UK, such as that of Parry et al. (2013) who obtained a maximum inventory of 6326 ± 1071 Bq m^{-2}. Equally, the annual flux is towards the upper end of values collated for wetlands of the world in Preiss et al. (1996), which mostly fall below 200 Bq m^{-2} yr^{-1}.

The ^{210}Pb supply rate is generally thought to correlate with rainfall (Preiss et al., 1996; Smith et al., 1997). Smith et al (1997) found that the supply rate for ^{210}Pb is 77 ± 14 Bq m^{-2} yr^{-1} for every 1000 mm of rainfall in the UK. In the study region, annual rainfall is c. 3000 mm yr^{-1} or greater (Marengo, 1998), predicting a flux of 231 ± 42 Bq m^{-2} yr^{-1} which accords well with the observed rate. The decline in ^{210}Pb activity with depth is exponential, as would be expected (Appleby, 2001), with the exception of the near-surface samples and the sample from 14-16 cm. In the sample from 2-4 cm , the low ^{210}Pb activity was the result of partial sample loss during preparation (N. Sanderson, pers. comm). This is unlikely to have a significant effect on the rest of the model. However, ^{210}Pb activity in the sample from 0-2 cm is also low.

A 'flattening' or relative fall in the ^{210}Pb activity curve near the surface (see Appleby, 2001), can be seen in ^{210}Pb data from many different studies (e.g. Malmer and Holm, 1984; MacKenzie et al., 1998; Olid et al., 2008). This can be the result of (after Appleby, 2001):

i) Bioturbation, for example by roots or insects near the peat surface
ii) Movement of ^{210}Pb in porewaters

iii) Accelerated accumulation rate

iv) Lack of $^{210}Pb/^{210}Po$ equilibrium at the time of measurement.

As the core was stored for four years prior to undertaking the measurements, the lack of equilibrium between ^{210}Pb and ^{210}Po is an unlikely causal factor. Given the high hydraulic conductivity (*K*) observed at the site (see Chapter 5), there is a strong likelihood that the cause of low activity in some peat layers could be the movement of ^{210}Pb in the near surface. High *K* values were observed at 50 cm depth and in the near surface where the peat is less compacted these values are likely to be higher, promoting the movement of soluble compounds. Although under anoxic conditions Pb is present in insoluble forms, where oxygen is available it can form soluble $PbSO_4$ (Damman, 1978), and the data available indicate that water tables are low enough for this to occur during the dry season even in Amazonian peatlands which are not domed (see Quistococha water table record, Chapter 5). Combined with the action of roots, this is likely to explain this particular anomaly.

Table 7.3: ^{210}PB activity determinations for the top 50 cm of the San Jorge peat core (SJO-2010-1). Note that ages are given in years AD. (Data collected in collaboration with Nicole Sanderson, as specified in Chapter 4). Analytical error is shown to 1 s.d.

Depth (cm)	^{210}Pb activity (Bq kg^{-1})	± total	Dry bulk density (g cm^{-3})	Unsupported ^{210}Pb activity (Bq kg^{-1})	Cum. Unsupported ^{210}Pb inventory (Bq m^{-2})	Age (AD)	Error (yrs)
0-2	375.34	10.86	0.125	365.77	228.68	2012.0	0.01
2-4	360.21	21.28	0.130	350.64	1162.45	2007.4	0.02
4-6	517.78	13.29	0.131	508.21	2275.79	2001.0	0.03
6-8	445.36	11.89	0.127	435.79	3470.06	1992.2	0.04
8-10	315.59	9.19	0.104	306.02	4233.24	1985.0	0.08
10-12	223.71	7.42	0.092	214.14	4705.94	1979.6	0.11
12-14	223.72	6.33	0.101	214.15	5138.44	1973.7	0.15
14-16	302.76	9.23	0.100	293.19	5639.13	1965.1	0.23
16-18	219.12	7.69	0.081	209.55	6042.17	1956.0	0.33
18-20	188.91	6.22	0.093	179.34	6401.17	1944.9	0.49
20-22	134.95	6.00	0.096	125.38	6690.37	1932.0	0.78
22-24	67.46	3.29	0.110	57.89	6882.54	1919.2	1.19
24-26	41.57	1.95	0.111	32.00	6979.25	1910.1	1.61
26-28	32.45	1.77	0.102	22.88	7034.67	1903.5	1.99
28-30	43.49	2.40	0.097	33.92	7089.14	1895.2	2.60
30-32	38.83	1.85	0.093	29.26	7147.55	1883.1	3.83
32-34	24.66	1.44	0.100	15.09	7190.38	1869.9	5.80
34-36	21.99	1.79	0.093	12.42	7216.01	1858.3	8.36
36-38	22.21	1.79	0.091	12.64	7238.89	1842.5	13.73
38-40	19.68	0.96	0.093	10.11	7259.85	1814.4	32.99
40-42	14.76	0.79	0.102	5.19	7274.87		
42-44	9.57	0.60	0.109	0.00	***^{210}Pb dating horizon***		
44-46	10.03	0.65	0.107				
46-48	11.03	0.78	0.115				
48-50	7.68	0.76	0.117				
Total ^{210}Pb inventory			7274.867	(Bq m^{-2})			
^{210}Pb supply rate			226.539	(Bq $m^{-2}yr^{-1}$)			

The anomaly at 14-16 cm could also be explained by a change in the peat accumulation rate. There is an abrupt increase in phytolith concentration at 16 cm depth. As discussed in chapter 6, this could indicate that there was a decrease in the accumulation rate at this time.

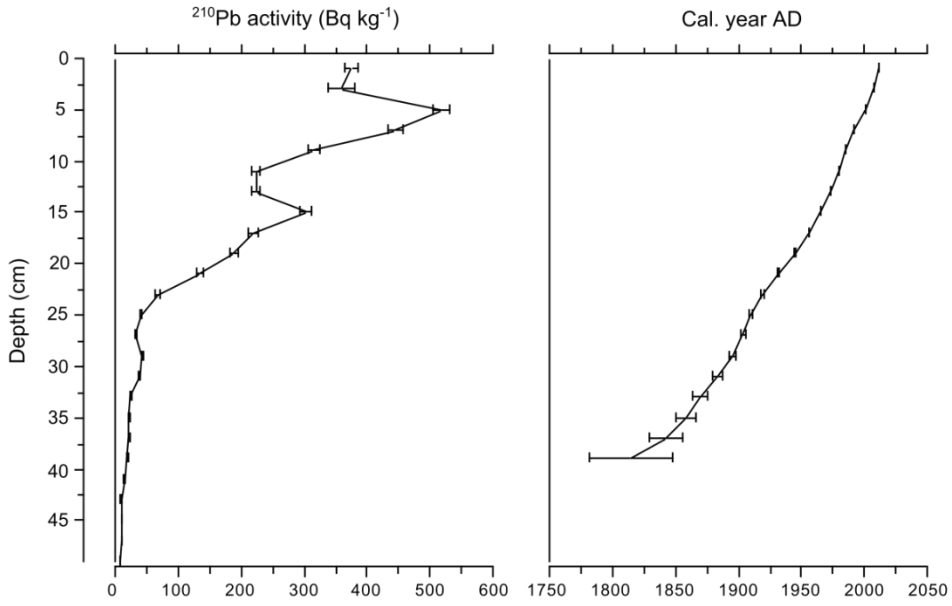

Figure 7.4: ^{210}Pb activity (Bq kg^{-1}) in the top 50 cm of the San Jorge profile (left), and the resulting CRS age model (right). Errors refer to the analytical error (1 s.d.) only (see Table 7.3).

7.5.3.2 Radiocarbon dating

Five radiocarbon dates were obtained for the top 240 cm in core SJO-2010-1; 240 cm marks the point at which pure peat accumulation initiated (see Chapter 9). Results of radiocarbon determinations are presented in Table 7.4. The dates were in sequence, but the date obtained at 90 cm returned an age which was significantly younger than those from 100-240 cm depth. This is discussed in the context of the age model in Section 7.5.3.2.

Table 7.4: Radiocarbon age determinations for the San Jorge peat core (SJO-2010-1). AMS radiocarbon dates were obtained from the NERC facility at East Kilbride (SUERC prefix), and at the ^{14}Chono radiocarbon laboratory (Queen's University Belfast; UBA prefix). Calibration was undertaken using the INTCAL13 curve. All samples are the < 180 μm peat fraction. Sample UBA-20285 was a humic acid extraction.

Laboratory code	Depth (cm)	^{14}C age (yrs BP)	Error (1 s.d)	δ^{13}C	Calibrated age (cal yr BP)
UBA-20285	90-92	282	22	-31.8	299-425
SUERC-54417	112-114	1,623	41	-29.0	1416-1564
SUERC-54418	144-146	1,759	41	-28.9	1610-1720
SUERC-54419	192-194	1,990	40	-28.8	1897-1989
SUERC-54422	238-240	2,173	41	-29.5	2120-2306

7.5.4 SJO-2010-1 age model

7.5.4.1 Lead-210 age modelling

In order to determine the age of a sample, the total supported and unsupported ^{210}Pb activity must be determined. The supported ^{210}Pb activity of a sample is that which is generated by the ongoing decay of isotopes in the uranium decay series. In ombrotrophic peatlands such as San Jorge, however, which are formed almost completely by the accumulation of organic matter, the supported ^{210}Pb component is likely to be very small (Appleby, 2008). Therefore, most ^{210}Pb activity in the samples is the result of unsupported ^{210}Pb, which is deposited on the peat surface directly from the atmosphere.

The ^{210}Pb activity data were translated into calendar ages using a constant rate of ^{210}Pb supply (CRS) model, after Appleby (2001):

$$t = \frac{1}{\lambda} Ln(\frac{A(0)}{A})$$

Where t is the age of the sample, λ is the decay constant of ^{210}Pb (0.03114 y^{-1}), A(0) is the total unsupported ^{210}Pb inventory, and A is the unsupported ^{210}Pb inventory underlying the sample.

A variety of other models can be used, and each is based on a different set of underlying assumptions (Table 7.5). Simple models such as the constant flux, constant sedimentation (CF-CS) model were originally formulated for use in lakes but make assumptions which are likely to be violated in peatlands (Appleby, 2001; see Table 7.5). The constant rate of supply (CRS) model has been found to be reliable in the majority of cases (Appleby, 2001), and CRS models are the most frequently used in peatlands (Appleby, 2008; Olid et al., 2013). Input of ^{210}Pb from atmospheric pollution can affect CRS models (Olid et al., 2013), and studies from elsewhere in South America show a general increase in lead deposition over the last c. 90 years, with a particular increase since 1945 (de Oliveira et al., 2009). However, this effect is likely to be less significant in the western Amazon. Although Pb is volatile and difficult to measure using ICP-OES, results obtained for San Jorge indicate that concentrations of Pb are low in the near-surface peats (see Chapter 9).

If ^{210}P activity varies with depth in a non-linear way when plotted on a log scale, this indicates that there have been changes in the accumulation rate and this therefore invalidates the Constant initial concentration (CIC) model (Appleby, 2001). In the case of San Jorge, it can be seen that while the decrease in ^{210}Pb activity with depth is

broadly linear, there are some variations and therefore the CRS model is likely to be more appropriate (Figure 7.5).

Table 7.5: Commonly applied models used to translate ^{210}Pb activity into age (summarised from Appleby and Oldfield, 1978; Appleby, 2001).

Model	*a-priori* assumptions	Applicability in peatlands
Constant rate of supply (CRS)	Unsupported ^{210}Pb flux is constant (accumulation rate can change through time)	Can be invalidated by recent changes in atmospheric ^{210}Pb input (pollution)
Constant initial concentration (CIC)	Assumes ^{210}Pb activity in surface layer is constant (therefore assumes constant accumulation rate)	Peats can decay and lose mass/volume, violating assumption of constant accumulation. Accumulation rates can change especially where there is a change in vegetation.
Constant flux, constant sedimentation (CF-CS)	Unsupported ^{210}Pb flux is constant AND accumulation rate is constant	Can be invalidated by recent changes in atmospheric ^{210}Pb input, and by peat decay or accumulation rate changes.

Shaw (2006) compared both CRS and CIC models in a set of cores from Glen Affric (Scotland); the two different models appeared to provide different information relating to the chronology of the cores. In particular the CIC model often helped to indicate where there may have been a change in accumulation rate (Shaw, 2006), even though it did not provide accurate age estimates. However, in the case of San Jorge, other proxy information is available to provide an indication of accumulation rate changes (e.g. pollen concentration data).

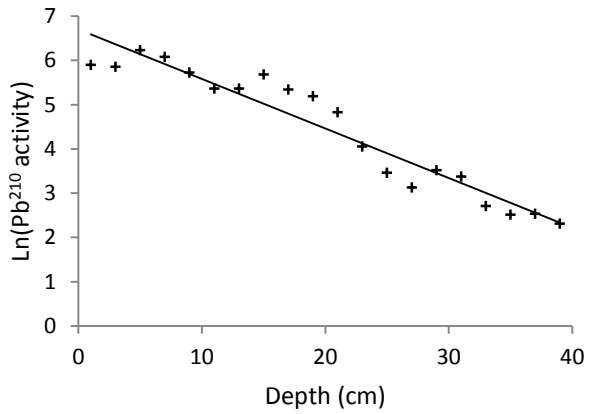

Figure 7.5: ^{210}Pb activity plotted on a log scale against depth for the San Jorge core. Where the accumulation rate has been constant, ^{210}Pb activity should be linear (Appleby, 2001; trend line shown). In this case there are some clear departures from the linear trend.

It has been argued that the ^{210}Pb content of overlying vegetation should also form part of the ^{210}Pb inventory (Olid et al., 2008), but this is practically impossible for forested peatlands such as San Jorge. The degree to which this might affect the ages is unknown, although Olid et al. (2008) found a total age underestimation of 16-22 years in a northern peatland with low-growing vegetation cover. Due to the heavy rainfall in the

study area, the quantity of ^{210}Pb intercepted by the overlying vegetation for more than a few months is likely to be minimal. However, the surface area of the overlying vegetation is also larger, and dust may settle and remain trapped in trees for long periods of time so further research may be required in this area.

Models based on ^{210}Pb are often validated using dates from other fallout radionuclides (Appleby, 2001), but in this case the model was compared to the projected ages for the upper part of the core derived from the ^{14}C age model. In a peatland where mobility of ^{137}Cs is highly likely, and ^{137}Cs concentrations may be low (as the site is in the southern hemisphere), this approach may be more valid. In the case of San Jorge, dating the upper part of the profile to the nearest year was not a key research aim, as it might be where researchers are seeking to establish recent pollution histories (e.g. Biester et al., 2007). Despite the potential problems noted with the ^{210}Pb profile, it is generally in good agreement with the age of the surface peat extrapolated from the ^{14}C date at 90 cm depth.

7.5.4.2 Age model incorporating Lead-210 and radiocarbon dates

A Bayesian model incorporating both ^{210}Pb and ^{14}C dates was produced for SJO-2010-1 (Figure 7.6). The large difference between UBA-20285 and the dates from lower in the core implies that there is a hiatus or period of slow accumulation between 90 cm and 112 cm depth. There is a marked peak in pollen and spore concentration at 96 cm which supports this inference (see Chapter 9). There is also a change in the core chemistry at this point, with reductions in concentrations of several major elements, and the transition to the uppermost pollen assemblage zone also occurs at between 96-104 cm. A hiatus was therefore defined in the age model at a depth of 100 cm. However, it is possible that peat accumulation did not totally cease at this stage, and although pollen concentrations are high pollen preservation is good. This would imply that the peat surface did not totally dry out, which would have resulted in the oxidation of pollen.

According to this age model, pure peat accumulation began at San Jorge between 2159-2366 cal yr BP. From 50-240 cm, the average accumulation rate is 1.3 mm yr^{-1}. However, across the hiatus (112-90 cm) this falls to 0.4 mm yr^{-1}. Excluding the hiatus, the average accumulation rate from 50-240 cm is 1.4 mm yr^{-1}. Accumulation rates in the upper part of the sequence, based predominantly on ^{210}Pb dates, averaged 2.3 mm yr^{-1}.

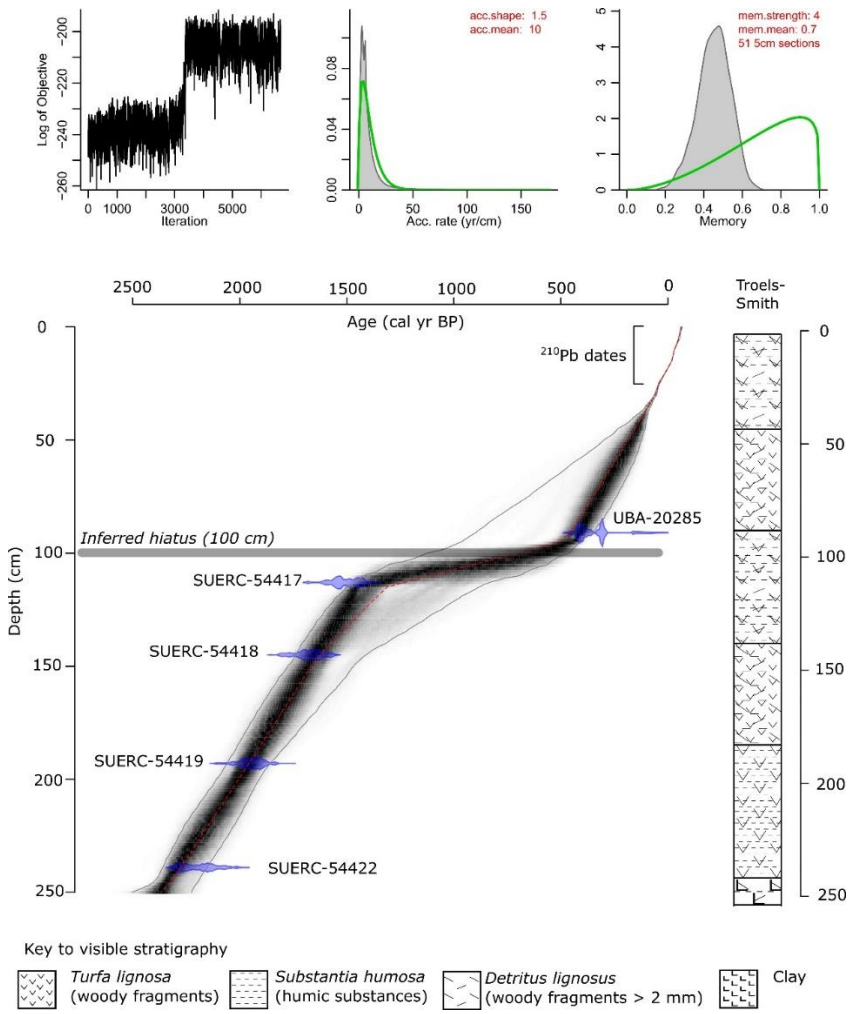

Figure 7.6: Bayesian age-depth model for the San Jorge peat core (SJO-2010-1), developed using the BACON software (Blaauw and Christen, 2011). The shaded area indicates the 95% probability interval of the model. The red line indicates the best-fit (most probable) age-depth relationship. A hiatus at 100 cm depth was incorporated into the model run, and ^{210}Pb dates from the CRS model were used for the uppermost 39 cm. Plots at the top of the figure show the Markov Chain Monte Carlo (MCMC) iterations, the accumulation rate prior (green) and posterior (shaded) curves, and the 'memory' prior (green) and posterior (shaded) curves. Instability in the MCMC iterations reflects the hiatus at 100 cm. Troels-smith stratigraphy has also been shown alongside the age-depth model for reference.

7.6 Discussion

7.6.1 'Old' carbon offset

The results of radiocarbon dating from QT-2010-3 confirm that there is a substantial offset in ages obtained from the lower, minerogenic part of the lake sequence. Picked plant fragments produced dates which were at least 989 yrs younger than bulk dates obtained from the same level (Table 7.2). This would imply an 'old' carbon contamination of 10-20% (Lowe and Walker, 1997; p. 246).

The findings made here support Räsänen et al. (1991), in that the previous date obtained for the age of the lake is certainly much older than its 'real' age. The modelled date for the level from which Räsänen et al. (1991) obtained their original date (c. 250

cm) is 6175-5746 cal yr BP. The oldest date obtained by this study, from a depth of 357-360 cm, was 4900 ± 67 cal. years BP, and as this was obtained from a part of the sequence which contained a substantial quantity of silt and had high magnetic susceptibility values, it seems likely that this layer slightly pre-dates the formation of the lake.

The identification of an old carbon offset calls into question the chronologies recently developed for three separate cores from Quistococha by Aniceto et al. (2014). They infer a hiatus in deposition between 4900 and 2700 cal yr BP, but this also coincides with the transition from clays to more organic rich sediments at the top of their cores. As can be seen in the chronology for QT-2010-3 developed by the present study, once the old carbon offset in the mineral-rich sediments is taken into account this hiatus disappears. This finding is in line with the sedimentology from QT-2010-3, which shows a gradual change from inorganic to organic sediments in line with continuous and unbroken sedimentation (see Chapter 8).

Further inconsistencies include the incongruity between the dates obtained by Aniceto et al. (2014) at 3-5 cm depth and those obtained by the present study; Aniceto et al. (2014) obtained a date of 500-520 cal yr BP in this part of their core, whereas in the present study sediments of this antiquity were only found several tens of centimetres further down (c. 32-34 cm). Although this could be interpreted in a number of ways (e.g. old carbon offset in the gyttja; differential sedimentation across the lake basin), it is likely that this discrepancy between the two studies is because Aniceto et al. (2014) failed to sample the upper part of the sequence. The inference that they failed to sample the upper part of the sequence is supported by the congruity between the palynology of QT-2010-3 and the peat cores from the present study. In particular, all show a recent decline in *Euterpe* type pollen over the last c. 460 years.

The influence of different coring techniques on the acquisition of sediments for study is sometimes difficult to infer, but based on the data from the present study it would appear that the vibracorer used by Aniceto et al. (2014) may have compacted (or failed to sample) the sediments. In the core obtained by the present study from approximately the same part of the lake using a side-sampling Russian-type corer, around 150 cm of organic sediments were retrieved. Aniceto et al. (2014) retrieved c. 60 cm of organic gyttja (which they describe as 'clay rich in organic matter'). It has been argued that, in corers where sediments are forced into a barrel or tube, incomplete sampling is the result of friction on the inner wall which creates a 'plug' and pushes aside sediment as the core is forced into the sediment (Wright, 1980). This is more likely to occur in soft sediments which are easier for the corer to push aside.

Hongve and Erlandsen (1979) also found that compaction of sediments can occur when using open barrel corers, and that compaction is more pronounced in soft organic sediments than in 'stiff' minerogenic layers. The arguments of both Wright (1980) and Hongve and Erlandsen (1979) support the inference that the vibracorer of Aniceto et al. (2014) caused compression of the gradational contact between clay and gyttja that can be seen in the core from this study, giving the false impression of a sharp contact (or hiatus).

7.6.2 'Young' carbon offset

Young carbon contamination from root penetration is probably the main source of contamination in the environment when dating a peat layer using radiocarbon (Wüst et al., 2008). However, Roucoux et al. (2013) showed that samples which were sieved to remove root contamination were in sequence with dated seeds and other plant macrofossils from the same core. The dates from Roucoux et al. (2013) are similar to the bulk dates from Lahteenöja et al. (2009a), who also manually removed visible root fragments. The basal dates for the cores from these two studies are within error of one another, and indistinguishable from the spread of dates produced by the present study for the peatland areas near to the lake (Figure 7.1).

Among the ten cores from Quistococha dated by the present study, only one sample seems to have been obviously affected (the basal sample from core QT-2011-1). Young carbon contamination is more likely to affect peat initiation dates in shallow cores, because the peat accumulation rate is slower and the base of the peat lies nearer to the surface and therefore is closer to active root growth.

Given the potential for old carbon to affect lakes and young carbon to affect peatlands, careful sample selection is vital to avoid the false appearance of diachroneity between records. Newnham et al. (2007), in a comparison of radiocarbon dates from pollen concentrates and the age of known tephra layers also found that lakes were less prone to young carbon contamination than peatlands, but did not find an old carbon effect in lakes. This suggests that recalcitrant old organic carbon contamination may only be a feature of floodplain lakes.

7.6.3 Implications for Holocene Amazonian records

Dating of bulk peat and lake sediment samples is commonplace in Amazonian palaeoecology; in many records, especially lakes, the frequently fine grained sediment contains few large macrofossils which can be used to provide a radiocarbon date. In core QT-2010-3, only a single large plant macrofossil was identified in the core

obtained, and in the lower part of the sequence small organic particles had to be carefully picked from the mineral-rich matrix, a time consuming process.

For this reason, the finding made here of a potentially large old carbon effect in floodplain sediments with a low organic content is significant. This effect was suggested as a possible hazard by Räsänen et al. (1991), but little attention has been given to sample selection when radiocarbon dating Amazonian lakes, and bulk dates are used as standard (with some exceptions: e.g. Weng et al., 2002). In some cases, bulk dates have been obtained on sediments which contain only 2-5% carbon (e.g. Irion et al., 2006). As Räsänen et al. (1991) first argued, and as the present study has also found, mineral rich Amazonian sediments contain a higher proportion of old carbon from eroded soils and other sources and therefore are particular prone to this effect.

This finding must cast doubt on the age models of some existing records, especially those from floodplain lakes. This has fundamental implications both for the timing of changes observed in Amazonian proxy records, as well as for our understanding of landscape processes, such as the migration of rivers and the time over which vegetation develops. It also makes it more likely that age models will contain apparent 'hiatuses' especially where records cross sedimentological boundaries between organic and inorganic sediments (see discussion above). In Amazonia, hiatuses in deposition are generally interpreted as representing drier climatic conditions (e.g. Ledru et al., 1998; Moreira et al., 2013; Aniceto et al., 2014), and therefore this could fundamentally affect our understanding of late Holocene climatic change.

7.7 Summary

Until the present study, there were no Amazonian peatlands with more than one radiocarbon dated core (see Chapter 3). This chapter has established a site chronology for Quistococha by obtaining basal peat initiation dates from multiple cores and by supplementing this with a well-dated lake sediment sequence. Chronologies have also been obtained for four cores from Quistococha which have been subjected to pollen analysis, with radiocarbon dates having been used to examine the timing of key vegetation changes. The implications for the timing of peat initiation at different points across the peatland are discussed in detail in relation to the model of peatland development for Quistococha in Chapter 10.

At San Jorge, the focus of dating has been on the top 240 cm (i.e. after pure peat began to accumulate) with a total of five radiocarbon dates providing the basis of a chronology. This has been supplemented in the top 50 cm by ^{210}Pb dating, which has

confirmed that peat accumulation is continuing at the present day, contrary to some domed Southeast Asian peatlands (Page et al., 1999).

In the lake core from Quistococha (QT-2010-3) and the core from San Jorge (SJO-2010-1) there is evidence for periods of slower accumulation or hiatuses. These are discussed further in Chapter 11, where potential climatic causes are examined.

8. Quistococha records: lake and peatland

8.1 Overview

This chapter contains the results of pollen and phytolith analysis for Quistococha, which includes data for four new peat core records and one lake sediment record. Supporting stratigraphic data are also provided, including a site survey of peat stratigraphy. This chapter presents the primary data only and the data are interpreted in Chapters 10 and 11.

8.2 Site stratigraphy

8.2.1 Background and approach

By comparison to the CICRA peatland (Madre de Dios, Peru) surveyed by Householder et al. (2012) which is 250 ha in size, Quistococha peatland covers almost double the area (c. 490 ha excluding the lake) and dense sampling of the kind which would allow an interpolated map of subsurface topography was impractical (ideally, depths would be measured every c. 100 m; 490 ha equates to 490 depth points). The general impassability of peatland terrain which results from the permanently waterlogged conditions, and the dense vegetation which requires paths to be cut with machete, also pose practical challenges.

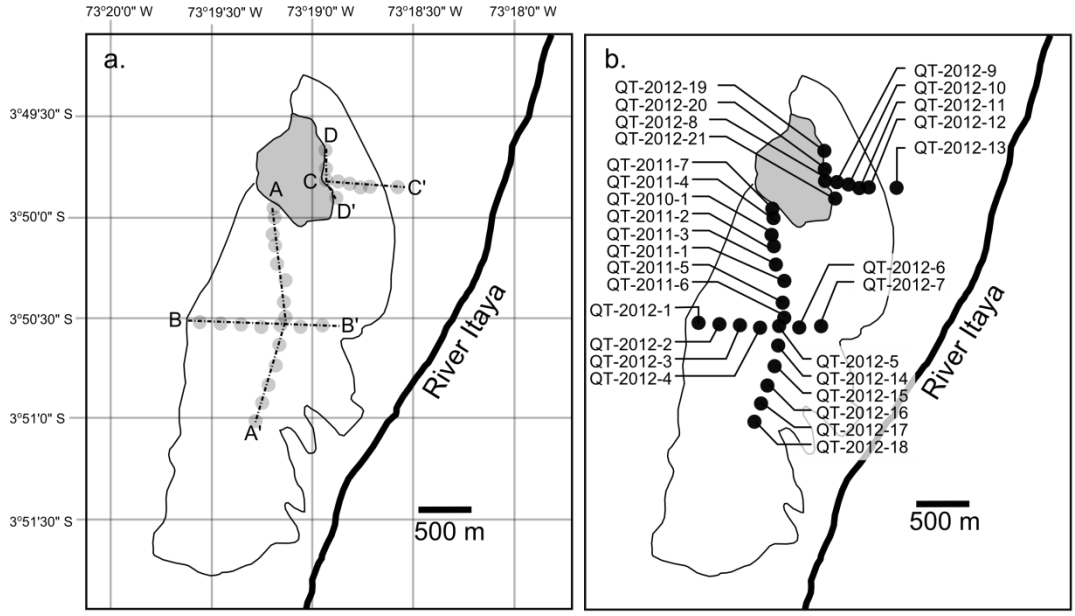

Figure 8.1: Sketch map of Quistococha lake and peatland showing a.) transects, for which the stratigraphy is illustrated in figures 8.2 – 8.5, and b.) core positions only. The approximate outline of the peatland is shown.

Therefore four transects were established (c. 5 km in total). Cores were located in order to establish the cross-section of the peatland basin along its two main axes, as well as to establish the nature of the transition from the lake to the peatland (Figure 8.1). This was

of importance for testing hypotheses relating to the rate and nature of peatland expansion (discussed in Chapter 10), particularly whether the peatland had expanded southwards over time. This peat stratigraphic survey also helped to inform the selection of cores for pollen analysis.

Table 8.1: Summary of the peat cores taken as part of this study as well as the core examined by Roucoux et al. (2013), QT-2010-1.

Core	Latitude	Longitude	Peat thickness (cm)
QT-2010-1	-3.83425	-73.32064	406
QT-2011-1	-3.83836	-73.31950	190
QT-2011-2	-3.83524	-73.32044	232
QT-2011-3	-3.83696	-73.32022	210
QT-2011-4	-3.83273	-73.32044	425
QT-2011-5	-3.84031	-73.31963	260
QT-2011-6	-3.84164	-73.31946	363
QT-2011-7	-3.83186	-73.32053	309
QT-2012-1	-3.84216	-73.32712	42
QT-2012-2	-3.84222	-73.32534	320
QT-2012-3	-3.84231	-73.32344	189
QT-2012-4	-3.84253	-73.32168	180
QT-2012-5	-3.84240	-73.31997	158
QT-2012-6	-3.84248	-73.31809	363
QT-2012-7	-3.84243	-73.31619	192
QT-2012-8	-3.82944	-73.31578	352
QT-2012-9	-3.82953	-73.31473	345
QT-2012-10	-3.82972	-73.31373	203
QT-2012-11	-3.83002	-73.31272	108
QT-2012-12	-3.83007	-73.31187	101
QT-2012-13	-3.83001	-73.30950	60
QT-2012-14	-3.84415	-73.32007	364
QT-2012-15	-3.84595	-73.32035	146
QT-2012-16	-3.84772	-73.32097	105
QT-2012-17	-3.84931	-73.32160	174
QT-2012-18	-3.85096	-73.32216	166
QT-2012-19	-3.32678	-73.31566	314
QT-2012-20	-3.82843	-73.31573	385
QT-2012-21	-3.83097	-73.31498	354

8.2.2 Description of site stratigraphy

The site stratigraphy is presented in figures 8.2-8.5. Descriptions of peat composition have been simplified to enable the main patterns to be observed across the basin. This interpretation was based on Troels-Smith (1955) classifications made in the field and in the laboratory, and on core photographs taken in the field. Four main units were identified, with some variation within these main peat types.

The first is a fibrous peat composed mainly of roots (typically Tl2DhSh1 or similar using the Troels-Smith classification), and tentatively identified as '*Mauritia* peat'. Peat of this composition is found in the upper part of all the cores. This identification was made with the support of the available pollen data (see Table 8.2). There are some differences in the depth at which '*Mauritia* peat' is first observed and the depth at which palm phytoliths and *Mauritia*-t. pollen become abundant in the cores; the two microfossil proxies become abundant at greater depth than the point at which '*Mauritia* peat' becomes discernible in the visible stratigraphy. This suggests that the microfossil

proxies are a more reliable indicator of the point at which *Mauritia/Mauritiella* became established but that equally, there may have been a period during which *Mauritia/Mauritiella* gradually increased in abundance until they caused a visible change in the litter being accumulated.

Table 8.2: Comparison between the inferred depth of '*Mauritia*' peat based on visible stratigraphy, peak in palm phytolith concentration (note: a lower peak has been indicated in brackets for QT-2012-10), and the depth at which *Mauritia*-t. exceeds 25% of the pollen sum.

Core	*Visible 'Mauritia'* peat Depth (cm)	Pollen: *Mauritia*-t. > 25 % Depth (cm)	Palm phytolith peak conc. Depth (cm)
QT-2011-2	103	130	100
QT-2012-9	90	96	96
QT-2012-10	92	112	16 (96-112)
QT-2012-18	78	96	96

The second peat unit is similar to the '*Mauritia* peat', in that it contains a large proportion of roots, but generally has a much more humified matrix (typically Tl2Sh2Dh+ or similar using the Troels-Smith classification).

The third unit was interpreted as a 'lake peat' (see Ruppert et al., 1993); it bore many similarities to the material found accumulating in the lake close to its margin at the present day (as seen in cores LC-1 and LC-9; see Figure 8.7). For example, it usually does not contain a matrix of roots, is often slightly green in colour, and occasionally contained visible leaf fragments. Leaves in particular are probably indicative of sub-aqueous accumulation (or possibly deposition) because leaves are rapidly destroyed unless they settle in anoxic water. The 'lake peat' differed considerably from the organic gyttja found in the other lake cores, which consisted of much smaller particles of organic matter (Ld3As1).

The fourth unit, found at the transition from peat into the underlying silty clay, is a mixture of clay and organic matter. Under the classification system of Wüst et al. (2003), this would be referred to as a "very high ash peat" or "muck" (as supported by the loss-on-ignition data for the four peat cores studied in detail, see below). The transition into higher loss-on-ignition peat was abrupt in many cores (< 10 cm), but in some this transition was very gradual. For example, in QT-2011-4 this transition occurred over c. 80 cm.

The maximum peat thickness recorded was 425 cm in a core adjacent to QT-2010-1; minimum peat thickness was 42 cm, in a core from the western margin of the peatland. Consistently thick accumulations of peat (>3 m) were found in the transect along the eastern lake margin (D-D'). However, in all other transects the peat thickness varied considerably, and in transects A-A' and B-B', the topography underlying the peatland was relatively undulating.

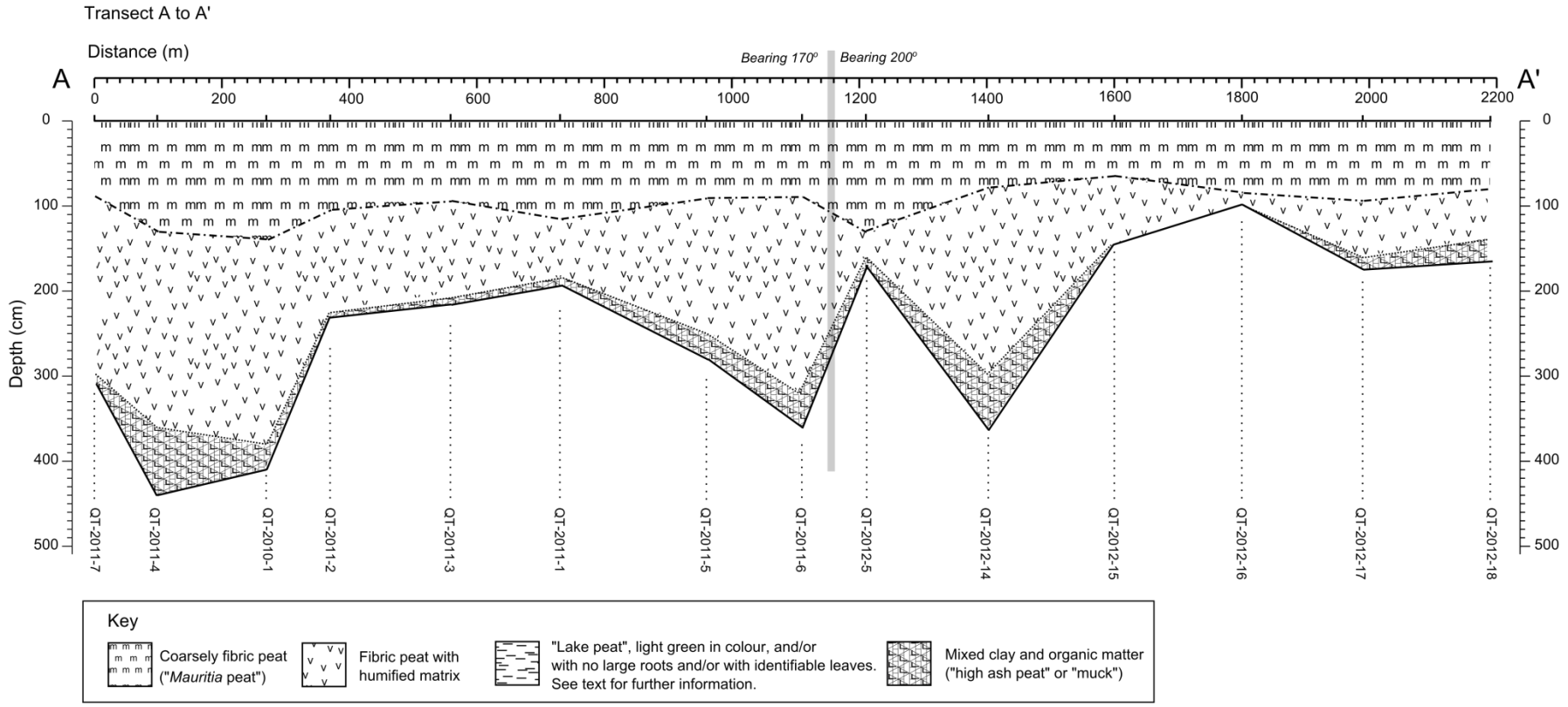

Figure 8.2: Transect A-A' showing peat composition. See figure 8.1 for transect map. The figure shows simplified peat compositional information in order to illustrate the broad patterns seen across the site (see text for further discussion). Core points are shown with tick marks and labelled at the bottom of the figure. The peatland is underlain by minerogenic sediments (silty clays) as discussed in the text and in Lawson et al. (2014). The grey line marks a change in the direction of the transect at marked on Figure 8.1. The surface of the peatland is assumed to be flat in this and subsequent figures .

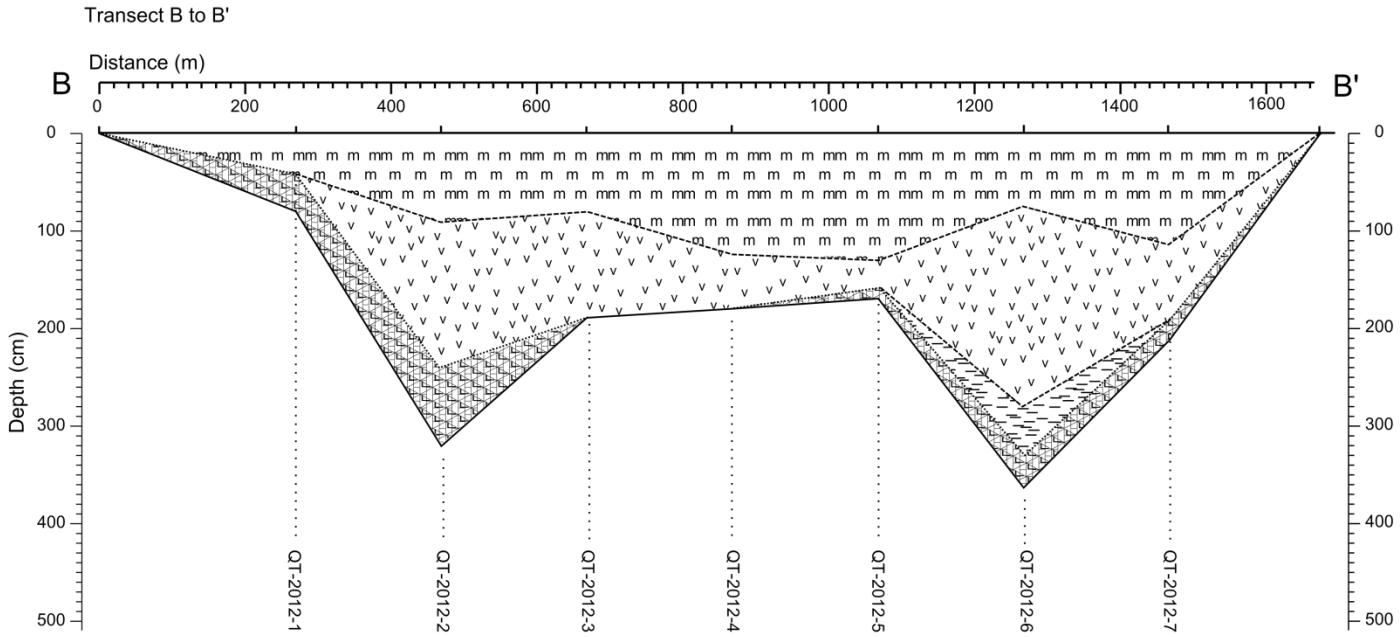

Figure 8.3: Transect B-B' showing peat composition (format follows that of Figure 8.2).

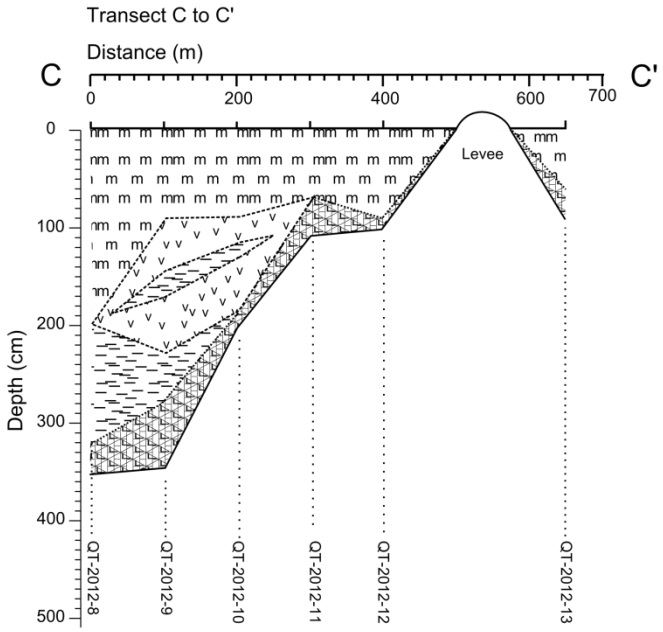

Figure 8.4: Transect C-C' showing peat composition (symbology follows that of Figure 8.2). Note that the absolute height of the levee above the peat surface is not known and is purely illustrative.

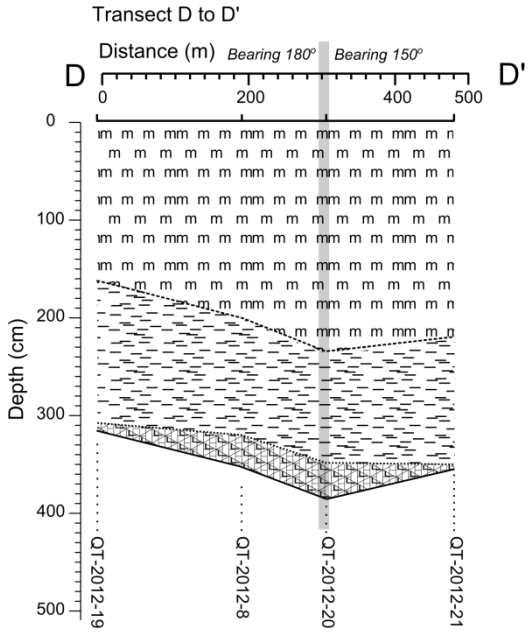

Figure 8.5: Transect D-D' showing peat composition (symbology follows that of Figure 8.2).Vertical grey line indicates the point at which the transect direction changes to follow the lake shoreline.

8.3 Lake Quistococha

This section summarises data collected for the lake at Quistococha. The main focus is on data for core QT-2010-3, a long sediment core, but some details of short 4 cm long surface samples are also given. For core QT-2010-3, all depths given here are relative to the sediment-water interface at 364 cm below the water surface. The chronology for QT-2010-3 is dealt with in Chapter 7.

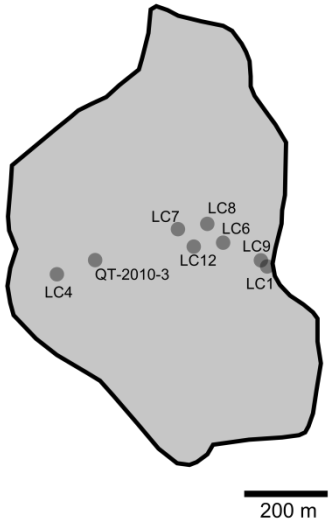

Figure 8.6: Sketch map of Quistococha lake showing the position of core QT-2010-3 and the short (4 cm) gravity cores collected to provide C and N reference values.

8.3.1 Loss-on-ignition, magnetic susceptibility, and visible stratigraphy

Loss-on-ignition (LOI) and magnetic susceptibility data (MS) for QT-2010-3 are presented alongside other stratigraphic information in Figure 8.8. LOI and MS measurements on this sequence were made by T.D. Jones in 2010. LOI was measured every 4 cm throughout the core, except from 0-32 cm depth where measurements were taken on sampled 5 cm subsections due to the high water content. Similarly, the high water content in the top of the core precluded the measurement of MS in the upper 30 cm. Below 30 cm, MS was measured every 2 cm to a depth of 364 cm (the base of the core).

From 276-364 cm the core consisted of silty clay, and is characterised by low LOI values and high MS (>20 *k*). There is a gradual decline in MS from 246 to 276 cm, where values drop to < 10 k. LOI values remain low across this interval and do not exceed 6%. MS and LOI remain low between 180 and 246cm; silty clay continues to dominate in the visible stratigraphy.

There is a transition to organic lake gyttja between 148-180 cm depth; there is little change in MS but LOI values increase from c. 5% to > 35 % across this interval. Fine, green organic gyttja (Ld3As1) is found from 0-148 cm, with some notable fluctuations in

LOI but with no change in the visible stratigraphy. No large plant macrofossils were observed in the core, except for a single leaf from a broad-leafed tree or shrub found at 88-89 cm. However, not all of the core material was systematically sieved and so there may have been a small number of larger leaves in the rest of the sediment.

8.3.2 Carbon and nitrogen content

8.3.2.1 Surface sample transect

In order to help interpret the C/N values from the lake and peatland, a transect of samples was analysed running from the lake margin towards the centre of the lake (see Figure 8.6). Samples were taken from 0-4 cm depth using a gravity corer in 2011. The results of total carbon and nitrogen measurements for these samples are shown in Figure 8.7.

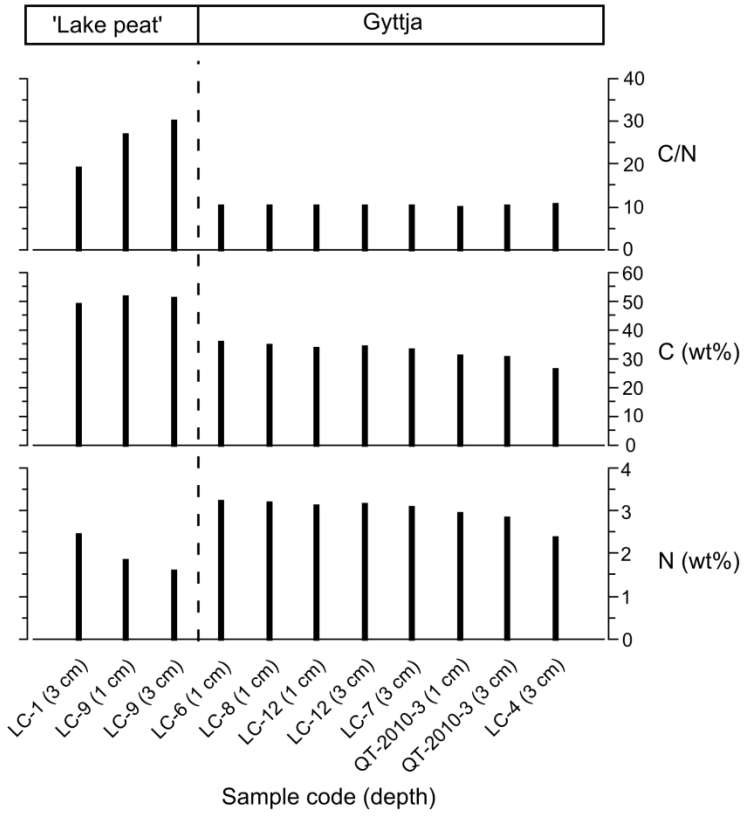

Figure 8.7: Carbon and Nitrogen data for short cores taken from lake Quistococha. Cores have been arranged in order of increasing distance from the eastern lake shore (see Figure 8.6 for core locations). Values from the top 4 cm of core QT-2010-3 have also been included. Samples have been broadly divided on the basis of their visible composition.

The lake gyttja was green in colour when sampled and composed of small (< 1 mm) unidentifiable particles of organic matter. Carbon and nitrogen values for the gyttja samples were all very similar, and with the exception of LC-4, carbon values ranged from 31-37 wt% and nitrogen values ranged from 2.9-3.3 wt%. LC-4, which was positioned

closest to the western lake shore, had lower nitrogen and carbon values than the other gyttja samples (2.4 wt% and 27 wt% respectively).

Surface samples collected within c. 20 m of the eastern lake margin contained more large identifiable plant fragments and were described as a 'lake peat'. These samples had a higher carbon concentration (49-53 wt%), and a lower nitrogen content (1.6-2.5 wt%) relative to the gyttja samples.

8.3.2.2 Lake core (QT-2010-3) C and N values

Lake core C and N concentrations are shown in Figure 8.8. In the lower part of the core from 356-266 cm, total carbon and nitrogen values are very low (<1 wt% and <0.1 wt% respectively). Between 356-308 cm, C/N ratios are around 9, but then fall steadily to their lowest value in the sequence (4.64) from 308 to 244 cm. This appears to be driven by a slight drop in the carbon content to 0.62-0.66 wt%. Nitrogen exceeds 0.1 wt% for the first time at 260 cm depth.

Between 244-236 cm, the C/N ratio increases to 6.2 and remains >5.5 between 236 and 184 cm. Carbon remains below 1.2 wt% across this interval, and nitrogen ranges from 0.10-0.16 wt%.

At 176 cm, carbon exceeds 1 wt% for the first time. From 161cm to 152 cm carbon increases from 5.94 wt% to 20.53 wt%, and remains above 20 wt% throughout the upper part of the core. The C/N ratio also increases across this interval from 12.8 at 176 cm to 16.4 at 152 cm, and from 152-72 cm it remains between 15 and 20.

The C/N ratio drops from 17.7 at 72 cm to 14.6 at 56 cm and remains between 14-15 up to a depth of 32 cm. There is then a marked decline in the C/N ratio in the top 32 cm of the core from 14.8 to 10.6 at 1 cm depth. Across this interval carbon content increases slightly from c. 30 wt% to 31.8 wt% at 1 cm, but nitrogen also increases from 1.9 wt% at 32 cm to its peak value of 3.0 wt% at 1 cm.

8.3.3 Pollen data for QT-2010-3

A total of 43 pollen samples were analysed from core QT-2010-3 from a depth of 1 cm to 330 cm below the sediment/water interface. The main pollen taxa are plotted against depth in Figure 8.9, and the minor taxa and spores are shown in Figures 8.10 and 8.11 respectively. A summary diagram plotted against time (according to the Bayesian age-depth model developed in Chapter 7) is shown in Figure 8.12. Pollen zones are described in Table 8.3, and indicator species identified for the core are summarised in Table 8.4, and are also shown in Figure 8.15 which shows the results of NMDS analysis.

Pollen preservation was generally good, although a greater proportion of damaged and indeterminable grains was observed in the lower, more mineral-rich part of the core.

Unknown pollen types did not exceed 10%. Pollen concentrations are lowest in zone QL-A and highest in zone QL-C, and varied from 20,100 to 184,300 grains cm^{-3}. Pollen influx largely mirrors the pollen concentration, with values ranging from 1,300 grains yr^{-1} to 12,500 grains yr^{-1}. Charcoal abundance was very low in zone QT-A (mostly < 500 fragments cm^{-3}), with increased abundance in the upper pollen zones (QL-B upwards). Peak pollen and charcoal concentrations were observed at the point in the core where accumulation was slowest (c. 90-100 cm).

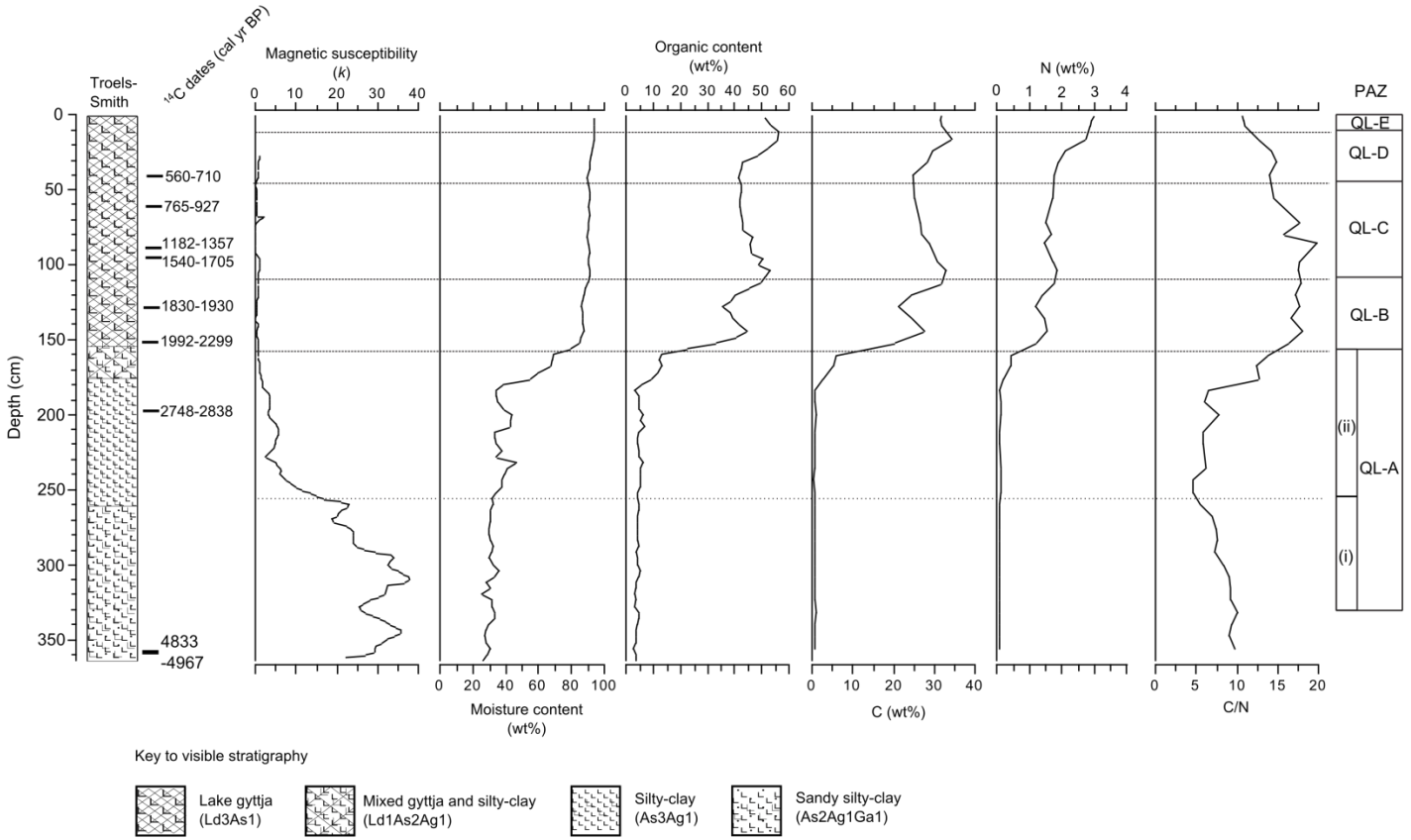

Figure 8.8: Summary data for the lake core (QT-2010-3). Core stratigraphy (Troels-Smith scheme) is shown alongside magnetic susceptibility, moisture content, organic content (loss-on-ignition), total carbon, nitrogen and C/N ratio. Radiocarbon dates (see Chapter 7 for further details) and pollen assemblage zones (PAZ) have been shown to facilitate comparison with other figures.

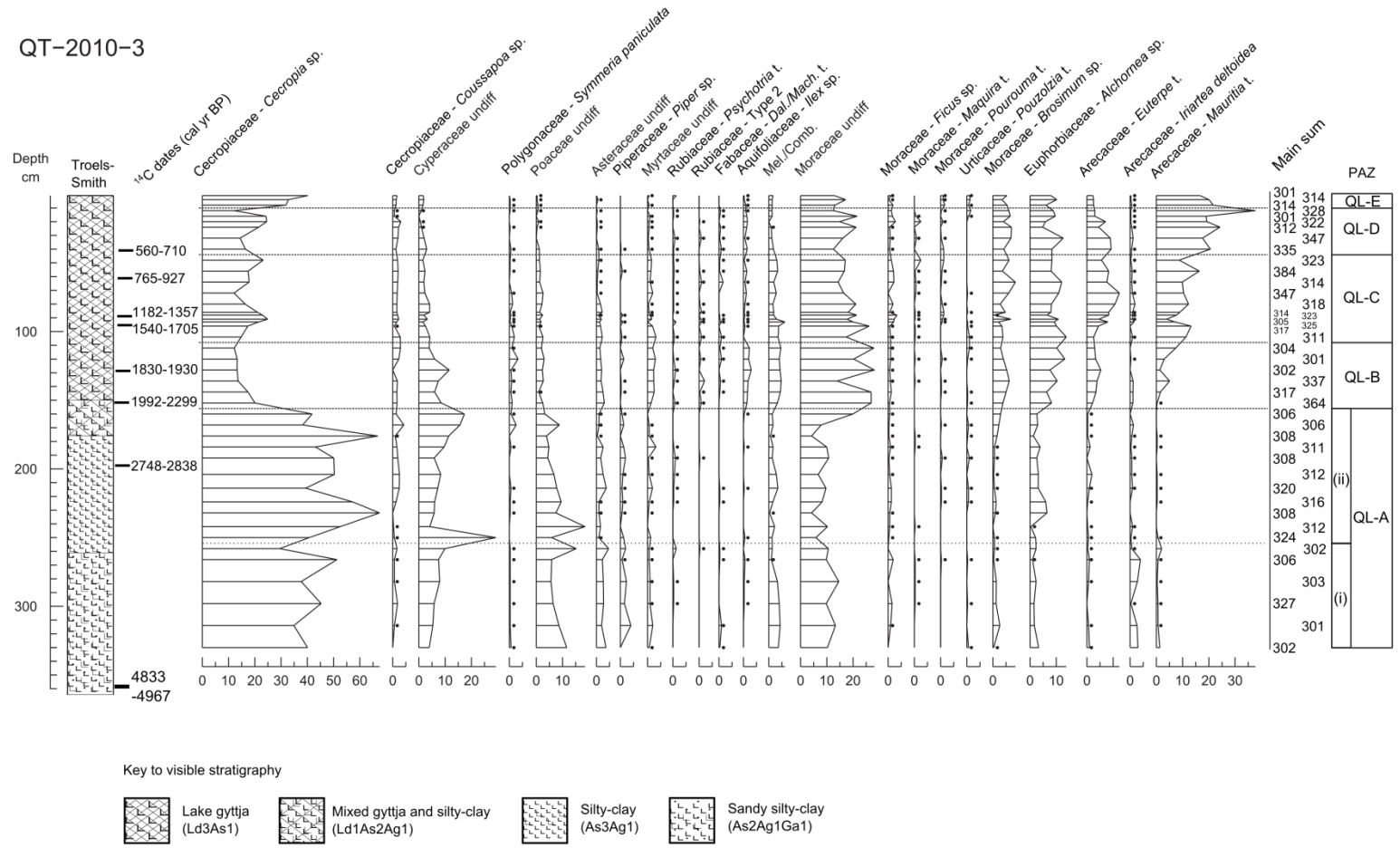

Figure 8.9: Main pollen taxa for the lake core (QT-2010-3) plotted against depth (percentage data). Some indicative minor taxa have also been included. Pollen assemblage zones (PAZ), radiocarbon dates, and stratigraphic observations have also been shown.

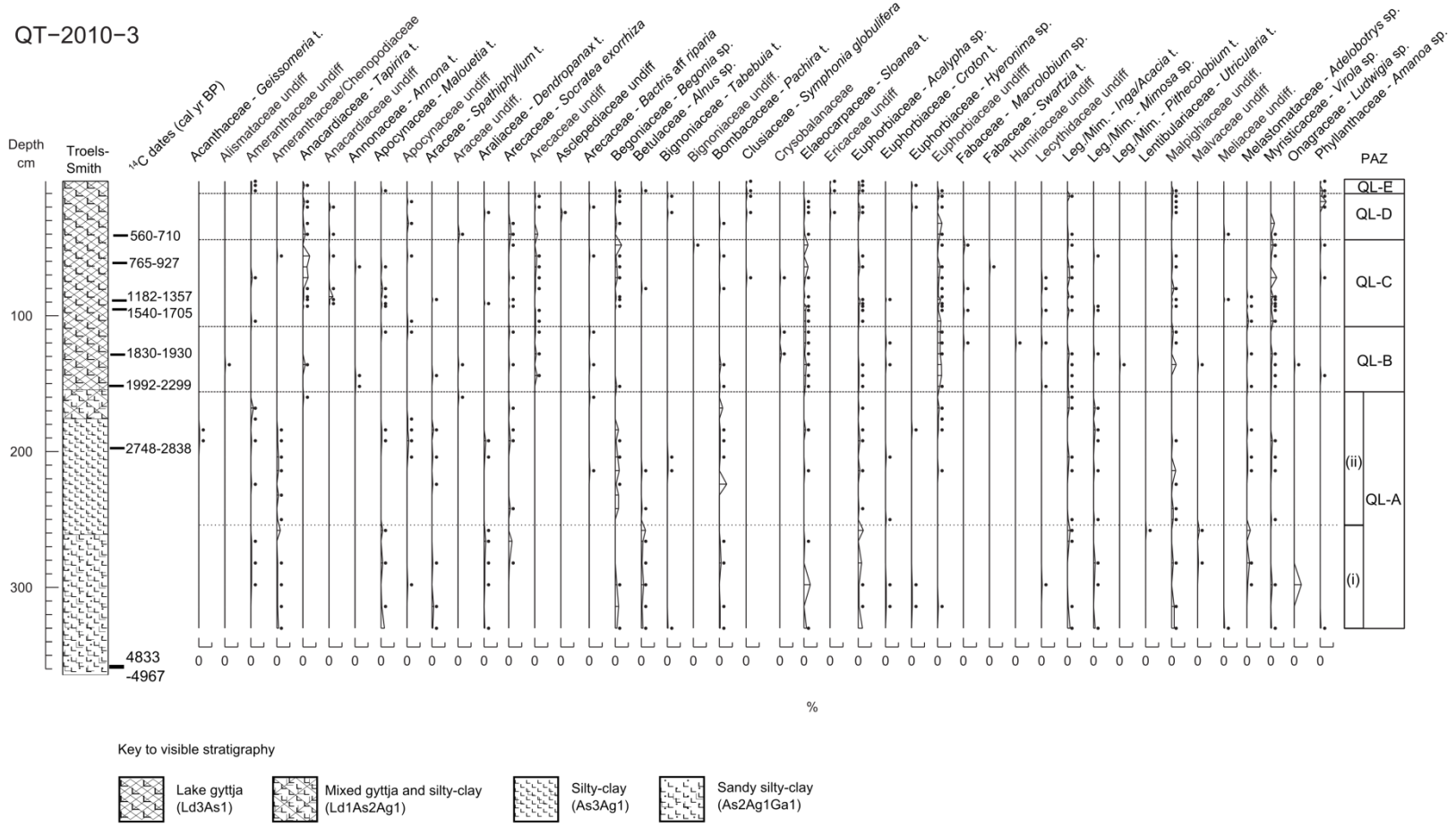

Figure 8.9 (contd.): Minor pollen taxa for the lake core (QT-2010-3) plotted against depth. Taxa are shown in alphabetical order according to family. Pollen assemblage zones (PAZ), radiocarbon dates, and stratigraphic observations have also been shown.

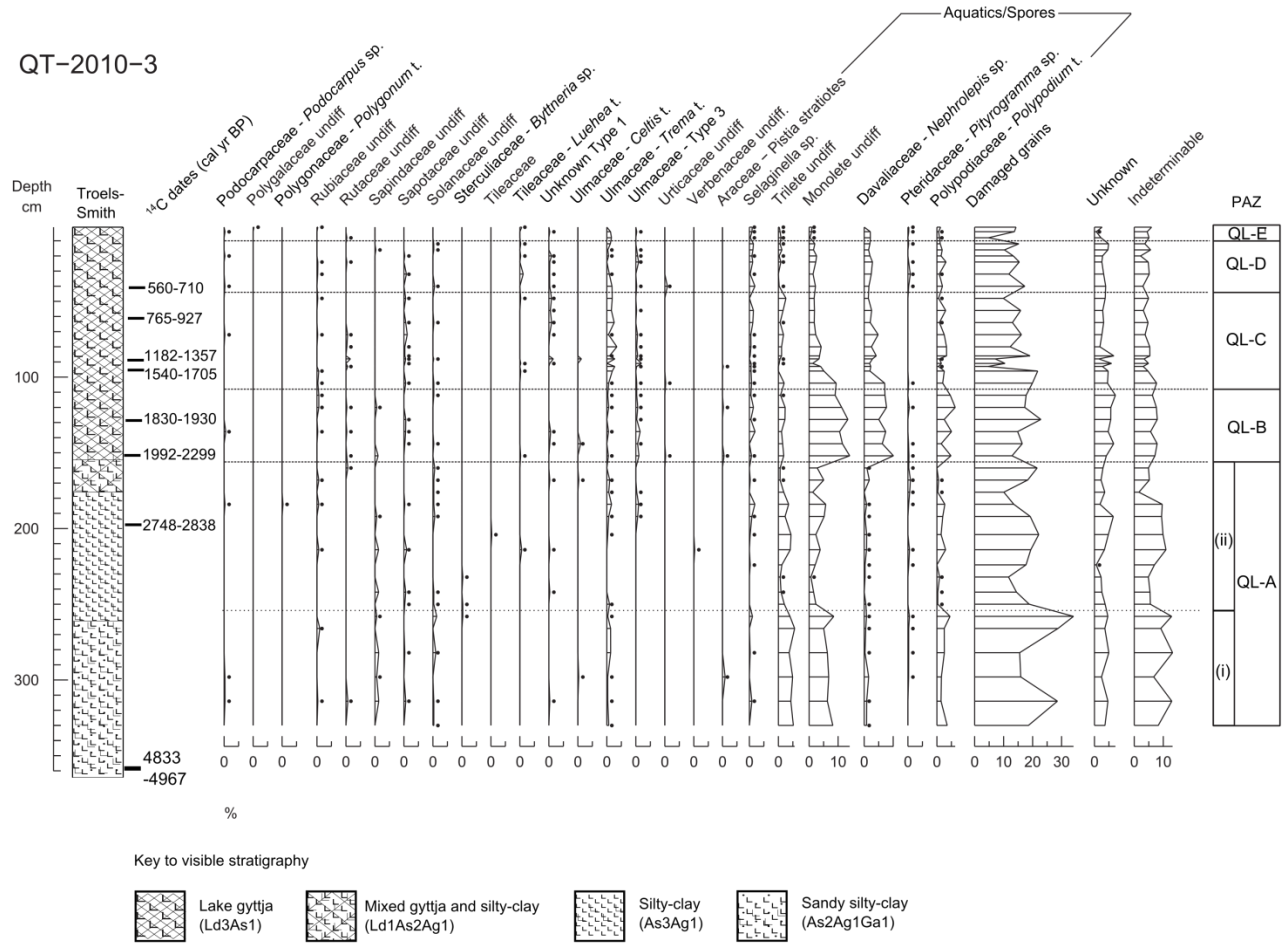

Figure 8.9 (contd.): Minor taxa (continued from figure 8.10), obligate aquatics (*Pistia stratiotes*), and spores for the lake core (QT-2010-3). The percentage of damaged grains (within the main sum), unknowns, and indeterminable (damaged) grains have also been shown. As in other figures, radiocarbon dates used in the age model (see Chapter 7) and visible stratigraphy have been shown to the left of the diagram.

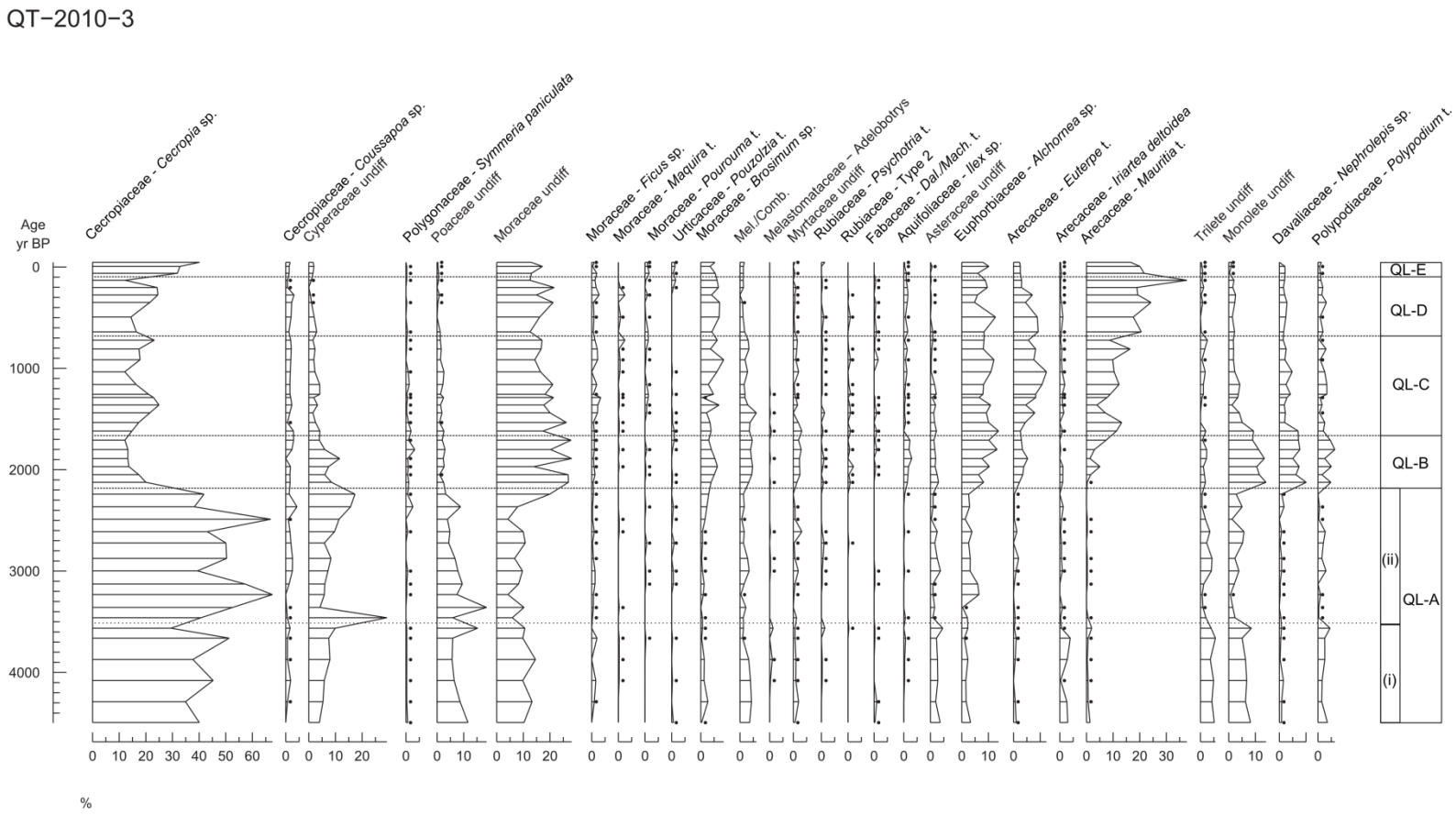

Figure 8.10: Summary pollen diagram for the lake core (QT-2010-3) showing taxa plotted against age (see Chapter 7 for age model).

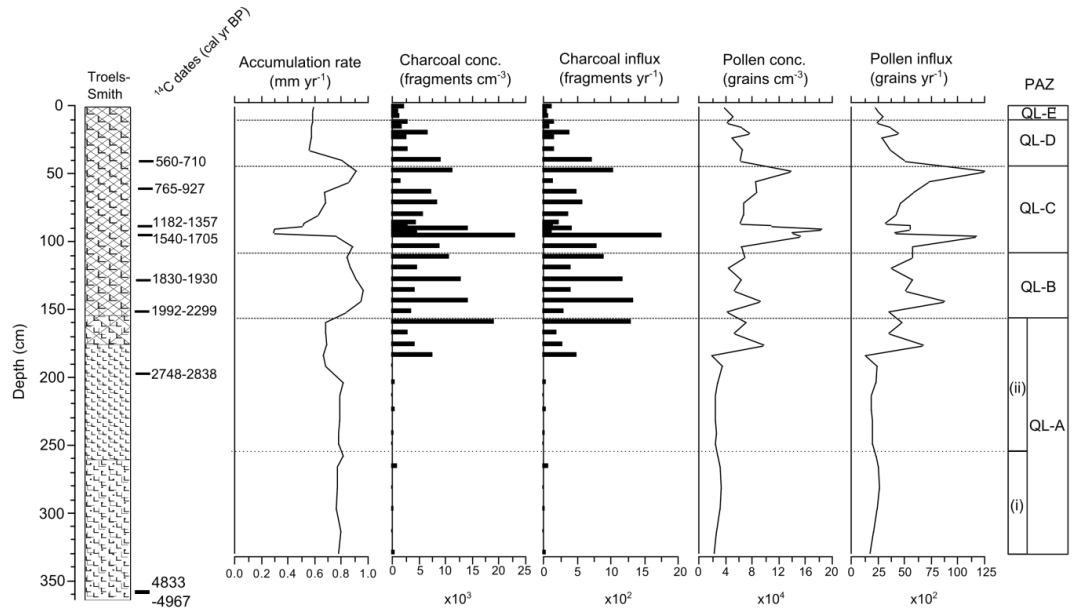

Figure 8.11: Concentration and influx data for the lake core (QT-2010-3): sediment accumulation rate (derived from Bayesian age-depth model in Chapter 7), charcoal concentration and influx, and pollen concentration and influx (main sum only). Visible stratigraphy (key shown in Figure 8.7), radiocarbon dates, and pollen assemblage zones (PAZ) have been shown to facilitate comparison with other figures.

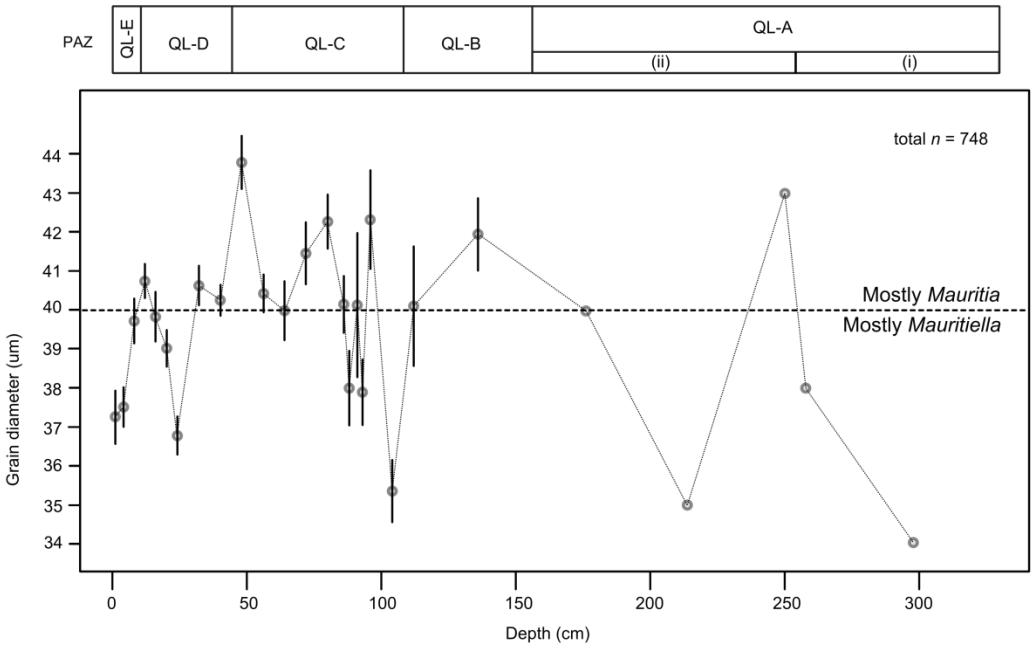

Figure 8.12: *Mauritia* t. grain diameter data plotted against depth for the lake core (QT-2010-3). Mean grain diameter is shown, and bars represent the standard error of the mean (points with no error bars have ≤4 measurements). Pollen assemblage zones (PAZ) are shown at the top of the figure. Dashed line marks the distinction between *Mauritia* and *Mauritiella* (discussed in Chapter 6). Only those core samples containing *Mauritia* t. pollen have been shown (grey line does not always connect adjacent core samples).

Table 8.3: Pollen assemblage zone summary descriptions for QT-2010-3 (the lake core). Zonation was undertaken using optimal splitting by sum-of-squares in Psimpoll (Bennett, 2007). Zones have been shown in stratigraphic order (i.e. the uppermost pollen zone is at the top of the table).

Zone (depths, *age*)	Summary of pollen assemblage zone characteristics
QL-E (1-10 cm, *94 to -46.5 cal yr BP*)	*Cecropia* sp. increases towards the top of this zone where it reaches 40%. *Alchornea* sp. (max. 10%) and Moraceae (max. 17%) continue to be moderately abundant. *Mauritia* t. remains abundant (max. 22%), and *Euterpe* t. is rare (max. 2.5%). All fern spore types are rare with many < 1% in the majority of samples.
QL-D (10-44 cm, *680 to 94 cal yr BP*)	*Mauritia* t. increases to >20% for the first time and peaks at the top of this zone (38%). *Euterpe* t. declines to 3% at the top of this zone, and Cyperaceae and Poaceae decline further, dropping to < 1% at the top of this zone. *Alchornea* sp. (max. 13%) and *Cecropia* sp. (max. 25%) remain abundant, and *Brosimum* sp. continues to be moderately abundant (max. 7%). Amongst the minor types, *Amanoa* sp. peaks towards the top of this zone (2%).
QL-C (44-108 cm, *1662 to 680 cal yr BP*)	Moraceae, *Alchornea* sp. and *Cecropia* sp. remain abundant. *Mauritia* t. is moderately abundant in this zone (max. 16%), as is *Euterpe* t. which peaks at 72 cm (12%). Cyperaceae declines to < 5%. Amongst the minor types, *Ilex* sp. declines from its values in the zone below, and is mostly < 1% in this zone. Asteraceae declines to < 1%. *Tapirira* t. peaks towards the top of this zone (max. 2.6%). *Trema* t. is most abundant in this zone (max. 3.5%).
QL-B (108-156 cm, *2175 to 1662 cal yr BP*)	*Cecropia sp.* declines to ≤ 20%. Moraceae increases to > 25%, and peaks in this zone at 128 cm (28%). Cyperaceae remains moderately abundant (max. 11.5%), but Poaceae declines to < 5%. *Brosimum* sp. increases to > 5% for the first time, and *Alchornea* sp. increases towards the top of this zone (max. 10%). *Mauritia* t. and *Euterpe* t. both increase to > 5% for the first time. Amongst the minor types, *Ilex* sp.*,* Asteraceae and Myrtaceae are consistently present. Several fern spore types are moderately abundant; *Nephrolepis* sp. (max. 10%), *Polypodium* t. (max. 6%), and Monolete spores (max. 14%) all peak in this zone.
QL-A (156-330 cm, *4494 to 2175 cal yr BP*)	QTL-A (ii): *Cecropia* sp. peaks in this subzone (67%) and is the dominant taxon. Cyperaceae and Poaceae also remain abundant, and Cyperaceae peaks at the base of the sub-zone (29%). *Alchornea* sp. becomes moderately more abundant than in sub-zone (i) but remains < 10%. Amongst the minor types, Asteraceae continues to be consistently present (max. 4%). QTL-A (i): *Cecropia* sp. dominant (max. 51%), with Moraceae, Poaceae and Cyperaceae also abundant. Amongst the minor types, *Piper* sp., Mel./Comb., Asteraceae, and *Iriartea deltoidea* are all consistently present. All fern spore types remain < 10%.

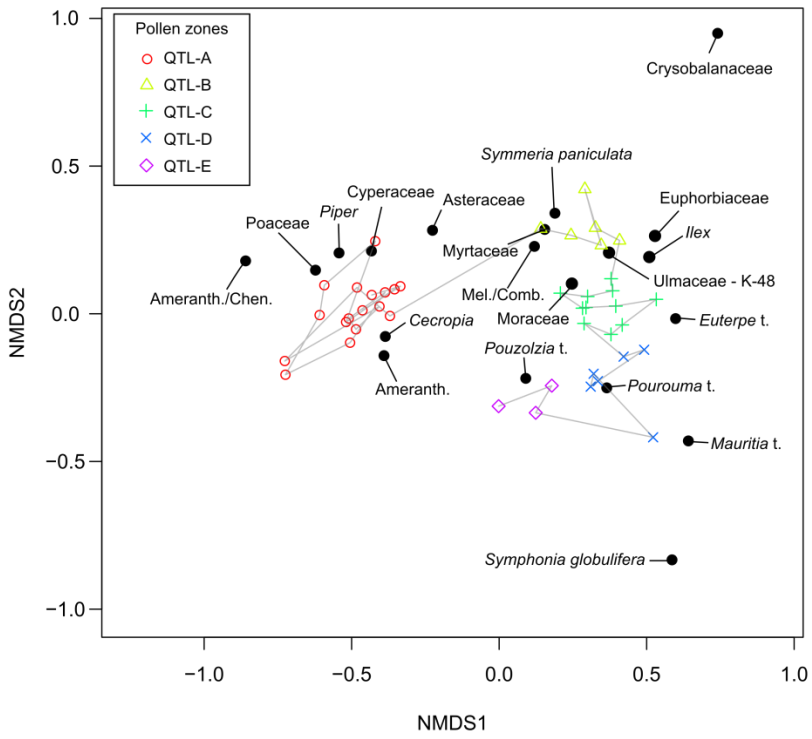

Figure 8.13: Results of NMDS analysis for QT-2010-3 showing the first two axes. Points represent individual samples within the four pollen zones, and taxa have been plotted which were found to be indicative of the different zones. Grey lines show the trajectory of change and connect samples which are adjacent to one another in the core.

Table 8.4: Indicator species identified for QT-2010-3. Taxa with indicator values > 0.25 have been shown, with their maximum percentage values within the zone for reference (2 s.f.).

Taxon	Pollen zone	*p* value	Indicator species value	Max. % in zone
Amaranthaceae	E	0.006	0.556	0.33%
Pourouma t.	E	0.011	0.457	1.6%
Pouzolzia t.	E	0.016	0.449	1.3%
Symphonia globulifera	E	0.024	0.411	0.33%
Mauritia t.	D	0.043	0.415	38%
Euterpe t.	C	0.047	0.368	12%
Symmeria paniculata	B	0.02	0.463	3.3%
Euphorbiaceae undiff.	B	0.013	0.459	1.6%
Ilex sp.	B	0.009	0.456	3.0%
Ulmaceae - type K48	B	0.031	0.431	1.5%
Myrtaceae	B	0.003	0.422	3.0%
Mel./Comb,	B	0.001	0.365	4.8%
Asteraceae	B	0.023	0.354	3.0%
Moraceae	B	0.011	0.295	28%
Crysobalanaceae	B	0.049	0.289	0.66%
Poaceae	A	0.001	0.614	15%
Amaranth./Chenopod.	A	0.006	0.606	1.3%
Piper sp.	A	0.008	0.525	3.9%
Cyperaceae	A	0.015	0.421	29%
Cecropia sp.	A	0.001	0.421	67%

8.4 Quistococha peatland: four records

Summary details are provided here of the results of analyses undertaken on four cores from Quistococha peatland: QT-2011-2, QT-2012-9, QT-2012-10, and QT-2012-18. Intact cores were taken at the base of each sequence to allow a closer examination of the clay-to-peat transition. In the rest of each sequence, sub-samples were taken in the field at 16 cm intervals.

8.4.1 Loss-on-ignition and visible stratigraphy

The four cores were described using the Troels-Smith (1955) scheme, and these data are shown alongside the pollen data in Figures 8.21-8.31 and the loss-on-ignition, carbon, and nitrogen data in Figures 8.16-8.19. Descriptions were based on observations made in the field and in the laboratory.

The loss-on-ignition (LOI) data are presented alongside the other stratigraphic and geochemical data collected for the cores in Figures 8.16-8.19. The organic content was determined by LOI at 500 °C every 2 cm in the basal cores and for each of the 16 cm sub-samples in the rest of each sequence.

All the cores exhibit a similar pattern. The organic content is very high in the upper part of the cores, which all consisted of pure (LOI > 65%) peat. The organic content is slightly lower in the upper part of QT-2012-18 (c. 87%) than in the other cores, which all had values that exceeded 94%.

At the base of each core there is a transition from the underlying clay to the overlying peat. In cores QT-2011-2, QT-2012-10, and QT-2012-18 there is a short, gradual transition where organic content gradually increases over a depth of 20-30 cm. However, in core QT-2012-9 there is a longer transition, and the underlying clay is separated from the overlying peat by a relatively thick (91 cm) layer of mixed clay and organic matter with varying LOI values.

8.4.2 Carbon and nitrogen concentration

Nitrogen content increases in the top 32 cm of all the cores, but in some cores (QT-2011-2) this appears to be part of a trend which extends further down the core to c. 1 m depth. The increase in nitrogen drives a reduction in C/N values in the top c. 100 cm of all the cores. Excepting the transition from the underlying clayey-silts at the base of the cores, the peat accumulations in all of the cores had high carbon values which exceeded 45 wt%. Peat carbon values were lowest in core QT-2012-18. As in the lake core and in QT-2010-1, the underlying clayey-silts had carbon values of < 2.5 wt%. In all cases, carbon values closely tracked loss-on-ignition.

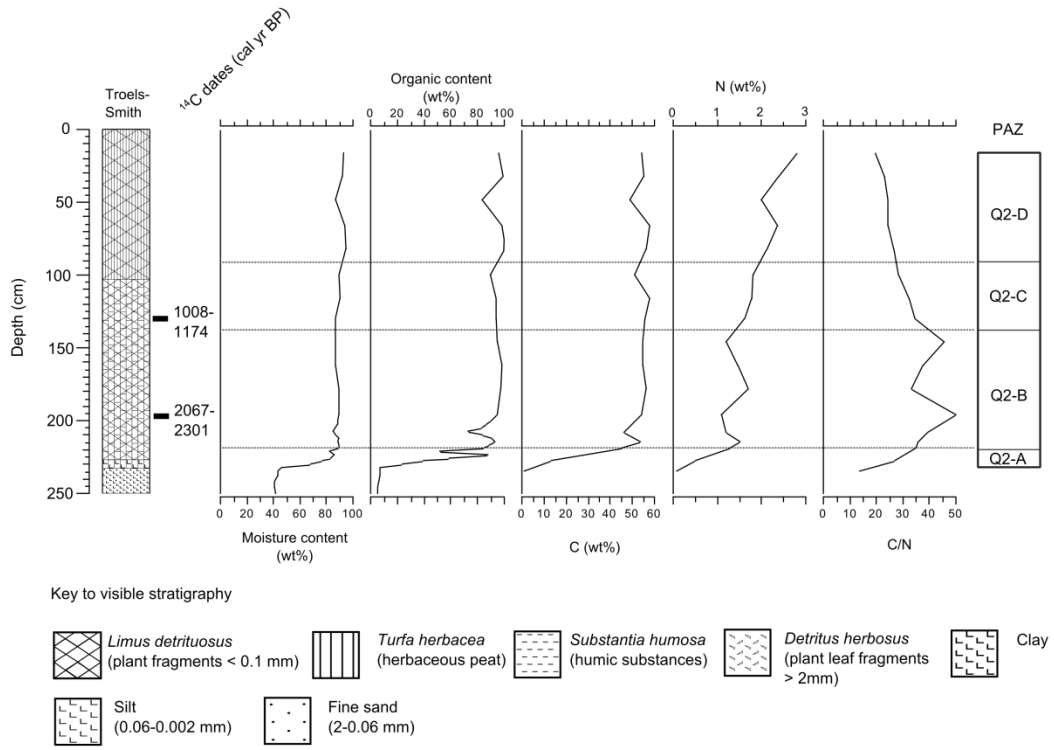

Figure 8.14 Core data for QT-2011-2. Peat stratigraphy (Troels-Smith scheme) is shown alongside moisture content, organic content (loss-on-ignition), total carbon, nitrogen and C/N ratio. Radiocarbon dates and pollen assemblage zones (PAZ) have been shown to facilitate comparison with other figures.

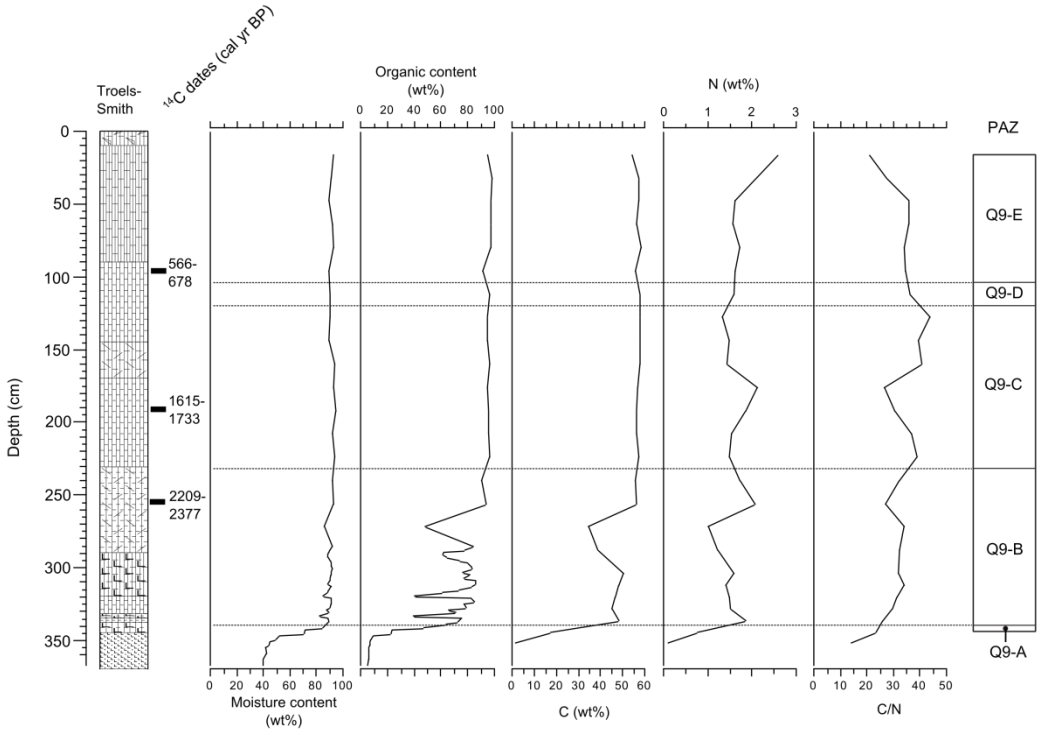

Figure 8.15: Core data for QT-2012-9. Format follows that of Figure 8.16. See Figure 8.14 for stratigraphic key.

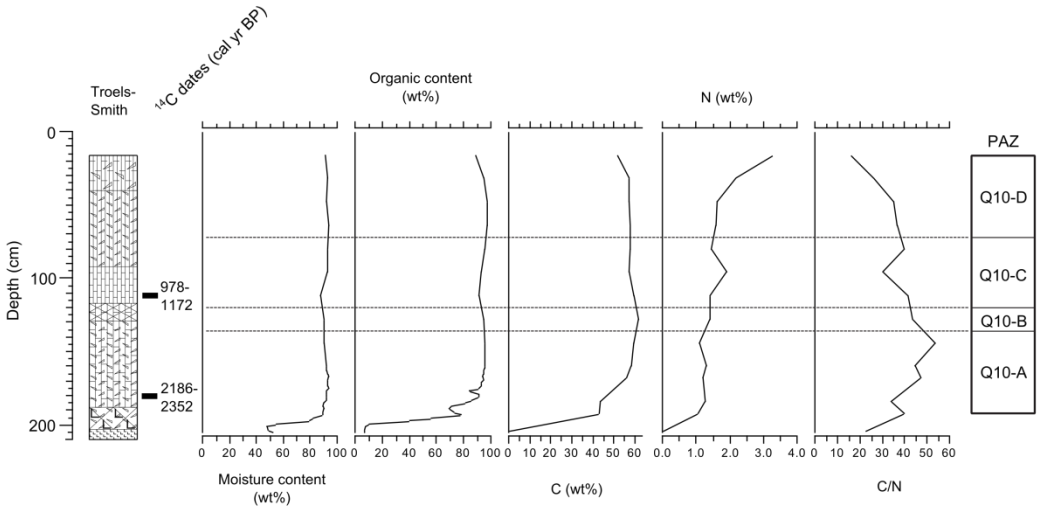

Figure 8.16: Core data for QT-2012-10. Format follows that of Figure 8.16. See Figure 8.14 for stratigraphic key.

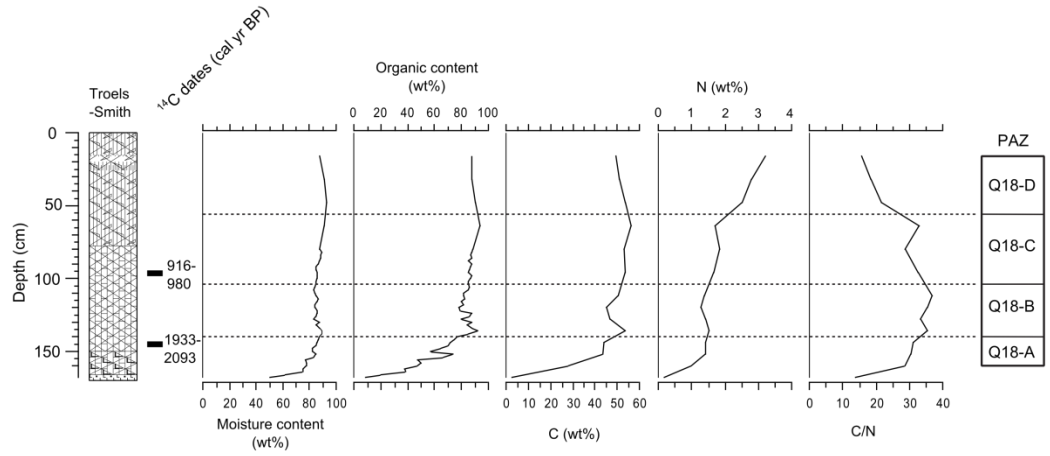

Figure 8.17: Core data for QT-2012-18. Format follows that of Figure 8.16. See Figure 8.14 for stratigraphic key.

8.4.3 Peatland pollen and phytolith data

8.4.3.1 Data collected

A total of 63 pollen samples were counted from across the Quistococha peatland, all with a main sum of > 300 grains (see Chapter 4). Sampling resolution was 16 cm, with a greater resolution of 8 cm towards the base of some of the cores. Fifteen samples were counted from core QT-2011-2, 24 samples from QT-2012-9, 12 from QT-2012-10 and 12 from QT-2012-18.

8.4.3.3 Description of the peatland pollen data

The percentage pollen data for the four peat cores studied from Quistococha are shown in Figures 8.21-8.31, and the key features of each pollen zone are described in Tables 8.9-8.12. Pollen concentrations are given alongside palm phytolith concentrations in

Figure 8.32. *Mauritia*-t. grain size data is plotted for the four cores in Figures 8.33-8.36. NMDS analysis and indicator species analysis are shown in Figures 8.37-8.40 and Tables 8.13-8.16 respectively.

As in the lake sediment core, pollen preservation was generally good; the highest proportion of indeterminable pollen was found in the basal sample of QT-2011-2 (13%), but in general indeterminable types were < 10% of the main sum. There is a general increase in damaged identifiable grains towards the top of the sequence which largely reflects the tendency of *Mauritia* t. pollen to crumple.

Pollen concentrations ranged from 21,000 to 542,000 in QT-2011-2, 17,700 to 419,400 in QT-2012-9, 20,700 to 1,376,000 in QT-2012-10 (the highest concentrations were at 128 cm and were caused by a high abundance of *Cecropia* pollen), and from 76,600 to 720,700 in core QT-2012-18. There was a peak in pollen concentration at a depth of c. 100 cm in all of the cores (discussed in more detail in Section 8.2). While pollen concentrations were generally good, achieving total counts >300 required the analysis of three slides in many cases. This was due to the large quantities of organic material which survived the pollen preparation.

Some common patterns can be found in the pollen stratigraphy of the four peat cores. As shown in the NMDS ordination plots, three of the peat cores show a similar trajectory from samples where Cyperaceae is indicative to samples rich in *Mauritia*-t., the main outlier being core QT-2012-10 where a range of minor taxa were indicative in the basal zone. The ordination of the lake core follows a similar trajectory, from zones where Cyperaceae and Poaceae are indicative taxa towards zones at the top of the core where *Mauritia*-t. is indicative and abundant. Although the pollen zones were defined independently, all the peat cores contained a high proportion of palm pollen in the top two zones, with *Mauritia*-t. being dominant in the upper zones. Grain size data reveal an increase in the proportion of *Mauritiella armata* pollen in the upper 50 cm of cores QT-2011-2, QT-2012-9, and QT-2012-10.

All of the cores contain at least one clear Myrtaceae peak, except QT-2012-18 where Myrtaceae pollen remains sparse throughout. There are two Myrtaceae peaks in core QT-2012-9, as in core QT-2010-1 (Roucoux et al., 2013). This contrasts with the lake core; although Myrtaceae is an indicative taxon in zone QL-B its abundance never exceeds 5%. This pattern can be seen in other taxa in the lake core; many are less abundant than in the peatland records (e.g. Rubiaceae pollen types, Asteraceae) while a small number of other taxa are more abundant in the lake core (e.g. *Cecropia,* Moraceae undiff.).

Symmeria paniculata pollen was abundant in the basal zones of QT-2011-2 and QT-2012-18, but present in only low quantities in cores QT-2012-9 and QT-2012-10. Cyperaceae pollen was also most abundant in the base of all the cores, although only present in low quantities in core QT-2012-10. Cyperaceae was particularly prevalent in the basal zones of core QT-2012-9, and was an indicative taxon in all of the cores except QT-2012-10.

Cecropia is most abundant towards the base of the most of the core cores, but is generally less abundant in QT-2012-18 than in the other cores. In core QT-2012-10 there is a substantial peak in *Cecropia* prior to the increase in palm pollen types. A stamen of *Cecropia* was identified in a pollen slide from QT-2012-9 at a depth of 328 cm (Figure 8.20).

There is also some particularly notable heterogeneity between the sequences. *Euterpe*-t. pollen is most abundant in QT-2012-10 and QT-2012-18; a clear phase is visible in both QT-2012-9 and QT-2011-2 but the abundance is generally lower. It is an indicative taxon in zone C all of the cores except QT-2012-9. There is a large *Ficus* peak in QT-2012-9 which is not visible in any of the other cores. Poaceae peaks can be clearly seen in QT-2012-9 and QT-2012-18 but no peak is seen in the other two cores, and Poaceae does not exceed 5% anywhere in QT-2012-10.

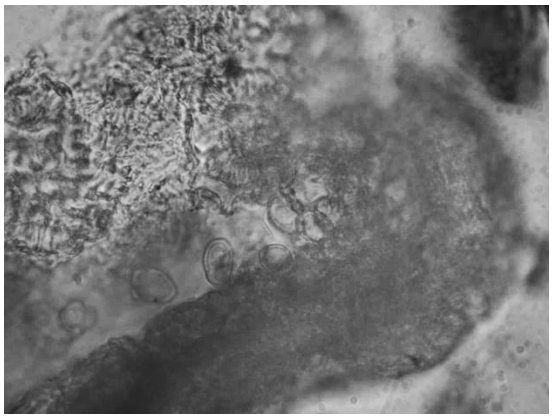

Figure 8.18: Intact anther of *Cecropia* observed in a pollen slide from core QT-2012-9 (328 cm depth), confirming the local presence of *Cecropia* at this point in the core.

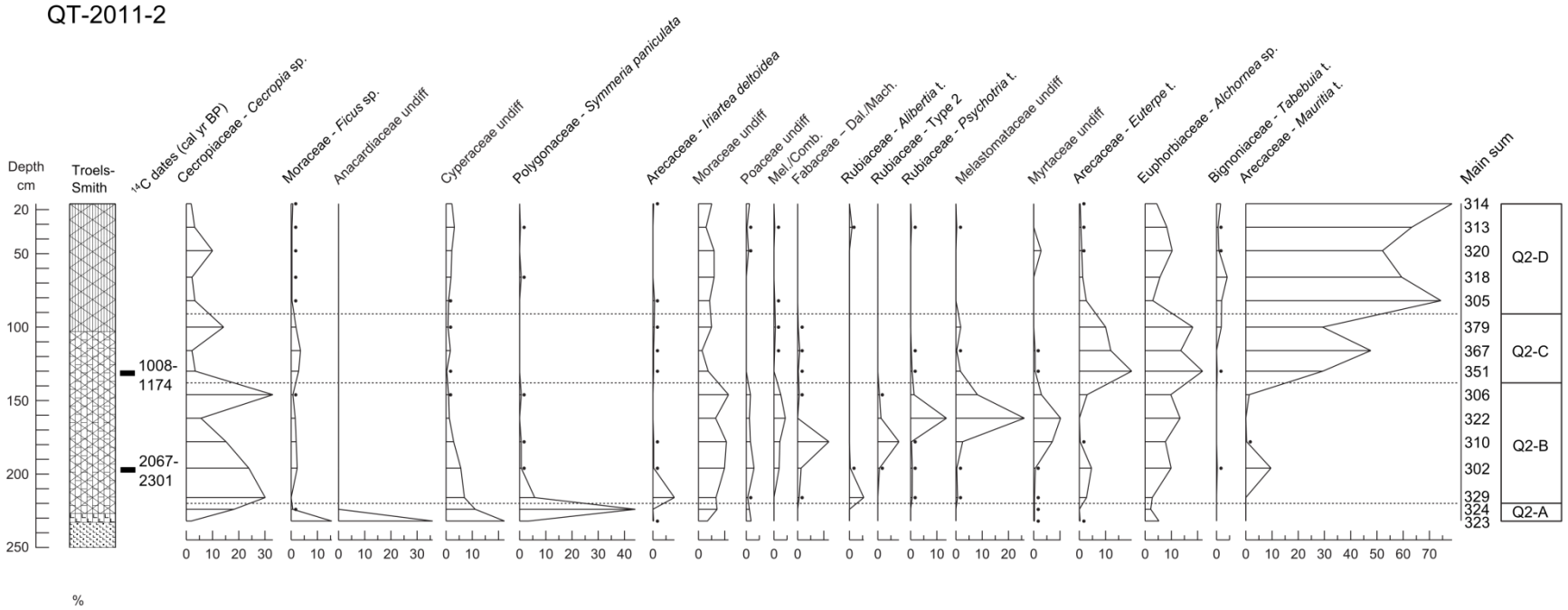

Figure 8.19: Main pollen taxa for the peat core QT-2011-2 plotted against depth. Some indicative minor taxa have also been included. Pollen assemblage zones, radiocarbon dates, and stratigraphic observations have also been shown. See Figure 8.14 for stratigraphic key.

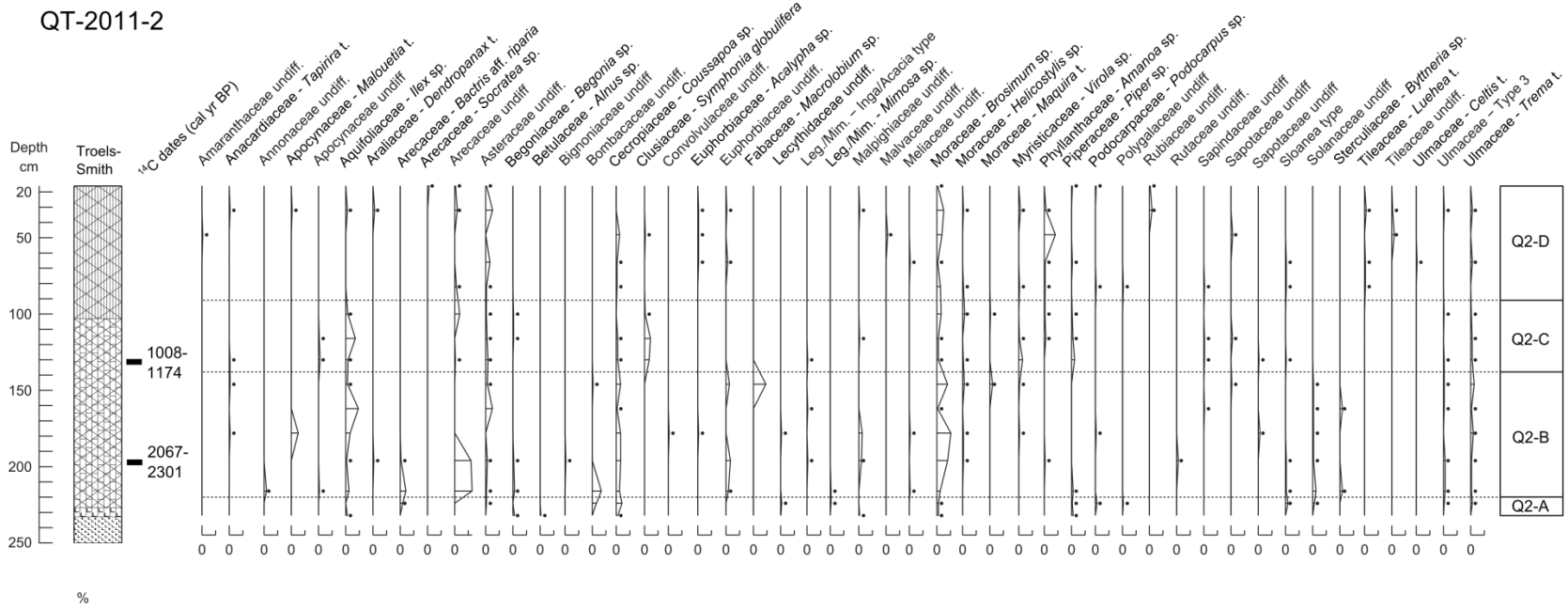

Figure 8.19 (contd.): Minor pollen taxa for the peat core QT-2011-2 plotted against depth. Taxa are shown in alphabetical order according to family. Pollen assemblage zones, radiocarbon dates, and stratigraphic observations have also been shown. See Figure 8.14 for stratigraphic key.

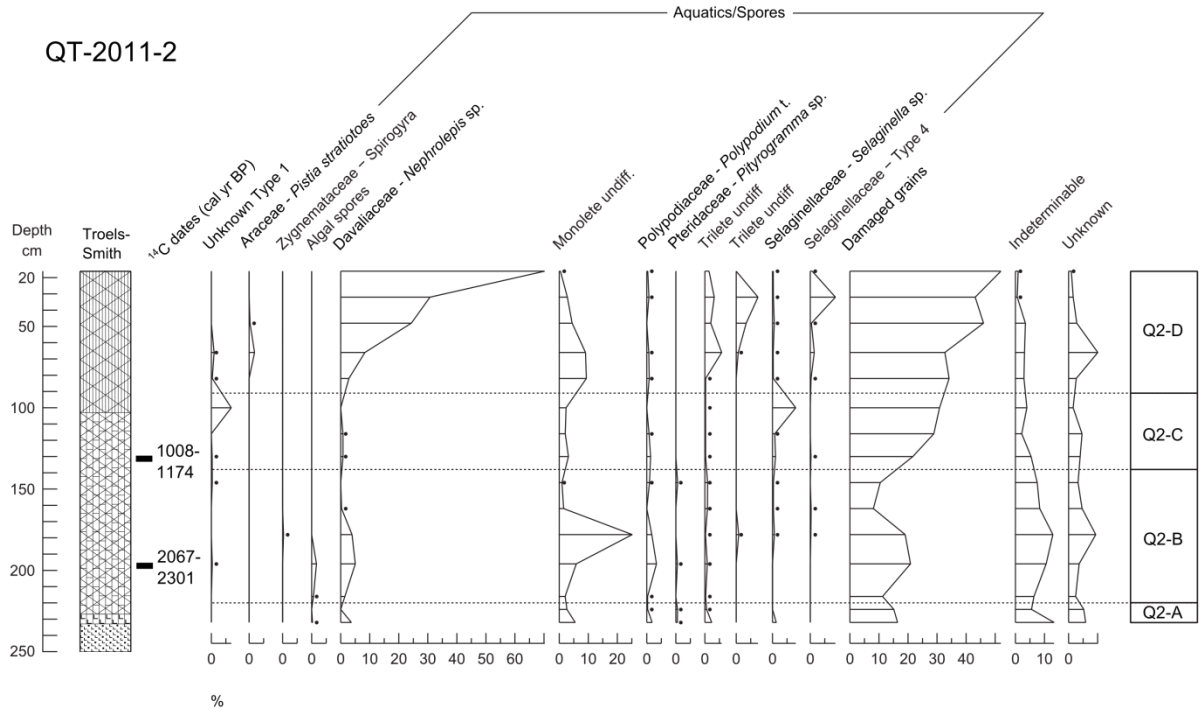

Figure 8.19 (contd.): Unknown taxa, obligate aquatics (*Pistia stratiotes*), and spores for peat core QT-2011-2. The percentage of damaged grains (within the main sum), unknowns, and indeterminable (damaged) grains have also been shown. Pollen assemblage zones, radiocarbon dates, and stratigraphic observations have also been shown. See Figure 8.14 for stratigraphic key.

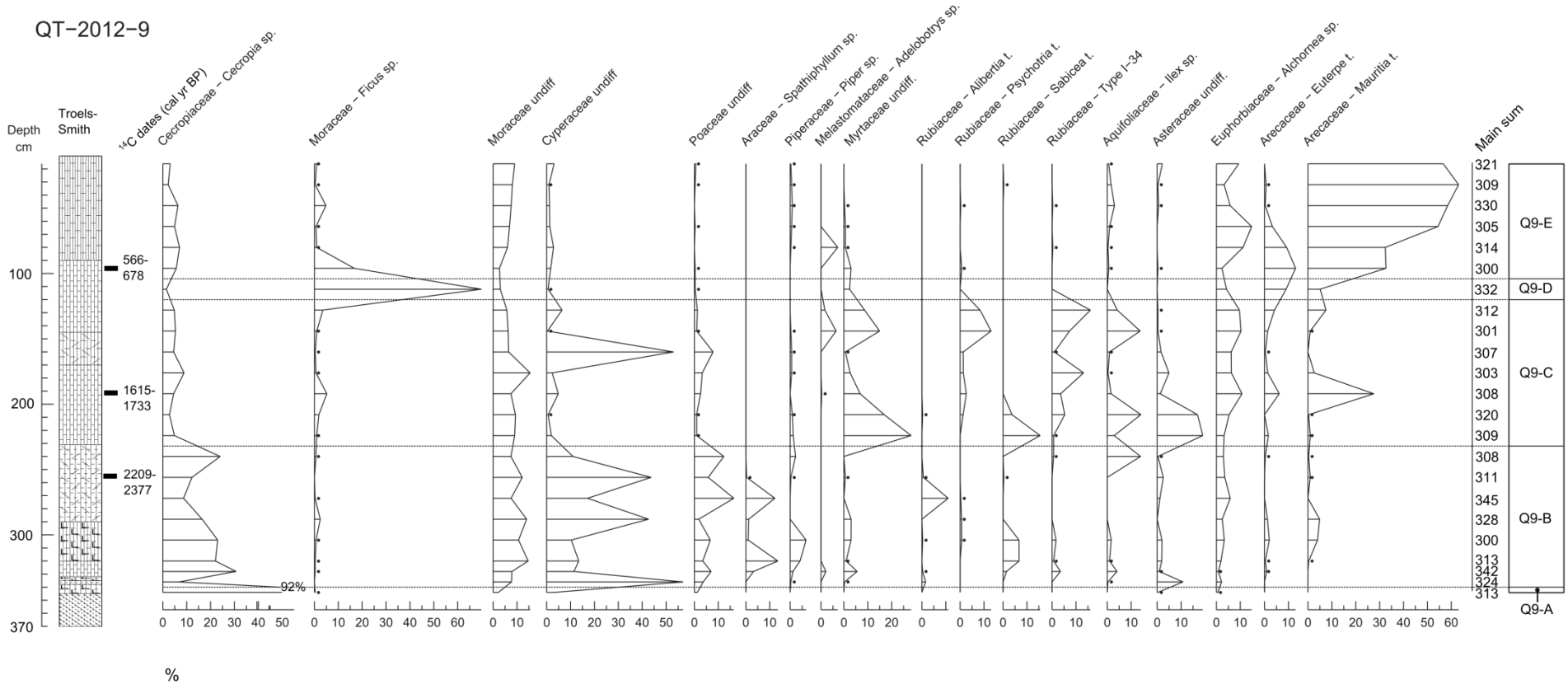

Figure 8.20 (contd.): Main pollen taxa for the peat core QT-2012-9 plotted against depth. Some indicative minor taxa have also been included. Pollen assemblage zones, radiocarbon dates, and stratigraphic observations have also been shown. See Figure 8.14 for stratigraphic key.

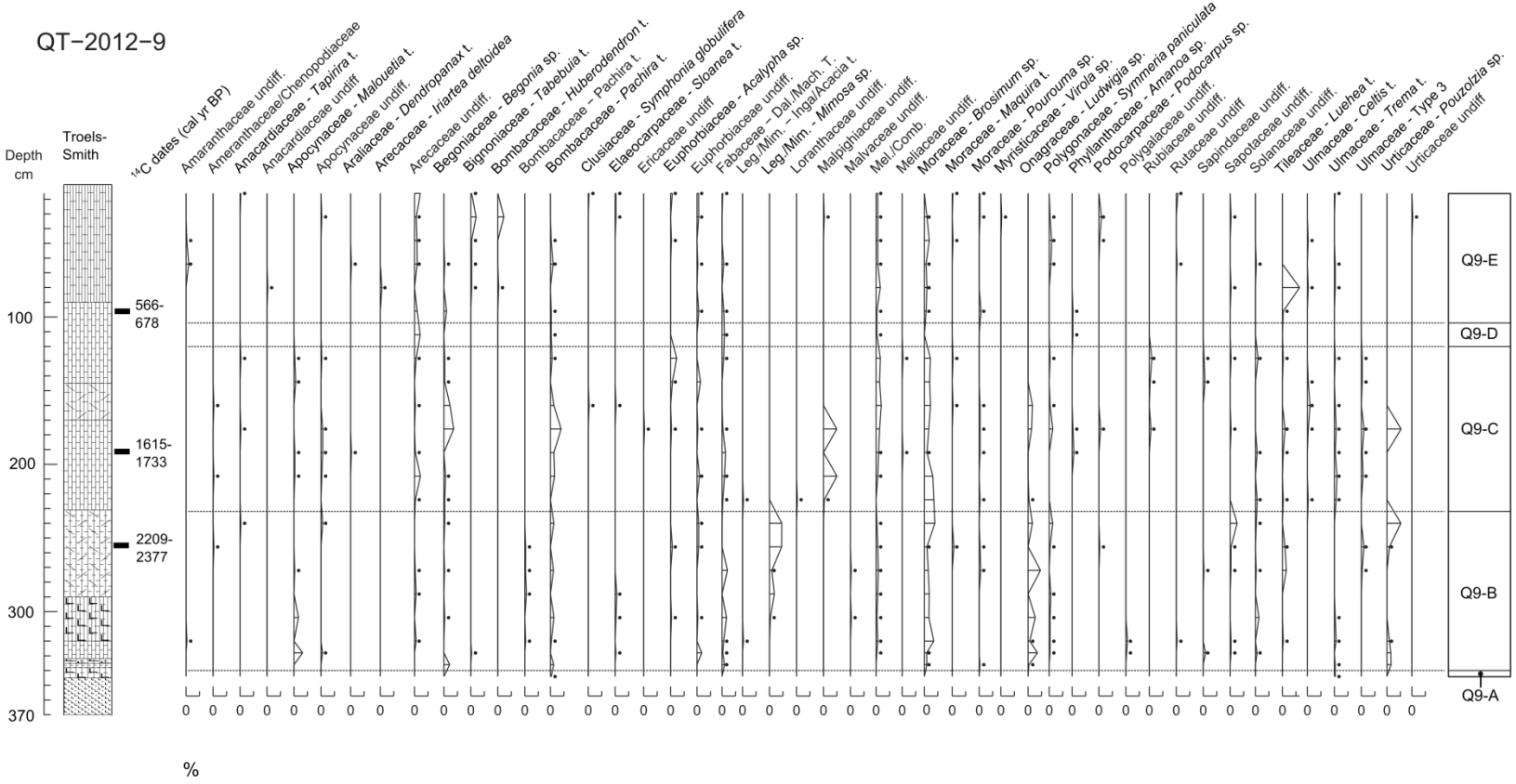

Figure 8.20 (contd.): Minor pollen taxa for the peat core QT-2012-9 plotted against depth. Taxa are shown in alphabetical order according to family. Pollen assemblage zones, radiocarbon dates, and stratigraphic observations have also been shown. See Figure 8.14 for stratigraphic key.

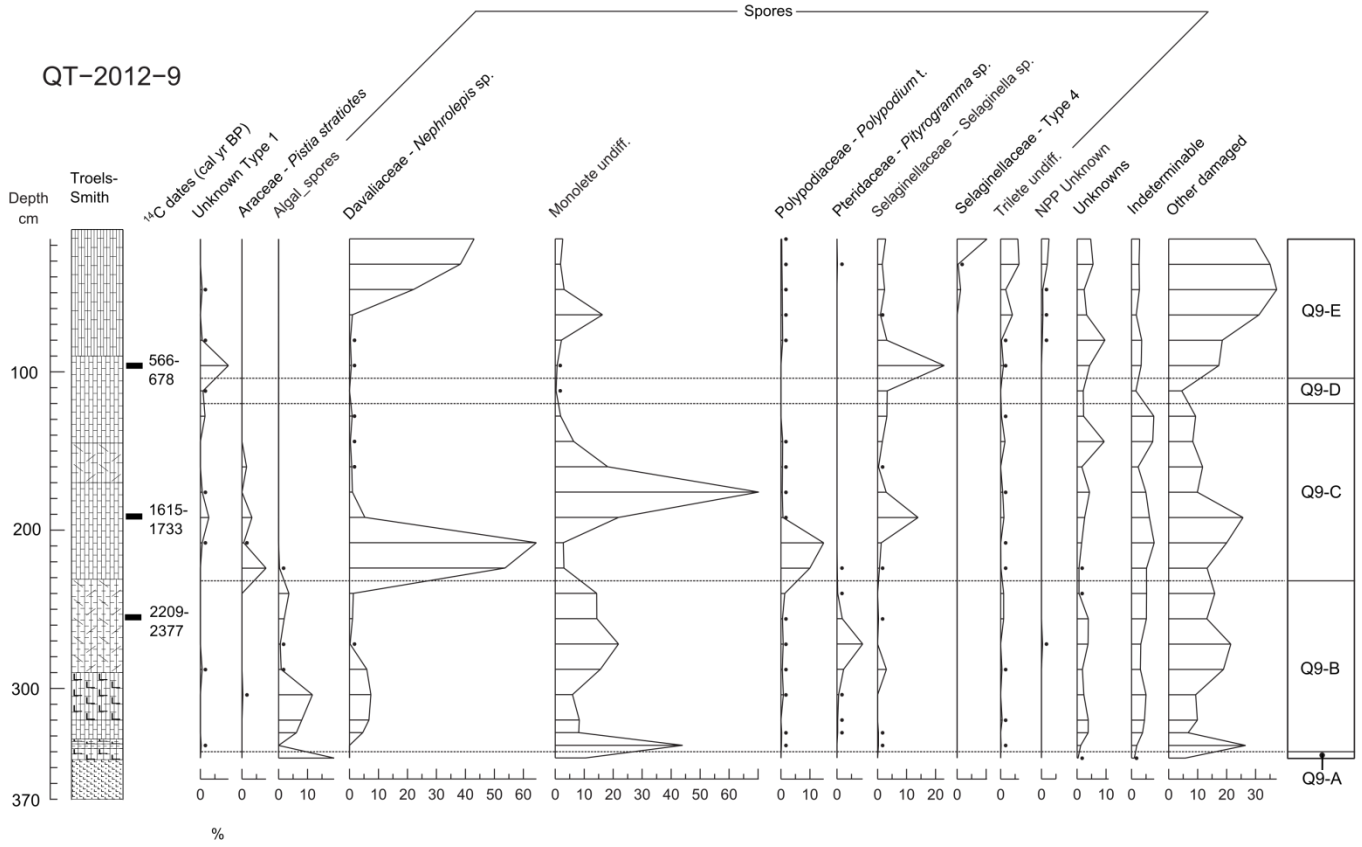

Figure 8.20 (contd.): Unknown types, aquatic taxa, and spores for the peat core QT-2012-9 plotted against depth. Pollen assemblage zones, radiocarbon dates, and stratigraphic observations have also been shown. See Figure 8.14 for stratigraphic key.

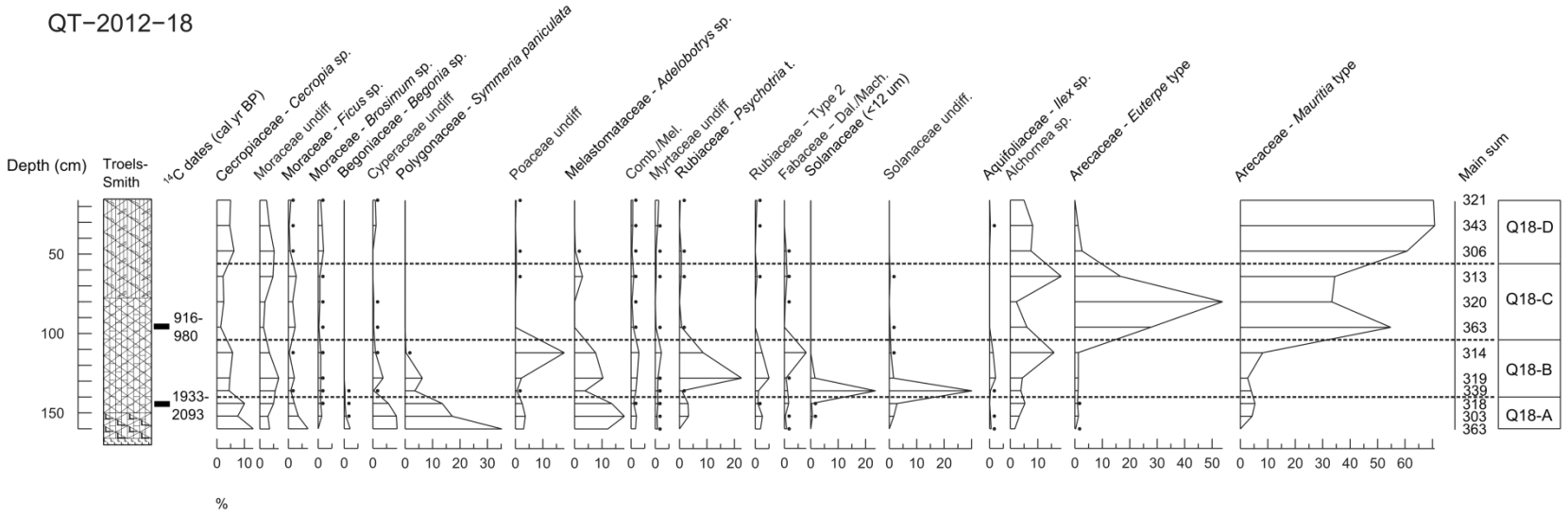

Figure 8.21: Main pollen taxa for the peat core QT-2012-18 plotted against depth. Some indicative minor taxa have also been included. Pollen assemblage zones, radiocarbon dates, and stratigraphic observations have been shown to facilitate comparison with other figures. See Figure 8.14 for stratigraphic key.

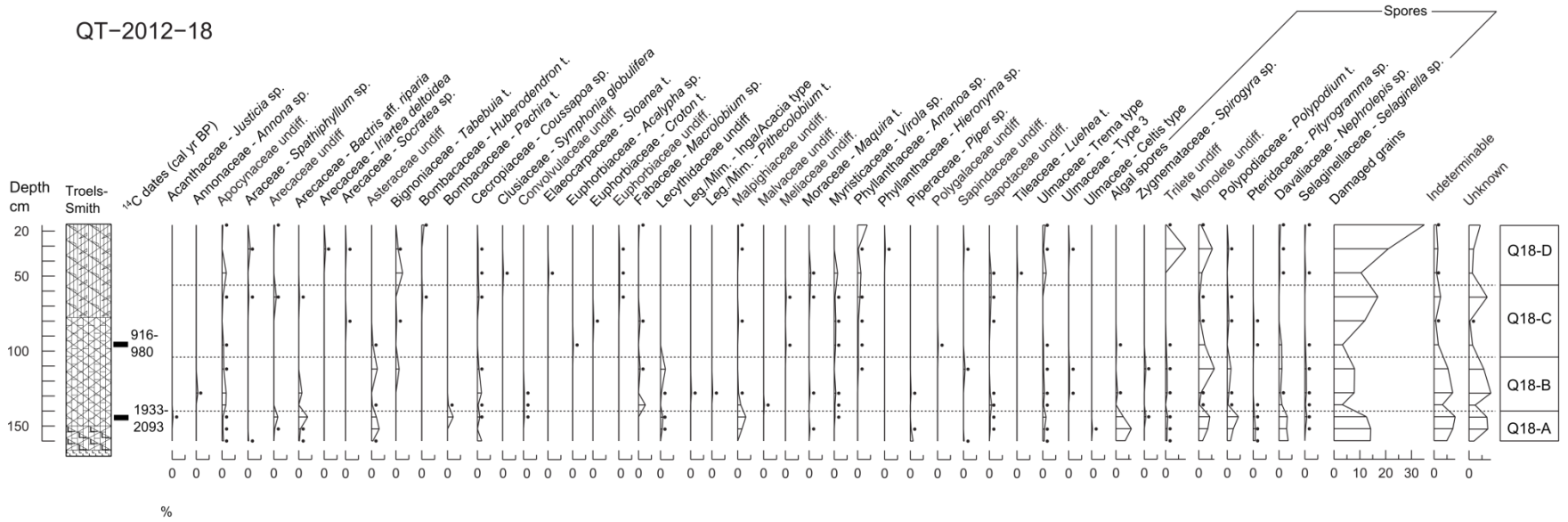

Figure 8.21 (contd.): Minor pollen taxa for the peat core QT-2012-18 plotted against depth. Taxa are shown in alphabetical order according to family. Pollen assemblage zones, radiocarbon dates, and stratigraphic observations have also been shown. See Figure 8.14 for stratigraphic key.

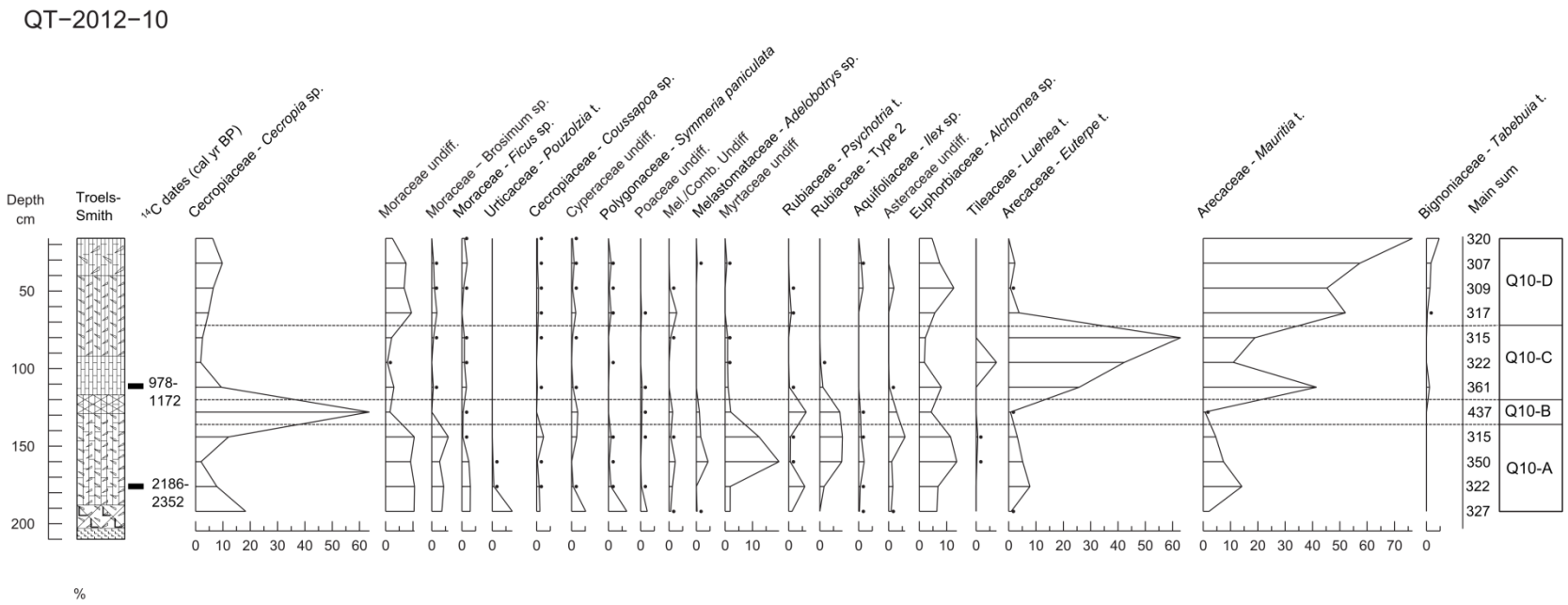

Figure 8.22: Main pollen taxa for the peat core QT-2012-10 plotted against depth. Some indicative minor taxa have also been included. Pollen assemblage zones, radiocarbon dates, and stratigraphic observations have also been shown. See Figure 8.14 for stratigraphic key.

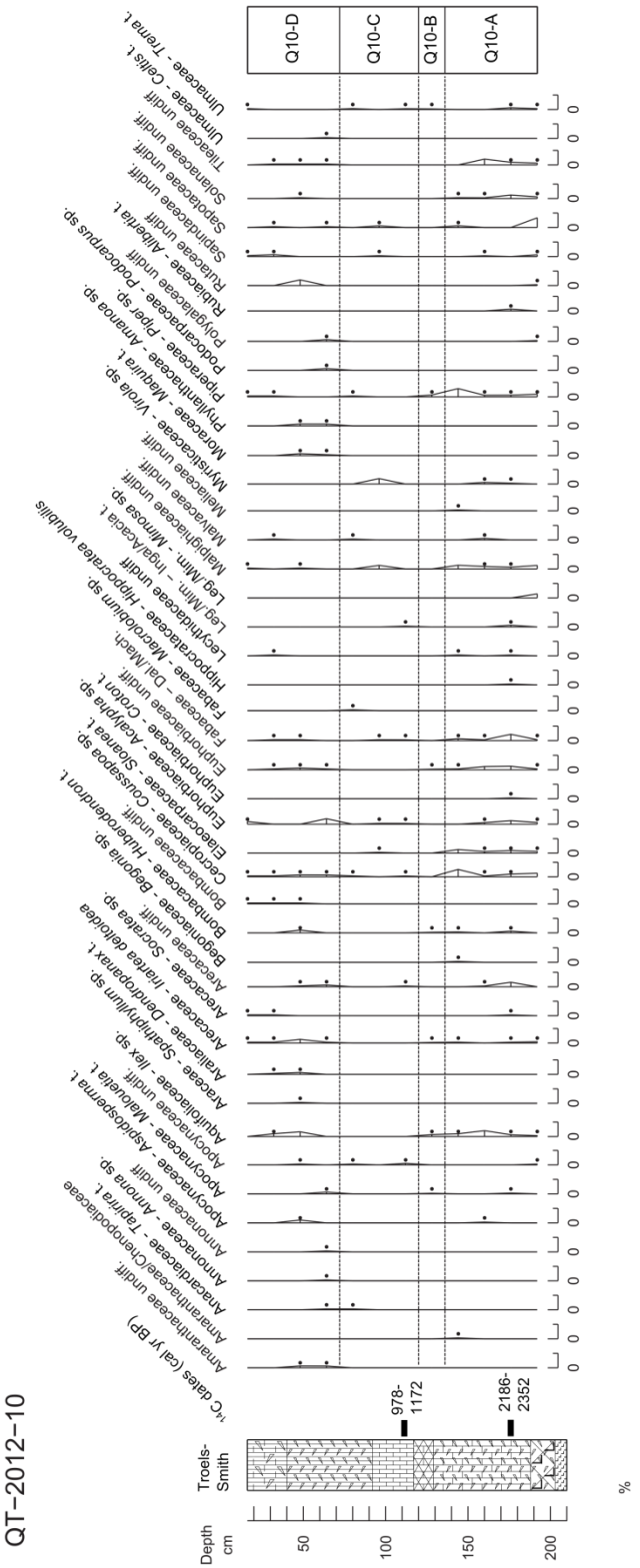

Figure 8.22 (contd.): Minor pollen taxa for the peat core QT-2012-10 plotted against depth. Taxa are shown in alphabetical order according to family. Pollen assemblage zones, radiocarbon dates, and stratigraphic observations have also been shown. See Figure 8.14 for stratigraphic key.

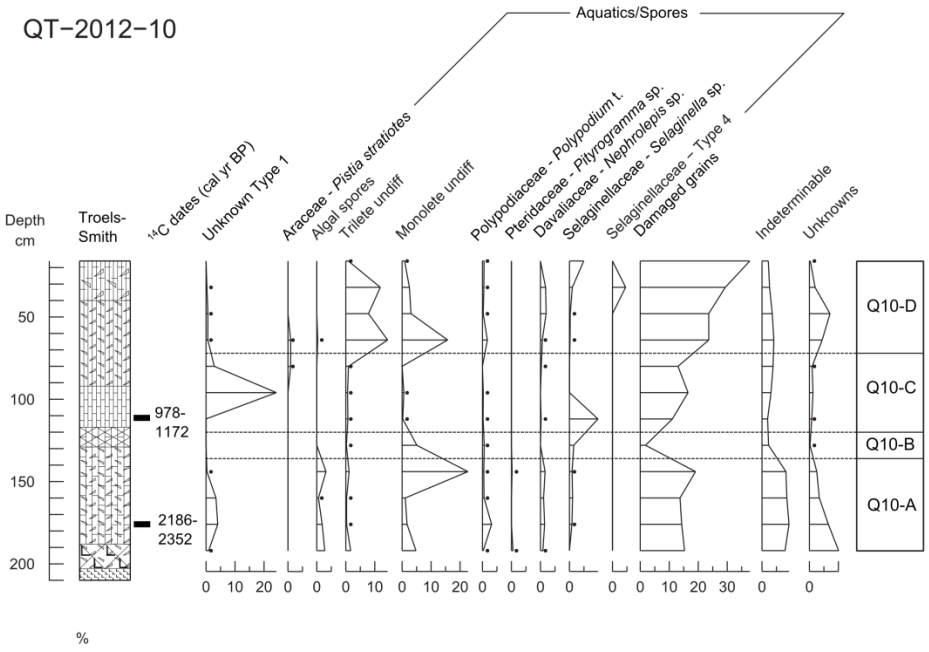

Figure 8.22 (contd.): Unknown taxa, obligate aquatics (*Pistia stratiotes*), and spores for peat core QT-2011-2. The percentage of damaged grains (within the main sum), unknowns, and indeterminable (damaged) grains have also been shown. Pollen assemblage zones, radiocarbon dates, and stratigraphic observations are shown to aid comparison with other figures. See Figure 8.14 for stratigraphic key.

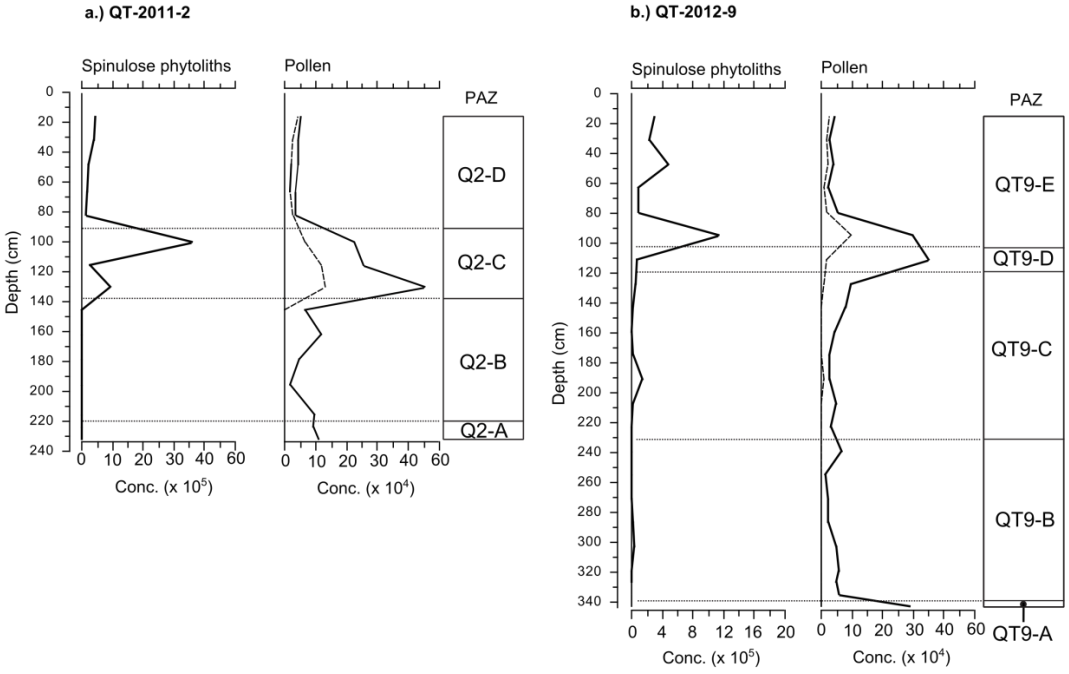

Figure 8.23 (continued over page): Pollen and phytolith concentrations per cm^3 for the four peat cores a.) QT-2011-2, b.) QT-2012-9, c.) QT-2012-10, and d.) QT-2012-18. Pollen zonation schemes have also been shown. For pollen concentrations, dashed line indicates *Mauritia* t. concentrations, and solid line denotes the concentration for the main pollen sum. (Note varying x-axis scales).

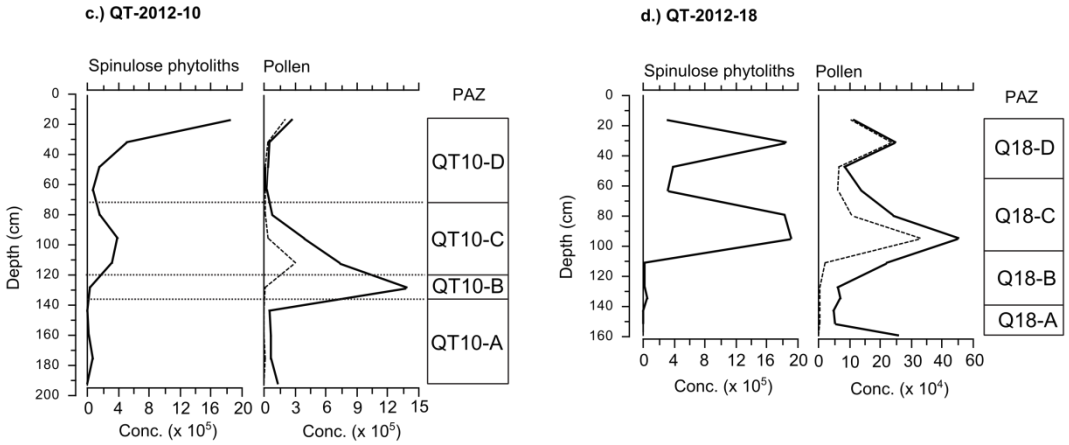

Figure 8.23 continued.

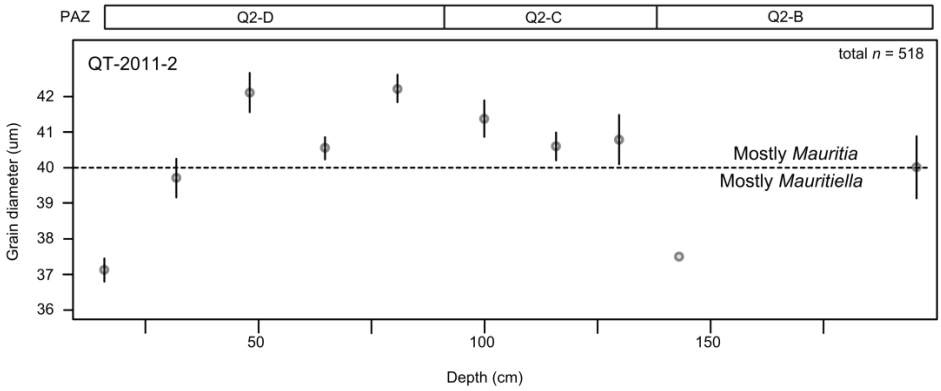

Figure 8.24: *Mauritia* t. grain diameter data plotted against depth for QT-2011-2. Mean grain diameter is shown, and bars represent the standard error of the mean (points with no error bars have ≤4 measurements). Pollen assemblage zones (PAZ) are shown at the top of the figure. Dashed line marks the distinction between *Mauritia* and *Mauritiella* which can be made on the basis of grain diameter as discussed in Chapter 6. Only those core samples containing *Mauritia* t. pollen have been shown.

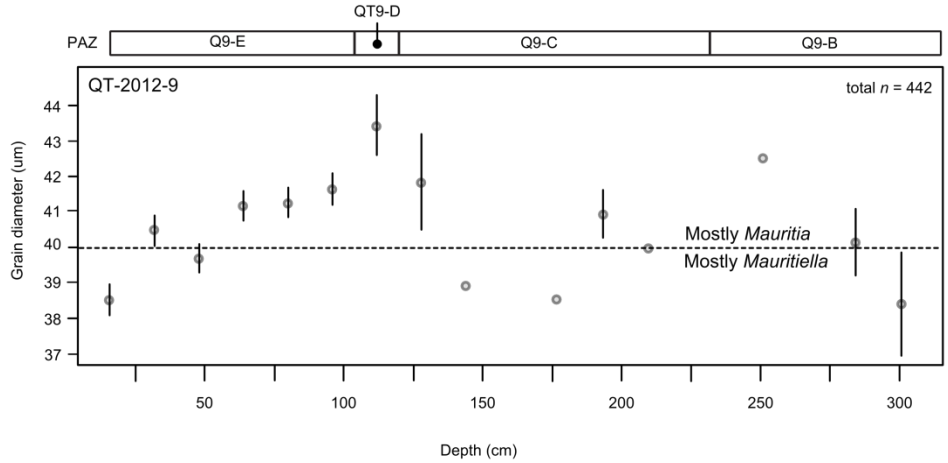

Figure 8.25: *Mauritia* t. grain diameter data plotted against depth for QT-2012-9. Format follows that of Figure 8.33. Note different depth scale.

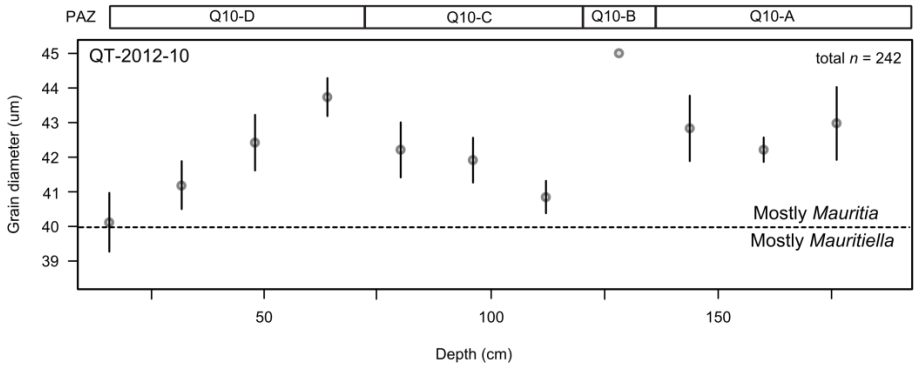

Figure 8.26: *Mauritia* t. grain diameter data plotted against depth for QT-2012-10. Format follows that of Figure 8.33. Note different depth scale.

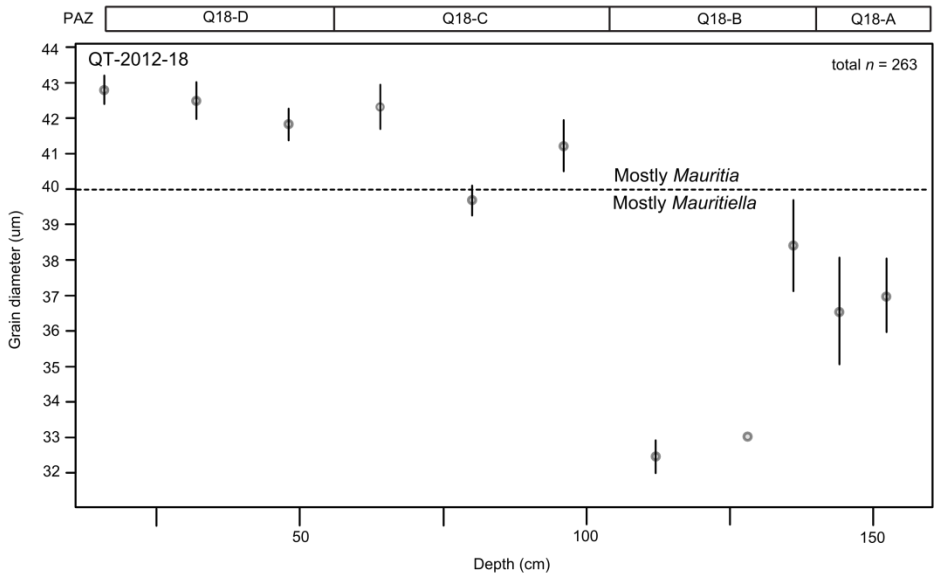

Figure 8.27: *Mauritia* t. grain diameter data plotted against depth for QT-2012-18. Format follows that of Figure 8.33. Note different depth scale.

Table 8.9: Pollen assemblage zone descriptions for QT-2012-18. Zonation was undertaken using optimal splitting by sum-of-squares in Psimpoll (Bennett, 2007). Zones have been shown in stratigraphic order (i.e. the uppermost pollen zone is at the top of the table). A summary of the palm phytolith data has also been provided. Indications of abundance refer to the maximum phytolith concentrations in a given zone, where 'extremely abundant' corresponds to >200,000 phytoliths cm^{-3}, 'present' corresponds to >5,000 phytoliths cm^{-3}, and 'rare' corresponds to < 1,000 phytoliths cm^{-3}. Phytoliths were absent from the basal zone, but this was due to HF treatment.

Zone (depths)	Pollen assemblage zone characteristics
Q18-D (56-16 cm)	*Mauritia* t. peaks in the top two samples of this zone (70%), but *Euterpe* t. pollen declines from its high values in the zone below to < 3%. Both *Alchornea* sp. and *Cecropia* sp. remain present but do not exceed 10%. Amongst the more minor taxa both *Amanoa* sp. (4%) and *Tabebuia* t. (3%) attain their peak abundance. **Spores:** Trilete spores peak in this zone (8%). **Palm phytoliths:** extremely abundant
Q18-C (104-56 cm)	*Euterpe* t. peaks in this zone, and *Mauritia* t. exceeds 25% for the first time (max. 55%). *Alchornea* sp. also peaks at the top of this zone (19%). Amongst the minor taxa, *Ficus* sp. exceeds 1% throughout. *Cecropia* sp. attains its lowest value in the whole of the core at the base of this zone. **Palm phytoliths:** extremely abundant

Q18-B (140-104 cm)	Poaceae (18%), *Psychotria* t. (23%), Dalbergia/Machaerium t. (8%), small < 12 um Solanaceae (24%) and Solanaceae undiff (30%) all peak within this zone. Cyperaceae is present but declines from its peak in the zone below and remains < 5%. *Adelobotrys* sp. also declines from its peak in the zone below but remains abundant (max. 10%). Amongst the minor types, this zone sees a peak in *Macrolobium* sp. (3%). **Palm phytoliths:** present
Q18-A (160-140 cm)	*Symmeria paniculata* peaks at the base of this zone (35 %), and is consistently abundant throughout (> 10 %). *Adelobotrys* (18%), *Cecropia* sp. (10%), *Ficus* sp. (7%) And Cyperaceae (9%) also peak in this zone. *Mauritia* t. and *Euterpe* t. pollen are present but remain low in abundance. Poaceae is consistently present but remains < 5%. Amongst the minor types, *Bactris* aff. *riparia* (3%), *Begonia* sp. (2%), and Asteraceae (3%) all peak in this zone. **Spores:** The ferns *Nephrolepis* sp. and *Polypodium* t. are most abundant in this zone but both remain < 5%. Algal spores are most abundant in this pollen zone. **Palm phytoliths:** all samples in zone HF treated

Table 8.10: Pollen assemblage zone summary descriptions for QT-2011-2. A summary of the palm phytolith data has also been provided (see caption for Table 8.9).

Zone (depths)	Pollen assemblage zone characteristics
Q2-D (91-16 cm)	*Mauritia* t. peaks in this zone (79%) and is the dominant taxon. *Alchornea* sp. declines to ≤ 10% from its peak values in the zone below. Amongst the minor taxa, *Amanoa* sp. peaks in this zone (4%). *Tabebuia* t. is consistently present, but remains uncommon (max. 2%). **Spores:** *Nephrolepis* sp. is abundant and increases towards to the top of this zone where it peaks at 70%. **Palm phytoliths**: extremely abundant
Q2-C (138-91 cm)	*Euterpe* t. increases to its peak at the base of the zone (20%) before declining to 10% at the top of the zone. *Mauritia* t. exceeds 25%. Amongst the minor types, *Symphonia globulifera* is consistently present. Moraceae undiff declines to ≤ 5% from its peak in the zone below. **Spores:** *Selaginella* sp. peaks in this zone 8%. **Palm phytoliths:** extremely abundant
Q2-B (220-138 cm)	Dalbergia/Machaerium t. (12%), Melastomataceae undiff (26%), Moraceae undiff. (11%), Myrtaceae undiff (10%), Psychotria t. (14%), and Rubiaceae Type I-34 (8%) all peak in this zone. *Mauritia* t. pollen exceeds 5% for the first time (10%). Amongst the rare types, *Alibertia* t. peaks at the base of this zone (5%). *Ilex* sp. and *Macrolobium* sp. also peak in this zone but do not exceed 5%. **Spores:** Monolete fern spores peak in this zone (25%). Algal spores are present in low numbers towards the base of the zone. **Palm phytoliths**: present
Q2-A (232-220 cm)	*Symmeria paniculata* (44%), Ficus sp. (15%), Cyperaceae (11%), and Anacardiaceae (36%) all peak in this zone. *Cecropia* sp. increases from 2% to 18% at the top of this zone. **Spores:** Fern spores are all low in abundance (< 6%). **Palm phytoliths:** all samples in zone HF treated

Table 8.11: Pollen assemblage zone summary descriptions for QT-2012-10. A summary of the palm phytolith data has also been provided (see caption for Table 8.9).

Zone (depths)	Pollen assemblage zone characteristics
Q10-D (16-72 cm)	*Mauritia* t. peaks in this zone (77%) and is the dominant taxon. *Cecropia* sp. and *Alchornea* sp. are moderately abundant throughout, but do not exceed 10% and 13% respectively. *Euterpe* t. declines from its peak in the zone below to < 5%. Amongst the rare types, *Tabebuia* t. is consistently present and peaks at the top of this zone (5%). **Spores:** Trilete spores are abundant throughout and reach their peak of 12%. **Palm phytoliths**: extremely abundant
Q10-C (72-120 cm)	*Euterpe* t. increases from 26% to its peak (63%) at the top of this zone and is the dominant taxon. *Mauritia* t. exceeds 25% for the first time (max. 41%). *Luehea* t. peaks at 7%, and and there is also a peak in Type Z-9 (24%). **Palm phytoliths:** extremely abundant
Q10-B (120-136 cm)	This zone consists of a single sample and is marked by the high abundance of *Cecropia* sp., which peaks in this zone (64%). *Psychotria* t. peaks in this zone (6%), and Type I-34 (max. 7%) is also moderately abundant. Amongst the minor taxa, Myrtaceae (max. 2%) and Asteraceae (max. 3%) are also present. **Palm phytoliths:** present
Q10-A (136-192 cm)	Myrtaceae increases from < 5% to its peak of 20%. *Alchornea* sp. peaks in this zone (14%) and *Psychotria* type is also moderately abundant (6%). *Cecropia* sp. is fairly abundant towards the base of this zone (max. 18%). There is a small peak in *Mauritia* t. at 176 cm (14%). There are also a number of peaks amongst the rarer taxa, such as *Pouzolzia* t. (7%), *Symmeria paniculata* (7%), Asteraceae (6%), and Adelobotrys sp. (4%). *Brosimum* sp. and *Ficus* sp. are consistently present but remain ≤ 6% and ≤ 3% respectively. **Spores:** Algal spores are low in abundance but consistently present throughout this zone. **Palm phytoliths:** present (note: basal sample HF treated)

Table 8.12: Pollen assemblage zone summary descriptions for QT-2012-9. A summary of the palm phytolith data has also been provided (see caption for Table 8.9).

Zone (depths)	Pollen assemblage zone characteristics
Q9-E (16-104 cm)	*Mauritia* t. expands from 5% in the zone below to its peak of 63% at 32 cm. *Euterpe* t. peaks at the base of this zone (13%) before declining to < 1% towards the surface. *Alchornea* sp. is also abundant and peaks at 64 cm (15%). *Luehea* t. (max. 6%) and Type Z-9 (max. 10%) also peak in the lower part of this zone. *Ficus* sp. is abundant in the lowermost sample in this zone (max. 16%) but declines to less than 1% at 16 cm. **Spores:** *Nephrolepis* sp. expands markedly towards the top of this zone (max. 43%). *Selaginella* sp. peaks towards the base of this zone (23%). **Palm phytoliths:** extremely abundant
Q9-D (104-120 cm)	This zone consists of a single sample and is characterised by a peak in *Ficus* sp. (70%). *Mauritia* t. is also present but in relatively low proportions (< 10%), and *Euterpe* t. is also present (max. 9%). **Palm phytoliths:** present
Q9-C (120-232 cm)	Myrtaceae has two definable peaks in this zone at 224 cm (28%) and 144 cm (15%). Several Rubiaceae types are moderately abundant in this zone; *Psychotria* t. peaks at 144 cm (13%), *Sabicea* t. peaks at 224 cm (16%), and Type I-34 peaks at 128 cm (16%).Cyperaceae is present but generally remains below 10%, except for a peak at 160 cm (53%). Poaceae remains moderately abundant (max. 8%). *Alchornea* sp. is consistently present (5-10%). Amongst the minor taxa, Malpighiaceae (5%) and *Pouzolzia* t. (5%) both peak in this zone. *Pistia stratiotes* is

	most common in this zone but does not exceed 10%. **Spores:** Both monolete spores and *Nephrolepis* sp. peak in this zone (70% and 64% respectively). **Palm phytoliths:** present
Q9-B (232-340)	Cyperaceae peaks in this zone and exceeds 10% throughout, but its abundance is variable (10-57%). Poaceae is also moderately abundant and peaks in this zone (17%). *Alibertia* t. is generally low in abundance but peaks in this zone (11%). Amongst the minor types, *Mimosa* sp. is present in low number (max 4.5%) towards the top of this zone. **Spores:** The fern *Pityrogramma* sp. peaks and is consistently present. Algal spores remain abundant throughout the lower half of this zone. **Palm phytoliths:** present
Q9-A (340-344)	This zone consists of a single sample and is dominated by the pollen of *Cecropia* sp., which peaks in this zone (91%). Poaceae, Asteraceae, Cyperaceae and *Alchornea* sp. are all present but in low abundance (< 5%). **Spores:** Algal spores are most abundant in this zone. **Palm phytoliths:** Sample HF treated

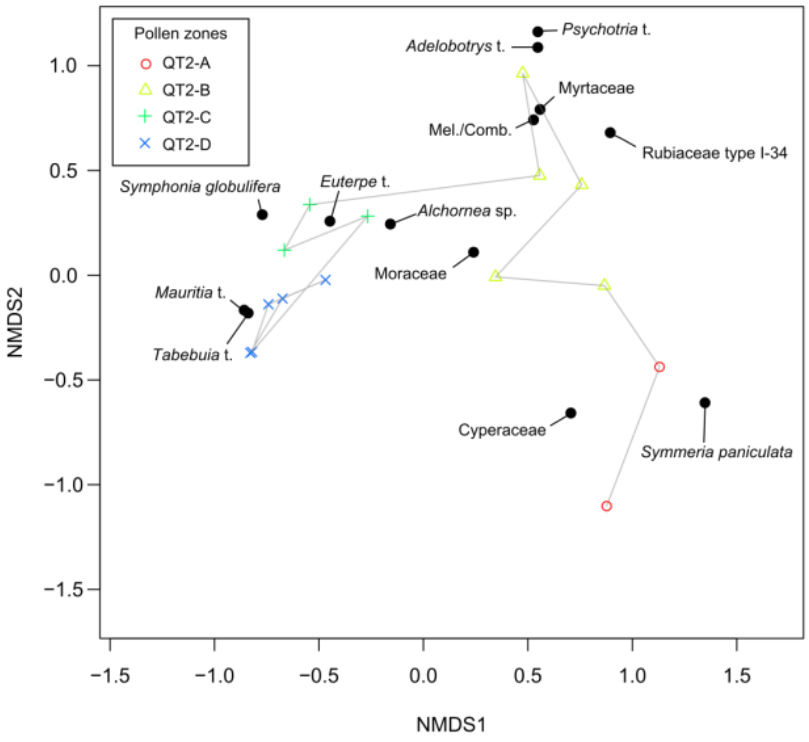

Figure 8.28: Results of NMDS analysis for QT-2011-2 showing the first two axes. Points represent individual samples within the four pollen zones, and indicator taxa have been plotted as points. Grey lines show the trajectory of change and connect samples which are adjacent to one another in the core.

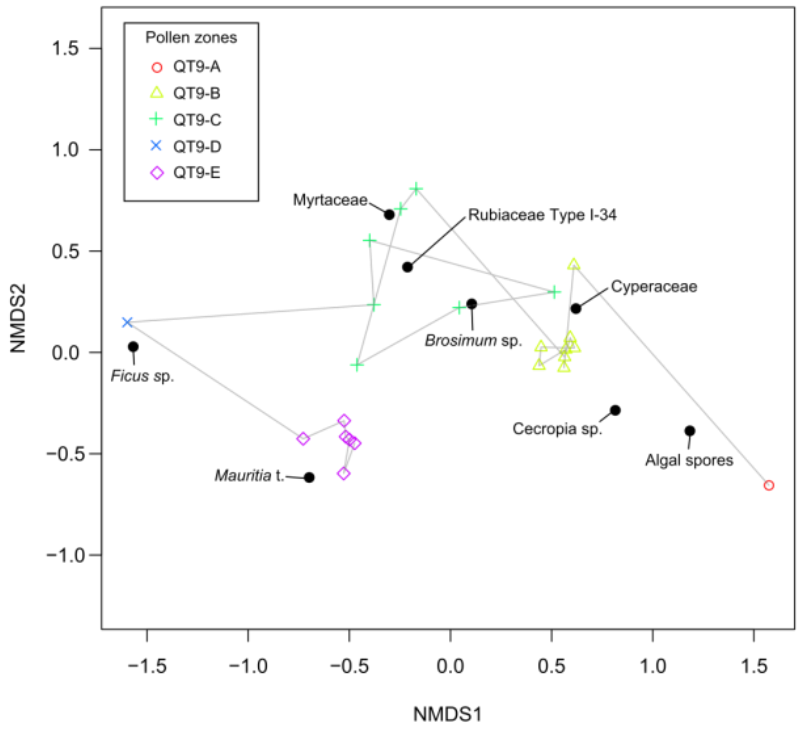

Figure 8.29: NMDS analysis for QT-2012-9 showing the first two axes. Format follows that of Figure 8.28

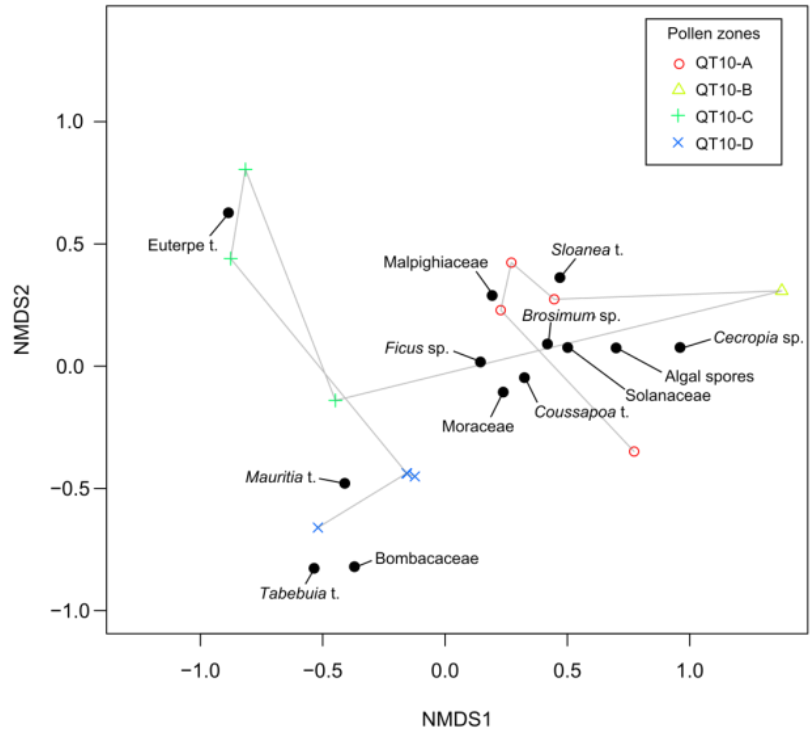

Figure 8.30: NMDS analysis for QT-2012-10 showing the first two axes. Format follows that of Figure 8.28.

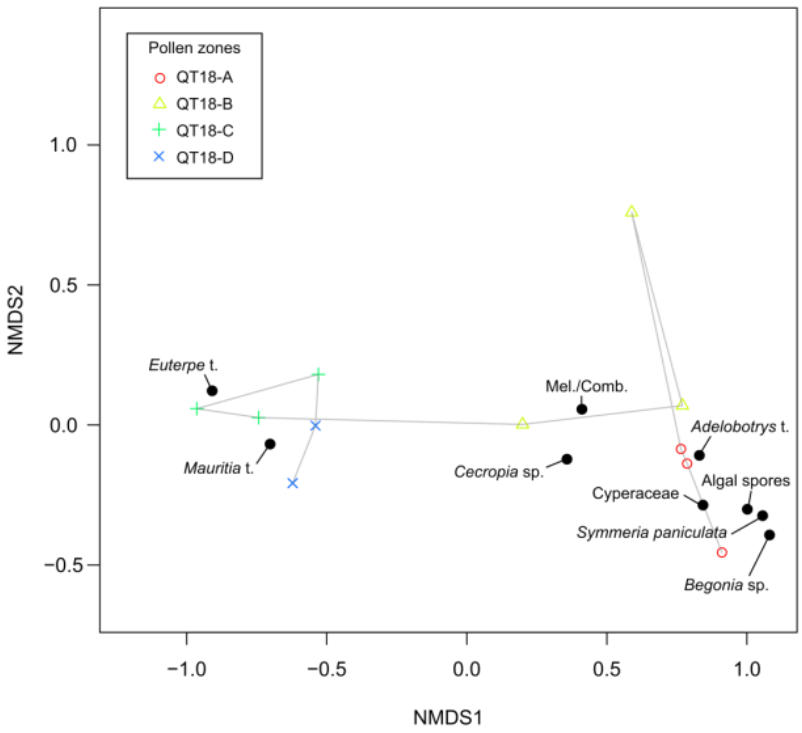

Figure 8.31: NMDS analysis for QT-2012-18 showing the first two axes. Format follows that of Figure 8.28.

Table 8.13: Indicator species identified for QT-2011-2. Taxa with indicator values > 0.25 have been shown, with their maximum percentage values within the zone for reference (2 s.f.).

Taxon	Pollen zone	*p* value	Indicator species value	Max. % in zone
Tabebuia t.	D	0.037	0.7121	4.1%
Mauritia t.	D	0.005	0.6349	79%
Symphonia globulifera	C	0.004	0.9573	2.2%
Euterpe t.	C	0.001	0.8025	20%
Alchornea sp.	C	0.002	0.4856	22%
Psychotria t.	B	0.027	0.9065	14%
Adelobotrys t.	B	0.031	0.8518	26%
Rubiaceae type I-34	B	0.038	0.8000	8.1%
Myrtaceae	B	0.031	0.7774	10%
Mel./Comb.	B	0.048	0.6823	4.3%
Moraceae	B	0.021	0.4037	11%
Symmeria paniculata	A	0.023	0.9320	44%
Cyperaceae	A	0.001	0.7211	22%

Table 8.14: Indicator species identified for QT-2012-9. Format follows Table 8.13.

Taxon	Pollen zone	*p* value	Indicator species value	Max. % in zone
Mauritia t.	E	0.001	0.812	63%
Ficus sp.	D	0.043	0.908	70%
Rubiaceae type I-34	C	0.001	0.886	16%
Myrtaceae	C	0.046	0.696	28%
Brosimum sp.	C	0.015	0.452	3.6%
Cyperaceae	B	0.021	0.631	57%
Algal spores	A	0.003	0.803	19%
Cecropia sp.	A	0.001	0.723	91%

Table 8.15: Indicator species identified for QT-2012-10. Format follows Table 8.13.

Taxon	Pollen zone	*p* value	Indicator species value	Max. % in zone
Tabebuia t.	D	0.016	0.842	4.7%
Bombacaceae	D	0.042	0.750	0.33%
Mauritia t.	D	0.002	0.647	77%
Euterpe t.	C	0.004	0.865	63%
Cecropia sp.	B	0.013	0.741	64%
Algal spores	A	0.001	0.965	3.2%
Sloanea t.	A	0.003	0.894	1.3%
Solanaceae	A	0.006	0.884	1.2%
Brosimum sp.	A	0.001	0.772	6.0%
Coussapoa	A	0.021	0.652	2.5%
Malpghiaceae	A	0.018	0.642	1.3%
Moraceae	A	0.001	0.509	11%
Ficus sp.	A	0.045	0.487	3.1%

Table 8.16: Indicator species identified for QT-2012-18. Format follows Table 8.13.

Taxon	Pollen zone	*p* value	Indicator species value	Max. % in zone
Mauritia t.	D	0.029	0.579	71%
Euterpe t.	C	0.024	0.906	54%
Mel./comb.	B	0.039	0.461	2.9%
Algal spores	A	0.025	0.929	5.9%
Begonia sp.	A	0.017	0.913	2.2%
Symmeria paniculata	A	0.018	0.860	35%
Cyperaceae	A	0.018	0.741	8.8%
Adelobotrys t.	A	0.023	0.627	18%
Cecropia sp.	A	0.027	0.450	13%

8.4.4 Palm phytolith stratigraphy

As summarised in Table 8.2 at the beginning of the chapter and illustrated in Figure 8.32, peaks in palm phytolith concentration were observed in all of the peat cores at a depth of 96-112 cm. This coincided with the increase in *Mauritia*-type pollen to > 25 % of the pollen sum, and also coincided with the main peak in *Mauritia*-t. pollen concentration in most of the cores. The highest concentration of palm phytoliths was observed in QT-2012-10, where concentrations reached 1.86 x 10^6 phytoliths cm^{-3}.

8.5 Summary

Quistococha peatland covers an area of c. 490 ha and transects of cores totalling c. 5 km were used to establish the shape of the underlying topography and the visible peat stratigraphy. These data were used to guide the selection of cores for detailed analysis.

A lacustrine sediment sequence from Quistococha itself was studied in detail (pollen analysis, C, N, LOI, and magnetic susceptibility), and modern reference samples for carbon and nitrogen were analysed from the lake to enable better interpretation of lake and peat sequences from Quistococha and similar peatlands, such as San Jorge (Chapter 9).

Four cores were chosen from the peatland for pollen analysis, and supporting data were also collected in the form of carbon, nitrogen, and loss-on-ignition measurements. Grain size data were collected for *Mauritia* t. pollen in order to allow finer taxonomic distinction, based on the study described in Chapter 6. Spinulose palm phytolith concentrations were also determined for the peat profiles.

These data are interpreted and discussed in Chapters 10 and 11, where they are used to establish a model for the development of Quistococha peatland and examine the main drivers of vegetation change in peatlands of the Western Amazon. The next chapter presents results from the peat core at taken at San Jorge.

9. The San Jorge peatland record

9.1 Introduction

This chapter contains the results of analyses undertaken on the core taken from San Jorge peatland (SJ0-2010-1). As mentioned in Chapter 3, San Jorge is a domed peatland and therefore differs from Quistococha in terms of its present attributes and nutrient status. As stated in Chapter 2, one of the key aims of this thesis is to determine the main drivers of vegetation change in Amazonian peatlands, but a particular aim was to determine the origin of the pole forest found at this site, which is unusual and rare in Amazonia. Zone by zone interpretations of this data are given prior to further discussions of the drivers of vegetation change in the context of the wider literature in Chapter 11.

9.2 Peat stratigraphy and geochemistry

Peat stratigraphic information and geochemistry are presented in Figure 9.1.

From 600-640 cm, the core consisted of inorganic sandy silt with a minor clay component. Magnetic susceptibility is highest across this interval, as is bulk density. Loss-on-ignition, carbon, nitrogen, C/N ratios and Ca/Mg ratios are all low. From 560-600 cm, the core contains a higher proportion of clay and less silt, and there is a general up-core decline in the bulk density.

From 240-560 cm, the core consisted of a mixture of fine clays and organic matter. Large pieces of wood were observed in parts of the core (297-301 cm, 352-354 cm), and some intact leaves were observed in the core at a depth of 465 cm. Bulk density remains low relative to the basal sediments (mostly < 0.25 g cm^{-3}), but some sections with higher bulk density are observed in association with increased clay content (as shown in the loss-on-ignition values). Loss-on-ignition values are highly variable (3.4-90%), and average 51%. Both C and N vary together in step with changes in organic content. Ca/Mg ratios remain low (< 20) throughout.

From 0-240 cm, the core consisted of pure fibrous peat (i.e. peat with loss-on-ignition values > 65%), which contained abundant small roots and twigs. The contact between the overlying peat and underlying mixed clay and organic matter is gradational but short, and loss-on-ignition values increase from 58% to 93% between 240 and 244 cm. The carbon content in this section is high and rises to > 60wt% at 208 cm depth. The carbon content drops notably by a few percent between 88 and 96 cm depth to below 60 wt% (this is not within the analytical uncertainty and is therefore likely a real decrease). Loss-on-ignition is also more variable within the upper 100 cm (relative to LOI from 100 to 200 cm), although it always remains above 90%. Nitrogen concentrations reach a

peak at 80 cm and are generally high, between 1.7 and 2.3wt%. The Ca/Mg ratio shows a marked decline from 47 to 16 between 112 and 128 cm depth, and remain below 20 up to the surface of the core.

9.3 Pollen and phytolith data

Pollen data were generated for the top 240 cm; in this upper section of the core loss-on-ignition values reveal pure peat accumulations with little inorganic residue. The pollen data indicate pronounced changes in composition through the upper 240 cm of SJO-2010-1. The results of pollen analyses are presented as percentage diagrams showing the main taxa and minor taxa plus spores (Figure 9.3), and pollen zones are described in Table 9.1. Pollen data have also been plotted against age using the chronology for the core developed in Chapter 7 (Figure 9.4). A diagram showing changes in total pollen and palm phytolith concentrations, as well as pollen influx, is shown in Figure 9.2.

Pollen preservation was good throughout the top 240 cm, with indeterminable damaged pollen < 10% throughout, and pollen concentrations (excluding spores and aquatics) between 13,900 and 980,000 grains cm^{-3}. Peak pollen concentrations occurred in the basal pollen zone (SJ-1), where the pollen assemblage is dominated by *Cecropia*. A second peak in pollen concentration occurred at 96 cm (667,000 grains cm^{-3}), towards the base of zone SJ-5, where *Mauritia*-t. is dominant.

Indicator species analysis showed that certain pollen types were significantly associated ($p < 0.05$) with each of the five zones (Table 9.2). These have also been shown in the biplot of the NMDS analysis (Figure 9.5). The identification of *Iriartea deltoidea* as an indicative taxon may be an artefact as there is only a single sample in zone SJ-3, and it is unlikely to be of ecological significance. The other indicative taxa are those which are more abundant such as *Mauritia*-t. and *Pistia*. The NMDS biplot is characterised by two groups: samples in zones SJ-3 and SJ-5 (containing abundant *Mauritia*-t. pollen) plot to the left of the diagram, whereas samples from zones SJ-2 and SJ-4 both plot to the right. This indicates a marked dissimilarity between these two groupings. Zone SJ-1, characterised by abundant *Cecropia* pollen, also has a notably lower axis 2 score.

The sample at 192 cm was prepared and counted twice to confirm that the presence of abundant *Mauritia*-t. pollen was not the result of accidental contamination; the low pollen concentration in the sample increases the risk that the pollen percentage might be affected by laboratory contamination of (for example) preparation tubes or sampling equipment. However, both samples from 192 cm were of identical composition (within counting uncertainty). The material could not have been a large piece of peat carried down from near-surface layers; the concentration of *Mauritia*-t. pollen was very low at 192 cm and the other taxa (especially spores) which are found at 192 cm are much less

abundant in the near-surface pollen zones (i.e. the overall composition of the sample suggests it could not be material derived purely from peat dragged down from the surface peats). A sample at 196 cm was prepared in order to establish whether the *Mauritia*-t. peak extended below the sample at 192 cm, and confirmed that *Mauritia*-t. pollen was moderately abundant (> 10%) in the immediately underlying peat layer.

Table 9.1: Pollen assemblage zone summary descriptions for SJO-2010-1. Zonation was undertaken using optimal splitting by sum-of-squares in Psimpoll (Bennett, 2007). A summary of the palm phytolith data has also been provided. Indications of abundance refer to the maximum phytolith concentrations in a given zone, where 'extremely abundant' corresponds to >200,000 phytoliths cm^{-3}, 'present' corresponds to >5,000 phytoliths cm^{-3}, and 'rare' corresponds to < 1,000 phytoliths cm^{-3}. Phytoliths were not absent from any of the zones.

Zone (depths)	Summary of pollen assemblage zone characteristics
SJ-5 (8-100-cm)	*Mauritia*-t. peaks in this zone (85%), as do *Alchornea* sp. (60%), *Ilex* sp. (20%), and *Euterpe*-t. palm pollen (17%). There is a second peak in *Cecropia* sp. mid-way through this zone (38%). **Spores:** Less abundant throughout this zone than in SJ-4. *Nephrolepis* sp. is abundant at the base of the zone (71%) but declines rapidly to low values at the top of the sequence. Selaginellaceae Type 4 reaches its peak abundance in the top 50 cm (3.3%). **Palm phytoliths:** Extremely abundant; peak concentration for the core occurs at 80 cm.
SJ-4 (100-188-cm)	There is a pronounced increase in *Pistia stratiotes* pollen, which peaks in this zone (93%), and along with Cyperaceae (max. 50%) is the dominant pollen type. Moraceae pollen (29%), and *Malouetia*-t. (21%) also peak in this zone. *Begonia* sp. peaks (max. 30%) and Poaceae is common (max. 15%), especially above 1.30 m depth. *Alchornea* sp. is persistently present but remains a fairly minor constituent (< 9%). *Trema* aff. *micrantha*, *Coussapoa* sp., *Piper* sp. and *Brosimum* sp. are all minor constituents (< 5%) but are most abundant in this zone. **Spores:** Extremely abundant; *Nephrolepis* sp. varies from < 5% to 74%, and round, sculptured trilete spores reach their peak abundance (54%). **Palm phytoliths:** Present **Note:** Non-pollen palynomorph *Spirogyra* sp. rare but present throughout this zone.
SJ-3 (188-194-cm)	This zone is marked by the first increases in both *Mauritia*-t. (increases to 65%). Cyperaceae declines relative to zone SJ-2, but remains common (8%). **Spores:** *Nephrolepis* sp. reaches its peak abundance (75%). **Palm phytoliths:** Present
SJ-2 (194-220-cm)	This zone is dominated by the pollen of Cyperaceae (max. 44%), Poaceae, which peaks in this zone (35%) and Asteraceae, which also peaks in this zone (39%). *Begonia* sp. is moderately abundant towards the top of the zone (13%). *Cecropia* sp. declines significantly from its peak values in SJ-1 to < 15%. **Spores:** Abundance of spores increases markedly from low values in SJ-1; Monolete spores reach their peak abundance (32%), and *Nephrolepis* increases towards the top of the zone (max. 40%). **Palm phytoliths:** Present
SJ-1 (220-240-cm)	This zone is dominated by the pollen of *Cecropia* sp., which peaks at 92%. Mel./Comb. are less abundant but also peak in this zone (8%). *Malouetia* is common at the top of this zone (10%), and Cyperaceae begins to increase (6%). Low percentages of various other taxa such as Moraceae (max. 9%) are also present. **Spores**: Low in abundance (no taxa exceed 7%). **Palm phytoliths:** Rare

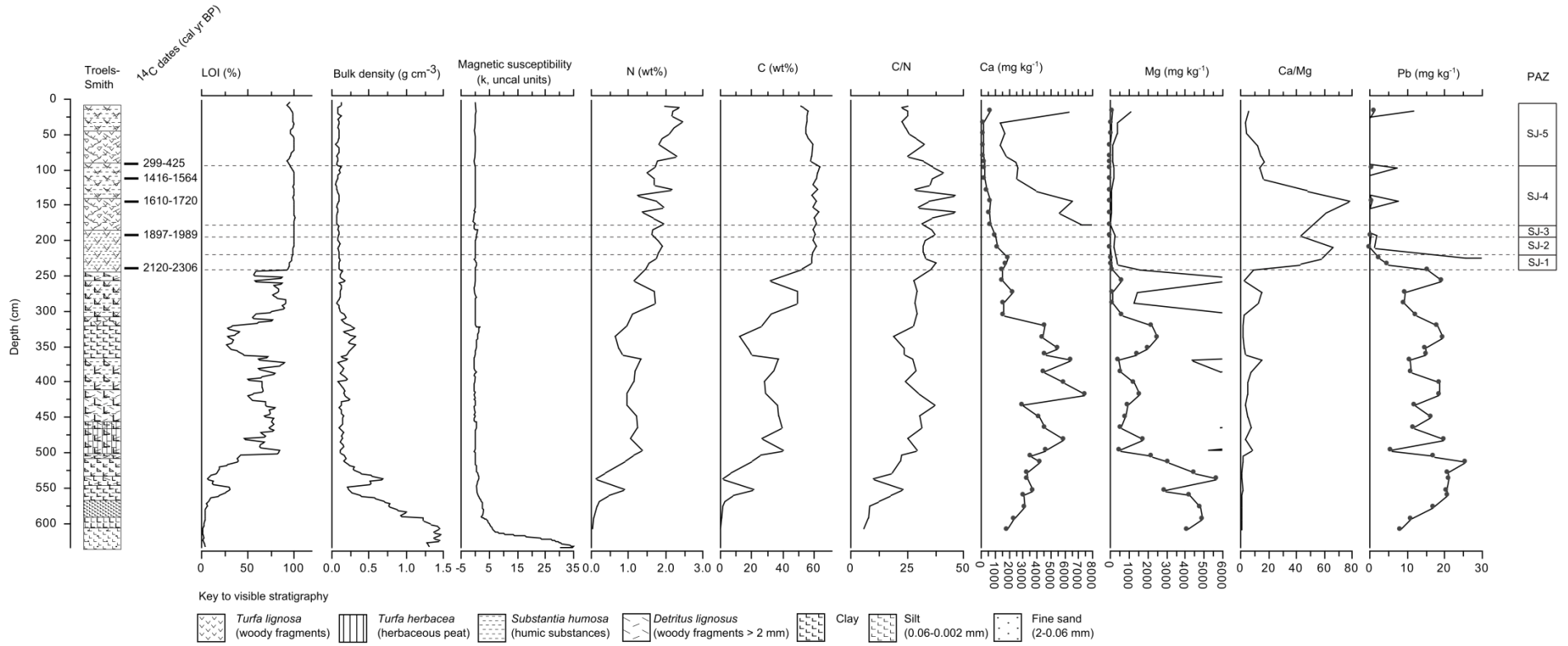

Figure 9.1: Core data for the San Jorge core (SJO-2010-1). Core stratigraphy (Troels-Smith scheme) is shown alongside organic content (loss-on-ignition), bulk density, magnetic susceptibility, total carbon, nitrogen, C/N ratio, Ca, Mg, Ca/Mg ratio, and Pb content. A single Ca/Mg ratio value has been omitted at 172 cm as it was unrealistically high, a result of low Mg values (likely due to low recovery). Radiocarbon dates (see Chapter 7 for further details) and pollen assemblage zones (PAZ) have been shown to facilitate comparison with other figures. LOI, bulk density, and magnetic susceptibility data were generated by T.D. Jones. A 10x exaggeration line has also been shown for Ca, Mg and Pb.

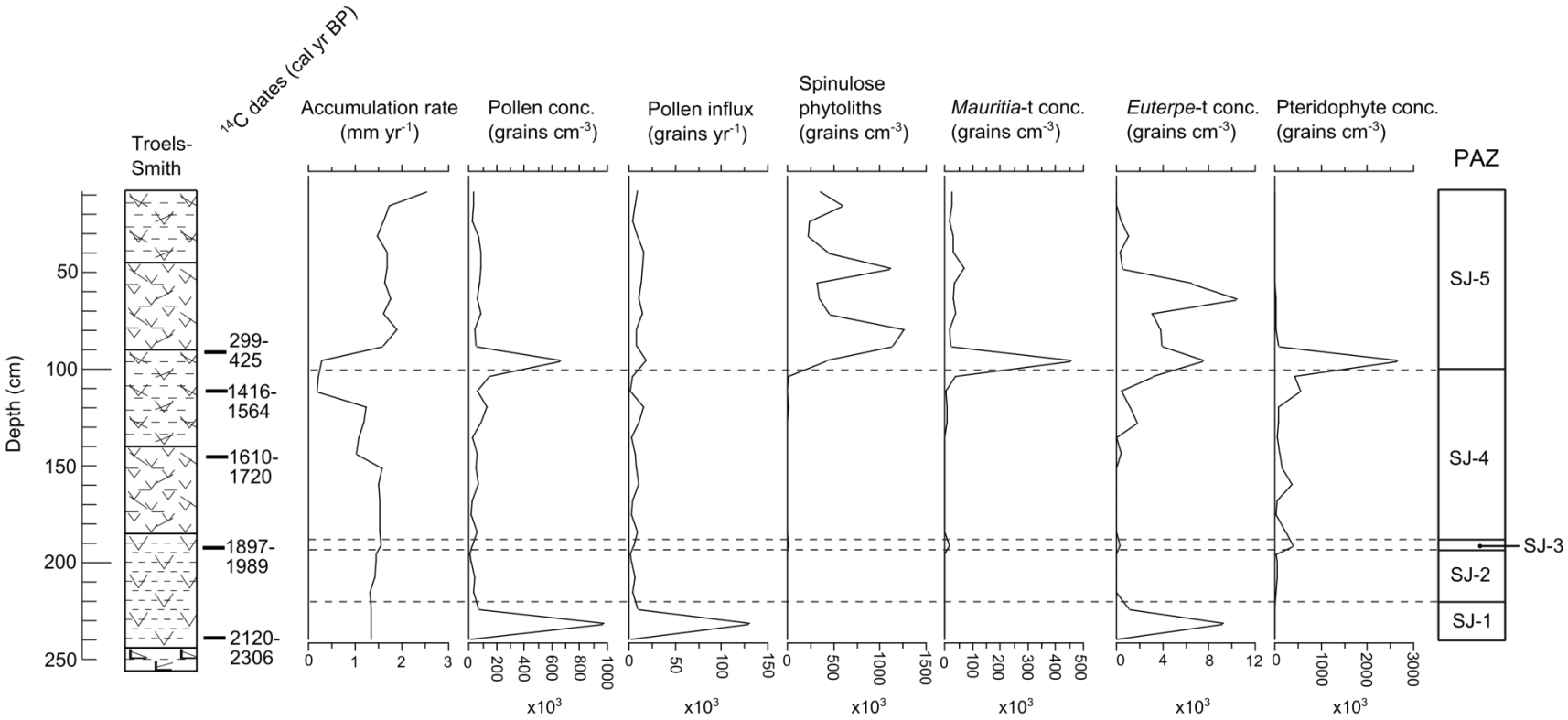

Figure 9.2: Concentration data plotted against depth for selected pollen taxa and for spinulose palm phytoliths in core SJO-2010-1. (Note the differing x-axis scales). Pollen influx and accumulation rate were calculated using the age model presented in Chapter 7.

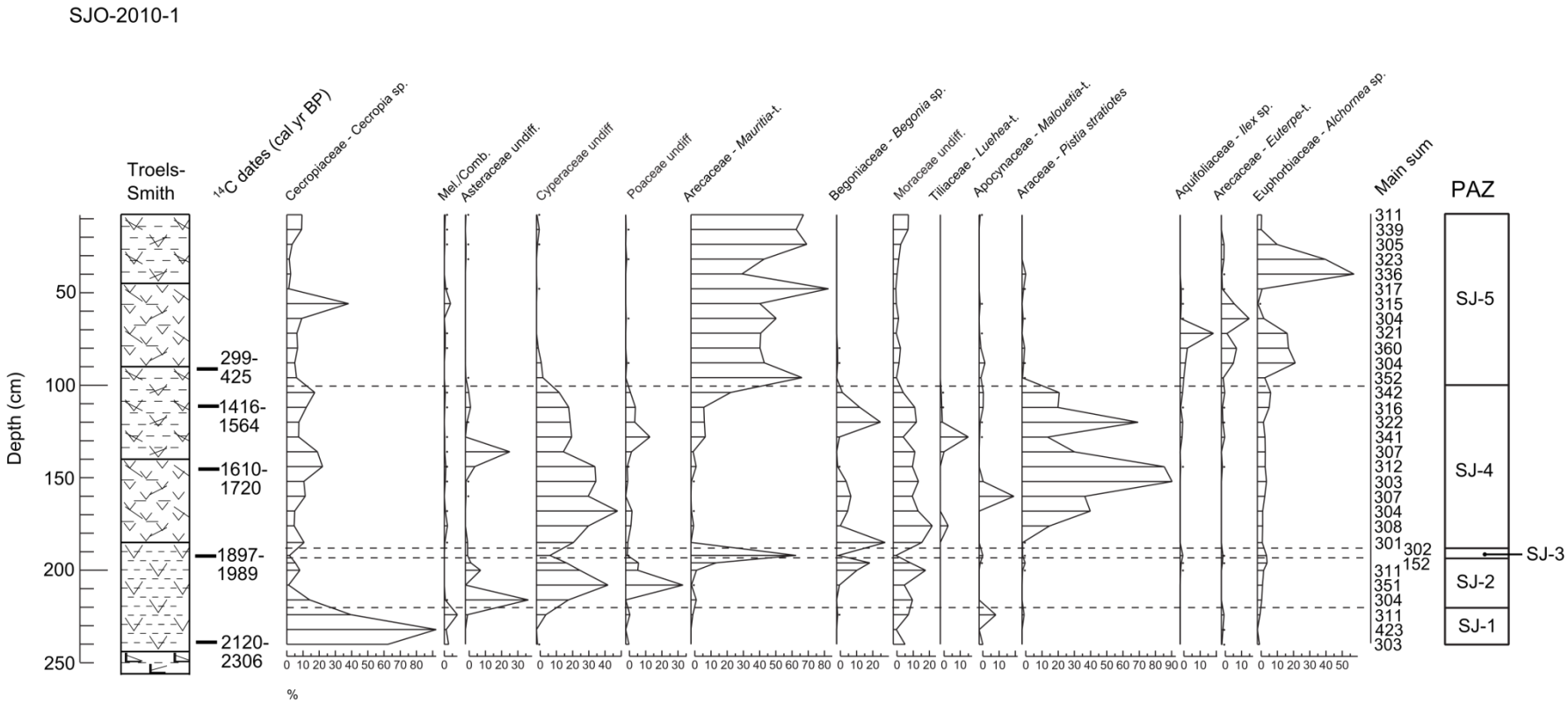

Figure 9.3: Percentage pollen diagram for the main taxa (> 5%) for core SJO-2010-1, plotted against depth. Pollen assemblage zones (PAZ) as defined using optimal splitting by sum-of-squares are also labelled to the right. Radiocarbon dates, stratigraphic observations (Troels-Smith), and the main pollen sum (excluding spores and obligate aquatic taxa) have also been shown.

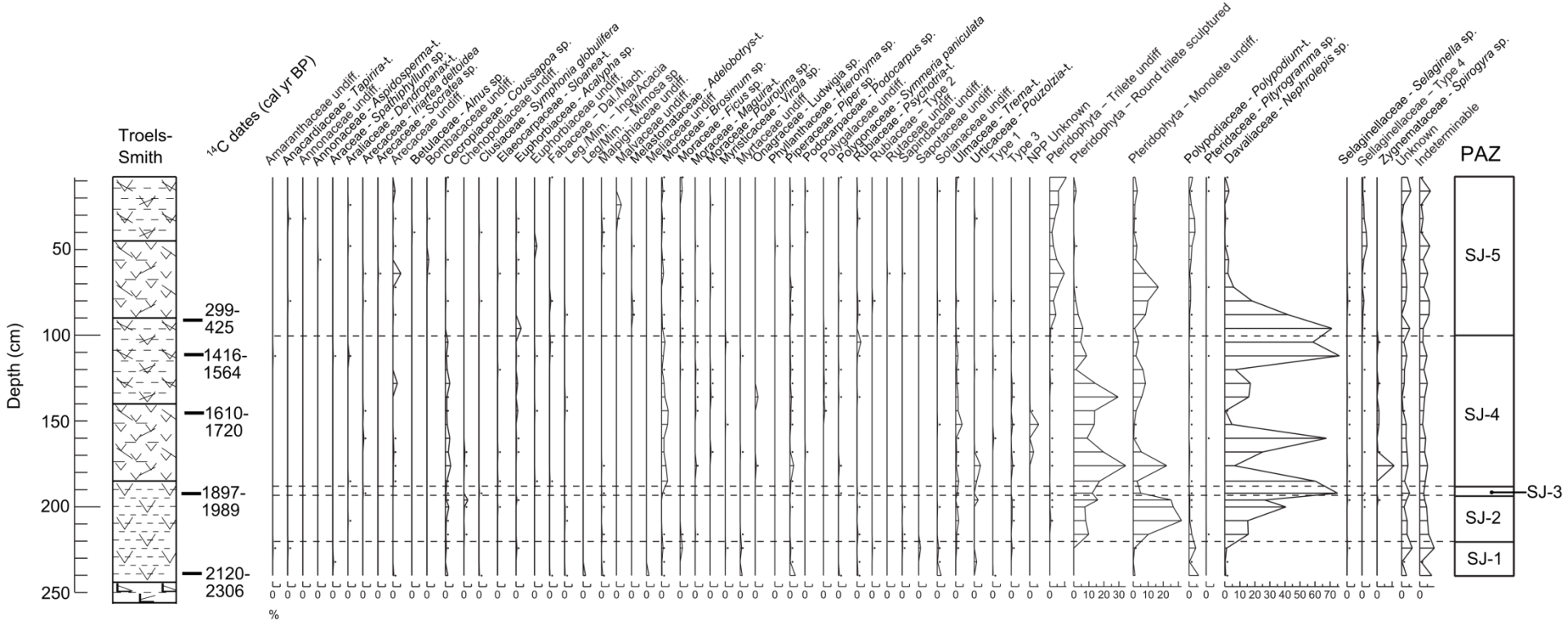

Figure 9.3 contd.: Percentage pollen diagram for selected minor taxa (<5 %) and pteridophyte spores for core SJO-2010-1, plotted against depth. Radiocarbon dates and stratigraphic information are shown to the left, pollen assemblage zones (PAZs) are labelled to the right.

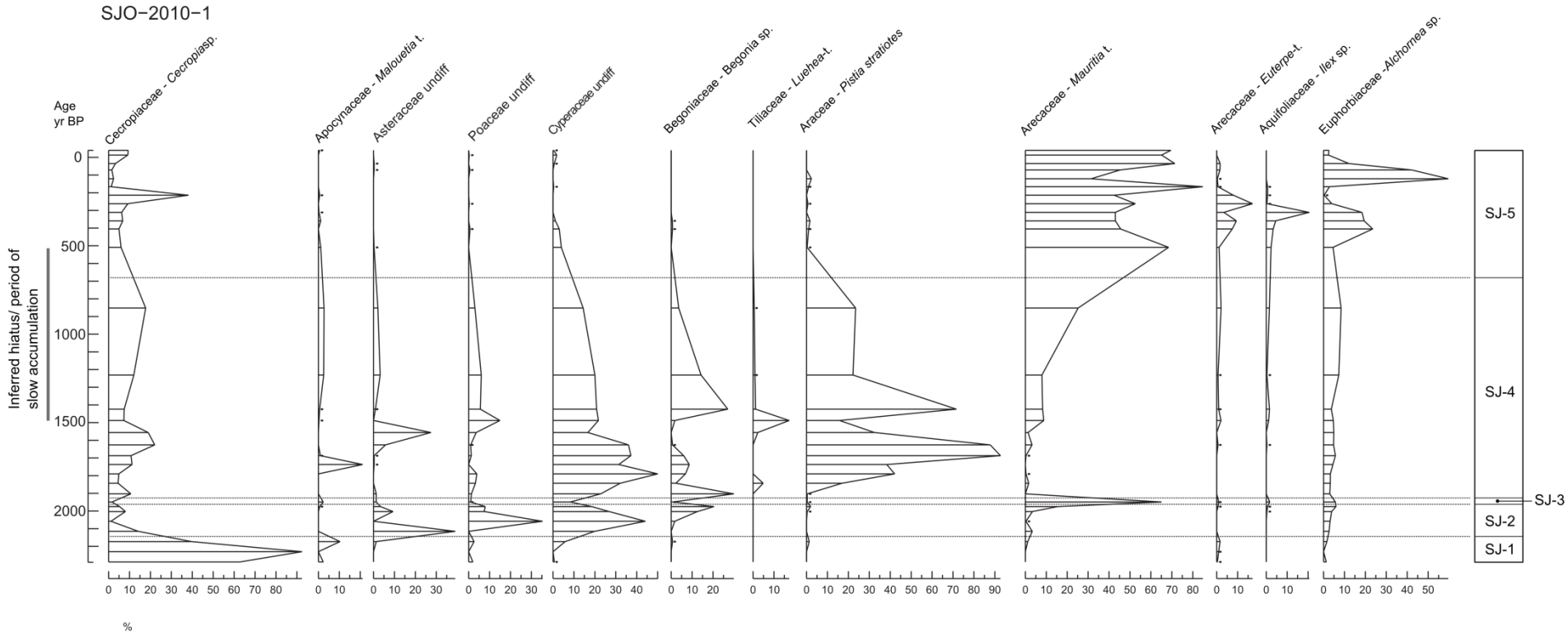

Figure 9.4: Summary pollen diagram for peat core SJ0-2010-1 showing taxa plotted against age (see Chapter 7 for age model). There is some uncertainty as to the precise age of samples during the period of slow accumulation.

Table 9.2: Results of indicator species analysis for SJO-2010-1, illustrating taxa which are strongly associated with the five pollen zones. Note that, as zone 3 comprised a single sample, this may distort the indicator species analysis.

Taxon	Zone	*p* value	Indicator species value	Max. in zone
Brosimum sp.	4	0.03	0.5076	4%
Pistia stratiotes	4	0.001	0.9310	93%
Mauritia-t.	3	0.02	0.5065	65%
Iriartea deltoidea	3	0.03	0.7595	0.3%
Chenopodiaceae	2	0.04	0.6940	3%
Cecropia sp.	1	0.005	0.7192	92%
Mel./Comb.	1	0.02	0.7776	8%
Solanaceae	1	0.03	0.8847	3%

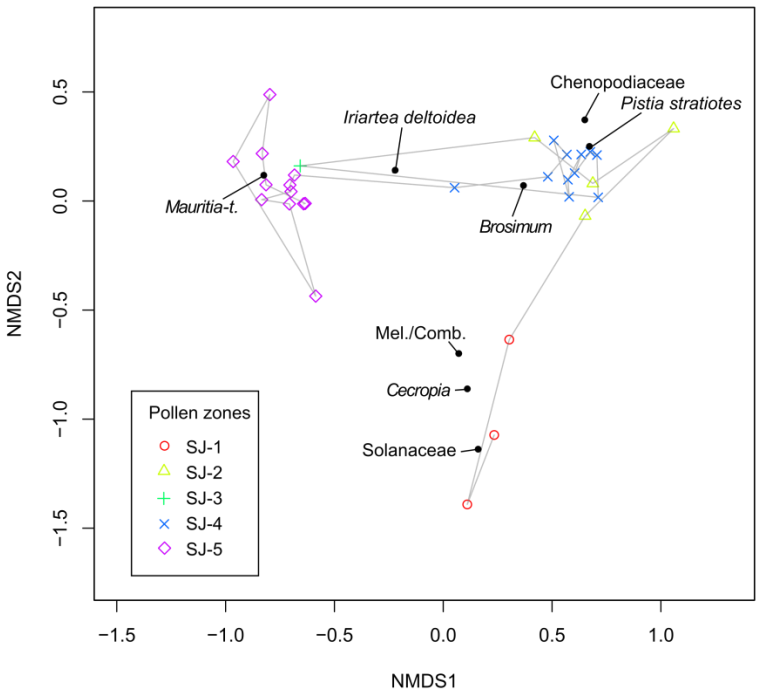

Figure 9.5 (left): Results of NMDS analysis for SJO-2010-1 showing the first two axes. Points represent individual samples within the five pollen zones, and taxa have been plotted which were found to be indicative of the different zones. Grey lines show the trajectory of change and connect samples which are adjacent to one another in the core.

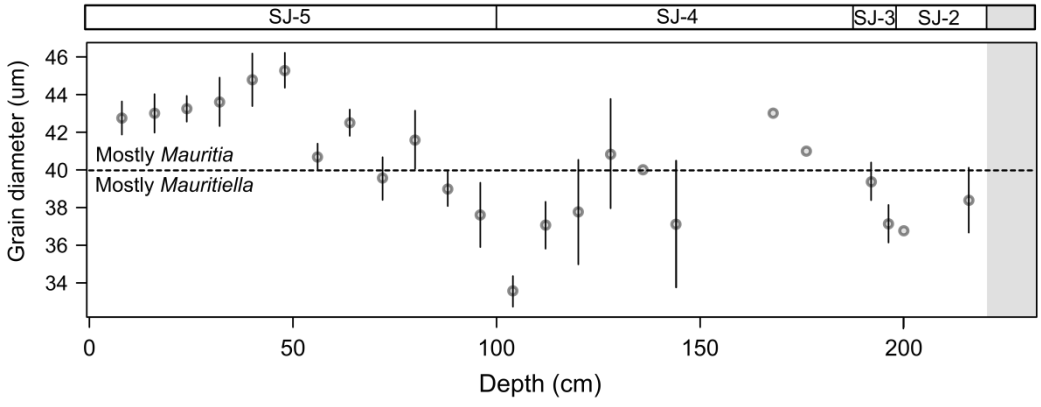

Figure 9.6: *Mauritia*-t. grain diameter data plotted against depth for SJO-2010-1. Mean grain diameter is shown, and bars represent the standard error of the mean (points with no error bars have ≤4 measurements). Pollen assemblage zones (PAZ) are shown at the top of the figure. Dashed line marks the distinction between *Mauritia* and *Mauritiella* which can be made on the basis of grain diameter as discussed in Chapter 6. Only those core samples containing *Mauritia*-t. pollen have been shown.

9.4 Discussion

9.4.1 Site-level interpretations

The discussion is structured using the pollen zonation, but all lines of evidence are discussed here to provide an indication of how the site at San Jorge has developed. Age ranges for the different pollen zones have been given to the nearest decade based on the age model in Chapter 7. Where they are used, term such as 'wetter' or 'drier' do not here refer to regional climatic changes but to changes in local site conditions. The potential role of climatic drivers is examined in Chapter 11 where comparisons are also made to data presented from Quistococha (Chapter 8). This serves to aid the observation of patterns common to both sites, and avoid repetition.

9.4.1.1 Lower section below the pollen record: 240–632 cm

The base of the core contains sediments consisting largely of silt and sand, with high magnetic susceptibility. The grain size is indicative of deposition in a moderately high-energy environment and probably indicates that these were laid down by an active channel of the Amazon. Similar sediments underlie the lake and peatland at Quistococha which have also been interpreted as evidence that it is an abandoned channel (see Chapter 10; Räsänen et al., 1991; Roucoux et al., 2013; Lawson et al., 2014).

The basal silts and sands are overlain by layers of mixed clays and organic matter ('muck' sensu Wüst et al., 2003), some of which have high (>50%) loss-on-ignition values. The suspended sediments of the main Amazon channel are mostly fine grained, and consist mostly of silts and clays (Irion et al., 1997), but the high clay content is indicative of low-energy depositional environments such as swales and lakes away from the main channel (Irion et al., 1997). The significant clay content is therefore evidence that the site had become cut off from the main channel. The C/N ratios are relatively high and are more typical of terrestrial vegetation (Meyers, 1994; see Chapter 4). It is possible that the site might have experienced alternating periods of higher and lower inorganic input from the river, perhaps resulting from periodic channel migration, controlling the relative proportion of organic material in the accumulating profile.

9.4.1.2 Zone SJ-1: 220–240 cm (2150-2290 cal yr BP)

The onset of peat accumulation is indicated by an increase in LOI from 58% to 93 % between 244 cm and 240 cm. This zone is dominated by the pollen of *Cecropia*, a light-demanding pioneer tree that typically colonizes floodplain areas following disturbance (Kalliola et al. 1991; Parolin, 2002). Although *Cecropia* forms a closed canopy very rapidly, these trees live for only c. 20 years, and so low-diversity *Cecropia* stands are quickly replaced by more diverse vegetation unless the forest is subjected to continued disturbance (Parolin, 2002).

Cecropia is a prolific pollen producer and is over-represented in Amazonian pollen records (Gosling et al., 2009), but where its abundance exceeds 15-20% this likely indicates that *Cecropia* is abundant at the core site (Roucoux et al., 2013). In zone SJ-1 *Cecropia* pollen exceeds 90%, and was therefore very likely locally abundant (Gosling et al., 2005). Although low in pollen percentage terms, palms may have formed a relatively significant part of the vegetation at this time. The pollen concentration data show that *Euterpe*-t. pollen reached concentrations similar to those seen in zone SJ-5 where its percentage abundance is higher; the percentage abundances in zone SJ-1 may be misleading due to the prolific pollen production of *Cecropia* (Gosling et al., 2005).

This pattern, with *Cecropia* pollen being abundant at the base of the peat profile, is also observed in several of the cores studied from Quistococha. Abundant *Cecropia* pollen is also found in the basal pollen zones of several records from wetland sites in Colombia (Urrego, 1997; Urrego et al., 2006). This may reflect the early stages of riparian succession, with *Cecropia* colonising recently exposed land surfaces (Salo et al., 1986).

9.4.1.3 Zone SJ-2: 194– 220 cm (1960-2150 cal yr BP)

In c. 150 years, the vegetation in zone SJ-1 is replaced by an open community dominated by Poaceae and Cyperaceae, and some other herbaceous taxa (*Begonia*, Asteraceae). Again this is very similar to the Quistococha record of Roucoux et al. (2013) and some of the other cores from that site (e.g. QT-2012-9; see Chapter 8). *Cecropia* drops to less than 15% and therefore it is unlikely that it was abundant at the core point; the open herbaceous vegetation at this time would have allowed *Cecropia* pollen from beyond the core site to be deposited. The abundant Asteraceae (subfamily Asteroideae) pollen at the base of this zone supports the interpretation that the early stages of vegetation development at San Jorge were related to riparian primary succession; *Tessaria* (Asteraceae; Asteroidea) is a common coloniser of recently exposed river sediments (Salo et al., 1986). However, it is unlikely that herbaceous taxa would have naturally replaced shrub taxa (Asteraceae) and *Cecropia* in an autogenically-driven succession. The presence of Cyperaceae and Poaceae likely reflects wetter conditions, and could reflect the deeper ponding of water at the site. *Cecropia* seeds cannot germinate under permanently waterlogged conditions (Parolin, 2002), and this may have been the reason why it was replaced by herbaceous taxa in zone SJ-2.

9.4.1.4 Zone SJ-3: 188–194 cm (1920-1960 cal yr BP)

The early Cyperaceae phase in the San Jorge pollen record is followed by a *Mauritia*-t. phase, which is accompanied by small quantities of *Ilex* and *Euterpe*-t. (< 3%). This phase is only brief, lasting less than c. 100 years. The pollen concentration for *Mauritia*-t. is lower across this interval than in the uppermost *Mauritia*-dominated zone (SJ-5), and

spores are extremely abundant (e.g. *Nephrolepis* reaches 75%). Cyperaceae is also still common (> 8%), and in combination with the low *Mauritia*-t. pollen concentrations this probably does not indicate a closed forest cover despite the high *Mauritia*-t. percentage. Instead there were probably a few individual trees amongst a generally herbaceous community; this inference is supported by the abundant spores of *Nephrolepis* (a gap coloniser; Tuomisto and Ruokolainen, 1994), and the pollen of other herbaceous, light requiring taxa such as *Begonia*. This might explain the brevity of the *Mauritia*-t. peak; the peak in SJ-3 may represent a single tree growing close to the core point at a time when there were only a few scattered individuals at the site.

A brief *Mauritia*-t. phase can also be seen in the pollen record of Behling et al. (2001) from Lago Calado in Brazil. This peak is somewhat lower (c. 15%) than that seen in SJO-2010-1, but also occurred early in the pollen sequence. This was interpreted as a *Mauritia* swamp which formed along the river margin, and as at San Jorge (see below) it was succeeded by an increase in aquatic pollen types which marked the formation of a lake system. At Lago Calado, this transition was inferred to have been caused by a change in sea level during the early Holocene (Behling et al., 2001), a less likely causal mechanism at San Jorge which is more than 2000 km from the sea. At San Jorge, the transition from SJ-3 to SJ-4 was probably caused by channel migration; this would explain the change from river marginal vegetation to aquatic vegetation, and can explain the necessary geomorphological changes required for the formation of a lake system.

9.4.1.5 Zone SJ-4: 100–188 cm (650-1920 cal yr BP)

The mixed *Mauritia* t. and Cyperaceae phase in SJ-3 is rapidly replaced (c. 100-150 years) by one which is dominated by Cyperaceae and *Pistia stratiotes*. This seems to reflect a shift towards wetter conditions at the site; *Pistia* is a free-floating aquatic plant which is common in the Amazon floodplain (Kalliola et al., 1991), and so this supports the inference that the vegetation consisted of aquatic macrophytes at this point in the site's history (see Figure 9.7 for a potential modern analogue). Cyperaceae and Poaceae also both frequently form part of shallow-water aquatic communities in tropical Peru (Kalliola et al., 1991; Piedade et al., 2010; also see Chapter 3). The spores of *Spirogyra*, a genus of algae, is also found in small quantities throughout this zone and is further evidence for the presence of open water. *Spirogyra* is in the family Zygnemataceae, and prefers oxygen-rich waters in shallow lakes or pools (Van Geel, 2001). It is most abundant at the base of this zone (176 cm) and may have declined as *Pistia stratiotes* became established and began to compete for light and nutrients.

The type of aquatic community inferred from the pollen data in this zone requires regular nutrient input; Junk and Piedade (1997) found that *Pistia* does not grow well in

nutrient-poor black water. The abundance of *Pistia* therefore suggests that there was some input of nutrient-rich water during the wet season, an inference supported by the relatively high Ca/Mg ratio across this interval (Shotyk, 1996; discussed in Chapter 4). The lack of significant clay content in this part of the sequence does not preclude continued flooding of the site, as many sites today are flooded annually without the deposition of significant quantities of sediment (discussed in Section 3.2).

The pollen data are contradicted somewhat by the geochemistry. C/N ratios for some temperate lakes (< 10: cf. Meyers, 1994) are lower than those for the gyttja in the lake core at Quistococha (Chapter 8), but those in the lake core are all < 20 whereas those above 240 cm at San Jorge never drop below 25. These higher values are more typical of C3 land plants (Meyers, 1994; Meyers & Lallier-Vergès, 1999). In the Carajas record (core CSS2: Absy, 1991; Sifeddine et al., 2001), high C/N ratios are associated with terrestrial pollen types, and zones dominated by *Isoëtes* spores are associated with low carbon concentrations and low C/N values (<15). The visible stratigraphy of SJ-4 is not typical of open lake sediments, with a distinct lack of fine gyttja observed in the core. However, the lake sediments from the margins of the lake at Quistococha are similar in appearance ('lake peat') and have a similar C/N ratio to the peats from this section of the San Jorge core (see Chapter 8). These may provide an analogue for the depositional environment in this part of the core, where the abundant aquatic pollen suggests that the material could be derived largely from floating macrophytes rather than lake algae. It is also plausible that the intrusion of roots could have altered the appearance of lake deposits that had been deposited previously (Walker, 1970). At the start of zone SJ-5 when there is an increase in *Mauritia* t. pollen, there would have been less than a metre of organic material from zone SJ-4 underlying any trees as they became established.

There are some other records from Amazonia which record an aquatic phase, but none could be found where *Pistia* was recorded in such abundance. It is possible that *Pistia* pollen has been inconsistently identified in the past (see Chapter 4). The Lake Comprida record contains abundant herbaceous taxa including Cyperaceae and Poaceae (Bush et al., 2000), and the Lake Gentry and Lago Calado cores record an aquatic phase with abundant *Sagittaria*, Poaceae, and Cyperaceae (Bush et al., 2007b; Behling et al., 2001). Bush et al. (2007b) record that this pollen assemblage is associated with a 'fibrous gyttja', which may be similar to the stratigraphy observed in SJO-2010-1 and lends support to the interpretation of zone SJ-4 given above.

Figure 9.7: A possible modern analogue for zone SJ-4: a lake in Manu National Park, Peru, where floating *Pistia stratiotes* and Cyperaceae have covered part of the lake surface. Open water can be seen in the background (Photograph courtesy of T. R. Baker).

9.4.1.6 Zone SJ-5: 8-100 cm (AD 1990-AD 1300)

The transition from the Cyperaceae- and *Pistia*-dominated assemblage in SJ-4 to a more closed, mixed palm forest, is associated with a long hiatus or period of slow accumulation in the core (Chapter 7; Figure 9.4). There is a marked peak in the pollen and spore concentration, followed by a peak in the palm phytolith concentration. These could be interpreted as a decrease in the peat accumulation rate, and hence may indicate locally drier conditions at this time (see Chapter 2, Figure 2.6). A mixed Poaceae, Cyperaceae, and *Pistia* phase is accompanied by the appearance of *Mauritia*, *Mauritiella*, and other Arecaceae as minor constituents towards the top of zone SJ-4, but this may reflect the mixing of non-contemporaneous pollen grains resulting from the slow accumulation rate. Alternatively, the increase in peatland taxa such as *Mauritia* alongside lake taxa such as *Pistia* could indicate the gradual encroachment of the peatland on a shrinking lake, implying that autogenic terrestrialisation was associated with the transition from SJ-4 to SJ-5.

At the onset of zone SJ-5, the pollen of *Alchornea* increases markedly in abundance, above the levels seen throughout the rest of the record, which suggests secondary forest encroaching on a disturbed area (Rondon et al., 2009). The increase in certain taxa, such as *Mauritia*-t., *Euterpe*-t. and *Ilex* is typical of the establishment of a palm-dominated forest, much like the aguajals found today at Quistococha and other sites (Roucoux et al., 2013; Aguajal Project database). Indeed, whether initiated by an external disturbance or otherwise, this could be typical of successionally-driven changes in peatland palm swamps. At Quistococha, a virtually identical pattern is observed whereby the early phase of palm swamp establishment is associated with *Mauritia*-t. and other Arecaceae

pollen, along with commonly associated taxa such as *Ilex* (cf. Roucoux et al., 2013; Chapter 8). This possible successional pattern is discussed further in Chapter 11.

There is a drop in pollen diversity above 50 cm depth, where *Euterpe*-t. pollen decreases in abundance. It is probable that this reduction represents the point at which the present pole forest vegetation became established at the site (discussed further below). There is some evidence to show that the establishment of the pole forest may have been associated with a disturbance event, as there is a significant peak in *Cecropia* at 56 cm depth and there is a peak in *Alchornea* at 40 cm depth which is indicative of secondary growth.

Apart from the Quistococha records (Chapter 8; Roucoux et al., 2013), there are several other published pollen records with assemblage zones dominated by *Mauritia*-t. Percentages in other records often remain below 10%, but there are many records where *Mauritia*-t. is present in greater proportions: for example, at Maxus 4 is exceeds 80% (Weng et al., 2002), at Anangucocha it reaches c. 40% (Frost, 1988), and at Lake Comprida (Bush et al. 2000), *Mauritia* is more abundant than all other pollen types combined, suggesting that it may have encroached upon the lake margins. High *Mauritia*-t. and *Mauritiella*-t. pollen values (> 40% in some cases) are found in two lake records (L. Carimagua, L. Sardinas) from the Llanos Orientales (Colombia). Both L. Sardinas and L. Carimagua are surrounded by *Mauritia* and *Mauritiella* respectively at the present day, and these communities have also been shown to have followed a herbaceous vegetation phase (Behling & Hooghiemstra, 1999). However, this is unlikely to provide a suitable analogue for the pollen record at San Jorge; in the Llanos Orientales, herbaceous taxa in the palaeoecological record are interpreted as representative of dry savannah vegetation.

The exceptionally high percentages of *Mauritia*-t. at San Jorge are matched by few other records (see above), but this is probably the result of pollen taphonomic processes. Most Amazonian records are derived from lake sediments, and therefore contain a higher proportion of anemophilous pollen (e.g. *Cecropia*; Moraceae: Gosling et al., 2005), whereas in a peatland pollen is also deposited directly underneath the vegetation (this is discussed in the context of the Quistococha records in Chapter 10). As can be seen in the lake core at Quistococha, although *Mauritia* and *Mauritiella* are dominant at the site today their pollen constitutes around 20% of the pollen assemblage against c. 80% in the peatland surface samples (Chapter 6).

9.4.2 The history of the pole forest

Pole forest of the kind growing at San Jorge is rare in lowland Amazonia, although small areas of similar forests growing on sandy substrates cover c. 3% of the Amazon basin

('white sand forests'; Fine et al., 2010), and until recently the composition of this kind of peatland forest was completely undescribed (see Chapter 3). The pollen data from the surface samples indicates that the pollen representation for the dominant pole forest tree species is poor, and even where only a few *Mauritia flexuosa* individuals are present these will entirely overwhelm the pollen signal (see Chapter 6). However, in the pollen record below 48 cm depth the pollen assemblage also contains more abundant *Euterpe*-t. pollen than in the upper layers, and therefore it can be inferred that there was a significant change in forest composition at this point. The *Mauritia*-t. grain size data also indicate a change to pure *Mauritia flexuosa* at this point (Figure 9.6). As *Mauritiella* is absent from the modern pole forest (see Chapter 3), this is also a significant transition. There is also a peak in phytolith concentrations at 48 cm which could indicate a shift towards drier conditions (see Chapter 2). Based on the age model for the core this transition is dated to between AD 1750-1850. The potential causes of this very recent change in forest composition are discussed further in Chapter 11.

9.4.3 Major elements and vegetation change

As at Quistococha (cf. Lawson et al., 2014), past changes in vegetation shown in the pollen record are accompanied by changes in the present peat chemistry. Following the inception of the peatland at around 240 cm, the most marked change in peat chemistry occurs at c. 112 cm. There is also a slight decrease in carbon content above 96 cm depth to below 60 wt%. These changes coincide with the transition from an assemblage with more herbaceous elements (Poaceae, Cyperaceae, *Begonia* sp.) and aquatic taxa (*Pistia stratiotes*) to one which is palm dominated (*Mauritia*-t., *Euterpe*-t..). The decrease in Ca/Mg ratio across this interval indicates that these changes were associated with reduced nutrient input (Shotyk, 1996; also see Chapter 4). The pollen data also support the inference that this transition represents a local change to drier conditions, with the decline of *Pistia* being particularly indicative. Further support for this suggestion comes in the form of the very high pollen concentration at 96 cm, which is associated with a slower accumulation rate or hiatus which would be expected during drier conditions (Page et al., 2004). The degree to which the change to drier conditions was related to localised hydrological changes or climatic change is discussed further in Chapter 11.

However, there are a number of notable differences between the geochemical profiles from the two sites, San Jorge and Quistococha. The first is that, at Quistococha, there is no general trend in C/N ratio or in the C and N content of the peat following peat initiation (see Lawson et al., 2014); the only notable feature is that there is a decrease in C/N ratio to around 15.2 in the uppermost 50 cm. At San Jorge, following peat initiation there appears to be a general decrease in C/N ratio from 240 cm upwards. The C

concentration remains virtually unchanged from 4-240 cm depth, but N concentrations increase gradually upwards. In the Slave Lake peatland (Canada), Kuhry and Vitt (1996) found that C/N ratios increase upwards towards the top of the core; they inferred that this was related to an initial loss of nitrogen in the upper, less water-logged, peat laters followed by carbon loss due to anaerobic decomposition in the lower peat layers. The pattern in the San Jorge core is therefore the opposite of that at Slave Lake. It seems probable therefore that the variation in C/N ratios reflect the changing origin of the litter (Meyers and Lallier-Vergès, 1999), more than the level of decomposition (Kuhry and Vitt, 1996).

Towards the top of the San Jorge core, the high N concentrations are likely related to the proximity to fresh leaf litter and recycling of this essential plant nutrient in the root zone (Weiss et al., 2002; Lawson et al., 2014). This pattern could also be explained by the direct addition of fresh litter in the form of live roots; a recent study in a forested Panamanian peatland has shown that roots are one of the main components of the peat in these systems (Hoyos-Santillan, 2014). This inference is supported by the visible stratigraphy at San Jorge. High N in the upper peats could also be explained by the rapid accumulation rates and therefore relatively young age of the peats compared to the site studied by Kuhry and Vitt (1996) which is c. 10,000 years old.

9.5 Summary

The first pollen data for a domed Amazonian peatland (San Jorge) have been presented. They indicate pronounced changes in vegetation composition which can be seen even at the family level. Palm forest became established at the site following largely herbaceous and aquatic communities during the earlier part of the peatland's development. This transition coincides with a hiatus or period of slow deposition identified by radiocarbon dating (Chapter 7). The 'pole' forest seen at the site today is difficult to detect in the pollen record (Chapter 6), but the modern forest seems to have appeared recently in the site's history, probably within the last two hundred years. This interpretation is supported by the identification of a *Mauritia flexuosa* dominated assemblage in the top 50 cm of the core on the basis of pollen grain size data, and ^{210}Pb dating (Chapter 7). The changes seen at the site are consistent with changes in local hydrological conditions and nutrient input, but whether these could in turn have been driven by late Holocene climate change will be explored in Chapter 11.

10. The development of Quistococha peatland

10.1 Introduction

10.1.1 Overview

This chapter first seeks to examine the applicability of conceptual models formulated for peatlands in other parts of the world, and to examine the necessity of a new model for the development of Quistococha. A conceptual model is then presented which combines a detailed palaeoenvironmental reconstruction with inferences about peatland developmental processes, and which provides a model of both vegetation development and peatland expansion for Quistococha. As part of the model development, the hypothesis that vegetation change occurred synchronously across the site is also tested. This in turn is connected to the discussion of developmental drivers in Chapter 11. In order to examine the role of allogenic drivers in peatland development, the synchroneity of changes in vegetation at different sites is discussed in Chapter 11, but this chapter examines the fundamental assumption that a single core is representative of the site as a whole, i.e. that:

i) Vegetation communities in the pollen record are similar across the site.

ii) Vegetation changes are synchronous across the site.

In particular, synchroneity between cores from different sites may well be meaningless if within-site changes are asynchronous. The Quistococha model draws on a combination of stratigraphic data, radiocarbon dates, and pollen analyses presented in this thesis and in Roucoux et al. (2013) and Lawson et al. (2014); the approach is similar to that of others who have formulated conceptual developmental models for some northern peatlands (Chapter 2). As discussed in Chapter 7, the chronology of the sequences studied by Aniceto et al. (2014) from the lake at Quistococha is potentially problematic, but the sedimentological evidence from that study is mentioned at some points in the discussion.

The model is not intended to be a general model for the development of peatlands in the Pastaza-Marañón basin as a whole, although it may be illustrative of some of the processes at work in these systems. Amazonian peatlands are diverse (Lähteenoja & Page, 2011), and a single model is unlikely to be representative of all peatlands found in this region. Further research is required into the development of other sites, particularly with regard to vegetation phases which may vary to a greater degree than peatland processes.

10.1.2 Applicability of other developmental models

In Chapter 2, the conceptual models of Anderson (1961) and Phillips & Bustin (1996) for Southeast Asian and Panamanian peatlands respectively were discussed. Although elements of these models have some applicability in Peru, they differ significantly from peatlands in Peru in terms of the allogenic influences on their development, and are not transferable to Amazonian peatlands. In particular, both describe peatlands which are close to or below sea level, a feature which affects their hydrology and, therefore, their long-term development. The Changuinola peatland is intersected by tidal channels, and peatland expansion is related to the progradation of a sea barrier (a natural berm) and tectonic subsidence (Phillips & Bustin, 1996). The Anderson (1961) model shows a peatland with no lake phase, where the flat surface, the low hydraulic gradient resulting from the proximity to sea level, and the impermeable substrate, provide the conditions for peat initiation. These models are also based on few radiocarbon dates (three in Anderson, 1961; four in Phillips & Bustin, 1996), and therefore must make assumptions about the process and rate of lateral expansion. Although these models are referred to later in this chapter, in more detailed discussions, alone they do not provide a strong basis for a conceptual model of Quistococha.

In Table 10.1, four other established conceptual models of peatland development have been outlined. Although there are numerous conceptual models for peatland development, these contrasting models encompass a range of common peatland processes, and cover differing combinations of terrestrialisation and paludification (described in Chapter 2). Constructed for temperate and sub-arctic peatlands, they present a number of testable hypotheses which can be used to assess their applicability, and these have been examined using the data obtained from Quistococha (Table 10.1). Peatland plant species will mostly differ between these models and those found in Amazonian peatlands (excepting perhaps Cyperaceae and Poaceae) and so have been excluded from the discussion.

The model of Kratz and Dewitt (1986) was based on earlier conceptual models of peatland development, and they termed this the ‘expanded classical model’. This model has some applicability at Quistococha, and at some points across the site (e.g. QT-2012-9) there is evidence that the initial phases of organic accumulation were from a floating mat. Ireland et al. (2013) have since noted that allogenic (climatically-driven) paludification also operated at Fallison Bog. However, in Chapter 7 the expansion of the peatland at Quistococha was shown to have occurred in two distinct phases (not a typical feature of paludification or terrestrialisation), so the ‘classical model’ does not appear to capture all of the processes of lateral expansion.

Table 10.1: Different bog developmental models formulated for northern peatlands (discussed in Chapter 2), including predictions which can be used to test their applicability, and how these relate to the observations from Quistococha. All models apart from that of Sjörs (1983) are for sites where lakes are present at some point during site development.

Conceptual model	***Fallison Bog Model (Expanded classical model)***	***Myrtle Lake Model***	***Swedish Model***	***New England model***
References	**Kratz and DeWitt (1986)**	**Heinselman (1963)**	**Sjörs (1983)**	**Anderson *et al.* (2003)**
Model summary	The lake is gradually filled in as floating mats of vegetation impinge on areas of open water.	The lake is self-perpetuating. A lake of sufficient size and depth cannot easily be colonised and filled in by floating mats of vegetation. The lake remains in the same position, accumulating its own lake sediments, as the peatland around it grows vertically.	Paludification is dominant process of lateral expansion. The peatland grows (or has grown in the past) mostly by gradually colonising adjacent areas of land.	Terrestrialisation of a lake is followed by paludification. Shallow peat areas contain younger peat directly on mineral substrate. Peatland growth is autogenically driven, with no direct climatic influence, and is controlled by basin shape.
Testable predictions	Terrestrialisation **A.** Tripartite sequence near to the modern lake (Lake sediments > Lake peat > Pure peat). **B.** Peat overhanging clear water (floating mat) **C.** Palynology shows aquatic taxa near base typical of the aquatic taxa which terrestrialised the lake margins.	Open water with little terrestrialisation **A.** No lake sediments underlying the peatland. **B.** No floating mats of vegetation. **C.** Possible erosive contact with the surrounding peatland which maintains the size of the lake and prevents terrestrialisation.	**A**. Peat initiation was not synchronous across the site. The gradual colonisation of peat results in a range of peat basal dates. **B**. Pollen assemblages near clay/peat contact contain mainly arboreal taxa (rather than aquatic taxa typical of terrestrialisation).	**A.** Paludified areas along site margins may be younger then terrestrialised areas. Shallow peat areas are younger than deeper areas, as peat accumulates in the deeper parts of the basin first before expanding on surrounding areas. **B.** Changes unlikely to be synchronous with other sites. No evidence of externally driven changes in development.
Corresponding patterns at Quistococha	**A.** Evidence of terrestrialisation in QT-2012-9 **B.** Floating mats are present at Quistococha but these are small and free floating; they do not seem to be attached to the adjacent peatland. Peatland margin appears erosive in places. **C.** Mostly in QT-2012-9, where *Pistia* and algal spores are present. Cyperaceae present at base in several cores; Cyperaceae is found in the floating mats at the present day but can be terrestrial.	**A.** Basal accumulations containing abundant Cyperaceae pollen in QT-2012-9 were probably laid down under aquatic or semi-aquatic conditions (algal spores also abundant in basal pollen zones). **B.** There are some floating mats still visible at the site, although these are small. **C.** Edge of the peatland does seem to be eroding in places at the present day.	**A**. Peat initiation occurs in two main phases during the early stages of site development. Some evidence for recent paludification along site margins where *'Mauritia'* peat sits directly on clay. **B**. QT-2012-10 does not exhibit an early herbaceous phase. QT-2012-18 has a *Symmeria* dominated zone near to the base indicative of flooded forest rather than floating mats, although this is alongside Cyperaceae.	**A.**Terrestrialisation at the site of QT-2012-9 occurs later than 'primary mire formation' on southern part of site. Thinner peat areas initiated at same time as thicker peat areas (e.g. QT-2011-2 vs QT-2010-1). **B.** Some evidence of changes synchronous with those at San Jorge (Chapter 11). Evidence of a disturbance event prior to establishment of *Mauritia* swamp (Cecropia phase in QT-2012-10).

Heinselman (1963) produced a model showing the persistence of Myrtle Lake through time, and again this seems to have some applicability at Quistococha. The observed erosive margins may indicate that the lake is too large to be easily terrestrialised at the present day and that wave action keeps the peatland from encroaching on the open water (see Chapter 3). It may also be the case that, in order to thrive, floating aquatic plants require abundant nutrients to be present in the water, and previous studies have shown that many do not grow in black water systems (Junk & Piedade, 1997; Chapter 3). Without an established aquatic community, encroachment on the lake by floating vegetation is severely limited today. However, there is evidence of earlier terrestrialisation (QT-2012-9), and therefore while the 'Myrtle Lake' model is a relatively close match for Quistococha it is not a perfect one.

The applicability of the Sjörs (1983) model is supported by the dominance of terrestrial pollen types in the base of some of the peat sequences studied (e.g. Q18-A; Q2-A), but in some cores there is evidence of an aquatic phase. The gradual paludification of the Sjörs (1983) model is also not found at Quistococha, where peat initiated across the whole site within a few hundred years (Chapter 7). It may well be the case that across much of the site, peat initiation occurred through paludification, but it is clear that the simple model of Sjörs (1983) does not capture the full range of processes at Quistococha.

The Anderson et al. (2003) model includes both terrestrialisation and paludification, and suggests that paludification follows an initial phase of terrestrialisation. However, in QT-2012-9 terrestrialisation occurs after peat initiation along the eastern site margin. Anderson et al. (2003) also conclude that paludification is largely controlled by subsurface topography, and in all the sites examined by Anderson et al. (2003) paludification occurred on shallower areas following the terrestrialisation of deeper basins. Low hydraulic conductivity peat trapped inflowing water at the peatland margins, aiding paludification (Anderson et al., 2003). There is certainly evidence from Quistococha which shows the important role that subsurface topography plays in determining peatland vegetation composition (discussed below in Section 10.4.2). However, the high hydraulic conductivity of peat in some Amazonian peatlands, including Quistococha, may hinder the process of paludification as described by Anderson et al. (2003). Furthermore, at Quistococha basal dates from shallow areas are generally similar in age as those from deeper areas; for example, peat initiation in QT-2010-1 and QT-2011-2 appears to have been synchronous within ^{14}C dating errors. Paludification of the site occurs in two main phases, and not continuously as would be expected if it had been autogenically driven. In peatlands where autogenic paludification has occurred in the absence of climate change, there should be a wide range of basal dates indicative of steady lateral expansion, with younger dates on shallower peat areas

(Anderson et al., 2003; Bauer et al., 2003). There is some further evidence of a climatic influence on peatland development at Quistococha in the form of a *Cecropia* phase (QT-2012-10, QT-2011-2) and a *Ficus* phase (QT-2012-9) which precede the main increase in *Mauritia*-t. in these cores (discussed further under Phase IV, and in Chapter 11).

Evaluation of the available peatland developmental models shows that whilst there are elements which can be applied to help describe and understand the processes operating at Quistococha, none of the four models discussed fully explains the patterns recorded at Quistococha. A new model including a different combination of processes is required to capture the full detail of site development. This is also essential if vegetation is to be incorporated.

10.1.3 The inclusion of allogenic processes in the model

The question of whether changes observed in the peatland archive are predominantly the result of internal or external processes has been a major motivation for research in this area (Foster and Wright, 1990; Lavoie et al., 2013). The rivers of the Amazon basin are some of the largest in the world, with the Amazon discharging more fresh water into the ocean each year than the next eleven largest rivers combined (Gupta, 2011), and the floodplain environment of the Pastaza-Marañón basin is geomorphologically dynamic (Lamotte, 1990; Kalliola et al., 1991; Räsänen et al., 1992). Any model of peatland development in this region must therefore include some aspect of disturbance if it is to fully illustrate the controls on peatland development over Holocene timescales. The abrupt changes seen in the peatland vegetation record imply some form of external driver (Payette, 1988), including channel avulsion and climatic change (Roucoux et al., 2013). Theoretically, rapid ecosystem changes can also occur at the result of autogenic processes (Scheffer et al., 2001), for example when the accumulation of peat causes a critical threshold to be crossed with respect to the water table depth (Granath et al., 2010), but many abrupt changes in peatlands have been linked to allogenic factors.

The influence of climate on peatlands can only be established by making comparisons with other sites (e.g. Anderson et al., 2003; Hughes and Barber, 2003). This section incorporates both palaeoenvironmental interpretations and inferences about peatland processes, but reserves substantive inferences about external drivers for Chapter 11. This allows a conceptual separation between site-based evidence of externally-driven change (e.g. high pollen concentrations could be interpreted as the result of low peat accumulation rates, for which one explanation could be drier climate), and inferences based on the synchroneity with other records drawn from the wider region. In palaeoecology, there are many lines of reasoning leading to the final interpretation, and it is important these can be followed straightforwardly.

10.2 Testing the synchroneity of vegetation change

Two key features of the pollen stratigraphy were targeted in order to test the synchroneity of vegetation changes seen across the peatland at Quistococha: a peak in *Mauritia*-t. seen in the lower part of several of the cores, and the increase in *Mauritia*-t. observed in the uppermost pollen zones in all of the cores Radiocarbon dates were obtained specifically to date these two features (see Chapter 8), and the results are discussed below.

10.2.1 The lower peak in *Mauritia*-type pollen

Although the rise of *Mauritia*-t. can be seen towards the top of all the cores, in some cores there is also an earlier peak in *Mauritia*-t. pollen across one or two samples below 160 cm depth. This peak varies in magnitude between different cores, from a maximum of 40% in QT-2010-1 to as little as 9.6% in QT-2011-2. There is no clear peak in QT-2012-18, and this feature is also unclear in the lake core (discussed further in Sections 10.2.2 & 10.2.3).

The timing of the lower *Mauritia*-t. peak differs in the pollen stratigraphy across the site (Table 7.1; Chapter 8; cf. Roucoux et al., 2013). In QT-2012-9, this peak in *Mauritia*-t. is dated to 1571-1817 (2σ) cal yr BP, whereas in QT-2010-1 it occurs earlier, between 1900-2000 cal yr BP (based on the QT-2010-1 age model). In QT-2012-10 and QT-2011-2, this peak appears to have occurred earlier than in both of the other cores. The early *Mauritia*-t. peak is synchronous in these two cores (within the errors of radiocarbon dating), and occurred between 2158-2358 cal yr BP in QT-2012-10 and between 2040-2308 cal yr BP in QT-2011-2. In both cores, this corresponds to the period immediately following peat initiation. Some caution may be required in inferring diachroneity between these shorter cores and QT-2010-1 due to the more 'compressed' chronostratigraphy in QT-2012-10 and QT-2011-2; the difference in age between samples 16 cm apart is much greater than in a longer core.

However, if the peak is genuinely time-transgressive across several cores, an internal driver must have caused the *Mauritia*-t. peaks; an external driver would be expected to cause a synchronous peak across the site. In the two cores where *Mauritia*-t. became established early, morphometric (or pollen grain size) data reveal an *M. flexuosa*-dominated assemblage in QT-2012-10 and a more mixed population with a greater proportion of *Mauritiella* in QT-2011-2. In QT-2012-18, where there is no lower peak in *Mauritia*-t. pollen (i.e. below the main increase at 96 cm), it appears that the *Mauritia*-t. grains largely consisted of *Mauritiella* at this time. In all of the cores, early assemblages are more mixed, and given that *Mauritiella* appears to be a less prolific pollen producer

than *Mauritia* (Chapter 6), it seems likely that *Mauritiella* was more prevalent than *Mauritia* during the earlier part of site development.

The reason for the time-transgressive nature of the lower *Mauritia*-t. peak in the pollen stratigraphy at Quistococha may therefore be due to the differing edaphic preferences of *Mauritia* and *Mauritiella.* These two palms do not always co-occur (Endress et al., 2013; Chapters 3 & 6), and have some physiological differences in their root morphology (Seubert, 1996). In a natural vegetation succession, these two palms could be expected to expand to occupy suitable parts of the site at different points in time. For example, although *Euterpe* and *Mauritiella* have similar adaptations which allow them to grow in waterlogged environments, such as pneumatophores, they differ in their spatial and temporal successional patterns (Urrego et al., 2006).

10.2.2 The second rise in *Mauritia*-type pollen

Across all of the peat cores, an increase of *Mauritia*-t. can be seen in the pollen stratigraphy in the top 150 cm or less. On the basis of pollen grain size data collected for the cores (see Chapter 8), we can infer that increases in both *Mauritia* and *Mauritiella* probably occurred together. *Tabebuia* is not a prolific pollen producer (Chapter 6), and therefore the persistent presence of its pollen in some of the cores (e.g. QT-2011-2, QT-2012-10) alongside *Mauritia* and *Mauritiella* likely indicates that it also became abundant across the site.

The timing of the increase in *Mauritia*-t., which represents the rise of the species which constitute the majority of individuals at the site today (see Chapter 3), appears to have been synchronous, with the exception of the area close to the lake shoreline (QT-2012-9). In cores QT-2011-2, QT-2012-10, QT-2012-18, the increase in *Mauritia*-t. pollen is dated to 916-1174 cal yr BP, and 900-1000 cal yr BP in QT-2010-1 (Roucoux et al., 2013), meaning that the increase is synchronous within the errors of radiocarbon dating in these cores (Figure 10.1). However, in QT-2012-9 this transition is dated to 566-676 cal yr BP. Therefore, as for the earlier peak in *Mauritia*-t. discussed in Section 10.2.1, the second *Mauritia*-t. increase occurred later at the lake margins than elsewhere on the site. In the lake core, the initial increase in Mauritia-t. occurs c. 1600 cal yr BP. However, a second significant increase in *Mauritia*-t. is seen in the lake core in zone QTL-D (40 cm: 541-707 cal yr BP) which also occurred after the increase in *Mauritia*-t. across the rest of the peatland. The vegetation growing around the immediate lake margin is likely to be better represented in the lake core pollen record, and so its stratigraphy is more likely to match that of QT-2012-9 than the other cores. The possible causes of the later increase in *Mauritia*-t. around the lake margins are discussed in Chapter 11.

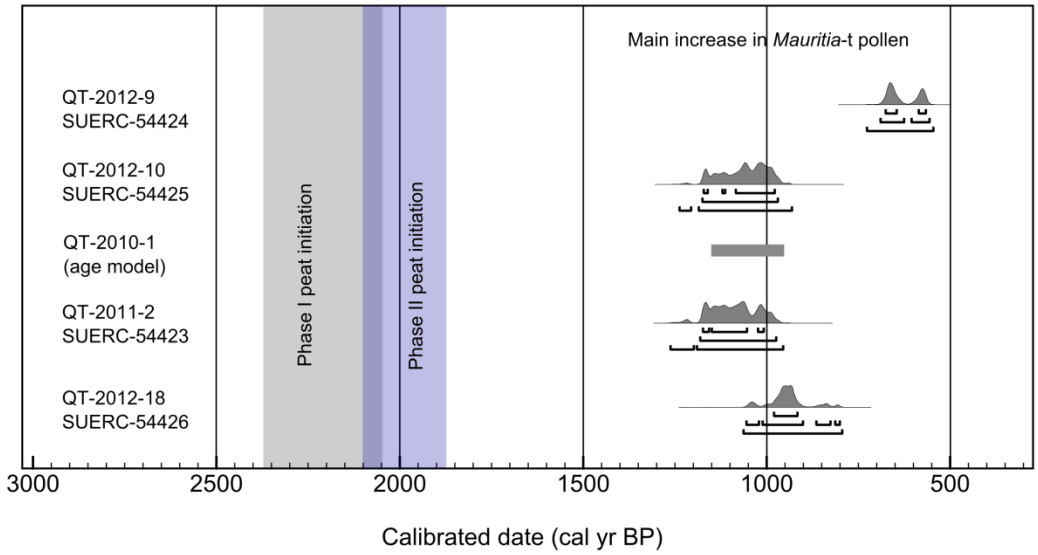

Figure 10.1: Radiocarbon dates for the main increase in *Mauritia*-t pollen seen across the peatland at Quistococha. Dates have been arranged in order from north to south, and the two main phases of peat initiation are shown for context (see below and Figure 7.1).

10.2.3 Differences between lake and peatland pollen records

The proportions of key taxa, and the points at which their abundances change, are markedly different between the lake and peatland records. Perhaps most significantly, *Mauritia*-t. pollen became abundant in the lake core from c. 1600 cal yr BP onwards (Chapter 11; Figure 11.2), much earlier than the increase seen in the peatland record where it occurs between 900-1170 cal yr BP (slightly later at 566-676 cal yr BP in the case of QT-2012-9).

There is controversy as to the pollination mechanism of *Mauritia flexuosa*, with some arguing that it is pollinated by small beetles (Coleoptera) of the Chrysomelidae and Nitidulidae families (Knudsen *et al*., 2001), and others that it is largely wind-pollinated (Rosa and Koptur, 2013). Alternatively, *Mauritia* may be ambophilous (i.e. be both wind and insect pollinated), although Rosa and Koptur (2013) suggest this is unlikely. If significant quantities of *Mauritia flexuosa* pollen can be transported on the wind, then the early increase in *Mauritia*-t. seen in the lake record may be the result of non-local expansion of *Mauritia* on the adjacent floodplain.

However, according to the Prentice-Sugita model of pollen transport (Prentice, 1985; Sugita, 1993; Davis, 2000), the pollen signal from vegetation close to a lake is an order of magnitude larger than for vegetation only a few hundred metres away. Wind speeds in tropical forests are very low; measurements from northern Colombia show mean wind speeds as low as 0.3 m s^{-1} beneath the canopy (Baynton et al. 1965). Rull (1998) also argues, based on studies of modern pollen dispersal, that *Mauritia* pollen is largely confined to areas where the trees themselves are growing. Therefore, the early increase

in *Mauritia*-t. seen in the lake core may still require a site-level explanation (i.e. one which involves changes across the peatland or around the lake margins, not on the floodplain beyond).

One possibility is that *Mauritia* and *Mauritiella* expanded along the site margins where the depth to the substrate is smaller, especially on the western part of the site. Although there are no significant peat accumulations along the western shoreline, *Mauritia flexuosa* can be seen growing there at the present day. In the area near to the artificial beach (c. 200 m west of QT-2011-7), *Mauritia flexuosa* can be found growing on an area of waterlogged soil with only a thin organic soil or peat layer. This environment is similar to that found at palm swamp sites near Jenaro Herrera investigated by the present study (see Chapter 3). *Mauritia* may have colonised this part of the site c. 1600 cal yr BP, explaining the early increase in the lake core, but have left little record in terms of peat accumulations.

Other differences between the lake record and the peatland records include the lower abundances of taxa such as Myrtaceae, *Symmeria*, *Psychotria*-t., *Ficus* and *Ilex* in the lake record. This difference is almost certainly the result of differing pollen dispersal mechanisms; for example, *Ficus* is insect pollinated and poorly dispersed (Horn and Ramirez, 1990). Myrtaceae, *Symmeria*, *Ilex*, and *Psychotria* are also all insect pollinated (Bush, 1995). The upper part of the lake core is dominated by taxa which are not generally well represented in the peat cores, such as *Cecropia* and Moraceae pollen, which have anemophilous pollination mechanisms. Moraceae pollen dominates the pollen rain from *terra firme* areas (Gosling et al., 2005, 2009), and therefore this signal likely represents the adjacent terrace areas and not the floodplain.

10.3 The development of Quistococha peatland

In this section, the development of the Quistococha peatland is discussed, and a conceptual model is proposed which makes reference to the data collected from across the peatland and presented in previous chapters (Figure 10.2 and Table 10.2). The period preceding peat initiation is also discussed; this period is not included in Figure 10.2 as this figure is intended to show changes in vegetation and at this time vegetation patterns are poorly constrained (it is also likely that much of the site was under water prior to peat initiation). This model seeks to illustrate the main developmental phases of Quistococha peatland, although it does not capture the fine detail of vegetation change as shown in the pollen diagrams. Whilst pollen data is often interpreted core by core, the aim here is to produce a chronology for the development of the peatland which draws together all of the evidence collected. Interpolations and inferences have been made in order to provide a fuller illustration of the site's history, but the transects and core

points used as a basis for these interpretations have been included in Figure 10.1 to indicate where the conceptual model is more speculative. Annotations have also been used for the same purpose. In the discussion, the terms 'deep' and 'shallow' have been used (rather than 'thick' and 'thin', terminology preferred for descriptions of modern peatlands by Lawson et al., 2015), as 'deeper' areas of the site were not necessarily occupied by 'thick' peat accumulations at the points in time under discussion.

Table 10.2: Key details of the developmental phases (illustrated in Figure 10.2) reconstructed for the Quistococha peatland from the six palaeoecological records for the site and the basal dates on six other cores. Chr. = the basis for the chronology of each phase (symbols given beneath table). Pollen zones with a 'QT' prefix refer to Roucoux et al. (2013). In contrast to normal geological convention, the oldest phase is given at the top to ensure congruity with the sequence shown in Figure 10.2.

Phase	Summary	Timing
I. Peat initiation	Peat initiated in the area within 800 m of the lake aided by the impermeable clay substrate. Pollen evidence indicates largely herbaceous vegetation with abundant Cyperaceae at this time. Some cores contain pollen which suggests the presence of taller trees (e.g. Anacardiaceae in QT-2011-2). *Symmeria* is an indicative taxon in QT-2010-1 but low in abundance. **Indicator taxa:** *Hevea*, *Symmeria paniculata*, Cyperaceae **Pollen zones:** Q2-A, Q9-B, Q10-A, QT-2	2,100-2,400 cal yr BP **Chr.:** P, R, L
II. Externally-controlled expansion through 'primary mire formation'	The peatland expanded to cover the southern part of the site through 'primary mire formation' as the influence of the river declined. *Symmeria paniculata*, a small tree tolerant of deep flooding, is prevalent across large parts of the site. Note that this phase overlaps somewhat with Phase I, a feature which likely results from radiocarbon dating uncertainties. **Indicator taxa:** *Symmeria paniculata*, *Adelobotrys*-t., *Begonia*, *Cecropia*, Cyperaceae, *Brosimum*, Moraceae, *Maquira*-t. **Pollen zones:** Q2-A, (Q9-B), Q10-A, Q18-A, QT-3	1,900-2,200 cal yr BP **Chr.:** P, R
III. Flooded forest	The site continued to be flooded annually, an inference supported by the presence of Myrtaceae. Shrubby taxa are prevalent across the site, especially Rubiaceae types such as *Psychotria*. Increase of *Mauritia*-t. in the lake core is interpreted as the result of *Mauritia* stands along the western lake margin. **Indicator taxa:** Myrtaceae, *Coussapoa*, Rubiaceae, Rubiaceae (type 2), Mel./Comb., *Adelobotrys*-t., *Psychotria*-t., *Brosimum*. **Pollen zones:** Q2-B, Q9-C, Q10-A, Q18-B, QT-4	1,900-1,100 cal yr BP [remnant around the lake until 566-678 cal yr BP] **Chr.:** P, R
IV. Mixed palm swamp	*Euterpe*-t. pollen phases are seen across the site, particularly in shallow peat areas (e.g. QT-2012-10, QT-2012-18). *Mauritia* and *Mauritiella* are both abundant across the site, especially in deeper peat areas (e.g. QT-2010-1). Peatland paludification (although relatively minimal) along the western site margin may have begun at this time, although this is based on stratigraphic evidence only (i.e. the presence of '*Mauritia*' peat only in core QT-2012-1). A second expansion of mixed palm swamp along the eastern lake margin was related to the delayed terrestrialisation of this area, and it is inferred that Myrtaceae and other flood tolerant taxa also lingered until this transition (Myrtaceae, although low in abundance, declines in the lake core c. 650 cal yr BP). **Indicator taxa:** *Euterpe*-t., *Symphonia globulifera*, *Alchornea*, *Ilex*. **Pollen zones:** Q2-C, Q9-D & Q9-E, Q10-C, Q18-C, QT-5	1,100 - 400 cal yr BP [second expansion: 566-678 cal yr BP] **Chr.:** P, R
V. Aguajal	The site as seen at the present day forms, with *Mauritia* and *Mauritiella* both very abundant. *Tabebuia* is found during Phase IV, but becomes more abundant in some cores during this phase. There is less variation in the vegetation between shallow and deep peat areas. **Indicator taxa:** *Mauritia*-t., *Tabebuia*-t., Bombacaceae. **Pollen zones:** Q2-D, Q9-E, Q10-D, Q18-D, QT-6	400 cal yr BP – present **Chr.:** R, L

L: Lake core R: QT-2010-1 (Roucoux et al., 2013) P: Peat cores, this study

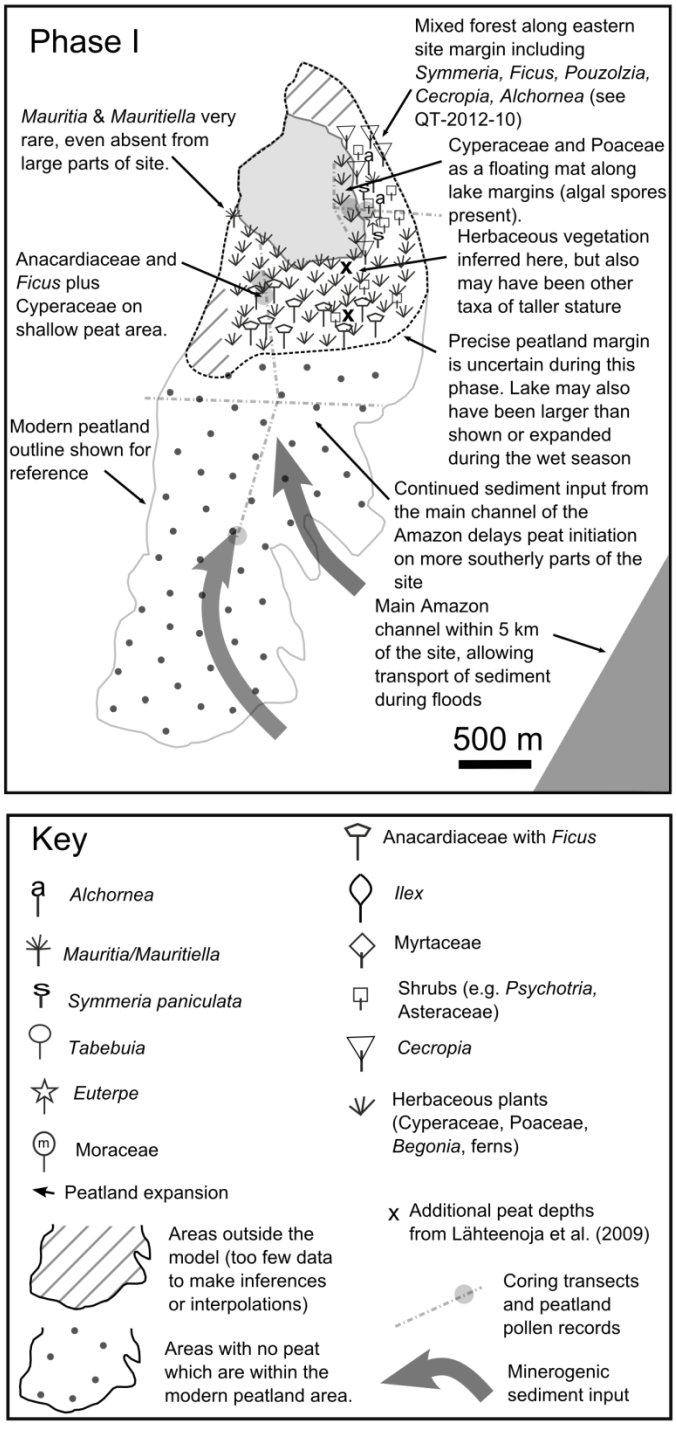

Figure 10.2: A conceptual model for the development of Quistococha peatland, showing five phases running from the point of peat initiation to the present. The model does not show the full detail of vegetation change as shown in the pollen diagrams, but aims to illustrate the main developmental phases and periods of peatland expansion. The position of the survey transects pollen records have been marked, and inferences away from these areas are more speculative (for positions of all cores and surrounding geomorphology, see Chapter 3). Two additional core points from a short transect by Lähteenoja et al. (2009a), which covered an area not measured by this study, have been used to aid interpretations (peat depths, marked 'x': northerly point = 300 cm, southerly point = 230 cm).

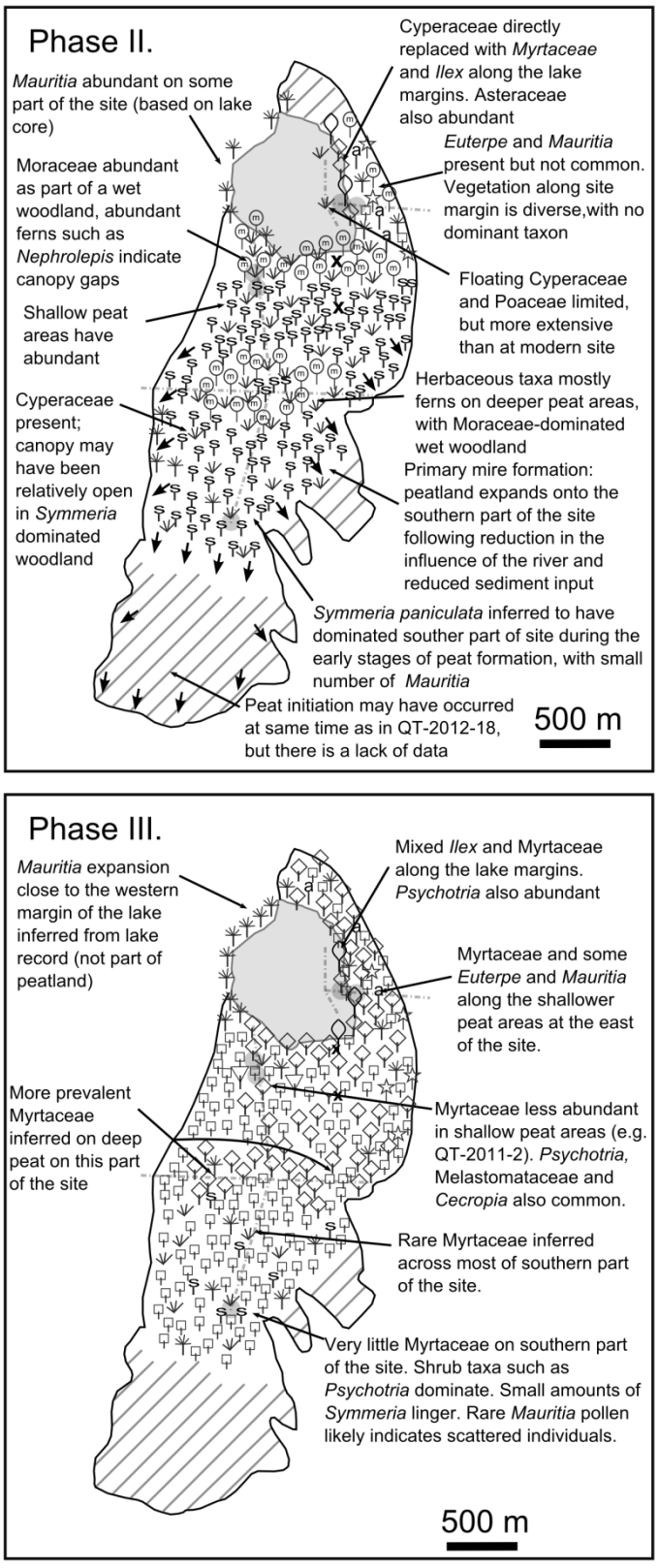

Figure 10.2 (contd): The development of Quistococha peatland.

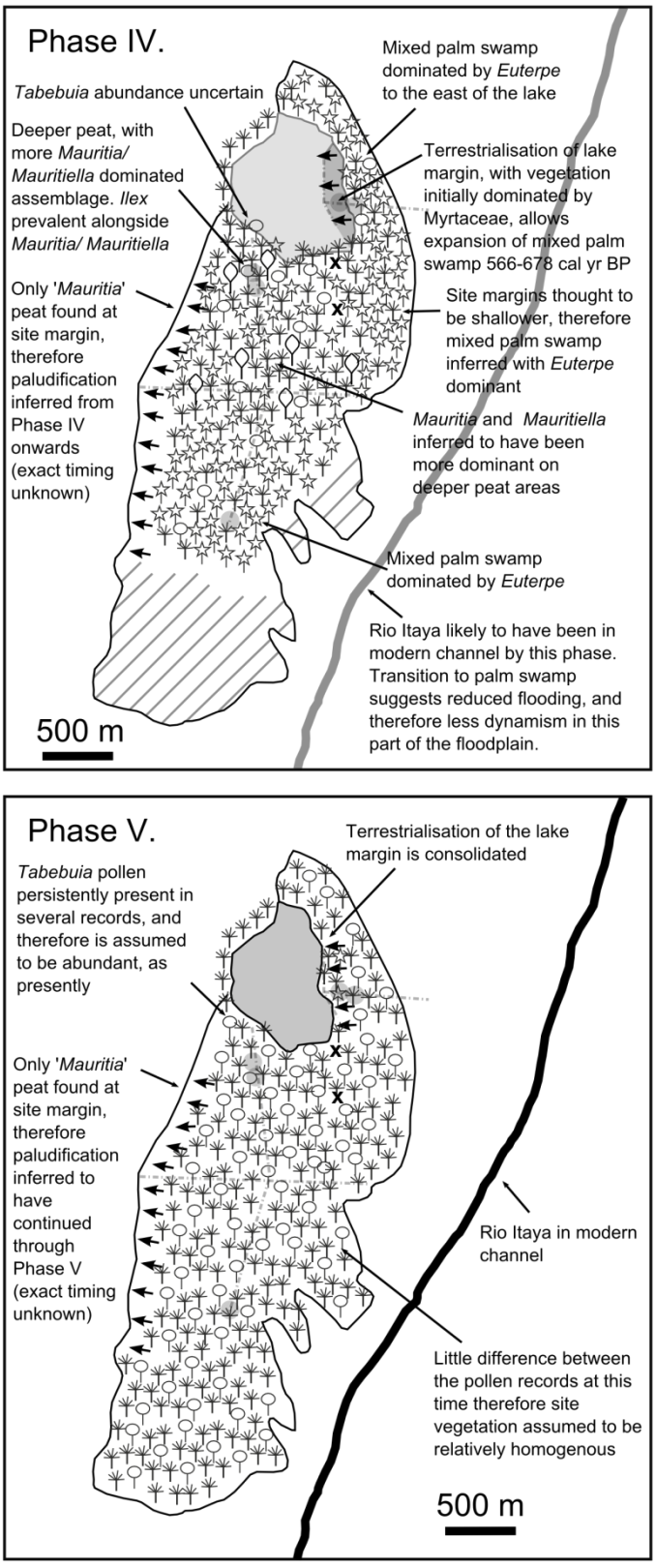

Figure 10.2 (contd): The development of Quistococha peatland.

The formation of the Quistococha basin

Most of the peatlands in the study region are likely to have formed in basins originally created by the Amazon River or its tributaries. The Ucayali and Marañón Rivers can be

characterised as meandering and weakly meandering (or anastomosing in places) respectively, and have a high sediment load (Räsänen et al., 1992). Channel sinuosity leads directly to the formation of oxbow lakes through neck and chute cut-off (Gay et al., 1998), and therefore (in this region) to the conditions which may be suitable for peat accumulation.

Quistococha is almost certainly the remnant of an oxbow lake, an inference that is supported by the presence of silts underlying the silty clays found in the lake core (see Chapter 8) and in QT-2010-1 (see Lawson et al., 2014). These imply a higher energy depositional environment, such as that of a river channel, rather than the low energy of the contemporary lake and peatland system. The clays underlying lake Quistococha are dominated by smectite (Aniceto et al., 2014), and are therefore similar to those of the main Amazon channel (Irion et al., 1997; Guyot et al., 2007).The presence of *Alnus* pollen, albeit in low quantities, implies an Andean origin for the minerogenic sediments below c. 210 cm in QT-2010-3 as *Alnus* is a montane taxon (suspended river sediments contain c. 1-2% *Alnus* in the central and western Amazon; Haberle, 1997). The breadth of Quistococha peatland (c. 1.6 km) is also consistent with it being an abandoned channel of the Amazon (c. 2 km wide at Iquitos), rather than a smaller tributary (for example, the Itaya River channel is only 85 metres wide). Therefore, the most parsimonious interpretation is that the site began life as a channel of the Amazon River, which has become isolated (also see Räsänen et al., 1991). By analogy with modern oxbow lakes (Constantine et al., 2010), the lake would still have been connected to the main channel during periods of high flow at this early stage, and there would have been a substantial amount of mineral sediment input which settled out in the still-water conditions of the lake. The amount of sediment input would have been determined to some extent by the original shape of the abandoned channel; 'neck' cut-offs receive smaller amounts of sediment than 'chute' cut-offs (Constantine et al., 2010). However, large parts of the lake would have infilled with silts and clays following isolation (accumulation in Amazonian floodplain lakes can average 3.5 mm yr^{-1}; Irion et al., 1997).

In the lake core, pollen assemblages in the sediments deposited before c. 2,100 cal yr BP are overwhelmingly dominated by the pollen of *Cecropia*, and the clays underlying the peatland have a similar pollen composition (as observed in the present study and by Roucoux et al., 2013). In the lake core, other pollen types are also consistently present during this period, such as the pollen of *Coussapoa*, a common várzea forest genus (Rudas Lleras and Prieto Cruz, 2005). The pollen of Cyperaceae and Poaceae is relatively abundant in the lake core before c. 2,100 cal yr BP and may indicate the presence of floating vegetation mats, similar in composition but potentially more extensive than

those found at the site today (see Chapter 3). Evidence for these mats can also be seen in QT-2012-9; clay-rich organic bands containing abundant Cyperaceae pollen and the pollen of other lake-marginal taxa such as Poaceae and *Spathiphyllum* precede the onset of peat accumulation. Although C/N ratios in QT-2012-9 do not conclusively indicate a lacustrine origin for the mixed clay and organic matter found in zone Q9-B (see Meyers, 1994), modern reference samples show that marginal lake sediments (within c. 20 m of the lake shoreline) are dominated by terrestrially derived material with a very similar C/N ratio to the peat found across the site (see Chapter 8). The inference that the vegetation represented by these pollen assemblages formed a floating mat is supported by the presence of algal spores in Q9-A (where they are an indicative taxon) and Q9-B.

Pistia stratiotes pollen is not common in the Quistococha cores (especially by comparison with the San Jorge core; see Chapter 9), suggesting that it never became well established at the site. It may have formed a minor part of the marginal aquatic vegetation (it is most common in Q9-B but never exceeds 10%), but its pollen is not present in any great abundance in the lake core (QT-2010-3). The small quantities could even indicate that its pollen was washed in with flood waters; *Pistia* is beetle pollinated and of low stature (Gibernau, 2003), and hence the pollen is unlikely to be blown in from neighbouring areas.

According to the lake core chronology (Chapter 7), this phase of the site's history may have continued for many hundreds of years prior to the beginning of pure peat accumulation. From the initial decline in magnetic susceptibility suggesting a decline in minerogenic sediment input (c. 246 cm; c. 3370 cal yr BP) to the transition into lake gyttja suggesting a substantial reduction in regular mineral sediment input from the river (c. 148 cm; c. 2080 cal yr BP) more than 1300 years passed.

Phase I: Peat initiation

During this phase, regular mineral sediment input from the river ceased on parts of the site, and it is at this stage that peat accumulation initiated at Quistococha. Although organic matter can accumulate as 'muck' in peatlands (Wüst et al., 2003; Lähteenoja et al., 2012), sediment necessarily dilutes the proportion of organic matter and therefore by definition pure peat accumulation is correlated with low allogenic mineral input. The input of sediment at the site must be separated from the concept of flooding, as when the river level rises a site may 'flood' but this water is not necessarily derived from the river itself but from rainwater unable to escape the site due to the high river level (cf. Mertes, 1997; also discussed in Chapter 3). Floodwater may also contain little suspended mineral material, particularly along black water rivers (Junk, 1983). The evidence from peat basal dates indicates that peat initiation was not synchronous across the site

(Chapter 7; Figure 7.1), but that it occurred in two separate phases. The earlier of the two phases coincides with the transition to organic accumulation seen in the lake core c. 2080 cal yr BP. In the area around the present lake, to a distance of around 800 m (core QT-2011-1), peat initiation occurred between 2100 and 2400 cal yr BP. Cores taken from shallower areas of peat (e.g. QT-2011-2) give basal radiocarbon dates within error of those from deeper areas (e.g. QT-2010-1) and therefore on this part of the site, paludification from deeper areas onto shallower areas does not seem to have occurred (contrary to the model of Anderson et al., 2003). In peatlands where this process has been inferred, it can take millennia for peat to paludify vertically onto shallower areas (cf. Anderson et al., 2003), and therefore would have required more time than that indicated by the Quistococha basal dates. However, on the more southerly parts of the site, deposition of minerogenic sediment from regular flooding appears to have delayed peat initiation.

To the south of the lake, there is also some evidence of an initial Cyperaceae phase in QT-2010-1, interpreted as a floating mat by Roucoux et al. (2013). At QT-2012-9 the floating mats inferred to have existed prior to peat initiation persisted during this early phase of peat accumulation. According to Roucoux et al. (2013), this phase lasted for c. 100 years at QT-2010-1. In the shallower peat cores, there is evidence of arboreal or shrub taxa; in QT-2011-2, for example, Anacardiaceae pollen is very abundant in the basal sample (transitional between peat and underlying clays). Although the open nature of the vegetation at this time may have allowed increased transport from *terra firme* trees, plants in the Anacardiaceae are insect pollinated meaning that this likely represents local presence (Bawa et al., 1985). In QT-2012-10 (zone Q10-A) a number of different taxa are found in the pollen record; small quantities of Cyperaceae pollen may not be indicative of presence at the core site and could have originated from the floating mats thought to occupy the lake at this time. *Symmeria paniculata*, Myrtaceae, *Pouzolzia*, and Asteraceae pollen are all found in low percentages. The most common species of *Pouzolzia* is *P. formicaria*, a liana of tahuampa forest (Gentry, 1993), and *Symmeria* is also tolerant of deep flooding (discussed below), supporting the inference that this was a diverse low-stature forest subjected to regular flooding. The low abundance of herbaceous taxa such as Cyperaceae and Poaceae in Q10-A, as well as the low abundance of ferns, imply that this part of the site probably had a closed canopy at this time.

Phase* II: *Externally-controlled expansion through 'primary mire formation'

The second phase of peat initiation is dated to between 1900 and 2200 cal yr BP (Chapter 7), and this occurred across the southern part of the site (cores QT-2012-5, QT-2012-6 and QT-2012-18). This step-like expansion implies that externally-driven

'primary mire formation' (sensu Sjörs, 1983) was the main cause of peatland expansion during this phase. The southern part of the site remained within the influence of the river for c. 200 years longer than the northern part, although cores were not obtained from the far southern part of the site (beyond QT-2012-18) and this part of the site may have continued to be affected by flooding and associated sediment input from the river for a more prolonged period (delaying peat initiation).

In the shallow, thinner peat area to the east of the lake represented by QT-2012-10, the vegetation during this phase was mixed and includes small numbers of palms (*Euterpe* and *Mauritia flexuosa*) and figs (*Ficus*), alongside low-stature shrub taxa such as *Psychotria* (Gentry, 1993). In the shallower areas represented by QT-2011-2 and QT-2012-18 *Symmeria paniculata* was dominant; its pollen is abundant in these cores and as *Symmeria* is insect pollinated (Bush, 1995), this likely indicates that it was locally abundant. *S. paniculata* is a specialist of low igapó forest (Worbes, 1997), and is adapted to long flood durations of more than 250 days per year (Ferreira and Stohlgren, 1999). In QT-2012-18, the interpretation that this phase represents a forest flooded for large parts of the wet season is supported by the presence of more minor pollen taxa such as *Bactris* aff. *riparia,* which is a low-growing palm predominantly associated with areas near to rivers which are flooded by black water (Gentry, 1993; Kahn and Moussa, 1994; Couvreur, 2011). Although the pollen suggests that this was a flooded forest, as in QT-2012-9, algal spores are also common in Q18-A, and are an indicative taxon in this zone. These could either have been washed in from other areas, or there could have to have been algal communities in standing water with good light availability on this part of the site.

In QT-2010-1, ferns such as *Nephrolepis* (indicative of forest gaps; Tuomisto and Ruokolainen, 1994) are abundant alongside various Moraceae pollen types. These are interpreted as being indicative of a wet woodland by Roucoux et al. (2013). For example, taxa such as *Maquira* and *Brosimum* are both known from floodplain forests; *Brosimum lactescens* is especially abundant in high várzea (Wittman et al., 2006). In QT-2012-9, Cyperaceae remains abundant until Myrtaceae increases in Phase III. In these deeper areas, the vegetation therefore seems to remain open at this stage.

Phase III: Flooded forest

Both to the east and south of the lake, the pollen record indicates the expansion of forest across all of the cores after the first c. 500 years of peat initiation, with the possible exception of QT-2012-18 (see below). Most cores show an increase in the pollen of trees and shrubs typical of flooded forest such as *Alchornea* (Q2-B), Myrtaceae (Q9-C), and *Ilex* (Q9-C) (Parodi and Freitas, 1990; Kalliola et al., 1991; Campbell et al., 1992; Wittman et

al., 2006). Myrtaceae phases are observed in all of the cores except for QT-2012-18; in the study region most Myrtaceae do not exceed 12 m in height (Figure 10.3; Rudas Lleras and Prieto Cruz, 2005). *Alchornea* species can grow as tall as 25 m (Rudas Lleras and Prieto Cruz, 2005), but can also take the form of shrubs such as *Alchornea castaneifolia,* which is common to the early stages of riparian successions (Kalliola et al., 1991).

Figure 10.3: A possible modern analogue for the community at Quistococha seen during Phase III, where parts of the site were occupied by a low-stature flooded shrub-forest. Picture shows Lake Charo (nr. R. Tahuayo) in July 2012 (dry season), with Myrtaceae and other low-stature trees growing in standing water in the foreground.

In the deeper cores (QT-2012-9 and QT-2010-1) there appear to be two Myrtaceae phases, separated by a phase with increased herbaceous vegetation such as Cyperaceae, Pteridophyte spores and, in QT-2012-9, an increase in *Mauritia* t. This interruption coincides with the probable hiatus observed in the Quistococha lake core (1500-1290 cal yr BP), and therefore could have been externally driven (discussed further in Chapter 11).

On the southern part of the site represented by QT-2012-18**,** the vegetation may have remained mostly low in stature, indicated by a predominance of Rubiaceae pollen types such as *Psychotria* (shrubs and small trees; Gentry, 1993) and a peak in Poaceae (see Q18-B). Given the later onset of peat initiation on this part of the site, it seems likely that the low vegetation stature was the result of continued influence from the river. In QT-2012-18, loss-on-ignition values remain below 90% in zone Q18-B indicating that there may also have been some continued sediment input, and perhaps a higher flood level than on the rest of the site.

Phase IV: Mixed palm swamp

The transition to '*Mauritia*' peat can be seen in the stratigraphy of cores from across the peatland. This transition was largely synchronous across the site, except in QT-2012-9 (Section 10.2.2). To the east of the lake there is some evidence that this phase may have followed a period of brief disturbance, as evidenced by the large quantity of *Cecropia* and *Ficus* pollen which underlies the increase in *Mauritia*-t. in cores QT-2012-10 and QT-2012-9 respectively. In the lake core, there is also a peak in *Cecropia* prior to the increase in *Euterpe*-t. pollen, which may reflect this feature of the peatland pollen stratigraphy, as QT-2012-10 is near the lake margin. There is no evidence for an increase in *Ficus* in the lake core but this is likely to be because *Ficus* is entemophilous and therefore its pollen is less well dispersed (Horn and Ramirez, 1990). In all of the cores, the increase in *Mauritia*-t. coincides with a peak in pollen and phytolith concentrations, a feature also seen at San Jorge (Chapter 9). This may indicate a period of slow accumulation, as identified in the San Jorge core, although the available radiocarbon dates are not spaced closely enough to determine whether this is the case. The possible causes of the change to *Mauritia*- and *Mauritiella*-dominated dominated vegetation (the start of Phase IV), including climatic change, are discussed in Chapter 11.

After this, peat accumulation occurred under a mixed palm assemblage or, at the site of QT-2010-1, a mixed *Mauritia*-t. and *Ilex* forest. The occurrence of mixed *Mauritia flexuosa* and *Euterpe precatoria* forest is common today in permanently waterlogged areas flooded by black water (Parodi and Freitas, 1990; Kvist and Nebel, 2001). It is towards the latter part of this stage that *Tabebuia* type pollen appears and remains consistently present in several of the records (e.g. QT-2011-2). As *Tabebuia* pollen is very poorly represented in the palaeoecological record, and is likely to be absent from the pollen record where present in low abundance (see Chapter 6), its appearance and subsequent continued presence in several of the cores is likely to indicate the establishment of *Tabebuia* across some areas of the site. However, in some core sites it is largely absent until Phase V (Q2-D, Q9-E, Q10-D, Q18-D, QT-6), and so it is difficult to be certain of the general abundance of *Tabebuia* across the whole site during Phase IV.

The underlying topography appears to have caused a difference in the forest composition between the shallow and deep peat areas, with *Mauritia*-t. being less abundant and *Euterpe*-t. being more abundant on the areas of shallower peat (cf. Q9-E & Q10-C in Chapter 8). There are two potential explanations. Firstly, the shallow peat areas may have been more poorly drained; at Caribou bog (Maine, USA), Comas et al. (2004) found that peat pools were more extensive in areas where the peat was shallow and the surface was in closer proximity to the impermeable substrate. Secondly, the difference could be explained by greater nutrient availability in shallow peat. For example, in QT-

2012-10, c. 70 cm of peat (or possibly more, accounting for subsequent decay and compression) would have underlain the mixed palm swamp when it became established. Although it is unlikely that living roots would have been able to penetrate to depths of 70 cm (Worbes et al., 1997; discussed below), the peat may have been shallow enough to allow nutrients transported in groundwater to have reached the root-zone (c. 30 cm deep). This hypothesis could be tested in future by analysing pore-water chemistry from peatland sites which have mixed palm swamp vegetation at the present day, and root growth studies of *Mauritia* and other peatland trees.

Phase V: Aguajal

In all of the peat cores, *Euterpe*-t. pollen declines to less than 5% in the uppermost pollen zone, and there is also a decline in *Ilex* in QT-2010-1. This pattern can also be seen in the lake core, where *Euterpe*-t. pollen gradually declines in the uppermost 30 cm (the last c. 460 cal yr). This change is quite gradual in QT-2011-2 and QT-2012-9 (where *Euterpe*-t. pollen does not exceed 20%), and more sudden in QT-2012-10 where *Euterpe*-t. pollen declines from > 60% to < 10 % between two samples.

In the other developmental phases there are generally notable differences in the pollen assemblage in the different cores, but in this final phase the pollen records all show a remarkable degree of consistency. One main difference is the prevalence of *Mauritia flexuosa* pollen in Q18-D, relative to the more mixed *Mauritia* and *Mauritiella* populations in the other cores (on the basis of pollen grain size data). It is possible that by Phase V, the accumulation of peat had progressed to the point where the topographic difference across most of the site had been removed. In all of the cores examined, a sufficient quantity of peat has accumulated (>190 cm) to cause the isolation of the modern vegetation from the mineral substrate. It has been suggested that root penetration is limited to the near-surface (top c. 30 cm) in igapó forests (Worbes, 1997), and the water table data for Quistococha peatland collected by the present study at one point remained within 27 cm of the surface even during the dry season (Chapter 5). Although many Amazonian trees are adapted to permanently water-logged conditions (e.g. through the growth of pneumatophores; Granville, 1974; Seubert, 1996), live root penetration to depths of c. 2 m is unlikely (Worbes, 1997). It is possible that this autogenic process has led to the convergence of vegetation composition across the site, which has culminated in the modern *Mauritia flexuosa-, Mauritiella armata-* and *Tabebuia insignis*-dominated assemblage.

In the lake sediment core there is an increase in *Cecropia* pollen from c. 20% to > 40% in the uppermost pollen zone which is not seen across the five records from the peatland itself. This feature of the lacustrine pollen record could be interpreted as due to either

increased disturbance of the forests in nearby floodplain areas by the Amazon river (i.e. increased channel movement) or increased man-made disturbance on the adjacent terrace. As the main channel of the Amazon River presently lies c. 10 km to the east of the site, it seems more likely that this reflects man-made disturbance, but natural disturbance associated with river dynamics cannot be ruled out. Possible areas of man-made disturbance include the adjacent terrace which has been opened up for grazing land and sand extraction, or along the levees to the eastern side of the site, which have been used periodically for agriculture (discussed further in Chapter 11).

10.4 Quistococha developmental model discussion

10.4.1 Lateral growth

Lateral peatland expansion can be seen as a type of autogenic succession driver; as certain plants colonise different areas (e.g. 'dry' areas at the peatland margin) they create a different hydrological environment ('hydrophytic habitat'; Tansley, 1935) which can be colonised by other plant species, and which is more conducive to peat formation. In most numerical models of peatland development, the potential for lateral growth is ignored in order to allow for simplification of model outputs and the emphasis is placed solely on vertical accumulation (e.g. Frolking et al., 2010; Baird et al., 2011). However, it has long been recognised that lateral expansion is an important part of peatland development; this occurs either via terrestrialisation or paludification (Anderson et al., 2003; processes are discussed more fully in Chapter 2).

Whereas in many northern peatlands, studies have shown continued (if episodic) expansion over the course of thousands of years (e.g. Bauer et al., 2003; Anderson et al., 2003; Ireland and Booth, 2011; Ireland et al., 2013), the model for Quistococha proposed here suggests that most lateral expansion occurs within the first few hundred years following peat initiation. The expansion of the peatland onto the southern part of the site was through externally-driven 'primary mire formation' (sensu Sjörs, 1983) and not gradual (autogenic) paludification. Whereas paludification results in the gradual spread of a peatland through changing conditions around the site margins (e.g. Anderson et al., 2003), in this case, continued sediment deposition from the river prevented peatland expansion for a period of c. 200 years. When the influence of the river declined, the impermeable riverine clay and relatively flat substrate topography created the poor drainage necessary for the largely simultaneous initiation of peat across the southern part of the site.

Following the initial expansion of the peatland during the early stages of its development the only clear evidence for peatland expansion is through terrestrialisation of the lake margins; this could have been climatically driven (Buell et al., 1968; Chapter

11). The limited role of terrestrialisation in the expansion of the Quistococha may be due to a lack of extensive macrophytic vegetation after Phase II, and there are few macrophytes in the modern lake (Chapter 3). This has probably aided the persistence of the lake, contrary to the 'classical model' of peatland development (Klinger, 1996; Kratz and deWitt, 1986). There is little evidence for lateral expansion at the modern site. '*Mauritia*' peat is found along the western margin, implying that this area was paludified during or after Phase IV, and this could represent ongoing expansion, but without radiocarbon dates it is hard to be certain. Peat accumulation may simply have been very slow on this part of the site (represented by QT-2012-1).

The model of peatland development described in Section 10.3 contains elements of all those given in Table 10.1. For example, the limited expansion of the peatland following its initial creation supports the Heinselman (1963) model which shows the persistence of peatland lakes through time as peat continues to accumulate around the margins. The size of the lake is likely maintained by ongoing processes, such as small-scale wave erosion and the lack of extensive macrophytic vegetation mats (Chapter 3).

The inability of numerical models to incorporate lateral expansion may therefore result in poor model outputs for the early stages of peat accumulation, when the size of the peatland expanded dramatically in a short period of time (≥ 1500 m in ≤ 500 years) by comparison with temperate peatlands (e.g. Anderson et al., 2003; Bauer et al., 2003). There is also strong evidence that paludification of the peatland at Quistococha was influenced by channel migration and geomorphological processes on the wider floodplain, and it may therefore be interesting to examine the effect of channel movement using numerical models of Amazonian peatland development.

10.4.2 Topography of the peatland bed

Much like the peatlands of formerly glaciated areas, many peatlands in the Amazon can be thought of as 'depressional' (cf. Ireland et al., 2013), which is to say that under current climatic conditions peat requires a waterlogged basin in which to begin accumulating (Lähteenoja et al., 2009, 2012; Householder et al., 2012). At present, no peatlands have been found on non-depressional surfaces in the Pastaza-Marañón basin, and floodplain sites without waterlogged basins (which can retain water all year round) investigated by the present study in the Jenaro Herrera area were not found to contain significant organic accumulations (Chapter 3). Lähteenoja et al. (2013) attributed the lack of peat in some sites in the Central Amazon to the topography; in places this allowed rapid run-off and therefore prevented water from ponding. Lähteenoja et al. (2013) assert that depressions are essential for peat inception and accumulation in Amazonia.

In depressional peatlands, it has been noted that basin shape exerts a strong influence on the development of the peatland and its associated vegetation (Walker, 1970; Anderson et al., 2003; Lavoie et al., 2013; Ireland et al., 2013). Various studies have demonstrated the influence of topography on peatland development in many northern peatlands, including several peatlands in Canada (Zoltai & Johnson, 1985; Bauer et al., 2003), Sweden (Almqvist-Jacobson and Foster, 1995), in New England (Anderson et al., 2003), at Caribou Bog (Maine, USA; Comas et al., 2004), and at Fallison Bog (Wisconsin, USA; Ireland et al., 2013).

The underlying topography of a peatland can influence peat accumulation and the vegetation growing on a site in several ways. In general, it acts through local changes to the hydrological regime, and in an Amazonian peatland we might expect subsurface topography to affect:

i) Surface drainage: Water will drain more rapidly from raised areas and pool in shallower areas. In a study of Swedish raised bog development, Almqvist-Jacobson and Foster (1995) state that where the angle of slope of the substrate is > 0.5%, drainage is too great to allow peat initiation, and hence vertical and lateral peatland expansion will be slowest in these areas. Whether this finding also applies to Amazonian peatlands is uncertain, in particular given the high water levels during the wet season which would lower the hydraulic gradient. Buttress roots can also act to slow surface runoff, a process reported from other tropical peatlands (Dommain et al., 2010). Surface drainage may become less important over time as peat accumulations fill the deeper parts of the basin (Almqvist-Jacobson and Foster, 1995).

ii) Water depth: Lower parts of the site will be more likely to trap the water necessary to create the anoxic conditions ideal for peat accumulation. This is particularly important for maintaining soil moisture during the dry season. They will also be flooded to a greater depth, and possibly also for longer periods, than shallower areas. Flood depth is not directly related to the accumulation of peat; sites near Jenaro Herrera which are annually flooded did not contain substantial organic accumulations (Chapter 3). However, in the floodplain of the Amazon, vegetation zonation is defined to a large degree by flood depth and duration (Junk & Piedade, 1997; Wittman et al., 2004), and therefore this will have an effect on the litter deposited, and hence indirectly affect peat properties (e.g. bulk density, hydraulic conductivity; Boelter, 1969).

iii) Subsurface flow: Even after peat has become established, the subsurface topography of the basin will guide groundwater flow (Comas et al. 2004). In

shallow peat areas, close proximity of the peat surface to the impermeable substrate can result in the ponding of water. At Quistococha this would affect trees which are less well-adapted to anoxic conditions in the root zone. This effect may apply even more strongly to Amazonian sites as a result of the high *K* fibrous peat, although different rates of decomposition and less fibrous peat types accumulated during the early part of site formation may mean that the *K* data presented in Chapter 5 cannot serve as an analogue for the early stages of peat accumulation.

The fast accumulation of peat in deeper areas results in the separation of the overlying vegetation from the mineral substrate, therefore changing the local nutrient status of the peat (and, conversely, slower accumulation maintains more minerotrophic conditions on the raised parts of the site). In the Holocene Peat Model, it is the separation of plants from the underlying substrate which drives the modelled succession (Frolking et al., 2010), and this may be a valid representation of the suituation at Quistococha (i.e. the distance from the peatland substrate could be used, in part, to drive plant successional changes in a numerical model). The shape of the basin will therefore play an important role in determining the evolution of the peatland vegetation which then begins to form. During the early history of the site, topography affects drainage and flood depth, and later it affects subsurface flow and access to nutrients in the substrate. Through ecohydrological feedbacks (Morris et al., 2011), the timing of vegetation changes can also be influenced by the underlying topography (e.g. late increase in *Mauritia*-t. in QT-2012-9). The underlying topography can therefore be thought of as a 'filter' which affects the way in which changes in external environmental conditions affect different parts of the site.

Householder et al. (2012) argued that the complex nature of the underlying topography found in tropical peatlands occupying abandoned channels likely contributes to the beta-diversity found within these systems, and noted that palm forest on deep peat can grade into open swamps on shallow peat (i.e. deeper areas of peat have different vegetation to shallower areas). The pollen analyses undertaken here on several cores have shown that deeper areas of the site have been occupied by noticeably different vegetation to that on shallow areas through time, which corroborates this inference. For example, shallower areas of peat have a more prominent mixed Arecaceae phase (e.g. QT-2012-10, QT-2012-18). Furthermore, as the site develops, topographic differences will be removed through peat accumulation, potentially driving a decrease in beta diversity (see Phase IV; Figure 10.4).

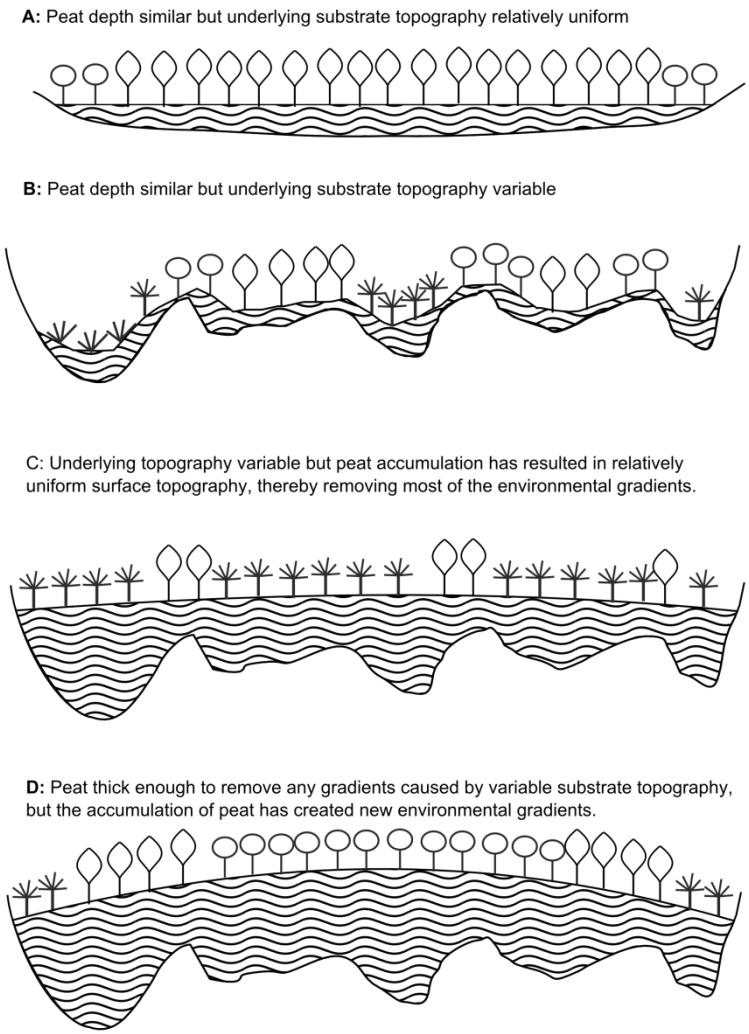

Figure 10.4: Hypothetical cross sections illustrating the interaction between peat depth and underlying topography with respect to the beta diversity of peatland vegetation. (Vegetation symbology is purely illustrative).

In temperate and arctic peatlands, microtopography is known to contribute to the diversity of habitats for bryophytes (Økland et al., 2008; Douda et al., 2012). However, Douda et al. (2012) also argued that, because herbaceous plants have deeper roots, microtopography has a lesser effect on their ability to access water and nutrients; they therefore respond more to coarser-scale heterogeneity which may be more closely linked to the underlying substrate topography. At present, the author could find no published studies directly examining the effect of the substrate topography on beta diversity in tropical peatlands, particularly through time, and this is therefore an avenue of further research. In Southeast Asian peatlands, peat depth and vegetation composition are often correlated (e.g. Page et al., 1999; Momose and Shimamura, 2002; Poesie et al., 2011), but this must be separated from the concept of substrate topographic variation. For example, peat depth could be broadly similar along a transect but the substrate topography could create many different habitats, and thereby drive a

high beta diversity by comparison with a transect where peat depth and underlying topography are both relatively uniform (Figure 10.4A).

One aspect which is often not considered by numerical models is that the geomorphology of peatland areas may also change through time as peat continues to accumulate. In the model of Anderson (1961) for peatlands in Southeast Asia, it is suggested that the levee at the edge of the peatland does not precede peat formation but that it accumulates as the water velocity drops during flood events and deposits sediment at the river edge (Figure 10.5). This is a difficult hypothesis to test at Quistococha using the available data; the dense mineral material of the levee is also difficult to sample, and may not contain material suitable for radiocarbon dating. Dating the basal peats in cores close to the levee (e.g. QT-2012-7, QT-2012-12, QT-2012-13) might allow the minimum age of this feature to be established, but would be unable to firmly demonstrate that it has not grown vertically over time. As shown in Figure 10.5, peat initiates when the levee is small, and accumulates as the levee grows. However, peat accumulations can be found beyond this hydrological margin at Quistococha (see Figure 8.4); therefore it is not a hard boundary between peatland and non-peatland areas as in the Anderson (1961) model. As such, it is likely that the levee at Quistococha pre-dates peat initiation, and has been instrumental in limiting the flow of water from the site along its eastern margin.

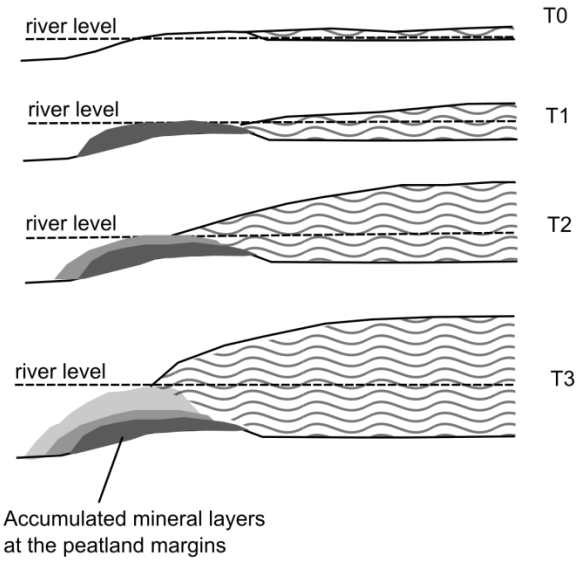

Figure 10.5: Accumulation of alluvium at the margins of a Southeast Asian peatland over time (T0, T1, T2, T3) as the mean river level rises (redrawn from Anderson, 1961).

10.5 Summary

Developmental models for Indonesian peatlands, Panamanian peatlands, temperate and sub-arctic peatlands do not fully apply to the peatland at Quistococha. Having reviewed the applicability of existing models, a conceptual model of site development for the site at Quistococha has been put forward. This chapter combines inferences about peatland

developmental processes with a detailed palaeoenvironmental reconstruction drawing on new and previously published data in the form of six pollen diagrams, 29 peat cores, a lake sediment sequence, and 22 radiocarbon dates from across the peatland, to form the basis of one of the most detailed conceptual models of peatland development for any tropical peatland site. This conceptual model differs from those reviewed in Section 10.1.2 (and in Chapter 2) in several ways, but particularly in terms of the influence of the river on peatland expansion. There is also evidence for the influence of climatic change, which may have driven the creation of the palm swamp in Stage IV, and which is discussed further in Chapter 11.

Peat initiation at Quistococha occurred in two main phases during the early period of peatland development (2,400-1,900 cal yr BP). Quistococha is covered in a relatively uniform aguajale swamp forest dominated by just three species at the present day (Chapter 3). However, the vegetation at the site was apparently more heterogeneous during earlier developmental phases. Topography plays a key role in creating site-level heterogeneity in vegetation, and as peat accumulates beta diversity decreases.

11. Drivers of Amazonian peatland vegetation change

11.1 Introduction

In Chapter 5, results from investigations were presented and discussed in order to establish the hydrological behaviour and sensitivity of three Amazonian peatlands. The water table logger installed at Quistococha demonstrated that, when rainfall becomes less frequent in the dry season, peatland water levels can fall quickly (c. 1.6 cm d^{-1}). Numerical models demonstrated that whilst the high hydraulic conductivity of the peat might contribute to rapid water losses, it is likely that most water is lost as a result of very high evapotranspiration rates. While further work would be desirable to add detail to our understanding of their hydrological behaviour, the results in Chapter 5 show that these Amazonian peatlands, like peatlands in other parts of the world (e.g. Ireland and Booth, 2011; Coffey et al., 2012; Ireland et al., 2013), are sensitive to reductions in net precipitation, particularly when it occurs during the dry season. Therefore, there is good reason to believe that peatlands like these may record past changes in climate, principally the length and severity of the dry season; low water tables could lead to increased oxidation and therefore peat decay, as well as vegetation changes visible in the palaeoecological record if sustained over several decades or more.

In Chapter 10, a developmental model for the site at Quistococha was presented, but establishing the influence of climate on peatland development is difficult using data obtained from only a single site. This chapter therefore complements Chapter 10 by making comparisons with data from other sites, particularly San Jorge (Chapter 9). Vegetation changes observed in pollen records from an individual site could be synchronous if driven by either local river dynamics (such as channel avulsion) or regional climate change. However, synchronous changes seen in pollen records at two or more hydrologically separate sites are likely to be driven by a common factor, most likely climatic change. Alternatively, asynchronous vegetation changes may have been driven by autogenic succession or by human impact, and these are also discussed in this chapter. The central aim of this chapter is to determine the main drivers of late-Holocene vegetation change in two Amazonian peatlands; as part of this, three key hypotheses will be tested:

- Vegetation changes seen in the peatland pollen records at Quistococha and San Jorge were synchronous.
- Vegetation changes in the peatland pollen records obtained were entirely driven by allogenic factors.

- Vegetation changes seen in the peatland pollen records at Quistococha and San Jorge were synchronous with climate events seen in other records from the wider region (see Chapter 2).

This chapter begins by exploring the evidence that autogenic, successional processes are important in driving vegetation change for the peatlands in the present study. Evidence for human occupation and impact is then examined. The evidence for climatically driven changes in the records from Quistococha and San Jorge is then discussed as a series of time slices, beginning with a period starting c. 1500 cal yr BP which was shown to be a period of slow peat accumulation (or a hiatus) at San Jorge in Chapter 7.

11.2 Evidence of successional processes

11.2.1 Vegetation changes driven by river dynamics

Evidence of vegetation change driven by river dynamics can be seen in the early history of the Quistococha peatland, as discussed in Chapter 10. In QT-2011-2, the basal pollen zone is dominated by Cyperaceae, *Ficus*, and *Symmeria paniculata,* and similarly in the basal zone of QT-2012-18 *Symmeria paniculata* is the dominant taxon with some Cyperaceae also present. In QT-2012-9, the deepest peat core in this study, the basal pollen zone is dominated by Cyperaceae with some Poaceae, as well as *Cecropia* and Moraceae pollen. Core QT-2010-1 also shows an early Cyperaceae phase. In all of the cores except QT-2012-10, Cyperaceae emerges as an indicative taxon in the lowermost pollen zones.

This pattern is one which is found throughout Amazonian floodplain communities (Junk and Piedade, 1997), i.e. the deeper-water parts of the site (QT-2012-9) are dominated by either herbaceous or aquatic taxa, and the shallower parts of the site and the levees which surround it are dominated by vegetation which is flood tolerant but of taller stature (QT-2012-2, QT-2012-18). Taxa such as *Ficus*, *Cecropia*, and to a lesser degree *Mimosa* which is found in Q9-B (the genus *Mimosa* includes herbaceous species; Gentry, 1993) are all typical of the early stages of riparian succession (Salo, 1986; Lamotte, 1990; Kalliola et al., 1991). Palm pollen is largely absent from the basal samples or is present in low abundance, and this is typical of early riparian successional communities (as established by repeat survey), *low restinga* and *tahuampa* areas (Salo, 1986; Nebel et al., 2001; forest types defined in Chapter 3). The lowest part of the peatland record below 216 cm at San Jorge is dominated by the pollen of *Cecropia* and Asteraceae, both common in early riparian successional communities in Amazonia (Salo, 1986; Kalliola et al., 1991). This early successional pattern is also similar to that seen in other pollen records. At Lake Coari (near Manaus, Brazil), the basal pollen samples are dominated by

Cyperaceae and Poaceae, which is then replaced (albeit over c. 650 years, a longer period of time than at Quistococha) by assemblages rich in *Symmeria* (Horbe et al., 2011). Yet where conditions remain suitable, some of these species can persist for long periods of time; for example, the record from Lake Surara (Brazil) shows that *Symmeria paniculata* can remain dominant for five thousand years (Absy, 1979; Chapter 2). In summary, the basal pollen samples in both peatlands are floristically similar to early-successional riparian communities (see above). It can therefore be inferred that the pattern of vegetation was largely the result of allogenic vegetation change (i.e. succession in combination with channel migration; Wittman et al., 2004) during the early formation of both peatlands. Fluvial influence appears to have declined during the later development of Quistococha (see Chapter 10).

11.2.2 Autogenic succession

Just as in temperate peatlands (Walker, 1970; Charman, 2002), the vertical accumulation of peat can cause autogenic vegetation change in tropical peatlands (Phillips et al., 1997; see Chapter 2). The accumulating layers of dead organic matter can result in the gradual separation of the surface vegetation from nutrients in the substrate and in groundwater (Hughes and Barber, 2003), as well as changes in the water level (Tansley, 1939). In the Holocene Peat Model, this is the main means by which plant succession is driven (Frolking et al., 2010). However, given the constant presence of allogenic forcings, it can be difficult to be certain that vegetation changes are totally autogenic (Payette, 1988). Swindles et al. (2012) also suggest through hydrological modelling that peatlands may show autogenic responses to climatic changes, and therefore the peatland archive may reflect a mixture of both internally and externally driven processes. For example, a climatic 'wetting' could be followed by an autogenic 'drying' at the peat surface through the accumulation of organic matter (Swindles et al., 2012).

At Quistococha, the palaeoecological data are best explained as the result of autogenic succession in core QT-2012-9. Although the initiation of the *Mauritia*-t. expansion in QT-2012-9 occurred c. 400 years after the expansion of *Mauritia*-t. pollen across the rest of the site, the core exhibits a similar series of subsequent vegetation phases. The initial phase (Q9-D and Q9-E) consists of a mixed *Euterpe*-t. and *Mauritia*-t. assemblage. There is then a decline in *Euterpe* t., leaving a mixed *M. flexuosa* and *M. armata* assemblage (based on pollen grain size data).

A similar sequence can be seen in the core from San Jorge. Following the increase in *Mauritia*-t. at 96 cm, *Euterpe* t. becomes common along with species such as *Ilex*, which

are also found in the early phases of palm swamp development at Quistococha (e.g. zone QT-5b in QT-2010-1). These elements then decline and are replaced by a pure *Maurita*-t. assemblage. This pattern can also be seen in the wetlands of the Chocó in Colombia (sites at San Martin and Villaneuva); *Euterpe oleraceae* occupies more poorly drained areas than *Mauritiella macroclada*, and this can be seen down core as *Euterpe* precedes *Mauritiella* in the pollen record (Urrego et al., 2006). In the Caquetá area of Colombia, *Euterpe precatoria* is also found to be more common in annually flooded sites than *Mauritia flexuosa* (Duivenvoorden, 1995). As such, Tansley's (1935) classic use of the term 'succession' could apply in this instance (see Chapter 2).

At Quistococha, there appears to be no relationship between the temporal succession and the modern distribution of plants across the site (Chapter 10). Earlier vegetation phases reconstructed from the pollen record include mixed *Euterpe* and *Mauritia* palm swamp, flooded forests with abundant Myrtaceae, and flooded forests with *Symmeria*, none of which can be seen at the site today (Chapters 8 and 10). However, at San Jorge the pollen data suggest that the spatial vegetation patterning seen at the site today may reflect the temporal succession (Figure 11.1). The pole forest was preceded by a palm swamp, and the palm swamp was in turn preceded directly by a lake; although the present lake itself was not reached during fieldwork at San Jorge, LANDSAT imagery shows a narrow ring of palm swamp around the lake margin (see Chapter 3). However, as Rydin and Jeglum (2006) remark, care must be taken when substituting space for time in the study of peatlands. There is no *a priori* reason to assume that the development of a peatland plant community will have followed a trajectory that is representative of spatial vegetation patterns across the site as a whole (Johnson and Miyanishi, 2008). In the case of tropical peatlands, some have several peat accumulating basins (Householder *et al*., 2012).

At San Jorge, if it was possible to see the site several hundred or a thousand years in the future, a different spatial succession might be observed which bears more similarity to sites such as Riñon (Figure 11.1; Lahteenoja et al., 2009a). At Riñon, the vegetation at the 'centre' of the peatland is open and treeless (Lähteenoja & Roucoux, 2010). Figure 11.1 uses San Jorge as a hypothetical example to show that the open areas seen at the 'centre' (which can be difficult to define in tropical peatlands) of other sites could be the result of remnant lakes which are still filling in and being colonised by trees and shrubs. The data from Quistococha discussed in Chapter 10 suggest that, providing that they survive the initial stages when the site is receiving mineral sediment from the river and organic matter is accumulating rapidly from floating vegetation mats, deep lakes may take thousands of years to fill in with sediment (the lake at Quistococha has persisted,

isolated from the main channel, for c. 3500 years). If the scenario in Figure 11.1 is the case, then, unlike Central American peatlands which often have an open 'bog-plain' as their climax vegetation (Phillips et al., 1997), in Amazonian peatlands the pole (or 'dwarf') forest found at sites such as Aucayacu (Swindles et al., 2014) and San Jorge may be the latest community currently known in the vegetation succession.

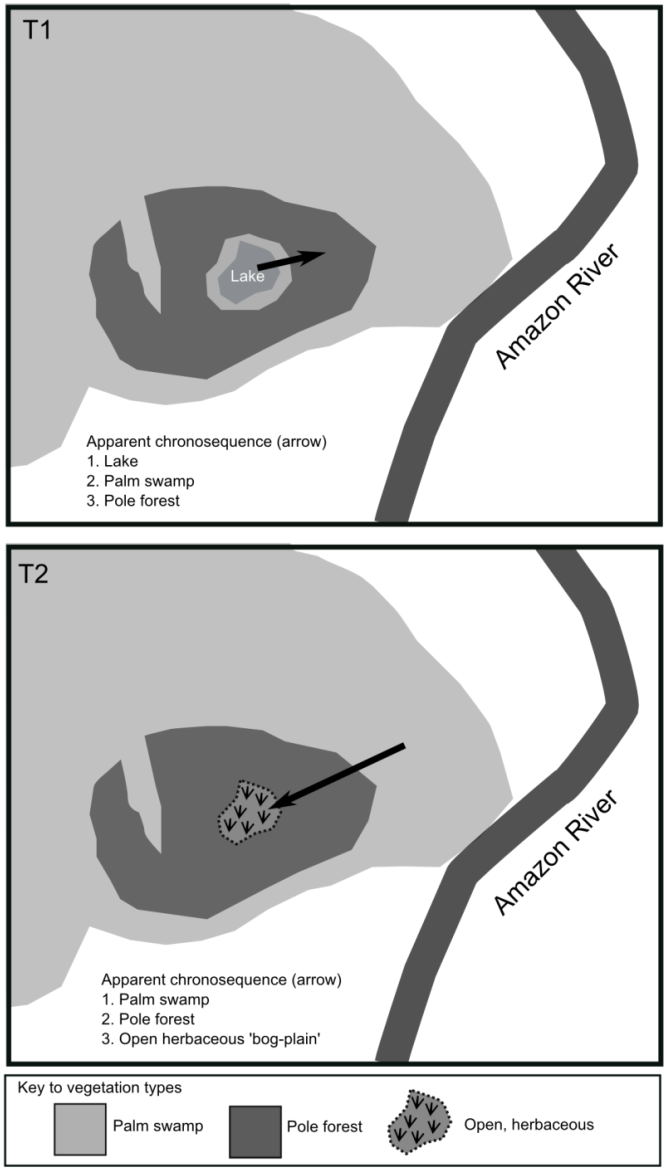

Figure 11.1: The appearance of different 'chronosequences' at different points in a site's history, using San Jorge peatland as an example. **T1** shows the current vegetation patterns as derived from LANDSAT imagery (see Chapter 3). In the 'classic model' (discussed in Chapter 2) the lake fills in from the margins, so the chronosequence extends from the lake outwards (see Ireland et al., 2012). **T2** shows a projected future time period where the lake has filled in with herbaceous vegetation. At this point in time, the 'chronosequence' appears to show the centre of the former lake as the latest successional community (as at Changuinola peatland, Panama; Phillips & Bustin, 1996). However, this would be quickly disproven using palaeoecological data, which should show a herbaceous community down core, overlying lake gyttja.

The increased understanding that has been gained from Quistococha and San Jorge allows new hypotheses to be formulated to guide future research, particularly to

examine in more detail the formation of open herbaceous areas seen at some peatland sites. In the dynamic landscape of the Amazonian floodplain, it may not be possible to make straightforward inferences about the age of sites from their present vegetation (Roucoux et al., 2013), or the temporal succession from the spatial distribution of their vegetation. Palaeoecological data are therefore critical for providing information relating to past and future vegetation changes.

A particular aim would be to establish whether open vegetation can develop as a late-successional community or, as the core from San Jorge suggests, this is always an early vegetation phase with respect to peatland development. This could have implications for peatland mapping by remote sensing (e.g. Jaenicke et al., 2008; Lähteenoja and Page, 2011). It could present some practical remote sensing difficulties, such as distinguishing between an old lake basin containing a large accumulation of 'lake peat' (found in the shallow water at the edge of the lake at Quistococha; Chapter 8) and a younger site with hardly any peat accumulated under the herbaceous (possibly floating) vegetation (as at Quistococha during the early stages of its development).

11.3 The record of human impact and occupation

According to Denevan's (1996) 'bluff model' of pre-Columbian settlement in Amazonia, human impacts are likely to have been greatest in those areas within a few kilometres of the rivers (see Chapter 2). These impacts would have taken the form of hunting, resulting in the removal of large herbivores which could transport seeds (see Chapter 3), and landscape alteration through burning (Bush et al. 2007b). Although there is abundant pottery, none of the archaeological sites in western Amazonia contain stone tools. Without stone tools it would have been very difficult for people to substantially alter or clear forests without the use of fire. As Mayle and Power (2008) show, the current fire return interval in western Amazonia is > 900 years, so charcoal is therefore a key indicator of human presence and impact in many palaeoecological records from Amazonia.

The peatland records at Quistococha and San Jorge all contain only sparse charcoal which occurs at extremely low concentrations. It is possible that people may have used peatland resources, such as palm leaves, or visited peatlands for hunting and foraging. However, clearance of peatlands does not seem to have occurred in pre-history at these two sites, as demonstrated by persistently abundant arboreal pollen and sparse microcharcoal. Furthermore, there is limited evidence for any impact by people on the *terra firme* forest in the Quistococha lake core. Pollen of the Moraceae family, typical of *terra firme* rainforest (Gosling et al., 2005), remains abundant throughout the last c.

2,200 cal yr. Even for a relatively large lake like Quistococha, more than 50% of the pollen likely comes from within c. 1 km of the lake shore (although dispersal varies for different taxa; cf. Davis, 2000; Sugita, 2007), and so large-scale local clearance should be visible. There could still have been small-scale clearance, but this was not substantial enough to be represented in the pollen record. Weng et al. (2002) also recorded little evidence of human impact in their cores from northern Ecuador, despite the presence of nearby archaeological sites.

The first increase in charcoal in the lake core is related to the change from minerogenic sediment to organic sediment and is dated to c. 2,450 cal yr BP. This is more likely to indicate a change in source area than the arrival of people at Quistococha; the minerogenic sediment derived from the main Amazon channel appears to contain little charcoal. However, this does coincide with the earliest known occupation on the adjacent river cliff, dated to 2350-2690 cal yr BP (i.e. they are within error; Rivas Panduro et al., 2006). What can be said with a high degree of certainty is that people were living in the vicinity of Quistococha around the time when the lake became fully isolated from the river, contrary to previous interpretations which suggested that people only occupied the site at Quistococha when it was connected to the main Amazon channel (Rivas Panduro et al., 2006). It should also be noted that the archaeological site at Quistococha lies between the main Amazon floodplain and the smaller Nañay River, which would have been within easy reach, and therefore the terrace area at Quistococha may have been ideal for the exploitation of multiple resources.

The presence of charcoal in the lake is continuous and therefore it seems likely that, while there is a gap in the archaeological evidence, people were present in the area near Quistococha persistently throughout the last c. 2,500 cal yr. The long fire return interval given by Mayle and Power (2008) is a reflection of the very low probability for natural fires in this region. The majority of soil cores taken in interfluvial areas in the western Amazon by McMichael et al. (2012) did not contain any charcoal, which indicates that natural fires are extremely rare and of a small scale. Therefore the persistent presence of charcoal in the Quistococha lake core is likely to be indicative of man-made fires.

The charcoal concentration data have almost certainly been affected by changes in the accumulation rate; peaks at 90-100 cm and 48 cm can be correlated with peaks in pollen concentration, which means that they do not reflect increased charcoal input from burning. Although the age model can correct this to some degree and therefore provide an indication of the charcoal influx, the spacing of the radiocarbon dates means that this is not always possible (particularly for the peak at 48 cm). The main decline in charcoal occurrence comes at 32-40 cm depth, dated to c. 500-640 cal yr BP. This could be due to

the reduced compaction in this part of the sequence, or be related to reduced burning, which could be related to changes in the environment which caused reduced human presence around Quistococha. In particular, the decline in charcoal coincides with the onset of pollen zone QT-7, the decline in Arecaceae pollen, the colonisation of the lake margins by *Mauritia* (core QT-2012-9), and could also correlate with a period of change at San Jorge (see below). However, another plausible explanation is that the decline in charcoal was as the result of a general reduction in human impact following Spanish conquest after AD 1492, which caused a decline in population across Amazonia for several centuries (see Chapter 2). In a review of radiocarbon dated charcoal horizons from Amazonia, Bush et al. (2008) also observed a decline in occurrence after c. AD 1600 which they correlated with the post-Columbian population collapse.

The palaeoecological record can provide some insights into resource use by those inhabiting the prehistoric settlement, but as with tropical pollen analysis there are taxonomic challenges. Specific identification of *Mauritia flexuosa* phytoliths is not possible, and the absence of clearly identified *Mauritia* phytoliths in existing reports from the archaeological site at Quistococha (S. Bozarth, unpublished data; Rivas Panduro, 2006) has previously been explained by the lack of overlap in terms of the period of settlement and the later expansion of *Mauritia* inferred from the QT-2010-1 pollen record (Roucoux et al., 2013). However, the lake record clearly shows that *Mauritia* was present in the vicinity during the period of occupation (Chapter 8). The data from the archaeological excavation reveal the presence of abundant unidentified spinulose phytoliths (S. Bozarth, unpublished data; Rivas Panduro, 2006), and these are the most abundant of all the phytolith types. These are likely the phytoliths of *Mauritia*, and this shows that either *Mauritia* was growing in the settlement or that those occupying the site were making use of its fruit (a modern ethnobotanical study has shown that *Mauritia* leaves are rarely used for thatch; Macia, 2004). The lack of large *Mauritia* fruit remains (e.g. seeds) at Quistococha challenges this hypothesis (Rivas Panduro, 2006; Roucoux et al., 2013), but these may have decayed or been disposed of elsewhere, and the abundant spinulose phytoliths still require an explanation. The only alternative is that these phytoliths are related to the cultivation of bromeliads such as pineapple (*Ananas comosus*) which produce similar phytoliths (cf. Piperno, 2006). Although early explorers did not record the cultivation of pineapple in the western Amazon, it was widely cultivated throughout South America (Collins, 1951). However, given that we now know from the lake record that *Mauritia* was present near to the archaeological site at Quistococha, it seems likely that this resource would have been exploited and that the unidentified phytoliths are indeed those of *Mauritia*.

Bromeliaceae and Arecaceae phytoliths can be differentiated by close examination of the echinae (Piperno, 2006), although this taxonomic distinction was not made at Quistococha. At an archaeological site in Colombia on the Caquetá River where *Mauritia* is similarly abundant, the number of *Mauritia* and other palm phytoliths was found to dramatically outweigh those of *Ananas comosus* (Morcote-Rios et al. 2013).

A large increase in *Cecropia* seen in the Quistococha lake sediment record occurred within the last century. This is accompanied by a decrease in the C/N ratio which is driven by an up-core increase in nitrogen from c. 2% to c. 3% which likely reflects the young age of the sediment. Nitrogen typically declines with increasing depth in the top 5-10 cm due to diagenesis as the nitrogen in dead organic matter, particularly in proteins and lipids, is lost through decomposition (Talbot, 2001). A less likely explanation is that this is the result of increased global anthropogenic nitrogen deposition over the last c. 50 years (Reay et al., 2008). *Cecropia* naturally occupies open and disturbed areas, but given the current distance of the site from the main channel of the Amazon, it seems likely that the increase in *Cecropia* is as a result of man-made rather than natural (e.g. blow-down) disturbance. The large scale clearance of land in this area, which has resulted from the expansion of Iquitos, the need for farm land, and the construction of roads, is likely to be the main cause. In the peatland records at Quistococha and San Jorge, there is also evidence of a recent peak in lead (Pb) within the uppermost parts (last c. 100 years) of the peat profile which is very likely the result of man-made emissions (Lawson et al., 2014). However, the peak in *Cecropia* seen in the lake at Quistococha is not observed in the peatland records where the abundance of *Cecropia* pollen has remained much the same for the last c. 2,000 years (with the exception of the peak in core QT-2012-10).

Pollen dispersal theory (see Davis, 2000) suggests that the small pollen source area of forested tropical peatlands makes them poor archives of landscape-scale environmental changes (e.g. Cole et al., 2015; also see Chapter 6), and a comparison of the results from the lake and peatland at Quistococha supports this prediction. Even the clearance of *terra firme* forest and the growth of Iquitos, Peru's fifth largest city, does not exhibit a clear signal in the peatland records. However, the charcoal in the Quistococha lake record strongly suggests that people have been living in the vicinity of Quistococha for the last c. 2,500 years.

11.4 Climatically driven changes

11.4.1 Peat initiation dates

Lähteenoja et al. (2012) state that the varying basal ages for peatlands in this region, which show no evidence for clustering around a particular time, imply that climate has not controlled peat initiation over the course of the late Holocene. However, care must be taken when inferring drivers based on peat initiation dates in this region for the following reasons:

i) The small number of study sites with basal dates (currently ten; see Chapter 3) prevents the detection of all but the most obvious patterns.

ii) Dated sites are not evenly distributed across the basin. Most sites are in the eastern part of the basin, and samples are generally biased towards sites which are accessible, near to the river. These are likely to be younger sites which have been more recently abandoned by the active channel.

iii) Peat initiation dates frequently vary substantially within sites elsewhere in the world (e.g. Anderson et al., 2003; Ireland et al., 2013); prior to this study, only single cores from sites in Amazonia had been dated. This study has attempted to establish how representative single cores can be at Quistococha (Chapter 7), and identified two phases of peat initiation at that site (see Chapter 10).

iv) Inappropriate sample selection can lead to errors when radiocarbon dating tropical peatlands (e.g. root contamination; see Chapter 7), and this can affect the inferred timing of peat initiation. As in this study, Lähteenoja et al. (2009a, 2012) excluded roots from their samples, and Lähteenoja et al. (2012) dated two samples from the base of each core, so this effect may be minor.

v) Organic accumulations being dated are not always 'peat', and the definition of a site as a peatland can vary. For example, this study has shown that the site at Charo designated as a peatland by Lähteenoja et al. (2009) has a low organic content (close to the threshold for peat) through much of the sequence (Chapter 3). Different processes may determine the accumulation of organic material lower on the floodplain where there is a large quantity of inorganic mineral input, versus sites where mineral input is negligible. At some sites (e.g. San Jorge), much of the accumulated material may have been laid down in a lake environment. Distinguishing between lake deposits and peats can be difficult, especially where detailed palaeoecological analyses are not undertaken.

Most peatlands in the Western Amazon are thought to have formed in abandoned channels, and therefore rely on channel migration to create suitable peat-forming sites (Lähteenoja et al., 2012). Climatic change may conceivably have an effect on channel migration by altering the discharge (and hence stream power; Hickin and Nanson, 1986), thereby changing the rate at which new sites are formed. However, the assumption that late Holocene climate change (reviewed in Chapter 2) would cause a sudden increase in the number of peatlands initiating could be false; it may only create the appropriate background conditions (i.e. moist conditions throughout the year to prevent peat oxygenation and decay).

There is evidence from Quistococha that the separation of the site from the influence of the river and the onset of peat accumulation coincided with a change in ENSO frequency and amplitude shown in the marine record of Rein et al. (2004, 2005) and others (see Chapter 2). Lähteenoja et al. (2009) made a similar observation regarding Quistococha and San Jorge, and the basal date for San Jorge obtained by the present study (see Chapter 7) confirms that peat initiation was synchronous at both sites within the errors of ^{14}C dating. However, it does not necessarily mean that climate has been a dominant driver of peat initiation in the wider region, as other sites exhibit a range of peat initiation dates (Chapter 3). Therefore answering this research question wholly convincingly would require peat initiation dates from a much larger number of sites. Preferably, this would also be combined with other analyses of peat stratigraphy (preferably including pollen analysis) to allow better interpretation of the significance of the dates obtained.

For all these reasons, the discussion here is not focussed on whether peat *initiation* in this region has been affected by climate. Instead, the discussion is focused on whether peatland vegetation change has been affected by climatic events in the late Holocene. Establishing whether this is the case is also of more relevance to potential near-future (next century) impacts on existing peatlands, and therefore to management schemes such as REDD+ (Miles & Kapos, 2009; Murdiyarso et al., 2010).

11.4.2 Evidence from palaeoecological data

The argument that tropical floodplain vegetation communities have been affected by Holocene climate changes is not a new one. Weng et al. (2002) reported late Holocene changes in Ecuadorian wetlands, with establishment of the modern wetland occurring at c. 1000 cal yr BP following a shift to drier conditions. Behling et al. (1999) and Behling and Hooghiemstra (1999) argued that sites in southern Colombia have experienced an observable change in climate during the late Holocene. Behling et al. (1999) also

mentioned the possible role of river dynamics and the potential for this to occlude the climatic signal.

The evidence from Quistococha and San Jorge shows that there was negligible sediment input at both sites after the initial period of establishment (with the possible exception of QT-2012-18 which has lower loss-on-ignition values down-core). Where slight drops in loss-on-ignition are observed, these frequently coincide with peaks in phytoliths and probably do not represent allochthonous mineral material. Based on the pollen data from Quistococha (e.g. *Symmeria*, Myrtaceae phases) the site was flooded annually until c. 1000 cal yr BP (Chapter 8; Roucoux et al., 2013). However, from the point of peat initiation c. 2300 cal yr BP this flooding did not result in a significant deposit of sediment. The process of flooding without sediment input can be seen at the site today. In 2012 the flood did not deposit an observable mineral sediment load across the site; this observation has also been made by Lähteenoja et al. (2012) at other peatlands in this region. As Mertes (1997) describes, the flow of groundwater and rainwater away from a site may be prevented by the river floodwater (also see Chapter 3). This means that sites can be flooded by water which does not originate in river channels, and which has no sediment load. As such, sediment input cannot be used as a reliable indicator of fluvial influence on vegetation development (i.e. the absence of sediment does not reliably indicate the absence of flooding). Distinguishing between climatically driven changes and changes driven solely by river dynamics therefore relies largely on the comparison of timings between different records from the region and the careful interpretation of palaeoecological and geochemical data.

11.4.2.1 Evidence for drier conditions 1500-500 cal yr BP

At San Jorge, the period around 1300 cal yr BP marks the beginning of a period of very slow accumulation which continued until c. 400 cal yr BP. When peat accumulation restarted, the open, aquatic community dominated by Cyperaceae and *Pistia* had been replaced by a mixed palm swamp (this marks the transition from pollen zone SJ-4 to SJ-5).

The evidence supports a period of slow accumulation at San Jorge, rather than removal (erosion) of layers by an active river channel to create an apparent hiatus. The very high concentration of pollen and phytoliths across this interval suggest that litter was still being laid down but that high decomposition rates removed most of the organic matter, leaving only recalcitrant particles behind (see Chapter 2). This also implies that the palms *Mauritia* and *Mauritiella* colonised this part of the peatland during the period of slow accumulation, as their phytoliths are very abundant in this part of the core

(especially at 96 cm). Although the chronology is uncertain from 90-112 cm, this implies only a short gap between the aquatic phase and the palm swamp which followed. There is a further argument which suggests peat was not removed by erosion by water: in order for peat to be eroded, a high-energy flow would be required that would likely have left traces in the San Jorge core (such as silts and clays).

A further possible explanation for the period of slow accumulation is that the shift from floating aquatic vegetation to forest was the result of a change in the local hydrology. In the Hudson Bay Lowlands (Canada), Glaser et al. (2004) found that vertical peatland growth was limited by the local hydrogeological conditions. In narrow interfluvial areas (i.e. areas where the centre of the peatland is close to a river channel), Glaser et al. (2004) found that high water table mounds could not be maintained and therefore the limit to vertical peat accumulation was rapidly reached. If a river channel migrates closer to the centre of a peatland, it can increase the hydraulic gradient and cause increased drainage, and therefore a fall in lake level (or peat water table) and reduced peat accumulation rates (Anderson et al., 2003; Glaser et al., 2004).

At San Jorge this seems an unlikely explanation for the period of slow accumulation as the chronology strongly suggests that peat with high loss-on-ignition values has accumulated continuously since at least AD 1800 until the present day (as shown by ^{210}Pb dating; Chapter 7); as such, the river channel would have to have been closer to the centre of the peatland than it is at present to create the hydraulic gradient required to cause water table draw down at the core site. The presence of peat accumulations in areas close to the river (seen eroding from the peatland margin in 2012) suggests that marginal parts of the peatland did not form part of the main river channel in the recent past (although peat accumulation rates in this region are high; Lähteenoja et al. 2009a). The hydrological models in Chapter 5 also cast doubt on a change in the hydraulic gradient as a possible explanation, due to the inability of subsurface flow to shed the water falling as rain under current climatic conditions. The draw-down in the centre of the modelled peatland is negligible, and it is only within c. 100 m of the peatland margin that there is significant water loss from subsurface flow (Chapter 5).

An alternative explanation could be that the lake at San Jorge was drained because of the removal of a natural barrier. If the *Pistia* and Cyperaceae-dominated lake at San Jorge was originally contained by a clay levee and that levee was removed by lateral movement of the river channel, it could cause rapid drainage and the colonisation of the site by trees such as *Mauritia flexuosa* (Scenario 1 in Figure 11.2). Householder et al. (2012) found that hydrological barriers help to maintain waterlogged conditions in peatlands in Madre de Dios (S. Peru), and a clay levee can be seen along the margin of

Quistococha peatland which may be critical to the accumulation of peat at that site (Chapter 8). As can be seen in *terra firme* forests at the present day, without the local conditions necessary for the ponding of water, organic matter is rapidly recycled even under wet climatic conditions (e.g. Scott et al., 1992; Sayer et al., 2010). There is evidence for the proximity of the river to the core point at San Jorge from c. 2,200-800 cal yr BP, in the form of high Ca/Mg ratios (characteristic of minerotrophy; Shotyk, 1996), and the pollen of floating aquatic plants (which require high nutrient input; Junk and Piedade, 1997). This hypothesis could be tested by a more extensive site survey to better establish the nature of the site's geomorphology.

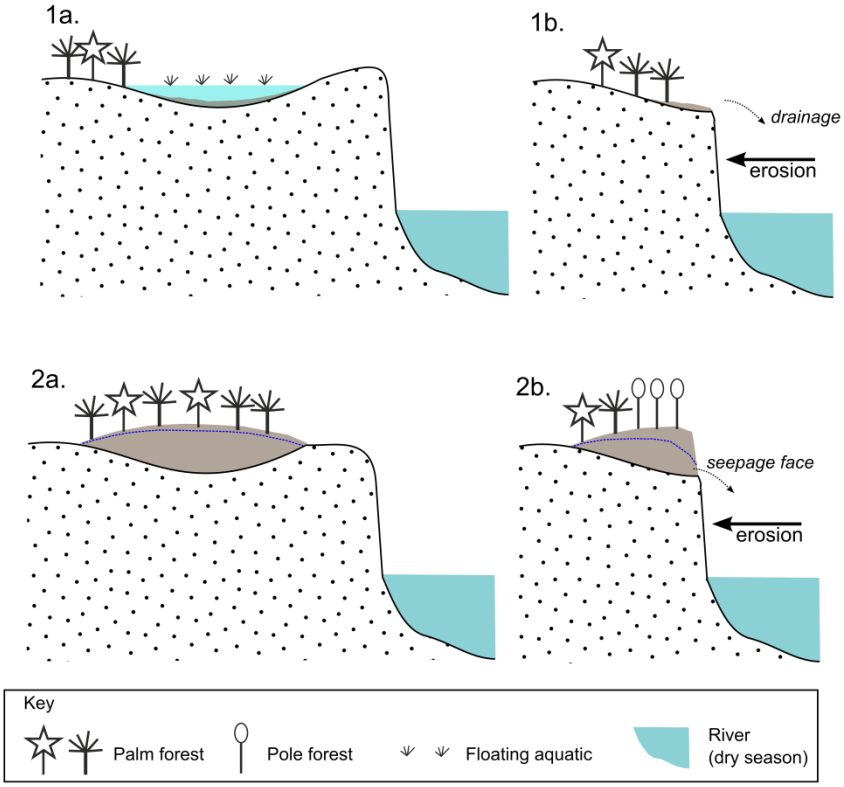

Figure 11.2: Examples of how river dynamics could indirectly effect peatland vegetation change across a site (cross-sections based on those in Puhakka et al., 1992). Erosion at the site margins could cause changes in the hydrological boundary conditions of a peatland. In Scenario 1, a lake with floating aquatic vegetation retained by a natural levee (1a) is affected by erosion by the river which causes the removal of the levee and drainage of the lake (1b). In Scenario 2, a domed peatland with a perched water table (2a) has its margin truncated, causing the previously isolated basin to drain more freely into the river (2b).

The period of slow accumulation at San Jorge could also have been caused by a period of dryer climate which lowered the water table and increased the rate of litter and peat decay. In terms of potential climatic causes, the slow accumulation could be related to the Medieval Climate Anomaly (see Figure 11.3), the precise timing and definition of which is variable (see discussion in Chapter 2), but which is thought by some authors to have been global in its extent (Graham et al., 2011). There is a parallel for this in the

palynological study by Morley (1981) of a peatland in Kalimantan, which showed an abrupt change from an open, herbaceous community (possibly a floating mat) consisting of Poaceae and *Lycopodium* to a peatland forest. Morley (1981) inferred that this transition was the result of mid-Holocene climate change, but had no absolute chronology (and therefore it is uncertain as to whether this transition was also marked by a hiatus or period of slow accumulation).

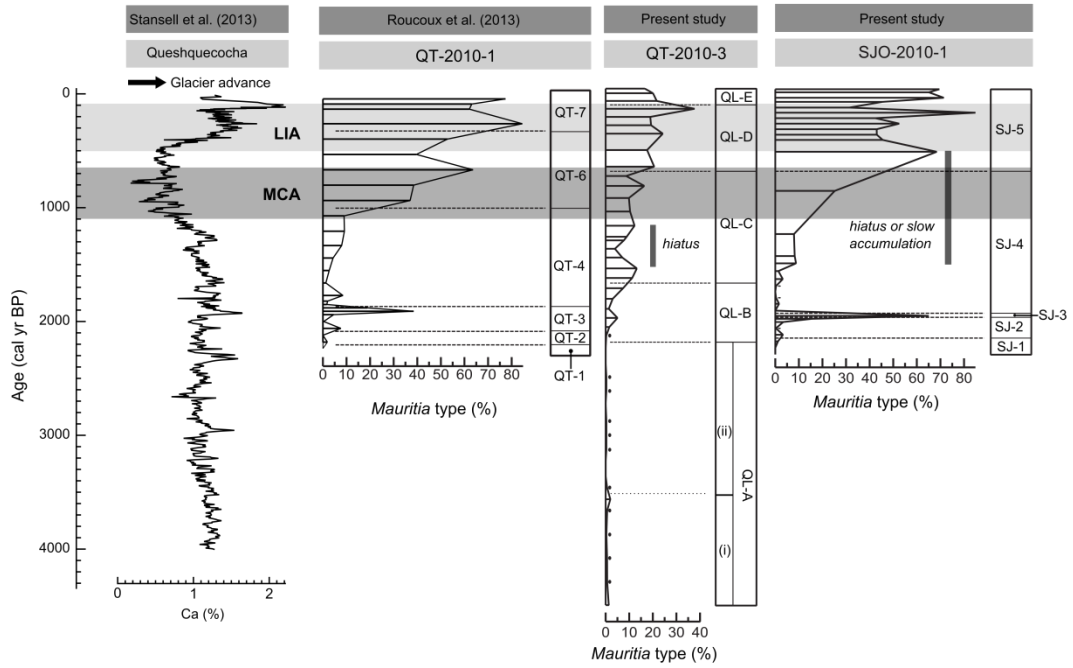

Figure 11.3: *Mauritia*-type percentage pollen curves and pollen assemblage zones for the well-dated lake and peat sequences currently available from Quistococha and San Jorge (Roucoux et al., 2013 and the present study), shown against the record of glacier advance and retreat from Queshquecocha, Andean Peru (Stansell et al., 2013). The Little Ice Age (LIA) and Medieval Climate Anomaly (MCA) have been marked (after Graham et al., 2011), but please see Chapter 2 for caveats relating to the timing of these climatic periods and figures illustrating other regional climate proxy records.

At Quistococha, the expansion of *Mauritia*-t. across the site c. 1000 cal yr BP is essentially synchronous within the errors associated with radiocarbon dating (with the exception of one core; Figure 10.1), which is interpreted as representing an allogenic cause. The expansion of *Mauritia*-t. coincides with the peak of the MCA seen in the Andes (Bird et al., 2011). The expansion of *Mauritia*-t. around the lake margin occurred later, and is dated to 566-676 cal yr BP; this is also detected in the lake core (zone QTL-D; see discussion in Chapter 10). Pollen grain size data indicate that the initial expansion of *Mauritia*-t. pollen in QT-2012-9 was dominated by the pollen of *Mauritia flexuosa*, rather than *Mauritiella armata* (Figure 8.34). The expansion of *Mauritia*-t. pollen in QT-2012-9 is coincident with the start of pollen zone QT-5b in QT-2010-1 (Roucoux et al., 2013), during which *Mauritia*-t. continues to increase and *Ilex* also increases in abundance. The

expansion of *Mauritia*-t. implies a drop in the water level or reduced flooding, as *Mauritia flexuosa* cannot tolerate flooding over c. 1.5 m depth (Nicholson, 1997), whereas the preceding phase is dominated by the pollen of Myrtaceae and other taxa adapted to more deeply flooded conditions (Parodi and Freitas, 1990; Kalliola et al., 1991; Campbell et al., 1992; Wittman et al., 2006).

Two radiocarbon dates indicate a period of slow accumulation in the lake at Quistococha between 1500-1290 cal yr BP, which correlates (within ^{14}C error) with the onset of slow accumulation at San Jorge, although accumulation rates in the lake seem to recover more quickly. In the tropics, reductions in lake sediment accumulation rate are generally taken as an indication of lower lake levels, and hence drier climate (e.g. Ledru et al., 1998; de Toledo and Bush, 2008; Aniceto et al., 2014). In the lake core the decrease in accumulation rate is accompanied by a drop in *Mauritia*-t. pollen proportions and an increase in *Cecropia*, which indicates disturbance, although this cannot be seen in any of the peat cores and *Mauritia*-t. does not become established until much later across the Quistococha peatland (Section 10.2.3). In peat core QT-2010-1 (Roucoux et al., 2013), a second peak in Cyperaceae at 224 cm occurs at the same time as the putative drop in lake level, and there are some indications that Myrtaceae declined between 1800 and 1500 cal yr BP (based on the QT-2010-1 age model). There is no clear evidence for a change in the geochemical record from QT-2010-1 (Lawson et al., 2014), although it is possible that the geochemical signal from this time period has been altered by post-depositional processes and nutrient recycling.

Sites from northern Ecuador, including Anañgucocha, L. Agrio, Limoncocha, and L. Santa Cecilia (Frost, 1988; Colinvaux et al., 1988), have recorded a period of increased rainfall and flooding c. 1100 cal yr BP (with some uncertainty in the chronology) . However, Liu and Colinvaux (1988) inferred a period of dry climate (1500-800 ^{14}C yr BP; c. 1350-770 cal yr BP based on a linear age model constructed by the present author) from their pollen record from L. Kumpaka (Southern Ecuador). The chronology of Liu and Colinvaux (1988) is also subject to uncertainty, and is based on a single bulk radiocarbon date (which may in turn be subject to old carbon error; Chapter 7), which does not bracket the event of interest. Weng et al. (2002) inferred a drier climate from c. 1000 cal yr BP in the Maxus 4 core from Northern Ecuador, which (conversely) terminated the *Mauritia* swamp growing at that site. Roucoux et al. (2013) also commented that the establishment of the palm swamp at Quistococha c. 1000 cal yr BP implies reduced flooding, and the San Jorge record supports the inference that this was a period of drier climate. The data from Quistococha and San Jorge therefore seems to

contrast with some of the records from northern Ecuador which show evidence for large floods around this time.

In the central Amazon (near Manaus, Brazil) Piperno and Becker (1996) found evidence of large natural fires in the form of charcoal from soil profiles; most of the radiocarbon dated charcoal fragments fell in the period from 1698 to 781 cal yr BP. Evidence for a period of dry climate is seen at Punta Laguna in the Yucatan c. 1365 cal yr BP, and coincides with a cultural event known as the 'Mayan Hiatus' (Curtis et al., 1996). A dry period has been recorded in other Central American archives, such as the Reflection Cave record which shows a change in $\delta^{13}C$ at this time (1400-800 cal yr BP) indicative of drier conditions (Polk et al., 2007). A peak in dust particle accumulation is also seen c. 1340 cal yr BP in the Quelccaya ice core (see Thompson et al., 1994), although there is no clear change in the $\delta^{18}O$ values indicative of a change in Atlantic SST (see Thompson et al., 1986; Thompson et al., 2013).

In summary, there is evidence from both Quistococha and San Jorge (but particularly San Jorge where there is a reduction in peat accumulation rate) for a reduction in rainfall in the period 1500-500 cal yr BP. Although changes in the local hydrology could provide alternative explanations for the changes seen at San Jorge, these are less convincing and a climatic cause is more likely. Dates and time frames for climatic change during the medieval period vary somewhat between different studies (Chapter 2), but there is evidence for a period of change in multiple archives across the world from 1000-600 cal yr BP (Mann et al., 2009; Graham et al., 2011). Sites elsewhere in the central and western Amazon also show evidence for a period of drier climate at this time (Weng et al., 2002; Piperno & Becker, 1996), and although the chronologies for some of these records are uncertain (e.g. Liu & Colinvaux, 1988), there is a growing body of evidence supported by proxy records of glacial retreat and Amazonian rainfall from the Andes (Bird et al., 2011; Stansell et al., 2013). Nevertheless, relative to the size of the western Amazon the number of well-dated records is small, and some isotopic records of rainfall in the Andes do not clearly show an anomaly during this period (Thompson et al., 1986; Thompson et al., 2013), highlighting the need for further work.

11.4.2.2 A wet-shift during the LIA c. 500-300 cal yr BP

In the Andean ice cores and lake isotopic records a period of cooler, wetter climate from c. 550-150 cal yr BP (Bird et al., 2011), usually correlated with the LIA, is the strongest and clearest of all the late Holocene climate events, and is the event which is most convincingly replicated across different climate proxy records (see Chapter 2). It was also of sufficient duration to have left an imprint in palaeoecological records.

At San Jorge, an increase in peat accumulation rate (following the period of slow accumulation discussed in Section 11.4.2.1) is dated to between 320-842 cal yr BP (c. 400 cal yr BP in the SJO-2010-1 age model); this could have been caused by an increase in the available moisture during the LIA (as indirectly recorded in the Andes), although there is uncertainty in the age model. This period is associated with increases in *Ilex* and *Euterpe*-t. pollen; species such as *Ilex inundata* are typical of flooded forests (*tahuampa*) in Amazonia (Gentry, 1993), in the Caquetá region of Colombia *Euterpe precatoria* is most common at flooded sites (Duivenvoorden, 1995). These changes are therefore consistent with a shift to wetter conditions, potentially a shorter or less severe dry season as peat accumulation rates are likely to respond more to dry season than wet season rainfall (Page et al., 2004; also see Chapter 5).

At Quistococha there is more equivocal evidence for changes during the period of the LIA. In QT-2010-1, *Ilex* declines in the top part of the record (from 80-100 cm; c. 400-600 cal yr BP), but the chronology in this part of the sequence is somewhat uncertain. A radiocarbon date at 50-52 cm was reported as 269-12 cal yr BP (Roucoux et al., 2013), which only indicates a very recent age for this part of the core. An increase in *Mauritia*-t. in zone QL-D appears to have begun during the MCA (see discussion in 11.4.2.1), and this persisted through the LIA, although the pollen grain size data from the lake core indicate that the relative populations of *Mauritia* and *Mauritiella* fluctuated throughout the last 600 years. The increase in *Mauritia*-t. in the lake core c. 600 cal yr BP may be related to the expansion of *Mauritia* around the lake margins, as seen in QT-2012-9 (discussed above), but elsewhere on the site this appears to occur later. In QT-2010-1, an increase in *Mauritia*-t. begins c. 400 cal yr BP. There is therefore a possibility that the late expansion of *Mauritia*-t. on different parts of the site could have been autogenically driven. The lack of a clear response to climatic change around the time of the LIA at Quistococha (by comparison with San Jorge) could be because San Jorge is domed and therefore more sensitive to changes in rainfall (although Ca/Mg ratios indicate that the site was not fully ombrotrophic at this stage). Ombrotrophic peatlands rely entirely on rainfall to maintain their soil moisture, whereas in minerotrophic peatlands groundwater flow can also help to maintain high peatland water tables (Charman, 2002).

11.4.2.3 Drier climate after 250 cal yr BP

Many South American proxy records show a change in climate after c. 250 cal yr BP. For example, the Quellcaya ice core shows a reduction in dust input after c. 250 cal yr BP and particularly after 150 cal yr BP (Thompson et al., 1986). The Galapagos diatom record from El Junco shows a gradual increase in lake depth from around 200 cal yr BP

onwards, perhaps responding to increased sea surface temperatures and therefore ENSO activity (Conroy et al. 2009). A recent change in conditions c. 150 cal yr BP is also observed in the Andean bog record from Papallacta, where a decrease in Poaceae pollen abundance is interpreted as a change to drier conditions (Ledru et al., 2013).

In two ocean core records from coastal Peru (Calao and Pisco; see Figure 2.2 for location map), Gutiérrez et al. (2009) report a change in ocean biogeochemistry c. 150 cal yr BP. The abundance of anchovy (*Engraulis ringens*) fish scales increases, as do direct proxies for upwelling and productivity such as TOC and diatom abundance (Gutiérrez et al., 2009). They argue this was the result of increasing ENSO activity and the northward migration of the ITCZ after the end of the LIA (also see Haug et al., 2001). Collated historical records also show an increase in ENSO frequency after c. 150 cal yr BP, with relatively few recorded events from the 250 cal yr BP onwards (Arteaga et al., 2006). However, it is unclear whether this might be a result of better record keeping during more recent times.

In summary, the period from 250 cal yr BP saw notable climatic changes in South America, defined by a northward movement of the ITCZ and an increase in ENSO activity which has continued throughout the Current Warm Period (see Table 2.1). At San Jorge, there is evidence for a change in forest composition above 50 cm depth (after c. 150 cal yr BP), which in tandem with the geochemical data can be interpreted as a shift towards drier, ombrotrophic conditions at the site (see Chapter 9). This drying may be consistent with an increase in ENSO frequency after the end of the LIA seen in the records discussed above (Arteaga et al., 2006; Conroy et al. 2009; Gutiérrez et al., 2009). As Hughes and Barber (2003) argue, a dry period may be all that is required to cause a shift to ombrotrophy, as it can help to isolate the vegetation from nutrients in groundwater (indeed, this can also affect nutrient supply in fens; see Wassen et al., 1989). An alternative hypothesis is that erosion of the site margin by the river could have resulted in an alteration of the hydraulic gradient, thereby causing a drop in water table (Scenario 2 in Figure 11.2). Parts of the peatland up to several hundred metres from the eroding face could have become drier, as the river created a larger hydraulic gradient and a fresh seepage face from which water drains. Erosion of the peatland margin was observed in 2012 (Chapter 3), and it is possible that this began during the relatively recent part of the site's history (i.e. from AD 1800). However, the hydrological model presented in Chapter 5 suggests that substantial draw-down of the water table at the centre of the site could not have been caused by a change in the hydrological boundary conditions alone.

At Quistococha there is little evidence for vegetation responses to climate change during the most recent part of the site's history. In the last c. 150 years, there is good reason to believe that human impact has been the main control on the lake pollen record (see Section 11.3). However, the *Mauritia*-t. grain size data do show an increase in the percentage of *Mauritiella* in the most recent part of many of the Quistococha records (generally within the top 32 cm), the main exception being QT-2012-18. At San Jorge, a more mixed *Mauritia* and *Mauritiella* assemblage forms part of an earlier vegetation phase which is followed by a phase where *Mauritia* only is present (currently as part of the pole forest). This could therefore indicate a reversed succession; the recent trend shows an increase in *Mauritiella* pollen, with similar proportions of pollen to that seen during the early formation of both San Jorge and Quistococha. However, without a more detailed knowledge of the environmental preferences of *Mauritia* and *Mauritiella* a causal mechanism is impossible to establish, and subtle changes in composition such as this could be autogenically driven or related to population dynamics.

Tabebuia-t. pollen is most abundant in the upper pollen zones of the peat sequences (e.g. Q18-D, Q10-D); the increase in *Tabebuia*-t. towards the top of the peat sequences from Quistococha, although small, is likely significant given the poor pollen representation of this taxon (Chapter 6). *Tabebuia barbata* is known from 'mid-level' blackwater communities (Worbes, 1997), and is known to tolerate long flooding and low nutrient availability (Ferreira and Prance, 1998). However, in the Caquetá area (Colombia), *Tabebuia insignis* is associated with reduced flooding, in contrast to species such as *Mauritiella aculeata* (Duivenvoorden, 1995). It is possible that in this case the increase in *Tabebuia*-t. pollen reflects a reduction in flood frequency, which could be related to drier conditions during the Current Warm Period (Bird et al., 2011), or could be autogenically driven as a result of increasing peat accumulation.

11.5 Summary

A summary of the discussion in this chapter is provided below with reference to the main hypotheses.

11.5.1. An ecologically-significant change in the peatland pollen records at Quistococha and San Jorge was synchronous.

Comparisons between the records at Quistococha and San Jorge reveal strong evidence for synchroneity. The main increase in *Mauritia*-t. appears to have occurred around the same time (c. 1000 cal yr BP) across Quistococha (with the exception of QT-2012-9, close to the lake margin) and at the core site at San Jorge (Figure 11.3). At San Jorge, the

core chronology during this time period is less certain due to the slow accumulation rate.

Comparison of the *Mauritia*-t. pollen curves (Figure 11.3) shows that the short peak in *Mauritia*-t. in QT-2010-1 at Quistococha was synchronous (within ^{14}C dating error) with a similar peak at San Jorge c. 1900 cal yr BP. However, the multi-core analysis at Quistococha has revealed that this peak occurs at different times in other peat cores (see discussion in Chapter 10), and is not discernible in the lake core (where *Mauritia*-t. increases c. 400 years earlier). Therefore the observed synchroneity between Quistococha core QT-2010-1 and San Jorge may be coincidental.

11.5.2 Changes in the peatland pollen records obtained were entirely driven by external factors.

In Chapter 10, it was argued that the increasing similarity of vegetation composition across the Quistococha peatland have resulted from long-term homogenisation of site topography through peat accumulation. However, with respect to the *points of change* (i.e. the precise timing of vegetation changes) there is only minimal evidence that internally-driven, autogenic succession is the dominant process at work in either site. Most changes seen in the pollen records at the two sites are most parsimoniously explained by succession which is allogenically driven either by river dynamics or climatic change. At Quistococha and San Jorge, a mixed palm swamp where *Euterpe* is more prevalent or is dominant in the assemblage precedes a change to an assemblage dominated by *Mauritia*-t. pollen with only small amounts of *Euterpe*-t. pollen. A similar pattern has been seen in the Chocó in Colombia, where *Euterpe* has been found to tolerate more waterlogged conditions (Urrego et al., 2006). It is hypothesised that the mixed palm swamp can be replaced by a purely *Mauritia*-dominated aguajal as a result of a change to a drier climate, or as a result of autogenic changes as peat accumulates thereby lowering the water table. At Quistococha, the change appears to be partly related to gradual peat accumulation, but the point of change is synchronous across the site and suggests that it was caused by a climatic drying. However, there is evidence for a wholly autogenic change in QT-2012-9, where the increase in *Mauritia*-t. occurs later than across the rest of the site and is related to the terrestrialisation of the lake margin.

11.5.3 Changes in the peatland pollen records at Quistococha and San Jorge were synchronous with climate events in other records from the wider region.

There is evidence that peatland vegetation changes, particularly those at San Jorge, correlate with periods of climatic change seen in proxy records from the wider region. Alternative hypotheses are discussed, but a major hiatus or period of slow accumulation

at San Jorge between 1300 and 450 cal yr BP coincides with a decrease in the South American summer monsoon recorded in isotopic records from the Andes (Bird et al., 2011), and records of Andean glacier retreat (Stansell et al., 2013). These have been attributed to the Medieval Climate Anomaly (MCA), thought to have been global in its extent (Graham et al., 2011). The expansion of *Mauritia*-t. pollen across the peatland at Quistococha also falls within this time frame, and largely coincides (with the exception of the increase in QT-2012-9) with the peak in MCA drying seen in the isotopic record from Lake Pumacocha in the Andes c. 900-1000 cal yr BP (Bird et al., 2011).

This is amongst the first evidence for an effect of late-Holocene climatic change on lowland vegetation communities in the western Amazon. That this can be most prominently seen at San Jorge suggests that upland rainforests may also have been affected: San Jorge is a domed site, and likely responded to changes in rainfall which could also have affected vegetation away from the floodplain in *terra firme* areas. There is a need for further research in these areas, and this may be achievable using short records (≤ 2000 years) found in forest hollows, such as the one identified near Jenaro Herrera during investigatory fieldwork as part of this study (Chapter 3; Roucoux et al., unpublished data).

12. Conclusions

This chapter summarises the main findings of this thesis, and places the work presented in the context of the wider literature, with the first four subheadings referring directly to the main aims presented in Chapter 2. Future avenues of research are then described, along with implications for tropical peatland conservation.

12.1 Hydrological behaviour in three Amazonian peatlands

Hydrological data have been presented from three peatlands (Buena Vista, Quistococha, and San Jorge). An annual record of water table fluctuations has shown that water levels can fall rapidly in the absence of rainfall (c. 1.6 cm d^{-1}), and field measurements have shown that the hydraulic conductivity of Amazonian peats is high by comparison with many northern peatlands (cf. Lewis et al., 2012), with some measurements as high as 0.11 cm s^{-1}. Hydrological models parameterised using the peat hydraulic conductivity measurements suggest that the majority of the water lost leaves peatlands via overland flow or evapotranspiration rather than subsurface flow. This data therefore confirms the potential sensitivity of peatlands to climatic change, and the need for palaeoecological data to establish the degree to which peatlands in the western Amazon have been affected by late Holocene climate events. Subsurface flow becomes more important towards the peatland margins, and the high hydraulic conductivity of the peat makes it vulnerable to the construction of drainage ditches (Holden et al., 2004). In peatlands with high hydraulic conductivity, fewer drainage ditches are required to effectively drain the peat, reducing the economic cost of the undertaking (Holden et al., 2004). At present, the author is not aware of any plans to drain peatlands for agricultural uses in Loreto, but if the region became more accessible to external markets then some peatland areas could be converted into oil palm plantations as has occurred on a large scale in Indonesia (see Chapter 1). Sites such as San Jorge, which is perched above the river level and hence would be relatively easy to drain, could be particularly vulnerable.

12.2 The first explicit model of Amazonian peatland development

The evidence from the present and previous studies strongly suggests that the peatland and lake at Quistococha are the remains of an abandoned channel of the Amazon (e.g. Räsänen et al., 1991). The peat basal dates collected as part of the research in this thesis show that peat initiation occurred in two main phases; peat accumulation began first in the vicinity of the modern lake (c. 2100-2400 cal yr BP), and then on more southerly parts of the site (c. 1900-2200 cal yr BP). However, this expansion likely occurred not as a result of terrestrialisation or paludification (which would have occurred more gradually), but through 'primary mire formation' (sensu Sjörs, 1983) when sediment input from the river declined. Authors often fail to distinguish between 'paludification'

(the gradual, largely autogenic spread of a peatland) and 'primary mire formation' (synchronous peat initiation across an area) in the literature (Sjörs, 1983), and the latter is a less common term. Ruppel et al. (2013) found that primary mire formation is a process mostly confined to coastal peatlands, and so its importance at Quistococha is somewhat unusual. Future research should seek to gather data specifically suitable for differentiating between paludification and primary mire formation (e.g. a range of basal dates from different parts of the peatland), and ensure that the processes are conceptually separated. However, in general, the conceptual model for Quistococha incorporates processes referred to in many other peatland development models (cf. Heinselman, 1963; Kratz & DeWitt, 1986; Anderson et al., 2003).

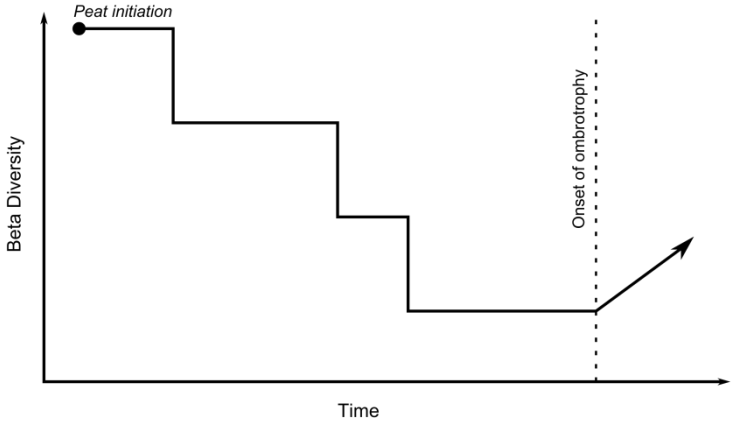

Figure 12.1: Figure representing changes in beta diversity through time in a hypothetical peatland. Immediately following peat initiation, topographic variation is high and the peatland includes a range of different habitats (i.e. beta diversity is high), but this declines as peat accumulates and reduces the topographic variation across the site. This gradual process is overprinted by externally-driven (e.g. Ireland et al., 2012) and internally-driven vegetation changes (internally driven non-linear behaviour can occur in ecosystems; Scheffer et al., 2001; Granath et al., 2010), resulting in a step-like reduction in beta diversity as vegetation communities persist and then change (usually rapidly, e.g. following a climatic event). As the peatland matures, peat accumulation creates domed, ombrotrophic areas, and causes a slight increase in beta diversity (e.g. marginal palm swamp may persist as a pole forest of differing composition develops in ombrotrophic areas). The step-like nature of the changes is supported by the pollen data.

Following the two main phases of peat initiation at Quistococha (see above), lateral growth through paludification and terrestrialisation was limited to small areas along the western margin and along the lake shoreline. The development of the vegetation across the peatland was strongly influenced by the topographic variation of the peatland substrate. This seems to have resulted in a general decline in beta diversity (at the site level) through time as peat accumulation reduced the differences in topography between parts of the site (Figure 12.1), confirming initial ideas expressed by Householder et al. (2012) that the beta diversity of tropical peatlands may be affected by their underlying substrate topography (i.e. beta diversity is likely to be higher on sites

with a more variable substrate topography; these are most likely to be younger peatlands closer to the main river channel).

12.3 The key drivers of vegetation change in two Amazonian peatlands

Palaeoecological data have been presented from two peatland sites at Quistococha and San Jorge. The data from Quistococha constitute the first detailed palaeoecological study of multiple cores from across an Amazonian peatland. Before the start of this project, existing work appeared to show continuous peat accumulation through the last 2000 years for the ten different peatland sites with radiocarbon dated profiles (e.g. Lähteenoja et al., 2009a). Given that the Pastaza-Marañón region is one of the wettest parts of the Amazon basin (Marengo, 1998), and the smooth age-depth curves of previous studies (Lähteenoja et al., 2009a, 2012), there was an assumption that conditions suitable for peat accumulation had persisted throughout the late Holocene (Lähteenoja, 2011). However, broad spacing of radiocarbon dates in a core can mask periods of slow deposition or hiatuses. At San Jorge, detailed dating of the top 240 cm, where peat accumulations with loss-on-ignition values greater than 95% are found, revealed a period of very slow accumulation from 1300-450 cal yr BP. There is evidence that the period of slow peat accumulation at San Jorge coincided with evidence for climatic change in some other South American palaeoclimate records (e.g. a period of ablation in Andean glaciers; Stansell et al., 2013), during what has become known as the Medieval Climate Anomaly (MCA) (and that accumulation may have resumed during the Little Ice Age). The MCA is a period of anomalous climate observed in many records globally (Graham et al., 2011). Graham et al. (2011) argue that the MCA saw changed to precipitation patterns across South and Central America, although it cannot always be clearly detected in proxy records from the region (e.g. $\delta^{18}O$ in Andean ice cores which derive their precipitation from the Amazon basin; Thompson et al., 2013). Charman et al. (2013) state that, as peat accumulation was faster in northern peatlands during the MCA than immediately before or after, carbon sequestration could be higher under projected future, warmer climates. The reduction in peat accumulation rate during this time at San Jorge suggests that peat accumulation rates at some sites in the Peruvian Amazon may also have declined during the MCA, although further data are needed to confirm the general nature of this result. At Quistococha, peat accumulation appears to have continued at a constant rate through this period, but further research should focus on applying closely-spaced radiocarbon dates in cores from other sites to establish whether they also contain observable hiatuses in peat accumulation.

There is, however, some evidence of a climatic effect on processes of peatland expansion from the multiple core study of Quistococha peatland. The pollen record from core QT-

2012-9 from the margin of the lake revealed that *Mauritia* and *Mauritiella* became abundant on this part of the site around 566-676 cal yr BP, significantly later than in the other cores. This expansion was likely caused by a reduction in lake level and therefore allogenically driven; it may have resulted from drier conditions during the MCA.

The palaeoecological data from San Jorge have also provided a unique insight into the formation of the pole forest at that site. Forests of a similar structure and floristic composition are found in non-peatland, 'white sand' areas, but are very rare (< 3% of the area) throughout the Amazon (Fine et al., 2010). The pole forest at San Jorge is young, and its formation c. AD 1800 is synchronous with changes in oceanic circulation recorded along the coast of Peru (Gutiérrez et al. 2009). This may be coincidental, but it is possible that this ecological transition, thought to have been accompanied by a shift to ombrotrophy, was climatically driven by changes in ENSO frequency after the end of the LIA. Dating the inception of the pole forest relied on the application of ^{210}Pb dating, the first time this technique has been applied in an Amazonian peatland, and this technique could be applied to constrain the timing of recent peatland vegetation at other sites. Further research should focus on whether other (domed) peatland sites show evidence of vegetation change at this time (c. AD 1800) in order to establish whether the cause was regional climate change.

12.4 Methodological implications for future research

This thesis has described pollen and spore types which will be of use in future palaeobotanical studies of tropical peatlands. Scanning electron microscopy (SEM) has revealed micron scale differences that can be used to make a taxonomic distinction between *Mauritia flexuosa* and *Mauritiella armata*. However, while SEM could be applied more than it is at present in tropical palaeoecology, precise grain size measurements can also allow greater taxonomic precision using normal light microscopy. The taxonomic work undertaken has allowed identifications which would otherwise have been difficult or uncertain, and has also revealed important findings as regards past vegetation patterns. A study of grain morphometry has allowed the confident splitting of *Mauritia flexuosa* and *Mauritiella armata* pollen (both common peatland trees), revealing vegetation changes which would have remained unknown (e.g. the shift to a *Mauritia flexuosa*-dominated assemblage in the top 50 cm at San Jorge). Identifying such changes is important when correlating peatland records and regional Holocene climate records, and at San Jorge has supported the inference that a change in forest type from palm swamp to pole forest may have been caused by climatic change after AD 1800.

There is still much scope for the refinement of tropical peatland pollen taxonomy. Obtaining flowers from tropical peatland trees can be practically challenging for a

number of reasons, such as intermittent flowering and the inaccessibility of flowers in the canopy. Further work should also focus on the potential of herbaceous taxa to provide insights into past edaphic conditions, and indeed further modern studies of plant distributions may be required which could be undertaken with palaeoecological applications in mind. Studies in the modern forest have generally focused on those elements which make the most significant contribution to the biomass (i.e. trees), and neglected the herbaceous elements such as ferns. In peatlands, not only could this give a false impression of their floristic diversity (some areas are occupied only by herbaceous taxa), but also understanding the distribution of herbaceous taxa in the modern environment could significantly increase our ability to interpret the palaeoecological record (see Chapter 6). Ferns are not only associated with particular forest types but are also sensitive to edaphic changes (Ruokolainen et al., 2007).

Palaeoecological studies of peatlands have usually focused on single cores taken from the deepest point; few have challenged the assumption that a single core can represent changes across the whole of a given site. The lack of good spatial resolution in palaeoecological studies has also been highlighted as an obstacle to the connection of modern ecological and palaeoecological disciplines (Birks, 1993). The five peat cores analysed at Quistococha by this study and by Roucoux et al. (2013) have shown that a single core can be broadly representative of the main vegetation phases which have occurred across most of the site, although differences did occur in timing and pollen assemblage between the cores. In particular, the main increase in *Mauritia*-t. at Quistococha appears to be largely synchronous across the site, but was delayed in the area directly adjacent to the eastern lake shoreline. This suggests that careful positioning of a small number of core points (in areas close to the lake margins, and in areas of deep and shallow peat) can capture the spatial variation with respect to palaeovegetation changes. Although data is still required from further multiple core studies to confirm the generality of these findings, this suggests that a greater research effort could be focused on obtaining records from different sites, rather than on within-site replication.

However, as has been found in studies of other tropical peatlands (Morley, 1981; Taylor, 2001), the examination of more cores can add important details relating to peatland development. For example, at Quistococha, other cores contained significant phases of *Symmeria* and *Euterpe* type pollen which were absent in the original core (QT-2010-1; Roucoux et al., 2013), which aided palaeoenvironmental interpretations of earlier vegetation communities and highlighted differences between shallow and deep (in terms of depth to the substrate) areas of the site.

12.5 Future work

There are a number of limitations to the work undertaken in this thesis. Our knowledge of Amazonian peatland palaeoecology remains relatively limited compared to that of peatlands elsewhere. In terms of site development, peatlands in other parts of the Pastaza-Marañón basin may have developed differently to the Quistococha and San Jorge peatlands; these two are both more than 50 km downstream of the junction where the Ucayali and Marañón rivers join to form the main Amazon channel and many peatlands lie upstream of this point. Further work is also needed to establish whether the hiatus observed at San Jorge is present in other domed peatlands. Older peatland sites could also provide insights into the early to mid-Holocene environment of this region, when other records from the region suggest that the ITCZ was in a different position and ENSO was less active (Chapter 2).

The adaptation of existing numerical peat accumulation models for use in tropical peatlands is also an important research goal. Creating numerical models is essential to determine the potential response of peatlands to man-made landscape change and global warming, particularly with regard to non-linear responses (Yu et al., 2011). In other regions of the world, palaeoecological data have served an important role as a means of testing numerical model outputs (Tuittila et al., 2013). As Lawrence and Slater (2008) have argued for northern peatlands, the aim for the next decade should be to couple numerical models for tropical peatlands (and their associated C fluxes) with global climate models. In this way, potential feedbacks between global climate and stored soil carbon can be included in our projections of future climatic change.

Although the hydrological work presented in this thesis provides new data that are essential to parameterise most numerical peat accumulation models (i.e. peat hydraulic conductivity measurements), there is still substantial scope for further work. As yet we have little knowledge of peat properties such as specific yield, the rate of litter addition in different peatland forest types, and peat decay rates. In the dynamic landscape of the Western Amazon, peatlands can be destroyed by the lateral migration of river channels, and these landscape scale processes will also require further exploration using, for example, a combination of fieldwork and remote sensing. Different rivers function in different ways; for example, as Puhakka et al. (1992) note, the sinuosity of major rivers such as the Marañón (braided/anastomosing) differ greatly from smaller rivers such as the Tigre (misfit meandering); Aucayacu, the oldest peatland dated so far in Amazonian Peru, is situated adjacent to the Tigre River (Lähteenoja et al. 2012; Swindles et al., 2014). This difference in river dynamics and sinuosity will have a local effect on the cycle of peatland creation and destruction.

12.6 Policy implications

The findings from San Jorge suggest that conservation for the sake of biodiversity and conservation for the sake of reducing carbon emissions may not always be compatible. The formation of the pole forest at San Jorge, a rare forest type, was preceded by a hiatus in peat accumulation, which likely indicates a period of increased peat decay. In the future, accumulation in some domed peatlands may be reduced as a result of climatic change, but this could also be associated with the creation of pole forests which accommodate rare plant assemblages and animal species. Peatland pole forests are similar in composition to white sand forests, which suggests they might share fauna too; surveys from elsewhere in Amazonian have shown that 3% of the bird species in white sand forest are not found in any other forest types (Borges, 2004). Alonso and Whitney (2003) also observed that several bird species were uniquely found in the white sand forests near Iquitos, and Lähteenoja et al. (2009b) recorded white sand bird species at San Jorge peatland. Such conflicts between biodiversity and carbon emissions could complicate conservation efforts undertaken through schemes such as REDD+ (Miles & Kapos, 2009; Murdiyarso et al., 2010). Further research is clearly also required into the modern ecology of domed peatlands in order to establish potential similarities and differences with white sand forests, including vertebrate diversity.

The western Amazon has been described as the 'core' of Amazonia; with high rainfall and lower seasonality than the rest of the basin it is seen as a refugial area for moist tropical rainforest species under most future climate change scenarios (Killeen and Solórzano, 2008). However, the results of the present study have shown that we must resist simplistic notions of 'refugia'; although the ecosystems of the western Amazon may continue to fall under the broad definition of moist tropical evergreen forest, there is evidence from the palaeoecological record that peatland ecosystems have responded to climatic changes in the late Holocene. Conservation strategies frequently assume that species distributions will remain constant (Froyd and Willis, 2008), but the palaeoecological record cautions against this assumption, particularly in Amazonian wetlands. The Quistococha model indicates that beta diversity across the site may decline on long timescales as peatland development progresses, and therefore that particular efforts should be made to limit human impact on active areas of the floodplain where young peatlands are forming.

Bibliography

Aaby, B., and Tauber, H. 1975. Rates of peat formation in relation to degree of humification and local environment, as shown by studies of a raised bog in Denmark. *Boreas*, 4: 1-17

Absy, M.L. 1979. A Palynological Study of Holocene Sediments in the Amazon Basin. PhD Thesis, University of Amsterdam.

Absy, M.L. 1991. Mise en évidence de quatre phases d'ouverture de la foret dense dans le sud-est de l'Amazonie au cours des 60,000 dernières annees. Première comparaison avec d'autres regions tropicales. *Comptes Rendus de l'Académie des Sciences, Série II*, 312: 673-678

Aguajal Project. (2011). Published online at http://atrium.andesamazon.org/research_project_list.php [accessed February 2011]

Alonso, J.A., and Whitney, B.M. 2003. New distribution records of birds from white-sand forests of the northern Peruvian Amazon, with implications for biogeography of northern South America. *The Condor*, 105: 552-566.

Almeda, F. 1981. The Mexican and Central American species of Adelobotrys (Melastomataceae). *Annals of the Missouri Botanical Gardens*, 68: 204-212

Almqvist-Jacobson, H., and Foster, D.R. 1995. Toward an Integrated Model for Raised-Bog Development: Theory and Field Evidence. *Ecology*, 76: 2503-2516.

Ambrósio, S.T., & De Melo, N.F. 2001. New Records of Pteridophytes in the Semi-Arid Region of Brazil. *American Fern Journal,* 91: 227-229.

Anderson, R.L., Foster, D.R., and Motzkin, G. 2003. Integrating lateral expansion into models of peatland development in temperate New England. *Journal of Ecology*, 91: 68-76

Andersen, S.T. 1980. Early and Late Weichselian chronology and birch assemblages in Denmark. *Boreas,* 9: 53-69.

Andersen S.T. 1960. Silicone oil as a mounting medium for pollen grains. *Danmarks Geologiske Undersøgelse* Series IV, 4: 1-24.

Anderson, J.A.R. 1961. The Ecology and Forest Types of the Peat Swamp Forests of Sarawak and Brunei in Relation to Their Silviculture. Unpublished PhD thesis, University of Edinburgh

Anderson, J.A.R., and Muller, J. 1975. Palynological study of a Holocene peat and a Miocene coal deposit from NW Borneo. *Review of Palaeobotany and Palynology,* 19: 291–351.

Andriesse, J.P. 1988. Nature and management of tropical peat soils. FAO Soils Bulletin 59, Food and Agriculture Organisation of the United Nations: Rome, Italy; 165.

Aniceto, K., Moreira-Turcq, P., Cordeiro, R.C., Fraizy, P., Quintana, I., and Turcq, B. 2014. Holocene paleohydrology of Quistococha Lake (Peru) in the upper Amazon Basin: Influence on carbon accumulation. *Palaeogeography, Palaeoclimatology, Palaeoecology.* DOI: 10.1016/j.palaeo.2014.08.018

Anshari, G., Kershaw, A.P., and van der Kaars, S. 2001. A Late Pleistocene and Holocene pollen and charcoal record from peat swamp forest, Lake Sentarum Wildlife Reserve, West Kalimantan, Indonesia. *Palaeoegeography, Palaeoclimatology, Palaeoecology,* 171: 213-228.

Anshari, G., Kershaw, A.P., van der Kaars, S., and Jacobsen, G. 2004. Environmental change and peatland forest dynamics in the Lake Sentarum area, West Kalimantan, Indonesia. *Journal of Quaternary Science,* 19: 637-655.

Antoine, P-O., De Franceschi, D., Flynn, J.J., Nel, A., Baby, P., Benammi, M., Caldero, Y., Espurt, N., Goswami, A., and Salas-Gismondi, R. 2006. Amber from western Amazonia reveals Neotropical diversity during the middle Miocene. Proceedings of the National Academy of Sciences, 103: 13595–13600

Appleby, P.G. 2001. Chronostratigraphic techniques in recent sediments. In: Last, W.M., and Smol, J.P. (eds) *Tracking Environmental Change Using Lake Sediments, Volume 1: Basin Analysis, Coring, and Chronological Techniques.* Kluwer: London, 171-203

Appleby, P.G., and Oldfield, F. 1978. The calculation of lead-210 dates assuming a constant rate of supply of unsupported ^{210}Pb to the sediment. *Catena,* 5: 1-8.

Appleby, P.G. 2008. Three decades of dating recent sediments by fallout radionuclides: a review. *The Holocene*, 18: 83-93

Arce-Nazario, J.A. 2007. Human landscapes have complex trajectories: reconstructing Peruvian Amazon landscape history from 1948 to 2005. *Landscape Ecology*, 22: 89–101

Armstrong, A.C. 1995. Hydrological model of peat mound form with vertically varying hydraulic conductivity. *Earth Surface Processes and Landforms,* 20: 473–477.

Arnold, J.R., and Libby, W.F. 1949. Age Determinations by Radiocarbon Content: Checks with Samples of Known Age. *Science,* 110: 678-680

Arteaga, K., Tutasi, P., and Jiménez, R. 2006. Climatic variability related to El Ni˜no in Ecuador – a historical background. *Advances in Geosciences*, 6: 237-241

Athens, J.S., and Ward, J.V. 1999. The Late Quaternary of the Western Amazon: climate, vegetation, and humans. *Antiquity*, 73: 287-302

Bacci, M.L. 2011. The Demise of the American Indios. *Population and Development Review*, 37: 161-165.

Baird, A.J., Eades, P.A., and Surridge, B.W.J. 2008. The hydraulic structure of a raised bog and its implications for ecohydrological modelling of bog development. *Ecohydrology,* 1: 289–298

Baird, A.J., Morris, P.J., and Belyea, L.R. 2012.The DigiBog peatland development model 1: rationale, conceptual model, and hydrological basis. *Ecohydrology,* **5**: 242-255. DOI: 10.1002/eco.230

Baird, A.J., Surridge, B.W.J., and Money, R.P. 2004. An assessment of the piezometer method for measuring the hydraulic conductivity of a Cladium mariscus—Phragmites australis root mat in a Norfolk (UK) fen. *Hydrological Processes* 18: 275–291.

Baker, P.A., Seltzer, G.O., Fritz, S.C., Dunbar, R.B., Grove, M.J., and Tapia, P.M. 2001. The History of South American Tropical Precipitation for the Past 25,000 Years. *Science*, 291: 64-643

Baker, T.R., Phillips, O.L., Malhi, Y., Almeida, S., Arroyo, L., Di Fiore, A., Erwin, T., Higuchi, N., Killeen, T.J., Laurance, S.G., Laurance, W.F., Lewis, S.L., Monteagudo, A., Neill, D.A., Núñez, P.V., Pitman, N.C.A., Silva, J.N.M., Martinez, R.V. 2004. Increasing biomass in Amazonian forest plots. *Philosophical Transactions of the Royal Society of London B.* 359: 353-365

Baker, W.J., Dransfield, J., and Hedderson, T.A. 2000. Phylogeny, Character Evolution, and a New Classification of the Calamoid Palms. *Systematic Botany* 25: 297-322

Ballhorn, U., Siegert, F., Mason, M., and Limin, S. 2009. Derivation of burn scar depths and estimation of carbon emissions with LIDAR in Indonesian peatlands. *Proceedings of the National Academy of Sciences,* 106: 21213-21218.

Barberi, M., Salgado-Labouriau, M.L., and Suguio, K. 2000. Paleovegetation and paleoclimate of "Vereda de Águas Emendadas", central Brazil. *Journal of South American Earth Sciences*, 13: 241-254

Barros, M.G. 2001. Pollination ecology of *Tabebuia aurea* (Manso) Benth. & Hook. and *T. ochracea* (Cham.) Standl. (Bignoniaceae) in Central Brazil cerrado vegetation. Brazilian Journal of Botany, 24: 255-261

Barton, A.M., Nurse, A.M., Michaud, K., and Hardy, S.W. 2011. Use of CART analysis to differentiate pollen of red pine (Pinus resinosa) and jack pine (P. banksiana) in New England. *Quaternary Research*, 75: 18-23.

Bauer, I.E., Gignac, L.D., and Vitt, D.H. 2003. Development of a peatland complex in boreal western Canada: lateral site expansion and local variability in vegetation succession and long-term peat accumulation. *Canadian Journal of Botany,* 81: 833-847.

Bauer, I.E. 2004 Modelling effects of litter quality and environment on peat accumulation over different time-scales. *Journal of Ecology,* 92: 661–674

Bawa, K.S., Bullock, S.H., Perry, D.R., Coville, R.E., and Grayum, M.H. 1985. Reproductive Biology of Tropical Lowland Rain Forest Trees. II. Pollination Systems. *American Journal of Botany*, 72: 346-356.

Baynton, H.W., Biggs, W.G., Hamilton, H.L., Sherr, P.E., Worth, J.J.B. 1965. Wind Structure in and above a Tropical Forest. *Journal of Applied Meteorology,* 4: 670-675

Beckwith, C.W., and Baird, A.J. 2001. Effect of biogenic gas bubbles on water flow through poorly decomposed blanket peat. *Water Resources Research*, 37: 551–558.

Beckwith, C.W., Baird, A.J., and Heathwaite, A.L. 2003. Anisotropy and depth-related heterogeneity of hydraulic conductivity in a bog peat. II: modelling the effects on groundwater flow. *Hydrological processes*, 17: 103–113.

Behling, H., and Hooghiemstra, H. 2000. Holocene Amazon rainforest–savannah dynamics and climatic implications: high-resolution pollen record from Laguna Loma Linda in eastern Colombia. *Journal of Quaternary Science*, 15: 687-695

Behling, H., and Hooghiemstra, H. 1998. Late Quaternary palaeoecology and palaeoclimatology from pollen records of the savannas of the Llanos Orientales in Colombia. *Palaeogeography, Palaeoclimatology, Palaeoecology*, 139: 251-267

Behling, H., and Hooghiemstra, H. 1999. Environmental history of the Colombian savannas of the Llanos Orientales since the Last Glacial Maximum from lake records El Pinal and Carimagua. *Journal of Paleolimnology*, 21: 461–476

Behling, H., Arz, H.W., Patzold, J., and Wefer, G. 2000. Late Quaternary vegetational and climate dynamics in northeastern Brazil, inferences from marine core GeoB 3104-1. *Quaternary Science Reviews*, 19: 981-994.

Behling, H., Berrio, J.C., & Hooghiemstra, H. 1999. Late Quaternary pollen records from the middle Caquetá river basin in central Colombian Amazon. *Palaeogeography, Palaeoclimatology, Palaeoecology*, 145: 193-213.

Behling, H., and da Costa, M.L. 2000. Holocene Environmental Changes from the Rio Curuá Record in the Caxiuaná Region, Eastern Amazon Basin. *Quaternary Research,* 53: 369-377.

Behling, H., Keim, G., Irion, G., Junk, W., and de Mello, J.N. 2001. Holocene environmental changes in the Central Amazon Basin inferred from Lago Calado (Brazil). *Palaeogeography, Palaeoclimatology, Palaeoecology*, 173: 87-101

Belyea, L.R., and Baird, A.J. 2006. Beyond 'The Limits to Peat Bog Growth": cross-scale feedback in peatland development. *Ecological Monographs* 76: 299–322.

Belyea, L.R., and Warner, B. 1994. Dating of the near-surface layer of a peatland in northwestern Ontario, Canada. *Boreas*, 23: 259-269.

Belyea, L.R. and Malmer, N. 2004. Carbon sequestration in peatland: patterns and mechanisms of response to climate change. *Global Change Biology* 10: 1043-1052.

Benavides, J.C., Vitt, D.H., and Kelman Wieder, R. 2013. The influence of climate change on recent peat accumulation patterns of *Distichia muscoides* cushion bogs in the high-elevation tropical Andes of Colombia. *Journal of Geophysical Research*, 118, 1627-1635.

Bendix, J. 2000. Precipitation dynamics in Ecuador and northern Peru during the 1991/92 El Niño: a remote sensing perspective. *International Journal of Remote Sensing,* 21: 533-548.

Bennett, K.D. 1996. Determination of the number of zones in a biostratigraphical sequence. *New Phytologist*, 132: 155-170

Bennett, K.D., 2007. PSIMPOLL (pollen plotting software). Available at http://chrono.qub.ac.uk/psimpoll/psimpoll.html (last accessed 20/9/14)

Berglund, B.E., Ralska-Jasiewiczowa, M., 1986. Pollen analysis and pollen diagrams. In: Berglund, B.E. (Ed.), *Handbook of Holocene Palaeoecology and Palaeohydrology*. John Wiley and Sons: Chichester, UK, 455–484.

Berrio, J.C., Behling, H., and Hooghiemstra, H. 2000. Tropical rain-forest history from the Colombian Pacific area: a 4200-year pollen record from Laguna Jotaordó. *The Holocene*, 10: 749-756

Betts, R.A., Cox, P.M., Collins, M., Harris, P.P., Huntingford, C., and Jones, C.D. 2004. The role of ecosystem-atmosphere interactions in simulated Amazonian precipitation decrease and forest dieback under global climate warming. *Theoretical and Applied Climatology*, 78: 157–175.

Biester, H., Bindler, R., Martinez-Cortizas, A., and Engstrom, D.R. 2007. Modeling the Past Atmospheric Deposition of Mercury Using Natural Archives. *Environmental Science and Technology*, 41: 4851–4860

Bird, B.W., Abbott, M.B., Vuille, M., Rodbell, D.T., Stansell, N.D., and Rosenmeier, M.F. 2011a. A 2,300-year-long annually resolved record of the South American summer monsoon from the Peruvian Andes. Proceedings of the National Academy of Sciences, 108: 8583-8588.

Bird, B.W., Abbott, M.B., Rodbell, D.T., and Vuille, M. 2011b. Holocene tropical South American hydroclimate revealed from a decadally resolvedlake sediment $\delta^{18}O$ record. *Earth and Planetary Science Letters*, 310: 192–202.

Birks, H.J.B. 1973. *Past and present vegetation of the Isle of Skye: a palaeoecological study*. Cambridge University Press: London.

Birks, H.J.B. 1993. Quaternary palaeoecology and vegetation science current contributions and possible future developments. *Review of Palaeobotany and Palynology*, 79: 153-177

Birks, H.J.B. 2007. Pollen methods and studies: Numerical Analysis Methods. In: Elias, S.A. (ed.) *The Encyclopedia of Quaternary Science, vol. 2.* Amsterdam: Elsevier, 2514-2521

Blaauw, M., 2010. Methods and code for 'classical' age-modelling of radiocarbon sequences. *Quaternary Geochronology,* 5: 512-518

Bodmer, R.E. 1990. Fruit patch size and frugivory in the lowland tapir (*Tapirus terrestris*). *Journal of Zoology,* 222: 121-128.

Bodmer, R.E., Eisenberg, J.F., and Redford, K.H. 1997. Hunting and the Likelihood of Extinction of Amazonian Mammals. *Conservation Biology*, 11: 460–466

Boelter, D.H. 1969. Physical properties of peat as related to degree of decomposition. *Soil Science Society of America Proceedings,* 33: 606–609.

Bolker, B.M., Brooks, M.E., Clark, C.J., Geange, S.W., Poulsen, J.R., Stevens, H.H., and White, J-SS. 2009. Generalized linear mixed models: a practical guide for ecology and evolution. *Trends in Ecology & Evolution,* 24: 127–135.

Borges, S.H. 2004. Species poor but distinct: bird assemblages in white sand vegetation in Jaú National Park, Brazilian Amazon. *Ibis*, 146: 114-124

Borren, W., Bleuten, W., and Lapshine, E.D. 2004. Holocene peat and carbon accumulation rates in the southern taiga of western Siberia. *Quaternary Research*, 61: 42-51

Bouwer, H. 1989. The Bouwer and Rice slug test – an update. *Ground Water,* 27: 304–309.

Bove, C.P. 1993. Pollen morphology of the Bignoniaceae from a south Brazilian Atlantic forest. *Grana*, 32: 330-337.

Bradshaw, H.W. 1981. Modern Pollen-Representation Factors for Woods in South-East England. *Journal of Ecology*, 69: 45-70

Brand, E.W., and Premchitt, J. 1980. Shape factors of cylindrical piezometers. *Géotechnique,* 30: 369–384.

Bridgham, S.D., Pastor, J., Janssens, J.A., Chapin, C., and Maltereff, T.J. 1996. Multiple limiting gradients in peatlands. *Wetlands*, 16: 45-65

British Standard BS 7755. 1995. British Standard BS 7755, section 3.9: ISO 11466. Soil Quality Part 3. Chemical methods Section 3.9 Extraction of trace elements soluble in aqua regia.

Bronk Ramsey, C., and Lee, S. 2013. Recent and planned developments of the program OXCAL. *Radiocarbon* 55: 720-730.

Bronk Ramsey. 1995. Radiocarbon calibration and analysis of stratigraphy: The OXCAL program. *Radiocarbon* 37: 425-430.

Bronk Ramsay, C. 2009. Bayesian analysis of radiocarbon dates. *Radiocarbon*, 51: 337-360

Bronk Ramsay, C. 2008. Deposition models for chronological records. *Quaternary Science Reviews*, 27: 42–60

Brönnimann, S., Xoplaki, E., Casty, C., Pauling, A., and Luterbacher, J. 2007. ENSO influence on Europe during the last centuries. *Climate Dynamics*, 28: 181-197

Bruijnzeel, L.A. 1990. Hydrology of Moist Tropical Forests and Effects of Conversion: a State of Knowledge Review. UNESCO International Hydrological Programme. http://unesdoc.unesco.org/images/0009/000974/097405eo.pdf.

Buell, M.F., Buell, H.F., and Reiners, W.A. 1968. Radial Mat Growth on Cedar Creek Bog, Minnesota. *Ecology*, 49: 1198-1199.

Buffam, I., Turner, M.G., Desai, A.R., Hanson, P.C., Rusak, J.A., Lottig, N.R., Stanley, E.H., and Carpenter, S.R. 2011.Integrating aquatic and terrestrial components to construct a complete carbon budget for a north temperate lake district. *Global Change Biology*, 17: 1193–1211

Bunting, M.J., and Warner, B.G. 1998. Hydroseral development in southern Ontario: patterns and controls. *Journal of Biogeography*, 25: 3-18

Bunting, M.J., and Whitehouse, N.J. 2008. Adding time to the conservation toolkit: palaeoecology and long term wetland function dynamics. *Biodiversity and Conservation*, 17: 2051–2054

Burn, M.J. and Mayle, F.E. 2008. Palynological differentiation between genera of the Moraceae family and implications for Amazonian palaeoecology. *Review of Palaeobotany and Palynology,* 149: 187-201.

Burnham, K.P., and Anderson, D.R. 2004. Multimodel Inference: Understanding AIC and BIC in Model Selection. *Sociological Methods & Research*, 33: 261-304

Burrows, C.J. 1990. *Processes of Vegetation Change.* Unwin Hyman: London

Bush, M.B. 1995. Neotropical Plant Reproductive Strategies and Fossil Pollen Representation. *The American Naturalist*, 145: 594-609

Bush, M.B. and Weng, M.B. 2006. Introducing a new (freeware) tool for palynology. *Journal of Biogeography*, 34: 377-380.

Bush, M.B., Miller, M.C., De Oliveira, P.E., & Colinvaux, P.A. 2000. Two histories of environmental change and human disturbance in eastern lowland Amazonia. *The Holocene,* 10: 543-553.

Bush, M.B., Silman, M.R., & Listopad, M.C.S. 2007b. A regional study of Holocene climate change and human occupation in Peruvian Amazonia. *Journal of Biogeography,* 34: 1342-1356

Bush, M.B., Silman, M.R., de Toledo, M.B., Listopad, C., Gosling, W.D., Williams, C., de Oliveira, P.E., & Krisel, C. 2007a. Holocene fire and occupation in Amazonia: records from two lake districts. *Philosophical Transactions of the Royal Society of London B*, 362: 209-218

Bush, M.B., Piperno, D.R., and Colinvaux, P.A. 1989. A 6,000 year history of Amazonian maize cultivation. *Nature,* 340: 303-305

Bush, M.B. & Silman, M.R. 2007. Amazonian exploitation revisited: ecological asymmetry and the policy pendulum. *Frontiers in Ecology and the Environment,* 5: 457–465

Bush, M.B., Moreno, E., De Oliveira, P.E., Asanza, E. & Colinvaux, P.A. 2001. The influence of biogeographic and ecological heterogeneity on Amazonian pollen spectra. *Journal of Tropical Ecology,* 17: 729-743

Cameron, C.C., Esterle, J.S., and Palmer, C.A. 1989. The geology, botany and chemistry of selected peat-forming environments from temperate and tropical latitudes. *International Journal of Coal Geology,* 12, 105-156.

Campbell, D.G., Stone, J.L., and Rosas, A. 1992. A comparison of the phytosociology and dynamics of three floodplain (*Várzea*) forests of known ages, Rio Jurua, western Brazilian Amazon. *Botanical Journal of the Linnean Society*, 108: 213-237

Cane, M.A. 2005. The evolution of El Niño, past and future. *Earth and Planetary Science Letters*, 230: 227–240

Carré, M., Azzoug, M., Bentaleb, I., Chase, B.M., Fontugne, M., Jackson, D., Ledru, M-P., Maldonado, A., Sachs, J.P., and Schauer, A.J. 2012. Mid-Holocene mean climate in the south eastern Pacific and its influence on South America. *Quaternary International*, 253: 55-66

Carson, J.F., Whitney, B.S., Mayle, F.E., Iriarte, J., Prümers, H., Watling, J. 2014. Environmental impact of geometric earthwork construction in pre-Columbian Amazonia. *Proceedings of the National Academy of Sciences,* 111: 10497-10502

Chamberlain, T.C. 1897. The Method of Multiple Working Hypotheses. *Journal of Geology,* 5: 837-848.

Chapman, S.B. 1964. The Ecology of Coom Rigg Moss, Northumberland: II. The Chemistry of Peat Profiles and theDevelopment of the Bog System. *Journal of Ecology*, 52: 315-321

Charman, D.J. 1992. Blanket mire formation at the Cross Lochs, Sutherland, northern Scotland. *Boreas*, 21: 53-72

Charman, D. 2002. *Peatlands and Environmental Change.* John Wiley and Sons: Chichester

Charman, D.J., Beilman, D.W., Blaauw, M., Booth, R.K., Brewer, S., Chambers, F.M., Christen, J.A, Gallego-Sala, A., Harrison, S.P., Hughes, P.D.M., Jackson, S.T., Korhola, A., Mauquoy, D., Mitchell, F.J.G., Prentice, I.C., van der Linden, M., De Vleeschouwer, F., Yu, Z.C., Alm, J., Bauer, I.E., Corish, Y.M.C., Garneau, M., Hohl, V., Huang, Y., Karofeld, E., Le Roux, G., Loisel, J., Moschen, R., Nichols, J.E., Nieminen, T.M., MacDonald, G.M., Phadtare, N.R., Rausch, N., Sillasoo, U., Swindles, G.T., Tuittila, E.-S., Ukonmaanaho, L., Väliranta, M., van Bellen, S., van Geel, B., Vitt, D.H., and Zhao, Y. 2013. Climate-related changes in peatland carbon accumulation during the last millennium. *Biogeosciences Discussions*, 9: 14327–14364

Chason, D.B., and Siegel, D.I. 1986. Hydraulic conductivity and related physical properties of peat, Lost River peatland, northern Minnesota. *Soil Science*, 142: 91-99

Chen, M. and Ma, L.Q. 2001. Comparison of Three Aqua Regia Digestion Methods for Twenty Florida Soils. *Soil Society of America Journal*, 65: 491–499

Clement, A.C., Seager, R., and Cane, M.A. 2000. Suppression of El Niño during the mid-Holocene by changes in the Earth's orbit. *Paleoceanography,* 15: 731-737.

Clement, C.R. 2006. Fruit trees and the transition to food production in Amazonia. In: Balee, W.L., and Erickson, C.L. (eds) *Time and Complexity in Historical Ecology: Studies in the Neotropical lowlands.* Columbia University Press: New York, 165-185

Clements, F.E. 1916. *Plant succession: an analysis of the development of vegetation*. Carnegie Institute of Washington Publication.

Clymo, R.S., Turunen, J., and Tolonen, K. 1998. Carbon accumulation in peatland. *Oikos,* 81: 368-388.

Coelho, C.B., and Esteves, L.M. 2008. Morfologia de esporos de pteridófitas do Parque Estadual das Fontes do Ipiranga (São Paulo, Brasil): 17-Pteridaceae. *Hoehnea*, 35: 91-98

Coffey, E.E.D., Froyd, C.A., and Willis, K.J. 2012. Lake or bog? Reconstructing baseline ecological conditions for the protected Galápagos Sphagnum peatbogs. *Quaternary Science Reviews*, 52: 60-74

Cohen, M.C.L., Behling, H., and Lara, R.J. 2005. Amazonian mangrove dynamics during the last millennium: The relative sea-level and the Little Ice Age. *Review of Palaeobotany and Palynology*, 136: 93-108

Cole, L.E.S., Bhagwat, S.A., and Willis, K.J. 2015. Long-term disturbance dynamics and resilience of tropical peat swamp forests. *Journal of Ecology*, 103: 16-30

Collins, J.L. 1951. Antiquity of the Pineapple in America. *Southwestern Journal of Anthropology*, 7: 145-155.

Colinvaux, P.A., and Schofield, E.K. 1976. Historical Ecology in the Galapagos Islands: II. A Holocene Spore Record from El Junco Lake, Isla San Cristobal. *Journal of Ecology,* 64: 1013-1028.

Colinvaux, P.A., Frost, M., Frost, I., Liu, K-B., & Steinitz-Kannan, M. 1988. Three Pollen Diagrams of Forest Disturbance in the Western Amazon Basin. *Review of Palaeobotany and Palynology,* 55: 73-81

Colinvaux, P.A., Bush, M.B., Steinitz-Kannan, M., & Miller, M.C. 1997. Glacial and Postglacial Pollen Records from the Ecuadorian Andes and Amazon. *Quaternary Research,* 48: 69-78

Colinvaux, P., De Oliveira, P.E., & Moreno, J.E. 1999. *Amazon Pollen Manual and Atlas.* Harwood: Amsterdam

Colinvaux, P.A., De Oliveira, P.E., Bush, M.B. 2000. Amazonian and neotropical plant communities on glacial time-scales: The failure of the aridity and refuge hypotheses. *Quaternary Science Reviews* 19: 141-169

Colinvaux, P.A., Irion, G., Räsänen, M.E., Bush, M.B., and Nunes de Mello, J.A.S. 2001. A paradigm to be discarded: Geological and palaeoecological data falsify the Haffer and Prance refuge hypothesis of Amazonian speciation. *Amazoniana,* 16: 609-646

Conroy, J.L., Restrepo, A., Overpeck, J.T., Steinitz-Kannan, M., Cole, J.E., Bush, M.B., and Colinvaux, P.A. 2009. Unprecedented recent warming of surface temperatures in the eastern tropical Pacific Ocean. *Nature Geoscience*, 2: 46-50.

Constantine, J.A., Dunne, T., Gay, H.P., and Kondolf, G.M. 2010. Controls on the alluviation of oxbow lakes by bed-material load along the Sacramento River, California. *Sedimentology*, 57: 389-407

Cooper, W.S. 1926. The Fundamentals of Vegetation Change. *Ecology*, 7: 391-413.

Correa-Metrio, A., Cabrera, K.R., and Bush, M.B. 2010. Quantifying ecological change through discriminant analysis: a paleoecological example from the Peruvian Amazon. *Journal of Vegetation Science,* 21: 695-704.

Cruz, F.W., Burns, S.J., Karmann, I., Sharp, W.D., Vuille, M., Cardoso, A.O., Ferrari, J.A., Dias, P.L.S., and Viana, O. 2005. Insolation-driven changes in atmospheric circulation over the past 116,000 years in subtropical Brazil. *Nature,* 434: 63-66.

Couvreur, T.L.P. 2011. Palms of the Lower Madidi River in northern Bolivia. *Palms*, 55: 37-45.

Curtis, J.H., Hodell, D.A., Brenner, M., 1996. Climate variability on the Yucatan Peninsula (Mexico) during the past 3500 years, and implication for Maya cultural evolution. *Quaternary Research,* 46: 37–47.

Curtis, J.H., Brenner, M., and Hodell, D.A. 1999. Climate change in the Lake Valencia Basin, Venezuela, ~12600 yr BP to present. *The Holocene*, 9: 609-619.

Curtis, J.T., and McIntosh, R.P. 1951. An upland forest continuum in the prairie-forest border region of Wisconsin. *Ecology*, 32: 476–496.

Couwenberg, J., Dommain, R., Joosten, H. 2010. Greenhouse gas fluxes from tropical peatlands in south-east Asia. *Global Change Biology,* 16: 1715-1732.

Dalby, A.P., Kumar, A., Moore, J.M., and Patterson, R.T. 2000. Preliminary survey of Arcellaceans (Thecamoebians) as limnological indicators in tropical Lake Sentani, Irian Jaya, Indonesia. *Journal of Foraminiferal Research*, 30: 135–142

Daly, D.C., Costa, D.P., & Melo, A.W.F. 2006. The 'salão' vegetation of Southwestern Amazonia. *Biodiversity and Conservation*, 15: 2905-2923.

Damman, A.W.H. 1978. Distribution and Movement of Elements in Ombrotrophic Peat Bogs. *Oikos,* 30: 480-495

D'Apolito, C., Absy, M.L., and Latrubesse, E.M. 2013. The Hill of Six Lakes revisited: new data and re-evaluation of a key Pleistocene Amazon site. *Quaternary Science Reviews*, 76: 140-155

Danielsen, F., Beukema, H., Burgess, N.D., Parish, F., Bruhl, C.A., Donald, P.F., Murdiyarso, D., Phalan, B., Reijnders, L., Struebig, M., and Fitzherbert, E.B. 2009. Biofuel Plantations on Forested Lands: Double Jeopardy for Biodiversity and Climate. *Conservation Biology,* 23: 348-358.

Dargie, G., Lewis, S., Lawson, I.T., Baird, A., Page, S., and Mitchard, E. 2012. Quantifying and understanding tropical peatland spatial distribution and carbon storage in Central Africa. *Proceedings of the 14th International Peat Congress, Stockholm.* http://www.peatsociety.org/document/quantifying-and-understranding-tropical-peatland-spatial-distribution-and-carbon-storage Accessed 28 May 2014

Davies, A.L., and Bunting, M.J. 2010. Applications of Palaeoecology in Conservation. *The Open Ecology Journal*, 3: 54-67

Davis, M.B. 2000. Palynology after Y2K – Understanding the Source Area of Pollen in Sediments. *Annual Review of Earth and Planetary Sciences*, 28: 1-18

De Granville, J.J. 1974. Aperçu sur la structure des pneumatophores de deux espèces des sols hydromorphes en Guyane. *Cahier O.R.S.T.O.M*, 23: 3-22

De Lima, N.E., Lima-Ribeiro, M.S, Tinoco, C.L., Terribile, L.C., & Collevatti, R.G. 2014. Phylogeography and ecological niche modelling, coupled with the fossil pollen record, unravel the demographic history of a Neotropical swamp palm through the Quaternary. *Journal of Biogeography,* 41: 673-686.

Demske, D., Tarasov, P.E., Nakagawa, T. 2013. Atlas of pollen, spores and further non-pollen palynomorphs recorded in the glacial-interglacial late Quaternary sediments of Lake Suigetsu, central Japan. *Quaternary International*, 290-291: 164-238.

De Oliveira, P.E., Barreto, A.M.F., and Suguio, K. 1999. Late Pleistocene/Holocene climatic and vegetational history of the Brazilian caatinga: the fossil dunes of the middle São Francisco River. *Palaeogeography, Palaeoclimatology, Palaeoecology*, 152: 319–337

De Oliveira, A.A., and Mori, S.A. 1999. A central Amazonian terra firme forest. I. High tree species richness on poor soils. *Biodiversity and Conservation*, 8: 1219–1244.

De Oliveira, S.M.B., Pessenda, L.C.R., Gouveia, S.E.M., Babinski, M., and Favaro, D.I.T. 2009. A geochemical and lead isotopic record from a small pond in a remote equatorial island, Fernando de Noronha, Brazil. *The Holocene*, 19: 439–448

De Toledo, M.B., and Bush, M.B. 2008. Vegetation and hydrology changes in Eastern Amazonia inferred from a pollen record. *Anais da Academia Brasileira de Ciências,* 80: 191-203

Denevan, W.M. 1996. A Bluff Model of Riverine Settlement in Prehistoric Amazonia. *Annals of the Association of American Geographers,* 86: 654-681.

Denevan, W.M. 1998. Comments on Prehistoric Agriculture in Amazonia. *Culture and Agriculture,* 20: 54-59.

Denevan, W.M. 2004. Semi-intensive Pre-European Cultivation and the Origins of Anthropogenic Dark Earths in Amazoniain. In: Glaser, B., and Woods, W.I. (eds) *Amazonian dark earths: explorations in space and time*. Berlin: Springer, 135-143

Denevan, W.M. 2006. Pre-European Forest Cultivation in Amazonia. In: Balée, W., and Erikson, C.L. (eds) *Time and Complexity in Historical Ecology: Studies in the Neotropical lowlands*. Columbia University Press: New York, 153-163

Dias Saba, M. 2007. *Morfologia polínica de Malvaceae: Implicações taxonômicas e filogeneticas.* Unpublished PhD thesis, Universidade stadual de Feira de Santana

Dommain, R., Couwenberg, J., and Joosten, H. 2010. Hydrological self-regulation of domed peatlands in south-east Asia and consequences for conservation and restoration. *Mires and Peat*, 6: 1-17

Dommain, R., Couwenberg, J., Glaser, P.H., Joosten, H., Suryadiputra, I.N.N. 2014. Carbon storage and release in Indonesian peatlands since the last deglaciation. *Quaternary Science Reviews*, 97: 1-32

Donald, A.M. 2003. The use of environmental scanning electron microscopy for imaging wet and insulating materials. *Nature Materials*, 2: 511-516.

Donders, T.H., Wagner-Cremer, F., and Visscher, H. 2008. Integration of proxy data and model scenarios for the mid-Holocene onset of modern ENSO variability. *Quaternary Science Reviews*, 27: 571-579

Douda, J., Doudová-Kochánková, J., Boublík, K., and Drašnarová, A. 2012. Plant species coexistence at local scale in temperate swamp forest: test of habitat heterogeneity hypothesis. *Oecologia*, 169: 523–534

Dransfield, J., Uhl, N.W., Asmussen, C.B., Baker, W.J., Harley, M.M., and Lewis, C.E. 2008. *Genera Palmarum: the Evolution and Classification of Palms.* RBG, Kew: London

Draper, F.C.H., Roucoux, K.H., Lawson, I.T., Mitchard, E.T.A., Honorio Coronado, E.N., Lahteenoja, O., Montenegro, L.T., Valderrama Sandoval, E., Zaráte, R., and Baker, T.R. 2014. The distribution and amount of carbon in the largest peatland complex in Amazonia. *Environmental Research Letters*, 9: 124017

Dufrene, M., and Legendre, P. 1997. Species Assemblages and Indicator Species: The Need for a Flexible Asymmetrical Approach. Ecological Monographs, 67: 345-366

Duivenvoorden, J.F. 1995. Tree species composition and rain forest environmental relationships in the middle Caquetá area, Colombia, North-western Amazonia. *Vegetatio*, 120: 91-113.

Dumont, J.F., Lamotte, S., Kahn, F. 1990. Wetland and upland forest ecosystems in Peruvian Amazonia: Plant species diversity in the light of some geological and botanical evidence. *Forest Ecology and Management*, 33/34: 125-139.

Dumont, J.F. 1993. Lake patterns as related to neotectonics in subsiding basins: the example of the Ucamara Depression, Peru. *Tectonophysics* 222: 69-78.

Dungait, J.A.J., Hopkins, D.W., Gregory, A.S., and Whitmore, A.P. 2012. Soil organic matter turnover is governed by accessibility not recalcitrance. *Global Change Biology*, 18: 1781-1796

Duque, A.J., Duivenvoorden, J.F., Cavelier, J., Sánchez, M., Polania, C., & León A. 2005. Ferns and Melastomataceae as Indicators of Vascular Plant Composition in Rain Forests of Colombian Amazonia. *Plant Ecology,* 178: 1-13.

Edwards, K.J. 1983. Quaternary palynology: multiple profile studies and pollen variability. *Progress in Physical Geography*, 7: 587-609

El-Daoushy, F. 1986. The value of ^{210}Pb in dating Scandinavian aquatic and peat deposits. *Radiocarbon*, 28: 1031-1040.

Endress, B.A., Horn, C.A., & Gilmore, M.P. 2013. *Mauritia flexuosa* palm swamps: Composition, structure and implications for conservation and management. *Forest Ecology and Management*, 302: 346-353.

Espinoza Villar, J.C., Guyot, J.L., Ronchail, J., Cochonneau, G., Naziano, F., Fraizy, P., Labat, D., de Oliveira, E., Ordonez, J.J., and Vauchel, P. 2009b. Contrasting regional discharge evolutions in the Amazon basin (1974-2004). Journal of Hydrology **375**: 297–311.

Espinoza Villar, J.C., Ronchail, J., Guyot, J.L., Cochonneau, G., Naziano, F., Lavado, W., de Oliveira, E., Pombosa, R., and Vauchel, P. 2009a. Spatio-temporal rainfall variability in the Amazon basin countries (Brazil, Peru, Bolivia, Colombia, and Ecuador). *International Journal of Climatology,* 29: 1574-1594.

Espinoza, J., Ronchail, J., Frappart, F., Lavado, W., Santini, W., and Guyot, J. 2013. The major floods in the Amazonas River and tributaries (Western Amazon basin) during the 1970 - 2012 period: A focus on the 2012 flood. *Journal of Hydrometeorology,* 14: 1000-1008

Esterle, J.S., 1990. *Trends in petrographic and chemical characteristics of tropical domed peats in Indonesia and Malaysia as analogues for coal formation*. PhD thesis, University of Kentucky.

Esterle, J.S., and Ferm, J.C. 1994. Spatial variability in modern tropical peat deposits from Sarawak, Malaysia and Sumatra, Indonesia: analogues for coal. *International Journal of Coal Geology,* 26: 1-41.

Esteves, L.M., and Coelho, C.B. 2007. Morfologia de esporos de pteridófitas do Parque Estadual das Fontes do Ipiranga (São Paulo, Brasil): Dennstaedtiaceae. *Hoehnea*, 34: 245-252

Faegri, K. and Iverson, J. 1989. Textbook of pollen analysis. John Wiley: Chichester, UK

Ferguson, K. 1986. Observations on the variation in pollen morphology of Palmae and its significance. *Canadian Journal of Botany*, 64: 3079-3090.

Ferraz-Vincentini, K.R., and Salgado-Labouriau, M.L. 1996. Palynological analysis of a palm swamp in Central Brazil. *Journal of South American Earth Sciences,* 9: 207-219.

Ferreira, L.V. and Prance, G.T. 1998. Structure and species richness of low-diversity floodplain forest on the Rio Tapajós, Eastern Amazonia, Brazil. *Biodiversity and Conservation,* 7: 585-596

Ferreira, L.V. 1997. Effects of the duration of flooding on species richness and floristic composition in three hectares in the Jaú National Park in floodplain forests in central Amazonia. *Biodiversity and Conservation,* 6: 1353-1363.

Ferreira, L.V., and Stohlgren, T.J. 1999. Effects of River Level Fluctuation on Plant Species Richness, Diversity, and Distribution in a Floodplain Forest in Central Amazonia. *Oecologia,* 120: 582-587.

Figuerido, J., Hoorn, C., van der Ven, P., and Soares, E. 2009. Late Miocene onset of the Amazon River and the Amazon deep-sea fan: Evidence from the Foz do Amazonas Basin. *Geology,* 37: 619-622.

Fine, P.V.A., García-Villacorta, R., Pitman, N.C.A., Mesones, I., and Kembel, S.W. 2010. A Floristic Study of the White-Sand Forests of Peru. *Annals of the Missouri Botanical Garden*, 97: 283-305

Finer, M., Jenkins, C.N., and Powers, J.B. 2013.Potential of Best Practice to Reduce Impacts from Oil and Gas Projects in the Amazon. PLoS ONE, 8: e63022.

Finsinger, W., and Tinner, W. 2005. Minimum count sums for charcoal concentration estimates in pollen slides: accuracy and potential errors. *The Holocene,* 15: 293-297

Flenley, J.R., King, A.S.M, Jackson, J., Chew, C., Teller, J.T., & Prentice, M.E. 1991. The late Quaternary vegetational and climatic history of Easter Island. *Journal of Quaternary Science,* 6: 85-115.

Foster, R.B. 1990. The Floristic Composition of the Rio Manu Floodplain Forest. In: Gentry A.H. (ed.) *Four Neotropical Rain Forests*. Yale University Press: London, 99-111

Foster, D.R. and Wright, H.E. 1990. Role of Ecosystem Development and Climate Change in Bog Formation in Central Sweden. *Ecology*, 71: 450-463

Fox, J. 2002. *Linear Mixed Models.* http://cran.r-project.org/doc/contrib/FoxCompanion/appendix-mixed-models.pdf (accessed December 2014).

Fraysse F, Pokrovsky O.S, Schott J, and Meunier J-D. 2009. Surface chemistry and reactivity of plant phytoliths in aqueous solutions. *Chemical Geology,* 258: 197-206.

Frodeman, R. 1995. Geological reasoning: Geology as an interpretive and historical science. *Geological Society of America Bulletin*, 107: 960-968.

Frolking, S., Roulet, N.T., Tuittila, E., Bubier, J.L., Quillet, A., Talbot, J., & Richards, P.J.H. 2010. A new model of Holocene peatland net primary production, decomposition, water balance, and peat accumulation. *Earth System Dynamics,* 1: 1-21

Frost, I. 1988. A Holocene Sedimentary Record from Anañgucocha in the Ecuadorian Amazon. *Ecology,* 69: 66-73.

Froyd, C.A. and Willis, K.J. 2008. Emerging issues in biodiversity & conservation management: The need for a palaeoecological perspective. *Quaternary Science Reviews*, 27: 1723-1732

Furch, K., and Junk,W.J. 1997. Physicochemical conditions in floodplains. In: Junk, W.J. (ed.), *The central Amazon floodplain: ecology of a pulsing system.* Springer: Berlin, 69–108.

Futymar, P., and Miller, N.G. 1986. Stratigraphy and genesis of the Lake Sixteen peatland, northern Michigan. *Canadian Journal of Botany,* 64: 3008-3019

Gagan, M.K., Hendy, E.J., Haberle, S.G., Hantaro, W.S. 2004. Post-glacial evolution of the Indo-Pacific Warm Pool and El Niño-Southern oscillation. *Quaternary International,* 118–119: 127–143

García, N.O. 1994. South American Climatology. *Quaternary International*, 21: 7-27

Gastony, G.T. 1974. Spore Morphology in the Cyatheaceae. I. The Perine and Sporangial Capacity: GeneralConsiderations. *American Journal of Botany,* 61: 672-680.

Gastony, G.J. and Tryon, R.M. 1976. Spore morphology in the Cyatheaceae. II. The Genera Lophosoria, Metaxya, Sphaeropteris, Alsophila and Nephelea. *American Journal of Botany,* 63: 738-758.

Gay, G.R., Gay, H.H., Gay, W.H., Martinson, H.A., Meade, R.H., and Moody, J.A. 1998. Evolution of cutoffs across meander necks in Powder River, Montana, USA. *Earth Surface Processes and Landforms*, 23: 651–662

Gentry, A.H. 1993. *A Field Guide to the Families and Genera of Woody Plants of Northwest South America (Colombia, Ecuador, Peru) with Supplementary Notes on Herbaceous Taxa*. London: University of Chicago Press.

Gentry, A.H., & Dodson, C. 1987. Contribution of Nontrees to Species Richness of a Tropical Rain Forest. *Biotropica,* 19: 149-156.

Gentry, A.H. and Tomb, A.S. 1979. Taxonomic Implications of Bignoniaceae Palynology. *Annals of the Missouri Botanical Garden*, 66: 756-777

Gibbard, P.L., Head, M.J., Walker, M.J.C., and the Subcommission on Quaternary Stratigraphy. 2010. Formal ratification of the Quaternary System/ Period and the Pleistocene Series/Epoch with a base at 2.58 Ma. *Journal of Quaternary Science*, 25: 96-102

Gibernau, M. 2003. Pollinators and Visitors of Aroid Inflorescences. *Aroideana*, 26: 73-91

Giudice, G.E., Morbelli, M.A., Piñeiro, M.R., Copello, M., and Erra, G. 2004. Spore Morphology of the Polypodiaceae from Northwestern Argentina. *American Fern Journal*, 94: 9-27

Glaser, P.H., Hansen, B.C.S., Siegel, D.I., Reeve, A.S., and Morin, P.J. 2004. Rates, pathways and drivers for peatland development in the Hudson Bay Lowlands, northern Ontario, Canada. *Journal of Ecology*, 92: 1036-1053.

Gleason, H.A. 1917. The Structure and Development of the plant association. *Bulletin of the Torrey Botanical Club* 44, 463-481.

Glenn-Lewin, P.C., Peet, R.K., and Éblen, T.T. 1992. Prologue. In: Glenn-Lewin, P.C., Peet, R.K., and Éblen, T.T. (eds) *Plant succession: Theory and prediction.* Chapman and Hall: London, 1-10.

Gloor, M., Brienen, R.J.W., Galbraith, D., Feldpausch, T.R., Schöngart, J., Guyot, J.-L., Espinoza, J.C., Lloyd, J., and Phillips, O.L. 2013. Intensification of the Amazon hydrological cycle over the last two decades. *Geophysical Research Letters*, 40: 1729-1733.

Goosse, H., Crespin, E., Dubinkina, S., Loutre, M-F., Mann, M.E., Renssen, H., Sallaz-Damaz, Y., and Shindell, D. 2012. The role of forcing and internal dynamics in explaining the ''Medieval Climate Anomaly''. *Climate Dynamics*, 39: 2847–2866

Gordon, A.D., and Birks, H.J.B. 1972. Numerical methods in Quaternary palaeoecology. *New Phytologist,* 71: 961-979.

Gosling, W.D., Mayle, F.E., Tate, N.J., & Killeen, T.J. 2009. Differentiation between Neotropical rainforest dry forest and savannah ecosystems by their modern pollen spectra and implications for the fossil pollen record. *Review of Palaeobotany and Palynology,* 153: 70-85

Gosling, W.D., Mayle, F.E., Tate, N.J. & Killeen, T.J. 2005. Modern pollen-rain characteristics of tall terra firme moist evergreen forest, southern Amazonia. *Quaternary Research,* 64: 284-297

Graham, N.E., Ammann, C.M., Fleitmann, D., Cobb, K.M., and Luterbacher, J. 2011. Support for global climate reorganization during the ''Medieval Climate Anomaly''. *Climate Dynamics*, 37: 1217–1245

Granath, G., Strengbom, J., and Rydin, H. Rapid ecosystem shifts in peatlands: linking plant physiology and succession. *Ecology*, 91: 3047-3056

Grimm, E.C. 1987. CONISS: a FORTRAN 77 program for stratigraphically constrained cluster analysis by the method of incremental sum of squares. *Computers & Geosciences*, 13: 13-35

Gupta, A. 2011. *Tropical Geomorphology.* Cambridge University Press: Cambridge

Gutiérrez, D., Sifeddine, A., Field, D.B., Ortlieb, L., Vargas, G., Chávez, F.P., Velazco, F., Ferreira, V., Tapia, P., Salvatteci, R., Boucher, H., Morales, M.C., Valdés, J., Reyss, J.-L., Campusano, A., Boussafir, M., Mandeng-Yogo, M., García, M., and Baumgartner, T. 2009. Rapid reorganization in ocean biogeochemistry off Peru towards the end of the Little Ice Age. *Biogeosciences*, 6: 835-848

Guyot, J.L., Jouanneau, J.M., Soarea, L., Boaventura, G.R., Maillet, N., and Lagane, C. 2007. Clay mineral composition of river sediments in the Amazon Basin. *Catena* 71, 340-356.

Haberle, S. 1997. Upper Quaternary Vegetation and Climate History of the Amazon Basin: Correlating Marine and Terrestrial Pollen Records. In: Flood, R.D., Piper, D.J.W., Klaus, A., and Peterson, L.C. (eds.) *Proceedings of the Ocean Drilling Program, Scientific Results, Vol. 155.* College Station, TX (Ocean Drilling Program), 382-396

Hansen, B.C.S, Rodbell, D.T., Seltzer, G.O., Leo, B., Young, K.R., Abbott, M. 2003. Late-glacial and Holocene vegetational history from two sites in the western Cordillera of southwestern Ecuador. *Palaeogeography, Palaeoclimatology, Palaeoecology,* 194: 79-108.

Haselhorst, D.S., Moreno, J.E., and Punyasena, S.W. 2013. Variability within the 10-Year Pollen Rain of a Seasonal Neotropical Forest and Its Implications for Paleoenvironmental and Phenological Research. PLoS ONE, 8: e53485.

Haug, G.H., Hughen, K.A., Sigman, D.M., Peterson, L.C., and Röhl, U. 2001. Southward Migration of the Intertropical Convergence Zone Through the Holocene. *Science,* 293: 1304-1308.

Hasseldonckx P. 1977. The Palynology of a Holocene Marginal Peat Swamp Environment in Johore, Malaysia. *Review of Palaeobotany and Palynology,* 24: 227-238.

Hatfield, R.G., and Stoner, J.S. 2013. Magnetic Proxies and Susceptibility. In: Elias, S.A. (ed.) *The Encyclopedia of Quaternary Science, vol. 2.* Amsterdam: Elsevier, 884-898.

Heckenberger, M.J., Kuikaro, A., Kuikaro, U.T., Russell, J.C., Schmidt, M., Fausto, C., Franchetto, B. 2003. Amazonia 1492: Pristine Forest or Cultural Parkland? *Science,* 301: 1710-1714

Heckenberger, M.J., Petersen, J.B., and Neves, E.G. 1999. Size and Permanence in Amazonia: Two Archaeological Examples from Brazil. *Latin American Antiquity,* 10: 353-376.

Heinselman, M.L. 1963. Forest Sites, Bog Processes, and Peatland Types in the Glacial Lake Agassiz Region, Minnesota. *Ecological Monographs* 33: 327-374.

Heinselman, M.L. 1970. Landscape Evolution, Peatland Types, and the Environment in the Lake Agassiz PeatlandsNatural Area, Minnesota. *Ecological Monographs*, 40: 235-261

Heiri, O., Lotter, A.F., and Lemcke, G. 2001. Loss on ignition as a method for estimating organic and carbonate content in sediments: reproducibility and comparability of results. *Journal of Paleolimnology*, 25: 101-110

Helama, S., Meriläinen, J., and Tuomenvirta, H. 2009. Multicentennial megadrought in northern Europe coincided with a global El Niño–Southern Oscillation drought pattern during the Medieval Climate Anomaly. *Geology*, 37: 175-178

Hendricks, M.R. 2010. *Introduction to physical hydrology.* Oxford University Press: Oxford

Hendy, E.J., Gagan, M.K., Alibert, C.A., McCulloch, M.T., Lough, J.M., and Isdale, P.J. 2002. Abrupt Decrease in Tropical Pacific Sea Surface Salinity at End of Little Ice Age. *Science*, 295: 1511-1514

Hickin, G.C., and Nanson, E.J. 1986. A statistical analysis of bank erosion and channel migration in western Canada. *Geological Society of America Bulletin*, 97: 497-504

Higgins, M.A., Ruokolainen, K., Tuomisto, H., Llerena, N., Cardenas, G., Phillips, O.L., Vásquez, R., Phillips, O.L., and Räsänen, M. 2011. Geological control of floristic composition in Amazonian forests. *Journal of Biogeography,* 38, 2136-2149.

Hilker, T., Lyapustin, A.I., Tucker, C.J., Hall, F.G., Myeni, R.B., Wang, Y., Bi, J., de Moura, Y.M., and Sellers, P.J. 2014. Vegetation dynamics and rainfall sensitivity of the Amazon. Proceedings of the National Academy of Sciences, 111: 16041–16046

Hill, T.R. 1996. Statistical Determination of Sample Size and Contemporary Pollen Counts, Natal Drackensberg, South Africa. *Grana,* 35: 119-124.

Hill, M.O., and Gauch, H.G. 1980. Detrended correspondence analysis: An improved ordination technique. *Vegetatio*, 42: 47-58

Hill, M.O. 1979. *TWINSPAN: a FORTRAN program for arranging multivariate data in an ordered two-way table by classifi- cation of the individuals and attributes*. Cornell University: New York

Hillen, R. 1984. Palynology of late quaternary sediments from various tropical lowland depositional environment. In: Bartstra, G-J., and Casparie, W.A. (eds), *Modern Quaternary Research in Southeast Asia 8.* Balkema: Rotterdam, 49-60

Hirano, T., Kusin, K., Limin, S., and Osaki, M. 2014. Evapotranspiration of tropical peat swamp forests. *Global Change Biology*, DOI: 10.1111/gcb.12653

Hobbs, N.B. 1986. Mire morphology and the properties and behaviour of some British and foreign peats. *Quarterly Journal of Engineering Geology and Hydrogeology,* 19: 7–80.

Hongve, D., and Erlandsen, A.H. 1979. Shortening of surface sediment cores during sampling. *Hydrobiologia*, 65: 283-287.

Hope, G., Chokkalingam, U., and Anwar, S. 2005. The stratigraphy and fire history of the Kutai Peatlands, Kalimantan, Indonesia. *Quaternary Research,* 64: 407-417.

Hoekman, D.H. 2007. Satellite radar observation of tropical peat swamp forest as a tool for hydrological modelling and environmental protection. *Aquatic conservation: marine and freshwater ecosystems,* 17: 265–275.

Hogg, A.G., Hua, Q. Blackwell. P.G., Niu, M., Buck, C.E., Guilderson, T.P., Heaton, T.J., Palmer, J.G., Reimer, P.J., Reimer, R.W., Turney, C.S.M., and Zimmerman, S.R.H. 2013a. SHCAL13 Southern Hemisphere calibration, 0–50,000 years cal BP. *Radiocarbon*, 55: 1889-1903.

Hogg, A., Turney, C., Palmer, J., Cook, E., and Buckley, B. 2013b. Is there any evidence for regional atmospheric 14C offsets in the southern hemisphere? *Radiocarbon*, 55: 1-6.

Holden, J., and Burt, T.P. 2002. Piping and pipeflow in a deep peat catchment. *Catena,* 48: 163–199.

Holden, J., Chapman, P.J., Labadz, J.C. 2004. Artificial drainage of peatlands: hydrological and hydrochemical process and wetland restoration. *Progress in Physical Geography*, 28: 95-123.

Holden, J. 2006. Peatland Hydrology. In: Martini, I.P., Martínez Cortizas, A., and Chesworth, W. (eds). *Peatlands: Evolution and records of environmental and climate changes.* London: Elsevier, 319-346.

Honorio Coronado, E.N., Dexter, K., Poelchau, M.F., Hollingsworth, P.M., Phillips, O.L., and Pennington, R.T. 2014. Ficus insipida subsp. insipida (Moraceae) reveals the role of ecology in the phylogeography of widespread Neotropical rain forest tree species. *Biogeography*. DOI:10.1111/jbi.12326

Honorio Coronado, E.N., Pennington, T.R., Freitas, L.A., Nebel, G., and Baker, T.R. 2008. Analysis of the floristic composition of the forests of Jenaro Herrera, Loreto, Peru. *Revista Peruana de Biología,* 15: 53-60

Hooijer, A., Page, S., Canadell, J.G., Silvius, M., Kwadijk, J., Wösten, H., and Jauhiainen, J. 2010. Current and future CO_2 emissions from drained peatlands in Southeast Asia. *Biogeosciences*, **7**: 1505–1514.

Householder, J.E., Janovec, J.P., Tobler, M.W., Page, S., and Lähteenoja, O. 2012. Peatlands of the Madre de Dios River of Peru: distribution, geomorphology, and habitat diversity . *Wetlands*, 32: 359–368.

Hoorn, C. 1993. Marine incursions and the influence of Andean tectonics on the Miocene depositional history of northwestern Amazonia: results of a palynostratigraphic study. *Palaeogeography Palaeoclimatology Palaeoecology,* 105: 267-309.

Hoorn, C. 1994. An environmental reconstruction of the palaeo-Amazon River system (Middle-Late Miocene, NW Amazonia). *Palaeogeography Palaeoclimatology Palaeoecology,* 112: 187-238

Hoorn, C., Guerrero, J., Sarmiento, G.A., and Lorente, M.A. 1995. Andean tectonics as a cause for changing drainage patterns in Miocene northern South America. *Geology,* 23: 237-240.

Hope, G., Chokkalingam, U., Anwar, S. 2005. The stratigraphy and fire history of the Kutai Peatlands, Kalimantan, Indonesia. *Quaternary Research* 64, 407-417.

Horbe, A.M.C., Behling, H., Nogueira, A.C.R, and Mapes, R. 2011. Environmental changes in the western Amazônia: morphological framework, geochemistry, palynology and radiocarbon dating data. *Anais da Academia Brasileira de Ciências,* 83: 863-874.

Horn, S.P., and Ramirez, W.B. 1990. On the Occurrence of Ficus Pollen in Neotropical Quaternary Sediments. *Palynology*, 14: 3-6.

Hou, X., and Jones, B.T. 2000. Inductively Coupled Plasma/Optical Emission Spectrometry. In: Meyers, R.A. (ed.). *Encyclopedia of Analytical Chemistry*. John Wiley & Sons: Chichester, 9468-9485

Householder, J.E., Janovec, J.P., Tobler, M.W., Page, S., and Lähteenoja, O. 2012. Peatlands of the Madre de Dios River of Peru: Distribution, Geomorphology, and Habitat Diversity. *Wetlands,* 32: 359-368.

Hovenkamp, P.H., and Miyamoto, F. 2005. A conspectus of the native and naturalized species of Nephrolepis (nephrolepidaceae) in the world. *Blumea,* 50: 279-322

Hoyos-Santillan, J. 2014. *Controls of Carbon Turnover in Tropical Peatlands.* Unpublished PhD thesis, University of Nottingham.

Hu, F.S., and Davis, R.B. 1995. Postglacial development of a Maine bog and paleoenvironmental implications. *Canadian Journal of Botany*, 73: 638-649

Hubbell, S.P., He, F., Condit, R., Borda-de-Agua, L., Kellner, J., & ter Steege, H. 2008. How many tree species are there in the Amazon and how many of them will go extinct? Proceedings of the National Academy of Sciences, 105: 11499-11504

Hughes, P.D.M, and Barber, K.E. 2003. Mire development across the fen–bog transition on the Teifi floodplain at Tregaron Bog, Ceredigion, Wales, and a comparison with 13 other raised bogs. *Journal of Ecology*, 91: 253-264

Hughes, P.D.M., and Dumayne-Peaty, L. 2002. Testing theories of mire development using multiple successions at Crymlyn Bog, West Glamorgan, South Wales, UK. *Journal of Ecology*, 90: 456–471

Hvorslev, M.J. 1951. Time Lag and Soil Permeability in Groundwater Observations. Waterways Experimental Station Bulletin 36, United States Army Corps of Engineers, Mississippi, USA.

Ineson, S. and Scaife. A.A. 2009. The role of the stratosphere in the European climate response to El Niño. *Nature Geoscience*, 2: 32-36

Ireland, A.W., and Booth, R.K. 2011. Hydroclimatic variability drives episodic expansion of a floating peat mat in a North American kettlehole basin. *Ecology,* 92: 11-18.

Ireland, A.W., Booth, R.K., Hotchkiss, S.C., and Schmitz, J.E. 2012. Drought as a Trigger for Rapid State Shifts in Kettle Ecosystems: Implications for Ecosystem Responses to Climate Change. *Wetlands*, 32:989-1000.

Ireland, A.W., Booth, R.K., Hotchkiss, S.C., and Schmitz, J.E. 2013. A comparative study of within-basin and regional peatland developmet: implications for peatland carbon dynamics. *Quaternary Science Reviews*, 61: 85-95.

Iriarte, J., Power, M.J., Rostain, S., Mayle, F.E., Jones, H., Watling, J., Whitney, B.S., McKey, D., 2012. Fire-free land use in pre-1492 Amazonian savannas. Proceedings of the National Academy of Sciences, 109: 6473-6478

Irion, G., Müller, J., Nunes de Mello, J., Junk, W.J. 1995. Quaternary geology of the Amazonian lowland. *Geo-Marine Letters,* 15: 172-178.

Irion, G, Junk, W.J., and de Mello, J.A.S.N. 1997. The Large Central Amazonian River Floodplains Near Manaus: Geological, Climatological, Hydrological, and Geomorphological Aspects. In: Junk, W.J. (ed). *The Central Amazon Floodplain: Ecology of a Pulsing System*. Springer: Berlin, 23-46

Irion, G., Bush, M.B., de Mello, J.A.N., Stüben, D., Neumann, T., Müller, G., Morais, J.O., and Junk, J.W. 2006. A multiproxy palaeoecological record of Holocene lake sediments from the Rio Tapajós, eastern Amazonia. *Palaeogeography, Palaeoclimatology, Palaeoecology*, 240: 523-535

Jaenicke, J., Rieley, J.O., Mott, C., Kimman, P., and Siegert, F. 2008. Determination of the amount of carbon stored in Indonesian peatlands. *Geoderma*, 147: 151-158.

Jaenicke, J., Wösten, H. Budiman, A. and Siegert, F. 2010. Planning hydrological restoration of peatlands in Indonesia to mitigate carbon dioxide emissions. *Mitigation and Adaptation Strategies for Global Change*, 15: 223-239

Jantz, N., and Behling, H. 2012. A Holocene environmental record reflecting vegetation, climate, and fire variability at the Páramo of Quimsacocha, southwestern Ecuadorian Andes. *Vegetation History and Archaeobotany*, 21: 169-185.

Jarosz, S.C. 2011.*The vegetation history of a tropical coastal peatland, southern Belize, in relation to plant succession and climatic influences: a pollen study*. Unpublished BSc thesis, Edinburgh.

Johnson E.A. and Miyanishi K. 2008. Testing assumptions of chronosequences in succession. *Ecology Letters,* 11: 419-431.

Jones, T.D., Lawson, I.T., Reed, J.M., Wilson, G.P., Leng, M. J., Gierga, M., Bernasconi, S.M., Smittenberg, R.H., Hajdas, I., Bryant, C.L., and Tzedakis, P. C. 2013. Diatom-inferred late Pleistocene and Holocene palaeolimnological changes in the Ioannina basin, northwest Greece. *Journal of Paleolimnology*, 49: 185-204

Jowsey, P.C. 1966. An Improved Peat Sampler. *New Phytologist*, 65: 245-248

Junk, W.J. 1983. Aquatic habitats in Amazonia. *Environmentalist,* 3: 24-34.

Kaandorp, R.J.G., Vonhof, H.B., Wesselingh, F.P., Pittman, L.R., Kroon, D., and van Hinte, J.E. 2005. Seasonal Amazonian rainfall variation in the Miocene Climate Optimum. *Palaeoegeography, Palaeoclimatology, Palaeoecology, 221: 1-6*

Kahn F. 1988. Ecology of Economically Important Palms in Peruvian Amazonia. *Advances in Economic Botany* 6: 42-49.

Kahn, F. & Mejia, K. 1990. Palm communities in wetland forest ecosystems of Peruvian Amazonia. *Forest Ecology & Management,* 33/44: 169-179

Kahn, F. and Moussa, F. 1994. Diversity and conservation status of Peruvian palms. *Biodiversity and Conservation*, 3: 227-241.

Kalliola, R., and Paitan, S.F. 1998. Presentación del estudio. *Annales Universitatis Turkuensis Ser A II,* 114: 11-15.

Kalliola, R., Salo, J., Puhakka, M., and Marjut, R. 1991. New Site Formation and Colonizing Vegetation in Primary Succession on the Western Amazon Floodplains. *Journal of Ecology*, 79: 877-901.

Keimowitz, A.R., Parisio, S., Adams, M.S., Interlichia, K., Halton, C., Kroenke, S., and Hubert, A. 2013. Identification of Ombrotrophic Bogs in the Catskill Mountains, NY by Geochemical and Isotopic Methods. *Wetlands*, 33: 355–364

Killeen, T.J., and Solórzano, L.A. 2008. Conservation strategies to mitigate impacts from climate change in Amazonia. *Philosophical Transactions of the Royal Society of London B,* 363: 1881–1888

Kirkham, D. 1945. Proposed method for field measurement of permeability of soil below the watertable. *Soil Science Society of America Proceedings*, 10: 58–68.

Klinger, L.F. 1996. The Myth of the Classic Hydrosere Model of Bog Succession. *Arctic and Alpine Research,* 28: 1-9

Koh, L.P., Miettinen, J., Liew, S.C., and Ghazoul, J. 2011. Remotely sensed evidence of tropical peatland conversion to oil palm. *Proceedings of the National Academy of Sciences,* 108: 5127-5132

Klute, A. 1965. Laboratory measurements of hydraulic conductivity of saturated soil. In Methods of Soil Analysis. Part 1: Physical and Mineralogical Properties, Black CA (ed.). American Society of Agronomy and Soil Science Society of America: Madison, WI; 210–221.

Knudsen, J.T., Tollsten, L., and Ervik, F. 2001.Flower Scent and Pollination in Selected Neotropical Palms. *Plant biology*, 3: 642-653

Kratz, T.K., and DeWitt, C.B. 1986. Internal Factors Controlling Peatland-Lake Ecosystem Development. *Ecology*, 67: 100-107.

Kubitzki, K. 1989. The ecogeographical differentiation of Amazonian inundation forests. *Plant Systematics and Evolution*, 162: 285-304.

Kuhry, P. 1988. Palaeobotanical-palaeoecological studies of tropical high Andean peatbog sections (Cordillera Oriental, Colombia). J. Cramer: Berlin. 241 pp.

Kuhry, P. and Vitt, D.H. 1996. Fossil Carbon/Nitrogen Ratios as a Measure of Peat Decomposition. *Ecology*, 77: 271-275.

Kvist, L.P., and Nebel, G. 2001. A review of Peruvian flood plain forests: ecosystems, inhabitants and resource use. *Forest Ecology and Management*, 150: 3-26

Lacourse, T., Mathewes, R.W., and Fedje, D.W. 2003. Paleoecology of late-glacial terrestrial deposits with in situ conifers from the submerged continental shelf of western Canada. *Quaternary Research*, 60:180-188.

Lähteenoja, O. 2011. *Carbon Dynamics and Ecosystem Diversity of Amazonian Peatlands*. Unpublished PhD thesis, University of Turku

Lähteenoja, O., Flores, B., and Nelson, B. 2013. Tropical Peat Accumulation in Central Amazonia. *Wetlands*, 33: 495-503.

Lähteenoja, O., and Page, S. 2011. High diversity of tropical peatland ecosystem types in the Pastaza-Marañón basin, Peruvian Amazonia. *Journal of Geophysical Research*, 116: G02025.

Lähteenoja, O., Reátegui, Y.R., Räsänen, M., Torres, D.D., Oinonen, M., and Page, S. 2012. The large Amazonian peatland carbon sink in the subsiding Pastaza-Marañón foreland basin, Peru. *Global Change Biology*, 18: 164–178.

Lähteenoja, O., and Roucoux, K.H. 2010. Inception, history and development of peatlands in the Amazon Basin. *PAGES news*, 18: 27-29

Lähteenoja, O., Ruokolainen, K., Schulman, L., and Oinonen, M. 2009a. Amazonian peatlands: an ignored C sink and potential source. *Global Change Biology,* 15: 2311–2320.

Lähteenoja, O., Ruokolainen, K., Schulman, L., and Alvarez, J. 2009b. Amazonian floodplains harbour minerotrophic and ombrotrophic peatlands. *Catena,* 79: 140–145.

Lamotte, S. 1990. Fluvial dynamics and succession in the Lower Ucayali River basin, Peruvian Amazonia. *Forest Ecology and Management*, 33/34: 141-156

Lapen, D.R., Price, J.S., and Gilbert, R. 2005. Modelling two-dimensional steady-state groundwater flow and flow sensitivity to boundary conditions in blanket peat complexes. *Hydrological Processes,* 19: 371–386.

Laurence, D.M., and Slater. A.G. 2008. Incorporating organic soil into a global climate model. *Climate Dynamics*, 30: 145-160

Lavigne, F., Degeai, J-P., Komorowski, J-C., Guillet, S., Robert, V., Lahitte, P., Oppenheimer, C., Stoffel, M., Vidal, C.M., Surono, Pratomo, I., Wassmer, P., Hajdas, I., Hadmoko, D.S., and de Belizal, E. 2013. Source of the great A.D. 1257 mystery eruption unveiled, Samalas volcano, Rinjani Volcanic Complex, Indonesia. *Proceedings of the National Academy of Sciences,* 110: 16742–16747

Lavoie, M., Pellerin, S., Larocque, M. 2013. Examining the role of allogenous and autogenous factors in the long-term dynamics of a temperate headwater peatland (southern Québec, Canada). *Palaeogeography, Palaeoclimatology, Palaeoecology* 386: 336-348

Lawson, I.T. 2001. *The Late Glacial and Holocene environmental history of Greece*. Unpublished PhD Thesis, University of Cambridge.

Lawson, I.T., Jones, T.D., Kelly T.J., Honorio Coronado, E.N., & Roucoux, K.H. 2014. The geochemistry of Amazonian peats. *Wetlands.* DOI: 10.1007/s13157-014-0552-z

Lawson, I.T., Kelly, T.J., Aplin, P., Boom, A., Dargie, G., Draper, F.C.H., Hassan, P.N.Z.B.P., Kaduk, J., Large, D., Murphy, W., Page, S.E., Roucoux, K.H., Sjögersten, S., Tansey, K., Waldram, M., & Wedeux, B.M.M. 2015. Improving estimates of tropical peatland area, carbon storage, and greenhouse gas fluxes. *Wetlands Ecology and Management.* DOI: 10.1007/s11273-014-9402-2

Ledru, M-P., Bertaux, J., and Sifeddine, A. 1998. Absence of Last Glacial Maximum Records in Lowland Tropical Forests. *Quaternary Research*, 49: 233–237

Ledru, M-P. 2002. Late Quaternary History and Evolution of the Cerrados as Revealed by Palynological Records. In: Oliveira, P.S., and Marquis, R.J. (eds) *The Cerrados of Brazil: Ecology and Natural History of a Neotropical Savanna.* Columbia University Press: New York, 33-50

Ledru, M-P., Samaniego, P., Vuille, M., Hidalgo, S., Herrera, M., and Ceron, C. 2013. The Medieval Climate Anomaly and the Little Ice Age in the eastern Ecuadorian Andes. *Climate of the Past*, 9: 307–321

Le Roux, G., and Marshall, W.A. 2011. Constructing recent peat accumulation chronologies using atmospheric fall-out radionuclides. *Mires and Peat*, 7(8): 1-14

Lewis, C., Albertson, J., Xu, X., and Kiely, G. 2012. Spatial variability of hydraulic conductivity and bulk density along a blanket peatland hillslope. *Hydrological Processes*, 26: 1527–1537.

Lewis, S.L, Phillips, O.L, Baker, T.R, Lloyd, J., Malhi, Y., Almeida, S., Higuchi, N., Laurance, W.F., Neill, D.A., Silva, J.N.M., Terborgh, J., Lezama, A.T., Marinez, R.V., Brown, S., Chave, J., Kuebler, C., Vargas, P.N., & Vincetti, B. 2004. Concerted changes in tropical forest structure and dynamics: evidence from 50 South American long-term plots. *Philosophical Transactions of the Royal Society of London B,* 359: 421-436

Li, W., Dickinson, R.E., Fu, R., Niu, G-Y., Yang, Z-L., and Canadell, J.G. 2007. Future precipitation changes and their implications for tropical peatlands. *Geophysical Research Letters,* 34:L01403.

Liu, K-B. & Colinvaux, P.A. 1988. A 5200-year history of Amazon rain forest. *Journal of Biogeography*, 15: 231-248

Ljungqvist, F.C. 2010. A new reconstruction of temperature variability in the extra-tropical Northern Hemisphere during the last two millennia. *Geografiska Annaler*, 92 A: 339‑351.

Lotter, A.F., Ammann, B., and Sturm, M. 1992. Rates of change and chronological problems during the late-glacial period. *Climate Dynamics,* 6: 233-239.

Lowe and Walker 1997

Lowe, J.J., and Walker, M.J.C. 1997. Reconstructing Quaternary Environments (2nd Edition). Prentice Hall: Harlow, England

Macía, M.J. 2004. Multiplicity in palm uses by the Huaorani of Amazonian Ecuador. *Botanical Journal of the Linnean Society*, 144: 149-159.

MacKenzie, A.B., Logan, E.M., Cook, G.T., and Pulford, I.D. 1998. Distributions, inventories and isotopic composition of lead in 210Pb-dated peat cores from contrasting biogeochemical environments: Implications for lead mobility. *The Science of the Total Environment,* 223: 25-35

Madanes, N., and Dadon, J.R. 1998. Assessment of the minimum sample size required to characterize site-scale airborne pollen. *Grana*, 37: 239-245

Maher, L.J. 1972. Nomograms for computing 0.95 confidence limits of pollen data. *Review of Palaeobotany and Palynology*, 13: 85-93

Mäkelä, E.M. 1996. Size distinctions between Betula pollen types – A review. *Grana,* 35: 248-256.

Makou, M.C., Eglinton, T.I., Oppo, D.W., and Hughen, K.A. 2010. Postglacial changes in El Niño and La Niña behaviour. *Geology* 38: 43-46.

Malhi, Y., Roberts, J.T., Betts, R.A., Killeen, T.J., Li, W., & Nobre, C.A. 2006a. Climate Change, Deforestation, and the Fate of the Amazon. *Science,* 319: 169-172

Malhi, Y., Wood, D., Baker, T.R., Wright, J., Phillips, O.L., Cochrane, T., Meir, P., Chave, J., Almeida, S., Arroyo, L., Higuchi, N., Killeen, T.J., Laurance, S.G., Laurance, W.F., Lewis, S.L., Monteagudo, A., Neill, D.A., Vargas, P.N., Pitman, N.C.A., Quesada, C.A., Salomao, R., Silva, J.N.M., Lezama, A.T., Terborgh, J., Martinez, R.V., & Vinceti, B. 2006b. The regional variation of aboveground live biomass in old-growth Amazonian forests. *Global Change Biology,* 12: 1107-1138

Malhi, Y., Aragão, L.E.O.C., Galbraith, D., Huntingford, C., Fisher, R., Zelazowski, P., Sitch, S., McSweeney, C., and Meir, P. 2009. Exploring the likelihood and mechanism of a climate-change-induced dieback of the Amazon rainforest. *Proceedings of the National Academy of Sciences,* 106: 20610-20615.

Malhi, Y., Roberts, J.T., Betts, R.A., Killeen, T.J., Li, W., and Nobre, C.A. 2008. Climate Change, Deforestation, and the Fate of the Amazon. *Science*, 319: 169-172

Malmer, N., and Holm, E. 1984. Variation in the C/N-Quotient of Peat in Relation to Decomposition Rate and Age Determination with ^{210}Pb. *Oikos,* 43: 171-182.

Mallick, K., Jarvis, A., Fisher, J.B., Tu, K.P., Boegh, E., and Niyogi, D. 2013. Latent Heat Flux and Canopy Conductance Based on Penman–Monteith, Priestley–Taylor Equation, and Bouchet's Complementary Hypothesis. *Journal of Hydrometeorology*, 14: 419-442

Mann, M.E., Cane, M.A., Zebiak, S.E., and Clement, A. 2005. Volcanic and Solar Forcing of the Tropical Pacific over the Past 1000 Years. Journal of Climate, 18: 447-456

Mann, M.E., Zhang, Z., Rutherford, S., Bradley, R.S., Hughes, M.K., Shindell, D., Ammann, C., Faluvegi, G., and Ni, F. 2009. Global Signatures and Dynamical Origins of the Little Ice Age and Medieval Climate Anomaly. *Science*, 326: 1256-1260

Mann, M.E., Fuentes, J.D., and Rutherford, S. 2012. Underestimation of volcanic cooling in tree-ring-based reconstructions of hemispheric temperatures. *Nature Geoscience*, 5: 202-205

Marchant, R., and Hooghiemstra, H. 2004. Rapid environmental change in African and South American tropics around 4000 years before present: a review. *Earth-Science Reviews,* 66: 217-260.

Marengo, J.A. 1998. Climatología de la zona de Iquítos, Perú. *Annales Universitatis Turkuensis Ser A II,* 114: 35–57.

Marengo, J.A. 1992. Interannual variability of surface climate in the Amazon Basin. *International Journal of Climatology*, 12: 853-863

Marengo, J.A. 2004 Interdecadal variability and trends of rainfall across the Amazon basin. *Theoretical and Applied Climatology*, 78: 79-96

Martin, L., Fournier, M., Mourguiart, P., Sifeddine, A., Turcq, B., Absy, M.L., and Flexor, J-M. 1993. Southern Oscillation Signal in South American Paleoclimate Data of the Last 7000 years. *Quaternary Research*, 39: 338-346.

Martinez Cortizas, A., Garcia-Rodeja, E., Pontevedra Pombal, X., Novoa Munoz, J.C., Weiss, D., and Cheburkin, A. 2002. Atmospheric Pb deposition in Spain during the last 4600 years recorded by two ombrotrophic peat bogs and implications for the use of peat as archive. *Science of the Total Environment*, 292: 33-44

Martínez, O.G, and Morbelli, M.A. 2009. The spores of *Pteris cretica* complex (Pteridaceae-Pteridophyta) in America. *Grana,* 48: 193-204.

Márquez, G.J., Morbelli, M.A., and Giudice, G.E. 2010. Spore morphology and ultrastructure of *Cyathea* (Cyatheaceae, Pteridophyta) species from southern South America. *Grana,* 49: 269-280.

Matos, F.B., Labiak, P.H., Sylvestre, L.S. 2009. A New Brazilian Species of the Genus Asplenium L. (Aspleniaceae). *American Fern Journal, 99*: 101-105.

Mayewski, P.A., Rohling, E.E., Stager, J.C., Karlén, W., Maasch, K.A., Meeker, L.D., Meyerson, E.A., Gasse, F., van Kreveld, S., Holmgren, K., Lee-Thorp, J., Rosqvist, G., Rack, F., Staubwasser, M., Schneider, R.R., and Steig, E.J. 2004. Holocene climate variability. *Quaternary Research*, 62: 243-255.

Mayle, F.E., and Beerling, D.J. 2004. Late Quaternary changes in Amazonian ecosystems and their implications for global carbon cycling. *Palaeogeography, Palaeoclimatology, Palaeoecology,* 214: 11–25.Mayle, F.E., Burbridge, R., and Killeen, T.J. 2000. Millennial-Scale Dynamics of Southern Amazonian Rain Forests. *Science,* 290: 2291-2294

Mayle, F.E., and Iriarte, J. 2014. Integrated palaeoecology and archaeology – a powerful approach for understanding pre-Columbian Amazonia. *Journal of Archaeological Science*, 51: 54-64

Mayle, F.E. and Power, M.J. 2008. Impact of a drier Early-Mid Holocene climate upon Amazonian forests. *Philosophical Transactions of the Royal Society B,* 363: 1829-1838

McCormac, F.G., Hogg, A.G., Blackwell, P.G., Buck, C.E., Higham, T.F.G, and Reimer, P.J. 2004. SHCAL04 Southern Hemisphere calibration 0-11.0 cal kyr BP. *Radiocarbon*, 46: 1087-1092.

McGregor, H.V., Fischer, M.J., Gagan, M.K., Fink, D., Phipps, S.J., Wong, H., and Woodroffe, C.D. 2013. A weak El Niño/Southern Oscillation with delayed seasonal growth around 4,300 years ago. Nature Geoscience, 6: 949-953

McKey, D., Rostain, S., Iriarte, J., Glaser, B., Birk, J.J., Holst, I., and Renard, D. 2010. Pre-Columbian agricultural landscapes, ecosystem engineers, and self-organized patchiness in Amazonia. *Proceedings of the National Academy of Sciences*, 107: 7823-7828

McMichael, C.H., Piperno, D.R., Bush, M.B., Silman, M.R., Zimmerman, A.R., Raczka, M.F., and Lobato, L.C. 2012. Sparse Pre-Columbian Human Habitation in Western Amazonia. *Science*, 336: 1429-1431

Melack, J.M., and Hess, L.L. 2011. Remote Sensing of the Distribution and Extent of Wetlands in the Amazon Basin. In: Junk, K.J., Piedade, M.T.F., Wittman, F., Schöngart, J., and Parolin, P. (eds) *Amazonian Floodplain Forests: Ecophysiology, Biodiversity and Sustainable Management.* Springer: London, 43-60

Mertes, L.A.K. 1997. Documentation and significance of the perirheic zone on inundates floodplains. *Water Resources Research*, 33: 1749-1762.

Meyers, P.A. 1994. Preservation of elemental and isotopic source identification of sedimentary organic matter. *Chemical Geology,* 114: 289-302

Meyers, P.A., and Lallier-Vergès, E. 1999. Lacustrine sedimentary organic matter records of Late Quaternary paleoclimates. *Journal of Paleolimnology,* 21: 345-372

Miettinen, J., and Liew, S.C. 2010. Degradation and development of peatlands in Peninsular Malaysia and in the islands of Sumatra and Borneo since 1990. *Land Degradation and Development,* 21: 285-296.

Mietinnen, J., Hooijer, A., Shi, C., Tollenaar, D., Vernimmen, R., Liew, S.C., Malins, C. and Page, S.E. 2012. Extent of industrial plantations on Southeast Asian peatlands in 2010 with analysis of historical expansion and future projections. *Global Change Biology – Bioenergy*, 4: 908-918.

Miles, L. and Kapos, V. 2008. Reducing Greenhouse Gas Emissions from Deforestation and Forest Degradation: Global Land-Use Implications. *Science*, 320: 1454-1455

Miller, G.H., Geirsdóttir, Á., Zhong, Y., Larsen, D.J., Otto-Bliesner, B.L., Holland, M.M., Bailey, D.A., Refsnider, K.A., Lehman, S.J., Southon, J.R., Anderson, C., Björnsson, H., and Thordarson, T. 2012. Abrupt onset of the Little Ice Age triggered by volcanism and sustained by sea-ice/ocean feedbacks. Geophysical Research Letters, 39: L02708

Minchin, P.R. 1987. An evaluation of the relative robustness of techniques for ecological ordination. *Vegetatio*, 69: 89-107

Mirmanto, E., Tsuyuzaki, S. & Kohyama, T. 2003. Investigation of the effects of distance from river and peat depth on tropical wetland forest communities. *Tropics*, 12: 287-294

Momose, K., and Shimamura, T. 2002. Environments and People of Sumatran Peat Swamp Forests I: Distribution and Typology of Vegetation. *Southeast Asian Studies*, 40: 75-86

Monteith, J.L. 1965. Evaporation and environment. *Symposium of the Society for Experimental Biology*, 19: 205-234.

Morcote-Rios, G. 2008. *Antiguos Habitantes en Ríos de Aguas Negras. Ecosistemas y Cultivos en el Interfluvio Amazonas-Putumayo*: *Colombia-Brasil.* Bogotá: Instituto de Ciencias Naturales, Universidad Nacional de Colombia.

Morcote-Rios, G., Raz, L., Giraldo-Cañas, D., Franky, C.E., and León Sicard. T. 2013. Terras Pretas de Índio of the Caquetá-Japurá River (Colombian Amazonia). *Tipití: Journal of the Society for the Anthropology of Lowland South America,* 11: 30-39

Moreira, L.S., Moreira-Turcq, P., Cordeiro, R.C., Turcq, B., Caquineau, S., Viana, J.C.C., Brandini, N. 2013. Holocene paleoenvironmental reconstruction in the Eastern Amazonian Basin: Comprido Lake. *Journal of South American Earth Sciences*, 44: 55-62

Morley, R.J. 1981. Development and Vegetation Dynamics of a Lowland Ombrogenous Peat Swamp in Kalimantan Tengah, Indonesia. *Journal of Biogeography,* 8: 383-404.

Morley, R.J 1982. A Palaeoecological Interpretation of a 10,000 Year Pollen Record from Danau Padang, Central Sumatra, Indonesia. *Journal of Biogeography,* 9: 151-190.

Morley, R.J. 2001. *Origin and evolution of tropical rain forests.* Chichester: Wiley.

Morley, R.J. 2013. Cenozoic ecological history of South East Asian peat mires based on the comparison of coals with present day and Late Quaternary peats. *Journal of Limnology*, 72: 36-59

Morris, P.J., Baird, A.J., Belyea, L.R. 2012. The DigiBog peatland development model 2: ecohydrological simulations in 2D. *Ecohydrology*, 5: 256–268 DOI: 10.1002/eco.229.

Morris, P.J., Belyea, L.R., and Baird, A.J. 2011. Ecohydrological feedbacks in peatland development: a theoretical modelling study. *Journal of Ecology*, 99: 1190–1201.

Moy, C.J. 1988. Variations of fern spore ultrastructure as reflections of their evolution. *Grana*, 27: 39-51

Moy, C.M., Seltzer, G.O., Rodbell, D.T., and Anderson, D.M. 2002. Variability of El Niño/Southern Oscillation activity at millennial timescales during the Holocene epoch. *Science*, 420: 162-165

Murdiyarso, D., Hergoualc'h, K., and Verchot, L.V. 2010. Opportunities for reducing greenhouse gas emissions in tropical peatlands. Proceedings of the National Academy of Sciences, 107: 19655–19660

Murillo, M.T. & Bless, M.J.M. 1974. Spores of recent Colombian Pteridophyta. I. Trilete spores. *Review of Palaeobotany and Palynology,* 18: 223-269.

Murillo, M.T. & Bless, M.J.M. 1978. Spores of recent Colombian Pteridophyta. II. Monolete spores. *Review of Palaeobotany and Palynology,* 25: 319-365.

Myers, T.P. 2004. Dark Earth in the Upper Amazon. In: Glaser, B., and Woods, W.I. (eds). *Amazonian Dark Earths: Explorations in Space and Time.* Springer: Heidelberg, 67-94.

Nagano, T., Osawa, K., Ishida, T., Sakai, K., Vijarnsorn, P., Jongskul, A., Phetsuk, S., Waijaroen, S., Yamanoshita, T., Norisada, M., and Kojima, K. 2013. Subsidence and soil CO2 efflux in tropical peatland in southern Thailand under various water table and management conditions. *Mires and Peat*, 11: 1-20

Nebel, G., Kvist, L.P., Vanclay, J.K., Christensen, H., Freitas, L., and Ruíz, J. 2001. Structure and floristic composition of flood plain forests in the Peruvian Amazon. I. Overstorey. *Forest Ecology and Mangement,* 150: 27-57

Neuzil, S.G. 1997. Onset and rate of peat and carbon accumulation in four domed ombrogenous peat deposits, Indonesia. In *Biodiversity and Sustainability of Tropical Peatlands*, Rieley JO, Page SE (eds) Samara Publishing: Cardigan. 55–72.

Neves, E.G. and Petersen, J.B. 2006. Political Economy and Pre-Columbian Landscape Transformations in Central Amazonia. In: Balée, W., and Erikson, C.L. (eds) *Time and Complexity in Historical Ecology: Studies in the Neotropical lowlands.* Columbia University Press: New York, 279-309

Newnham, R.M., Vandergoes, M.J., Garnett, M.H., Lowe, D.J., Prior, C., and Almond, P.C. 2007. Test of AMS ^{14}C dating of pollen concentrates using tephrochronology. *Journal of Quaternary Science*, 22: 37-51

Nicholson B. 1997. Aguajal Swamp Forests of the Peruvian Amazon. In: Rieley, J.O., and Page, S.E. (eds.) *Biodiversity and Sustainability of Tropical Peatlands*. Samara Publishing: Cardigan, 267-270.

Nowicke, J.W., and Takahashi, M. 2002. Pollen morphology, exine structure and systematics of Acalyphoideae (Euphorbiaceae), Part 4: Tribes Acalypheae pro parte (Erythrococca, Claoxylon, Claoxylopsis,

Mareya, Mareyopsis, Discoclaoxylon, Micrococca, Amyrea, Lobanilia, Mallotus, Deuteromallotus, Cordemoya, Cococceras, Trewia, Neotrewia, Rockinghamia, Octospermum, Acalypha, Lasiococca, Spathiostemon, Homonoia), Plukenetieae (Haematostemon, Astrococcus, Angostyles, Romanoa, Eleutherostigma, Plukenetia, Vigia, Cnesmone, Megistostigma, Sphaerostylis, Tragiella, Platygyna, Tragia, Acidoton, Pachystylidium, Dalechampia), Omphaleae (Omphalea), and discussion and summary of the complete subfamily. *Review of Palaeobotany and Palynology*, 121: 231-336

Nugroho, K., Gianinazzi, G., and Widjaja-Adhi, I.P.G. 1997. Soil hydraulic properties of Indonesian peat. In: Rieley, J.O., and Page, S.E. (eds) *Biodiversity and Sustainability of Tropical Peatlands*. Samara Publishing: Cardigan, 147–155.

Nuñez-Iturri, G., and Howe, H.F. 2007. Bushmeat and the fate of trees with seeds dispersed by large primates in a lowland rain forest in Western Amazonia. *Biotropica*, 39: 348–354.

Obando, L.M., and Malavassi, L.R. 1993. Geology of peat deposits of Costa Rica. Revista Geologica de América Central, 15: 33-40.

Økland, R.H., Rydgren, K., and Økland, T. 2008. Species richness in boreal swamp forests of SE Norway: The role of surface microtopography. *Journal of Vegetation Science,* 19: 67-74

Olid, C., Garcia-Orellana, J., Martinez-Cortizas, A., Masque, P., Peiteado, E., and Sanchez-Cabeza, J-A. 2008. Role of Surface Vegetation in 210Pb-Dating of Peat Cores. *Environmental Science and Technology*, 42: 8858-8864.

Olid, C., Garcia-Orellana, J., Masqué, P., Martínez Cortizas, A., Sanchez-Cabeza, J.A., and Bindler, R. 2013. Improving the ^{210}Pb-chronology of Pb deposition in peat cores from Chao de Lamoso (NW Spain). *Science of the Total Environment,* 443: 597-607.

Oppo, D. W., Rosenthal, Y. and Linsley, B. K. 2009. 2,000-year-long temperature and hydrology reconstructions from the Indo-Pacific warm pool. *Nature*, 460: 1113-1116

Pacienda, M.L., and Prado, J. 2005. Effects of forest fragmentation on pteridophyte diversity in a tropical rain forest in Brazil. *Plant Ecology,* 180: 87-104.

Page, S.E., Rieley, J.O., Shotyk, Ø.W., and Weiss, D. 1999. Interdependence of peat and vegetation in a tropical peat swamp forest. *Philosophical Transactions of the Royal Society of London B*, 354: 1885-1897

Page, S.E., Siegert, F., Rieley, J.O., Boehm, H-D.V., Jaya, A. & Limin, S. 2002. The amount of carbon released from peat and forest fires in Indonesia during 1997. *Nature,* 420: 61-65

Page, S.E., Rieley, J.O., and Banks, C.J. 2011. Global and regional importance of the tropical peatland carbon pool. *Global Change Biology,* 17: 798–818.

Page, S.E., Rieley, J.O., and Wüst, R. 2006. Lowland tropical peatlands of Southeast Asia. In Peatlands: Evolution and records of environmental and climate changes, Martini IP, Martínaz-Cortizas A, Chesworth W. (eds): 145–172.

Page, S.E., Wüst, R.A.J., Weiss, D., Rieley, J.O., Shotyk, W., and Limin, S.H. 2004. A record of Late Pleistocene and Holocene carbon accumulation and climate change from an equatorial peat bog (Kalimantan, Indonesia): implications for past, present and future carbon dynamics. *Journal of Quaternary Science,* 19: 625-635.

Päivänen, J. 1973. Hydraulic conductivity and water retention in peat soils. *Acta Forestalia Fennica,* 129: 1–70.

Pajunen, H. 1997. Physical and Chemical Properties of Peat in Rwanda, Central Africa. *Geological Survey of Finland Bulletin*, 394: 1-61.

Parodi, J.L., and Freitas, D. 1990. Geographical aspects of forested wetlands in the Lower Ucayali, Peruvian Amazonia. *Forest Ecology and Management*, 33/34: 157-168

Parolin, P., Adis, J., Rodrigues, W.A., Amaral, I., and Piedade, M.T.F. 2004. Floristic study of an igapó floodplain forest in Central Amazonia, Brazil (Tarumã-Mirim, Rio Negro). *Amazoniana,* 18: 29-47.

Parolin, P., Lucas, C., Piedade, M.T.F, and Wittman, F. 2010. Drought responses of flood-tolerant trees in Amazonian floodplains. *Annals of Botany,* 105: 129-139.

Parolin, P. 2002. Life history and environment of *Cecropia latiloba* in Amazonian floodplains. *Revista da Biologia Tropical,* 50: 531-545.

Parry, L.E., Charman, D.J., and Blake, W.H. 2013. Comparative dating of recent peat deposits using natural and anthropogenic fallout radionuclides and Spheroidal Carbonaceous Particles (SCPs) at a local and landscape scale. *Quaternary Geochronology,* 15: 11-19.

Payette, S. 1988. Late-Holocene Development of Subarctic Ombrotrophic Peatlands: Allogenic and Autogenic Succession. *Ecology* 69, 516-531.

Pearsall, D.M. 1994. Investigating New World tropical agriculture: Contributions from phytolith analysis. In: Hather, J. (ed.) *Tropical Archaeobotany: Applications and New Developments*. Routledge: London, 115-138

Pennington, W. 1964. Pollen analyses from the deposits of six upland tarns in the lake district. *Philosophical Transactions of the Royal Society of London B,* 248: 205-244.

Pereira, L.A.R., Calbo, M.E.R., and Ferreira, C.J. 2000. Anatomy of Pneumatophore of *Mauritia vinifera* Mart. *Brazilian Archives of Biology and Technology, 43: 1-7*

Pajunen, H. 1997. Physical and Chemical Properties of Peat in Rwanda, Central Africa. *Geological Survey of Finland Bulletin,* 394: 1-61.

Penman, H.L. 1948. Natural Evaporation from Open Water, Bare Soil and Grass. *Proceedings of the Royal Society of London A*, 193: 120-145.

Pessenda, L.C.R., Gouveia, S.E.M., Aravena, R., Boulet, R., and Valencia, E.P.E. 2004. Holocene fire and vegetation changes in southeastern Brazil as deduced from fossil charcoal and soil carbon isotopes. *Quaternary International*, 114: 35-43

Pessenda, L.C.R., Gouveia, S.E.M., de Souza Ribeiro, A., De Oliveira, P.E., and Aravena, R. 2010. Late Pleistocene and Holocene vegetation changes in northeastern Brazil determined from carbon isotopes and charcoal records in soils. *Palaeogeography, Palaeoclimatology, Palaeoecology*, 297: 597–608

Phillips, S., and Bustin, R.M. 1996. Sedimentology of the Changuinola peat deposit: Organic and clastic sedimentary response to punctuated coastal subsidence. *Geological Society of America Bulletin*, 1996: 794-814

Phillips, S., Rouse, G.E., Bustin, R.M. 1997. Vegetation zones and diagnostic pollen profiles of a coastal peat swamp, Bocas del Torro, Panamá. *Palaeoegeography, Palaeoclimatology, Palaeoecology,* 128: 301-338.

Phillips, O.L., Malhi, Y., Higuchi, N., Laurence, W.F., Núñez, P.V., Vásquez, R.M., Laurence, S.G., Ferreira, L.V., Stern, M., Brown, S. & Grace, J. 1998. Changes in the Carbon Balance of Tropical Forests: Evidence from Long-Term Plots. *Science,* 282: 439-442

Piedade, M.T.F., Junk, W., D'Ângelo, S.A., Wittman, F., Schöngart, J., Barbosa, K.M.d.N., and Lopes, A. 2010. Aquatic herbaceous plants of the Amazon floodplains: state of the art and research needed. *Acta Limnologica Brasiliensia*, 22: 165-178

Piperno, D.R., and Stothert, K.E. 2003. Phytolith evidence for early Holocene Cucurbita domestication in Southwest Ecuador. *Science,* 299: 1054-1057.

Piperno, D.R. 2006. *Phytoliths: A comprehensive guide for archaeologists and paleoecologists*. Altamira: Oxford

Pitman, N., Vriesendorp, C., Moskovits, D. K., von May, R., Alvira, D., Wachter, T., Stotz, D.F., and del Campo, A. (eds.). 2011. *Perú: Yaguas-Cotuhé. Rapid Biological and Social Inventories Report 23*. The Field Museum: Chicago.

Poesie, E.S., Shimamura, T., Page, S.E., Ninomiya, I., and Limin, S. 2011. Species composition and phylogenetic diversity in a tropical peat swamp forest, Central Kalimantan, Indonesia. *Tropics*, 19: 93-105

Polak, A.M. 1992. *Major timber trees of Guyana: a field guide*. The Tropenbos Foundation: Wageningen

Polak, E. 1933. Ueber Torf und Moor in Nieder-landisch Indien. *Proceedings of the Koninklijke Nederlandse Akademie Van Wetenschappen* 30, 1-85.

Polissar, P.J., Abbott, M.B., Wolfe, A.P., Vuille, M., and Bezada, M. 2013. Synchronous interhemispheric Holocene climate trends in the tropical Andes. Proceedings of the National Academy of Sciences, 110: 14551-14556

Polk, J.S., van Beynen, P.E., and Reeder, P.P. 2007. Late Holocene environmental reconstruction using cave sediments from Belize. *Quaternary Research,* 68: 53–63

Poulsen, A.D., & Nielsen, I.H. 1995. How Many Ferns Are There in One Hectare of Tropical Rain Forest? *American Fern Journal,* 85: 29-35.

Poulsen, A.D. & Balslev, H. 1991. Abundance and cover of ground herbs in an Amazonian rain forest. *Journal of Vegetation Science,* 2: 315-322.

Poveda, G., Waylen, P. R., and Pulwarty, R. 2006. Modern climate variability in northern South America and southern Mesoamerica. *Palaeogeography, Palaeoclimatology,* Palaeoecology, 234: 3‐27.

Preiss, N., Mélières, M-A., and Pourchet, M. 1996. A compilation of data on lead 210 concentration in surface air and fluxes at the air-surface and water-sediment interfaces. *Journal of Geophysical Research*, 101: 28847-28862.

Price, J.S. 1992. Blanket bog in Newfoundland. Part 2. Hydrological processes. *Journal of Hydrology,* 135: 103–119.

Proctor, M.C.F., McHaffie, H.S., Legg, C.J., and Amphlett, A. 2009. Evidence from water chemistry as a criterion of ombrotrophy in the mire complexes of Abernethy Forest, Scotland. *Journal of Vegetation Science*, 20: 160–169

Prous, A. & Fogaca, E. 1999. Archaeology of the Pleistocene-Holocene boundary in Brazil. *Quaternary International,* 53/54: 21-41

Prychid, C.J., Rudall, P.J., and Gregory, M. 2004. Systematics and Biology of Silica Bodies in Monocotyledons. *The Botanical Review*, 69: 377-440

Puhakka, M., Kalliola, R., Rajasilta, M., and Salo, J. 1992. River types, site evolution and successional vegetation patterns in Peruvian Amazonia. *Journal of Biogeography*, 19: 651-665

Punt, W., Hoen, P.P., Blackmore, S., Nilsson, S. & Le Thomas, A. 2007. Glossary of pollen and spore terminology. *Review of Palaeobotany and Palynology,* 143: 1-81.

Räsänen, M.E., Salov, J.S., and Jungner, H. 1991. Holocene floodplain lake sediments in the Amazon: ^{14}C dating and palaeoecological use. *Quaternary Science Reviews,* 10: 363–372.

Räsänen, M., Neller, R., Salo, J., and Jungner, H. 1992. Recent and ancient fluvial deposition systems in the Amazon foreland basin, Peru. *Geological Magazine,* 129: 293-306.

Rasmusson, E.M., and Wallace, J.M. 1983. Meteorological Aspects of the El Nino/Southern Oscillation. *Science*, 222: 1195-1202

Reay, D.S., Dentener, F., Smith, P., Grace, J., and Feely, R.A. 2008. Global nitrogen deposition and carbon sinks. Nature Geoscience, 1: 430-437

Renberg, I. The HON-Kajak sediment corer. *Journal of Paleolimnology*, 6: 167-170.

Reuter, J., Stott, L., Khider, D., Sinha, A., and Cheng, H., and Edwards, R.L. 2009 A new perspective on the hydroclimate variability in northern South America during the Little Ice Age. *Geophysical Research Letters,* 36: L21706.

Rein, B., Lückge, A., Reinhardt, L., Sirocko, F., Wolf, A., and Dullo, W-C. 2005. El Niño variability off Peru during the last 20,000 years. *Paleoceanography*, 20: PA4003

Rein, B., Lückge, A., and Sirocko, F. 2004. A major Holocene ENSO anomaly during the Medieval period. *Geophysical Research Letters*, 31: L17211

Reimer, P.J., Bard, E., Bayliss, A., Beck, J.W., Blackwell, P.G., Bronk Ramsey, C., Buck, C.E., Edwards, R.L., Friedrich, M., Grootes, P.M., Guilderson, T.P., Haflidason, H., Hajdas, I., Hatté, C., Heaton, T.J., Hoffman, D.L., Hogg, A.G., Hughen, K.A., Kaiser, K.F., Kromer, B., Manning, S.W., Niu, M., Reimer, R.W., Richards, D.A., Scott, M., Southon, J.R., Staff, R.A., Turney, C.S.M., and van der Plicht, J. 2013. IntCal13 and Marine13 radiocarbon age calibration curves 0–50,000 years cal BP. *Radiocarbon*, 55: 1869-1887

Rivas Panduro, S., 2006. *Projecto de investiacion excavaciones arqueologicas en Quistococha Loreto-Amazonia Peruana.* Informe presentado al Instituto Nacional de Cultura, RNA Nº CR-0350/COARPE Nº 040328

Rivas Panduro, S., Panaifo Texeira, M., Oyuela-Caycedo, A., Zimmerman, A., 2006. Informe preliminar sobre los hallazgos en el sitio archeológico de Quistococha, Amazonía peruana. *Boletin de Estudios Amazonicos*: 1, 79–98

Rodbell, D.T., Bagnato, S., Nebolini, J.C., Seltzer, G.O., Abbott, M.B. 2002. A Late Glacial–Holocene Tephrochronology for Glacial Lakes in Southern Ecuador. *Quaternary Research,* 57: 343–354

Rodbell, D.T., Seltzer, G.O., Anderson, D.M., Abbott, M.B., Enfield, D.B., and Newman, J.H. 1999. An ~15,000 year record of El Niño driven alluviation in southwestern Ecuador. *Science*, 283: 516-520

Roddaz, M., Baby, P., Brusset, S., Hermoza, W., and Darrozes, J.M. 2005. Forebulge dynamics and environmental control in Western Amazonia: The case study of the Arch of Iquitos (Peru). *Tectonophysics,* 399: 87-108.

Rondon, X.J., Gorchov, D.L., and Cornejo, F. 2009. Tree species richness and composition 15 years after strip clear-cutting in the Peruvian Amazon. *Plant Ecology*, 201: 23-37

Roosevelt, A.C., Lima da Costa, M., Lopes Machado, C., Michab, M., Mercier, N., Valladas, H., Feathers, J., Barnett, W., Imazio da Silveira, M., Henderson, A., Silva, J., Chernoff, B., Reese, S., Holman, J.A., Toth, N., & Schick, K. 1996. Paleoindian Cave Dwellers in the Amazon: The Peopling of the Americas. *Science,* 272: 373-384

Roosevelt, A.C., Housley, R.A., da Silveira, M.I., Maranca, S., and Johnson, R. 1991. Eighth Millennium Pottery from a Prehistoric Shell Midden in the Brazilian Amazon. *Science*, 254: 1621-1624.

Rosa, E., and Larocque, M. 2008. Investigating peat hydrological properties using field and laboratory methods: application to the Lanoraie peatland complex (southern Quebec, Canada). *Hydrological Processes*, 22, 1866-1875.

Rosa, R.K., and Koptur, S. 2013. New findings on the pollination biology of Mauritia flexuosa (Arecaceae) in Roraima, Brazil: Linking dioecy, wind, and habitat. *American Journal of Botany*, 100: 613-621

Rose, N.L., Harlock, P.G., Appleby, P.G., and Battarbee, R.W. 1995. Dating of recent lake sediments in the United Kingdom and Ireland using spheroidal carbonaceous particle (SCP) concentration profiles. *The Holocene,* 5: 328-335.

Roucoux, K.H., Lawson, I.T., Jones, T.D., Baker, T.R., Coronado, E.N., Gosling, W.D., Lähteenoja, O. 2013. Vegetation development in an Amazonian peatland. *Palaeogeography, Palaeoclimatology, Palaeoecology,* 374: 242–255.

Roubik, D.W., & Moreno, J.E. 1991. Pollen and Spores of Barro Colorado Island. *Monographs in Systematic Botany (36.)* Missouri Botanical Garden: Missouri, USA

Rovner, I. 1971. Potential of opal phytoliths for use in paleoecological reconstruction. *Quaternary Research*, 1: 343-359.

Rudas Lleras, A, and Prieto Cruz, A. 2005. *Flórula del Parque Nacional Natural Amacayacu, Amazonas, Colombia.* Missouri Botanical Gardens Press: Missouri, USA

Rull, V. 1998. Biogeographical and evolutionary considerations of *Mauritia* (Arecaceae), based on palynological evidence. *Review of Palaeobotany and Palynology*, 100: 109 122

Rull, V. 1999. A palynological record of a secondary succession after fire in the Gran Sabana, Venezuela. J. Quat. Sci. 14, 137-152.

Rull, V. 2001. A morphometric study of early Miocene Mauritiidites from Northern South America: palaeoecological and evolutionary implications. *Grana* 40: 163-167.

Rull, V., and Montoya, E. 2014. *Mauritia flexuosa* palm swamp communities: natural or human-made? A palynological study of the Gran Sabana region (northern South America) within a neotropical context. *Quaternary Science Reviews*, 99: 17-33.

Ruokolainen, K., Tuomisto, H., Macía, M.J., Higgins, M.A., Yli-Halla, M. 2007. Are floristic and edaphic patterns in Amazonian rain forests congruent for trees, pteridophytes and Melastomataceae? *Journal of Tropical Ecology,* 23: 13-25.

Ruppel, M., Väliranta, M., Virtanen, T., and Korhola, A. 2013. Postglacial spatiotemporal peatland initiation and lateral expansion dynamics in North America and northern Europe. *The Holocene*, 23: 1596-1606

Ruppert, L.F., Neuzil, S.G., Cecil, C.B., and Kane, J.S. 1993. Inorganic constituents from samples of a domed and lacustrine peat, Sumatra, Indonesia. *Geological Society of America Special Papers*, 286: 83-96

Rydin, H., and Jeglum, J. 2006. *The Biology of Peatlands.* Oxford: Oxford University Press.

Salo, J., Kalliola, R., Häkkinen, I., Mäkinen, Y., Niemelä, P., Puhakka, M., and Coley, P.D. 1986. River dynamics and the diversity of Amazon lowland forest. *Nature*, 322: 254-258

Salovaara, K.J, Cárdenas, G.G, and Tuomisto, H. 2004. Forest classification in an Amazonian rainforest landscape using pteridophytes as indicator species. *Ecography,* 27: 689-700

Salino, A., Almeida, T.E., Smith, A.R., Gómez, A.N., Kreier, H-P., & Schneider, H. 2008. A New Species of *Microgramma* (Polypodiaceae) from Brazil and Recircumscription of the Genus Based on Phylogenetic Evidence. *Systematic Botany,* 33: 630-635

Sandgren, P. and Snowball, I. 2001. Application of mineral magnetic techniques to paleolimnology. In: Last, W.M., and Smol, J.P. *Tracking Environmental Change Using Lake Sediments: Volume 2: Physical and Geochemical Methods.* Dordrecht: Kluwer, 217-237

Sandweiss, D.H., Maasch, K.A., Burger, R.L., Richardson, J.B., Rollins, H.B., and Clement, A. 2001. Variation in Holocene El Niño frequencies: Climate records and cultural consequences in ancient Peru. *Geology,* 29: 603-606.

Sayer, E.J., and Tanner, E.V.J. 2010. Experimental investigation of the importance of litterfall in lowland semi-evergreen tropical forest nutrient cycling. *Journal of Ecology*, 98: 1052-1062

Sayok, A.K., Nik, A.R, Melling, L., Samad, R.A., and Efransjah, E. 2007. Some characteristics of peat in Loagan Bunut National Park, Sarawak, Malaysia. In: Rieley J.O., Banks C.J., Ragjagukguk, B. (eds) *Proceedings of the International Symposium and Workshop in Tropical Peatland, Yogyakarta, 27-29 August 2007*, 95–100.

Scheffer, M., Carpenter, S., Foley, J.A., Folke, C., and Walker, B. 2001. Catastrophic shifts in ecosystems. *Nature*, 413: 591-596

Schellekens, J., Bruijnzeel, L.A., Scatena, F.N., Bink, N.J., and Holwerda, F. 2000. Evaporation from a tropical rain forest, Luquillo Experimental Forest, eastern Puerto Rico. *Water Resources Research* 36: 2183-2196.

Schöngart, J., Wittman, F., Worbes, M., Piedade, M.T.F., Krambeck, H-J., and Junk, W.J. 2007. Management criteria for *Ficus insipida* Willd. (Moraceae) in Amazonian white-water floodplain forests defined by tree-ring analysis. *Annals of Forest Science*, 64: 657-664

Schulman, L., Ruokolainen, K., Tuomisto, H. 1999. Parameters for global ecosystem models. *Nature,* 399: 535–536

Schwing, F.B., Murphree, T., deWitt, L., and Green, P.M. 2002. The evolution of oceanic and atmospheric anomalies in the northeast Pacific during the El Niño and La Niña events of 1995–2001. *Progress in Oceanography*, 54: 459-491

Scott, D.A., Proctor, J., and Thompson, J. 1992. Ecological studies on a lowland evergreen rain forest on Maracá Island, Roraima, Brazil. II. Litter and nutrient cycling. *Journal of Ecology* 80: 705-717

Seager, R., Graham, N., Herweijer, C., Gordon, A.L., Kushnir, Y., and Cook. E. 2007. Blueprints for Medieval hydroclimate. *Quaternary Science Reviews*, 26: 2322–2336

Seltzer, G., Rodbell, D. and Burns, S. 2000. Isotopic evidence for late Quaternary climatic change in tropical South America. *Geology*, 28: 35-38

Seubert, E. 1996. Root anatomy of palms II: Calamoideae. *Feddes Repertorium*, 107: 43-59

Shaw, E.M. 1994. *Hydrology in Practice (3rd Edition).* Chapman and Hall: London

Shaw, E.H. 2006. *A palaeoecological investigation of long-term stand-scale ecological dynamics in semi-open native pine woods: Contributing to conservation management in east Glen Affric*. Unpublished PhD thesis, University of Sterling.

Shotyk, W., 1988. Review of the inorganic geochemistry of peats and peatland waters. *Earth-Science Reviews*, 25: 95-176.

Shotyk, W. 1996. Natural and anthropogenic enrichments of As, Cu, Pb, Sb, and Zn in ombrotrophic versus minerotrophic peat bog profiles, Jura Mountains, Switzerland. *Water, Air, and Soil Pollution,* 90: 375–405.

Shuttleworth, W.J. 2007. Putting the 'vap' into evaporation. *Hydrology and Earth System Sciences*, 11: 210-244

Silva, R.J.F., and Potiguara, R.D.d-V.2009. Leaf ergastic substances of Amazonian species of *Oenocarpus* Mart. (Arecaceae): histochemical and ultrastructural characterization. *Acta Amazonica,* 39: 793-798

Sierra, C.A., del Valle, J.I., Orrego, S.A., Moreno, F.H., Harmon, M.E., Zapata, M., Colorado, G.J., Herrera, M.A., Lara, W., Restrepo, D.E., Berrouet, L.M., Loaiza, L.M., and Benjumea, J.F. 2007.Total carbon stocks in a tropical forest landscape of the Porce region, Colombia. *Forest Ecology and Management*, 243: 299-309

Sifeddine, A., Martin, L., Turcq, B., Volkner-Ribeiro, C., Soubiès, F., Cordeiro, R.C., and Suguio, K. 2001. Variations of the Amazonian rainforest environment: a sedimentological record covering 30,000 years. *Palaeogeography, Palaeoclimatology, Palaeoecology,* 168: 221-235.

Sjögersten, S., Black, C.R., Evers, S., Hoyos-Santillan, J., Wright, E.L., and Turner, B.L. 2014. Tropical wetlands: A missing link in the global carbon cycle? *Global Biogeochemical Cycles*. DOI: 10.1002/2014GB004844

Sjörs, H. 1983. Mires of Sweden. In: Gore, A.J.P. (ed.) *Ecosystems of the world. 4B. Mires: swamp, bog, fen and moor.* Elsevier: Amsterdam, 69-94.

Stansell, N.D., Rodbell, D.T., Abbott, M.B., and Mark, B.G. 2013. Proglacial lake sediment records of Holocene climate change in the western Cordillera of Peru. *Quaternary Science Reviews*, 70: 1-14

Steinhilber, F., Beer, J., and Frohlich, C. 2009. Total solar irradiance during the Holocene. *Geophysical Research Letters*, 36: L19704.

Stockmarr, J. 1971. Tablets with spores used in absolute pollen analysis. *Pollen et Spores*, 13: 615-621.

Sugita, S. 1993. A model of pollen source area for an entire lake surface. *Quaternary Research,* 39: 239–44

Sugita, S. 2007. POLLSCAPE model. In: Elias, S.A. (ed.) *The Encyclopedia of Quaternary Science, vol. 2.* Amsterdam: Elsevier, 2561-2570

Surridge, B.W.J., Baird, A.J., Heathwaite, A.L. 2005. Evaluating the quality of hydraulic conductivity estimates from piezometer slug tests in peat. *Hydrological Processes,* 19: 1227–1244.

Swindles G.T, Morris P.J, Baird A.J, Blaauw M. and Plunkett G. 2012. Ecohydrological feedbacks confound peat-based climate reconstructions. *Geophysical Research Letters*, 39: L11401.

Swindles, G.T., Reczuga, M., Lamentowicz, M., Raby, C.L., Turner, T.E., Charman, D.J., Gallego-Sala, A., Valderrama, E., Williams, C., Draper, F., Honorio Coronado, E.N., Roucoux, K.H., Baker, T., and Mullan, D.J. 2014. Ecology of Testate Amoebae in an Amazonian Peatland and Development of a Transfer Function for Palaeohydrological Reconstruction. *Microbial Ecology*, 68: 284-298

Takahashi, H., Yonetani, Y. 1997. Studies on microclimate and hydrology of peat swamp forest in Central Kalimantan, Indonesia. In: Rieley J.O., and Page S.E. (eds) *Biodiversity and Sustainability of Tropical Peatlands.* Samara Publishing: Cardigan, 179-187.

Talbot, M.R. 2001. Nitrogen isotopes in palaeolimnology. In: Last, W.M., and Smol, J.P. *Tracking Environmental Change Using Lake Sediments: Volume 2: Physical and Geochemical Methods.* Dordrecht: Kluwer, 401-439

Tansley, A.G. 1935. The use and abuse of vegetational concepts and terms. *Ecology*, 16: 284-307.

Tansley, A.G. 1939. *The British Islands and Their Vegetation.* Cambridge University Press: Cambridge.

Taylor, D., Yen, O.H., Sanderson, P.G., and Dodson, J. 2001. Late Quaternary peat formation and vegetation dynamics in a lowland tropical swamp: Nee Soon, Singapore. *Palaeoegeography, Palaeoclimatology, Palaeoecology,* 171:269-287

Terborgh, J., and Andresen, E. 1998. The composition of Amazonian forests: patterns at local and regional scales. *Journal of Tropical Ecology,* 14: 645-664.

Ter Braak, C.J.F., and Prentice, I.C. 1988. A theory of gradient analysis. *Advances in Ecological Research*, 18: 271-317

Ter Steege, H., Sabatier, D., Castellanos, H., Van Andel, T., Duivenoorden, J., De Oliveira, A.A., Ek, R., Lilwah, R., Maas, P., and Mori, S. 2000. An analysis of the Floristic composition and diversity of Amazonian forests including those of the Guiana Shield. *Journal of Tropical Ecology,* 16: 801-828

Thompson, L.G., Mosley-Thompson, E., Davis, M.E., Zagorodnov, V.S., Howat, I.M., Mikhalenko, V.N., Lin, P.-N. 2013. Annually Resolved Ice Core Records of Tropical Climate Variability over the Past ~1800 Years. *Science*, 340: 945-950

Thompson, L.G., Mosley-Thompson, E., Davis, M.E., Lin, P.-N., Henderson, K.A., Cole-Dai, J., Bolzan, J.F., Liu, K.-B. 1995. Late Glacial Stage and Holocene Tropical Ice Core Records from Huascarán, Peru. *Science*, 269: 46-50.

Thompson, L.G., Davis, M.E., and Mosley-Thompson, E. 1994. Glacial Records of Global Climate: A 1500-Year Tropical Ice Core Record of Climate . *Human Ecology*, 22: 83-95

Thompson, L. G., Mosley-Thompson, E., Dansgaard, W., and Grootes, P. M. 1986. The Little Ice Age as recorded in the stratigraphy of the tropical Quelccaya ice cap. *Science,* 234: 361-364.

Tolonen, K. and Turunen, J. 1996. Accumulation rates of carbon in mires in Finland and implications for climate change. *The Holocene*, 6: 171-178

Troels-Smith, J. 1955. *Karakterisering af Løse Jordater.* Geological Society of Denmark/Rietzels Forlag: Copenhagen.

Troxler, T.G., Ikenaga, M., Scinto, L., Boyer, J.N., Condit, R., Perez, R., Gann, G.D., and Childers, D.L. 2012. Patterns of Soil Bacteria and Canopy Community Structure Related to Tropical Peatland Development. *Wetlands,* 32: 769-782

Tuittila, E-S., Juutinen, S., Frolking, S., Väliranta, M., Laine, A.M., Miettinen, A., Seväkivi, M-L., Quillet, A., and Merilä, P. 2012. Wetland chronosequence as a model of peatland development: Vegetation succession, peat and carbon accumulation. *The Holocene*, 23: 25-35

Turetsky, M.R., Manning, S.W., and Wieder, R.K. 2004. Dating recent peat deposits. *Wetlands*, 24: 324-256

Turner, T.E., Swindles, G.T., and Roucoux, K.H. 2014. Late Holocene ecohydrological and carbon dynamics of a UK raised bog: impact of human activity and climate change. *Quaternary Science Reviews*, 84: 65-85

Turunen, J., Tomppo, E., Tolonen, K., and Reinikainen, A. 2002. Estimating carbon accumulation rates of undrained mires in Finland-application to boreal and subarctic regions. *The Holocene*, 12: 69-80

Tuomisto, H., and Poulsen, A.D. 1996. Influence of Edaphic Specialization on Pteridophyte Distribution in Neotropical Rain Forests. *Journal of Biogeography,* 23: 283-293.

Tuomisto, H., and Poulsen, A.D. 2000. Pteridophyte diversity and species composition in four Amazonian rain forests. *Journal of Vegetation Science,* 11: 383-396.
Tuomisto, H., Poulsen, A.D., and Moran, R.C. 1998. Edaphic distribution of some species of the fern genus *Adiantum* in Western Amazonia. *Biotropica,* 30: 392-399.
Tuomisto, H. and Ruokolainen, K. 1994. Distribution of Pteridophyta and Melastomataceae along an edaphic gradient in an Amazonian Rain Forest. *Journal of Vegetation Science,* 5: 25-34.
Tuomisto, H., Ruokolainen, K., Poulsen, A.D., Moran, R.C., Quintana, C., Cañas, G., and Celi, J. 2002. Distribution and Diversity of Pteridophytes and Melastomataceae along Edaphic Gradients in Yasuní National Park, Ecuadorian Amazonia. *Biotropica,* 34: 516-533.
Turetsky, M.R., Manning, S.W., and Kelman Wieder, R. 2004. Dating recent peat deposits. *Wetlands*, 24: 324-356.
Turner, T.E., Swindles, G.T., and Roucoux, K.H. 2014. Late Holocene ecohydrological and carbon dynamics of a UK raised bog: impact of human activity and climate change. *Quaternary Science Reviews*, 84: 65-85
Turunen, J., Tahvanainen, T., Tolonen, K., 2001. Carbon accumulation in West Siberian mires, Russia. *Global Biogeochemical Cycles*, 15: 285-296.
Urban, N. R., Eisenreich, S. J., Grigal, D. F. & Schurr, K. T. 1990. Mobility and diagenesis of Pb and Pb-210 in peat. *Geochimica Et Cosmochimica Acta*, 54, 3329-3346.
Urrego L.E. 1997. Los Bosques Inundables del Medio Caquetá. Estudios en la Amazonia Colombiana XIV, Fundación Tropenbos, Bogotá.
Urrego, L.E., Molina, L.A., Urrego, D.H., and Ramíriez, L.F. 2006. Holocene space-time succession of the Middle Atrato wetlands, Chocó biogeographic region, Colombia. *Palaeoegeography, Palaeoclimatology, Palaeoecology,* 234: 45-61.
Van Andel, T.R. 2003. Floristic composition and diversity of three swamp forests in northwest Guyana. *Plant Ecology,* 167: 293-317
Van Breukelen, M.R., Vonhof, H.B., Hellstrom, J.C., Wester, W.C.G., and Kroon, D. 2008. Fossil dripwater in stalagmites reveals Holocene temperature and rainfall variation in Amazonia. *Earth and Planetary Science Letters,* 275: 54–60
Van der Hammen, T., and Hooghiemstra, H. 2000.Neogene and Quaternary history of vegetation, climate, and plant diversity in Amazonia. *Quaternary Science Reviews*, 19: 725-742
Van Geel, B. 2001. Non-pollen palynomorphs. In: Smol, J.P., Birks, H.J.B., and Last, W.M. (eds). *Tracking Environmental Change Using Lake Sediments. Volume 3: Terrestrial, Algal, and Siliceous indicators.* Dordrecht: Kluwer
Vercoutere, K., Fortunati, U., Muntau, H., Griepink, B., and Maier, E.A. 1995. The certified reference materials CRM 142 R Light Sandy Soil, CRM 143 R Sewage Sludge Amended Soil and CRM 145 R Sewage Sludge for quality control in monitoring environmental and soil pollution. *Fresenius' Journal of Analytical Chemistry*, 352: 197-202
von Post, L. 1924. Das genetische System der organogenen Bildungen Schwedens. Comité International de Pédologie IV, Communication No. 22: 287-304.
van der Kaars S, Penn D, Tibby J, Fluin J, Dam R.A.C, Suparan P. (2001) Late Quaternary palaeoecology, palynology and palaeolimnology of a tropical lowland swamp: Rawa Danau, West-Java, Indonesia. *Palaeoegeography, Palaeoclimatology, Palaeoecology*, 171: 185-212.
Van der Hammen T. and Hooghiemstra H. (2000) Neogene and Quaternary history of vegetation, climate, and plant diversity in Amazonia. *Quaternary Science Reviews* 19, 725-742
Vasquez, R., and Gentry, A.H. 1989. Use and Misuse of Forest-Harvested Fruits in the Iquitos Area. *Conservation Biology*, 3: 350-361.

Waddington, J.M., Morris, P.J., Kettridge, N., Granath, G., Thompson, D.K., and Moore, P.A. 2014. Hydrological feedbacks in northern peatlands. *Ecohydrology*, 8: 113-127

Wagner, W.H. 1974. Structure of Spores in Relation to Fern Phylogeny. *Annals of the Missouri Botanical Garden*, 61: 332-353.

Walker, D. 1970. Direction and rate in some British post-glacial hydroseres. In: Walker, D. and West, R.G. (eds) *Studies in the Vegetational History of the British Isles*. Cambridge University Press: Cambridge, 117-139

Walker, M., Johnsen, S., Rasmussen, S. O., Popp, T., Steffensen, J.-P., Gibbard, P., Hoek, W., Lowe, J., Andrews, J., Björck, S., Cwynar, L. C., Hughen, K., Kershaw, P., Kromer, B., Litt, T., Lowe, D. J., Nakagawa, T., Newnham, R., and Schwander, J. 2009. Formal definition and dating of the GSSP (Global Stratotype Section and Point) for the base of the Holocene using the Greenland NGRIP ice core, and selected auxiliary records. *Journal of Quaternary Science*, 24: 3-17

Waller, M.P. 1998. An Investigation into the Palynological Properties of Fen Peat through Multiple Pollen Profiles from South-Eastern England. *Journal of Archaeological Science*, 25: 631–642

Wang, X., Auler, A.S., Edwards, R.L., Cheng, H., Cristalli, P.S., Smart, P.L., Richards, D.A., and Shen, C-C. 2004, Wet periods in northeastern Brazil over the past 210 kyr linked to distant climate anomalies. *Nature*, 432: 740-743

Wanner, H., Beer, J., Bütikofer, J., Crowley, T.J., Cubasch, U., Flückiger, J., Goosse, H., Grosjean, M., Joos, F., Kaplan, J.O., Küttel, M., Müller, S.A., Prentice, I.C., Solomina, O., Stocker, T.F., Tarasov, P., Wagner, M., and Widmann, M. 2008. Mid- to Late Holocene climate change: an overview. *Quaternary Science Reviews*, 27: 1791–1828

Wassen, M.J., Barendregt, A., Bootsma, M.C., and Schot, P.P. 1989. Groundwater chemistry and vegetation gradients from rich fen to poor fen in the Naardermeer (the Netherlands). *Vegetatio*, 79: 117-132.

Watling, J. and Iriarte, J. 2013. Phytoliths from the coastal savannas of French Guiana. *Quaternary International,* 287: 162-180

Waughman, G.J. 1980. Chemical Aspects of the Ecology of Some South German Peatlands. *Journal of Ecology*, 68: 1025-1046

Weber, M., Halbritter, H., and Hesse, M. 1999. The Basic Pollen Wall Types in Araceae. *International Journal of Plant Sciences*, 160: 415-423

Weiss, D., Shotyk, W., Rieley, J., Page, S., Gloor, M., Reese, S., and Martínaz-Cortizas, A. 2002. The geochemistry of major and selected trace elements in a forested peat bog, Kalimantan, SE Asia, and its implications for past atmospheric dust deposition. *Geochimica et Cosmochimica Acta*, 66: 2301–2323.

Weng, C., Bush, M.B., & Athens, J.S. 2002. Holocene climate change and hydrarch succession in lowland Ecuador. *Review of Palaeobotany and Palynology*, 120: 73-90.

Wesselingh, F.P., Räsänen, M.E., Irion, G., Vonhof, H.B., Kaandorp, R., Renema, W., Romero Pittman, L., and Gingras, M. 2001. Lake Pebas: a palaeoecological reconstruction of a Miocene, long-lived lake complex in western Amazonia. *Cenozoic Research*, 1: 35-81

Wesselingh, F.P., Hoorn, M.C., Guerrero, J., Räsänen, M.E., Romero Pitman, L., and Salo, J. 2006. The stratigraphy and regional structure of Miocene deposits in western Amazonia (Peru, Colombia and Brazil), with implications for late Neogene landscape evolution. *Scripta Geologica*, 133: 291-322

Whitney, B.S., Mayle, F.E., Punyasena, S.W., Fitzpatrick, K.A., Burn, M.J., Guillen, R., Chavez, E., Mann, D., Pennington, R.T. and Metcalfe, S.E. 2011. A 45 kyr palaeoclimate record from the lowland interior of tropical South America. *Palaeogeography, Palaeoclimatology, Palaeoecology*, 307: 177-192.

Whitney, B.S., Dickau, R., Mayle, F.E., Soto, D.J., Iriarte, J., 2013. Pre-Columbian landscape impact and agriculture in the Monumental Mound region of the Llanos de Moxos, lowland Bolivia. *Quaternary Research,* 80: 207–217

Witte, H.J.L., and van Geel, B. 1985. Vegetational and environmental succession and net organic production between 4500 and 800 b.p. reconstructed from a peat deposit in the western dutch coastal area (assendelver polder). *Review of Palaeobotany and Palynology*, 45: 239-300

Wittman, F., Junk, W.J., and Piedade, M.T.F. 2004. The varzea forests in Amazonia: flooding and the highly dynamic geomorphology interact with natural forest succession. *Forest Ecology and Management* ,196: 199-212.

Wittman, F., Schöngart, J., Montero, J.C., Motzer, T., Junk, W.J., Piedade, M.T.F., Queiroz, H.L., and Worbes, M. 2006. Tree species composition and diversity gradients in white-water forests across the Amazon Basin. *Journal of Biogeography*, 33: 1334-1347

Willis, K.J., Araújo, M.B., Bennett, K.D., Figueroa-Rangel, B., Froyd, C.A., and Myers, N. 2007. How can a knowledge of the past help to conserve the future? Biodiversity conservation and the relevance of long-term ecological studies. *Philosophical Transactions of the Royal Society of London B.,* 362: 175-186

Willis, E.H., Tauber, H., Münnich, K.O. 1960. Variations in the atmospheric radiocarbon concentration over the past 1300 years. *American Journal of Science Radiocarbon Supplement*, 2: 1-4.

Wösten, J.H.M., Van den Berg, J., Van Eijk, P., Gevers, G.J.M., Giesen, W.B.J.T., Hooijer, A., Aswandi, Idris, Leenman, P.H., Satriadi Rais, D., Siderius, C., Silvius, M.J., Suryadiputra,N., TricahyoWibisono, I., 2006. Interrelationships between hydrology and ecology in fire degraded tropical peat swamp forests. *International Journal of Water Resources Development*, 22: 157–174.

Wösten, J.H.M., Clymans, E., Page, S.E., Rieley, J.O., Limin, S.H. 2008. Peat–water interrelationships in a tropical peatland ecosystem in Southeast Asia. *Catena*, 73: 212-224

Worbes, M. 1997. The Forest Ecosystem of the Floodplains. In: Junk, W.J. (ed). *The Central Amazon Floodplain: Ecology of a Pulsing System*. Springer: Berlin, 223-265.

In Biodiversity and Sustainability of Tropical Peatlands, Rieley JO, Page SE (eds) Samara Publishing: Cardigan. 179–187.

Wright, H.E. 1980. Cores of soft lake sediments. *Boreas*, 9: 107-114

Wüst, R.A.J. 2001. 2001. *Holocene evolution of the intermontane Tasek Bera peat deposit, Peninsular Malaysia: controls on composition and accumulation of a tropical freshwater peat deposit.* Unpublished PhD thesis, University of British Columbia, Canada.

Wüst, R.A., Bustin, R.M., and Lavkulich, L.M. 2003. New classification systems for tropical organic-rich deposits based on studies of the Tasek Bera Basin, Malaysia. *Catena*, 53: 133-163

Wüst, R.A.J, Jacobsen, G.E, van der Gaast, H, and Smith, A.M. 2008. Comparison of radiocarbon ages from different organic fractions in tropical peat cores: Insights from Kalimantan, Indonesia. *Radiocarbon*, 50: 359-372.

Yan, H., Sun, L., Wang, Y., Huang, W., Qiu, S., and Yang, C. 2011. A record of the Southern Oscillation Index for the past 2,000 years from precipitation proxies. *Nature Geoscience,* 4: 611-614

Young, K.R., and Leon, B. 1989. Pteridophyta species diversity in the central Peruvian Amazon: importance of edaphic specialisation. *Brittonia*, 41: 388-395

Yu, Z., Campbell, I.D., Vitt, D.H., and Apps, M.J. 2001. Modelling long-term peatland dynamics. I. Concepts, review, and proposed design. *Ecological Modelling*, 145: 197–210

Zoltai, S. C., and Johnson, J.D. 1985. Development of a treed bog island in a minerotrophic fen. *Canadian Journal of Botany*, 63: 1076- 1085.

Appendix

A.1 Pollen descriptions

Descriptions follow the form and terminology used by Colinvaux et al. (1999). Text in brackets refers to the origin of the samples; where necessary, the herbarium code has been provided (K = Royal Botanical Gardens, Kew).

Tabebuia insignis var. monophylla Sandwith [T.R. Baker, F.C. Draper, & T.J. Kelly, field samples, Peru]

Grains monad, isopolar, radially symmetric; Tricolporate, but with often invisible endopore; Exine tectate 1 µm thick; Sexine reticulate, homobrochate; Colpi as long as grain, often closed but wide when open, equatorially constricted, clear margo along margin of colpi; Polar area c. 7 µm; Prolate to subprolate, c. 32-38 µm x 18- 28 µm.

Mauritia flexuosa L. [see Table 6.1 for sample details]

Grains monad, heteropolar, bilaterally symmetric; Monoporate, frequently inaperturate; Exine tectate, 1-2 µm thick (ornamentation excluded); Sexine echinate and micro-scabrate; spines bottle-shaped and capitate, 5-10 µm in length x 1.5 µm wide at base; Scabrae sub-micron in size (c. 0.8 µm in length x 0.25 µm width), cover entire grain surface; Pore irregular circle/oval, c. 5 µm diameter; Amb circular/oval, often irregular; Grains mostly 41- 48 µm long (excluding echinae).

Mauritia carana Wallace [K000526864]

Grains monad, heteropolar, bilaterally symmetric; Monoporate, frequently inaperturate; Exine tectate, c. 1 µm thick (ornamentation excluded); Sexine echinate and micro-scabrate; Spines bottle-shaped, 2.5- 6 µm in length x 1.5 µm wide at base; Pore irregular circle/oval, c. 5 µm diameter; Amb circular/oval, often irregular; Grains mostly 42-47 long (excluding echinae).

Mauritiella armata (Mart.) Burrett [Jenaro Herrera herbarium, Peru]

Grains monad, heteropolar, bilaterally symmetric; Monoporate, frequently inaperturate; Exine tectate, c. 1-3 µm thick (ornamentation excluded); Sexine echinate and micro-scabrate; Spines bottle-shaped, 5-7 µm in length x 1.5 µm wide at base; Scabrae sub-micron in size (c. 0.3 µm x 0.3 µm), cover grain surface, each being c. 0.3 µm apart; Pore irregular circle/oval c. 4 µm diameter; Amb circular, often irregular; grains mostly 32 to 37 µm long (excluding echinae).

Mauritiella macroclada (Burret) Burret [K000526929]

Grains monad, heteropolar, bilaterally symmetric; Monoporate, occasionally inaperturate; Exine tectate, c. 1.5-2.5 µm thick (ornamentation excluded); Sexine echinate; Spines thin and of relatively uniform thickness from base to tip, mostly 3-4 µm in length but occasionally longer; Pore irregular circle/oval c. 4-5 µm diameter; Amb circular; Grains mostly 28-33 µm long (excluding echinae).

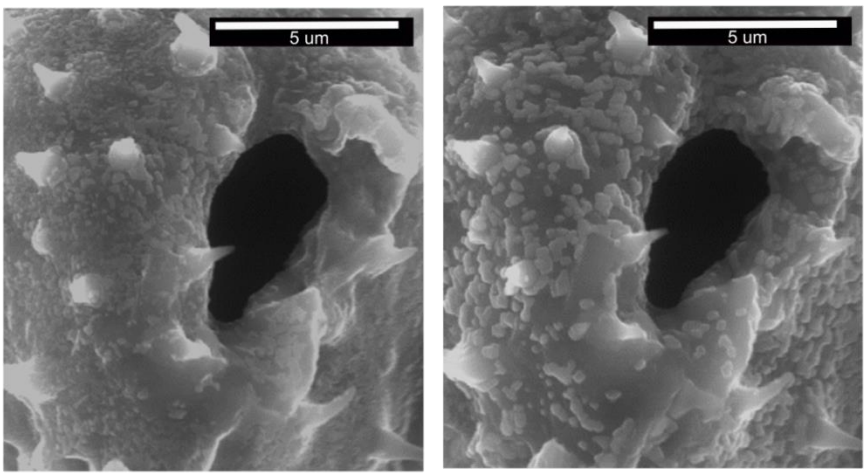

Figure A.1: Observations of surface sculpture for a *Mauritia* type pollen grain in a wet, un-coated palaeoecological sample taken from Quistococha peatland. In contrast to the stable sub-micron surface sculptures observed in gold-coated samples, surface artefacts were seen to form on grains during the period of observation (two to three minutes) when wet sub-fossil samples were subjected to SEM analysis. Echinae appear to have been affected by the vacuum and are more tapered than those seen in Figures 6.7 and 6.8. The lack of gold-coating also meant that charge accumulated on the pointed echinae and made obtaining high-quality images challenging.

A.2 Fern spore descriptions

At the beginning of each description, information relating to the specimens investigated is given in brackets [Collector(s), Date; Herbarium name, herbarium specimen number. SEM = specimen examined using scanning electron microscopy. NLM = specimen examined using normal light microscopy]. Descriptions follow the form used by Colinvaux et al. (1999). Data on the length (L) and depth (D) of the spores (in μm) is summarised in three figures; minimum—mean—maximum. Values have been rounded to the nearest μm. Terminology follows that laid out in Punt et al. (2007), except for 'wings' which refer to definable (generally rounded) protuberances from the perine, and 'ridges' which refer to irregular, thickened protuberances from the perine. Especially distinctive or characteristic features have been underlined.

Monolete types

Asplenium cirrhatum Rich., Willd. [H. Tuomisto, 1997; Turku, 353916.]
Monolete; Heteropolar; Bilaterally symmetric; Sclerine up to 8 μm thick; Perine present with thin and irregularly undulating membrane, joining into ridges, microreticulate (luminae <0.5 μm); Laesura straight, narrow, around ½ length of grain, with thin margo c. 0.5 μm; Amb elliptical; Plano-convex in lateral view. (L: 29—32—38), (D: 15—19—22).

Asplenium pearcei Baker. [H. Tuomisto, 2007; Turku 585244.]
Monolete; Heteropolar; Bilaterally symmetric; Sclerine up to 4 μm (excluding pointed wings), pointed wings up to 25 μm in length (psilate); Perine present with long, pointed, joining into thin ridges, and mixed striate and scabrate sculpture; Laesura straight, narrow, just over ½ length of grain; Amb elliptical; Plano-convex in lateral view. (L: 25—28—33), (D: 16—20—24).

Asplenium serratum L. [H. Tuomisto, 1997; Turku, 356305.]
Monolete; Heteropolar; Bilaterally symmetric; Sclerine up to 8 μm thick; Perine present with thin and irregularly undulating membrane, joining into ridges, microreticulate (luminae <0.5 μm) ; Laesura straight, opened, around ½ length of grain, with thin margo c. 0.5 μm; Amb elliptical; Plano-convex in lateral view. (L: 33—37—40), (D: 19—21—23).

Bolbitis nicotianifolia Alston. [H. Tuomisto, 1999; Turku, 586078.]
Monolete; Heteropolar; Bilaterally symmetric; Sclerine up to 9 μm, exine c. 1 μm; Perine present with thin and irregular membrane, often joining into ridges, apparently sparsely scabrate (scabrae <1 μm); Laesura straight, broad, open, around ½ length of grain; Amb elliptic; Plano-convex in lateral view. (L: 33—37—42), (D: 23—26—30).

Campyloneurum fuscosquamatum Lellinger. [H. Tuomisto & A.R. Smith, 1999; Turku, 586626.]
Monolete; Heteropolar; Bilaterally symmetric; Sclerine around 1 μm thick, densely verrucate (verrucae c. 2 μm, separated by a gap of c. 1 μm); Perine absent; Laesura straight, quite broad, just less than ½ length of grain; Amb elliptical; Plano-convex in lateral view. (L: 38—50—60), (D: 24—30—35).

Campyloneurum phyllitidis C. Presl. [H. Tuomisto, 1997; Turku, 356120. (NLM), (SEM).]
Monolete; Heteropolar; Bilaterally symmetric; Sclerine 1-1.5 μm, finely verrucate (verrucae mostly <1 μm); Perine absent; Laesura straight, broad, around ½ length of grain; Amb elliptical; Plano-convex in lateral view. (L: 54—61—73), (D: 17—25—30).

Diplazium bombanasae Rosenst var. *petiolulatum,* Stolze . [A.R. Smith, 1999; Turku, 587103.]
Monolete; Heteropolar; Bilaterally symmetric; Sclerine up to 6 μm; Perine present, thin and undulating membrane, joining into ridges, very finely scabrate (scabrae <0.5 μm); Laesura 2/3 length grain, straight, open, broad, with thin margo c. 1 μm; Amb elliptical; Plano-convex in lateral view. (L: 32—36—40), (D: 18—22—25).

Elaphoglossum discolor (Kuhn) C. Chr. [(1) H. Tuomisto, 1990; Turku, 316887. (2) H. Tuomisto, J.T. Mickel, 1996; Turku, 354392.]
Monolete; Heteropolar; Bilaterally symmetric; Sclerine up to 10 μm thick; Perine present with thin and irregular undulating membrane, winged, microreticulate (luminae <0.5 μm); Laesura straight, relatively narrow, around 1/3 length of spore; Amb elliptical; Plano-convex in lateral view. (L: 27—31—36), (D: 14—19—23).

Elaphoglossum flaccidum (Fée) T.Moore. [H. Tuomisto, 1997; Turku 353985.]
Monolete; Heteropolar; Bilaterally symmetric; Sclerine up to 6 μm thick, perine; Perine present with thin and irregular undulating membrane, winged, microreticulate (luminae <0.5 μm); Laesura straight, narrow, 1/3 length of spore; Amb elliptical; Plano-convex in lateral view. (L: 27—30—33), (D: 16—18—20).

Elaphoglossum nigrescens (Hook.) Diels. [Moran, 1996; Turku 579343.]
Monolete; Heteropolar; Bilaterally symmetric; Sclerine up to 6 μm thick, densely scabrate (scabrae <1 μm); Perine present with thin, continuous, undulating membrane; Laesura straight, often broad, ½ length of grain; Amb elliptical; Plano-convex in lateral view. (L: 40—44—49), (D: 24—28—33).

Lomagramma guianensis (Aubl.) Ching. [Hanna Tuomisto, 1991; Turku 316881.]
Monolete; Heteropolar; Bilaterally symmetric; Sclerine up to 15 μm, exine c. 1.5 μm; Perine present with thin membrane often joining into ridges, microreticulate (luminae <0.5 μm), but microreticulum obscured somewhat by scabrae (<1μm); Laesura c. ½ length of grain, straight, narrow, slightly open, with margo 1 μm wide; Amb elliptical; Plano-convex in lateral view.(L: 40—49—56), (D: 24—32—36).

Microgramma percussa (Cav.) de la Sota. [H. Tuomisto, 1999; Turku 587240.]
Monolete; Heteropolar; Bilaterally symmetric; Sclerine up to 2 μm thick (including ornamentation), densely verrucate (verrucae c. 3 μm separated by a gap of c. 1 μm) with closely packed verrucae; Laesura straight, narrow but occasionally broad, around ½ length of grain; Amb elliptical; Plano-convex in lateral view. (L: 42—49—53), (D: 24—31—35).

Microgramma reptans (Cav.) A.R.Sm. [A.R. Smith, 1999; Turku 587263.]
Monolete; Heteropolar; Bilaterally symmetric; Sclerine up to 2 μm thick (including ornamentation), densely verrucate (verrucae 1-2 μm separated by a gap of c. 1 μm); Laesura straight, broad, around ½ length of grain; Amb elliptical; Plano-convex in lateral view. (L: 34—40—45), (D: 20—25—30).

Microgramma thurnii (Baker) R.M. Tryon & Stolze. [(1) A.R.Smith 1999; Turku, 587251. (2) H. Tuomisto, 1997; Turku, 355966.]
Monolete; Heteropolar; Bilaterally symmetric; Sclerine up to 3 μm thick (including ornamentation), densely verrucate (verrucae large, square in side view, ≤ 5 μm across, separated by relatively wide gap of c. 3-4 μm); Laesura straight, around ½ length of grain; Amb elliptical; Plano-convex in lateral view. (L: 38—46—52), (D: 24—29—37).

Nephrolepis biserrata Schott. [(1) H. Tuomisto, 1997; Turku, 354071. (NLM). (2) H. Tuomisto, 1999; Turku, 587265. (SEM).]
Monolete; Heteropolar; Bilaterally symmetric; Sclerine around 1.5 μm, reticulate, can appear 'pitted', with irregular, bumpy surface; Perine absent; Laesura c. ½ length of grain, straight, opened, with thin margo <1 μm wide; Amb elliptical; Plano-convex in lateral view. (L: 25—29—34), (D: 14—17—20).

Nephrolepis pectinata (Willd.) Schott. [Smith, 1999; Turku, 587266.]
Monolete; Heteropolar; Bilaterally symmetric; Sclerine around 1.5 μm, reticulate, can appear 'pitted', with irregular, bumpy surface; Perine absent; Laesura c. ½ length of grain, straight, opened, with thin margo <1 μm wide; Amb elliptical; Plano-convex in lateral view. (L; 26—31—36), (D: 15—18—21).

Nephrolepis rivularis (Vahl.) Mett. Krug. [(1) H. Tuomisto, 1990; Turku, 317252. (NLM). (2) Moran, 1996; Turku, 359573. (SEM).]
Monolete; Heteropolar; Bilaterally symmetric; Sclerine around 2 μm, reticulate, often appears 'pitted', with irregular, bumpy surface; Perine absent; Laesura 2/3 length of grain, straight, with thin margo <1 μm wide; Amb elliptical; Plano-convex in lateral view. (L: 26—31—36), (D: 16—19—23).

Polybotrya caudata Kunze. [H. Tuomisto, 1992; Turku, 318422.]
Monolete; Heteropolar; Bilaterally symmetric; Sclerine up to 12 μm thick, apparently densely scabrate (scabrae <1 μm); Perine present with thin, continuous, undulating membrane, winged; Laesura straight, ½ length of grain; Amb elliptical; Plano-convex in lateral view. (L: 35—43—49), (D: 16—27—33).

Polybotrya osmundacea Willd. [H. Tuomisto, 1992; Turku, 317956.]
Monolete; Heteropolar; Bilaterally symmetric; Sclerine up to 1.5 μm thick, apparently finely scabrate (scabrae <1 μm) or psilate; Perine absent; Laesura straight, indistinct, thin, around ½ length of grain; Amb elliptical; Plano-convex in lateral view. (L: 32—39—46), (D: 17—22—26).

Polypodium adnatum Wall. [H. Tuomisto, 1999; Turku, 587182.]
Monolete; Heteropolar; Bilaterally symmetric; Sclerine c. 3 μm (inc. sculpture), verrucate (verrucae large, plate-like); Perine absent; Laesura straight, narrow, margo c. 1 μm wide; Amb elliptical; Plano-convex in lateral view. (L: 36—41—46), (D: 21—24—26).

Polypodium bombycinum Maxon. [H. Tuomisto, 1999; Turku, 587199.]
Monolete; Heteropolar; Bilaterally symmetric; Sclerine around 2 μm, scabrate (scabrae mostly <1 μm) in some cases joining into rugulate surface sculpture; Perine absent; Laesura ¾ length of grain, opened, broad, with thin margo c. 1 μm wide; Amb elliptical; Plano-convex in lateral view. (L: 42—51—60), (D: 26—32—36).

Polypodium caceresii Sodiro. [H. Tuomisto, A.R. Smith, 1999; Turku, 587211.]
Monolete; Heteropolar; Bilaterally symmetric; Sclerine c. 3.5-4 μm (inc. sculpture), verrucate (verrucae very large, plate-like, 4-8 μm across, irregular); Perine absent; Laesura straight, narrow, margo c. 1 μm wide; Amb elliptical; Plano-convex in lateral view. (L: 38—42—45), (D: 21—25—28).

Polypodium polypodoides (L.). [H. Tuomisto, A.R.Smith, 1999; Turku, 587437.]
Monolete; Heteropolar; Bilaterally symmetric; Sclerine around 2.5 μm, coarsely scabrate (scabrae 1 μm), occasionally with degraded verrucae; Perine absent; Laesura 3/5 length of grain, opened, broad, with thin margo <1 μm wide; Amb elliptical; Plano-convex in lateral view. (L: 35—44—50), (D: 20—25—30).

Tectaria antioquiana (Baker) C. Chr. [H.Tuomisto, 2007. Turku, 588821]
Monolete; Heteropolar; Bilaterally symmetric; Sclerine c. 10 μm (c. 1 μm excluding perine); Perine present, microreticulate (luminae <0.5 μm), thin and irregular membrane joining into ridges/wings; Laesura straight, c. ½ length of grain; Amb elliptic; Lateral view plano-convex. (L: 30—35—39), (D: 19—22—25).

Thelypteris ancyriothrix (Rosenst.) A.R.Sm. [H. Tuomisto, 1999; Turku, 587795.]
Monolete; Heteropolar; Bilaterally symmetric; Sclerine up to 7 μm, exine c. 1 μm; Perine present with irregular membrane and thickened ridges, with very subtle microreticulum (luminae <0.5 μm); Laesura indistinct; Amb elliptic; Plano-convex in lateral view. (L: 26—30—33), (D: 14—18—21).

Thelypteris interrupta (Willd) B.C.Stone. [H. Tuomisto, 1991; Turku, 317713.]
Monolete; Heteropolar; Bilaterally symmetric; Sclerine up to 7 μm, exine c. 1 μm; Perine present, generally densely scabrate (scabrae <1 μm) bordering on rugulate in parts, with underlying microreticulum (luminae <0.5 μm); Laesura c. 3/5 grain, straight, narrow, slightly open; Amb elliptical; Plano-convex in lateral view. (L: 31—44—53), (D: 18—26—31).

Triplophyllum funestum (Kunze) Holttum. [H. Tuomisto, A.R. Smith 1999; Turku, 589224.]
Monolete; Heteropolar; Bilaterally symmetric; Sclerine up to 10 μm, exine c. 1 μm; Perine present with thin and undulating membrane occasionally joining into ridges, densely scabrate (scabrae coarse, mostly <1 μm), with underlying microreticulum; Laesura indistinct, but often

marked by parallel ridges in perine; Amb elliptic; Plano-convex in lateral view. (L: 37—42—47), (D: 23—27—30).

Trilete types

Adiantum humile Kunze. [H. Tuomisto, 1999; Turku, 588462.]
Trilete; Heteropolar; Radially symmetric; Sclerine c. 1 μm, microreticulate; Perine absent; Laesurae slightly sinuous with thin margo (≤ 1 μm); Amb subtriangular-concave. (L: 27—30—35).

Adiantum obliquum Willd. [H. Tuomisto, 2007; Turku, 588551.]
Trilete; Heteropolar; Radially symmetric; Sclerine c. 2 μm, densely scabrate on distal and proximal faces (scabrae fine, <0.5 μm); Perine absent; Laesurae slightly sinuous, narrow, opened, with thin margo (<1 μm); Amb subtriangular-concave. (L: 40—46—53).

Adiantum terminatum Kunze, Miq. [H.Tuomisto, A.R. Smith, 1999; Turku, 586314.]
Trilete; Heteropolar; Radially symmetric; Sclerine c. 1.5 μm, densely scabrate on distal and proximal faces (scabrae fine, <0.5 μm); Perine absent; Laesurae straight, broad, opened; Amb subtriangular. (L: 32—34—39).

Adiantum tomentosum Klotzsch. [A.D. Poulsen, 1988; Turku, 317412.]
Trilete; Heteropolar; Radially symmetric; Sclerine c. 1 μm, densely scabrate on distal and proximal faces (scabrae fine, <0.5 μm); Perine absent; Laesurae slightly sinuous, opened, with thin margo (<1 μm); Amb subtriangular-concave. (L: 24—28—31).

Cyathea macrosora (Baker) Domin. [H. Tuomisto, 2007; Turku, 585950.]
Trilete; Heteropolar; Radially symmetric; Sclerine c. 2 μm, thickening at angles up to 3 μm, densely scabrate on distal and proximal faces (scabrae fine, <0.5 μm); Perine generally absent, but where present consists of thin undulating membrane, with ridges; Laesurae mostly straight but occasionally sinuous, opened, with thin margo (c. 0.5 μm); Amb subtriangular. (L: 45—55—74).

Metaxya rostrata C. Presl. [H. Tuomisto, 1990; Turku, 317562.]
Trilete; heteropolar; radially symmetric; Sclerine c. 1 μm, microreticulate; Perine present, thin and undulating membrane, joining into ridges in places; Laesurae almost full radius of grain in many cases, and protrude above the surface of the spore, relatively straight with thin margo (c. 1 μm); Amb subtriangular. (L: 25—30—35).

Pityrogramma calomelanos (L.) Link. [H.Tuomisto, 1999; Turku, 587323.]
Trilete; Heteropolar; Radially symmetric; Sclerine c. 1 μm, reticulate on distal face, rugulate on proximal face; Zona thick, up to 5 μm; Laesurae straight, narrow, with thin margo (<1 μm); Amb subtriangular-semiconcave. (L: 35—42—49).

Pteris altissima Poir. [H.Tuomisto, 1999; Turku, 587480.]
Trilete; Heteropolar; Radially symmetric; Sclerine c. 1.5 μm, rugulate on distal face, rugulate to verrucate on proximal face; Zona up to 4 μm; Perine absent; Laesurae straight, often quite broad, with margo c. 1.5 μm wide; Amb subtriangular-semiconcave. (L: 28—33—38).

Pteris propinqua J. Agardh. [H. Tuomisto, 1999; Turku, 587458.]

Trilete; Heteropolar; Radially symmetric; Sclerine 1-1.5 μm, rugulate on distal face, densely scabrate on proximal face (scabrae <1 μm); Zona up to 3 μm; Perine absent; Laesurae narrow, fairly straight; Amb subtriangular-semiconcave. (L: 30—35—40).

Saccoloma inaequale (Kunze) Mett. [H. Tuomisto, 1997; Turku, 354222.]
Trilete; Heteropolar; Radially symmetric; Sclerine c. 1.5 μm, striate (striae <1 μm); Perine absent; Laesurae straight with thin margo (<1 μm); Amb subtriangular. (L: 29—33—40).